Sediment Transport in Alluvial Channels 1963-65

GEOLOGICAL SURVEY PROFESSIONAL PAPER 462

This volume was published as separate chapters A–I

UNITED STATES DEPARTMENT OF THE INTERIOR

STEWART L. UDALL, *Secretary*

GEOLOGICAL SURVEY

William T. Pecora, *Director*

CONTENTS

[The letters designate separately published chapters]

(A) Discharge of sands and mean-velocity relationships in sand-bed streams, by Bruce R. Colby.
(B) Vertical distribution of velocity and suspended sediment, Middle Rio Grande, New Mexico, by Carl F. Nordin, Jr., and George R. Dempster, Jr.
(C) A preliminary study of sediment transport parameters, Rio Puerco near Bernardo, New Mexico, by Carl F. Nordin, Jr.
(D) Scour and fill in sand-bed streams, by Bruce R. Colby.
(E) An analysis of some storm-period variables affecting stream sediment transport, by H. P. Guy.
(F) Sediment transport in the Rio Grande, New Mexico, by Carl F. Nordin, Jr., and Joseph P. Beverage.
(G) Effects of water temperature on the discharge of bed material, by B. R. Colby and C. H. Scott.
(H) Bedload equation for ripples and dunes, by D. B. Simons, E. V. Richardson, and C. F. Nordin, Jr.
(I) Summary of alluvial channel data from flume experiments, 1956–61, by H. P. Guy, D. B. Simons, and E. V. Richardson.

Discharge of Sands and Mean-Velocity Relationships in Sand-Bed Streams

By BRUCE R. COLBY

SEDIMENT TRANSPORT IN ALLUVIAL CHANNELS

GEOLOGICAL SURVEY PROFESSIONAL PAPER 462-A

UNITED STATES GOVERNMENT PRINTING OFFICE, WASHINGTON : 1964

UNITED STATES DEPARTMENT OF THE INTERIOR

STEWART L. UDALL, *Secretary*

GEOLOGICAL SURVEY

Thomas B. Nolan, *Director*

For sale by the Superintendent of Documents, U.S. Government Printing Office
Washington, D.C. 20402 -

CONTENTS

	Page
Definitions	v
Symbols	vi
Abstract	A1
Introduction	1
Concept of sediment transportation	2
Complexity of sediment and streamflow relationships	2
Simplifying assumptions	3
Bedload discharge	4
Meyer-Peter and Müller equation	4
Einstein equations	5
Bagnold equation	6
Major variables	7
Suspended-sediment discharge	7
Concentration immediately above the bed layer	7
Vertical distribution of sediment concentration	8
The classical equation for sediment of one fall velocity	8
Theoretical and observed distributions	9
Equation for flow over dune beds	11
Total sediment discharge	13
General methods of computation	13
Fine sediment	13
Effects of major factors	A15
Mean velocity	15
Natural streams	15
Flumes	18
Shear	20
Shear velocity computed from mean velocity	24
Stream power	24
Depth	25
Viscosity	29
Water temperature	29
Concentration of fine sediment	32
Graphs for computing discharge of sands	34
Basic information	34
General method of analysis	34
Determining the discharges of sands from the graphs	37
Probable accuracy of the graphs	37
Experimental errors in basic information	37
Data included in the study	38
Stream reaches and flume investigations not included in the study	40
Applications	43
Deficiencies of basic information	44
Conclusions	45
References	46

ILLUSTRATIONS

		Page
FIGURE 1.	Bedload discharges, computed with the Meyer-Peter and Müller equation, as functions of RS and mean velocity	A5
2.	Relationship of Φ_* to Ψ_* for individual size ranges	6
3.	z_1 plotted against z_m	10
4.	z_1 plotted against k_1 for shallow streams in Nebraska	12
5.	$z_1 u_*$ plotted against k_1 for shallow streams in Nebraska	12
6.	Distribution of concentrations of different sediment sizes at a stream vertical	14
7.	Discharge of sands plotted against mean velocity for Niobrara River near Cody, Nebr	16
8.	Discharge of sands plotted against mean velocity for Middle Loup River at Dunning, Nebr	16
9.	Curves of relationship between discharge of sands and mean velocity for stations on Pigeon Roost Creek in Mississippi	17
10.	Discharge of sands plotted against mean velocity for the Rio Grande in New Mexico and for some diversions from it	18
11.	Discharge of sands plotted against mean velocity for Rio Puerco near Bernardo, N. Mex	19
12.	Discharge of sands plotted against mean velocity for Mississippi River at St. Louis, Mo	19
13.	Curves showing relationship between discharge of sands and mean velocity for five sand-bed streams at average temperatures of about 60° F	20
14.	Curves showing relationship between discharge of sands and mean velocity for some flume experiments with two sands	21
15.	Curves showing relationship between discharges of sands and mean velocity for some flume experiments	22
16.	Discharges of sands plotted against parameters that are related to the force which moves sediment particles	23
17.	Effect of depth and water temperature on the relationship between discharge of sands and mean velocity, as computed from a somewhat revised Einstein procedure	26
18.	Schematic diagram showing the general reasons for variability of effect of depth on the relationship of bed-material discharge to velocity	27

Page

FIGURE 19. Empirically determined graph of the effect of depth on the relationship between discharge of sands and mean velocity ---- A28
20. Effect of depth on the relationship between discharge of sands and shear velocity computed from mean velocity ---- 28
21. Effect of depth on the relationship of concentration of sands to mean velocity ---- 29
22. Adjustment for effect of water temperature on the discharge of sands, Niobrara River near Cody, Nebr ---- 30
23. Effect of water temperature on the discharge of sands in four natural streams ---- 30
24. Approximate effect of water temperature and concentration of fine sediment on the relationship of discharge of sands to mean velocity ---- 31
25. Comparison of computed and observed discharges of sands for Rio Puerco near Bernardo, N. Mex ---- 33
26. Relationship of discharge of sands to mean velocity for six median sizes of bed sands, four depths of flow, and a water temperature of 60°F ---- 36
27. Comparison of computed and observed discharges of sands for natural streams that were included in the study ---- 39
28. Comparison of computed and observed discharges of sands for flume data that were included in the study ---- 41
29. Comparison of computed and observed discharges of sands for stream reaches that were not included in the study ---- 42
30. Comparison of computed and observed discharges of sands for flume data that were not included in the study ---- 43

DEFINITIONS

Antidunes are roughly symmetrical sand waves that are about in phase with similar water waves. This definition includes as antidunes the roughly symmetrical sand waves that may exist below relatively quiet and symmetrical standing waves on the water surface.

Bars are extensive raised areas or ridges, larger than dunes in the same flow, on the bed of a stream whose bottom shifts readily, at least at high flow.

Bed layer is the layer through which the bedload moves. It is usually considered to be only a few grain diameters thick.

Bedload is the sediment that moves by sliding, rolling, or skipping on or very near the streambed and is supported mainly by the bed rather than by the turbulence of the flow.

Bed material is the sediment of those particle sizes that are found in appreciable quantity in the streambed. It is classified according to particle size rather than mode of transportation or location in the cross section.

Bed sediment is the sediment on the streambed.

Bed sand is bed sediment within the size range of sand.

Concentration is a ratio of the weight of sediment to the weight of the water-sediment mixture. In this paper it is the weight ratio of the sediment that is transported through a stream cross section or part of a cross section to the water-sediment mixture that moves through the same area during the same time interval.

Dunes are somewhat irregularly spaced mounds of loose sand. Their upstream faces are usually gently inclined as compared with their much steeper downstream faces.

Fall velocity of a sediment particle is the rate at which the suspended particle settles with respect to the surrounding fluid.

Fine sediment as the term is used in this paper is the sediment that is finer than 0.062 mm.

Froude number is the ratio of the velocity of flow to the square root of the product of the gravity constant and the depth of flow.

Grain roughness is the boundary roughness that results solely from the sizes of the stationary particles without any effect from the configuration of the bed or banks.

Mean velocity is the velocity that is obtained by dividing the flow by the perpendicular area of section through which the flow passes. Usually, the mean velocity is computed for the whole cross section of a stream, but sometimes a mean velocity is computed for part of a flow.

Measured discharge of sediment or of sands is the discharge of sediment or sands that is usually determined directly from streamflow and depth-integrated sediment samples, which generally are obtained by sampling the flow from the water surface to within 0.3 or 0.4 foot of the streambed.

Median particle size is the size for which 50 percent of the sediment by weight is finer.

Plane bed is a relatively smooth and firm sand bed that is free of ripples, dunes, and antidunes and, consequently, has low resistance to flow.

Resistance to flow is an inclusive term for the total resistance to flow in a channel.

Roughness of bed or banks is a boundary irregularity and is usually expressed as a linear measure of the effective size of the irregularities of bed or banks.

Sand is sediment particles that have diameters between 0.062 and 2.0 mm.

Sand-bed stream is a reach of stream whose bed is composed almost entirely of cohesionless, shifting sand and whose channel is not confined by walls of rough rock or other material that would cause unusually high turbulence throughout much of the flow.

Sediment discharge is the rate at which weight of sediment moves through a cross section perpendicular to the direction of flow.

Shear per unit area of the streambed is the product of the specific weight of water-sediment mixture, the depth of flow, and the energy gradient.

Shear velocity is the square root of the product of the gravity constant, the depth of flow, and the energy gradient.

Shear velocity with respect to the grains or particles is a concept used by Einstein (1950) and is the shear velocity that can be computed from the energy gradient and a particular hydraulic radius R'.

The square root of the ratio of R' to the hydraulic radius R equals the ratio of the actual mean velocity to the mean velocity that would exist if all resistance to flow were due to the stationary particles on the bed.

Shear velocity computed from mean velocity is the shear velocity that can be computed from a known mean velocity with the use of an equation such as the one Einstein (1950) derived from work by Keulegan (1938).

Size class or **size range** is a definitely limited range of sediment particles that are grouped together because their behavior can be reasonably well represented by some one particle size such as the geometric mean size, which is the square root of the product of the upper and lower limiting sizes.

Suspended sediment (suspended load) or **suspended sand** is sediment or sand that is supported by the upward components of turbulent currents or by colloidal suspension if the sediment particles are very small.

Standard fall velocity is the average rate at which a particle would eventually settle if falling alone in quiescent distilled water of infinite extent and at a temperature of 24° C.

Unmeasured sediment discharge is the difference between total sediment discharge and measured sediment discharge.

SYMBOLS

A and B	Dimensionless constants used as 0.047 and 0.25, respectively, by Meyer-Peter and Müller (1948).
A_1	Dimensionless constant used by Bagnold (1956). It may be about 9.
B_1	Dimensionless constant used by Bagnold. It varies slowly with particle size.
a	Distance above the streambed.
C	Chezy C, which is equal to $\bar{u}/\sqrt{RS}$.
c	Concentration of sediment. Concentration at a is denoted by c_a and at y by c_y.
D	Particle size expressed as a diameter or the geometric mean diameter of a size range.
D_m	Effective diameter of the bed-material mixture (the particle size of uniform sediment) and equal to $\Sigma D i_b$ for bed sediment of a range of sizes.
D_{35}	Particle size for which 35 percent of the bed material by weight is finer. Subscripts 50, 65, and 90 have comparable meanings. Hence, D_{50} is the median particle size.
d	Depth of flow.
g	The gravity constant.
i_b	Fraction by weight of bed sediment in a size range.
K_r	A measure of resistance to flow and equal to the mean velocity $\bar{u}$ divided by the quantity $(R^{2/3}S^{1/2})$.
K_r'	A comparable measure of the flow resistance due only to the resistance of the stationary grains, and for metric units it can be computed from $26/(D_{90})^{1/6}$ in which D_{90} is the particle size, in meters, for which 90 percent of the bed sediment by weight is finer.
K_1, K_2, K_3	Constants.
k	The turbulence constant, which is about 0.40 for clear-water flow and certain types of boundary roughness but may vary widely for sediment-laden flow and dune roughness.
k_s	A linear measure of roughness that may be assumed to equal D_{65} if the bed roughness is due wholly to the roughness of the stationary grains.
k_1	The form of k that is computed from the vertical distribution of velocity over a dune bed or other rough bed.
L	Length of channel reach.
l_e	The mixing length.
q_B	Bedload discharge per foot of width in terms of weight of sediment per unit time.
q_B'	Bedload discharge per unit width in terms of underwater weight of sediment per unit time.
R	The hydraulic radius, which equals average depth of flow when the bank resistance is negligible.
R'	The hydraulic radius with respect to the grains or particles. It is the hydraulic radius that could be used to compute velocity if all the resistance to flow were due to the stationary sediment particles.

S The energy gradient.

u Time-averaged velocity at a point. A subscript may be used to indicate distance of the point above the streambed.

$\bar{u}$ Mean velocity, which is computed by dividing the streamflow by the area of the cross section.

u_m Shear velocity computed from mean velocity and equal to $0.40\bar{u}/[2.30 \log (12.27 xd/D_{65})]$.

u_* Shear velocity and equal to $\sqrt{gRS}$.

u_*' Shear velocity with respect to the sediment particles and equal to $\sqrt{gR'S}$.

v Average vertical velocity of the upward- or downward-moving water in turbulent flow.

W Channel width.

w Fall velocity of a sediment particle or particles.

x A dimensionless parameter to cover the transition from hydraulically smooth to hydraulically rough boundaries.

y Distance above the streambed.

z Theoretical exponent for vertical distribution of sediment of one fall velocity or a narrow range of fall velocity and equal to $w/(0.40u_*)$ for uniform flow over a plane bed.

z_m The form of z that can be computed from $w/(0.40u_m)$.

z_o The form of z for flow over dunes or other rough beds and equal to $w/(k_1u_*)$.

z_1 Exponential measure of the actual distribution of sediment with depth as determined from a logarithmic plot of concentration for a size range against $(d-y)/y$.

log Logarithm to the base 10.

$\log_e$ Logarithm to the base e.

β Declination of the bed surface below the horizontal; $\cos \beta$ generally can be considered to equal unity and be disregarded.

γ Specific weight of water-sediment mixture.

γ_f Specific weight of the fluid.

γ_s Specific weight of the sediment particles.

θ_F A dimensionless measure of the apparent tangential stress due to action of external forces on the fluid and equal to $[\rho_f/(\rho_s-\rho_f)](RS/D)$.

θ_t That value of θ_F (determined by extrapolation) at which sediment particles begin to move on a rippled sand bed.

ν Kinematic viscosity.

ρ_f Density of the fluid.

ρ_s Density of the sediment particles.

Φ Intensity of bedload transportation for uniform bed sediment.

Φ_* Intensity of bedload transportation for a size range of nonuniform bed sediment.

Ψ Function for correlating effect of flow with intensity of sediment transportation.

Ψ_* Function Ψ as adjusted by Einstein (1950, p. 37) for an individual size range.

DISCHARGE OF SANDS AND MEAN-VELOCITY RELATIONSHIPS IN SAND-BED STREAMS

By Bruce R. Colby

ABSTRACT

Theories of sediment movement and general observation provide the basis for a practical concept of sediment transportation in sand-bed streams. This concept covers bedload discharge, the concentrations of sediment of different size ranges immediately above the bed layer, and the vertical distribution of suspended sediment of different size ranges within the flow. According to the concept, the bedload discharge per unit width depends mostly on the velocity near the streambed, the fall velocities of the bed sediment, and the depth of flow. Immediately above the bed layer, the concentrations of sands in the different size ranges are determined mainly by the bedload discharge of the different size ranges, the depth of the bed layer, the velocity of flow through the bed layer, and the probable continuity of the concentrations from the bed layer to the suspended sediment immediately above the bed layer. The concentrations of suspended sands within the different size ranges at any level in the flow depend on the concentrations immediately above the bed layer and the rate at which the concentrations decrease with distance above the bed layer. The rate of decrease of sediment concentration in each size range can be computed, but only roughly, from the ratio of the fall velocity to the shear velocity.

An analysis of the relationships of discharge of sands per foot of width to the controlling factors that were indicated or suggested by the general concept of sediment transportation showed approximate major effects of several variables as follows:

1. Mean velocity or, as an alternative factor, shear velocity computed from mean velocity has a dominant effect on the discharge of sands in most sand-bed streams. At a cross section of a sand-bed stream a reasonably close relationship usually exists between discharge of sands and mean velocity unless water temperature changes greatly or unless the concentration of fine sediment is high and variable. The curve of relationship for one sand-bed stream may approximately apply for some other sand-bed streams.
2. Shear and stream power each has a dominant effect, somewhat similar to that of mean velocity, on the discharge of sands except for the uncertainty of the relationship when the resistance to flow is variable.
3. For moderate to high velocities and shallow flows, discharge of sands per foot of width varies somewhat but not greatly for changes in median diameter of the bed material from 0.30 to 0.80 mm. However, the effect of particle size on the discharge of sands may be large at low velocities in any depth of flow or at high velocities in deep flows.
4. Depth sometimes has a large effect on the relationship between discharge of sands per foot of width and any one of the four measures of the force or the energy that causes sediment movement, and the effect varies complexly with changes in velocity and particle size.
5. If other factors remain constant, an increase in viscosity as a result of a decrease in water temperature causes an increase in discharge of sands because the change in viscosity causes a decrease in the fall velocity of the sand grains. In much the same way, a high concentration of fine sediment may increase the apparent viscosity of the water and thus decrease the fall velocities of the sand grains.

Graphs based on the empirical relationships of discharge of sands to major variables were prepared for a wide range of velocity, depth, water temperature, and concentration of fine sediment; they provide a method for quickly approximating the discharge of sands in sand-bed streams. In spite of many inaccuracies in the available data and uncertainties in the graphs, about 75 percent of the sand discharges that were used to define the relationships were less than twice or more than half of the discharges that were computed from the graphs of average relationship.

The agreement of computed and observed discharges of sands for sediment stations whose records were not used to define the graphs seemed to be about as good as that for stations whose records were used.

INTRODUCTION

Two practical objectives of sedimentation research are to understand the effects of major factors on sediment discharge in streams and to develop methods for computing the sediment discharge. An understanding of the effects of the major factors is essential to evaluate correctly the somewhat incomplete and inexact information available on sediment discharge and on the behavior of sediment-laden streams. Methods for computing sediment discharge are needed in studies and computations relating to channel design and maintenance, sediment yields from drainage basins, rates of scour or fill in natural or artificial channels, and depletion of reservoir storage by sediment accretion.

Because sediment transportation varies with complex characteristics of sediment and flow, an

727-985 O - 64 - 2

accurate and always applicable method for determining sediment discharge from characteristics of drainage basins, transported sediment, and streamflow may never be developed. If such a method is ever devised for all types of sediment, drainage areas, channels, and flows, it is likely to be unmanageably complex and generally impracticable because of the large amount of field information and the complicated office procedures that would be necessary. However, the relating of sediment discharge to characteristics of streamflow is much simplified (although it still remains difficult) if the sediment discharge is computed for only those particle sizes generally present in the streambed in appreciable quantities and if only streams with beds of sand are considered.

The main purpose of this paper is to indicate in as simple, accurate, and practical a form as possible the major relationships between the discharge of sands in sand-bed streams and the characteristics of flow and sediment. Secondary purposes are to provide a rapid method for computing the discharge of sands in sand-bed streams and to show deficiencies in the information that is necessary to define more accurately the relationships between discharge of sands and characteristics of flow and sediment.

Because the relationships are complex and are inexactly defined, they have been expressed in graphs rather than in equations. The graphs are based on laboratory and field information and on a general concept of the theories and equations of sediment transportation. They express the discharge of sands for flows as shallow as 0.1 foot and as deep as 100 feet, although for the deepest flows the graphs are poorly defined extrapolations. Bed-material sizes on the graphs are shown only as median diameters and range from 0.1 to 0.8 mm. The relationships for the largest and the smallest sizes are based to a considerable degree on extrapolation.

First, a concept of sediment transportation is given on the basis of recognized theories and personal observations of water and sediment discharge. It provides a background for understanding the major factors that can be expected to affect the discharge of sands in sand-bed streams. Then, the quantitative effects of the major factors as empirically defined by available information are individually shown and discussed. Finally, graphs are given for computing the approximate discharge of sands in sand-bed streams; and the probable accuracy, limitations, and possible improvements of the graphs and relationships are suggested.

Studies on which this paper is based were made over a period of several years; some were made while the writer was working for the Agricultural Research Service, U.S. Department of Agriculture.

Unpublished data for Pigeon Roost Creek in northern Mississippi and its tributaries were used in some of the studies and were from the files of the Agricultural Research Service, University, Miss. Much unpublished information collected by the Geological Survey was made available by: D. M. Culbertson, district engineer, for streams in Nebraska and for the Mississippi River at St. Louis, Mo.; J. M. Stow, district chemist, for streams in New Mexico and for the Colorado River; D. B. Simons, project chief, for flume investigations at Fort Collins, Colo.; and T. F. Hanly, district engineer, for streams in the Bighorn River basin in Wyoming.

CONCEPT OF SEDIMENT TRANSPORTATION

An understanding of the causes of sediment movement by streamflow and the general pattern of the movement is necessary for developing sound relationships for computing sediment discharge. Such a concept cannot be precise, however, partly because our knowledge is not complete and partly because our minds cannot wholly grasp the complexities of all the complete and detailed relationships involved in sediment transportation. Fortunately, a concept of sediment movement in flowing water may be adequate for many studies if it includes approximately correct interrelationships of major factors and characteristics of the flow, the sediment particles, and the sediment discharge. An attempt will be made to state a useful concept in terms of theories, equations, and observations of streamflow and sediment movement.

The statement of this concept is divided into several parts. The complexity of sediment transportation is explained briefly; then, the assumptions made to simplify and to limit the scope of the studies and the relationships for this paper are stated. Next, each of the two general modes of sediment discharge—bedload discharge and suspended-sediment discharge—are discussed separately; and finally, the total discharge of sediment at a cross section is considered.

COMPLEXITY OF SEDIMENT AND STREAMFLOW RELATIONSHIPS

The relationships of sediment discharge to characteristics of sediment, drainage basin, and streamflow are complex because of the large number of variables involved, the problems of expressing some variables simply, and the complicated relationships among the

variables. At a cross section of a stream, the sediment discharge may be considered to depend: on depth, width, velocity, energy gradient, temperature, and turbulence of the flowing water; on size, density, shape, and cohesiveness of particles in the banks and bed at the cross section and in upstream channels; and on the geology, meteorology, topography, soils, subsoils, and vegetal cover of the drainage area. Obviously, simple and satisfactory mathematical expressions for such factors as turbulence, size and shape of the sediment particles in the streambed, topography of the drainage basin, and rate, amount, and distribution of precipitation are very difficult, if not impossible, to obtain.

The concentration of the moving sediment is generally nonuniform both laterally and vertically in the cross section, and each sediment size (more precisely, sediment of each fall velocity) will have a vertical and lateral distribution that differs from the distribution of sediment of any other size. Similarly, the depth, velocity, turbulence, shear, and other characteristics of flow vary, sometimes widely, across a stream. Thus, a single value such as an average depth, a mean velocity, or a median particle size may be a somewhat unsatisfactory measure of depth, velocity, or particle size for a cross section. Furthermore, the lateral and vertical distributions of sediment and flow depend partly on nearby cross sections and on channel alinement. The flow may be over a relatively firm and smooth bed or over bars, dunes, or antidunes; and the bed configuration may vary laterally, longitudinally, and with time. In addition, sediment particles interfere with each other at high concentrations, and the chemical composition of the water may affect the degree of flocculation of fine sediment. Because the flow pulsates and the coarse sediment tends to discharge erratically both in time and in lateral position in the flow, observations of velocity, discharge of coarse sediment, and slopes of the water surface must be made carefully over a considerable period of time to obtain satisfactory averages. An adequate knowledge of these difficulties indicates that (a) sediment discharge cannot, in general, be precisely computed from characteristics of the flow, the sediment, and the drainage basin and (b) some assumptions are necessary to reduce the problem of sediment transportation to manageable proportions.

SIMPLIFYING ASSUMPTIONS

The assumptions made for this study should be well understood because they limit significantly the scope and applicability of the discussions and results. The derived relationships should only be applied to compute discharge of sands for streams and cross sections that have characteristics reasonably consistent with the assumptions.

When one cross section is compared with others, sediment discharge is assumed to be proportional to width if other major variables are constant from section to section. Thus, sediment discharge is computed and discussed in terms of discharge per unit width. The assumption does not imply a uniform distribution of sediment discharge across a section. It implies only that the sediment discharge through two sections should be about proportional to width if the sections have the same mean velocity, average depth, bed sediment, water temperature, and concentration of fine sediment.

Mean velocity, average depth, and average shear at a cross section are assumed to be acceptable measures of the actual nonuniform velocities, depths, and shears across the section. Obviously, this assumption will not always be satisfactory. Some irregular cross sections should be subdivided into parts, and separate computations of sediment discharge should be made for each part. However, the error in using a mean velocity for an entire nonuniform cross section may be partly compensated, or even overcompensated, for by the assumption that sediment discharge is proportional to stream width.

For example, if 30 feet of the width of a 100-foot section is shallow and has a very low velocity, almost the entire discharge of sands may be within the other 70 feet of width. The mean velocity may be only a few percent lower for the whole section than for the 70-foot width (mean velocity is weighted with width and depth, not with width alone). Hence, even though the discharge of sands may vary as the third or fourth power of the mean velocity, the computed decrease in discharge of sands per foot of width for the 100-foot width as compared with the 70-foot width will be partly compensated, or even overcompensated, for when multiplication is by 100 feet rather than by 70 feet.

Cross sections for determining sediment discharges are assumed to be in reasonably straight reaches of channel.

The bed sediment is considered to be adequately represented by the median particle size, although for certain somewhat extreme conditions of flow, such as the beginning of sediment movement, low discharges of sands, or deep flows, the assumption is not generally satisfactory.

The discharge of fine sediment is assumed to be more closely related to supply of fine sediment in the

drainage basin than to conditions of flow at a cross section, and hence no attempt is made to compute the discharge of fine sediment from characteristics of the flow at a cross section. (However, some attention is given to the effect of high concentrations of clay on the discharge of sands.) This assumption is in line with findings of Einstein and Chien (1953) that the discharge of fine sediment theoretically follows the same laws as the discharge of sands but that limitations on sampling the fine bed sediment and on applying the laws make the computation of the discharge of fine sediment impracticable and unreliable. Theoretically, the dividing size between sediment too fine to have its discharge related satisfactorily to characteristics of flow at a cross section and sediment whose discharge can be so related should vary with mean velocity and other factors. For this paper the dividing size, which is arbitrary because no sharp division exists, has been selected as 0.062 mm., the lower limit of sand sizes.

Only stream reaches whose beds are composed almost entirely of nearly cohesionless sand and whose channels are not confined between rough rock walls are considered. Such walls may cause unnaturally high turbulence for a given mean velocity and depth.

BEDLOAD DISCHARGE

When water flows very slowly over a bed of sand, none of the sand grains may move. If velocity near the bed is slowly increased, a critical velocity will be reached at which some sand grains occasionally move along the bed for short distances and then stop. Obviously, this critical velocity is somewhat indefinite because initial movement of the grains depends on the arrangement of the grains and on local variations of velocity. Hence, Einstein (1950) related the picking up of the grains from the bed and the beginning of movement to the probability of individual grains to move. This reasonable concept of Einstein indicates that any critical velocity can only be an inexact and partly arbitrary measure of the beginning of significant bedload movement.

If the velocity near the bed is greater than critical, sand grains move intermittently by rolling, sliding, or skipping along the bed. The movement is within a very thin layer, called the bed layer, a few grain diameters thick. (The bed-layer concept is, of course, inexact, especially for a dune bed and a wide range of grain sizes in the bed sediment.) The grains which thus move in the bed layer and which are supported mainly by contact with the streambed compose the bedload. In general, the rate of travel of these grains while in motion and the frequency with which the grains begin intermittent movement depend on the velocity of flow near the bed. Obviously, the particle sizes of bed sediment and the difference in density between the sediment and the water are also significant factors that affect bedload discharge. The viscosity of the fluid probably also has an appreciable effect. There are three generally known procedures by different investigators for computing bedload discharge.

MEYER-PETER AND MÜLLER EQUATION

A reasonably simple and evidently fairly accurate formula for bedload discharge was developed by Meyer-Peter and Müller (1948). For channels having negligible bank friction, the formula may be written

$$\gamma_f(K_r/K_r')^{3/2}RS=A(\gamma_s-\gamma_f)D_m+B(\gamma_f/g)^{1/3}(q_B')^{2/3}, \quad (1)$$

in which

- γ_f and γ_s are the specific weights, respectively, of the fluid and the sediment particles;
- K_r is a measure of resistance to flow and equals the mean velocity $\bar{u}$ divided by $(R^{2/3}S^{1/2})$;
- K_r' is a comparable measure of the flow resistance due only to the resistance of the stationary grains and for metric units can be computed from $26/(D_{90})^{1/6}$. D_{90} is the particle size, in meters, for which 90 percent of the bed sediment by weight is finer;
- R is the hydraulic radius, which equals average depth of flow when the bank resistance is negligible;
- S is the energy gradient;
- A and B are dimensionless constants that may be used as 0.047 and 0.25, respectively;
- D_m is the particle size of uniform sediment and equals ΣDi_b for bed sediment of a range of sizes; i_b is the fraction by weight of sediment of a size D in the streambed;
- g is the gravity constant; and
- q_B' is the bedload discharge per unit width by weight under water.

Equation 1 for bedload discharge, in foot-pound-second units, when γ_s is equal to 165 pounds per cubic foot, can be written as

$$(K_r/K_r')^{3/2}RS=0.077D_m+0.0050(q_B')^{2/3}.$$

For convenience, the bedload discharge per foot of width can be expressed in terms of the dry weight per foot of width (q_B) through the relationship

$$(q_B')^{2/3}=[(165-62.4)/165]^{2/3}(q_B)^{2/3}$$

and equation 1 becomes

$$(K_r/K_r')^{3/2}RS=0.077D_m+0.0036q_B^{2/3}. \quad (2)$$

According to equation 2, no bedload moves until the left-hand side exceeds $0.077D_m$. For high velocities and small particle sizes, $0.077D_m$ becomes relatively small. If it is disregarded and (K_r/K_r') is constant, the computed bedload discharge varies as $(RS)^{3/2}$ or as the third power of the mean velocity if the Chezy C is constant.

The ratio K_r/K_r' in equation 2 equals the ratio of the actual mean velocity to the mean velocity if all resistance to flow were due to the bed roughness that the grains would cause if stationary on a plane streambed. (The equation is based on assumed negligible bank friction.) A convenient way to evaluate K_r/K_r' in foot-pound-second units is to compute the ratio of the actual velocity to the velocity that can be determined from an equation of the type given by Keulegan (1938) and from a roughness equal to the D_{65} size of the bed material as suggested by Einstein (1950). In whatever way the ratio is computed, K_r/K_r' is an adjustment that makes the left side of equation 2 vary much more closely with mean velocity than with RS or with shear with respect to the particles rather than with γRS.

The close relationship between bedload discharges computed from the Meyer-Peter and Müller equation and mean velocity can readily be shown by an example for a cross section of Pigeon Roost Creek near Byhalia, Miss. Within a narrow range of depths and shears, two considerably different flows may occur at a particular depth at this cross section because of differences in configuration of the streambed. The bed sediment at the cross section is cohesionless sand that has a median diameter of 0.40 mm. D_m in equation 2 is 0.45 mm, and D_{90} is 0.66 mm. Bedload discharges were computed from equation 2 for five velocities and depths of flow; the three lowest velocities were over dune beds, and the two highest were over plane beds or a combination of plane bed and antidune bed. The computed bedload discharges increase rapidly and consistently as mean velocity increases, but a break exists in their relationship to RS. (See fig. 1.) Evidently, RS may be a poor measure of the bedload discharge unless RS is adjusted by some factor, such as K_r/K_r', that corrects for the effect of changes in resistance to flow that are due to changes in bed roughness.

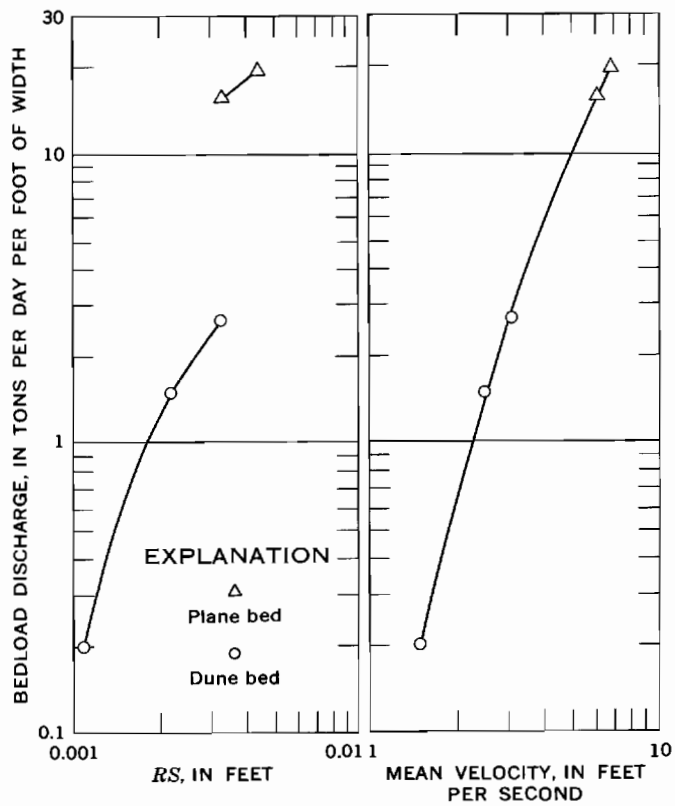

FIGURE 1.—Bedload discharges, computed with the Meyer-Peter and Müller equation, as functions of RS and mean velocity.

EINSTEIN EQUATIONS

Einstein (1950) suggested a comprehensive procedure for the computation of bed-material discharge from the characteristics of flow and bed sediment. In this procedure, the part of the bed-material discharge that is bedload was computed on the basis of the probability of movement of particles at the bed surface as related to intensity of flow. Einstein's bedload equations for uniform sediment can be written

$$\Phi=\frac{q_B}{\rho_s g}\left(\frac{\rho_f}{\rho_s-\rho_f}\frac{1}{gD^3}\right)^{1/2},$$

in which ρ_f and ρ_s are densities of the fluid and the sediment particles, respectively. Also,

$$\Psi=\frac{\rho_s-\rho_f}{\rho_f}\frac{D}{R'S}$$

and

$$\Phi=f(\Psi).$$

For constant densities and for one consistent system of units of measurement these three equations of Einstein's become

$$\begin{aligned} q_B&=K_1D^{3/2}\Phi \\ &=K_1D^{3/2}f\left(\frac{K_2D}{R'S}\right), \end{aligned} \tag{3}$$

and K_1 and K_2 are constants. R' is the hydraulic radius that could be used to compute velocity if all the resistance to flow were due to the roughness that might be caused by the sediment particles if stationary on the bed.

Einstein used R' in equations based on work by Keulegan (1938), but R' can be used equally well in a Manning equation; that is, R' can be stated in terms of R, the actual hydraulic radius (or average depth of flow for negligible bank friction), as

$$\bar{u}=K_r R^{2/3} S^{1/2}$$
$$=K_r'(R')^{2/3} S^{1/2};$$

hence

$$R'=R(K_r/K_r')^{3/2}.$$

Einstein's equation for q_B then may be written, in which K_3 is a constant, as

$$q_B=K_3 D^{3/2} f\left[\frac{D}{(K_r/K_r')^{3/2} RS}\right].$$

Thus, Einstein's parameter for the effect of flow on bedload discharge of uniform particle size is like that used in the Meyer-Peter and Müller equation (see eq. 2). Einstein's graph of the function (fig. 2) shows, of course, that Φ_* and, hence, q_B increase as $D/[(K_r/K_r')^{3/2} RS]$ decreases.

Einstein stressed the need for the adjustment from R to R', an adjustment that ties the bedload discharge more closely to mean velocity than to RS. However, he computed the relationship between R and R' through the use of a curve (Einstein, 1950, fig. 5) that may be a good average but sometimes does not apply well (Brooks, 1958, p. 588–589).

If the bed sediment is not uniform in size, the Einstein procedure requires considerable adjustment of Φ and Ψ. The adjusted quantities for individual size classes or size fractions of bed sediment are Φ_* and Ψ_*. Einstein's graph of Φ_* as a function of Ψ_* (fig. 2) shows a rapid decrease of bedload discharge when the velocity, as measured by $R'S$, becomes low in relation to the particle size; that is, when Ψ_* becomes large. The bedload discharge of a size fraction is directly proportional to the percentage by weight of that size fraction in the bed sediment. In other words, if the percentage of bed sediment in a size range is doubled but Φ_* remains constant, the bedload discharge of that size range is also doubled. The statement of proportionality does not mean that the bedload discharges for different size fractions are in direct proportion to the relative percentages of the size fraction in the streambed.

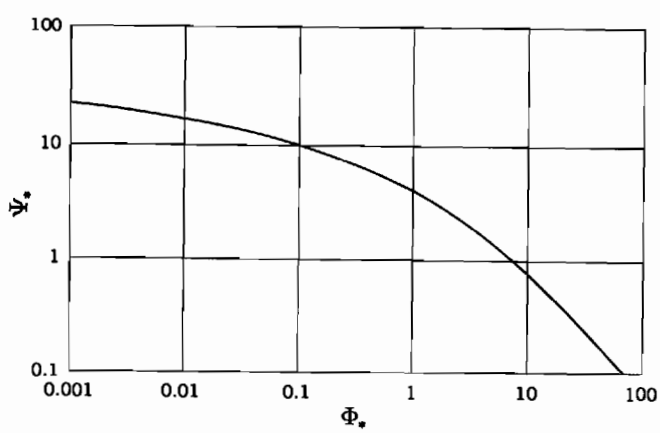

FIGURE 2.—Relationship of Φ_* to Ψ_* for individual size ranges. From Einstein (1950, fig. 11).

BAGNOLD EQUATION

Using a different approach from that of Einstein, Bagnold (1956) derived a formula for computing bedload discharge similar to Einstein's. For bed sediment of uniform size, his equation (Bagnold, 1956, eq 42c) is

$$q_B=A_1 B_1 K_1 D^{3/2}\sqrt{\cos\beta}(\theta_F-\theta_t)\theta_F^{1/2}, \qquad (4)$$

in which

- A_1 is a dimensionless constant that may be about 9,
- B_1 is a dimensionless constant that varies slowly with particle size,
- K_1 is the same constant that was used in equation 3,
- θ_F is a dimensionless measure of the apparent tangential stress due to action of external forces on the fluid and equals $[\rho_f/(\rho_s-\rho_f)](RS/D)$,
- θ_t is that value of θ_F (determined by extrapolation) at which sediment particles begin to move on a rippled sand bed, and
- β is declination of the bed surface below the horizontal, and $\cos\beta$ generally can be considered to equal unity and be disregarded.

Except for the use of R instead of R', Bagnold's θ_F is the reciprocal of Einstein's Ψ. Of course, the bedload discharge increases as θ_F increases or as Ψ decreases. Also, for a particular grain size, for constant densities, and for moderately high velocities—for which θ_t becomes relatively insignificant—the bedload discharge according to equation 4 is about proportional to $(RS)^{3/2}$. For these stated conditions, the bedload discharge is also about proportional to the third power of the mean velocity if the Chezy C is constant.

A major difference between the Bagnold equation for computing bedload discharges and the equations of Einstein or Meyer-Peter and Müller is that Bagnold made no direct provision for the effect of changing resistance caused by changing bed configuration (if θ_t is intended to be such an adjustment, it is inadequate for most natural streams); that is, Bagnold used

neither an R' instead of R nor a K_r/K_r' ratio. If RS is as inadequate a measure of bedload discharge as figure 1 indicates that it may sometimes be, Bagnold's equation may generally not be as applicable as the equations of Einstein and Meyer-Peter and Müller.

MAJOR VARIABLES

The general concept of bedload discharge and certain mathematical statements of the concept indicate that no sediment may move as bedload at very low velocities. At relatively high velocities, the bedload discharge may vary roughly with the third power of the mean velocity. Hence, mean velocity—or more exactly, velocity near the streambed—must be a highly significant variable in the computation of bedload discharge. Shear (or RS) is an alternate major variable and might be used rather than velocity, but an adjustment of the shear from total shear to shear with respect to the particles evidently is required for changing bed roughness. If mean velocity is used as a parameter of bedload discharge, depth can be expected to affect bedload discharge because for a given velocity near the streambed the mean velocity usually increases as the depth of flow increases.

The emphasis here placed on mean velocity as a measure of bedload discharge is wholly consistent with the usual concept that shear with respect to the particles is a major parameter of bedload discharge. Unfortunately, shear with respect to the particles can at present be obtained only indirectly and often inexactly except for flow over plane beds. Usually it can be computed as accurately from mean velocity and depth as in any other way. Thus, mean velocity is a practical and convenient measure of bedload discharge to substitute for shear with respect to the particles.

Another significant variable is the bed sediment. The size of the bed sediment, as measured by the median diameter and the size distribution, has three noteworthy effects on bedload discharge. One effect is that particle size largely determines the velocity that is necessary near the bed to start appreciable sediment movement. Particle size also partly determines resistance to flow because it directly determines grain roughness and affects bed configuration. A third effect is that particles of different sizes discharge at different rates even though the velocity near the bed is constant.

The properties of the fluid may also affect the discharge of sands as bedload. The density of the fluid is included in each of the three bedload equations that were discussed, but the practical effect of changes in the different densities of fluid and sediment is usually small because these densities are generally about constant in sand-bed streams. Changes in viscosity of the fluid or of the fluid-sediment mixture seem to have an effect on the relationship of shear to mean velocity because these changes may modify the bed configuration.

Thus for sand-bed streams, the discharge per foot of width of sands as bedload can be expected to vary mainly with mean velocity, depth of flow, median particle size or median fall velocity of bed sediment, and size distribution of the bed sediment. If the velocity near the bed could be satisfactorily determined, perhaps the only other major parameter that would usually have to be considered in determining bedload discharge in sand-bed streams would be the sizes of the bed sediment.

SUSPENDED-SEDIMENT DISCHARGE

Although in sand-bed streams much more sand is generally discharged as suspended sediment than as bedload, bedload discharge was discussed first because it forms a base to which the suspended sediment adjusts itself. The most direct relationship of suspended sediment to bedload results from continuity of the concentrations of suspended sediment of each size range at the upper surface of the bed layer; that is, the concentrations of suspended sediment immediately above the bed layer depend on the concentrations within the bed layer. Suspended-sediment concentrations at higher levels in the flow depend, in turn, on the concentrations immediately above the bed layer and on the vertical attenuation of the concentrations of sediment of the different sizes from the bed layer upward.

CONCENTRATION IMMEDIATELY ABOVE THE BED LAYER

If the velocity near the streambed is great enough, some sand grains, perhaps usually the lightest or the fastest moving ones, escape from the bed layer by hydraulic lift, aerodynamic lift (R. E. Glover, written communication, 1960), or other mechanical or hydraulic action. Grains that rise above the bed layer may be supported by the turbulence of the flow and thus become suspended sediment rather than bedload. Of course, if the flow contains suspended sediment, some particles of the suspended sediment are continually settling into the bed layer. The ready interchange of particles from bedload to suspended load or of suspended load to bedload means that the suspended-sediment concentration just above the bed layer adjusts itself to changes in discharge of bedload.

Einstein (1950) used the assumption that the concentration of each particle size of suspended sediment at the upper surface of its own 2-grain-diameter bed

layer was equal to the concentration of that particle size in the bed layer. This assumption may be only approximate, and the idea of separate thicknesses of bed layer for each particle size may be somewhat unrealistic. However, changes in the concentration of suspended sediment of each size class at the upper surface of the bed layer should be roughly proportional to changes in concentration of particles of that size class within the bed layer. If the thickness of the bed layer and the average velocity in the bed layer remain constant, changes in the concentration of sediment of a given size class in the bed layer will be proportional to changes in bedload discharge of that size class of sediment. Hence, the same variables that determine the bedload discharge will mainly determine the suspended-sediment concentrations at the upper surface of the bed layer and immediately above it. Thus, the major variables that affect concentration of suspended sediment immediately above the bed layer are mean velocity, depth of flow, and particle sizes or fall velocities of the bed material.

VERTICAL DISTRIBUTION OF SEDIMENT CONCENTRATION

A detailed discussion of the concepts that relate to the vertical distribution of suspended sediment seems to be necessary for two reasons. The first reason is that much more sand is transported in most streams as suspended sediment than as bedload. The second reason is that the factors affecting the vertical distribution of sediment are incompletely defined and their relationships to the discharge of sands are complex. Available experimental data are generally inadequate to determine the factors and their relationships except, perhaps, for narrow ranges of the factors. Therefore, empirical analysis of the data should be based on as adequate and practical an understanding of the basic concepts as can be obtained.

By definition, suspended sediment is supported by the vertical currents in turbulent flow. These currents exist because of vertical eddies or random vertical movements of some parts of the flow relative to other parts of the flow. The amount of the vertical movement in either direction is largely a function of the time-averaged horizontal velocity, although roughness of the channel boundary and other factors have considerable effect. Hence, the mean velocity of a stream is a rough measure of the turbulent currents that suspend sediment. If the water surface and the streambed are plane and parallel, any upward movment of part of the flow must be balanced by a downward movement of another part of the flow. If the sediment particles were uniformly distributed in the turbulent flow and did not settle with respect to it, the rate of upward sediment movement, like the rate of upward water movement, would on the average equal the rate of downward sediment movement through any area of plane parallel to the water surface.

Because sediment particles settle with respect to the surrounding water, vertical equilibrium requires that the number of sediment particles raised by the upward components of flow must exceed the number lowered by the downward components of flow. Thus, equilibrium may be reached if the upward movement of water starts at a lower altitude where the concentration is comparatively high and if the downward movement of water starts from a higher altitude where the concentration is comparatively low. The sediment in both upward and downward components of the flow is assumed to move an appreciable distance before mixing with other water. If this vertical distance of movement before mixing is the same for all particle sizes, the ratio of the number of particles that starts moving upward to the number that starts moving downward is directly related to the fall velocity; that is, in a particular flow the fall velocity is a measure of the rate of change of concentration with distance above the streambed. For a constant fall velocity, an increase in turbulence means an increase in the vertical movements of the flow and results in a lower rate of change of concentration with distance above the streambed. Thus, the major parameters that determine vertical variation of concentration of sediment in a flow are fall velocity and turbulence. Mean velocity is probably the best available measure of turbulence, although relative roughness of the channel boundary is likely to affect the relationship between mean velocity and turbulence.

THE CLASSICAL EQUATION FOR SEDIMENT OF ONE FALL VELOCITY

The theoretical equation for the vertical distribution of concentration of suspended sediment of a particular fall velocity was given by Rouse (1937) and was restated by Einstein (1950, p. 17) in the familiar form

$$\frac{c_y}{c_a}=\left(\frac{d-y}{y}\,\frac{a}{d-a}\right)^z \tag{5}$$

and

$$z=\frac{w}{ku_*}, \tag{6}$$

in which

c_y is the concentration at a distance y above the streambed,

c_a is the concentration at a distance a above the streambed,

d is the depth of flow,
w is the fall velocity of the particles,
k is the turbulence constant, and
u_* is the shear velocity and is equal to $\sqrt{gRS}$

The exponent z is the theoretical slope of a log-log graph of concentration of sediment of one fall velocity against $(d-y)/y$ and increases as the rate of change of the concentration with depth increases. When z is zero, the vertical distribution of concentration is uniform.

Equation 5, in which z is defined as in equation 6, is the classical equation for the vertical distribution of suspended sediment. Theoretically, it can be used to compute the vertical distribution of concentration of suspended sediment of any particular fall velocity in turbulent flow over a plane bed that is parallel to the water surface if the suspended sediment concentration is known at any one distance above the streambed.

THEORETICAL AND OBSERVED DISTRIBUTIONS

Observed vertical distributions of sediment concentration in a natural stream (Anderson, 1942) and in a laboratory flume (Vanoni, 1946) checked equation 5 to the extent that the log-log graphs of concentration against $(d-y)/y$ defined approximately straight lines. However, the slope z_1 determined from a line was usually different from the theoretical slope z computed from equation 6. Vanoni (1946) and Ismail (1952) considered that the coefficient of sediment transfer is not the same as the coefficient of momentum transfer. Einstein and Chien (1954) suggested other changes in the relatively simple assumptions on which equations 5 and 6 are based in order to make z and z_1 agree better. However, they apparently restricted their explanations to flows over plane beds, whereas equation 6 is likely to be less accurate for flows over dune beds than for flows over plane beds. Their suggestions merit careful study but are generally too complicated and uncertain for use at the present time.

Because the vertical distribution of sediment concentration is an important phase of sediment transportation particularly in deep flows, equation 6 is here examined to show some possible uncertainties and inaccuracies that involved in its use. A few of the uncertainties and inaccuracies result directly from the assumptions on which the equation is based. Each of the variables w, k, and u_* is considered individually.

The variation of z_1 with fall velocity can be defined experimentally from the concentrations and size analyses of sediment samples that are collected at several points on a vertical during a short period of time when the turbulent flow over a sand bed is reasonably constant. A value of z_1 for each size range at a vertical can readily be determined by plotting. Because ku_* is the same for all size ranges, the values of z_1 for the different size ranges should vary in proportion to the fall velocities of representative particles from each size range, if the numerator of the right side of equation 6 is correct. However, the values of z_1 thus determined for sands in the Enoree River (Anderson, 1942) did not increase as rapidly as the values of z and were generally smaller for the coarser particles than the corresponding values of z computed from equation 6. Similarly, Colby and Hembree (1955) found that the values of z_1 for different ranges of sand sizes in several natural streams varied roughly with about the 0.7 power of the fall velocity as computed from equations given by Rubey (1933). The relationship of z_1 to fall velocity was based on the slopes of lines that might be drawn through points on figure 3 for a given time and cross section. The first power of the fall velocity from the Rubey equations evidently is an inadequate measure, at least for sands, of the change in z_1 with change in particle size within a given flow. The vertical distributions of concentration of the coarse sizes of sediment are more uniform than equations 5 and 6 indicate that they should be.

The first power of the mean velocity may be an inadequate measure of the change of z_1 with particle size for any one of several reasons or for a combination of reasons. These reasons include the possible effects of using an average vertical velocity rather than a range of vertical velocities and of disregarding higher order terms for the concentration gradients of coarse sediments (Einstein and Chien, 1954). Other possible reasons are mass movement of water and sediment from the bed upward, inapplicability of a laboratory determination of fall velocity of a representative particle of a size range as a measure of the effective fall velocity in the turbulent flow of a natural stream, and inadequacy of the assumptions regarding the mixing length.

On figure 3 the wide vertical scatter, which is relatively consistent from one size range to another, indicates that $0.40u_m$ does not satisfactorily show the effect that the characteristics of the flow have on z_1, at least for these shallow flows that were mostly over dune beds. Colby and Hembree (1955, p. 75) suggested that large variations in k might explain much of this vertical scatter. Hence, the significance and variability of k, especially for flow over dune beds, may help to explain differences between z and z_1.

727-985 O - 64 - 3

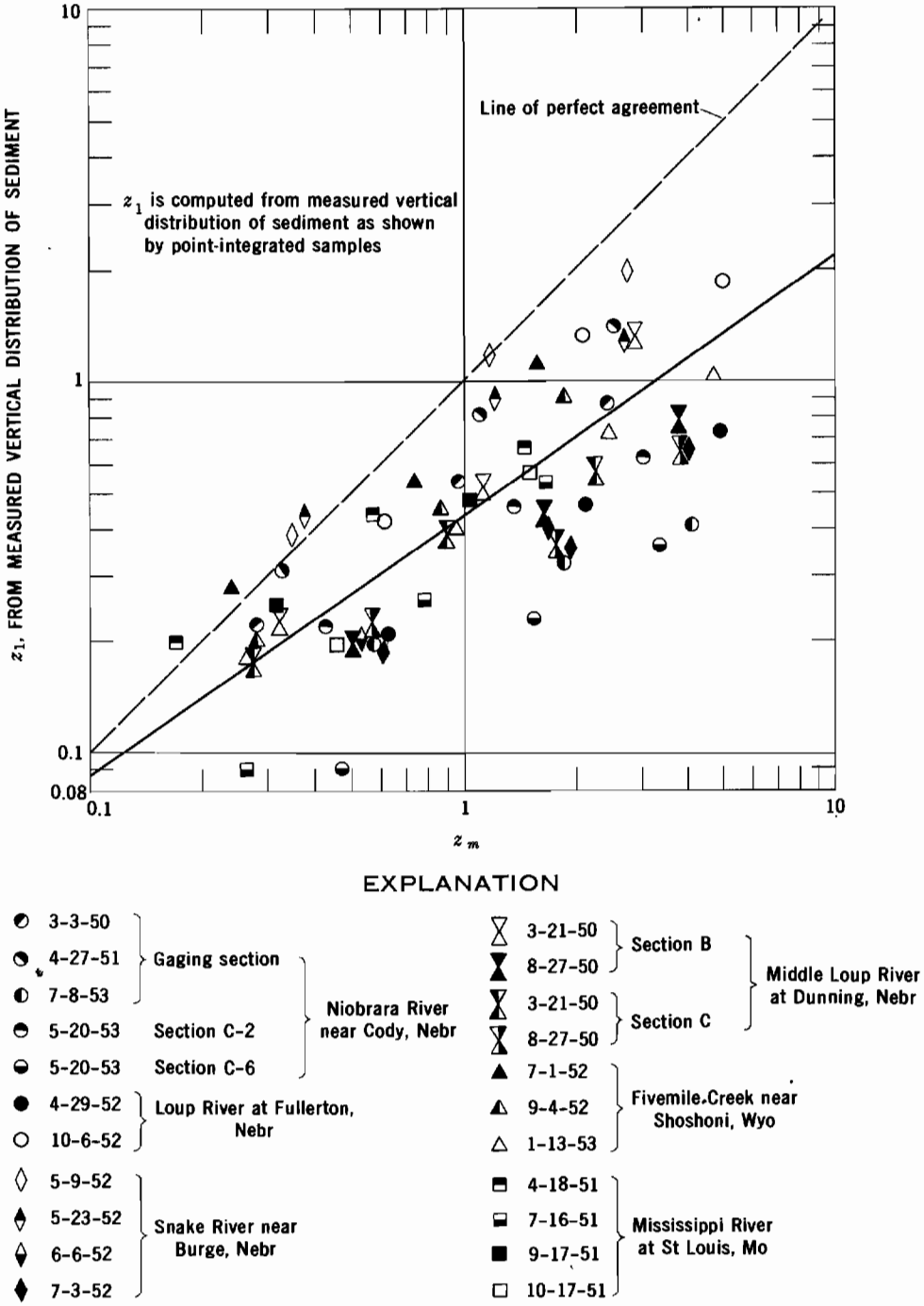

FIGURE 3.—z_1 plotted against z_m. $z_m = w/(0.40u_m)$ and $u_m = 0.40\bar{u}/[2.30 \log (12.27\, xd/D_{65})]$. From Colby and Hembree (1955, fig. 40).

EQUATION FOR FLOW OVER DUNE BEDS

The equations of the type given by Keulegan (1938) for mean velocity $\bar{u}$ and for time-averaged velocity at a point u_y may be written, respectively,

$$\bar{u}/2.30=\frac{u_*}{k}[1.09+\log\ (xd/k_s)] \tag{7}$$

$$u_y/2.30=\frac{u_*}{k}[1.48+\log\ (xy/k_s)], \tag{8}$$

in which

- x is a dimensionless parameter to cover the transition from hydraulically smooth to hydraulically rough boundaries, and
- k_s is a linear measure of roughness and may be taken equal to D_{65} (the size for which 65 percent of the bed material by weight is finer) if the roughness is due wholly to grain roughness.

Usually, k_s is large and is not known for flow over dune beds, and therefore these equations cannot then be used to compute velocities directly. Equation 8, however, shows that the difference in point velocity at distances $10y$ and y above the streambed is $2.30u_*/k$, which is the same as the difference for flow over a plane bed provided that equations 7 and 8 apply; that is, the vertical distribution of velocity depends on the total shear over a dune bed the same as it does over a plane bed, if equation 8 is applicable.

Three types of information indicate that equations (7) and (8) do not necessarily apply to shallow flows over dune beds. The first type shows that the vertical-velocity distribution changes (and hence k changes) as the measuring vertical is shifted with respect to a dune. For example, in the Middle Loup River at Dunning, Nebr., two values of k computed from vertical distributions of velocity at the crest of a dune were 0.32 and 0.62 as compared to k values of 0.11 and 0.19 for verticals in a trough downstream from the crest. A second type of information shows that some k's as computed from equation (8) and from observed vertical distributions of velocity are much higher than 0.40 for shallow flows over dune beds (Hubbell and Matejka, 1959, p. 71), whereas, in general, k values for flows that transport bed material in appreciable quantity probably should be somewhat lower than 0.40 (Einstein and Chien, 1954). The third type of information, obtained by Sayre and Albertson (1959) for clear-water flow, rigid boundaries, and fixed baffles, shows that the k computed from an equation similar to equation (7) differs from the k computed from an equation similar to equation (8) for the same flow if the baffles are spaced too widely apart. In other words, the vertical distribution of velocity is determined partly by position of the vertical with respect to a baffle if the spacing of baffles is wide. The variability of vertical velocity distribution and k from place to place in the clear-water flow is consistent to that for the Middle Loup River at Dunning. On the basis of these three types of information, the k that is computed from the vertical distribution of velocity in flow over a dune bed or other rough bed is here called "k_1" because it may not be a true turbulence constant.

Although k_1 may not be a true turbulence constant, it seems to have a relationship—as it logically should—to the vertical distribution of sediment concentration as was shown by Hubbell and Matejka (1959, p. 71 and fig. 36). They used values of k_1 (k in their terminology) that were computed by averaging the values of k_1 for individual verticals in the cross section and found that z_1 for shallow flows in some sand-bed streams in Nebraska varied inversely with about the 0.6 power of k_1. For this paper, the k_1 values for the cross sections were recomputed from a vertical-velocity difference and a shear velocity that were averages of figures for the individual verticals. The recomputed k_1 values give less weight to a high k_1 at an individual vertical than did the k values that were used for a cross section by Hubbell and Matejka. In general, the z_1 values vary inversely with about the 0.8 power of the recomputed k_1 values. (See fig. 4.) The quantity z_1u_* also varies inversely with about the 0.8 power of k_1 (fig. 5), whereas equation (6) indicates that it should vary inversely with the 1.0 power of k_1. The difference may result from the fact that an abnormally high k_1 is usually higher than the k_1 for the surrounding flows; that is, the vertical distribution of sediment is probably partly determined by the k_1 at nearby verticals; hence, the average or effective k_1 may often be lower than an abnormally high observed k_1 even though the observed k_1 is itself an average for perhaps three to five verticals.

The use of u_* in equation 6 was not accepted by Einstein (1950), although he obtained u_* in his derivation. He computed z from the equation

$$z=w/(0.40u_*'). \tag{9}$$

In this equation, u_*' or the shear velocity with respect to the particles is the shear velocity that can be computed from the energy gradient and the part of the hydraulic radius that relates to the movement of sediment particles on the bed; that is, Einstein used the mean velocity equation

$$\bar{u}=\frac{2.30u_*'}{0.40}\log\ (12.27xR'/D_{65}). \tag{10}$$

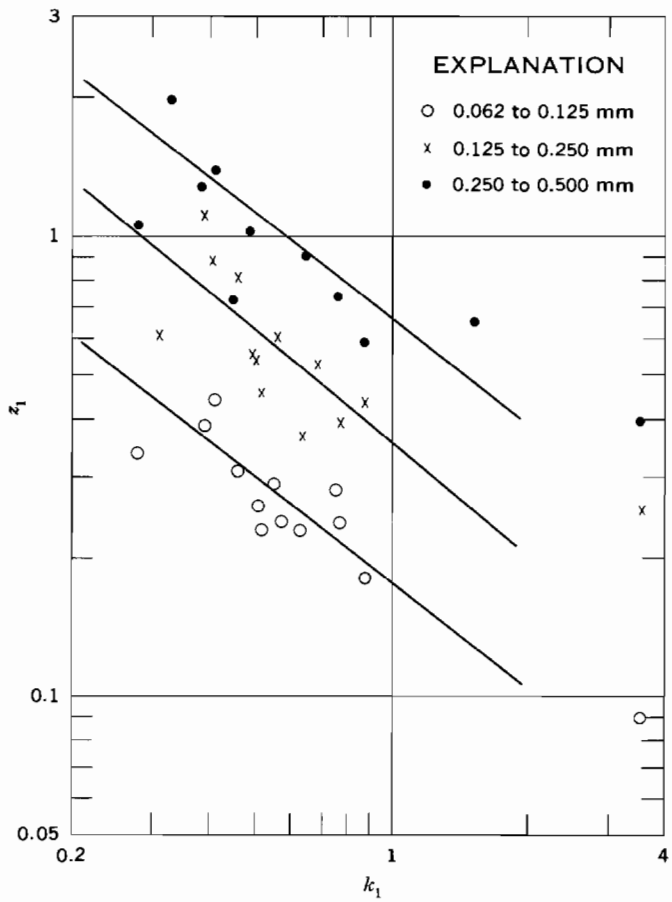

FIGURE 4.—z_l plotted against k_l for shallow streams in Nebraska.

As D_{65} is only a small fraction of the total roughness of a dune bed, a comparison of equations 7 and 10 shows that $u_*'/0.40$ must be much smaller for flow over dune beds than u_*/k_1 (k_1 rather than k because the constant may not be a true turbulence constant). Whether k_1 is about equal to 0.40 or is larger than 0.40, u_* must be considerably larger than u_*' for flow over dune beds, and for such flow the two kinds of shear velocity are by no means equivalent.

A reexamination of Einstein's development (1950, p. 14–17) of equation 6 does not seem to indicate that u_*' should be substituted for u_* in this equation. Einstein used the equation for the vertical distribution of suspended sediment at equilibrium in the form

$$\frac{dc_y}{d_y}=\frac{-c_y w}{vl_e/2}.$$

He then evaluated the product of the average vertical water movement v and the mixing length l_e from the equation for momentum exchange to obtain

$$\frac{dc_y}{c_y}=\frac{-wddy}{u_*^2(d-y)}\frac{du_y}{dy}.$$

By differentiation of equation 8 with k_1 rather than k

$$du_y/dy=u_*/(k_1y).$$

Hence,

$$\frac{dc_y}{c_y}=\frac{-w}{k_1u_*}\frac{ddy}{y(d-y)}. \tag{11}$$

For convenience define z_o by the equation

$$z_o=w/(k_1u_*). \tag{12}$$

Equation 11 can now be integrated from a distance a to a distance y above the streambed to obtain

$$\frac{c_y}{c_a}=\left(\frac{d-y}{y}\frac{a}{d-a}\right)^{z_o},$$

which is the same as the classical equation 5 except for the change from k to k_1 in the exponent. If equation 8 applies, k_1 equals k, and the classical equation should apply to flow over a dune bed provided that the equation for momentum exchange also applies to flow over a dune bed. Of course, the equation for momentum exchange is somewhat questionable for flow over a dune bed, especially if the dune height is relatively large in comparison to the depth of flow.

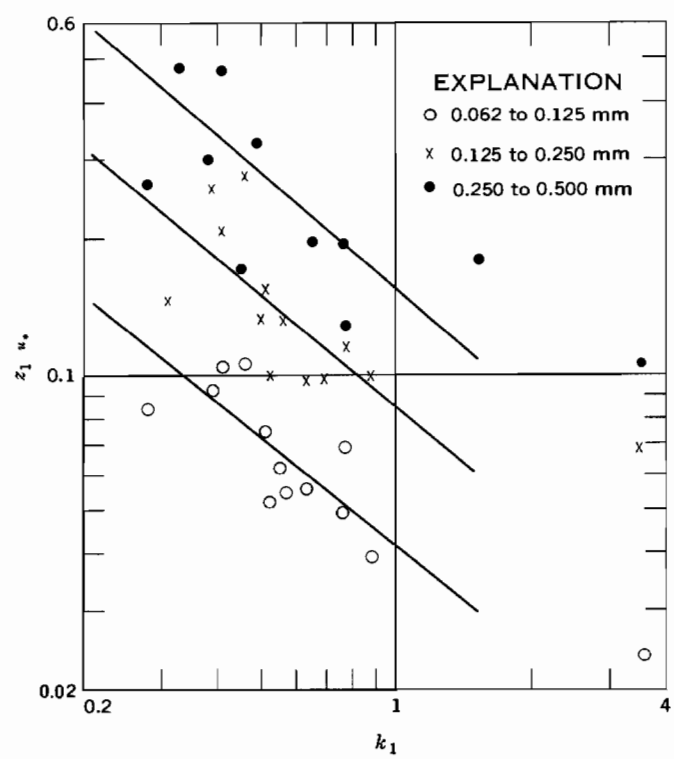

FIGURE 5.—$z_l u_*$ plotted against k_l for shallow streams in Nebraska.

The difference between z_0 from equation 12 and z from equation 9 is usually large for flow over dune beds. If k_1 differs appreciably from k, it is usually larger than 0.40. Also, u_* for flow over dune beds is usually much larger than u_*'. Hence, the product $k_1 u_*$ is usually much larger than 0.40 u_*', and the computed vertical distributions of sediment concentration that are based on $k_1 u_*$ are much more uniform than those that are based (as Einstein suggested) on $0.40 u_*'$.

In summary, the vertical distribution of sediment concentration of a particular size range becomes more uniform as the shear velocity and k or k_1 increase and as the fall velocity decreases. However, the classical equation for the vertical distribution holds only inexactly and is especially questionable for flow over dune beds. Hence, a procedure like Einstein's (1950) for computing the discharge of bed material, although based on generally sound concepts, is unlikely to give consistently accurate computations of suspended-sediment discharge particularly for flow over dune beds.

TOTAL SEDIMENT DISCHARGE

Some general relationships involved in the computation of the total sediment discharge at a cross section can be visualized from figure 6, which is consistent with the preceding explanations of a concept of sediment transportation. The figure was prepared for flow at a depth of 5.0 feet and at a mean velocity of 3.5 feet per second over a dune bed and for a bed material in which D_{35} and D_{65} are 0.0007 and 0.001 foot, respectively. (The same depth and energy gradient might be associated with a plane bed, but the velocity would then be much greater and the vertical distributions of concentration would be different.) The vertical distribution of sediment concentration varies widely from one particle size to another.

The complicated interrelationships indicated by the general concept of sediment transportation and partly illustrated by figure 6 preclude any simple modeling in a flume of the sediment transportation in a river. Although many phases of sediment transportation can well be studied in the laboratory, flume investigations, in the absence of satisfactory model laws, are basically studies of sediment transportation in small channels rather than model studies of the sediment transportation in natural streams.

The complexity of sediment and flow relationships and the difficulties of modeling sediment transportation suggest extreme caution in the use of compound parameters, whether dimensionless or not, in studies of sediment transportation. Even the simple ratio d to D can be highly misleading if used as a parameter, because the effect of doubling the depth d is often much different from the effect of dividing the particle size D by 2.

GENERAL METHODS OF COMPUTATION

The total sediment discharge at a cross section of a stream is the sum of the bedload discharges and the suspended-sediment discharges of all particle sizes. The bedload discharge either can be computed directly as a whole or can be obtained by adding the computed bedload discharges for the different size ranges. It must be computed by individual size ranges if the concentrations of suspended sediment by size ranges are to be based on the bedload discharges. The computation of suspended-sediment discharge can be made from defined distributions, such as those shown on figure 6, by multiplying average velocity and average concentration within each of several layers of flow, adding the products for all the layers of flow, and converting the sum of the products to a convenient rate, such as tons per day. Thin layers of flow should be selected at depths where the concentration and velocity change rapidly as the distance above the bed changes.

FINE SEDIMENT

The discharge of the fine sediment can seldom be computed from the characteristics of the bed sediment and of the flow at a cross section by the general procedure that can be used, though inexactly, for coarser sediment such as sand. As Einstein and Chien (1953) have pointed out, the two main reasons preventing this type of computation for fine sediments are that (a) a representative sample of the fine sediment in the upper layer of the streambed can seldom be obtained especially under high flows and (b) the relative amount of the fine sediment in this upper layer changes rapidly. (Silt and clay together are roughly equivalent to "wash load" as the term was used by Einstein and Chien.) Thus, the relative amount of fine sediment at the surface of the streambed is seldom known; hence, the bedload discharge of the fine sediment usually cannot be computed with any reasonable accuracy. The bedload discharge of the fine sediment is so small as compared to the discharge of suspended fine sediment that it could be disregarded, except that the only theoretical way of computing the concentration and discharge of the suspended fine sediment is based directly on the bedload discharge. As figure 6 indicates, a small percentage of fine sediment at the streambed may provide a base for much suspended fine sediment.

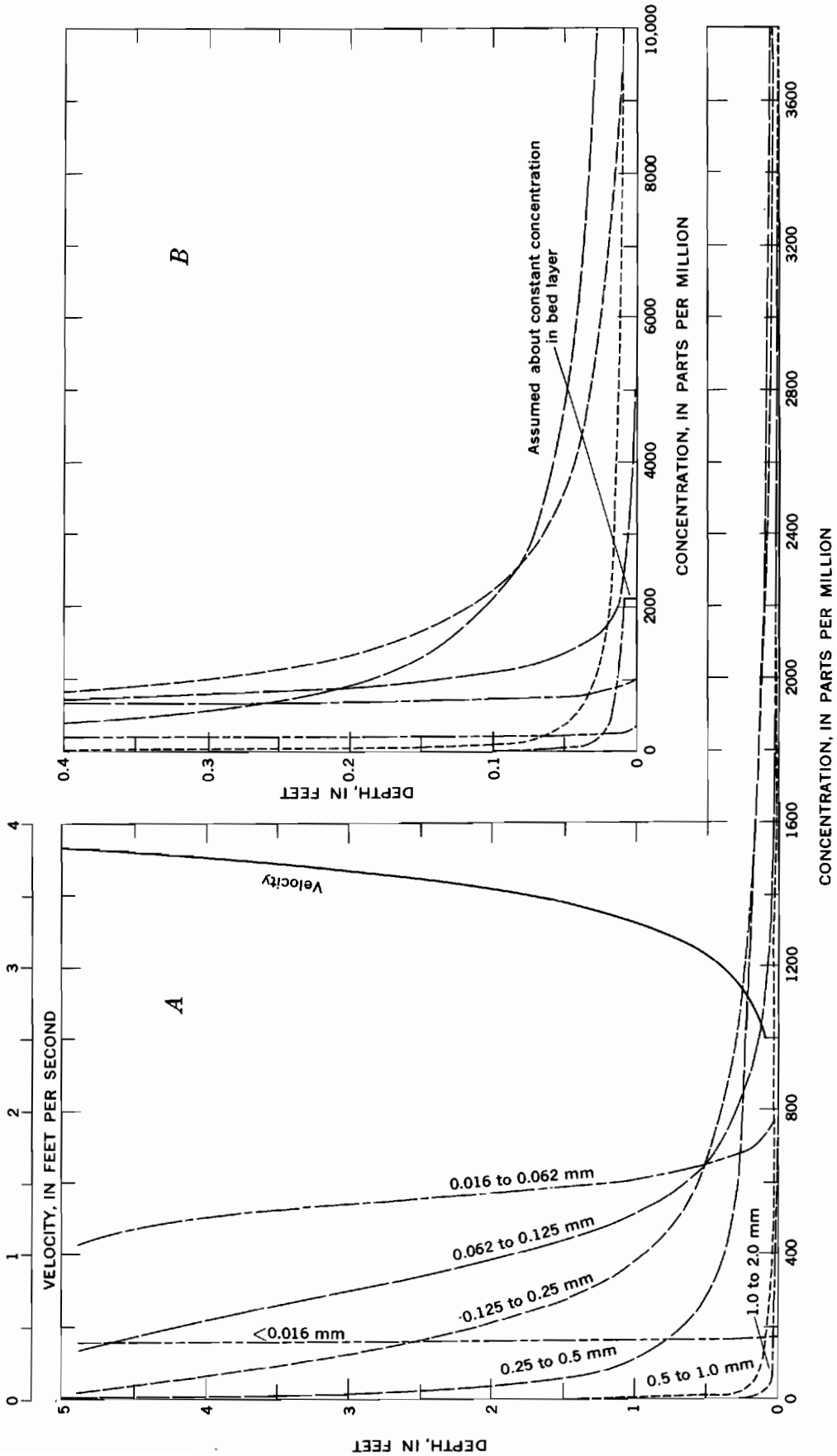

FIGURE 6.—Distribution of concentrations of different sediment sizes at a stream vertical.

High concentrations of fine sediment in a flow increase the discharge of the coarser sediment because they decrease the fall velocity of the suspended sediment and may modify the bed configuration (D. B. Simons, E. V. Richardsons, and W. L. Haushild, written comm.). The fine sediment seems to affect sediment transportation by changing the apparent viscosity of the mixture of water and sediment. The effect of the fine sediment should be comparable to the effect of a decrease in water temperature, but the effect of high concentrations of fine sediment may be much greater than the effect of usual changes of the temperature of natural streams.

EFFECTS OF MAJOR FACTORS

The preceding discussion of the concept of sediment transportation indicates the major variables that probably control the discharge of sands in sandbed streams through the effect of these variables on bedload discharges, suspended-sediment concentrations immediately above the bed layer, and vertical distributions of suspended-sediment concentrations. The quantitative effect of individual variables can be approximately defined, at least for some flows and streams cross sections, by a type of graphical analysis. An important part of the analysis is to determine which of four possibly interchangeable variables—namely, mean velocity, shear, shear velocity computed from mean velocity, or stream power—shows the closest and most useful relationship to the discharge of sands. Of course, shear velocity computed from mean velocity is the type of shear velocity with respect to the particles that is computed from a known mean velocity with the use of an equation such as equation 10.

Three general assumptions or limitations should be kept in mind in the following discussions. One is that the assumed bed material of the streams is relatively cohesionless sands. Another is that discharge of sands in these streams is equivalent to the sum of the bedload discharge and the suspended discharge of bed material. The third is that discharge of sands is proportional to the width of stream; this assumption, in effect, excludes some highly irregular cross sections from the studies but does permit the use of discharge of sands per foot of width as the usual unit for expressing the rate of transportation of sands through a cross section.

MEAN VELOCITY

Probably the simplest measure of the force that moves sediment in a stream is the mean velocity. Studies by Gilbert (1914), Colby (1957), and Rottner (1959) have shown an approximate relationship between the discharge of bed material in shallow flows or near the streambed and roughly the third power of the mean velocity, except for low velocities. Hence, the relationship of discharge of sands per unit width of stream to mean velocity was investigated in detail for natural streams and less extensively for flumes.

NATURAL STREAMS

Total discharges of sands for Niobrara River near Cody, Nebr., show a close relationship to mean velocity. (See fig. 7.) (For this and other curves that involve a relationship of discharge of sediment to mean velocity or to other variables, the sediment discharge is considered to be the statistically dependent variable; that is, each curve is drawn to show, as well as possible, the average sediment discharge for each of several narrow ranges of the independent variable.) These total discharges of sands were measured at a contracted section 1,900 feet downstream from the gaging-station section where velocities, depths, and widths of flow and particle sizes of the bed sediment were determined (Colby and Hembree, 1955). The median size of the bed sediment was about 0.28 mm. The total discharges of sands have the usual inaccuracies inherent in sampling suspended sands at a somewhat unsatisfactory cross section. Also, at times some appreciable gain or loss of sands must have occurred between the two sections. No adjustment was applied for change in water temperature. In spite of the inaccuracies, the scatter of points from the average curves of figure 7 is not excessive.

An average curve of discharge of sands per foot of width against mean velocity was also defined (fig. 8) from information given by Hubbell and Matejka (1959) for Middle Loup River at Dunning, Nebr. Sections *A*, *B*, *C*, and *E*, at which velocities, depths, and widths of flow and particle sizes of the bed sediment were determined, have average widths of roughly 280, 70, 80, and 150 feet, respectively. Section A is about 1.4 miles upstream from the turbulence flume where total sediment discharges were measured (Benedict, Albertson, and Matejka, 1955), and section *E* is about 700 feet downstream from the flume. Section *B* is about 1,200 feet and section *C* is less than 100 feet upstream from the flume. Median particle size of the bed material at the four sections is about 0.32 mm. Rough adjustments for changes in water temperature were applied before the total discharges of sands were plotted on figure 8. A single curve represents the average relationship fairly well for all four sections.

Total discharges of sands (data from the files of the Agricultural Research Service, U.S. Dept. of

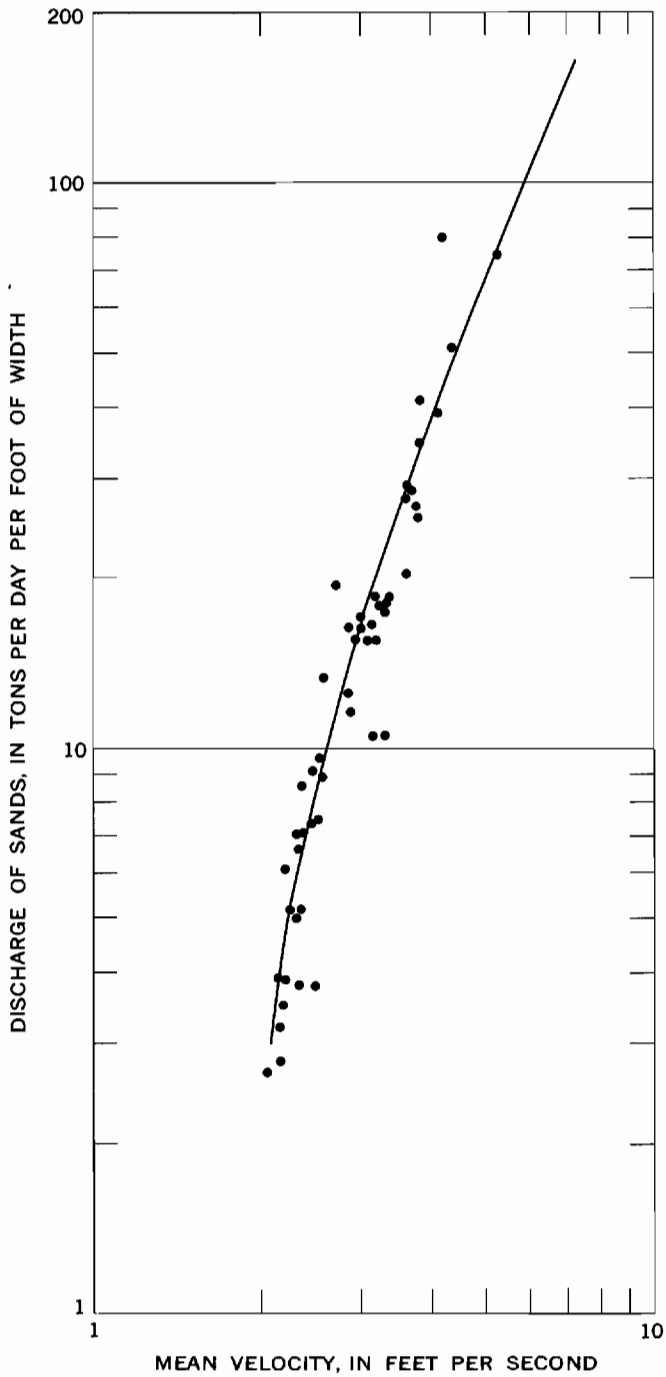

FIGURE 7.—Discharge of sands plotted against mean velocity for Niobrara River near Cody, Nebr. (Data unadjusted for water temperature.)

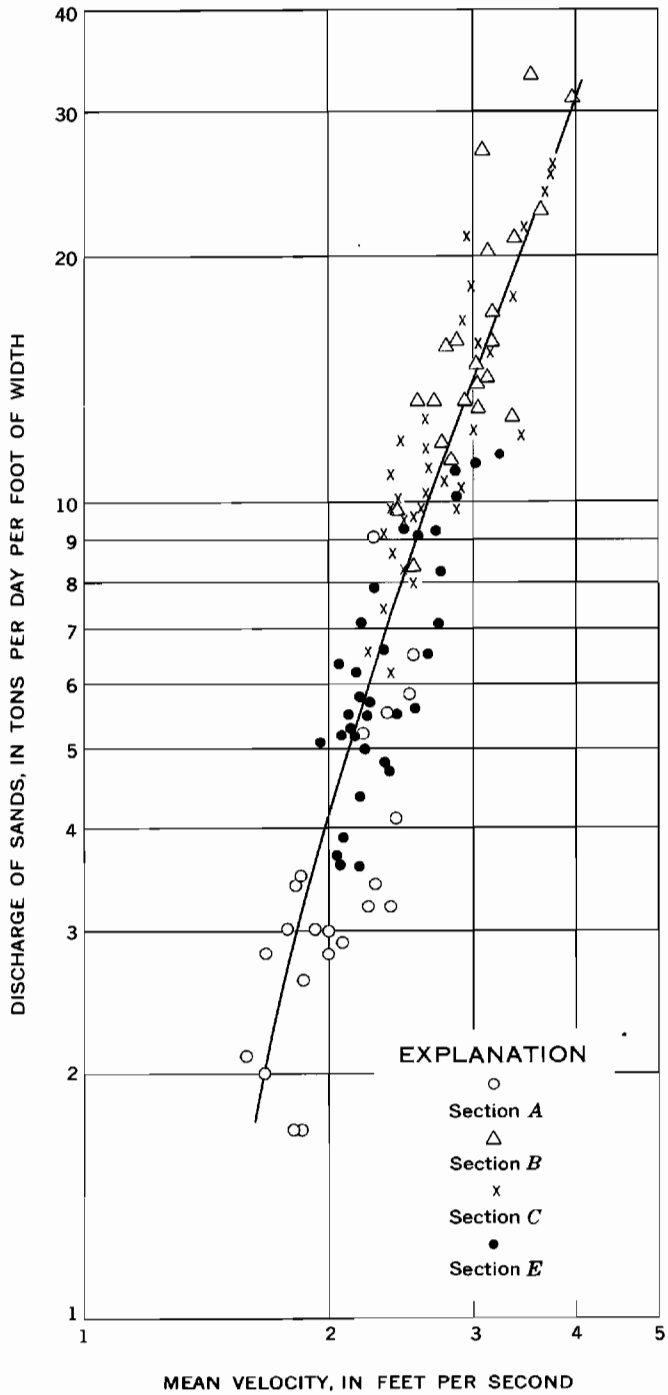

FIGURE 8.—Discharge of sands plotted against mean velocity for Middle Loup River at Dunning, Nebr. (Data roughly adjusted for water temperature.)

Agriculture, University, Miss.) for several stations on Pigeon Roost Creek or its tributaries in Mississippi were approximately determined by adding estimates of unmeasured sediment discharges to measured discharges of sands. These total discharges were plotted against mean velocity to define the six average curves that are indicated by broken lines on figure 9. Each of five of the broken curves is for an individual sediment station, and the sixth is a composite curve that is based on only a few determinations for each of several sediment stations. Median diameter of the bed sands is about 0.40 mm. at all stations. The unmeasured sediment discharges, mostly of sands, were estimated from a graphical

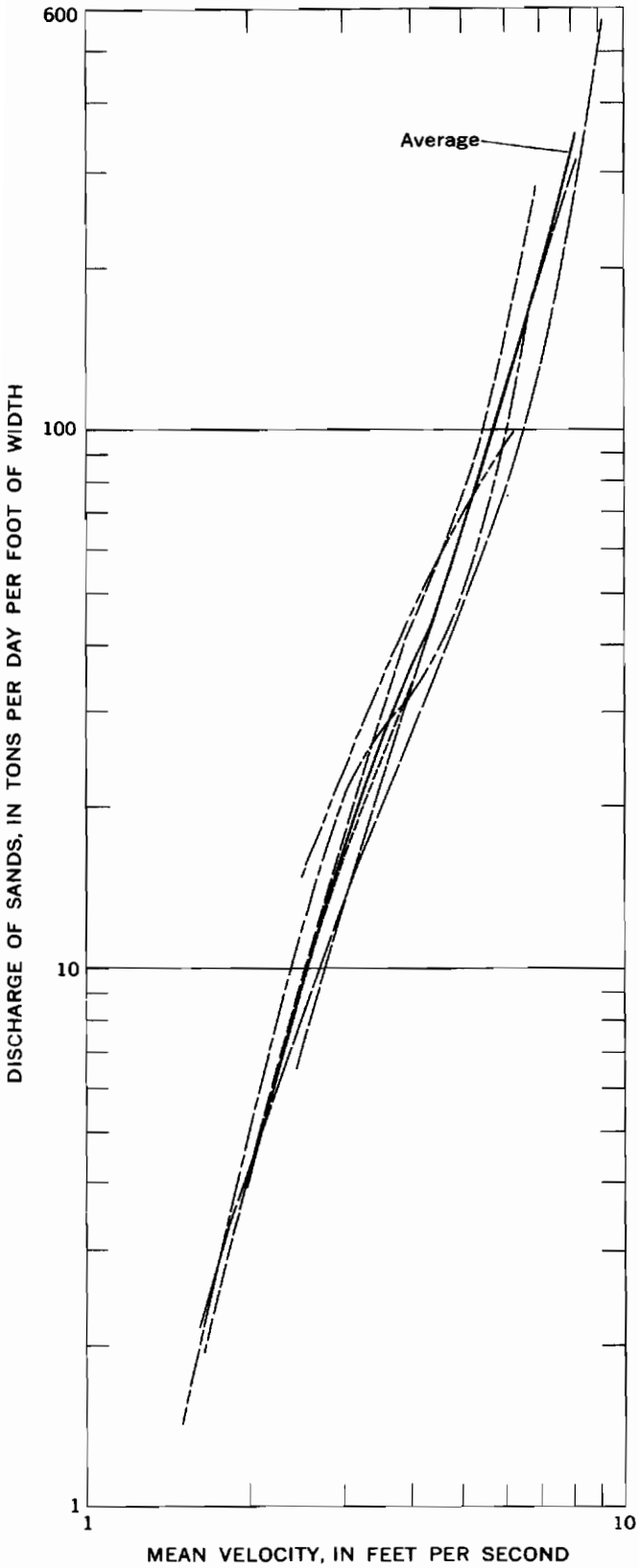

FIGURE 9.—Curves of relationship between discharge of sands and mean velocity for stations on Pigeon Roost Creek in Mississippi. (Data unadjusted for water temperature.)

727-985 O - 64 - 4

relationship to mean velocity (Colby, 1957). Hence, the unmeasured portion of the total discharge of sands was based partly on mean velocity. Also, the mean velocities for the high flows at several of the stations were determined by measuring from bridges where the streambed scoured locally. Most measurements of high flows were made on falling stages when the mean velocity under a bridge may have been appreciably lower than the mean velocity away from the bridge. In general, the six curves are reasonably consistent and may be roughly expressed by the single continuous curve of figure 9.

Total discharges of sands for stations on the Rio Grande or diversions from it in New Mexico were obtained from unpublished computations that were made by J. K. Culbertson and D. Q. Matejka according to the modified Einstein procedure (Colby and Hembree, 1955) and were used to define a curve of relationship to mean velocity. (See fig. 10.) Two total discharges of sands in the Rio Grande near Socorro, N. Mex., and one near San Antonio, N. Mex., were made when most of the flow originated in the drainage basin of the Rio Puerco and contained very high concentrations of clay and silt. The plotted points for the three determinations when the concentration of fine sediment was very high are circled on figure 10. The circled points indicate discharges of sands that are roughly three to eight times greater than the discharges of sands from the average curve for times when the concentrations of fine sediment were low.

Total discharges of sands for Rio Puerco near Bernardo, N. Mex., where concentrations of silt plus clay are on the order of 100,000 ppm (parts per million) or more on many rises, have only a rough relationship to mean velocity (fig. 11). They are generally very high as compared with total discharges indicated by an estimated curve for which factors such as velocities, depths, and bed-materials sizes are similar but the concentration of fine sediment is low. The effect of the high concentrations of fine sediment apparently is very large. It is reasonably consistent with the laboratory findings of D. B. Simons, E. V. Richardson, and W. L. Haushild (written communication).

For a large stream, Mississippi River at St. Louis, Mo., the total discharges of sands plot fairly close to an average curve of relationship to mean velocity. (See fig. 12.) They were based on measured discharges of sands plus unmeasured sediment discharges that were estimated from the same graphs used for the unmeasured sediment discharges of Pigeon Roost

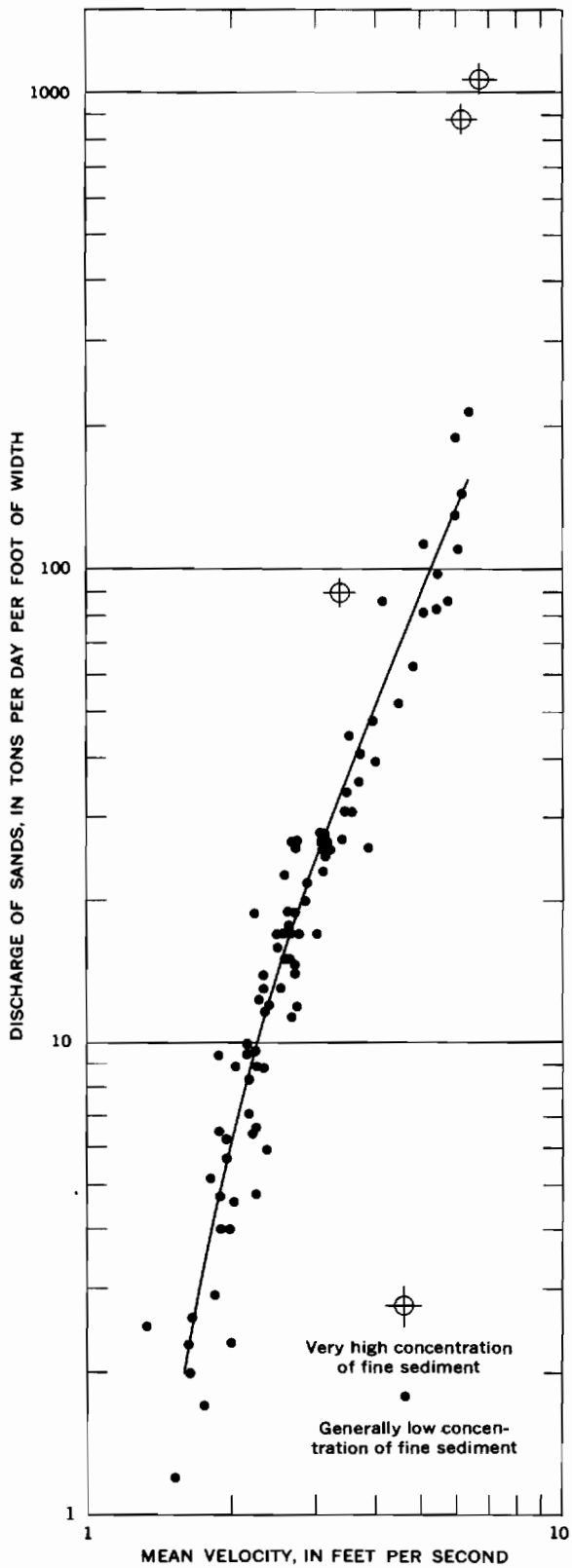

FIGURE 10.—Discharge of sands plotted against mean velocity for the Rio Grande in New Mexico and for some diversions from it. (Data unadjusted for water temperature.)

Creek. Hence, these unmeasured sediment discharges are related to mean velocity. However, the relationship of measured discharge of sands to mean velocity (P. R. Jordan, written communication) seems to be equally as consistent as the relationship of figure 12.

Scatter of total discharges of sands from an average relationship such as that of figures 7, 8, 10, or 12 is generally less for a single and reasonably uniform cross section — for example, the cross section of Niobrara River near Cody, Nebr. — than for a group of cross sections or for an irregular cross section.

Curves showing relationship between discharge of sands per foot of stream width and mean velocity for the Niobrara River, the Middle Loup River, Pigeon Roost Creek, the Rio Grande, and the Mississippi River are rather surprisingly consistent (fig. 13) and can be used to estimate quickly and roughly the discharge of sands in many sand-bed streams. The average water temperature is about 60° F. for each curve. Of course, the somewhat steeper slope of the curve for the Mississippi River is due to the fact that any particular mean velocity occurs at greater depths in the Mississippi River than in the shallower streams. However, in general, a sand-bed stream seems to have not only a reasonable close relationship between discharge of sands per foot of width and mean velocity at a cross section, but the relationship defined for one cross section may apply approximately for other sand-bed streams if bed-material sizes and depths are not greatly different and if the concentrations of silt plus clay are not unusually high.

FLUMES

The discharge of sands per foot of width for a series of flume experiments with the same bed sediment and constant water temperature usually shows a fairly close relationship to mean velocity. (See fig. 14). However, in a flume whose slope can be adjusted, a particular mean velocity may occur over a wide percentage range of depths. Thus, some scattering of points on figure 14 is caused by changes in depth, but some is caused by changes in water temperature, by unidentified factors, or by experimental error. Except for the effect of depth, the scatter of the observed discharges of sands about an average curve would probably be considerably less for most flume experiments in which a constant bed material is used that it would be for similar mean velocities at a cross section of a natural stream where the determinations are likely to be less accurate and where the lateral distributions of depth, velocity, and sediment discharge generally are less uniform. If the mean velocities in a flume are much lower than in a natural stream, they may be in

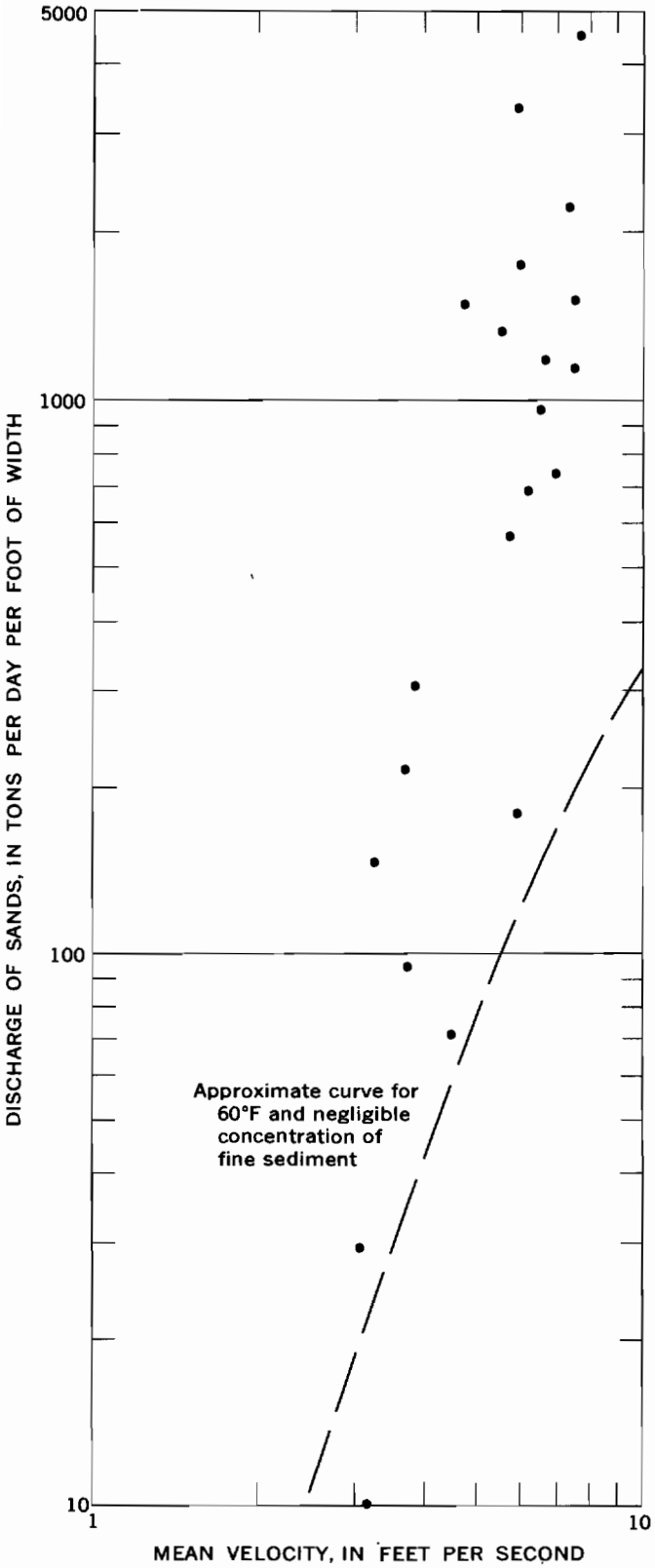

FIGURE 11.—Discharge of sands plotted against mean velocity for Rio Puerco near Bernardo, N. Mex. (Data unadjusted for water temperature.)

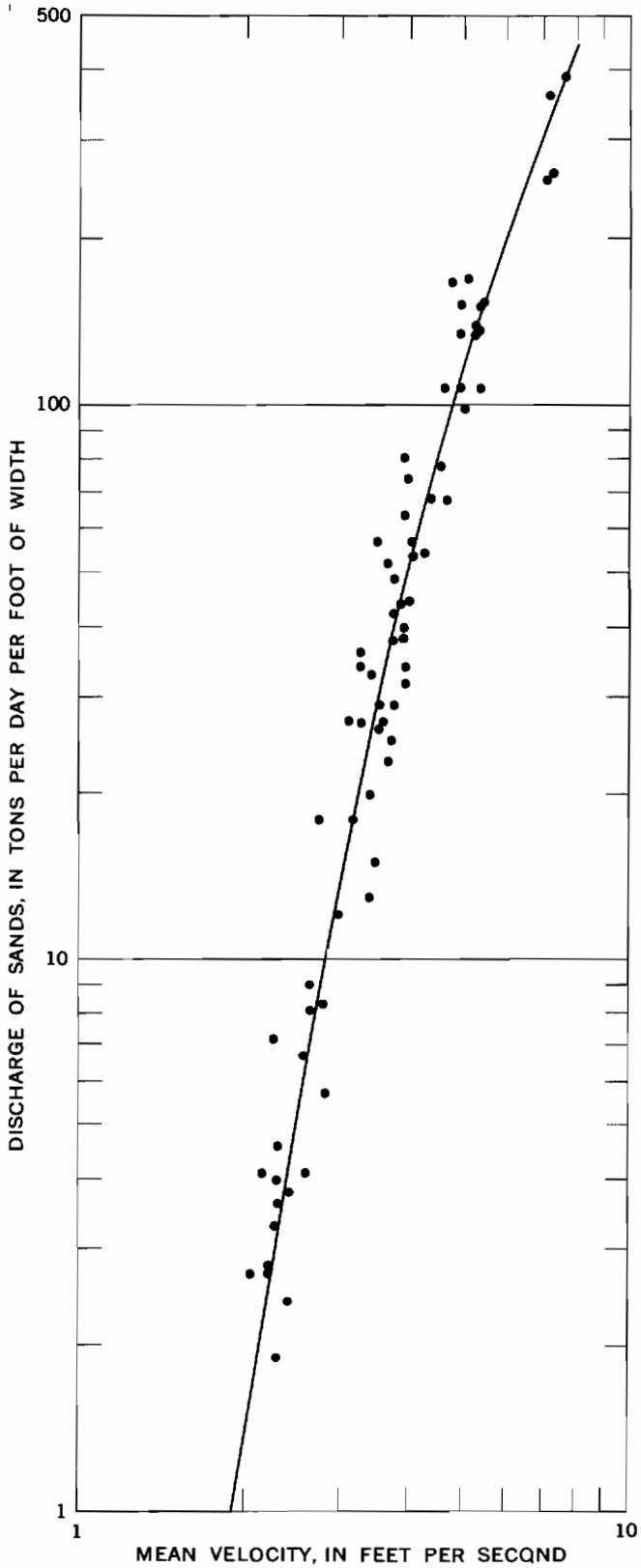

FIGURE 12.—Discharge of sands plotted against mean velocity for Mississippi River at St. Louis, Mo. (Data unadjusted for water temperature.)

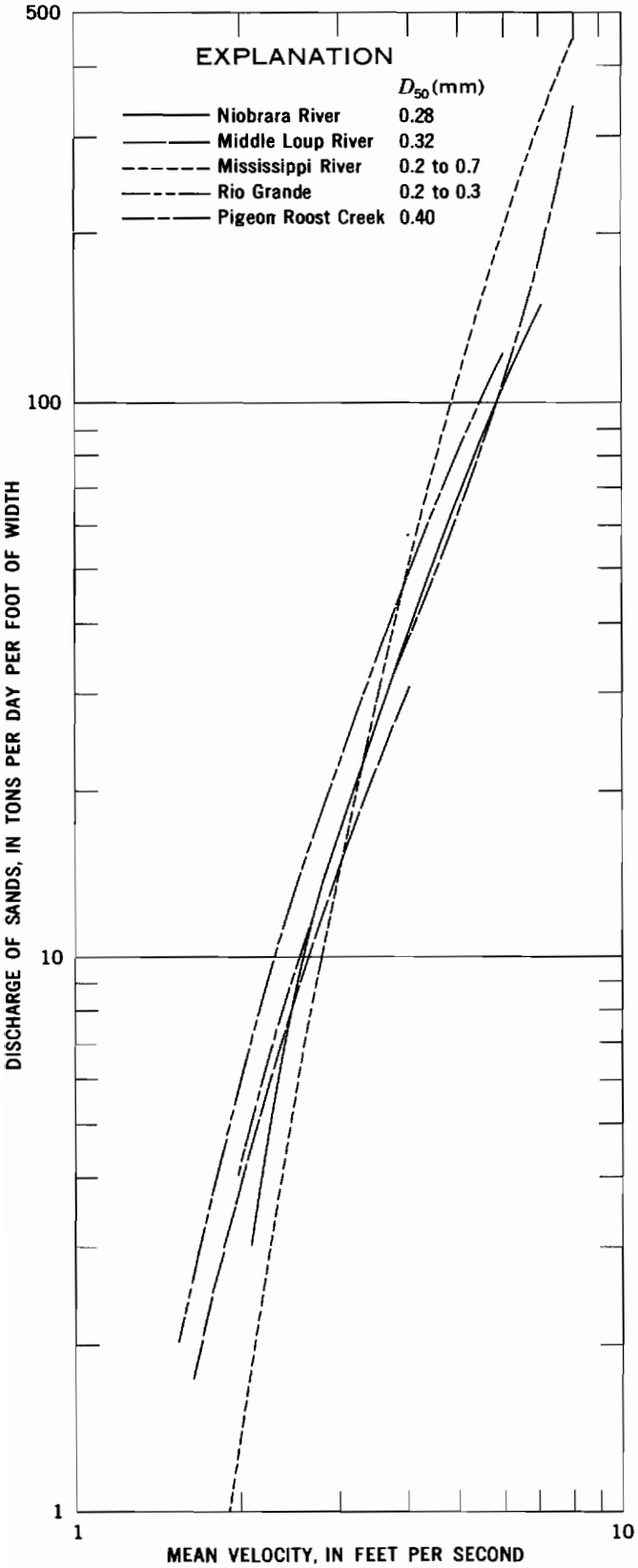

FIGURE 13.—Curves showing relationship between discharge of sands and mean velocity for five sand-bed streams at average temperatures of about 60° F.

the range for which the discharge of sands is very sensitive to small changes in velocity, depth, and size distribution of the bed sediment.

The main reason for the curvature of the lines showing average relationship on figure 14 is that the discharges of sands are plotted against mean velocity rather than against mean velocity minus the critical velocity at which movement of significant amounts of sand begins. If 0.8 and 0.7 foot per second are subtracted from the mean velocities for the left and right curves of figure 14, respectively, straight lines can be substituted for the curves.

The average relationships of discharges of sands to mean velocity for flume experiments differ considerably among themselves and especially for shallow flows are rather inconsistent with the relationship for Niobrara River near Cody, Nebr. (See fig. 15.) Much of the disagreement is due to differences in sizes of bed sediment or in depth. Because of the divergence among the curves for flumes, the comparative consistency of the curves for natural streams (fig. 13) probably would not have been predicted from flume experiments.

SHEAR

Shear or tractive force is an obvious measure of the force that may cause sediment to move and has been widely used as a parameter of sediment discharge. Shear in the form of a shear velocity is directly proportional to mean velocity if the Chezy C is constant. Thus, if resistance to flow as expressed by C were always constant, mean velocity and shear velocity could be used interchangeably as parameters of discharge of sands in sand-bed streams. The choice between those two parameters should be made, therefore, mainly on the basis of which one has the more consistent relationship to the discharge of sands when resistance to flow is variable.

Other factors should also be considered in making a choice between mean velocity and shear as a measure of the discharge of sands. Shear can be used directly in the design of a channel, whereas mean velocity for channel design normally must be computed from the shear. However, if the discharge of sands is more closely related to mean velocity than to shear, the problem of the relationship of mean velocity to shear cannot be avoided. Also, canals usually are designed for velocities that are slow enough to be in the range of flow over dune beds, and in this range the major change of roughness at the transition from dunes to a smoother bed does not enter the computations. In a natural stream

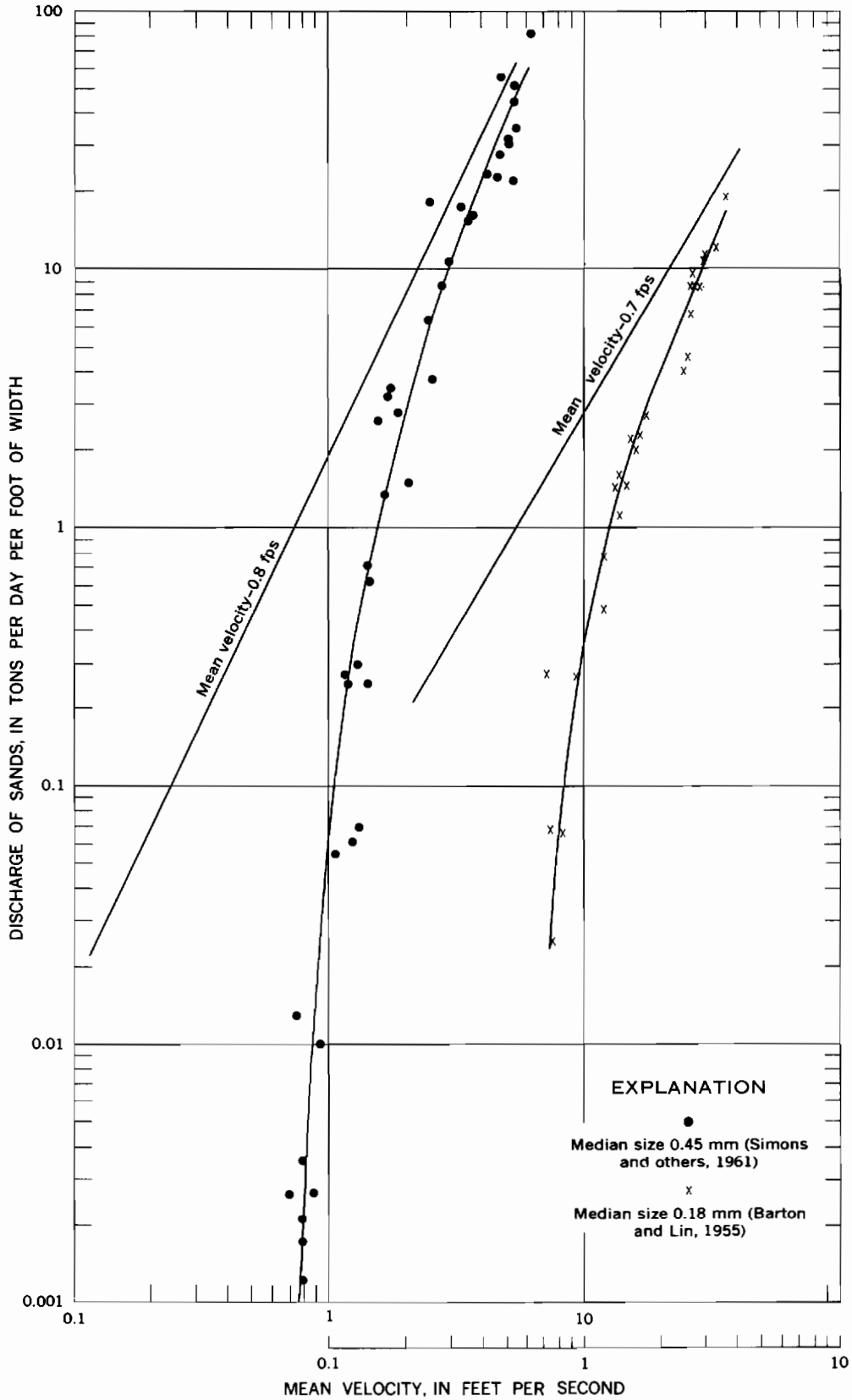

FIGURE 14.—Curves showing relationship between discharge of sands and mean velocity for some flume experiments with two sands. (Data unadjusted for water temperature and depth.)

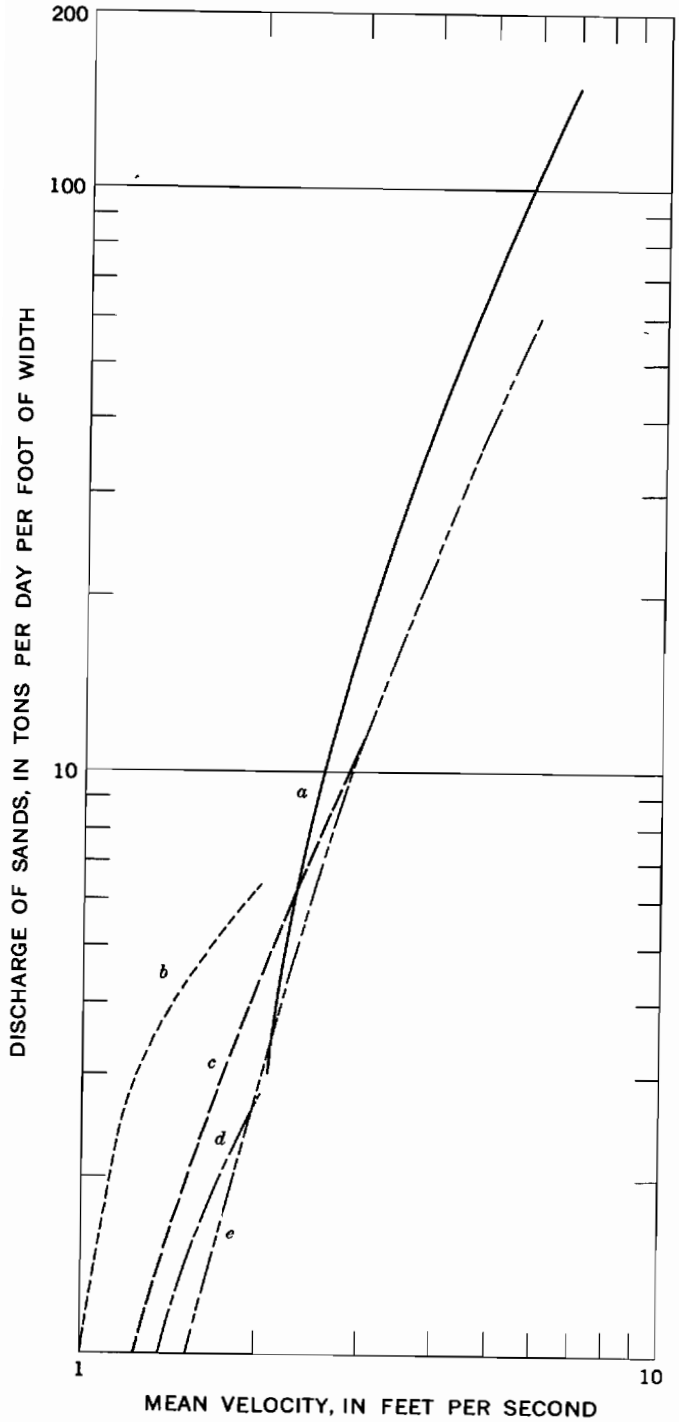

		D_{50} (mm)	Approx depth (ft)
a	Niobrara River	0.28	1.0 -6.0
b	Brooks (1958)	.088	0.15-0.3
c	Barton and Lin (1955)	.18	0.3 -1.4
d	Brooks (1958)	.145	0.15-0.3
e	Simons and others (1961)	.45	0.25-1.0

FIGURE 15.—Curves showing relationship between discharges of sands and mean velocity for some flume experiments. (Data unadjusted for water temperature and depth.)

at a particular time, the mean velocity usually can be determined experimentally more easily than the shear. For channels that are not uniform laterally, the average depth of flow ordinarily used to compute shear is weighted with lateral distance in contrast to mean velocity, which is weighted with the product of lateral distance and depth; that is, average depth is equal to the area divided by the width, but mean velocity is equal to the streamflow divided by the area, which is the product of the average depth and the width. Thus, the areas of highest velocity in a cross section usually are given more weight in computing the mean velocity than in computing the average depth because the velocities generally are highest where the flow is deepest.

The discharges of sands reported by Simons, Richardson, and Albertson (1961) and plotted against mean velocity on figure 14 indicate an approximate relationship (fig. 16) to shear. For easy comparison with stream power, the discharges of sands are replotted against the 3/2 power of the shear and the cube of the mean velocity. At a shear of about 0.07 to 0.10 pound per square foot (a shear to the 3/2 power of about 0.018 to 0.030), the range in discharge of sands at a particular shear is large. From independent experiments that were made mostly within a similar range of uncertain relationship, Brooks (1958) concluded that neither the velocity nor the sediment discharge is a single-valued function of the shear. Although the conclusion applies to only a narrow range of shears in most natural streams if the bed material, water temperature, and energy gradient are constant, within this range the shear is not an acceptable measure of the mean velocity or of the discharge of sands. The range of uncertain relationship between discharge of sands and shear differs considerably from one stream to another and cannot be acccurately predicted at the present time from characteristics of the channel. Hence, the shear is at times an undependable measure of the discharge of sands.

A conclusion by Barton and Lin (1955, p. 21, 37) that the bed-material concentration may be a function only of resistance to flow is a further indication of the relatively poor relationship of discharge of sands to shear. Of course, the reason for some relationship between bed-material discharge and resistance to flow is that mean velocity depends both on resistance to flow and on shear, and the relationship either to resistance to flow or to shear is an incomplete part of the more basic relationship to mean velocity. In other words, shear at constant resistance to flow is a measure

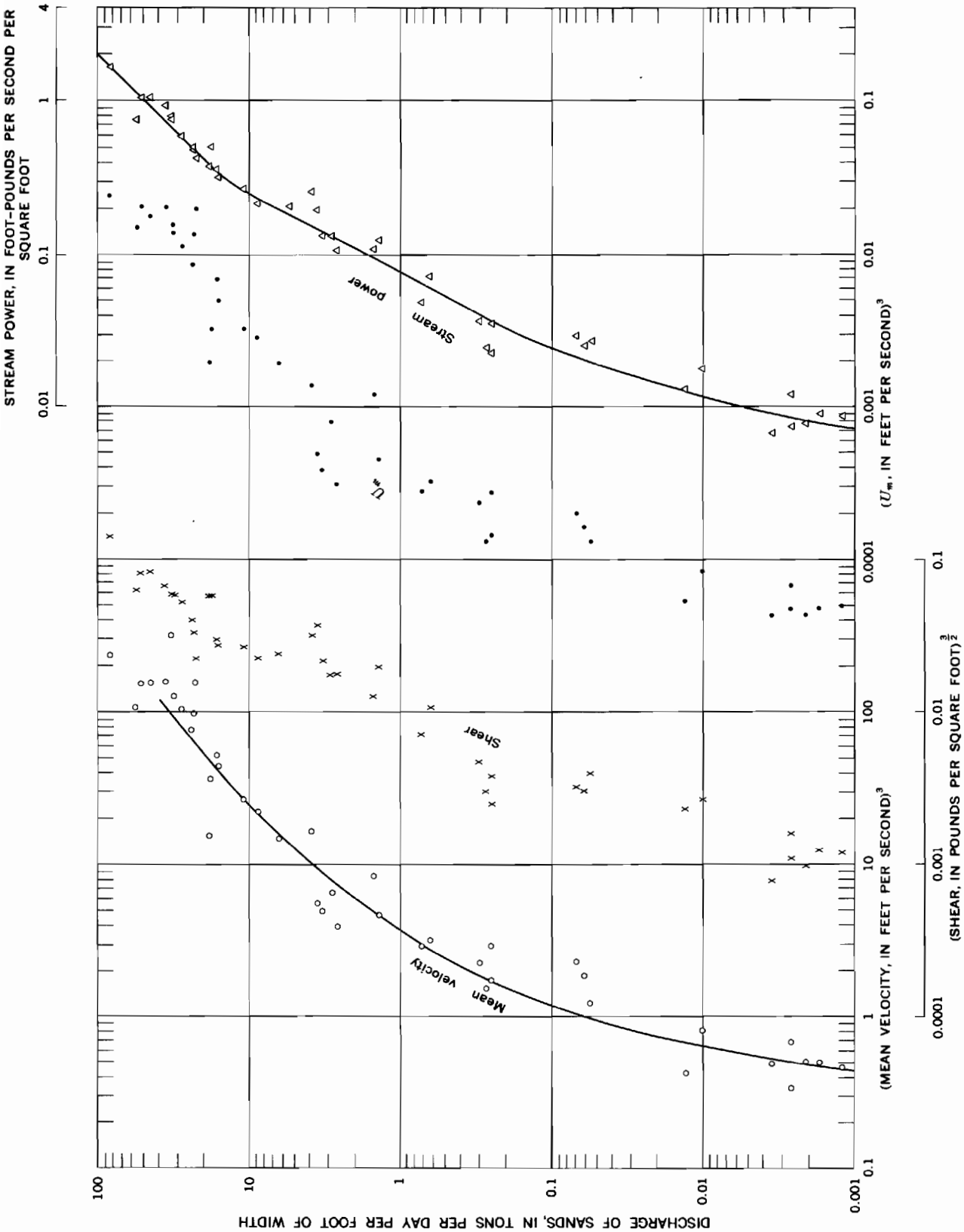

FIGURE 16.—Discharges of sands plotted against parameters that are related to the force which moves sediment particles. (Data unadjusted for water temperature and depth.) u_* is shear velocity computed from mean velocity.

of mean velocity and discharge of bed material, and resistance to flow at constant shear is also a measure of mean velocity and discharge of bed material.

SHEAR VELOCITY COMPUTED FROM MEAN VELOCITY

Einstein (1950, p. 9–10) used a shear velocity with respect to the grains, which is the shear velocity that can be computed from the hydraulic radius with respect to the grains. This hydraulic radius with respect to the grains or particles is the hydraulic radius that can be used with the energy gradient to compute mean velocity from equation 10. However, the use of this hydraulic radius, R', under the logarithm sign in the equation is questionable. The shear velocities used in this paper were computed from known mean velocities and from equation 10 except that d or R was substituted for R' under the logarithm sign.

The same discharges of sands that were plotted against the mean velocity cubed and against the 3/2 power of the shear show no discontinuity in their relationship to the shear velocities computed from mean velocity. Hence, this type of shear velocity has a major advantage over shear as a measure of the discharge of bed material. The scatter about an average curve is, of course, approximately the same whether mean velocity or shear velocity computed from mean velocity is used as the independent variable. However, as will be shown later, the effect of depth on the relationship between discharge of sands and shear velocity computed from mean velocity is somewhat different from that on the relationship between discharge of sands and mean velocity. Except for the difference in effect of depth, the choice between mean velocity and shear velocity computed from mean velocity is based mostly on convenience and simplicity of use.

STREAM POWER

"Stream power" is a term for the rate at which a stream loses energy. It has been discussed as a measure of the discharge of sediment by Cook (1935) and Bagnold (1960), but its relationship to sediment discharge is not simple, as Cook indicated. Specifically, the stream power of a volume of water in a reach of river L units long and W units wide is equal to the product of the weight of the water in the reach and the loss of energy head per unit time. Hence, the stream power for low concentrations of sediment and of dissolved solids and in pound-foot-second units is 62.4 $LWd\bar{u}S$. For unit width and length of channel the stream power is 62.4 $dS\bar{u}$ or the product of shear and mean velocity.

If the Chezy C were constant, the stream power would be directly proportional to the third power of the mean velocity and would be neither a better nor a worse parameter than mean velocity. However, when C varies, the shear is a somewhat inadequate measure of the discharge of sands. Hence, the stream power also is a poor measure of the discharge of sands when C varies widely, as it does within the range of shear at which a dune bed changes to a plane or antidune bed. In other words, the discontinuity in the relationship between discharge of sands and shear at about a shear of 0.07 to 0.10 pound per square foot also exists in the relationship between discharge of sands and stream power but is partly obscured by the inclusion in stream power of mean velocity.

Any continuous curve that might be drawn to represent the experimental relationship between discharge of sands and stream power on figure 16 obviously cannot be as smooth and consistent as the curve for the relationship to the cube of the mean velocity. A comparison of the two curves of figure 16 suggests some conclusions with respect to stream power.

At velocities high enough to cause plane or antidune beds, the resistance to flow should be reasonably constant; hence, all curves showing relationship between discharge of sands and one of the independent variables of figure 16 should have about the same slope. Curves showing relationship of discharge of sands to mean velocity or to shear velocity computed from mean velocity are smooth and continuous and merge gradually into the slope for high velocity. In fact, as was shown (fig. 14) for two sands, the relationship between discharge of sands per foot of width and mean velocity minus the velocity at which sediment begins to move significantly is about a straight-line relationship. No constant quantity can be subtracted from the cube of the mean velocity to obtain a straight-line relationship to the discharge of sands. Similarly, no constant stream power can be subtracted from the stream power on figure 16 to define a straight-line relationship between discharge of sands and stream power. This fact and objections based on theoretical physics make very questionable the usefulness of Bagnold's suggestion (1960, p. 4) that a power threshold should be used for the beginning of sediment movement.

The relationship between discharge of sands and stream power is poor within the range of stream power from about 0.10 to 0.30 foot-pound per second per square foot, because within this range the shear has little relationship either to mean velocity or to discharge of sands. Above and below this range, the curve showing the relationship of discharge of sands to stream power is much like that to the cube of the

mean velocity. The break in the relationship occurs at the transition from dunes below this range to a plane bed or antidunes above this range and is caused by the unsatisfactory independent variable. It can be eliminated by using mean velocity or shear velocity computed from mean velocity as the independent variable.

At high discharges of sands, the scatter of points about a curve showing average relationship is less from stream power than for any of the other three independent variables that were used on figure 16. This relatively good agreement for one set of experiments at high discharges of sands may or may not be characteristic.

A reasonably constant concentration of sands is indicated by the approximately 45° slope of the curve showing the relationship between the discharge of sands and stream power at high flows and at high discharges of sands. At a particular reach of a sand-bed stream, the slope of the energy gradient usually varies comparatively little with changes in depth. Hence, if the depth is quadrupled, the mean velocity should double provided that the Chezy C remains constant, and the flow per foot of width should be eight times greater for the deeper flow. For the concentration of sands to remain constant, the discharge of sands should increase eightfold or in proportion to the cube of the mean velocity.

DEPTH

The effect of depth on the relationship of discharge of sands to any one of the four independent variables —namely, mean velocity, shear, shear velocity computed from mean velocity, and stream power—is different from the effect of depth on the relationship of discharge to any of the other three variables. It can be defined more accurately for the relationships of discharge of sands to mean velocity or to shear velocity computed from mean velocity than for the relationships to shear or to stream power.

The complicated effect of depth of flow on the relationship of discharge of sands to mean velocity at different water temperatures can be shown qualitatively by the results of many computations of discharge of sands. The computations were made according to a procedure that was based mostly on the work of Einstein (1950) and for a natural bed of unconsolidated sand whose D_{35}, D_{50}, and D_{65} sizes were about 0.35, 0.40, and 0.45 mm, respectively. They were made for many different combinations of depth and mean velocity and usually for water temperatures of 40°, 60°, and 80°F. The main departures from the Einstein procedure were the use of shear velocities computed from the mean velocities and of some assumptions with regard to the vertical distribution of sediment concentrations. These assumptions were probably fairly accurate for flow over dune beds but resulted in too great discharges of sands at high velocities. A qualitative graph based on these computations (fig. 17) indicates the dominant general relationship between discharge of sands and mean velocity. It also indicates a complex effect of depth on this dominant relationship. At constant low velocities, an increase in depth is accompanied by a decrease in discharge of sands; but at constant high velocities, an increase in depth is accompanied by an increase in discharge of sands. At some intermediate constant velocities, depth has little effect on the relationship between discharge of sands and mean velocity. At constant mean velocity, the effect of depth varies somewhat, but not greatly, as the water temperature changes.

The general reason for the variable effect is easily understood in broad outline, although the actual computation of bed-material discharges for different depths is inexact and complicated. If mean velocity is low—perhaps 2 feet per second—and if water flows in a shallow stream over a sand bed whose median diameter is 0.3 or 0.4 mm, a certain amount of bed material (as generally indicated by the curves of velocity and concentration on figure 18) will be discharged, mostly near the streambed. If the mean velocity is constant at 2 feet per second and if the flow is deep, the velocity near the streambed will be lower and the amount of bed material discharged will be less, both at the bed and throughout the original shallow depth of flow, than they were in the shallow stream. Only a little bed material will be discharged in suspension in the additional depth of flow. Hence, the total bed-material discharge is likely to be less for a given low mean velocity when the flow is deep than when it is shallow. On the other hand, if the mean velocity is high—perhaps 6 feet per second—the bed-material discharge is greater in a shallow flow than in a layer of equal depth at the bottom of a deep flow because of the difference in velocity near the streambed. However, the difference in the bed-material discharge in this layer near the bed is more than balanced by the discharge of bed material in the superposed layer of the deeper flow. (See fig. 18.)

If enough information is available for one bed material and one water temperature and for a wide range of depths and mean velocities, the effects of mean velocity and depth on the discharge of bed material can be determined by the empirical definition of a graph similar to figure 17. Even information for different water temperatures and different bed materials can be analyzed by trial-and-error procedures to

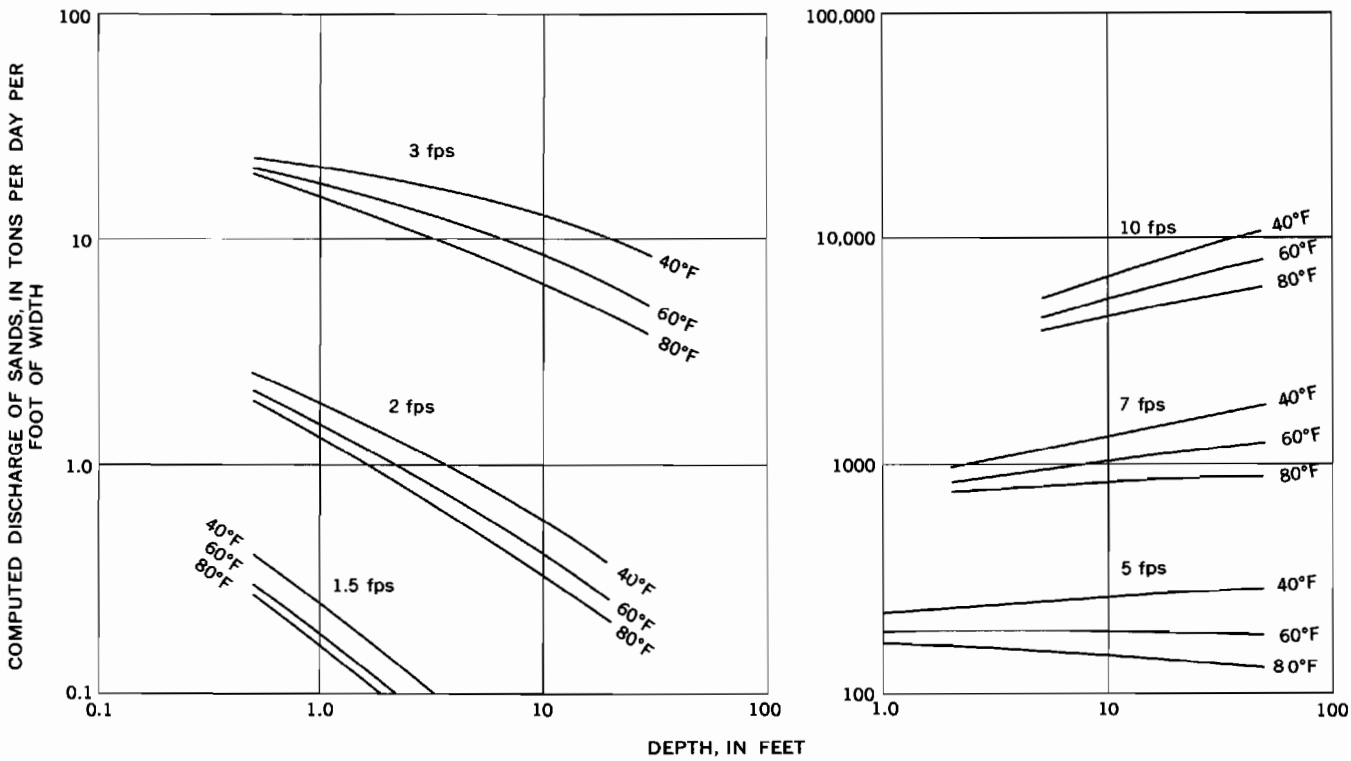

FIGURE 17.—Effect of depth and water temperature on the relationship between discharge of sands (0.40 mm median diameter of the bed sands) and mean velocity, computed from a somewhat revised Einstein procedure. From Colby (1961, fig. 1).

define a graph of empirical relationship of discharge of sands to mean velocity and to depth. (See p. 34–35.) Such a relationship for a water temperature at 60° F and bed sediment having a 0.30-mm median diameter is shown on figure 19. Qualitatively, the relationships of figures 17 and 19 are similar in spite of the difference in particle size and in method of determination; but quantitatively, figure 19 is much more accurate than figure 17. The fundamental soundness of the Einstein procedure is well shown, at least for the assumed bed sand, by the general qualitative agreement of the computed effects with the empirically defined effects of mean velocity, depth, and water temperature.

For a median particle size of 0.30 mm and a water temperature of 60°F, about the same discharge of sands is indicated for a mean velocity of 3.0 feet per second whether the depth is 1.0 foot or 100 feet. Of course, if the line on figure 19 for a mean velocity of 3.0 feet per second were defined more accurately, it might have a somewhat different shape and position.

The effect of depth varies somewhat with changes in particle size. The mean velocities at which depth has little apparent effect on the relationship between discharge of sands and mean velocity are about 1.6, 2.2, and 3.5 feet per second for bed sediments of 0.10–, 0.20–, and 0.40–mm median diameters, respectively, according to empirically defined graphs similar to figure 19. To some extent an increase in mean velocity at constant particle size has about the same effect as a decrease of particle size at constant mean velocity.

Only a small apparent effect of depth on discharge of sands in natural streams was indicated by the relative consistency of the relationship between discharge of sands and mean velocity for different streams. (See fig. 13.) These streams generally have mean velocities, depths, and sizes of bed sediments for which changes in depth should have comparatively little effect, according to figure 19. However, compared with shallower streams, the deeper flows of the Mississippi River at St. Louis result in lower discharges of sands at low velocities and higher discharges of sands at high velocities.

Some inconsistencies of the relationships between discharge of sands in flumes and mean velocity (fig. 15) are explainable on the basis of the effect of depth and particle size. Not only are the depths in flume experiments usually shallow, but they may decrease as the velocities increase. At a high velocity the discharge of sands, especially fine sands, is likely to be far lower in a shallow flow in a flume than at the same mean velocity in a deep river. In contrast, at a low velocity the discharge of sands is likely to be higher in a shallow flow in a flume than at the

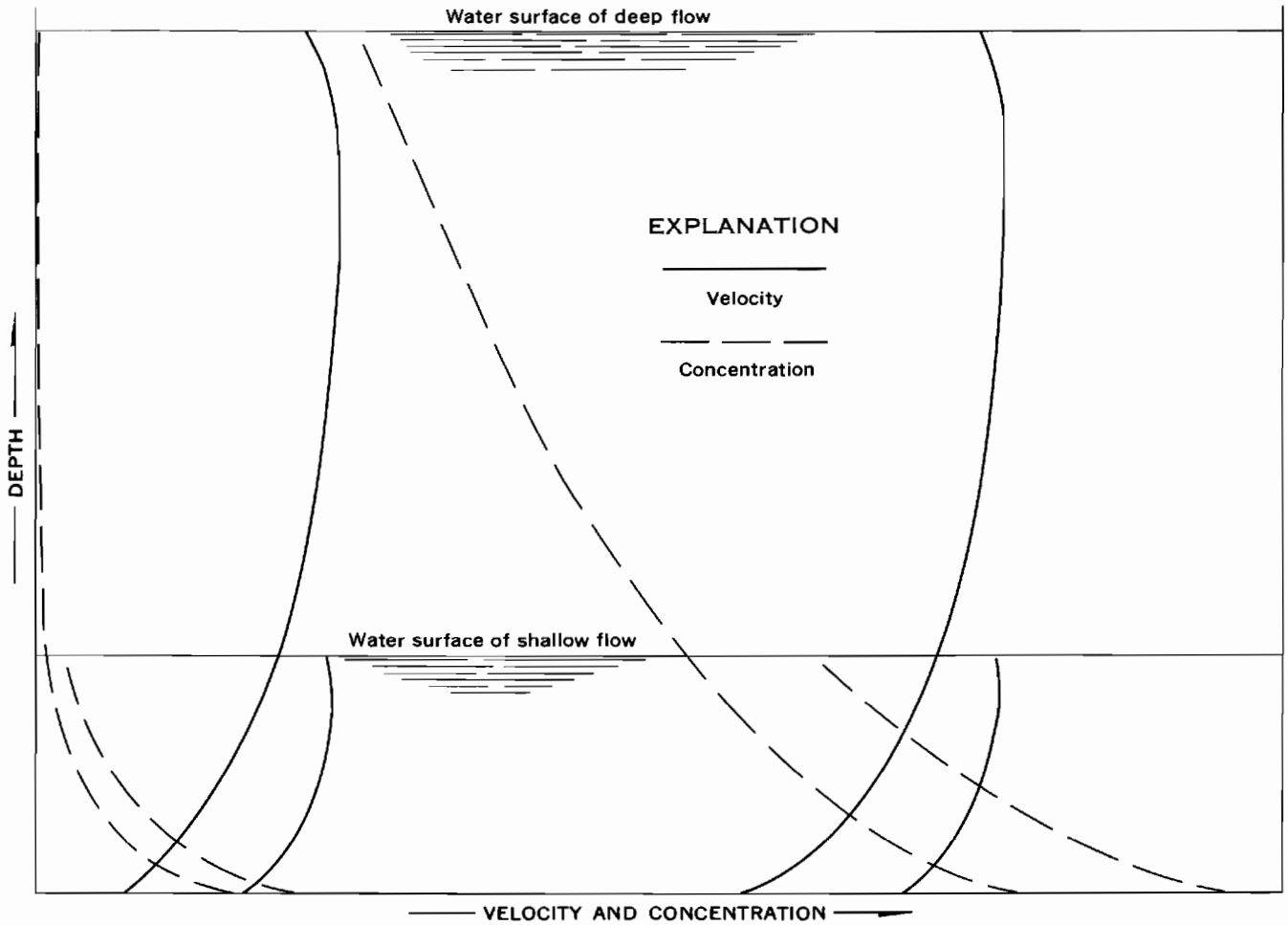

FIGURE 18.—Schematic diagram showing the general reasons for variability of effect of depth on the relationship of bed-material discharge to velocity. From Colby (1961, fig. 3).

same mean velocity in a deep river. Thus, the rate at which the discharge of sands increases with respect to the mean velocity is usually greater in a natural stream than in a flume and in a deep river than in a shallow stream. Also, the depth effect becomes increasingly large at low velocities, and the velocities in flumes—particularly for a given type of bed configuration—are generally low as compared with those in rivers.

The effect of depth on the relationship between discharge of sands and shear velocity computed from mean velocity differs somewhat from the effect on the relationship between discharge of sands and mean velocity but can be computed readily from figure 19 for a median diameter of 0.30 mm and a water temperature of 60°F. The computations require the solving of equation 10 by graphic or algebraic trial and error to obtain values of the shear velocity computed from the mean velocity for many different combinations of depth and velocity. The discharges of sands corresponding to these combinations can then be plotted against depth and shear velocity computed from mean velocity to obtain a reasonably simple pattern of depth effect. (See fig. 20.) One advantage of this depth effect is that it is always in the same direction; that is, at constant shear velocity computed from mean velocity, the discharge of sands increases as the depth increases if there is any appreciable discharge of sands. However, the rate of increase in the discharge of sands is slow at low shear velocities computed from mean velocities, but the rate becomes progressively greater as the shear velocity computed from the mean velocity increases. In many flume experiments, the effect of depth on the relationship between discharge of sands and shear velocities computed from mean velocities would be simpler to use than the effect of depth on the relationship between discharge of sands and mean velocities. In computations for natural streams, the latter effect of depth is smaller and, hence, is generally easier to apply with reasonable accuracy.

The effect of depth on the relationship between discharge of sands and shear is somewhat indefinite except when shear is about proportional to mean velocity or to shear velocity computed from mean velocity. When shear has this relationship, the effect of depth on the relationship of discharge of sands to mean velocity or to shear velocity computed from mean velocity can be applied.

The effect of depth on the relationship between discharge of sands and stream power is a combination of the effects on the relationships to mean velocity and to shear. It is, therefore, both complex and sometimes indfinite. If the Chezy C is constant and if a change in hydraulic radius is exactly compensated by an inverse change in energy gradient so that RS remains constant, the depth effect on the relationship of discharge of sands to stream power can be determined from figure 19 for a median particle size of 0.30 mm and a water temperature of 60°F. If the mean velocity is 3.0 feet per second, median diameter is 0.30 mm, and shear and water temperature are constant, the indicated discharge of sands remains nearly unchanged as the depth increases from about 1 foot to 100 feet. For a lower mean velocity such as 1.5 feet per second, the discharge of sands decreases rapidly as the depth increases at constant shear. If the Chezy C varies, as it does when the bed configuration changes, the effect of depth on the relationship between discharge of sands and stream power becomes more complex and is somewhat indefinite. It is indefinite because the compound parameter stream power is also somewhat indefinite in the sense that doubling the shear may cause a different effect than doubling the mean velocity.

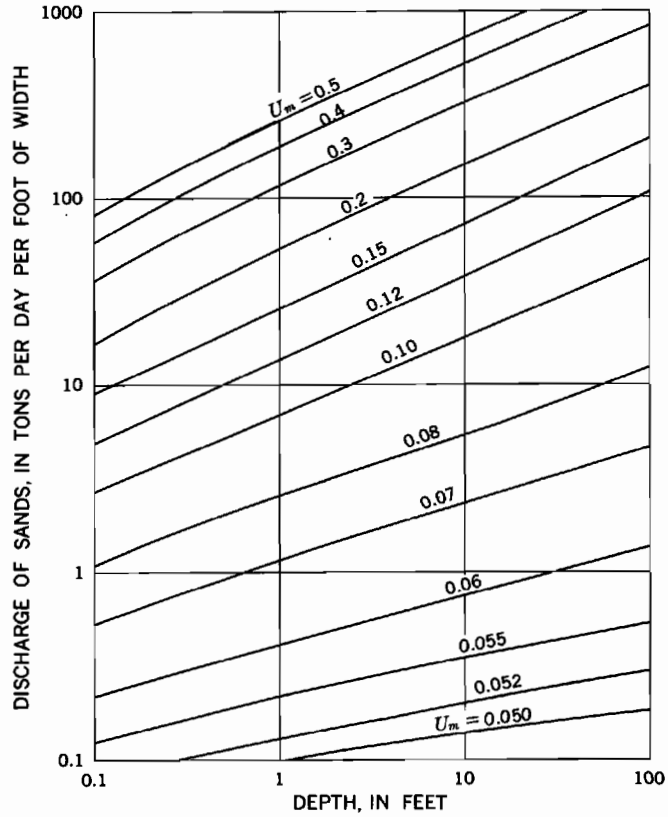

FIGURE 20.—Effect of depth on the relationship between discharge of sands and shear velocity computed from mean velocity. (Water temperature 60°F, and median diameter of bed sands 0.30 mm.)

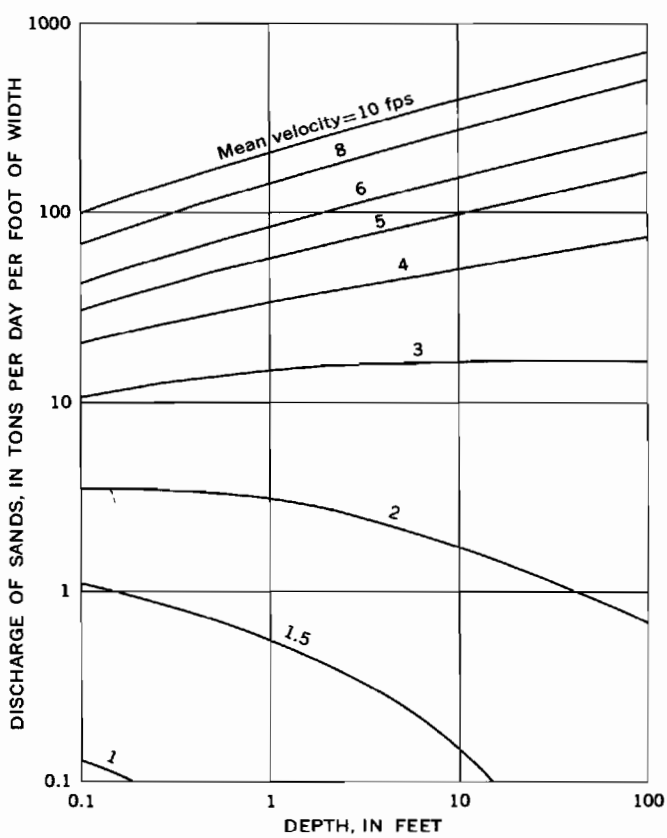

FIGURE 19.—Empirically determined graph of the effect of depth on the relationship between discharge of sands and mean velocity. (Water temperature 60 °F, and median diameter of bed sands 0.30 mm.)

The effect of depth on relationships that involve concentrations of sands should also be understood because it seriously limits the usefulness of concentration of sands as a measure of the rate of sediment movement. The effect of depth on the relationship between concentration of sands and mean velocity for flow over a sand bed whose median particle size is 0.30 mm is large and variable. (See fig. 21, which is plotted directly from the information on fig. 19.) Also, the effect of depth on the relationship between the concentration of sands and mean velocity obviously will differ considerably from one particle size to another. The effect of depth on the relationship of concentration of sands to mean velocity is large and

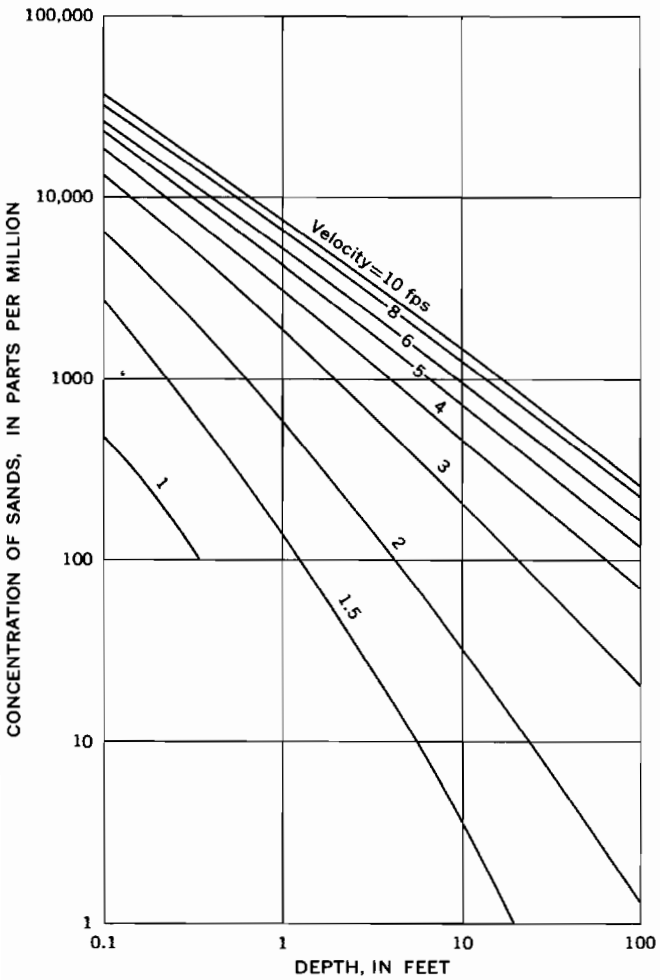

FIGURE 21.—Effect of depth on the relationship of concentration of sands to mean velocity. (Water temperature 60°F, and median diameter of bed sands 0.30 mm.)

variable; therefore, the concentration of sands is a relatively meaningless parameter of rates of sediment transportation as compared to discharge of sands per foot of width, unless both particle size and depth of flow are stated or are kept within narrow ranges. Hence, the concentration of sands may be significant in a flume study of about equal depths of flow over a particular bed of sand, but any attempts to relate concentrations of sands at a cross section in a flume to concentrations at a cross section in a natural stream are likely to be unfruitful. The effect of depth is also large and variable on the relationships of concentration of sands to shear, to shear velocity computed from mean velocity, or to stream power.

VISCOSITY

According to the concept of sediment transportation, viscosity has an effect on the thickness of the laminar sublayer, but its major effect on the relationship between discharge of sands and mean velocity is through its influence on the fall velocities of the particles and thus on the vertical distributions of sediment of different sizes. The percentage effects of changes in water temperature on the discharge of sands obviously varies with velocity, depth, and particle size. If the concentrations of the different particle sizes and the vertical distributions of the concentrations could be computed accurately, the effect of a change in viscosity could also be determined accurately, although the computations would be rather complex and tedious. Unfortunately, the vertical distributions of concentration cannot now be accurately computed, especially for flows over dune beds. Until vertical distributions of sands are more accurately predictable, somewhat oversimplified adjustments based mainly on empirical analysis of available field and flume information may be more practical measures of the effect of viscosity on the discharge of sands than are more theoretical adjustments.

The viscosity of water or the apparent viscosity of a water-sediment mixture can be changed appreciably by variations in water temperature or in concentrations of fine sediment. The relationship between the viscosity of distilled water and water temperature is accurately known. In contrast, high concentrations of fine sediment have a large and less readily defined effect on the apparent viscosity of the water-sediment mixture (D. B. Simons, E. V. Richardson, and W. L. Haushild, written commun.; J. C. Mundorff, written commun.). The effect varies not only with concentration of the fine sediment but with characteristics of the fine sediment. The effects of changes in water temperature and in concentration of fine sediment on discharge of sands are sometimes too large to be disregarded.

WATER TEMPERATURE

The effect of water temperature at a particular cross section can be approximated with trial-and-error multiple correlation. Usually, the size and the composition of the bed sediment at a particular cross section of a sand-bed stream are fairly constant with respect to time and flow, and either the relationship between depth and velocity is reasonably constant or the velocity is in the range for which depth has little effect on the relationship between discharge of sands and mean velocity. Hence, the effect of changes in depth at a particular mean velocity is likely to be small, and the discharge of sands at the cross section is controlled mainly by mean velocity and water temperature if concentrations of fine sediment are not high. An average curve drawn through the observed discharges of sands plotted against mean velocities for Niobrara

River near Cody, Nebr. (fig. 7), gives an approximation of the effect that a change in mean velocity has on the average discharge of sands. The ratio of each observed discharge of sands to the average discharge of sands from the curve of figure 7 at that mean velocity can be computed and then plotted against water temperature. (See fig. 22.) Although the points

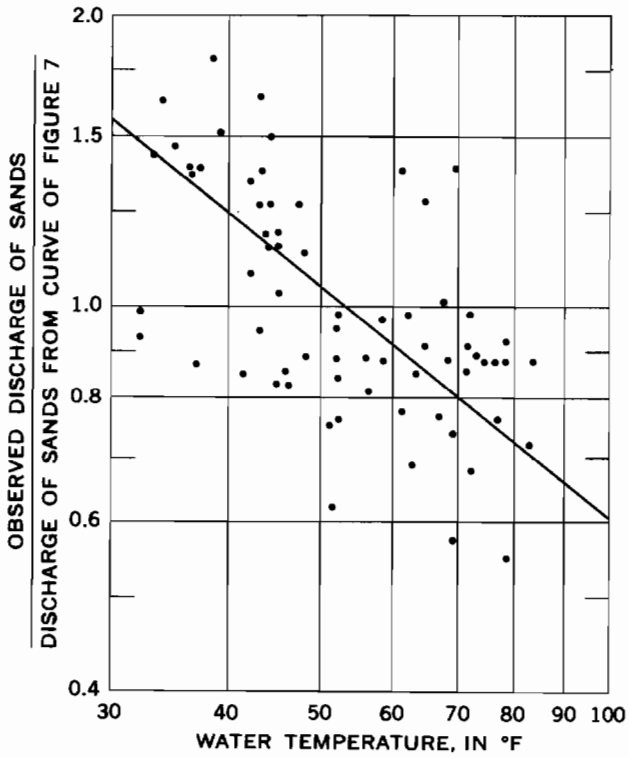

FIGURE 22.—Adjustment for effect of water temperature on the discharge of sands, Niobrara River near Cody, Nebr.

scatter widely, in general the discharge of sands decreases as the temperature increases.

The curves of figure 7 and 22 are only first approximations of the relationships that they represent. Second approximations can be obtained by using the curve of figure 22 to adjust the observed discharges of sands to equivalent sand discharges for a constant temperature of, for example, 60°F. The temperature-adjusted discharges of sands can then be plotted to obtain a second approximation of an average curve of relationship of discharge of sands to mean velocity. This second approximation is, of course, for a temperature of 60°F. Next, the ratio of each observed discharge of sands (unadjusted) to the average discharge of sands from the curve of second approximation can be plotted against water temperature to obtain the second approximation of the effect of changes in water temperature. For the discharge of sands in Niobarara River near Cody, the second approximation for the effect of temperature changes did not seem to differ significantly in slope from the curve of figure 22.

The effect of water temperature on discharge of sands, defined by trial-and-error multiple correlation, for three sediment stations is surprisingly consistent. (See fig. 23.) It also agrees approximately with the computed effect of temperature (fig. 17) for usual combinations of depth and velocity (for example, 10 feet and 7.0 feet per second or 2.0 feet and 3.0 feet per second) in natural flows over a bed material whose median diameter is 0.40 mm. However, the percentage effect shown on figure 17 is generally a little smaller for the 0.40-mm bed sand than for the somewhat finer bed sands at the three sediment stations for which the temperature effect was empirically defined.

A complete expression of the temperature effect might be made in terms of several graphs, each for a different median size of bed material and each similar to figure 17. However, presently available information is inadequate to define such graphs accurately either empirically or theoretically.

In the absence of such detailed and accurate graphs, an oversimplified relationship indicated by the dashed curves on figure 24 is suggested as a practical measure of the effect of water temperature on the discharge of sands in sand-bed streams. It is based on figures 18 and 23 and on general considerations of the effect of viscosity on the discharge of sands. It may be satis-

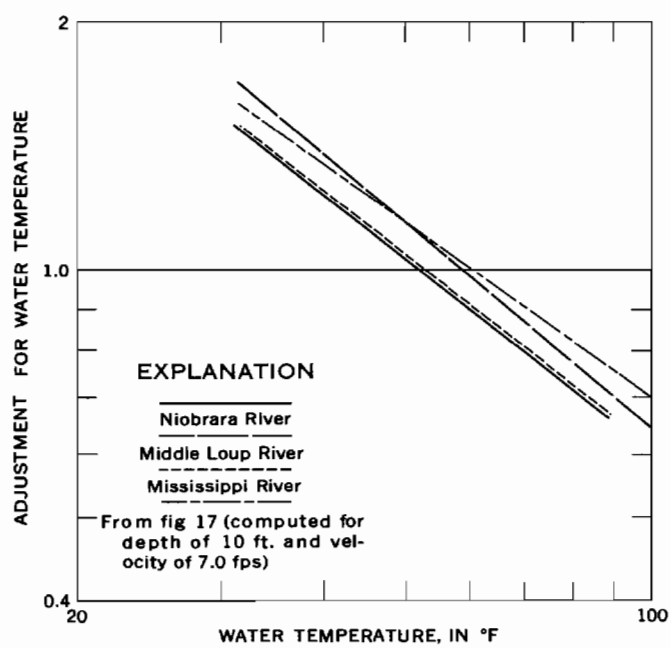

FIGURE 23.—Effect of water temperature on the discharge of sands in four natural streams.

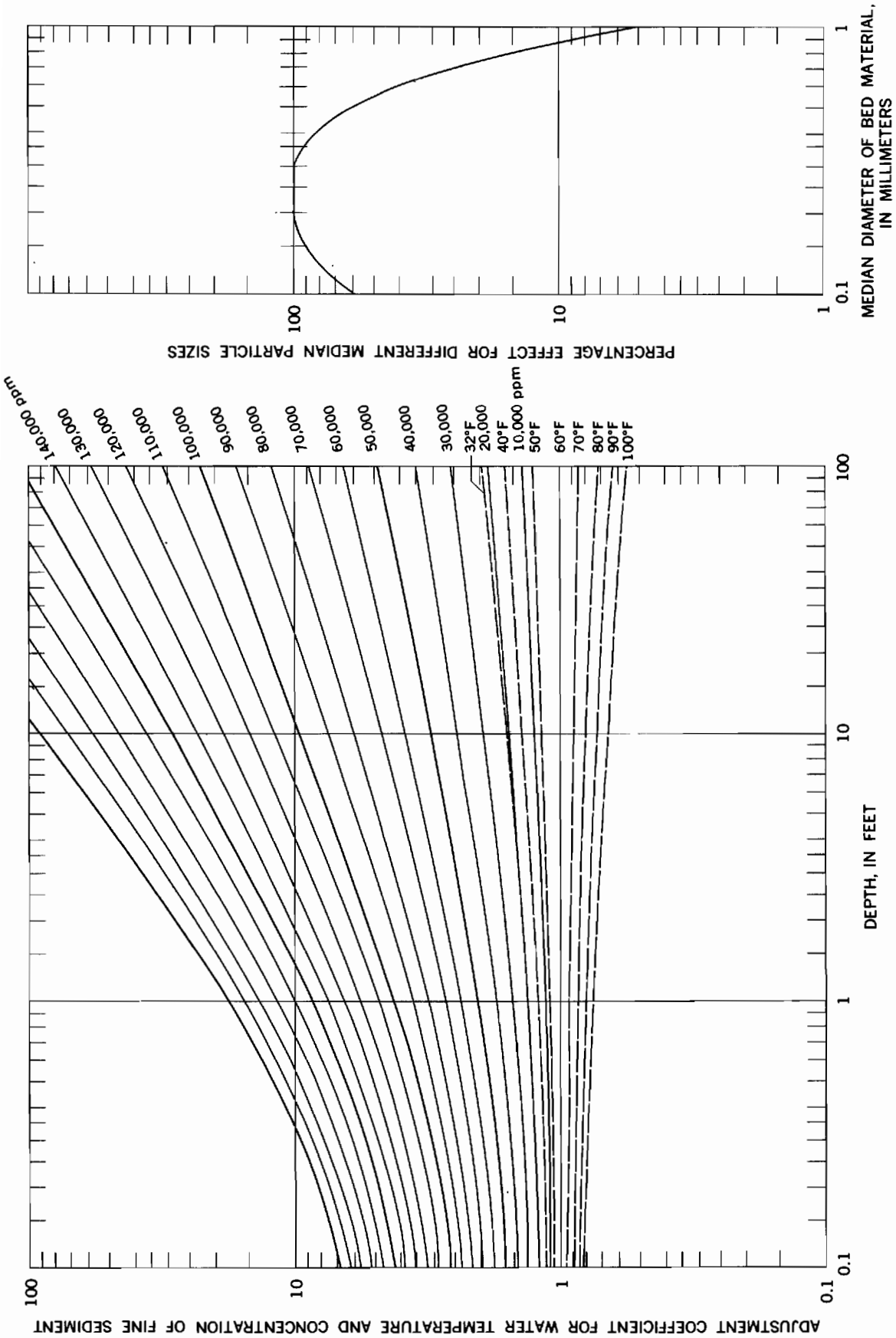

FIGURE 24.—Approximate effect of water temperature and concentration of fine sediment on the relationship of discharge of sands to mean velocity.

factorily accurate for most natural streams whose bed sands have median diameters of 0.20 to 0.40 mm but may be very inaccurate for some other particle sizes, for very low velocities, or for very deep flows. A theoretically accurate temperature correction would be different for each particle size of sand in suspension and presumably cannot be made without a more exact knowledge of the vertical distribution of sediment than is now available. Fortunately, the temperature correction generally is rather small, and a large percentage error in the correction usually causes only a moderate percentage error in discharge of sands.

A curve for making rough estimates of adjustments for different particle sizes is also given on figure 24, but it may be very inexact for some particle sizes. This curve and its usage will be discussed in more detail later.

CONCENTRATION OF FINE SEDIMENT

According to D. B. Simons, E. V. Richardson, and W. L. Haushild (written commun.), a high concentration of fine sediment has an effect on the fall velocity of sands that is explainable in terms of the change that the fine sediment causes in the apparent viscosity of the water-sediment mixture. Their laboratory investigations showed that the median fall diameter of each of three sands decreased as the concentration of suspended fine sediment increased. Roughly four times as high a concentration of kaolin as of "bentonite" was required to decrease the median fall diameter by equal amounts. (However, the fine material that Simons, Richardson, and Haushild called "bentonite" contained about 25 percent of particles coarser than 0.004 mm and about 3 percent coarser than 0.062 mm. In this paper the term "bentonite" when inclosed in quotation marks refers specifically to the fine sediment that they used.) Although these laboratory findings show the great effect that high concentrations of fine sediment have on the discharge of sands, they cannot be used directly to indicate the effect in natural streams.

To some extent the effect of an increase in concentration of fine sediment is equivalent to a decrease of water temperature. Median fall diameters of 0.19 and 0.29 mm were decreased about as much by an increase of 40,000 ppm of "bentonite" as by a change in water temperature from 100° to 32°F. The same general equivalence can be established between the change in concentration of "bentonite" that will cause a given change in apparent viscosity of the water-sediment mixture and the change in water temperature that will cause an equal change in the viscosity of distilled water.

For concentrations of "bentonite" on the order of 50,000 ppm or less, an adjustment cofficient for their effect on the discharge of sands can be estimated on the basis of the indicated equivalent effect of a particular concentration of "bentonite" and a given change in water temperature; that is, if the temperature and the concentration of fine sediment affect the relationship of discharge of sands to mean velocity only through changes in viscosity or apparent viscosity, the adjustment coefficient can be approximated on figure 24 on the basis of the curves already drawn on that figure for water temperature. However, the extension of the graph to high concentrations of "bentonite" would obviously be very questionable if based only on the relationship to water temperature.

A crude idea of the adjustment coefficients for high concentrations of fine sediment can be obtained from information for Rio Puerco near Bernardo, N. Mex., whose sediment concentrations frequently are very high. Usually, the discharge of sands at a given mean velocity, especially a high mean velocity, is far greater (fig. 11) than that for flows over a bed of roughly similar sand in the Rio Grande or other streams. However, discharges of sands may be unusually high (fig. 10) in the Rio Grande at infrequent times when the concentrations of fine sediment are high. The clay carried by the Rio Puerco and the Rio Grande is probably bentonite or similar fine material, but appreciable quantities of the fine sediment are silt. Because 25 percent of the "bentonite" used in the laboratory studies consisted of particles coarser than clay, the fine material of the Rio Puerco and the Rio Grande probably is similar to the "bentonite." The ratios of observed discharges of sands (roughly adjusted to a water temperature of 60°F) for Rio Puerco near Bernardo to discharges of sands from the estimated curve for low concentrations of fine sediment (fig. 11) were plotted on a draft of figure 24. The ratios together with extrapolations from the curves for lower concentrations of fine sediment on figure 24 were used to define the adjustment coefficients for high concentrations of "bentonite" or of the fine sediment that is transported by the Rio Puerco.

Discharges of sands computed from figure 24 average roughly the same as the observed discharges of sands for the Rio Puerco, but the observed discharges tend to be somewhat higher at high flows and lower at low flows. (See fig. 25.) Although the percentage differences between computed and observed discharges of sands are rather large, the adjustments of figure 24 can be used to remove most of the wide departures of the observed discharges of sands in the Rio Puerco from the approximate curve (fig. 11) for

low concentrations of fine sediment. Of course, the adjustments of figure 24 are unlikely to apply as well to other streams as to the Rio Puerco for which they were defined.

Presumably, the adjustment coefficients for water temperature and for concentration of fine sediment can be multiplied together to obtain a single adjustment coefficient for the combined effects of water temperature and concentration of fine sediment on the relationship between discharge of sands and mean velocity.

Adjustment coefficients similar to those on figure 24 will certainly vary with changes in bed-material size, but the relative effects of the different factors that affect the coefficients have not been satisfactorily evaluated. Hence, the right-hand diagram of figure 24 is only a guess at the relative effect of concentration of fines or of water temperature for different median sizes of bed sediment. The effect is stated in percent, and the adjustments on the main diagram of figure 24 are assumed to be for a median size of bed sediment of 0.20 to 0.30 mm and to represent 100 percent. Of course, the adjustment coefficients from the main diagram of figure 24 are not to be directly multiplied by percentages from the right-hand diagram; rather, the adjustment coefficients minus 1.00 are to be multiplied by the percentages. For example, if an adjustment coefficient from the main diagram is 1.50 and the median diameter of the bed sediment is 0.50 mm, the adjustment for the effect of viscosity would be 60 percent of 0.50 or 30 percent. The final adjustment coefficient would be 1.30.

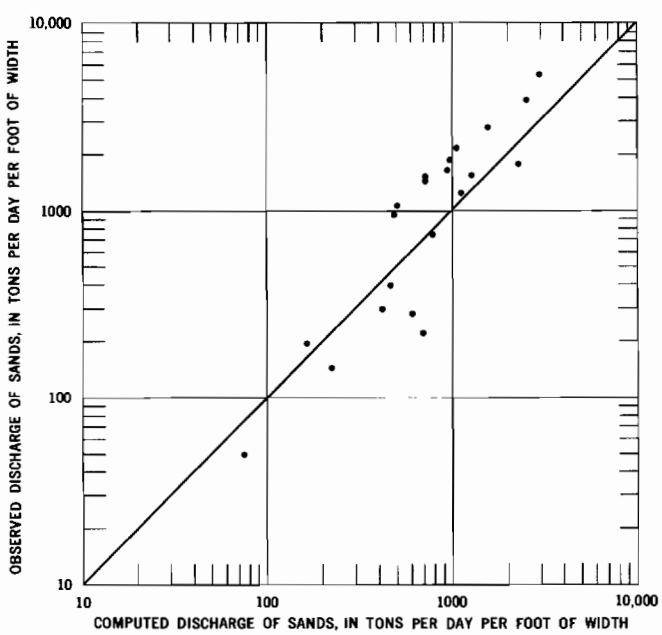

FIGURE 25.—Comparison of computed and observed discharges of sands for Rio Puerco near Bernardo, N. Mex.

If the fine sediment transported by a stream is mostly kaolin, the adjustments of figure 24 might be used as a very rough estimate after the concentrations of fines is divided by four (D. B. Simons, E. V. Richardson, and W. L. Haushild, written commun.). The effects of high concentrations of other fine sediments or of mixtures of fine sediments are scarcely known at all. Also, the chemical character and the concentration of the dissolved solids in the flow probably control to an appreciable degree the effect of any particular high concentration of fine sediment.

At times, the fine sediment may deposit on or in the top layers of the streambed if the concentrations are very high and if the velocities near the bed are relatively low. The presence of fine sediment at the surface of the bed may reduce the discharge of sands. If the free movement of the sand particles at the surface of the bed is known to be inhibited by the fine sediment, the discharge of sands may be relatively low, and the adjustments of figure 24 should not be applied.

The adjustment for the effect of high concentrations of fine sediment on the discharge of sands could be based on the assumption that the fall velocity of a sand particle is the only measure of size that has an appreciable effect on the discharge of the sand. In other words, a sand bed whose median particle size is 0.40 mm might be assumed to have the same discharge of sands for a given condition of flow as a bed whose median particle size was 0.20 mm if the concentration of fine sediment was high enough to reduce the fall velocity of the 0.40 mm sand to that of a 0.20 mm sand. This type of adjustment was not made for two main reasons. First, in shallow flows the discharge of sands seems to increase appreciably if the concentration of fine sediment is greatly increased even for ranges of depth and velocity at which a decrease in particle size of the bed sands apparently causes little increase in the discharge of sands. Second, knowledge of the relationship of the discharge of sands to mean velocity and depth is very inexact for sands that have as low fall velocities as those of 0.25 to 0.40 mm sands when settling through water that contains very high concentrations of fine sediment.

In general, the effect of fine sediment on the relationship between discharge of sands and mean velocity is highly complex and poorly understood. The effect, although sometimes very large in natural streams, has usually been disregarded in the computation of discharges of sands or bed material. The relatively simple adjustments suggested here are

intended to give only a rough idea of (a) the actual relationships and (b) the possibly large effect of concentration of fine sediment on the discharge of sands. Computed discharges of sands that are based on these adjustments for high concentrations of fine sediment are likely to be very inaccurate. However, the comparatively minor adjustments for concentrations of fine sediment lower than perhaps 50,000 ppm may usually be realistic for flows in most natural streams whose bed materials have median diameters of 0.20 to 0.40 mm.

GRAPHS FOR COMPUTING DISCHARGE OF SANDS

The complicated relationships involving major factors that control the discharge of sands in sand-bed streams can probably be better understood from graphs than from mathematical equations. Also, the discharges of sands can be computed more readily from graphs than from equations. Hence, graphs were prepared to indicate the relationships of discharge of sands to the major factors that affect the discharge of sands. The general concept of sediment transportation gives an idea of qualitative relationships to be expressed by the graphs; but until sediment transportation is better understood, the quantitative definition of the graphs must depend mainly on field and laboratory information.

BASIC INFORMATION

A graph such as the one (fig. 19) for a bed sand whose median diameter is 0.30 mm could be defined readily if enough accurate determinations of discharge of sands were available for a particular size of bed sand, for low concentrations of fine sediment, and for one water temperature. Enough determinations would require discharges of sands for a wide range of depths and velocities. In the absence of enough accurate information, a few graphs, each similar to that of figure 19 and each for a different size of bed sand, were approximated from somewhat random and sometimes questionably accurate data. None of the flume or field information was collected specifically for this analysis of the discharge of sands.

Total discharges of bed material over beds of sand were tabulated for many flume investigations, but no attempt was made to investigate all flume studies of bed-material discharge because the relationships were to be defined mainly for field streams. Particularly helpful were published data from flume experiments that were reported by Gilbert (1914), Barton and Lin (1955), Simons, Richardson, and Albertson (1961), and Brooks (1958).

Field data on the discharge of sands for several streams in different parts of the United States were tabulated and studied. Sand discharges for Middle Loup River near Dunning, Nebr. (Hubbell and Matejka, 1959), and for Niobrara River near Cody, Nebr. (Colby and Hembree, 1955), were approximately total discharges. They were based on measurements of bed-material discharge at cross sections where velocity and turbulence were high enough to suspend practically the entire sediment discharge of the stream. Widths and mean velocities were measured at nearby cross sections where the flow was over beds of sand whose median diameter was determined by sampling. For most other sand-bed streams in this study, the total discharges of sands were not so directly determined, and only the measured discharges of sands were known. For these streams, the total discharges of sands usually had been computed in local offices from the modified Einstein procedure (Colby and Hembree, 1955), but some were computed locally or by the writer from measured discharges of sands and from the relationship of unmeasured sediment discharge to mean velocity (Colby, 1957). Thus, total discharges of sands based partly on indirect computations were used for Elkhorn River near Waterloo, Nebr. (Beckman and Furness, 1962), the lower Colorado River (U.S. Bureau of Reclamation, 1958), Pigeon Roost Creek and tributaries in northern Mississippi (unpublished information, Agricultural Research Service, U.S. Dept. of Agriculture, University, Miss.), Mississippi River at St. Louis, Mo., the Cedar, Little Blue, North Loup, and South Loup Rivers in Nebraska, and the Rio Grande and the Rio Puerco in New Mexico (unpublished information, U.S. Geol. Survey, Lincoln, Nebr., or Albuquerque, N. Mex.).

GENERAL METHOD OF ANALYSIS

Graphical analysis of the information on the discharge of sands consisted in eliminating progressively the approximate effect of one variable after another. On the basis of the assumption that discharge of sands is proportional to stream width, all discharges of sands were expressed in tons per day per foot of stream width. These discharges for a single cross section or sometimes for a combination of cross sections were then usually plotted against mean velocity to define a relationship that applied specifically to each section or combination of sections. For some sections, the ratios of observed discharges of sands to the discharges from the average curve were plotted against water temperature to obtain the approximate effect of water temperature (fig. 22, for example) on the relationship between discharge of sands and mean

velocity. After the effect of water temperatures had been defined for a few cross sections (fig. 23), the discharges of sands per foot of width were roughly adjusted to a water temperature of 60°F, if the water temperature were known.

The next major step in the graphical analysis was to define the separate graphs showing the effect of depth (such as fig. 19) on bed sands of different median diameters. Each temperature-adjusted discharge of sands for a median diameter of bed sands between about 0.06 and 0.90 mm was plotted against depth on the graph sheet for the selected median diameter (0.10, 0.20, 0.30, 0.40, 0.60, or 0.80 mm) that was closest to the reported median diameter. The mean velocity was noted beside each plotted point. Some discharges of sand over beds whose median diameter was, for example, about 0.25 mm were plotted on graphs for both the nearest smaller and the nearest larger median diameter. Lines for different mean velocities were drawn on each of the six graphs on the basis of the plotted points and judgment. The general form of the graph of figure 19 was used as a guide. On parts of a graph for which data were insufficient, somewhat contradictory, or entirely lacking, rough estimates were made by comparison among the six graphs or by consideration of the general concept of sediment transportation. Then the six graphs were redrawn as relationships between discharge of sands and mean velocity for each of four depths of flow; the median size of the bed sands was used as a second independent variable. The smoothing of the curves for these relationships, which were first approximations of the graphs of figure 26, removed any large inconsistencies from one median size of bed sand to another. Smoothing of the graphs was continued by replotting alternately in the form of figure 19 and in the form of figure 26 until a reasonably consistent set of curves (fig. 26) was obtained. The form of figure 26 was selected rather than that of figure 19, because the interpolation for the effect of depth can usually be made more conveniently and accurately than the interpolation for the effect of mean velocity.

The derivation of figure 24 for the effect of changing water temperature and for the effect of high concentartion of fine sediment has already been discussed.

The effect of bed configuration on the relationship between mean velocity and discharge of sands may sometimes be large and is likely to be most evident in natural streams at the cross sections that are uniform laterally. One of the dashed curves of figure 9, the curve for Pigeon Roost Creek near Byhalia, Miss., has a flatter slope at mean velocities of 3.0 to 5.0 feet per second than at either lower or higher mean velocities, and the flatter slope coincides with the transition from a dune bed to a plane bed. A distinguishing characteristic of the channel at this station is lateral uniformity, which results in a change of bed configuration at about the same time across most of the channel width. In natural streams, changes in bed configuration usually occur gradually; that is, a change usually affects only a small part or strip of the streambed at first and then spreads over more of the bed. Thus, at any one time only part of the width of the bed is likely to be plane unless the channel is unusually uniform laterally. According to D. B Simons (written commun.), flume experiments have shown considerably lower discharges of sands for a given mean velocity over a plane bed than over an antidune bed. Such a relationship might be explainable, at least in part, by the fact that the turbulence for a given mean velocity, depth, viscosity, and particle size should be less over a plane bed than over a dune or antidune bed. Although no adjustments have been applied in this paper for differences in bed configuration and none may be generally required for most natural streams, the discharge of sands should be expected to be considerably lower over a plane bed than for the same velocities and depths over irregular sand beds.

The available information was inadequate for determining the usually minor effects of such factors as the variations or scattering of particle size, velocity, or depth about the median or mean. Obviously, the variation of particle size of the bed material about the median diameter may sometimes appreciably affect the discharge of sands, perhaps especially at low flows. A nonuniform lateral distribution of velocity and depth may also have a large effect on the discharge of sands at some irregular cross sections. If an appreciable part of a cross section is shallow and has a low velocity as compared with the rest of the section, the discharge of sands may well be computed separately for each of two or more parts of the cross section.

The graphical analysis of the data, which is largely based on judgment and evaluation of complex factors, would not be exactly duplicated if the study were repeated. Obviously, the adequacy and accuracy of the analysis cannot be directly stated but can be crudely indicated by comparison of observed discharges of sands with discharges computed from the results of the graphical analysis. This comparison and an evaluation will be made as a part of the discussion of probable accuracy of sand discharges that are determined from the final graphs.

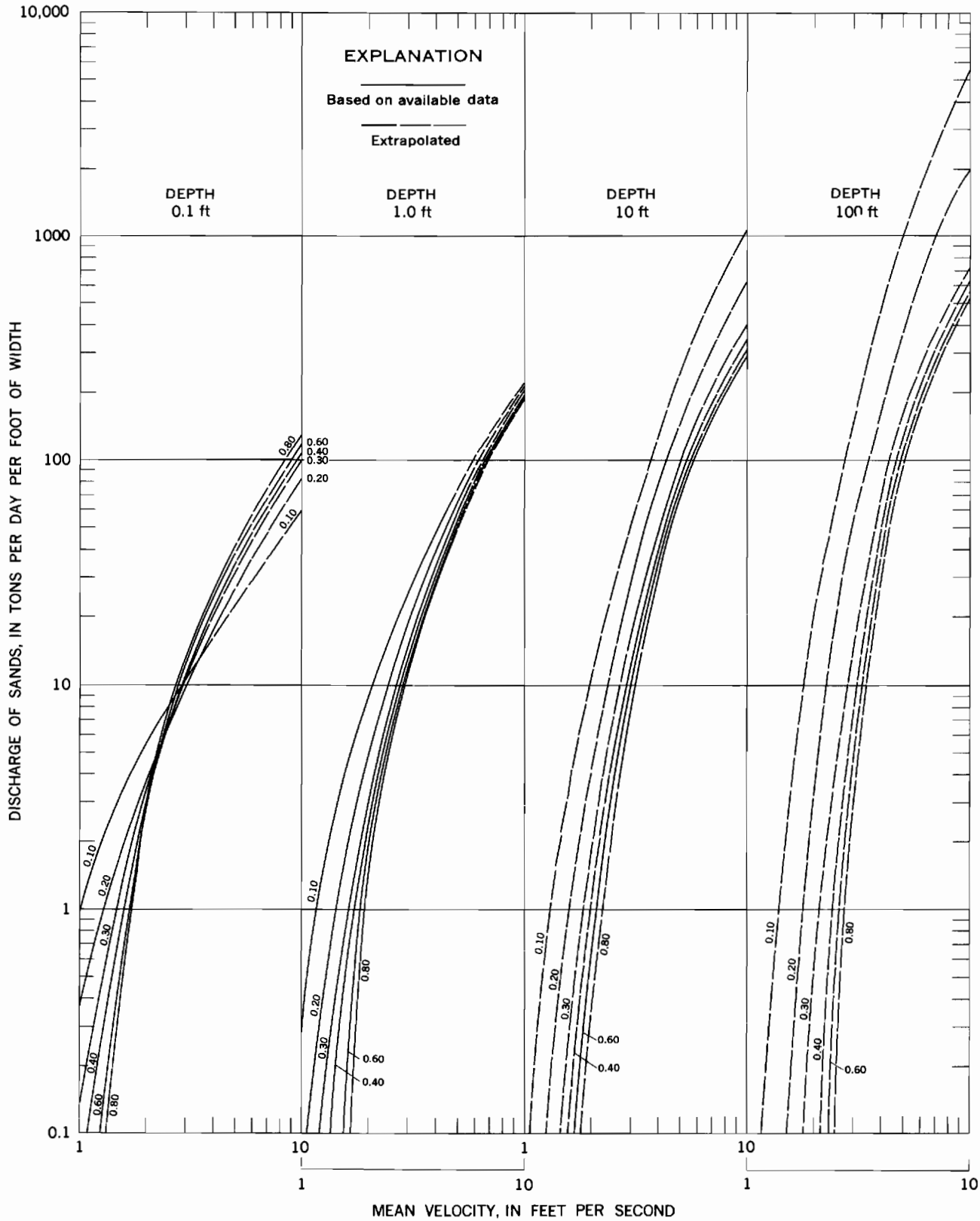

FIGURE 26.—Relationship of discharge of sands to mean velocity for six median sizes of bed sands, four depths of flow, and a water temperature of 60° F.

DETERMINING THE DISCHARGES OF SANDS FROM THE GRAPHS

The discharge of sands in a sand-bed stream can be computed from the empirical graphs according to one or more of three methods. The choice of a method depends mainly on the number of variables that need to be considered in the computation. If the velocity, depth, bed-material sizes, water temperature, and concentration of fine sediment are within the general range for which the curves of figure 13 were defined, the effect of variables other than mean velocity may perhaps be disregarded, and the discharge of sands per foot of width may be taken with reasonable accuracy from one of the curves of figure 13. However, if the depth effect is likely to be appreciable, the discharge of sands should be determined from figure 26. If concentrations of fine sediment are high and water temperatures differ considerably from 60°F, the discharge of sands from figure 26 should be adjusted according to figure 24. Examples show the computation of the discharge of sands according to each of the three methods.

First method—discharge of sands based on figure 13

Selected data for example 1:

Mean velocity	ft per sec	2. 70
Depth	ft	3. 5
Median size of bed sediment	mm	0. 37
Water temperature	° F	65
Concentration of fine sediment	ppm	1, 500

Summary of the computations: Because the size of bed material is about that for Pigeon Roost Creek, the discharge of sands per foot of stream width can be taken directly as 11 tons per day per foot of width from the curve for Pigeon Roost Creek on figure 13. (If computed by the second method, the result is about 8.5 tons per day per foot.)

Second method—discharge of sands based on figure 26

Selected data for example 2:

Mean velocity	ft per sec	6. 2
Depth	ft	15. 5
Median size of bed sediment	mm	0. 26
Water temperature	° F	57
Concentration of fine sediment	ppm	650

Summary of the computations: From figure 26 the indicated discharges of sands are by interpolation for median size about 188 and 400 tons per day per foot for depths of 10 and 100 feet, respectively. Interpolation for the depth of 15.5 feet can be made by guess, by use of a simple diagram, or with a straightedge on a sheet of log-log paper to obtain 210 tons per day per foot. This discharge of sands can be quickly checked against a discharge of 220 tons per day per foot that might be picked directly from the curve (fig. 13) for the Mississippi River at St. Louis, Mo. Thus, the first method can usually be used as an easy check for major errors in computations by the second method.

Third method—discharge of sands based on figures 24 and 26

Selected data for example 3:

Mean velocity	ft per sec	6. 5
Depth	ft	4. 8
Median size of bed sediment	mm	0. 43
Water temperature	° F	75
Concentration of fine sediment, mostly bentonite	ppm	33, 000

Summary of the computations: From figure 26 the discharges of sands are about 92 and 150 tons per day per foot of width for depths of 1.0 and 10 feet, respectively. Hence, about 130 tons per day per foot of width can be interpolated for the depth of 4.8 feet. The adjustment coefficient from figure 24 for 75°F and a depth of 4.8 feet is 0.86 for a median diameter of 0.20 or 0.30 mm. Also, the adjustment coefficient for 33,000 ppm of fine sediment, mostly bentonite, is 1.92 for a median diameter of 0.20 to 0.30 mm, and the total adjustment coefficient is 1.92×0.86 or 1.65. According to the right-hand graph of figure 24, the effect of a change in viscosity or apparent viscosity is only 78 percent as large for the median diameter of 0.43 mm as for a median diameter of 0.20 or 0.30 mm. Therefore, 78 percent of $(1.65-1.00)$ or 0.51 is added to 1.00 to obtain the estimated adjustment coefficient for the median diameter of 0.43 mm. The 130 tons per day per foot multiplied by 1.51 gives 196 tons per day per foot, which could well be rounded to 200 tons per day per foot because the discharge of sands ordinarily should not be determined to more than two significant figures. The discharge of sands from the curve of figure 13 for Pigeon Roost Creek is about 150 tons per day per foot.

PROBABLE ACCURACY OF THE GRAPHS

Three phases of the probable accuracy of the graphs for computing the discharge of sands need consideration. In order of their discussion, these phases are the experimental errors inherent in the basic field and laboratory information, the accuracy of the definition of the graphs for the data that were included in the study, and the applicability of the graphs to discharges of sands for streams that were not included in the study.

EXPERIMENTAL ERRORS IN BASIC INFORMATION

A major difficulty in an evaluation of the probable accuracy of the graphs is that the amount of experimental error in individual determinations of discharge of sands is seldom known satisfactorily. However, the fact of appreciable experimental error can be easily established. For example, rather wide variations of concentration of suspended sediment (mostly but not all sands) were measured at a turbulence flume in Middle Loup River at Dunning, Nebr., by Benedict, Albertson, and Matejka (1955). Also, C. F. Nordin and J. K. Culbertson (written commun.) reported two sets of suspended-sediment samples at about the same times and at nearly steady flow at each of seven sections in Rio Grande near Barnalillo, N. Mex.; these samples, although probably collected more care-

fully than most samples, showed considerable percentage differences in the concentrations of sands. To the nearest whole percent, the differences between the two concentrations of silt plus clay for a cross section ranged from 0 to 8 percent and averaged 3 percent for the seven cross sections. The differences between the two concentrations of suspended sands ranged from 3 to 33 percent and averaged 20 percent. Such differences as these (which probably are reasonably typical) between individual determinations of average concentration of suspended sands at a cross section indicate proportional errors in the measured discharges of the suspended sands. (Actually, these differences are, of course, measures of consistency rather than of absolute accuracy.) In addition to differences in carefully determined discharges of sands at a cross section, wide differences in measured discharges of sands may occasionally result from the collection in a suspended-sediment sample of sands from the bed layer or the streambed unless the excess sand is noted immediately and the sampling is repeated. Most experienced field men consider that sampled concentrations of suspended sands are likely to be much too large at times but are unlikely to be much too small. Usually several individual determinations of the discharge of sands may be required to establish an accurate average discharge of sands for a particular time and flow. Even in a flume experiment for which conditions of flow and sediment discharge are likely to be more constant than in field investigations, the sampling of sands may have to be continued over a period of a few hours in order to establish an accurate average discharge of sands.

Because the average discharge of sands during a period of steady flow is the discharge that should correlate with characteristics of the flow and the bed sand, departures from this average are considered to be experimental errors. Thus, the experimental error is a measure of the difference between an experimentally determined or computed discharge of sands and the average discharge of sands in the same flow at a steady state. It is not the difference between the experimentally determined or computed discharge of sands and the actual instantaneous discharge of sands at that time. Therefore, because of short-time fluctuations in the discharge of sands, the experimental error may be large even though the determination of the instantaneous discharge of sands was accurate.

At many of the high flows and sometimes at rather low flows per foot of width, the mean velocities used in this study were determined from bridges where the sand bed is affected by local scour and where piers may cause turbulence that is relatively high as compared to the mean velocity. In general, the discharges of sands per foot of width at bridge sections are likely to be larger than they would be for the same velocities in representative reaches of channel away from the bridges.

Lateral distributions of depth and velocity are sometimes so far from uniform that the reported means are not good measures of the discharge of sands. However, inaccuracies that are caused in the relationships of discharge of sands to mean velocity and to depth by poor lateral distributions are more strictly failures in analysis of the data than experimental errors.

If the slope of the water surface is used as a parameter of the discharge of sands, considerable experimental error should be expected in the determinations of slope, unless the total fall through the reach is large enough to be determined accurately and unless several observations of the slope are made and averaged.

Total discharges of sands in field streams are generally measurable only at very constricted sections or at structures that have been designed for the determination of the total sand discharges of the stream. The widths, depths, and velocities at such places are not useful measures of the discharge of sands in sand-bed streams. If useful relationships are to be obtained, the discharges of sands at these places must be correlated with widths, depths, and velocities at nearby reaches of channel where the streambed is mostly cohesionless sand. Obviously, temporary net scour or net fill and the short-time fluctuations in discharge of sands even at constant flow make uncertain any individual determinations of total discharge of sands in terms of conditions of flow at another cross section.

In most streams, only part of the discharge of sands is measured, and the rest is computed somewhat indirectly. The computation of part of the discharge of sands introduces error because the procedures for computing the unmeasured discharges of sands are by no means exact and because some of the procedures depend on the measured concentrations of sand, which are themselves inexact. The probable inaccuracy of the computation of the discharge of unmeasured sands is known only roughly.

DATA INCLUDED IN THE STUDY

The many and complicated steps involved in the graphical analysis cannot readily be reproduced or explained in detail in this paper and were partly based on judgment. Hence, the probable accuracy of the graphs on figures 24 and 26 is difficult to

evaluate or to state. A practical measure of the probable accuracy for data that were included in the study can be obtained by comparing the discharges of sands computed from figures 24 and 26 with the original observed discharges of sands. (The term "observed discharges" is used for simplicity even though for many field streams the "observed discharges" of sands are partly based on indirect computations of the unmeasured discharges of sands.) Because many observations were used in the graphical analysis, an arbitrary selection was made for the test of accuracy. Within each set of field or flume data, the first, sixth, eleventh, sixteenth, etc., determinations were selected. Thus, at least one observation was included from each set of data.

Although the difference between the computed and the observed discharge of sands sometimes is large, especially for low velocities and shallow depths, the general relationship for field sand-bed streams is reasonably good. (See fig. 27.) Of about 200 indi-

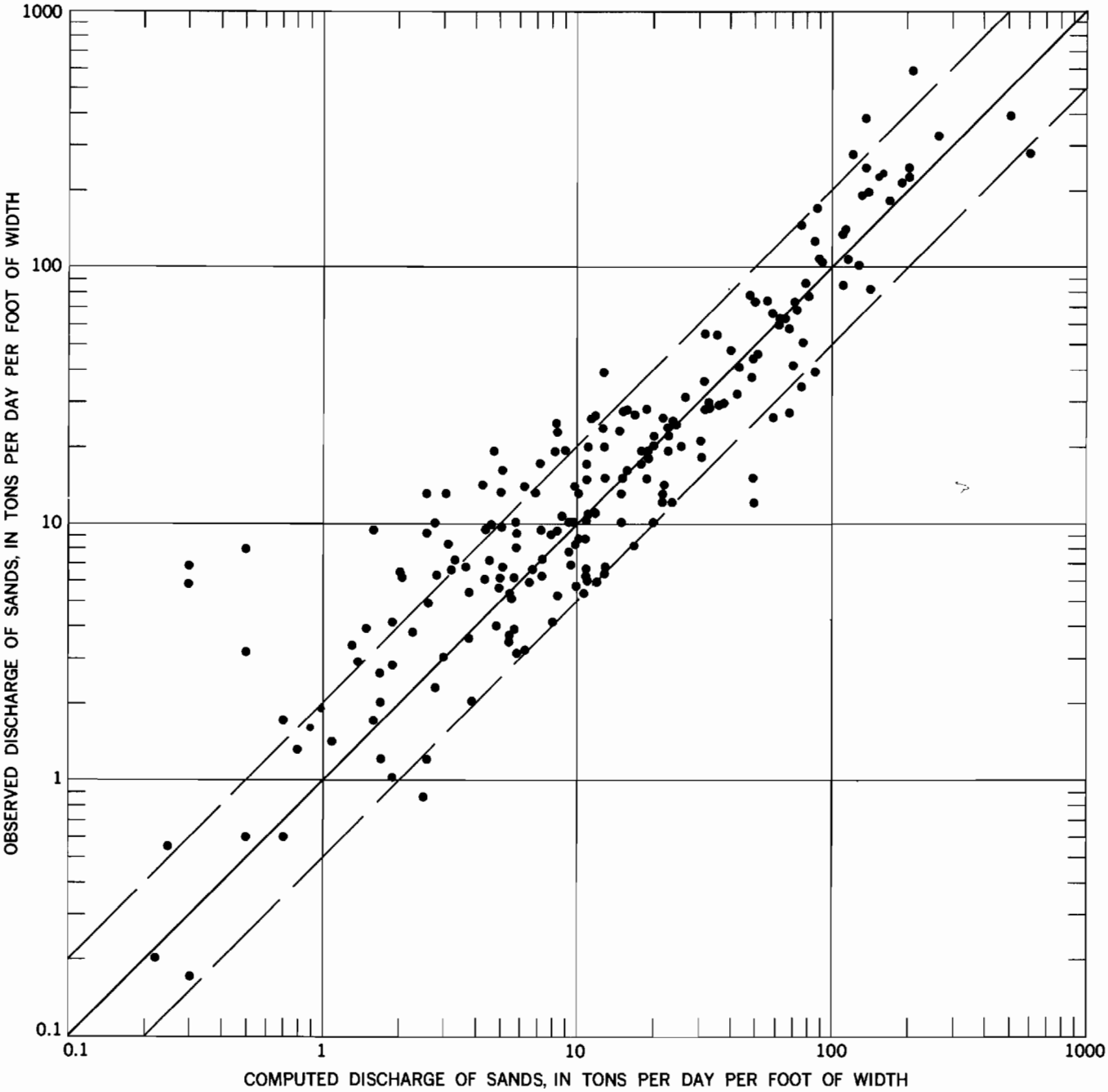

FIGURE 27.—Comparison of computed and observed discharges of sands for natural streams that were included in the study.

vidual comparisons, about three-fourths of the observed discharges of sands are within limits that are 100 percent larger and 50 percent smaller than the computed discharges of sands. The widest percentage differences and proportionately the fewest close agreements are for shallow depths and low mean velocities. Usually in field sand-bed streams the lateral distributions of depth and velocity are more uneven for shallow flows, especially perhaps in very wide channels, than for deep flows. Also, at low velocities the percentage effects of small changes in particle size or in mean velocity may be large. For example, at a depth of 1 foot and for a median particle size of 0.30 mm, a change in mean velocity from 1.50 to 1.70 feet per second slightly more than doubles the discharge of sands, according to figure 26. The differences in tonnage of the computed and the observed discharges of sands at these low velocities and shallow depths are usually insignificant in terms of the annual discharge of sands for creeks and rivers even though the percentage difference is large.

At low depths and mean velocities, a somewhat better average agreement between computed and observed discharges of sands in natural streams could be obtained by revising the curves of figures 26, but such a change is probably not worthwhile until the reasons for the differences at low flows are better understood. Perhaps some differences are due to nonuniformity of the cross sections and could be partly removed by subdividing the cross sections into parts and then computing the discharge of sands separately for each of the parts. Disagreement may also be caused by different bed configurations at the same mean velocity.

The agreement between the computed and the observed discharges of sands is a little better for flows over sand beds in flumes (fig. 28) than in natural streams. Any change in figure 26 that would make the computed discharges of sands agree better with the observed discharges of sands from 1 to 10 tons per day per foot of width in natural streams would make the agreement poorer for the discharges of sands in flumes. Obviously, separate graphs like those of figure 26 could be prepared for natural streams and for flumes, or an arbitrary adjustment could be applied to the computed discharges of sands for low flows in natural streams. However, such procedures may not be desirable at this time.

STREAM REACHES AND FLUME INVESTIGATIONS NOT INCLUDED IN THE STUDY

Of course, really significant tests of the accuracy of the derived graphs should be based on the total discharge of sands at stream reaches for which information was not used to define the graphs. Some unpublished information for such reaches of natural streams was available in the files of the Geological Survey at Lincoln, Nebr., and Worland, Wyo. Also, two computations of total discharges of sands at individual verticals in the Missouri River at Omaha, Nebr., were furnished by Lloyd C. Fowler, U.S. Army Corps of Engineers, Omaha, Nebr. The observed discharges of sands in natural streams were determined by the modified Einstein procedure. The flume investigations by the U.S. Waterways Experiment Station (1935) were not used to define the graphs, so about every fifth run that had an observed discharge of sands greater than 0.1 ton per day per foot of width was selected as a check on the probable accuracy of the graphs for flume flows.

The comparison between the computed discharges of sands and the observed discharges of sands for cross sections that were not used to define the graphs is generally good for the cross sections that are relatively uniform and moderately deep and that have dependable basic information. The comparison was relatively much poorer for some of the other cross sections. (See fig. 29.) The computed and observed discharges of sands agree rather closely for the individual verticals of Missouri River at Omaha and for the cross sections of Niobrara River near Valentine, Nebr., Snake River near Burge, Nebr., and Bighorn River at Thermopolis, Wyo. The Popo Agie River near Riverton, Wyo., is not a sand-bed stream, although the beds of many pools are mostly sand. Also, the samples on which the size of the bed material for the Popo Agie River is based were collected more than a year after the dates for which the discharges of sands were observed. Probably because of the incomplete sand cover, the observed discharges of sands are somewhat lower than 50 percent of the computed discharges of sands. In general, shallow cross sections, such as those of Fivemile, Muddy, and Badwater Creeks and Pavillion drain, have considerably greater observed discharges of sands than computed discharges of sands. Beaver Creek near Arapahoe, Wyo., although its flows were rather shallow, does have a close relationship between observed and computed discharges of sands. The cross sections of Badwater Creek at Bonneville, Wyo., in addition to being shallow, are nonuniform laterally at low flow and have very high concentrations of fine sediment. In general, the graphs of figures 24 and 26 seem to represent the discharges of sands as well for these stream reaches that were not included in their definition as for the stream reaches that were included.

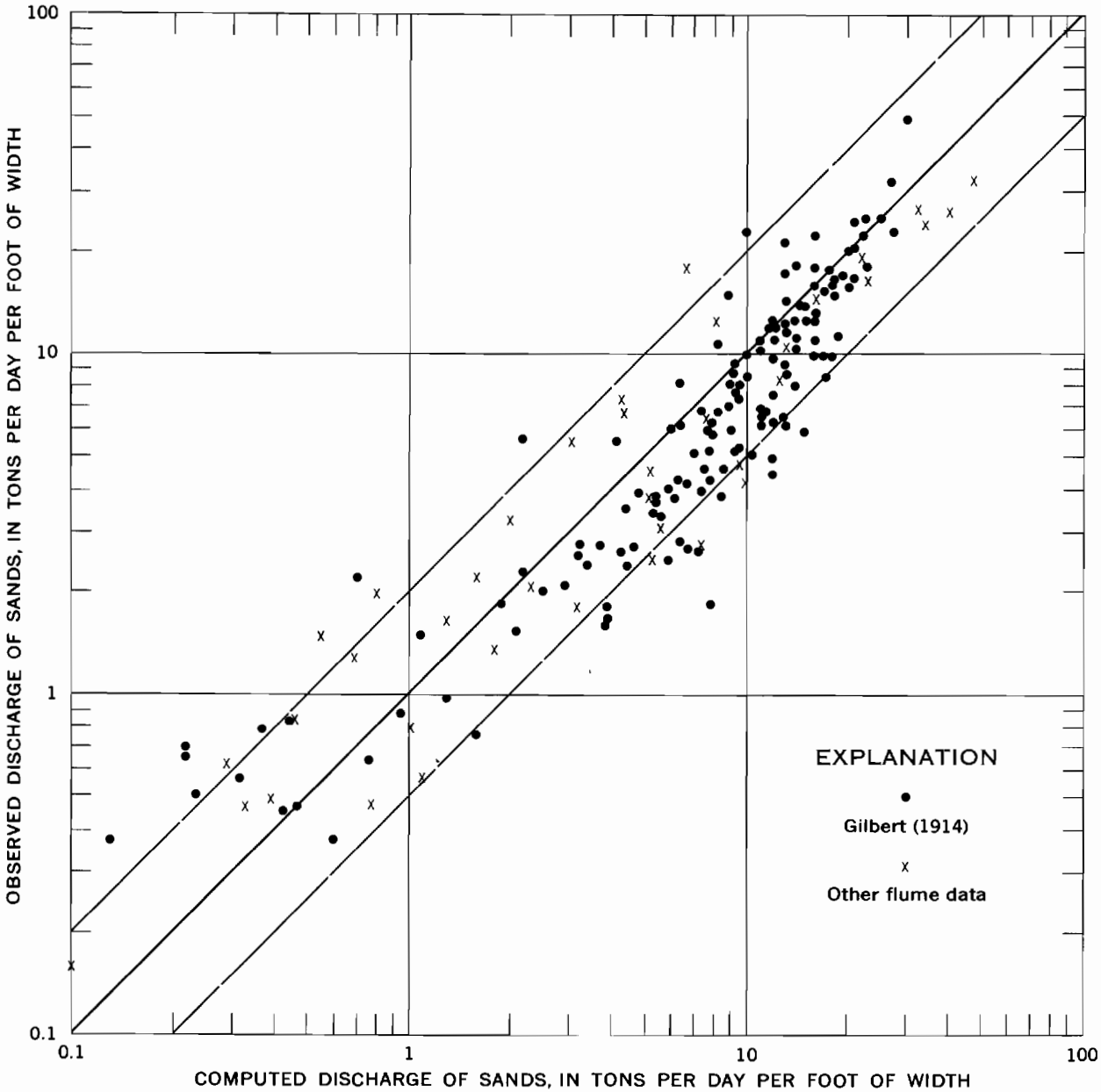

FIGURE 28.—Comparison of computed and observed discharges of sands for flume data that were included in the study.

For flume investigations, the graphs of figures 24 and 26 do not apply as well to the discharges of sands that were reported by the U.S. Waterways Experiment Station (fig. 30) as they did to the discharges of sands that were used to define the graphs. Perhaps the observed discharges of sands from the Waterways Experiment Station studies were lower than those from other flume studies because of relatively more coarse particles in several of their sands. The inconsistencies may be due, at least partly, to differences in bed configuration at about the same shallow depths and velocities. Sand 6 (U.S. Waterways Experiment Station, 1935), for example, had very little sand that was appreciably finer than the median particle size but had considerable sand that was considerably coarser than the median particle size. Observed discharges of sand 6 were very low as compared with the computed discharges of sands.

On the basis of figures 27 through 30, the graphs of figures 24 and 26 probably provide a means of computing fairly consistent discharges of sands at a particular cross section. However, especially for shallow flows and low velocities, the effects of some factors that vary from one stream or flume to another or from one sand to another are not yet satisfactorily represented by the graphs. Although the graphs

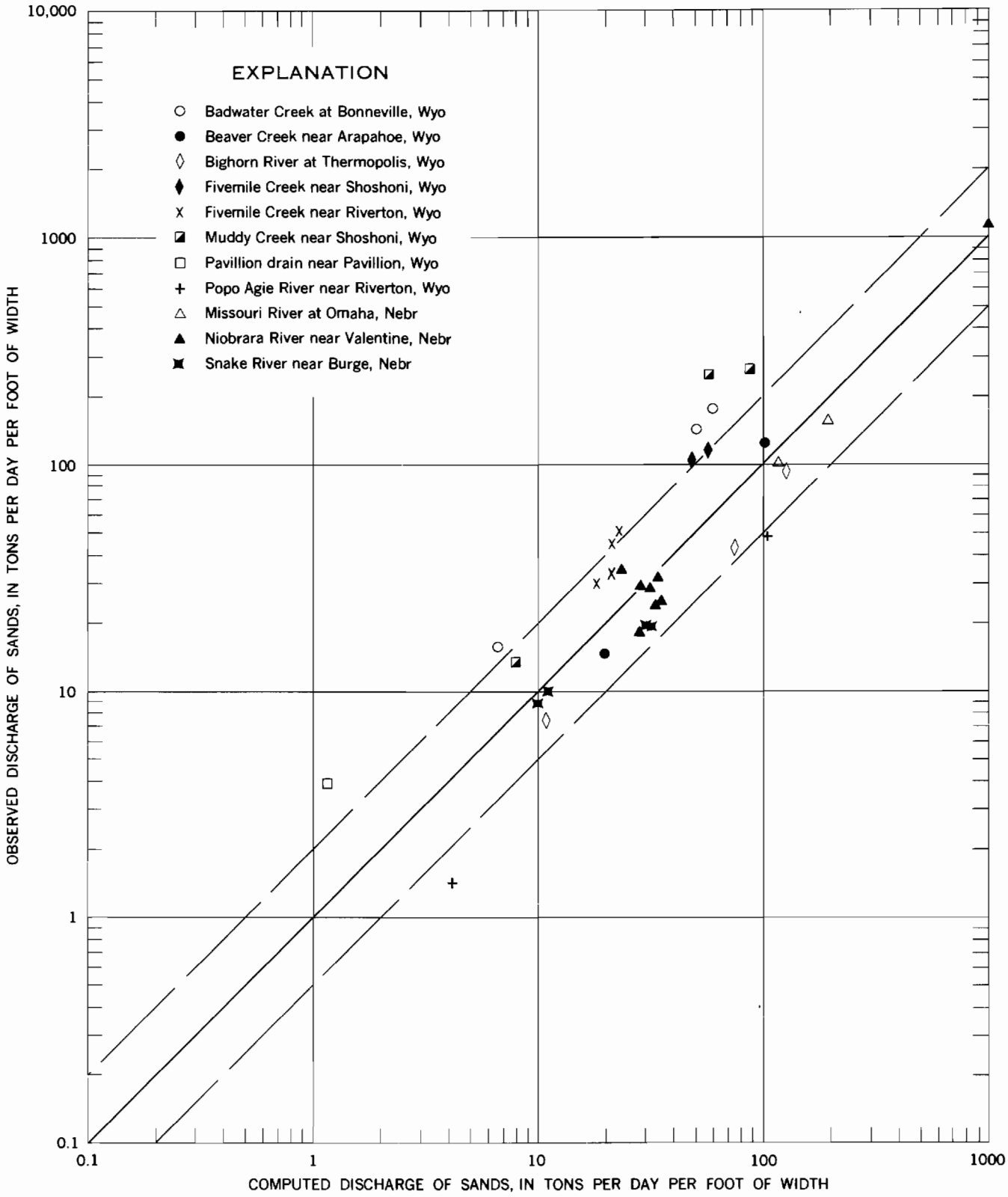

FIGURE 29.—Comparison of computed and observed discharges of sands for stream reaches that were not included in the study.

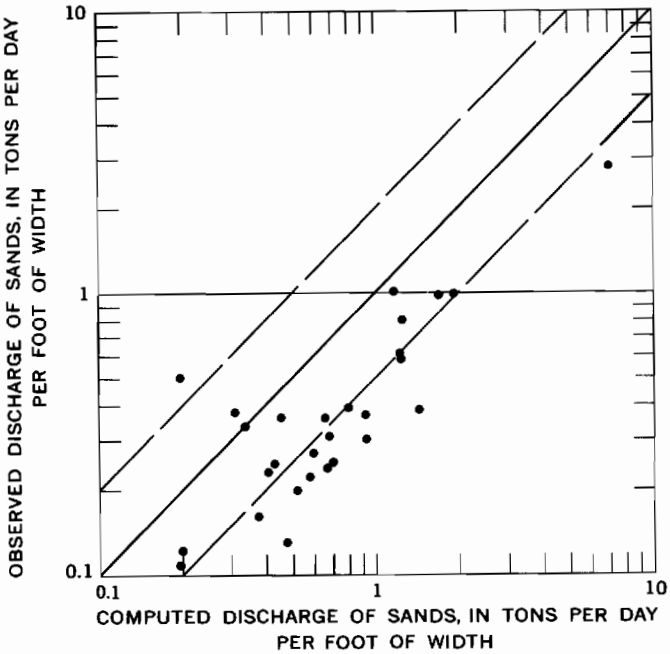

FIGURE 30.—Comparison of computed and observed discharges of sands for flume data (U.S. Waterways Experiment Station, 1935) that were not included in the study.

cannot be used to obtain highly accurate discharges of sands in sand-bed streams, they provide a quick and reasonably accurate procedure for computing the average discharge of sands for many sand-bed streams.

The graphs are applicable only to sand-bed streams that do not have unusually rough confining walls or distinct pools and riffles (except, perhaps, at very low flow). Even though the bed of a stream is composed of cohesionless sand, the graphical relationships may not apply well at narrow sections that are confined between rough rock walls. Rough rock walls, such as those at the cableway on the Colorado River near Grand Canyon, Ariz., may cause considerably more turbulence than would normally exist for a combination of velocity and depth; as was previously pointed out, the vertical distribution of the sands is determined by the turbulence, which seems to be at least partly dependent on the total shear rather than on the shear with respect to the sediment particles.

APPLICATIONS

The empirically defined graphs have two obvious general uses. One is to show the effect on the discharge of sands of a change in any major variable. The other is to compute the approximate discharge of sands in flows over sand beds.

In addition to the two general uses, more specialized applications of the graphs also can be made. For example, the average relationship at a particular cross section between discharge of sands and mean velocity for a water temperature of about 60°F can be readily approximated from the graphs of figure 26 if the median diameter of the bed sands and the widths, depths, and mean velocities are known for one or two low, medium, and high streamflows.

The change is velocity from a wide to a narrow cross section along a reach of stable channel can also be approximated on the basis of continuity of flow and of discharge of sands. Because a large change in discharge of sands usually accompanies a small change in mean velocity, the mean velocity must change comparatively little from one cross section to another along a stable reach of channel. This relative constancy of mean velocity has sometimes been noted in terms of a tendency for the area of cross section to remain about constant along a reach of sand-bed channel at steady flow. According to tht curves of figure 13, an increase of 100 percent in width might be compensated (a constant discharge of sands might be maintained from one cross section to the other) by a 25– or 30–percent decrease in mean velocity.

The large changes in discharge of sands for small changes in mean velocity help to explain channel configuration. For example, a particular flow per foot of width can occur at a wide range of depths and mean velocities; but, if that flow transports a given discharge of sands per foot of width, the velocity and depth become fixed within narrow limits for a given water temperature and for low concentrations of fine sediment. In broad terms, a particular discharge of sands per foot of width largely determines the mean velocity that must exist in a stable reach of a sand-bed stream, which has a particular size of bed sands. The mean velocity and the rate of flow per foot of width largely determine the depth of flow and hence the slope if the resistance to flow is known. (However, within certain ranges of depth, velocity, particle size, and water temperature, the resistance to flow may change widely and be somewhat indeterminate.)

In a channel reach that is not at equilibrium, the probable rate of net scour or net fill may be approximated from the graphs, provided that the flow-duration curves, the channel widths, and the velocities for given rates of streamflow can be predicted for each end of the reach.

An understanding of the effect of a few major factors on the discharge of sands may aid in understanding the effect of other factors. For example, the effect of high concentrations of fine sediment on the discharge of sands in natural streams was not

generally recognized for many years because the relationship of the discharge of sands per foot of width to mean velocity had not been defined for low concentrations of fine sediment. As soon as the dominant relationship to mean velocity was known, the effect of the high concentrations of fine sediment became obvious for such a stream as the Rio Puerco.

DEFICIENCIES OF BASIC INFORMATION

Because of the number of variables, the wide ranges in value of the variables, and the complex interrelationships among the variables, the empirical determination of the major graphs in this paper should have been based on a large amount of accurate information that was collected specifically for this study. Unfortunately, the available field and flume data were all collected for purposes other than this study and are deficient in coverage of the ranges of the variables, in applicability to the specific relationships to be defined, and to some extent in accuracy. Lack of accuracy was due partly to the necessity for computing the unmeasured part of the discharge of sands for most sediment stations but probably more to differences between measured discharge of sands and the correct time average for the cross section when samples were collected. A correct time average of discharge of sands is an average over a long enough period of time to eliminate both random and short-term cyclical variations in discharge of sands.

Adequate field information for a particular median diameter of bed sand should cover at least the usual range and combinations of depths and velocities in sand-bed streams in enough detail to define a graph like that of figure 19. The information is definitely inadequate if significant parts of such a figure must be based on estimates, interpolations, or extrapolations as was necessary to some extent for all the different median sizes of bed sands. For most particle sizes, available information is inadequate or entirely lacking especially for high velocities and for deep flows. Therefore, discharges of sands for Mississippi River at St. Louis are particularly helpful because they are for deep flows and some are for moderately high velocities.

Field information on total discharges of sands is wholly inadequate to define a graph like that of figure 19 for median diameters of bed sands smaller than 0.10 mm or larger than 0.50 mm for most combinations of depth and mean velocity.

The effect of water temperature on the relationship of discharge of sands to mean velocity has been defined empirically for only a few streams and then only for the usual combinations of depths and mean velocity in those streams. The somewhat similar but sometimes much larger effect of concentration of fine sediment on the discharge of sands is based mostly on a few laboratory studies and on the discharges of sands in Rio Puerco near Bernardo. More experimental data on the effect of water temperature and of high concentrations of fine sediment in field streams are badly needed.

Information applicable and sufficiently accurate to define possible effects of such usually minor factors as the lateral variation of velocity at a given mean velocity is almost entirely lacking. Also, the effects of deviation of sizes of the bed sands from the median size have been obscured by the scarcity of precise and pertinent information. The bed configuration is seldom known from available information for field streams; hence, the effect of bed configuration on the relationship between discharge of sands and mean velocity is difficult to establish.

The empirical determination of the relationships of discharges of sands in sand-bed streams to the major factors that control such discharges could be made more exact and dependable by a planned program for obtaining the needed coverage and accuracy of field information. Such a program should include at least the following procedures:

1. Determine the probable accuracy of the basic information on the discharge of sands in natural streams either by studying the accuracy of sediment discharges in general or by repeating individual field observations, particularly of concentration of sands, often enough to obtain a practical measure of the consistency of measured discharges of sands.
2. Determine by measurement the total discharges of sands in streams other than the Niobrara and the Middle Loup Rivers; that is, obtain more determinations of the discharge of sands at cross sections where all or nearly all the sands are in suspension and can be sampled and then relate these total discharges of sands to characteristics of the flow and the bed sands at nearby cross sections where the stream has a sand bed. These other streams should preferably have other bed-material sizes and combinations of depth and mean velocity than the Niobrara and the Middle Loup Rivers.
3. Use the total discharges of sands from procedure 2 to confirm or to revise the present methods of computation so that discharges of unmeasured sands can be determined with acceptable accuracy in any sand-bed stream for which suitable information on flow and measured sediment discharge is available.

4. Use the total discharges of sands from procedure 2 as part of the basis for determining or improving individual graphs similar to the graph of figure 19 for bed sands whose median diameters are 0.10, 0.20, 0.30, 0.40, 0.60, 0.80, and 1.00 mm.
5. Complete the definition of these graphs. Obtain measured discharges of sands for particle sizes, depths, and mean velocities for which total discharges of sands could not be measured; add to the measured discharges the computed unmeasured discharges of sands; and define the graphs from the computed total discharges of sands.
6. Obtain accurate determinations of discharges of total sands (either measured or partly unmeasured) at the same cross sections and flows but at widely different water temperatures to define the effect of water temperature through the range of usual combinations of depth, velocity, and bed-material size.
7. Investigate in the laboratory the fall velocities of sand grains in water that contains high concentrations of different combinations of clays and silts of usual mineralogical compositions. Also, study the effect of changes in the dissolved solids in the flow on the effect of high concentrations of different fine sediments on the discharge of sands.
8. Check the effect of fine sediments as indicated by the laboratory studies against the apparent effect on the discharge of sands in natural streams.

After the major effects have been clearly defined, develop a program for the determination of the effects of usually minor variables on the discharge of sands. Presumably, such a program may require the careful control and evaluation of all major factors in order that relatively minor effects can be discerned.

CONCLUSIONS

The discharge of sands in a sand-bed stream depends on many variables whose effects are complicated and interrelated. Hence, no precise relationship between discharge of sands and characterics of the flow and sediment can be expected.

Flume investigations can provide much helpful information on sediment transportation; but, until scale effects are understood more completely, flume investigations of the discharge of sands are not model studies of the discharge of sands in field streams.

The use of discharge of sands per foot of width as a measure of the rate of transportation of sands is based directly on the assumption that, if other factors remain constant, the discharge of sands is in proportion to stream width. Although this assumption is not precisely correct, it seemed to afford a reasonable basis for comparison of sand discharges in streams of greatly different widths.

Concentration of sands is a poor basis for comparison of discharge of sands with the factors that control that discharge in natural streams because the concentration varies greatly with depth of flow. However, for a narrow range of depths in a set of flume experiments, concentration of sands may be a fairly satisfactory measure of transportation of sands.

For the velocities and depths at which most of the sand is transported in many natural streams, the discharge of sands per foot of width does not vary greatly with changes in the depth of flow.

Shear, which has been widely used as a measure of the discharge of sediment, is sometimes a poor measure. When the roughness of the channel changes, the discharge of the coarse sediment generally is more closely related to the mean velocity than to the shear. However, the vertical distribution of sands may vary more nearly with total shear than with shear velocity with respect to the particles.

When discharge of sands per foot of width at one cross section is plotted against mean velocity, a reasonably good relationship is usually defined for that cross section, unless the concentration of fine sediment is high and variable.

The relationships between discharge of sands per foot of width and mean velocity may be much the same for one cross section as for another, provided that differences in depth, water temperature, concentration of fine sediment, or size of bed sand are not excessively large. The agreement in relationships indicates that mean velocity is a dominant measure of the discharge of sands per foot of width in many sand-bed streams.

The relationship to mean velocity implies that mean velocity must be relatively constant from one cross section to another along a reach of sand-bed channel. If mean velocity were to change appreciably, the discharge of sands per foot of width would change much more than the mean velocity. Such a velocity change would require very large percentage differences in width. Otherwise more sands would be discharged at one section that the other, and the channel would aggrade or degrade.

Shear velocity computed from mean velocity correlates with discharge of sands about as well as mean velocity. The effect of depth on the relationship between discharge of sands and shear velocity computed from mean velocity is, however, somewhat different than on the relationship between discharge

of sands and mean velocity. The effect of depth indicates that for flume investigations shear velocity computed from mean velocity may be a more convenient parameter (because of a smaller and more consistent depth effect) than mean velocity and that for field streams mean velocity is the more convenient parameter because of the smaller effect of depth for many combinations of depth and mean velocity.

Stream power, the product of shear and mean velocity, may be a good measure of discharge of sands when roughness is about constant, but it is unsatisfactory for variable roughness.

The effect of depth on the relationships between discharge of sands per foot of width and mean velocity, shear, shear velocity computed from mean velocity, or stream power is complex and variable and may be large. The effect of depth is usually easier to apply to the relationship of discharge of sands to mean velocity or to shear velocity computed from mean velocity than to the relationship of discharge of sands to shear or to stream power. The effect of depth also largely determines the use of discharge of sands per foot of width rather than concentration as a measure of the discharge of sands.

Qualitatively, the effects of mean velocity, depth, and water temperature on the discharge of sands can be computed, for some streams at least, from the Einstein procedure.

Median particle size of the bed sands has an appreciable effect on the discharge of sands especially at low velocities in shallow flows and at either low or high velocities in deep flows.

The discharge of sands increases as the water temperature decreases, but the change is usually small as compared with changes that may be caused by variations in mean velocity or in depth.

High concentrations of fine sediment, especially of bentonite, may greatly increase the discharge of sands per foot of width even though velocity, depth, and water temperature are kept constant.

The method of analysis that is suggested for determining empirically the effects of major factors on the discharge of sands is limited by the available information, but it gives relationships that should be helpful in understanding the relative effects of different major factors.

The empirically defined graphs provide a basis for rapid estimation of the discharge of sands in sand-bed streams. The accuracy of the estimated discharges should be reasonably satisfactory for many sand-bed streams. Accuracy, however, may be poor for bed sands whose median diameters are outside the range of 0.15 to 0.50 mm, for unusually low or high velocities, for deep flows, for turbulence that is unusually high in comparison to mean velocity, or for high concentrations of fine sediment.

The graphs are applicable only to streams whose beds are composed of nearly cohesionless sands and whose banks do not have the unusually high roughness that might be caused by rock walls that constrict the flow.

REFERENCES

Anderson, A. G., 1942, Distribution of suspended sediment in a natural stream: Am. Geophys. Union Trans., 23d ann. mtg., pt. 2, p. 678–683.

Bagnold, R. A., 1956, The flow of cohesionless grains in fluids: Royal Soc. [London] Philos. Trans., v. 249, p. 235–297.

Bagnold, R. A., 1960, Sediment discharge and stream power—a preliminary announcement: U.S. Geol. Survey Circ. 421, 23 p.

Barton, J. R., and Lin, Pin-Nam, 1955, A study of the sediment transport in alluvial channels: Civil Eng. Dept., Colorado State Univ., Fort Collins, Colo., 43 p., 21 figs., and app.

Beckman, E. W., and Furness, L. W., 1962, Flow characteristics of Elkhorn River near Waterloo, Nebr.: U.S. Geol. Survey Water-Supply Paper 1498–B, 34 p.

Benedict, P. C., Albertson, M. L., and Matejka, D. Q., 1955, Total sediment load measured in turbulence flume: Am. Soc. Civil Engineers Trans., v. 120, p. 457–484.

Brooks, N. H., 1958, Mechanics of streams with movable beds of fine sand: Am. Soc. Civil Engineers Trans., v. 123, p. 526–594.

Colby, B. R., 1956, Relationship of sediment discharge to streamflow: U.S. Geol. Survey open-file rept.

——— 1957, Relationship of unmeasured sediment discharge to mean velocity: Am. Geophys. Union Trans., v. 38, p. 708–717.

——— 1961, Effect of depth of flow on discharge of bed material: U.S. Geol. Survey Water-Supply Paper 1498–D, 12 p.

Colby, B. R., and Hembree, C. H., 1955, Computations of total sediment discharge, Niobrara River near Cody, Nebr.: U.S. Geol. Survey Water-Supply Paper 1357, 187 p.

Cook, H. L., 1935, Outline of the energetics of stream-transportation of solids: Am. Geophys. Union Trans., pt. 2, p. 456–463.

Einstein, H. A., 1950, The bed-load function for sediment transportation in open channel flows: U.S. Dept. Agriculture Tech. Bull. 1026, 70 p.

Einstein, H. A., and Chien, Ning, 1953, Can the rate of wash load be predicted from the bed-load function?: Am. Geophys. Union Trans., v. 34, p. 876–882.

——— 1954, Second approximation to the solution of the suspended load theory: California Univ. Inst. Eng. Research, Missouri River Div. sediment ser. 3, 30 p., 12 figs.

Gilbert, G. K., 1914, Transportation of debris by running water: U.S. Geol. Survey Prof. Paper 86, 263 p.

Hubbell, D. W., and Matejka, D. Q., 1959, Investigations of sediment transportation, Middle Loup River at Dunning, Nebr.: U.S. Geol. Survey Water-Supply Paper 1476, 123 p.

Ismail, H. M., 1952, Turbulent transfer mechanism and suspended sediment in closed channels: Am. Soc. Civil Engineers Trans., v. 117, p. 409–446.

Keulegan, G. H., 1938, Laws of turbulent flow in open channels: U.S. Natl. Bur. Standards, Jour. Research, v. 21. p. 707–741.

Meyer-Peter, R., and Müller, R., 1948, Formulas for bed-load transport: Internat. Assoc. Hydraulic Structures Research, 2d mtg., Stockholm, Sweden, p. 39–64.

Rottner, J., 1959, A formula for bed-load transportation: La Houille Blanche, p. 301–307.

Rouse, Hunter, 1937, Modern conceptions of the mechanics of fluid trubulence: Am. Soc. Civil Engineers Trans., v. 102, p. 463–505.

Rubey, W. W., 1933, Settling velocities of gravel, sand, and silt particles: Am. Jour. Sci., 5th ser., v. 25, no. 148, p. 332.

Sayre, W. W., and Albertson, M. L., 1959, The effect of roughness spacing in rigid open channels: Civil Eng. Dept., Colorado State Univ., Fort Collins, Colo., 78 p.

Simons, D. B., Richardson, E. V., and Albertson, M. L., 1961, Flume studies using medium sand (0.45mm): U.S. Geol. Survey Water-Supply Paper 1498–A, 76 p.

U.S. Bureau of Reclamation, 1958, Interim report, total sediment transport program, lower Colorado River basin: Sedimentation Sec., Hydrology Br., Div. Proj. Inv., 175 p.

U.S. Waterways Experiment Station, 1935, Studies of river bed materials and their movement with special reference to the lower Mississippi River: Paper no. 17, Vicksburg, Miss., 161 p.

Vanoni, V. A., 1946 Transportation of suspended sediment by water: Am. Soc. Civil Engineers Trans., v. 111, p. 67–102

○

Vertical Distribution of Velocity and Suspended Sediment Middle Rio Grande New Mexico

By CARL F. NORDIN, JR., *and* GEORGE R. DEMPSTER, JR.

SEDIMENT TRANSPORT IN ALLUVIAL CHANNELS

GEOLOGICAL SURVEY PROFESSIONAL PAPER 462-B

UNITED STATES GOVERNMENT PRINTING OFFICE, WASHINGTON : 1963

UNITED STATES DEPARTMENT OF THE INTERIOR

STEWART L. UDALL, *Secretary*

GEOLOGICAL SURVEY

Thomas B. Nolan, *Director*

For sale by the Superintendent of Documents, U.S. Government Printing Office
Washington, D.C., 20402

CONTENTS

	Page
Abstract	B1
Introduction	1
Purpose and scope	1
Acknowledgments	1
Description of reaches	1
Measured data	2
General approach	3
Velocity distribution	B4
Mean velocity	6
Suspended-sediment distribution	7
Effects of high concentrations on fall velocity	12
Conclusions	13
Basic data and computed parameters	14
References cited	20

ILLUSTRATIONS

	Page
FIGURE 1. Location and sketch map	B2
2. Definition sketch	2
3. Variation of velocity with depth	4
4. Variation of k with concentration	5
5. Variation of k with $C/\sqrt{g}$	5
6. Bar-resistance curve, Bernalillo and Socorro	7
7. Bar-resistance curve, Bernalillo, 1952	7
8. Variation of concentration with $(D-y)/y$, Bernalillo	8
9. Variation of concentration with $(D-y)/y$, Socorro	8
10. Variation of Z_1 with Z and Z_k	9
11. Size distribution of bed material	10
12. Variation of Z_1 and fall velocity	11
13. Variation of k and β	12
14. Qualitative relation of velocity and sediment distribution	12
15. Variation of fall velocity with concentration	13
16. Comparison of computed Z values	13

TABLES

TABLE 1. Velocity distribution	B14
2. Suspended-sediment distribution	16
3. Basic data	18
4. Computed parameters	19
5. Basic data and computed parameters for the average of 13 cross sections through a 16,000-foot reach, Rio Grande near Bernalillo, N. Mex	19

SYMBOLS

Symbols		Units
a	Reference distance above the bed	ft
c	Concentration of suspended sediment	ppm
$C/\sqrt{g}$	Dimensionless Chezy coefficient	0
C_1	A constant	0
C_r	A coefficient of discharge	0
d_{35}	Particle size for which 35 percent of the bed material by weight is finer, as determined by sieve analysis	mm
d_{50}	Particle size for which 50 percent of the bed material by weight is finer	mm
d_{65}	Particle size for which 65 percent of the bed material by weight is finer	mm
dy	Increment of distance above stream bed	ft
D	Depth of flow at a vertical	ft
$\overline{D}$	Mean depth of flow in a cross section	ft
g	Acceleration of gravity	ft per sec^2
i	An exponent	0
j	An exponent	0
k	The coefficient of turbulent exchange	0
K_s	A length parameter	ft
m	Slope of semilogarithmic graph of velocity versus depth for a single vertical	ft per sec
$\overline{m}$	Average slope of velocity versus depth for all verticals in a cross section	ft per sec
q_s	Transport rate of suspended sediment	lb per sec per ft
P_w	Wetted perimeter	ft
R	Hydraulic radius	ft
R'	Hydraulic radius with respect to the sand grain	ft
R''	Hydraulic radius with respect to dunes and bars	ft
S	Water surface slope	0
S_e	Energy slope	0
V	Velocity at a point	ft per sec
$\overline{V}$	Mean velocity	ft per sec
V_*	Shear velocity	ft per sec
x	A correction factor for transition from smooth to rough boundary	0
y	Distance above stream bed	ft
Z	Computed exponent for vertical distribution of suspended sediment using $k=0.4$	0
Z_1	Exponential measure of the actual distribution of suspended sediment	0
Z_k	Computed exponent for vertical distribution of suspended sediment using $k=(2.3/m)V_*$	0
β	Factor of proportionality between ϵ_s and ϵ_m	0
γ	Specific weight of water	lb per ft^3
δ'	Thickness of laminar sublayer	ft
Δ	An increment of change	0
ϵ_m	Momentum transfer coefficient	0
ϵ_s	Sediment transfer coefficient	0
ν	Kinematic viscosity	ft^2 per sec
ρ_f	Density of fluid	slugs per ft^3
ρ_s	Density of sediment	slugs per ft^3
τ_0	Tractive force on the bed	lbs per ft^2
ψ'	A flow intensity parameter	0
ω	Fall velocity of sediment particles	ft per sec

VERTICAL DISTRIBUTION OF VELOCITY AND SUSPENDED SEDIMENT, MIDDLE RIO GRANDE, NEW MEXICO

By Carl F. Nordin, Jr. and George R. Dempster, Jr.

ABSTRACT

Samples of suspended sediment and measurements of velocity at 3 to 5 points in a vertical are used to define vertical sediment concentration and velocity profiles for cross sections in reaches of the Rio Grande near Bernalillo and Socorro, and of the Rio Puerco near Bernardo, N. Mex.

Velocity profiles show the velocity to vary logarithmically with depth. The coefficient of turbulent exchange, k, is found to decrease systematically for the transition zone and upper regime flow. For lower regime flow, k varies from about 0.4 to 1.2, indicating three-dimensional flow effects.

Assuming a conventional logarithmic velocity equation to be applicable, it is found that the range of values of K_s, the height of the representative roughness element, is dependent upon the condition of the channel bed. The ratio of maximum to minimum K_s is about 20,000 for lower regime flow, 40 for transition and upper regime flow, and 4 for flow over a clay-armored bed. However, the relation of the average K_s value to the average representative bed-material size for each of the reaches is about constant, and is approximately 400 times greater than d_{65}, the size of bed material for which 65 percent by weight is finer.

The Einstein-Barbarossa bar-resistance curve is shown to describe frictional losses for individual cross sections of the Bernalillo and Socorro reaches with reasonable accuracy. Twenty of the 23 computed values of mean velocity are within 25 percent of the measured values. When an average cross section is used for the Bernalillo reach, the computed mean velocities are within 15 percent of the measured values.

Suspended sediment is more uniformly distributed through a vertical than predicted by conventional theory. The measured exponent of the sediment distribution, Z_1, varies with about the 0.55 power of the fall velocity. The fall velocity is reduced appreciably by the presence of high concentrations of suspended fine material.

The ratio of the sediment transfer coefficient to the momentum transfer coefficient, β, appears to be a direct function of particle size and bed configuration. For a given particle size the highest values of β are associated with upper regime flow, while for lower regime flow, β values are close to unity.

INTRODUCTION

PURPOSE AND SCOPE

The purpose of this report is to present measured values of vertical velocity and suspended-sediment concentration distributions, and to compare the measured values with values computed from theoretical considerations. Some of the variables in the distribution equations are analysed. In addition, one method of estimating mean velocity is discussed.

Data are presented for 23 observations in reaches of the Rio Grande near Bernalillo and the Rio Grande near Socorro, N. Mex. Limited data for the Rio Puerco, a tributary to the Rio Grande, also are included to indicate some of the effects of high suspended-sediment concentrations. Data for the Rio Grande near Bernalillo and near Socorro were collected during the period 1953–54 as part of a cooperative program between the U.S. Geological Survey and the U.S. Bureau of Reclamation to study sediment transport in the Middle Rio Grande, N. Mex.

This report is one of several utilizing available data for the Middle Rio Grande basin for studies of sediment-transport parameters in sand-bed streams.

ACKNOWLEDGMENTS

This report was written under the supervision of J. M. Stow, district chemist, and J. K. Culbertson, hydraulic engineer, Quality of Water Branch, Albuquerque District, N. Mex.

Appreciation is expressed to A. A. Fischback, Jr., district engineer, Surface Water Branch, Oklahoma City, Okla., and others for their cooperation.

DESCRIPTION OF REACHES

Velocity and suspended-sediment concentration distributions were measured in two reaches of the Rio Grande: Rio Grande near Bernalillo, and Rio Grande near Socorro, N. Mex. In addition, several observations were obtained for a single cross section on the Rio Puerco near Bernardo. A location and sketch map of the reaches is shown in figure 1.

The Bernalillo reach is located approximately 3 miles southwest of Bernalillo and 9 miles downstream from the Jemez River. The right bank at the upstream portion of the reach is a high bluff composed of calcareous sandstone. The bluff veers away from the

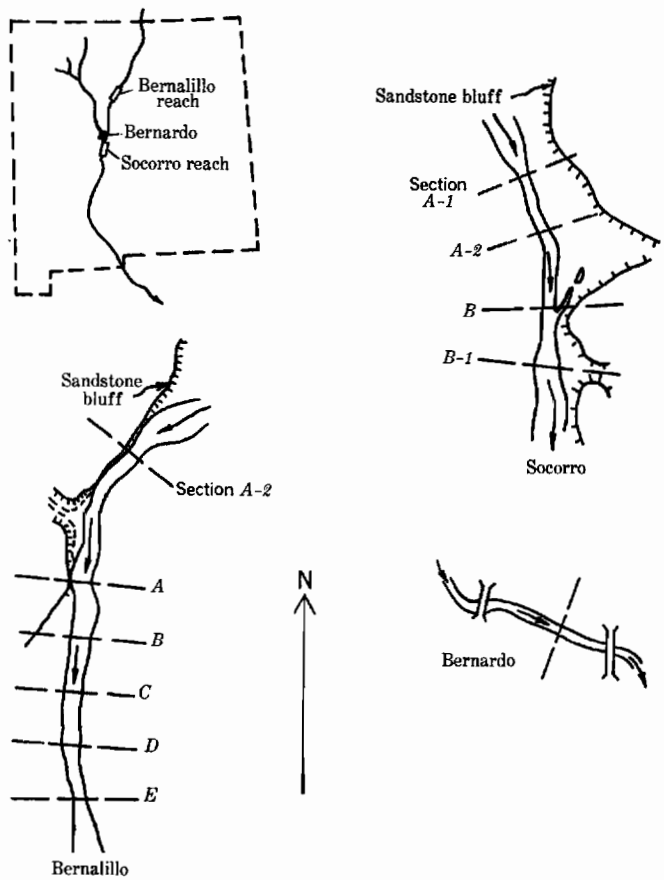

FIGURE 1.—Location and sketch maps of Rio Grande near Bernalillo, Rio Grande near Socorro, and Rio Puerco near Bernardo, N. Mex.

river about 200 yards downstream from the uppermost cross section. Throughout the rest of the reach, both banks consist of a mixture of sand, silt, and clay, and are partially stabilized by vegetation. The reach is laterally unconfined except at section A–2, which is the site of a U.S. Geological Survey gaging station. The reach is about 7,000 feet in length.

The Socorro reach is approximately 28 miles downstream from the mouth of the Rio Puerco and a quarter of a mile northeast of Socorro. Both banks of the reach consist of silty clay and are partially stabilized by vegetation. The reach diverges somewhat and is about 4,000 feet in length.

The Bernardo reach is located about 1 mile southwest of Bernardo and 3 miles upstream from the mouth of the Rio Puerco. This is the site of a U.S. Geological Survey gaging station. Both banks consist of silty clay and are stabilized by vegetation. The cross section is located about midway of a slightly converging reach approximately 630 feet in length immediately downstream from the gaging station. The reach has a sand bed, but for the several observations presented, the bed was armored with a layer of clay and silt 0.1–0.6 foot thick.

MEASURED DATA

Basic data for 26 observations of velocities and suspended-sediment concentrations are shown in tables 1 and 2.

Velocities were measured with a Price current meter and samples of suspended sediment were collected at points in the vertical with a US P–46 sampler or a modified DH–48 hand sampler. Suspended-sediment samples were analyzed for particle-size distribution by the pipette-visual accumulation tube method. Vertical distributions of velocity and suspended sediment were defined at approximate equal centroids of flow at each cross section. The number of centroids varied from 2 to 5, except in one case, where 15 velocity profiles were obtained. The number of points in a vertical varied from 3 to 5 and were obtained at approximate equal $(D-y)/y$ horizons. Concentrations shown in table 2 were determined from a composite of samples for the indicated horizons. Figure 2 is a

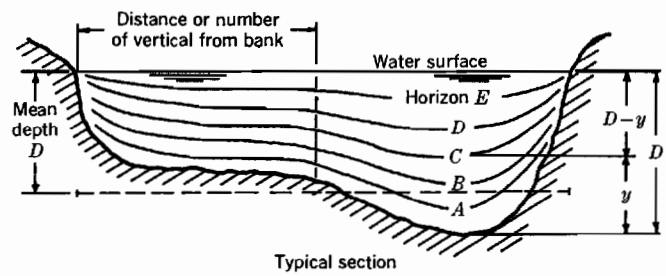

FIGURE 2.—Definition sketch of equal $(D-y)/y$ horizons, any cross section.

definition sketch showing equal $(D-y)/y$ horizons in any cross section. Verticals were numbered consecutively from the right bank.

Obtained concurrently with velocity and suspended-sediment samples were water discharge, width, mean depth, mean velocity, water temperature, water-surface slope, and bed-material samples. These data are shown in table 3.

Water-surface slopes for the Bernalillo and Socorro reaches were determined as the slope of the line fitted by method of least squares through the plotted water-surface profile. Particle-size distributions of bed-material samples were determined by seiving. Values of d_{65}, d_{50}, and d_{35}, where the subscript denotes the percent finer by weight, were read from a logarithmic probability plot of size distribution. These data were furnished by the United States Bureau of Reclamation.

Water-surface slopes in the Bernardo reach were determined by dividing the difference in water-surface elevation between two cross sections by the distance between the two sections.

For the data herein, the width-depth ratio is large and it is assumed $R=D$ for a cross section. For

practical purposes, the flow is considered uniform and $S_e=S$; also bank friction is considered to be negligible.

GENERAL APPROACH

The equation for suspended-sediment discharge per unit width for two-dimensional flow is given by

$$q_s=\gamma\int_a^D V_y c_y dy \tag{1}$$

where

q_s=the transport rate of suspended sediment between the depths a and D
γ=the average unit weight of the water-sediment mixture
a=reference depth
D=flow depth
V_y=flow velocity at depth y
c_y=concentration at depth y

In order to integrate equation 1, V_y and c_y must be expressed as functions of y.

The velocity distribution for two-dimensional open-channel flow over a rough boundary as presented by Keulegan (1938) is

$$\frac{V_y}{V_*}=\frac{2.3}{k}\log_{10}\frac{y}{K_s}+C_1 \tag{2}$$

where

$V_*=\sqrt{gRS_e}$=shear velocity
k=von Karman coefficient of turbulent exchange
y=distance above bed
K_s=a length parameter
C_1=a constant
g=acceleration due to gravity
R=hydraulic radius
S_e=energy gradient

Equation 2 is not generally applicable for flow over an alluvial boundary, but in this report the equation will be used throughout as a basis for comparison with measured velocity distributions.

The equation for sediment suspension was introduced by O'Brien (1933) as

$$\omega c=\epsilon_s\frac{dc}{dy} \tag{3}$$

where

ω=the fall velocity of the sediment particle.
c=concentration of suspended sediment.
$\epsilon_s\frac{dc}{dy}$=rate of upward transfer of suspended sediment from turbulent exchange.

Rouse (1937) showed that equation 3 could be integrated to yield an equation for the distribution of the relative concentration of the suspended sediment as

$$\frac{c_y}{c_a}=\left(\frac{D-y}{y}\cdot\frac{a}{D-a}\right)^Z \tag{4}$$

where

c_y=concentration of a grain size at depth y above bed.
c_a=concentration of a grain size at reference level a above bed.
Z=theoretical exponent of the distribution equation given by

$$Z=\frac{\omega}{\beta k V_*} \tag{5}$$

where

β=ratio of the transfer coefficient for sediment (ϵ_s) to the momentum transfer coefficient (ϵ_m).

In the derivation of equations 4 and 5, it was assumed that

$$\epsilon s=\epsilon_m$$

$$\beta=\frac{\epsilon_s}{\epsilon_m}=1$$

and

$$k=0.4$$

The general forms of equations 2 and 4 are well established, but the solution to the suspended-sediment transport rate is not completely formulated. Neither k nor K_s is constant and the exponent Z given by equation 5 does not agree with Z_1, the exponent that fits the measured data.

Equation 2 may be integrated over a representative vertical to obtain mean velocity. Keulegan (1938) has shown that the mean velocity for open-channel flow over a wholly rough surface of a rigid boundary may be expressed as

$$\frac{\overline{V}}{V_*}=6.25+5.75\log\frac{R}{K_s} \tag{6}$$

where

$\overline{V}$=mean velocity.

The constant 6.25 is a mean value, and varies with several factors such as effect of the shape of section, the free surface, and nonuniform distribution of the tractive forces at the boundary. For sand-grain roughness only, such as flow over a flat sand bed, K_s assumes the value of a representative grain size or an equivalent height of the roughness elements. For natural river sediments, Einstein (1950) used the value of d_{65} for K_s. In many natural channels with flow over an alluvial bed, K_s is greater than d_{65} owing to the presence of dunes and bars on the bed.

The quantitative relation between dune characteristics and the roughness parameter K_s is not known. Flume studies with rigid boundaries (Sayre and Albertson, 1961) have shown that roughness conditions are dependent upon the relative size and spacing of the roughness elements and that the overall boundary roughness can be expressed as one parameter in the velocity equation. If the relative size and spacing of dunes and bars in a natural channel could be measured, a more complete evaluation of K_s could be made. Sonic-sounding equipment offers possibilities in this field. Sonic-sounding equipment has been used in the Mississippi River (Carey and Keller, 1957) and in the

laboratory (Richardson, Simons, and Posakony, 1961), but the information obtained is more qualitative than quantitative and thus is not subject to a rigorous mathematical analysis.

Several flume and field studies present qualitative information on the relations between resistance coefficients and bed configuration. The forms of bed roughness observed in flume studies using 0.28 mm and 0.45 mm median-diameter sand have been described in detail by Simons and Richardson (1961). They indicate that flow may be classified into lower regime and upper regime with a transition zone between, and that both resistance and sediment transport are intimately related to flow regime. The lower and upper flow regime classification is based upon magnitude of resistance to flow, bed and water surface configuration, and mode and magnitude of sediment transport. The bed roughness for lower regime flow is ripples or dunes or both, the resistance to flow is large, and the bed material transport rate is low. For upper regime flow, the bed is relatively plane, standing waves or antidunes may be present on the water surface, the flow resistance is low, and the rate of transport of bed material is relatively high. These general regimes of flow are applicable to natural streams. Culbertson and Dawdy (1963) and Dawdy (1961) have shown that these different regimes of flow occur in the Rio Grande and in many other sand-bed streams.

VELOCITY DISTRIBUTION

Typical velocity profiles (fig. 3) show that the velocity distributions fit a logarithmic law. It is noted that lateral variation of velocity distribution and depth occur in the cross section. For practical purposes, mean values of velocity and depth are used.

Values of the Von Karman coefficient of turbulent exchange (k) can be computed from a form of equation 2 as

$$\frac{V_1-V_2}{\log y_1-\log y_2}=\frac{2.3}{k}V_*=m \qquad (7)$$

where V_1 and V_2 are the velocities at depth y_1 and y_2, respectively, and m is the slope of the velocity profile in feet per second change per log cycle of depth; thus

$$k=\frac{2.3}{m}V_* \qquad (8)$$

The average k for a cross section was computed using $\overline{m}$ and V_* where $\overline{m}$ is the average of the individual m values of all the verticals in a cross section and $V_*=\sqrt{g\overline{D}S}$. The values of $\overline{m}$ and k are shown in table 4. Values of k vary widely, ranging from 0.15 to 1.20. For the Socorro reach and Bernardo cross section, the values of k appear to vary systematically

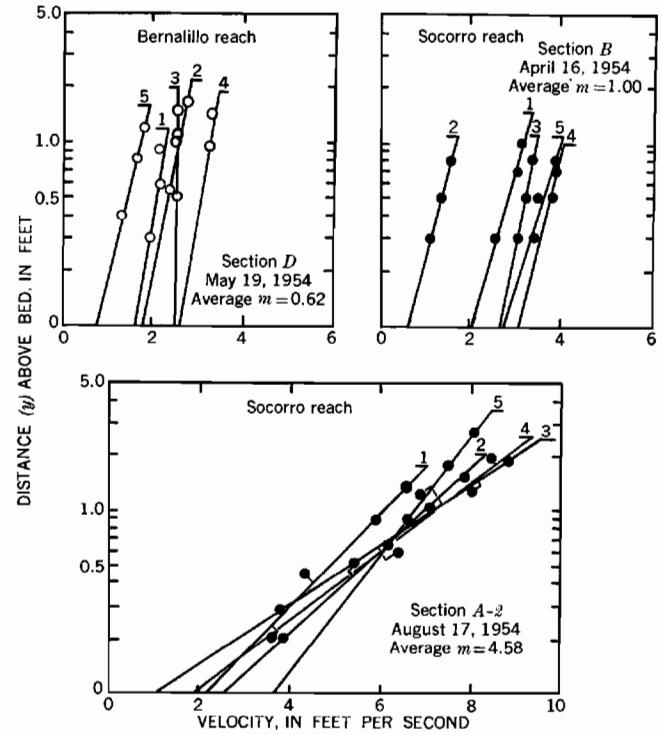

FIGURE 3.—Variation of velocity with depth, Rio Grande near Bernalillo and Socorro.

and are generally less than 0.4. Conversely, the Bernalillo values appear to be random and generally are greater than 0.4, varying from 0.35 to 1.2.

Flume and river measurements show that the k for sediment-laden flow generally varies from the 0.4 that was determined by Nikuradse for pipe flow with clear water. Vanoni and Brooks (1957) and Ismail (1951) suggested that sediment dampens the turbulence and reduces the momentum transfer. In effect, this results in a reduction of k. Einstein and Chien (1955) measured the reduction of k by the amount of turbulent energy spent in supporting the sediment in suspension. The rate at which frictional energy is spent per unit weight of fluid per unit time in supporting the sediment in suspension was expressed as

$$\sum\frac{c_s\omega}{\overline{V}S_e}\,\frac{\rho_s-\rho_f}{\rho_s} \qquad (9)$$

where c_s=average concentration by weight of a given particle size, and Σ signifies the summation of the concentrations and fall velocities of all the particle sizes present. Values of k plotted versus equation 9 in figure 4 show wide scatter. Socorro and Bernardo data generally follow the predicted trend, while the Bernalillo data show no definite trend. Dashed lines on the figure indicate the approximate scatter of points from which the relation was defined by Einstein and Chien. About half of the 26 points fall within or close

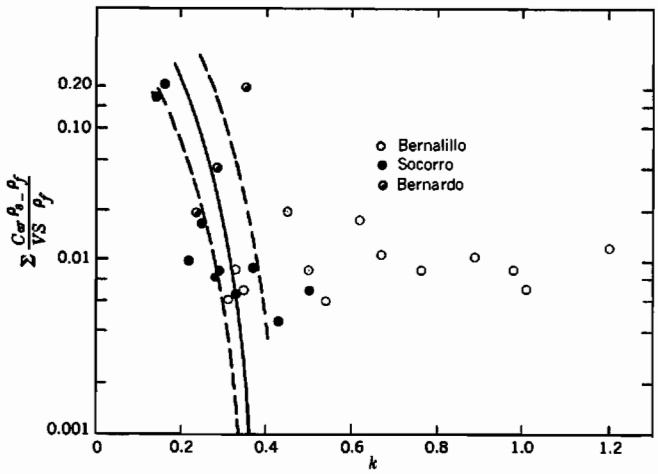

FIGURE 4.—Variation of k with concentration, Rio Grande near Bernalillo, Socorro, and Rio Puerco near Bernardo. Dashed lines indicate approximate envelope of points used to define the relation. From Einstein and Chien, 1955.

to the envelope. Values of equation 9 for the data herein are shown in table 4. That portion of the summation for particle size less than 0.062 mm was obtained by assuming all material was in a size range of 0.002–0.062 mm and then using a fall velocity based on the geometric mean size of this class.

Chien (1954) suggested that k may change with roughness if the height of the roughness elements are comparable to the mean depth of flow. Field observations in the Bernalillo reach show that the height of dunes in fully developed lower regime flow is often equal to or greater than one-half the mean depth. Under such conditions, extreme lateral variations in a cross section may occur and the flow may exhibit three dimensional characteristics.

Figure 5 shows the variation of k with $\overline{V}/V_* = C/\sqrt{g}$. In this figure there is no quantitative measure of the dune height, but a qualitative measure of bed configuration based on the three regimes of flow may be shown

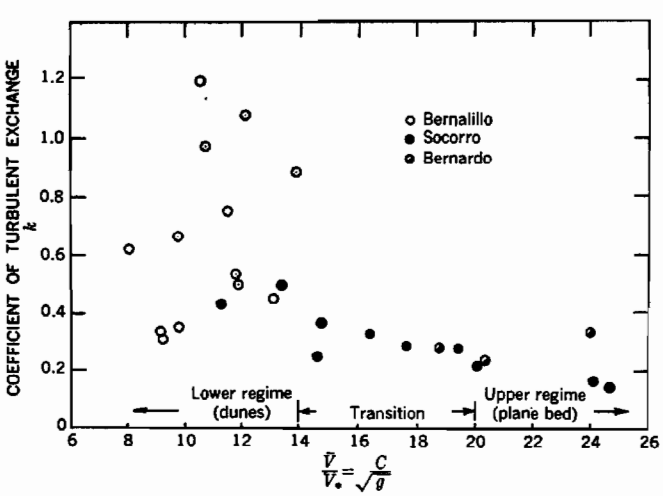

FIGURE 5.—Variation of k with $C/\sqrt{g}$.

The $C/\sqrt{g}$ values indicated on the figure for the various flow regimes are based on field observations where bed configuration was verified by probing. These $C/\sqrt{g}$ values are in close agreement with those reported by Simons and Richardson (1961). The figure clearly indicates that extreme variations of k occur for flow over a dune bed.

Sayre and Albertson (1961) reported k values ranging from 0.34 to 2.77 as determined by the velocity-profile method (equation 8) for clear-water flow with isolated roughness baffles. However, from the slope of the average lines drawn through plots of V/V_* versus relative roughness, they determined that the average or "integrated" k was in fact a constant, with a value of 0.38. They attribute the wide variation in k values determined from the velocity-profile method to three-dimensional flow effects and large scale vortices, and they conclude that equation 8 is not adequate to define k where such flow conditions exist. The wide range of k values for flow over a dune bed shown in figure 5 probably reflects the same effects that were reported by Sayre and Albertson.

The decreasing value of k with increasing $C/\sqrt{g}$ for transition and upper regime flow may or may not be related to changing roughness. Because sediment transport generally increases with an increase in $C/\sqrt{g}$, the decrease of k may be attributed, in part, to a concentration effect.

Although k may not be adequately defined for flow over a dune bed, the velocity for such flow is still proportional to the logarithm of the depth. If a form of equation 2 applies, and if k attains a near-constant value of about 0.4, the proportionality factor between V and log y does not equal the shear velocity V_*, but must assume a much smaller value. From equation 7, the proportionality factor is approximately equal to $\overline{m}/5.75$. Einstein (1950) introduced a shear velocity with respect to the grain roughness, V_*', which is less than V_*. For the data in table 4, the factor of proportionality between velocity and the logarithm of the depth, $\overline{m}/5.75$, is considerably less than Einstein's V_*'.

Regardless of the value of the proportionality factor relating velocity to the logarithm of the depth, if equation 2 applies with $C_1=8.5$ as given by Keulegan, the value of K_s may be determined from a plot of V versus log y by extrapolating the line through the plotted point to intercept the ordinate at zero velocity. This follows from equation 2, where the velocity must equal zero when the logarithm of $30.2y/K_s$ equals zero.

Values of K_s for each cross section were determined for the data in table 4 by two methods: first, as the average of the K_s values for the individual verticals read from the V versus log y plots extrapolated to intercept the ordinate at zero velocity; second, by plot-

ting mean velocity $\overline{V}$ at $y=0.4\overline{D}$ on semilog paper, and extending a line with slope $\overline{m}$ to intercept the ordinate at zero velocity. For any given cross section, the values of K_s computed by the two methods vary appreciably but are of the same order of magnitude; therefore, the two values were averaged to obtain the K_s shown in table 4.

The values of $\overline{m}$ and K_s in table 4 were defined from a limited number of verticals, and thus may not describe accurately the average velocity distribution in a cross section. Even so, for a given reach, the range of values of K_s and the ratio of the average K_s to the average d_{65} should provide an indication of bed-configuration effects on velocity distributions. These data are shown in the table below.

For Bernalillo, where flow was in lower regime, K_s varies by a factor of about 20,000. Flow in the Socorro reach was mostly in transition or upper regime, and the ratio of maximum to minimum K_s is 48. At Bernardo the bed was armored with clay, the flow was comparable to flow over a rigid boundary, and K_s varies by a factor of 4. These values indicate clearly the extreme influence which bed configuration has on velocity distributions.

It is significant that the mean value of K_s is much greater than d_{65}, even for the clay-armored bed of the Rio Puerco, which was relatively free of irregularities. The values of the ratio of the mean K_s to d_{65} are remarkably constant, considering the wide differences in bed conditions for the three reaches. That such similarities should be fortuitous seems unlikely. The data tabulated below suggest that although the bed condition dictates the range of K_s values, it is the size of the bedmaterial and not the bed configuration which determines the mean K_s. For the range of conditions examined, the mean K_s is about 400 times as great as d_{65}.

In the foregoing discussion, no consideration was given to the correction factor for the transition from smooth to rough boundaries (Rouse, 1937). Inclusion of the factor could alter the values of K_s by as much as 20 percent.

MEAN VELOCITY

Where the relative effects of bed configuration on flow resistance are minor, mean velocity may be predicted with reasonable accuracy by using empirical formulas of the Manning or Chezy type with coefficients based upon a grain-size roughness.

Two empirical formulas which attempt to predict the relation between bed configuration and flow resistance have been proposed (Liu and Hwang, 1959; Einstein and Barbarossa, 1952).

Summary of K_s values

Reach	K_s, in ft			K_s max	d_{65} ft	Mean K_s	Bed condition
	minimum	maximum	mean	K_s min		d_{65}	
Bernalillo	0.000086	1.86	0.47	22,000	0.00121	388	Dunes.
Socorro	.020	.95	.27	48	.00072	375	Transition and plane bed.
Bernardo	.03	.11	.078	4	.0002	390	Clay-armored.

Liu and Hwang presented a formula of the Chezy type

$$\overline{V}=C_r R^i S^j \tag{10}$$

where C_r and the exponents, i and j, are functions of bed configuration and particle size of the bed material. It has been shown that Liu's criterion for the prediction of bed configuration is not applicable to the Rio Grande data (Culbertson and Nordin, 1960).

Einstein and Barbarossa (1952) introduced an approach to the determination of flow resistance where the total resistance was divided into two parts, one due to the sand-grain roughness, and the other due to bars, dunes, and the general irregularities of the channel bed. The velocity equation given by Einstein and Barbarossa was

$$\frac{\overline{V}}{V_*'}=5.75 \log_{10}\left(12.27 \frac{R'x}{K_s}\right) \tag{11}$$

where

K_s=the representative grain roughness d_{65}.
R'=the hydraulic radius with respect to the sand grain.
x=a correction factor for channels which are not hydrodynamically rough and is given as a function of $\frac{K_s}{\delta'}$.
δ'=the theoretical thickness of the laminar sublayer, which is equal to $\frac{11.6\nu}{V_*'}$.
ν=the kinematic viscosity.

That part of the resistance due to bars and dunes was expressed as a functional relation between the dimensionless resistance factor, V/V_*'', and flow intensity, ψ', where $V_*''=\sqrt{gR''S}$, the shear velocity with respect to the dunes and bars, and

$$\psi'=\frac{\rho_s-\rho_f}{\rho_f} \quad \frac{d_{35}}{R'S_e} \tag{12}$$

ρ_s and ρ_f=the densities of the sediment and fluid respectively.
and d_{35}=representative grain diameter of bed material.

The functional relation of $\overline{V}/V_*''$ to ψ', called the bar-resistance curve, was defined from average cross sections and representative slopes for reaches in several natural channels. For a given mean depth, slope, and bed material, the mean velocity may be computed by

trial and error from equations 11 and 12 and several graphs presented by Einstein. The accuracy with which mean velocity may be predicted depends upon the accuracy with which the $\overline{V}/V_*''-\psi'$ relation expresses frictional losses due to bars, dunes, and other irregularities on the bed for the channel under consideration. Vanoni and Brooks (1957) and Vanoni and others (1961) have discussed the applicability of the bar-resistance curve for flume data and for some limited natural-channel data.

The graphical method presented by Vanoni and Brooks was used to compute values of $\overline{V}/V_*''$ and ψ' for the Bernalillo and Socorro data. These values, listed in table 4, are plotted in figure 6 and show reasonable agreement with the predicted relation. Of 23 computed values of mean velocity using the Einstein-Barbarossa approach, 20 are within 25 percent of the measured values. Some scatter on the plot may be attributed to the use of $k=0.4$ in the velocity equation and to the use of data at individual cross sections.

From the manner in which the bar-resistance curve was derived, the curve should describe conditions for a reach of a natural unconfined channel. The relations do not necessarily apply to an individual cross section. Vanoni and Brooks (1957) apply data for several cross sections of the Bernalillo reach to the bar-resistance curve. On the basis of the scatter of the points for these individual cross sections, they conclude that the 1952 data "do not lend confidence to the bar-resistance curve." Figure 7 shows the 1952 Bernalillo data using average conditions for 13 cross sections through a 16,000-foot reach. All computed values of mean velocity are within 15 percent of the measured mean

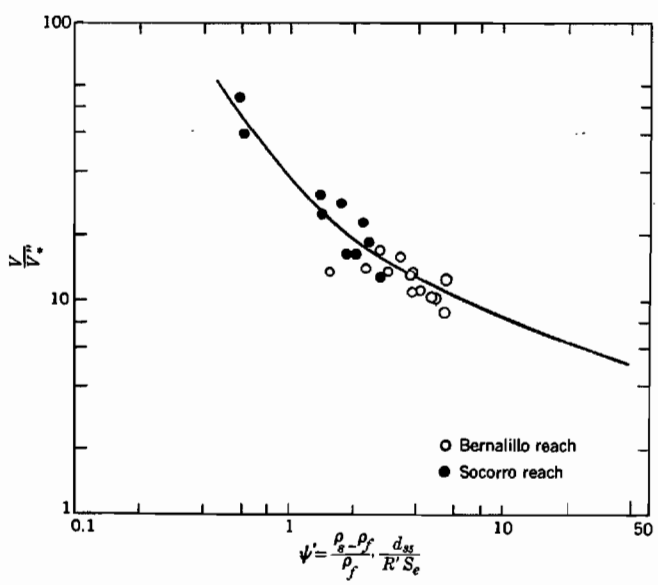

FIGURE 6.—Einstein-Barbarossa bar-resistance curve for Rio Grande near Bernalillo and near Socorro. Curve from Einstein and Barbarossa, 1952.

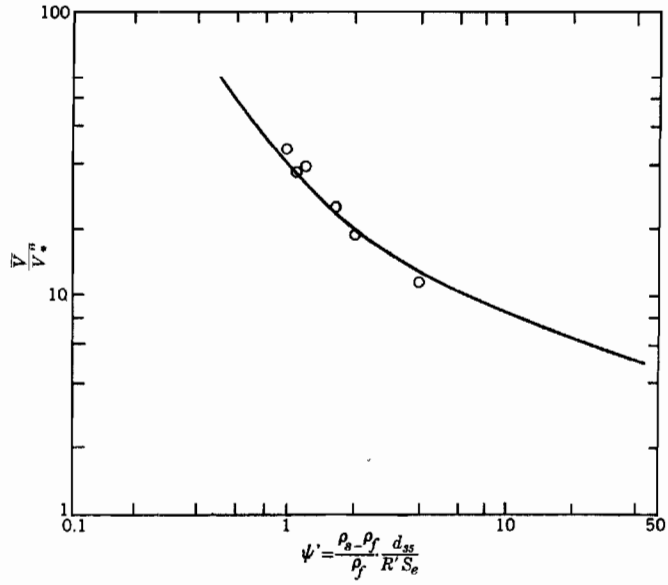

FIGURE 7.—Einstein-Barbarossa bar-resistance curve for Rio Grande near Bernalillo, 1952 data. Curve from Einstein and Barbarossa, 1952.

velocities. Basic data for these calculations are given in table 5.

From figures 6 and 7, it is concluded that mean velocity may be predicted within reasonable limits by the Einstein-Barbarossa method for the Rio Grande near Bernalillo and near Socorro.

SUSPENDED-SEDIMENT DISTRIBUTION

The vertical distribution of suspended-sediment concentration for several size ranges was determined from particle-size analysis of point-integrated samples. Data for the Bernalillo, Socorro, and Bernardo reaches are shown in table 2. The data show that suspended sediment less than 0.062 mm in diameter was almost uniformly distributed throughout the depth of flow. The vertical distribution of suspended sediment greater than 0.062 mm in diameter was defined for three size classes: 0.062–0.125 mm, 0.125–0.250 mm, and 0.250–0.50 mm. Theoretical distributions for these size classes were computed using the fall velocities from figure 5 of "Inter-Agency Report No. 4," 1941, for the geometric mean of the size class.

Equation 4 plotted logarithmically is a straight line with a slope,

$$Z_1=\frac{\log c_y}{\log \frac{D-y}{y}}=\text{measured exponent of suspended-sediment distribution.}$$

which may be read directly from the logarithmic plot of c versus $(d-y)/y$. Figures 8 and 9 are typical plots using several sets of data from table 2. The plots show that log c varies directly with log $(D-y)/y$, thus the distribution function is of the correct form.

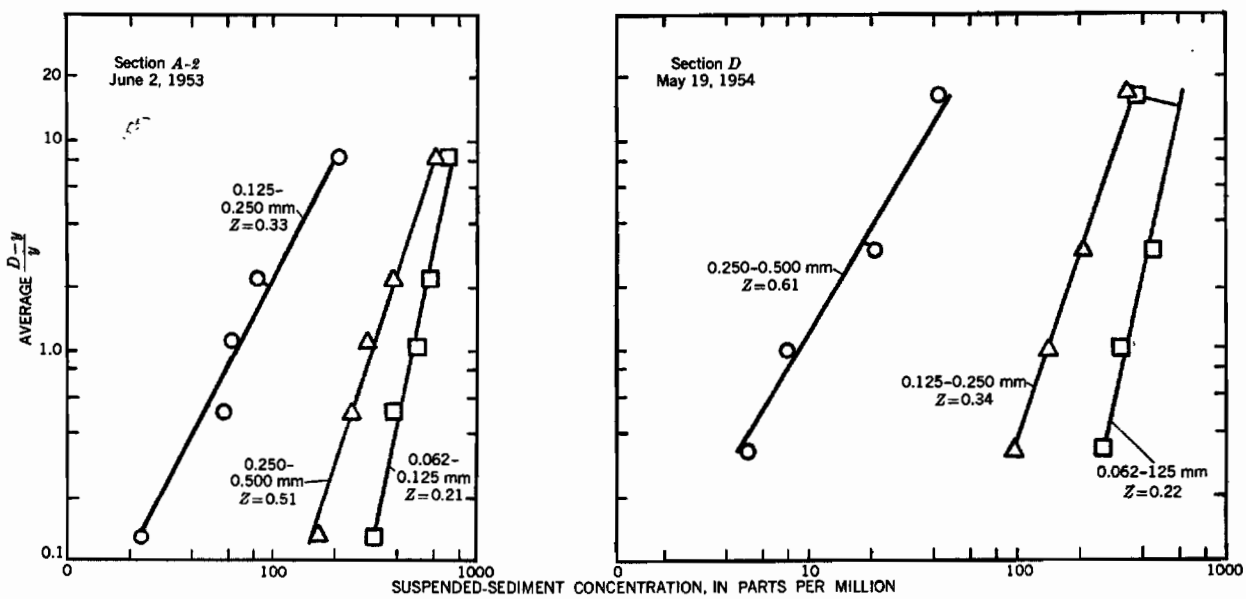

FIGURE 8.—Variation of concentration with $(D-y)/y$, Rio Grande near Bernalillo.

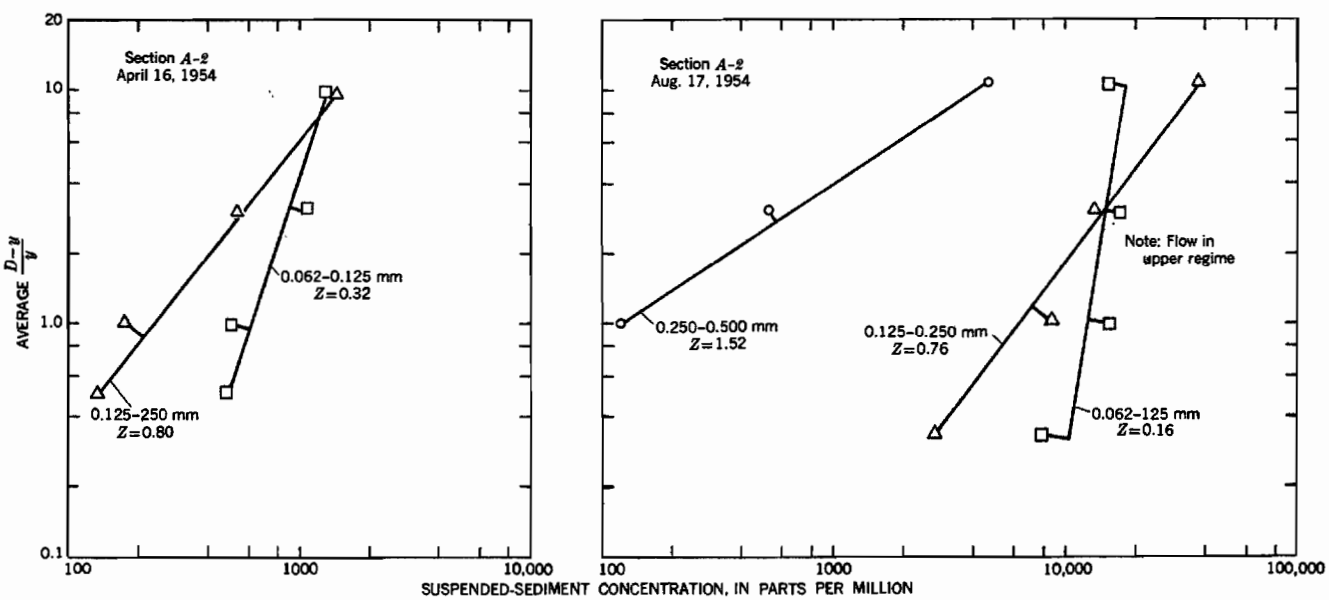

FIGURE 9.—Variation of concentration with $(D-y)/y$, Rio Grande near Socorro.

Values of Z may be calculated from equation 5, using the original assumptions as previously mentioned ($\beta=1$, $k=0.4$). An alternate Z, designated Z_k, can be calculated assuming $\beta=1$ and using the computed k from equation 8. Values of Z_1, and $\beta=Z_k/Z$, are shown in table 4.

Figure 10 shows the plots of Z_1 versus Z and Z_k for the three size classes used herein. For small Z or Z_k values, Z_1 is generally in close agreement with Z or Z_k. For large Z or Z_k values, Z_1 is smaller than Z or Z_k, indicating the suspended sediment is distributed more uniformly than the theory would predict. The deviation of the computed exponent from the measured exponent becomes greater with increasing particle size. This is typical of the results found by Anderson (1942), Colby (1955), and others.

Points on the Z_1 versus Z plot in figure 10 tend to group by reach along the ordinate (Z_1) and by particle size along the abscissa (Z). Grouping by particle size in Z values is indicative of the limited range in shear velocity, V_*. On the Z_1 versus Z_k plot, the points scatter and are more random, but the trend by reach is still evident. This apparent difference between Z_1's for the Bernalillo, Socorro, and Bernardo data may be

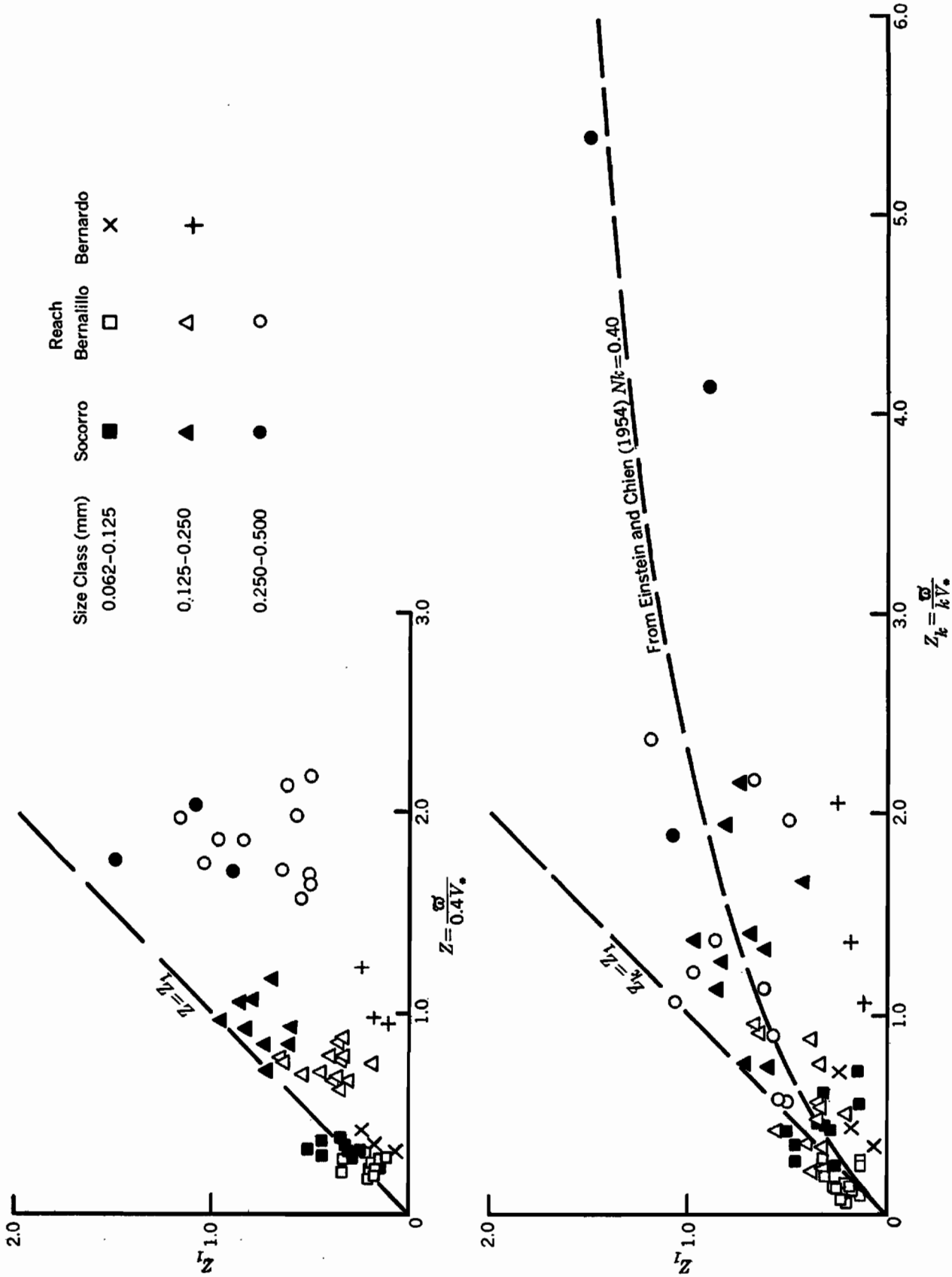

FIGURE 10.—Variation of Z_1 with Z and Z_k.

attributed to the marked difference in average size of bed material (fig. 11) and to individual characteristics peculiar to each reach.

The curves in figure 11 are the average of the size distributions of bed material shown in table 3. The median diameter of bed material in the Socorro reach was about 0.19 mm compared to 0.30 mm in the Bernalillo reach. The median diameter of bed material for the Bernardo data was in the clay-size range.

Some of the characteristics that may influence Z_1 values for the different reaches are flow regime and bed conditions. The Bernalillo data have low $\overline{V}/V_*''$ values for a given ψ' (fig. 6) and high k's for low $C/\sqrt{g}$ values (fig. 5), thus indicating the persistence of dunes

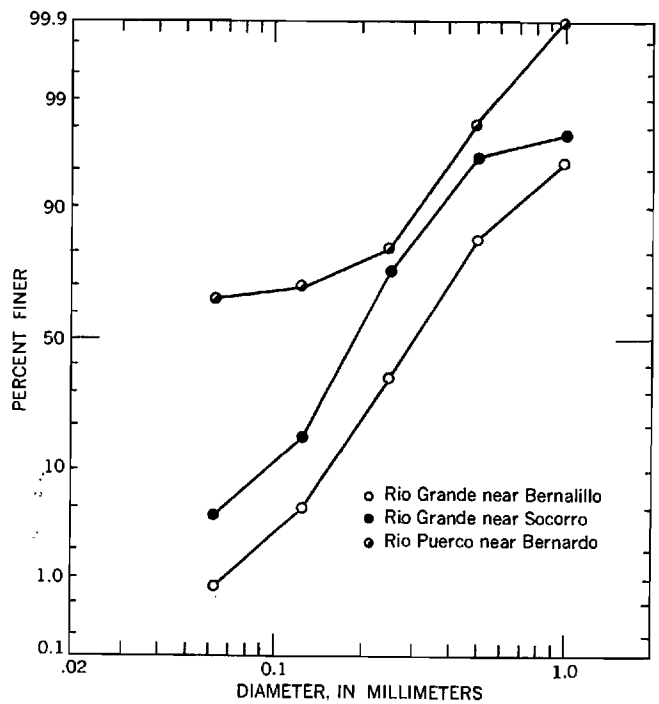

FIGURE 11.—Average particle-size distribution of bed material.

in this reach. The flow in the Socorro reach is mostly in transition and upper regime, while at Bernardo the bed was armored with clay. The launching of the particles into suspension may be different from a dune bed than from a plane bed. The suspended sand in the Bernardo reach is probably not from the bed, but is supplied from an upstream source. All these factors contribute to the apparent difference of the measured suspended-sediment distributions for Bernalillo, Socorro, and Bernardo.

Figure 12 shows Z_1 to vary curvilinearly with the fall velocity. For comparison, curves showing the variation of Z_1 with the 0.55 power of the fall velocity are plotted on the figure for the Bernalillo and Socorro reaches. When one point is high, the corresponding points for adjacent size classes are also high. Colby and Hembree (1955) found Z_1 to vary with the 0.7 power of the fall velocity in the Niobrara River. The suspended-sediment distribution is relatively more uniform for the Rio Grande than for the Niobrara River.

Vanoni (1946) and Ismail (1952) proposed that ϵ_s is not the same as ϵ_m but is related by the factor of proportionality $\beta=\epsilon_s/\epsilon_m$ where β seems to be a function of particle size. Also

$$Z_1=\frac{\omega}{\beta k V_*}=\frac{Z_k}{\beta};\ \beta=\frac{Z_k}{Z_1}$$

thus β indicates the deviation of Z_1 from Z_k.

Ismail (1952) found ϵm affected only through changes in k when sand was present. Values of ϵ_m could not be measured directly but could be evaluated by studying ϵ_s and the relations between ϵ_m and ϵ_s. He found that $\beta=1.5$ for a 0.10 mm sand and 1.3 for a 0.16 mm sand.

Figure 13 shows the comparison of k and β for the three size classes used herein. Trend by size class is evident. When the value of β for one size class is large, the corresponding β's for the other size classes are also high. Thus the trend is consistent within itself. β and k are intimately related. It is noted that at $k=0.4$, average values of β are approximately 0.85, 1.4, and 2.2 or greater for the 0.062–0.125 mm, 0.125–0.250 mm, 0.250–0.500 mm size classes, respectively. The value 1.4 compares favorably with Ismail's value of 1.3 for 0.16 mm sand. Ismail's k values were slightly less than 0.4. From Ismail's findings, β decreased with increasing particle size. For the data herein, β increases with increasing particle size and with decreasing roughness. It is of special interest that β values are closest to 1.0 for lower regime flow, where k values vary upward to about 1.2; while for upper regime flow, where k ranges from about 0.2 to 0.4, β varies upward to about 9. This indicates that for flow over a dune bed the predicted suspended-sediment distribution follows approximately the measured distribution; for flow over a plane bed, the predicted suspended-sediment distribution deviates considerably from the measured distribution. On the other hand, measured velocity distribution for upper regime flow follows a predicted distribution ($k\approx0.4$), while for lower regime flow the velocity distribution is more uniform than predicted ($k\gg0.4$). These relations are shown qualitatively in figure 14.

Einstein and Chien (1954) presented several approaches to the solution of the suspended load theory using various assumptions on the nature of the mixing length and turbulence characteristics. All of the approaches are cumbersome and require that experimentally determined constants be selected on the basis of measured data. The approach which most closely

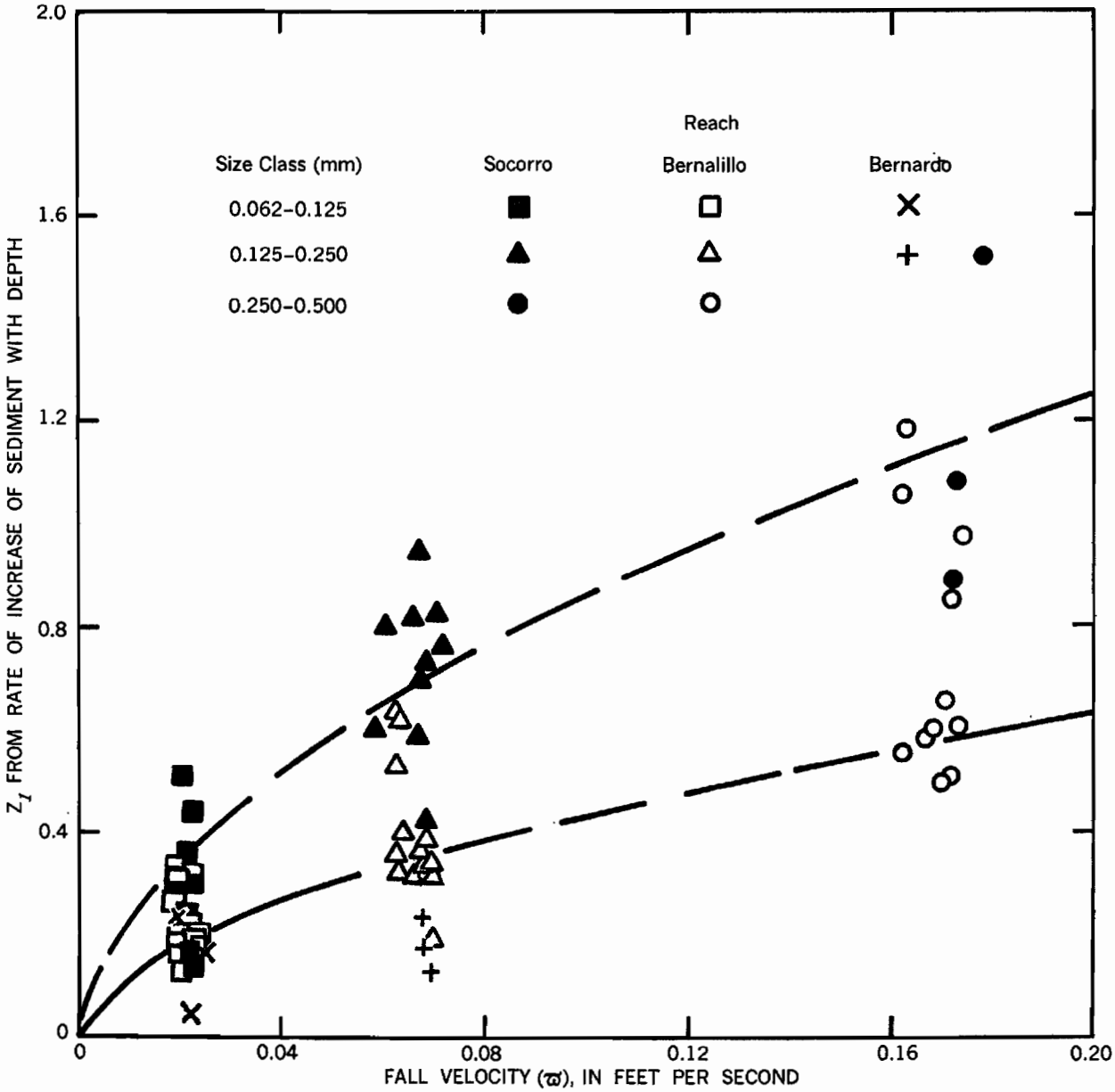

FIGURE 12.—Variation of Z_1 and fall velocity.

fits the measured suspended-sediment distribution herein is given by the following equation:

$$\frac{c_y}{c_a}=\left[\frac{1-\sqrt{\frac{D-a}{D}}}{1-\sqrt{\frac{D-y}{D}}}\right]^{\frac{Z}{1+NkZ}}\left[\frac{1+\sqrt{\frac{D-a}{D}}}{1+\sqrt{\frac{D-y}{D}}}\right]^{\frac{Z}{1-NkZ}}\left[\frac{\sqrt{\frac{D-a}{D}}+NkZ}{\sqrt{\frac{D-y}{D}}+NkZ}\right]^{\frac{2Z}{N^2k^2Z^2-1}} \quad (13)$$

where

N=an experimentally determined constant
$Z=\omega/kV_*$

In deriving this equation, Einstein and Chien assumed that the turbulence was unsymmetric. Equation 13 using a value of $Nk=0.4$ is shown on figure 10. The equation generally fits the trend of the measured data throughout the range of values. It should be noted that the distribution function given by equation 13 is changed from the functional relation of equation 4, but the suspended-sediment distribution can still be approximated by a straight line for a plot of c versus $(D-y)/y$ on a logarithmic plot. For small Z values in equation 13.

$$\frac{c_y}{c_a}\rightarrow\left(\frac{D-y}{y}\cdot\frac{a}{d-a}\right)^Z$$

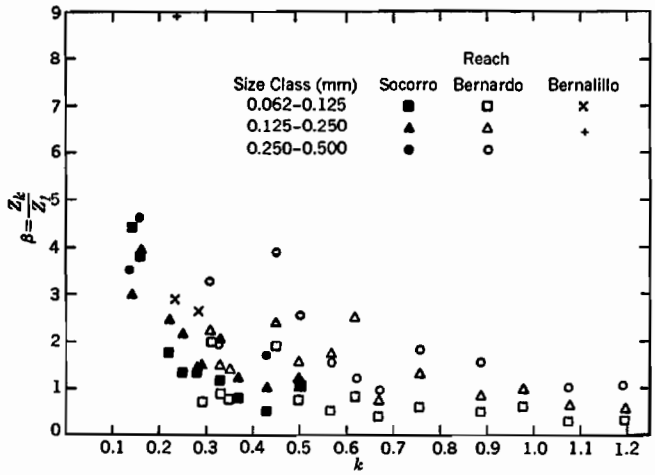

FIGURE 13.—Variation of k and β.

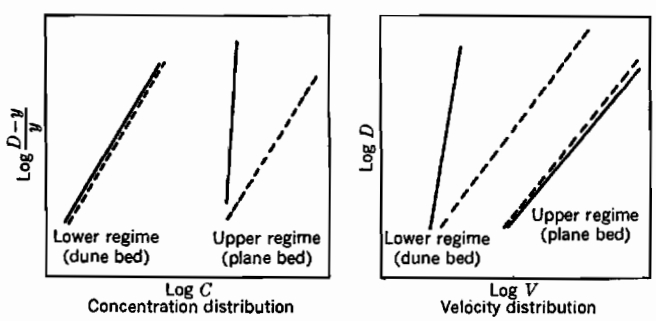

FIGURE 14.—Qualitative relation of predicted and measured velocity and suspended-sediment distribution for lower regime flow and upper regime flow. Predicted distribution, dashed line; measured distribution, solid line.

Einstein and Chien (1954) favored an approach where mixing length and velocity fluctuations of turbulent flow follow certain probability distributions, and the higher derivative terms of the concentration gradient are included. For low Z values, this approach does not fit the data herein as well as that given by equation 13.

Einstein (1950) used the shear velocity with respect to the sand grain, V_*', in equation 5 to compute the distribution exponent Z. Values of Z computed in this manner show the same trend as indicated in figure 10. Because $V_*'<V_*$, the values of Z deviate even further from the measured values than those computed using V_*. Vanoni and Brooks (1957) have questioned the use of V_*' in computing the distribution exponent Z.

In modifying the suspended-sediment distribution theory, Einstein and Chien (1954) used $V_*=\sqrt{gDS}$ to compute values of Z. Presumably, the flow was over a plane bed, and it was implied that for flow over a dune bed, V_*' should be used. For most field data, V_*' is less than V_*, even for upper regime flow; that is, there are always some additional frictional losses beyond those due to the grain roughness only. Thus, in using the approaches suggested by Einstein and Chien, and in defining the constants, for example N in equation 13, it is important that the shear velocity used in computing the values of Z be consistent throughout.

Einstein and Chien (1955) also suggest that k from the graphical relation of figure 4 be used in computing Z. For the data presented herein, the relation does not define the value of k for lower regime flow.

EFFECTS OF HIGH CONCENTRATIONS ON FALL VELOCITY

The observations of velocity and concentration distributions for the Rio Puerco near Bernardo and for the Rio Grande near Socorro (August 17, 1954) were obtained in flows which carried high concentrations of fine material (<0.062 mm) in suspension. The Socorro flow was inflow from the Rio Puerco.

The Rio Puerco flows intermittently. Concentrations of fine material of 100,000 ppm (parts per million) are common, and concentrations up to 400,000 ppm are not unusual. Core samples of the bed of the Rio Puerco show the bed material to be a fine sand with a size distribution similar to that of the Socorro reach ($d_{50}\approx 0.20$ mm). As flow recedes, clay impregnates the bed to a depth of about 0.6 foot. When the bed dries, this clay-impregnated layer hardens into an armor coating.

When the bed of the Rio Puerco is armored with clay, the concentrations of suspended sand are low, probably because the material is not readily available for transport. When the clay layer is broken up, and flow is over the sand bed, the capacity of the Rio Puerco to transport sand is several times greater than the capacity of a stream with comparable flow of clear water or flow carrying negligible concentrations of fine material. The major factors which contribute to this increased capacity for transport are the increase in viscosity and mass density of the fluid and the concurrent decrease in the fall velocity of the sediment (Simons and others, 1961).

The general effects of concentration on fall velocity in sedimentation chambers have been investigated ("Inter-Agency Report No. 12, 1957"), but the overall effects of high concentrations under natural stream conditions are not known. Figure 15 shows the apparent reduction in fall velocity at 24°C for various concentrations of fine material for the geometric mean diameters of the three size classes used in this report. This figure was developed from visual accumulation tube analyses of bed material in clear water and in native water of the Rio Puerco with varying concentrations of suspended fine material. The reduction in fall velocity thus includes the effects of the dissolved solids as well as the effects of the fine material.

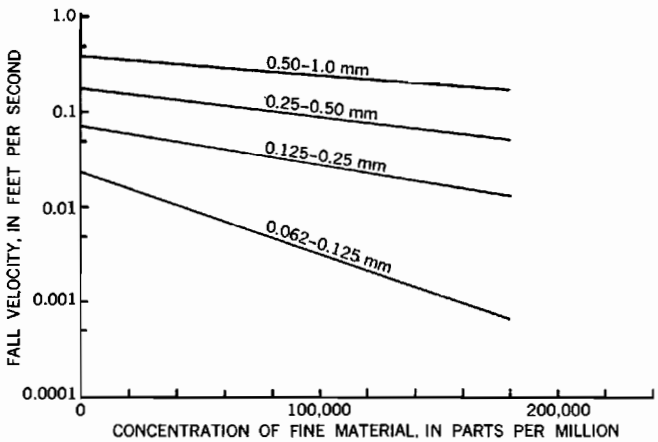

FIGURE 15.—Variation of fall velocity with concentration of fine material.

Figure 15 was developed from limited data and should be considered tentative. The reduction of fall velocity with increased concentration in the visual accumulation tube is probably not quantitatively comparable to the reduction in fall velocity which actually occurs in the stream, but figure 15 shows clearly that the effect of concentration on fall velocity is appreciable for the range of conditions encountered in the Rio Puerco flow. If the fall velocities from figure 15 are assumed applicable in computing Z, values of the computed sediment distribution exponent show much closer agreement with the measured exponent Z_1 for the high concentration flows at Bernardo and Socorro (fig. 16). The effect of concentration on fall velocity for concentrations less than about 10,000 ppm in the Rio Puerco and middle Rio Grande is negligible for practical purposes.

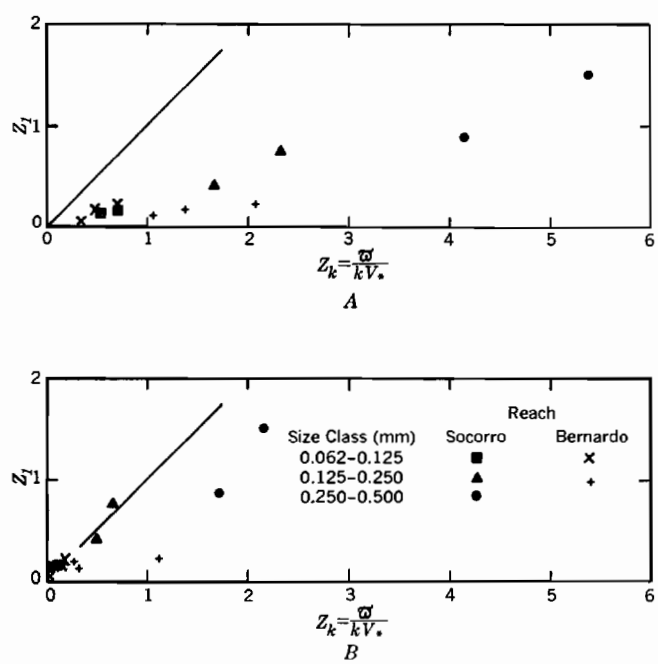

FIGURE 16.—Comparison of measured sediment distribution exponent, Z_1, with the exponent, Z_k, computed (a) using fall velocities in distilled water, and (b) using fall velocities from figure 15.

CONCLUSIONS

For the data presented, measured values of vertical velocity and suspended-sediment concentration distributions were compared with values predicted from theoretical considerations. The data included observations of flow in lower regime, transition zone, several in upper regime, and several with high suspended-sediment concentrations. Results and conclusions, some of which may be applicable only for this study, are summarized as follows:

1. For flow over a dune bed, the predicted suspended-sediment distribution follows approximately the measured distribution, and the velocity distribution is more uniform than predicted; while for flow over a plane bed, the predicted suspended-sediment distribution deviates considerably from the measured distribution, and the velocity distribution follows approximately the predicted distribution.
2. Mean velocity for the Rio Grande near Bernalillo and near Socorro is adequately described by the Einstein-Barbarossa bar-resistance relation.
3. For a given reach the range of values for K_s depends on bed configuration. However, the average value of K_s for a reach does not appear to be related to bed configuration, but depends upon size of bed material. For the three reaches, the average value of K_s is approximately 400 times as large as d_{65}.
4. The value of the coefficient of turbulent exchange, k, decreases with high concentration for upper regime flow; and varies widely for lower regime flow, probably due to a three-dimensional flow effect. There is not apparent effect of concentration on k for flow over a dune bed. The coefficient k appears to decrease with decreasing bed roughness as measured indirectly by $C/\sqrt{g}$ for transition and upper regime flow.
5. The suspended sediment is distributed more uniformly than conventional theory predicts. The deviation of the measured exponent, Z_1, from the computed exponent, Z, becomes greater with increasing particle size. Differences between measured and computed values of Z are due to flow regime, to size of bed material, and to the effects of the concentrations of suspended fine material.
6. The measured exponent, Z_1, varies with about the 0.55 power of the fall velocity.
7. The factor of proportionality β increases with increasing particle size and with decreasing roughness. Values of β are closest to 1.0 for flow over a dune bed.
8. Fall velocity is effectively decreased in flows with concentrations greater than about 10,000 ppm.

BASIC DATA AND COMPUTED PARAMETERS

TABLE 1.—*Velocity distribution*

Date	Reach	Section	No. of vertical	Temp	D	Horizon A		Horizon B		Horizon C		Horizon D		Horizon E	
						y	v	y	v	y	v	y	v	y	v
				°F	ft	ft	ft per sec	ft	ft per sec	ft	ft per sec	ft	ft per sec	ft	ft per sec
6–2–53	Bernalillo	A–2	1	------	3.0	0.30	2.68	1.00	3.26	1.50	3.58	2.00	3.58	2.70	3.38
			2	------	3.0	.30	2.75	1.00	3.10	1.50	3.38	2.00	3.51	2.70	3.54
			3	71	2.6	.30	3.74	.80	3.94	1.20	4.08	1.70	4.04	2.20	3.99
			4	70	3.0	.30	1.84	1.00	3.30	1.50	4.28	2.00	4.66	2.70	4.38
			5	70	2.6	.30	3.26	.80	3.90	1.20	4.04	1.70	4.28	2.20	4.54
			6	70	2.7	.30	3.51	.80	3.82	1.20	3.74	1.70	3.74	2.20	3.74
			7	70	2.5	.30	2.45	.80	3.70	1.20	3.74	1.70	3.90	2.20	3.94
			8	71	2.5	.30	2.87	.80	3.00	1.20	3.00	1.70	2.81	2.20	2.75
			9	71	2.5	.30	1.88	.80	2.36	1.20	2.75	1.70	2.81	2.20	2.72
			10	71	2.4	.30	2.08	.80	2.18	1.20	2.30	1.60	2.25	2.10	2.28
			11	71	2.5	.30	1.84	.80	1.88	1.20	2.36	1.70	2.62	2.20	2.65
			12	71	4.0	.40	2.08	1.20	2.20	2.00	2.50	2.80	2.75	3.60	2.81
			13	71	5.0	.50	1.48	1.40	2.01	2.30	2.53	3.10	2.75	4.50	2.90
			14	72	5.0	.50	2.87	1.50	3.00	2.50	3.00	3.50	2.81	4.50	2.75
			15	71	5.4	.50	1.01	1.70	2.10	2.70	2.53	3.80	2.72	4.90	2.65
4–53	do	A–2	1	62	2.5	.30	3.35	.80	4.18	1.30	4.38	1.70	4.38	2.20	4.18
			2	62	2.0	.30	2.87	.60	3.21	1.00	2.93	1.40	2.90	1.70	2.62
			3	63	2.5	.30	3.26	.80	3.38	1.30	3.70	1.70	3.74	2.20	3.74
		A	1	------	3.5	.30	3.72	1.00	4.09	1.75	4.36	2.50	4.36	3.20	4.25
			2	------	4.6	.40	4.36	1.20	4.59	2.30	5.06	3.20	5.18	4.20	4.84
			3	------	4.6	.40	4.74	1.20	5.00	2.30	5.44	3.20	5.06	4.20	4.50
		C	1	70	1.6	.30	.75	.60	1.06	.80	1.21	1.00	1.50	1.30	1.61
			2	71	2.7	.30	2.56	.80	3.07	1.40	3.14	1.90	3.32	2.40	3.08
			3	71	3.2	.40	1.21	1.00	3.10	1.60	3.51	2.20	3.90	2.80	3.94
		E	1	------	3.8	.50	3.43	1.20	3.76	1.90	4.02	2.60	4.06	3.30	4.15
			2	------	1.6	.30	2.61	.55	2.67	.80	2.86	1.05	2.77	1.30	2.74
			3	70	2.1	.30	3.25	.70	3.51	1.10	3.38	1.50	3.30	1.80	3.07
4–13–54	do	B	1	61	1.5	.20	1.38	.38	1.88	.75	2.24	1.20	2.34	------	------
			2	61	1.1	.20	1.88	.28	2.15	.55	2.20	.88	1.96	------	------
			3	61	1.7	.20	1.23	.42	2.10	.85	2.15	1.36	2.29	------	------
			4	62	1.5	.20	1.08	.38	1.47	.75	1.92	1.20	2.00	------	------
			5	63	2.5	.20	1.84	.62	2.80	1.25	3.43	2.00	3.64	------	------
		C	1	63	1.5	.20	1.58	.38	1.80	.75	1.96	1.20	1.94	------	------
			2	64	.8	.20	1.88	.20	1.96	.40	2.22	.64	1.73	------	------
			3	64	1.1	.20	2.49	.28	2.49	.55	2.61	.88	2.42	------	------
			4	64	2.5	.20	1.23	.62	1.92	1.20	2.05	2.00	2.00	------	------
			5	63	4.4	.20	1.50	1.10	3.02	2.20	3.33	3.52	3.50	------	------
		D	1	63	2.0	.30	.43	.50	.78	1.00	2.33	1.50	2.28	------	------
			2	63	1.9	.30	1.16	.50	1.12	1.00	2.33	1.40	2.50	------	------
			3	63	1.6	.30	2.47	.40	2.42	.80	2.80	1.10	2.80	------	------
			4	63	1.8	.30	1.72	.50	1.90	.90	2.15	1.30	2.33	------	------
			5	63	2.2	.30	2.65	.60	2.77	1.10	2.89	1.70	2.89	------	------
		E	1	62	1.7	.30	2.13	.50	2.13	.80	2.30	1.20	2.50	------	------
			2	62	2.7	.30	1.14	.60	1.40	1.20	1.66	2.20	1.90	------	------
			3	62	2.0	.30	2.23	.40	2.20	.80	2.40	1.50	2.47	------	------
			4	62	2.5	.30	1.10	.60	1.28	1.20	1.82	2.00	2.42	------	------
			5	61	2.1	.30	1.50	.60	1.86	1.10	1.92	1.60	1.90	------	------
5–19–54	do	B	1	70	4.7	.20	3.05	1.18	3.57	2.35	3.97	3.52	4.02	------	------
			2	69	4.6	.20	2.80	1.15	3.50	2.30	3.97	3.45	4.36	------	------
			3	68	2.6	.20	3.32	.65	4.06	1.30	4.25	1.95	4.36	------	------
			4	67	1.8	.20	1.51	.45	2.00	.90	2.49	1.35	2.86	------	------
			5	65	1.9	.20	1.84	.48	2.20	.95	2.05	1.42	2.05	------	------
		C	1	72	5.0	.15	1.32	1.25	2.67	2.50	3.13	3.75	3.20	------	------
			2	74	1.6	.15	.84	.40	1.62	.80	1.54	1.20	1.08	------	------
			3	74	2.0	.15	1.76	.50	2.05	1.00	1.70	1.50	2.15	------	------
			4	73	2.1	.15	1.58	.52	2.25	1.05	2.49	1.58	2.55	------	------
			5	73	2.1	.15	1.84	.52	2.25	1.05	2.49	1.58	2.44	------	------

TABLE 1.—*Velocity distribution*—Continued

Date	Reach	Section	No. of vertical	Temp	D	Horizon A		Horizon B		Horizon C		Horizon D		Horizon E	
						y	*v*	*y*	*v*	*y*	*v*	*y*	*v*	*y*	*v*
				°F	*ft*	*ft*	*ft per sec*	*ft*	*ft per sec*	*ft*	*ft per sec*	*ft*	*ft per sec*	*ft*	*ft per sec*
5-19-54		D	1	72	1.2	.30	1.94	.60	2.18	.90	2.13	------	------	------	------
			2	72	2.2	.55	2.37	1.10	2.50	1.65	2.77	------	------	------	------
			3	73	2.0	.50	2.53	1.00	2.47	1.50	2.53	------	------	------	------
			4	73	1.9	.48	3.02	.95	3.24	1.42	3.32	------	------	------	------
			5	73	1.6	.40	1.31	.80	1.62	1.20	1.79	------	------	------	------
		E	1	71	2.9	.72	4.01	1.45	4.36	2.16	4.69	------	------	------	------
			2	71	2.1	.50	3.02	1.05	3.64	1.60	3.76	------	------	------	------
			3	70	1.5	.38	2.96	.75	3.02	1.12	2.68	------	------	------	------
			4	69	2.4	.60	1.94	1.20	2.28	1.80	2.47	------	------	------	------
			5	67	1.1	.25	2.28	.55	2.77	.85	2.53	------	------	------	------
4-16-54	Socorro	A-1	1	51	2.7	.30	1.67	.50	2.34	1.40	3.14	2.20	3.58	------	------
			2	54	2.8	.30	4.08	.50	4.57	1.40	5.48	2.30	5.86	------	------
			3	54	3.5	.30	3.07	.50	3.38	1.80	4.98	3.00	5.97	------	------
			4	56	3.0	.30	3.30	.50	4.38	1.50	4.30	2.50	4.38	------	------
			5	59	1.4	.30	.39	.50	.49	.70	.63	1.10	.74	------	------
		A-2	1	56	1.3	.20	2.99	.32	3.43	.65	3.88	.90	4.06	------	------
			2	57	.7	.20	3.30	.18	3.97	.35	4.15	.42	4.45	------	------
			3	58	1.3	.20	2.99	.32	4.06	.65	4.45	.90	4.64	------	------
			4	59	.9	.20	1.84	.22	2.53	.45	2.86	.60	2.99	------	------
			5	60	1.1	.20	1.03	.28	1.38	.55	1.80	.75	1.88	------	------
		B	1	71	1.5	.30	2.59	.70	3.07	1.00	3.14	------	------	------	------
			2	70	1.1	.30	1.17	.50	1.39	.80	1.58	------	------	------	------
			3	69	1.1	.30	3.07	.50	3.25	.80	3.38	------	------	------	------
			4	68	1.0	.30	3.44	.50	3.82	.70	3.90	------	------	------	------
			5	68	1.1	.30	3.44	.50	3.51	.80	3.90	------	------	------	------
		B-1	1	71	2.8	.20	1.26	.70	2.10	1.40	2.05	1.90	1.96	------	------
			2	72	4.0	.20	1.96	1.00	2.49	2.00	2.34	2.80	2.15	------	------
			3	72	4.1	.20	3.05	1.00	3.88	2.05	4.15	2.90	4.50	------	------
			4	72	3.3	.20	3.04	.82	4.45	1.65	4.74	2.30	5.44	------	------
			5	72	1.0	.20	2.05	.25	2.92	.50	3.72	.73	3.60	------	------
5-21-54	do	A-1	1	67	3.4	.20	2.27	.85	2.65	1.70	2.96	2.55	3.09	------	------
			2	68	1.8	.20	2.83	.45	3.47	.90	3.93	1.35	4.20	------	------
			3	69	1.3	.20	3.34	.30	3.84	.65	4.30	1.00	4.69	------	------
			4	70	1.0	.20	3.32	.25	3.68	.50	4.20	.75	4.20	------	------
			5	71	1.2	.20	2.77	.30	3.02	.60	3.54	.90	3.61	------	------
		A-2	1	65	1.2	.20	2.77	.30	3.16	.60	3.61	.90	3.76	------	------
			2	67	1.1	.20	3.47	.28	3.76	.55	4.01	.83	4.36	------	------
			3	66	1.1	.20	3.32	.28	3.54	.55	3.97	.83	4.20	------	------
			4	67	1.1	.20	2.83	.28	3.09	.55	3.68	.83	3.80	------	------
			5	68	1.5	.20	2.65	.38	3.02	.75	3.40	1.12	3.68	------	------
		B	1	75	2.4	.20	1.45	.60	1.60	1.20	1.58	1.80	1.64	------	------
			2	73	.8	------	------	.20	2.71	.40	3.12	.60	3.16	------	------
			3	72	.8	.20	2.96	.25	3.24	.40	3.47	.60	3.47	------	------
			4	72	.7	------	------	.20	3.16	.35	3.58	.52	3.40	------	------
			5	71	.9	------	------	.22	2.96	.45	3.28	.68	3.20	------	------
		B-1	1	75	.9	.20	2.65	.30	3.02	.45	3.40	.70	3.32	------	------
			2	75	1.3	.20	2.96	.30	3.16	.65	3.84	1.00	3.93	------	------
			3	75	.8	------	------	.20	3.24	.40	3.76	.60	3.64	------	------
			4	75	1.7	.20	1.46	.42	1.53	.85	1.38	1.28	1.53	------	------
			5	75	2.0	.20	3.09	.50	3.48	1.00	3.80	1.50	3.97	------	------
8-17-54		A-1	1	70	2.2	.20	3.07	.55	3.66	1.10	3.90	1.65	4.76	------	------
			2	71	2.9	------	------	.72	6.56	1.45	8.31	2.18	8.74	------	------
			3	72	3.2	------	------	.80	5.65	1.60	7.29	2.40	8.74	------	------
			4	72	2.0	.20	3.74	.50	4.76	1.00	6.19	1.50	6.44	------	------
			5	73	2.8	.20	2.81	.70	3.78	1.40	4.71	2.10	4.87	------	------
		A-2	1	74	1.8	.20	3.66	.45	4.38	.90	5.95	1.35	6.63	------	------
			2	------	2.1	.20	3.92	.52	5.48	1.05	7.13	1.58	7.90	------	------
			3	------	2.5	.30	3.90	.60	6.44	1.25	6.91	1.90	8.92	------	------
			4	------	2.6	------	------	.65	6.25	1.30	8.10	1.95	8.49	------	------
			5	78	3.6	------	------	.90	6.63	1.80	7.54	2.70	8.10	------	------

TABLE 1.—*Velocity distribution*—Continued

Date	Reach	Section	No. of vertical	Temp	D	Horizon A		Horizon B		Horizon C		Horizon D		Horizon E	
						y	*v*	*y*	*v*	*y*	*v*	*y*	*v*	*y*	*v*
				°*F*	*ft*	*ft*	*ft per sec*	*ft*	*ft per sec*	*ft*	*ft per sec*	*ft*	*ft per sec*	*ft*	*ft per se*
7–10–61	Bernardo	------	1	------	2. 6	. 30	2. 92	. 70	3. 28	1. 10	3. 80	1. 60	3. 97	2. 20	3. 97
			2	------	2. 5	. 30	2. 86	. 70	3. 43	1. 20	3. 72	1. 70	3. 97	2. 10	3. 97
8–18–61	do	------	1	75	3. 6	. 50	3. 20	1. 00	3. 88	2. 00	4. 25	3. 00	4. 54	------	------
			2	75	2. 6	. 50	3. 43	1. 10	3. 97	1. 60	4. 15	2. 10	4. 15	------	------
19–61	do	------	1	74	5. 8	. 50	3. 80	1. 00	4. 25	2. 20	4. 84	3. 40	5. 18	4. 60	5. 18
			2	74	4. 8	. 50	4. 45	. 80	4. 48	1. 80	4. 69	2. 80	4. 88	3. 80	5. 12

TABLE 2.—*Suspended-sediment distribution*

Date	Reach	Section	Horizon	Average $\frac{D-y}{y}$	Concentration, ppm of indicated sizes: <0.0625	0.0625–0.125	0.125–0.25	0.25–0.50	Total
					mm	*mm*	*mm*	*mm*	
6– 2–53	Bernalillo	A–2	A	8. 28	1, 300	726	637	207	2, 870
			B	2. 17	1, 310	569	396	85	2, 360
			C	1. 07	1, 240	500	284	63	2, 090
			D	. 50	1, 240	398	239	58	1, 930
			E	. 13	1, 150	309	168	23	1, 650
4–53	do	A–2	A	6. 78	840	489	403	59	1, 790
			B	2. 19	1, 070	381	156	16	1, 620
			C	. 95	907	386	261	27	1, 580
			D	. 46	861	287	169	13	1, 330
			E	. 15	837	291	169	33	1, 330
		A	A	10. 54	802	656	821	80	2, 360
			B	2. 73	796	572	396	45	1, 810
			C	1. 00	804	451	270	15	1, 540
			D	. 43	704	368	159	9	1, 240
			E	. 09	719	282	144	6	1, 150
		C	A	6. 44	895	355	334	76	1, 660
			B	2. 08	830	314	208	18	1, 370
			C	. 98	775	248	117	9	1, 150
			D	. 49	734	248	124	15	1, 120
			E	. 16	753	191	81	5	1, 030
		E	A	5. 64	774	334	434	48	1, 590
			B	2. 03	827	222	291	40	1, 380
			C	. 97	821	238	258	34	1, 350
			D	. 46	763	189	165	14	1, 130
			E	. 18	675	156	120	6	956
4–13–54	do	B	A	15. 6	3, 090	988	1, 250	188	5, 520
			B	2. 98	2, 920	537	431	27	3, 920
			C	1. 00	2, 870	361	200	10	3, 440
			D	. 25	2, 720	270	105	----------	3, 100
		C	A	19. 6	2, 890	567	859	44	4, 360
			B	2. 98	2, 620	344	305	43	3, 310
			C	1. 00	2, 670	315	272	23	3, 280
			D	. 25	2, 720	267	191	10	3, 180
		D	A	18. 0	2, 550	769	1, 120	330	4, 930
			B	2. 81	2, 810	344	315	107	3, 580
			C	. 98	2, 730	241	178	29	3, 170
			D	. 36	2, 740	230	92	3	3, 070
4–13–54	do	E	A	21. 0	3, 100	749	1, 300	604	5, 810
			B	3. 11	2, 840	357	350	61	3, 610
			C	1. 17	2, 770	304	240	23	3, 340
			D	. 31	2, 750	246	135	13	3, 150

TABLE 2.—*Suspended-sediment distribution*—Continued

Date	Reach	Section	Horizon	Average $\frac{D-y}{y}$	Concentration, ppm of indicated sizes				
					<0.0625	0.0625–0.125	0.125–0.25	0.25–0.50	Total
					mm	*mm*	*mm*	*mm*	
5-19-54	Bernalillo	B	A	30.2	2,850	710	1,150	456	5,180
			B	2.99	2,880	454	431	116	3,880
			C	1.00	2,880	476	381	76	3,810
			D	.33	2,760	403	264	45	3,470
		C	A	24.6	2,490	863	1,200	439	4,990
			B	3.02	2,390	482	302	32	3,210
			C	1.00	2,380	440	240	18	3,080
			D	.33	2,300	377	199	6	2,880
		D	A	16.8	2,390	382	348	44	3,160
			B	2.99	2,370	444	210	21	3,040
			C	1.00	2,270	323	142	8	2,740
			D	.33	2,360	267	95	5	2,720
		E	A	19.0	2,900	715	1,120	327	5,110
			B	3.12	2,890	388	237	11	3,530
			C	1.00	2,760	258	170	3	3,260
			D	.32	2,760	252	96	3	3,110
4-16-54	Socorro	A-1	A	26.0	6,490	1,620	2,740	154	11,000
			B	4.36	5,390	1,120	897	----------	7,410
			C	.97	5,240	641	408	----------	6,280
			D	.22	4,840	313	148	----------	5,300
		A-2	A	9.60	5,890	1,310	1,450	17	8,680
			B	3.02	5,660	1,050	560	----------	7,270
			C	1.00	5,200	512	176	----------	5,880
			D	.50	5,180	488	134	----------	5,810
		B	A	10.6	6,390	1,290	626	42	8,350
			B	2.87	6,270	755	232	----------	7,260
			C	1.15	5,740	399	203	----------	6,340
			D	.41	5,400	405	65	----------	5,870
		B-1	A	29.4	6,660	1,850	2,460	316	11,300
			B	3.02	5,720	661	564	14	6,960
			C	1.00	5,520	376	158	6	6,060
			D	.42	5,580	326	109	12	6,030
5-21-54	do	A-1	A	7.70	14,300	2,220	1,660	36	18,200
			B	3.06	13,900	1,050	431	----------	15,400
			C	1.00	13,600	754	160	----------	14,500
			D	.32	13,600	525	43	----------	14,200
		A-2	A	5.00	15,200	2,590	2,230	100	20,100
			B	2.95	15,000	1,570	564	----------	17,100
			C	1.00	14,800	1,060	242	----------	16,100
			D	.33	14,500	544	91	----------	15,100
		B	A	6.60	13,500	1,000	465	----------	15,000
			B	3.52	13,800	1,040	444	----------	15,300
			C	1.00	13,300	649	169	----------	14,100
			D	.33	12,900	612	109	----------	13,600
		B-1	A	5.70	13,000	1,620	2,020	67	16,700
			B	2.88	13,300	1,120	680	----------	15,100
			C	1.00	12,900	778	250	----------	13,900
			D	.32	12,600	475	106	----------	13,200
8-17-54	do	A-1	A	12.6	109,000	13,700	18,100	5,000	147,000
			B	3.00	110,000	10,800	11,200	396	132,000
			C	1.00	107,000	10,500	6,880	250	125,000
			D	.33	105,000	8,380	4,010	118	118,000
		A-2	A	10.8	100,000	15,600	38,500	4,770	159,000
			B	3.04	100,000	17,700	13,600	528	132,000
			C	1.00	98,900	15,100	7,810	122	122,000
			D	.33	99,100	8,140	2,750	----------	110,000

TABLE 2.—*Suspended-sediment distribution—Continued*

Date	Reach	Section	Horizon	Average $\frac{D-y}{y}$	Concentration, ppm of indicated sizes				
					<0.0625	0.0625–0.125	0.125–0.25	0.25–0.50	Total
					mm	*mm*	*mm*	*mm*	
7–10–61	Bernardo		A	7.33	66,400	475	881		67,800
			B	3.27	65,600	398	265		66,300
			C	1.08	65,700	265	199		66,200
			D	.47	64,900	261	131		65,300
			E	.19	65,200	196	131		65,500
8–18–61	do		A	4.20	177,000	410	374		178,000
			B	1.36	177,000	357	357		178,000
			C	.62	177,000	391	355		178,000
			D	.24	177,000	268	250		178,000
19–61	do		A	9.60	128,000	1,970	1,520		132,000
			B	4.90	127,000	1,870	1,330		130,000
			C	1.66	128,000	1,790	1,320		131,000
			D	.71	128,000	1,860	1,130		131,000
			E	.26	125,000	1,850	955		128,000

TABLE 3.—*Basic data*

Reach	Date	Section	Q	W	$\bar{D}$	$\bar{V}$	Ave. temp.	Slope	Composition of bed material: Percent finer than indicated size					d_{33}	d_{50}	d_{65}
									0.062	0.125	0.250	0.500	1.000			
			cfs	*ft*	*ft*	*ft per sec*	°*F*	*ft per ft*	*mm*	*mm*	*mm*	*mm*	*mm*	*mm*	*mm*	*mm*
Bernalillo	6–2–53	A–2	2,150	270	2.56	3.11	71	[a] 0.000826	0.7	4.1	27.8	86.6	97.9	0.27	0.32	0.37
	4–53	A–2	2,090	270	2.48	3.12	62	.000826	.5	3.7	34.1	74.3	91.0	.25	.33	.42
		A	1,970	397	1.69	2.94	66	.000826	1.0	6.0	32.9	89.4	97.4	.25	.30	.35
		C	2,070	376	2.36	2.33	71	.000826	.3	1.8	16.9	57.8	87.8	.35	.42	.60
		E	1,780	268	2.47	2.69	70	.000826	.6	4.5	43.7	94.8	99.0	.23	.26	.31
	4–13–54	B	1,200	432	1.42	1.96	62	.000864	.5	12.4	45.7	96.3	99.7	.21	.26	.30
		C	1,160	370	1.45	2.17	63	.000864	.9	6.1	43.0	90.4	97.3	.35	.37	.56
		D	1,160	399	1.53	1.89	63	.000864	1.2	7.5	40.2	84.9	96.3	.23	.29	.35
		E	1,200	265	1.98	2.30	62	.000864	1.0	5.9	35.5	80.5	95.1	.25	.31	.38
	5–19–54	B	1,450	434	1.33	2.51	68	.000864	1.0	5.6	34.8	82.4	94.5	.25	.31	.38
		C	1,430	383	1.96	1.90	73	.000864	.7	4.3	30.6	76.2	94.5	.26	.27	.41
		D	1,410	401	1.50	2.35	73	.000864	.6	3.7	34.5	81.6	94.1	.25	.31	.38
		E	1,430	266	1.95	2.75	70	.000864	1.0	5.2	36.9	90.4	98.1	.25	.30	.35
Socorro	4–16–54	A–1	697	175	1.53	2.60	55	.000758	3.6	16.7	68.1	83.2	84.2	.15	.17	.19
		A–2	697	241	1.00	2.90	58	.000758	4.2	19.9	87.4	99.3	99.9	.15	.17	.19
		B	697	447	.66	2.36	69	.000980	5.4	25.1	85.7	98.7	99.4	.14	.16	.19
		B–1	697	202	1.44	2.40	72	.000980	1.7	10.0	67.2	94.5	98.2	.18	.21	.24
	5–21–54	A–1	891	222	1.16	3.45	69	.000844	3.2	16.6	76.5	96.5	99.1	.16	.19	.22
		A–2	900	233	1.20	3.21	67	.000844	4.7	21.4	88.0	99.2	99.8	.14	.16	.19
		B	874	327	1.07	2.50	73	.00100	8.8	29.0	89.8	99.2	99.6	.13	.15	.18
		B–1	840	368	.91	2.51	75	.00100	2.3	11.3	79.2	98.4	99.0	.16	.19	.21
	[b] 8–17–54	A–1	3,600	258	2.30	6.07	72	.000855	5.3	12.6	53.4	94.4	99.4	.19	.24	.29
		A–2	3,550	234	2.38	6.37	76	.000855	2.6	7.7	48.3	97.7	99.3	.21	.25	.29
Bernardo	7–10–61		403	82.0	1.71	2.88	72	.000385	53.3	70.8	92.3	99.8	100.0	.0092	.048	.10
	8–18–61		636	90.0	2.08	3.40	75	.00049	84.8	88.7	96.9	99.7	100.0			
	19–61		2,380	119	4.47	4.46	74	.00024	65.6	69.3	81.1	98.2	100.0			

[a] Estimated on basis of adjoining values.
[b] Flow on this day is from Rio Puerco.

TABLE 4.—*Computed parameters*

Reach	Date	Sec.	$\overline{m}$	k	K_s	V_*	$\frac{\overline{V}}{V_*''}$	ψ'	$\sum \frac{C_s \omega}{\overline{V} S_s} \frac{\rho_s - \rho_f}{\rho_s}$	$\frac{C}{\sqrt{g}}$	Z_1			$\beta = Z_k/Z_1$		
											0.062 −0.125	0.125 −0.250	0.250 −0.500	0.062 −0.125	0.125 −0.250	0.250 −0.500
			fps		*ft*	*fps*					*mm*	*mm*	*mm*	*mm*	*mm*	*mm*
Bernalillo	6–2–53	A–2	1.20	0.501	0.50	0.261	13.9	1.59	0.0092	11.9	0.21	0.33	0.51	0.81	1.57	2.57
	4–53	A–2	.55	1.08	.00035	.257	14.4	2.35	.0070	12.1	.21	.35	.56	.34	.65	1.05
		A	.55	.888	.000086	.212	17.4	2.70	.0107	13.9	.19	.40	.58	.59	.87	1.53
		C	1.84	.313	1.86	.250	10.4	4.76	.0062	9.32	.14	.38	.66	2.00	2.29	3.30
		E	.49	1.20	.00042	.256	11.8	2.93	.0123	10.5	.22	.37	.50	.33	.59	1.10
	4–13–54	B	1.32	.348	.50	.199	11.1	4.25	.0070	9.85	.34	.63	-----	.84	1.43	-----
		C	.47	.982	.0072	.202	12.7	5.57	.0091	10.7	.16	.32	-----	.63	1.00	-----
		D	1.44	.330	1.36	.206	10.2	5.00	.0090	9.17	.32	.62	1.19	.92	1.51	1.99
		E	.81	.666	.29	.234	11.0	3.82	.0107	9.83	.26	.53	1.06	.49	.76	.98
	5–19–54	B	.99	.447	.11	.192	16.1	3.40	.0198	13.1	.13	.32	.50	1.91	2.40	3.92
		C	.87	.620	1.32	.233	8.85	5.47	.0178	8.12	.18	.19	.98	.87	2.53	1.22
		D	.62	.758	.054	.204	13.5	3.80	.0091	11.5	.22	.34	.61	.66	1.32	1.84
		E	.99	.542	.092	.233	13.8	2.97	.0061	11.8	.31	.32	.86	.57	1.71	1.58
Socorro	4–16–54	A–1	1.66	.247	.69	.178	16.5	2.10	.0169	14.6	.29	.60	-----	1.42	2.20	-----
		A–2	1.54	.215	.22	.144	29.0	1.77	.0102	20.1	.32	80	-----	1.80	2.45	-----
		B	1.00	.332	.079	.144	23.6	2.28	.0068	16.4	.36	.69	-----	1.26	2.03	-----
		B–1	1.13	.434	.098	.213	13.0	2.71	.0046	11.3	.44	.73	1.08	.55	1.02	1.73
	5–21–54	A–1	1.44	.283	.060	.177	32.0	1.41	.0084	19.5	.31	.95	-----	1.39	1.41	-----
		A–2	1.44	.289	.076	.181	25.9	1.46	.0090	17.7	.51	.82	-----	.79	1.52	-----
		B	.85	.504	.020	.186	16.8	1.91	.0072	13.4	.25	.59	-----	.96	1.21	-----
		B–1	1.06	.372	.044	.171	19.0	2.41	.0095	14.7	.44	.83	-----	.82	1.34	-----
	8–17–54	A–1	3.52	.165	.44	.252	61.8	.62	.110	24.1	.14	.42	.89	3.83	3.93	4.65
		A–2	4.58	.129	.95	.256	90.4	.59	.090	24.7	.16	.76	1.52	4.42	3.04	3.54
Bernardo	7–10–61	------	1.36	.238	.11	.141	------	------	.0197	20.4	.24	.23	-----	2.96	8.91	-----
	8–18–61	------	1.46	.285	.094	.181	------	------	.0364	18.8	.17	.18	-----	2.65	7.61	-----
	19–61	------	1.21	.354	.030	.186	------	------	.103	24.0	.05	.12	-----	6.80	8.83	-----

TABLE 5.—*Basic data and computed parameters for the average of 13 cross sections through a 16,000-foot reach, Rio Grande near Bernalillo, N. Mex.*

Date	Q	P_w	R	b	V	T	S	Bed material (mm)		ψ'	V/V_*''
								d_{35}	d_{65}		
1952	*cfs*	*ft*	*ft*	*ft*	*ft per sec*	*°F*	*ft per ft*				
4–25	2,820	454.0	1.63	452	3.83	61	0.00090	0.230	0.330	1.61	25.7
5–12	6,440	485.2	2.35	477	5.65	64	.00086	.278	.406	.96	47.1
6–17	6,120	477.3	2.41	475	5.32	72	.00086	.270	.385	1.04	36.4
20	4,775	429.5	2.20	427	5.09	72	.00086	.290	.420	1.16	38.9
26	2,800	384.3	2.04	382	3.57	70	.00085	.260	.375	1.99	19.5
7–24	2,030	424.4	1.95	422	2.46	78	.00088	.283	.405	3.94	11.9

REFERENCES CITED

Anderson, A. G., 1942, Distribution of suspended sediment in a natural stream: Am. Geophys. Union Trans. 23d Ann. Mtg., pt. 2, p. 678–683.

Carey, W. C., and Keller, M. D., 1957, Systematic changes in the beds of alluvial rivers: Am. Soc. Civil Engineers Jour., v. 83, no. HY 4.

Chien, Ning, 1954, The present status of research on sediment transport: Am. Soc. Civil Engineers Proc., separate no. 565, 33 p.

Colby, B. R. and Hembree, C. H., 1955, Computations of total sediment discharge, Niobrara River near Cody, Nebraska: U.S. Geol. Survey Water-Supply Paper 1357, 187 p.

Culbertson, J. K., and Dawdy, D. R., 1963, A study of fluvial characteristics and hydraulic variables, middle Rio Grande, New Mexico: U.S. Geol. Survey Water-Supply Paper 1498–F.

Culbertson, J. K., and Nordin, C. F., 1960, Discussion of discharge formula for straight alluvial channels: Am. Soc. Civil Engineers Jour., v. 86, no. HY 6.

Dawdy, D. R., 1961, Depth-discharge relations of alluvial streams—discontinuous rating curves: U.S. Geol. Survey Water-Supply Paper 1498–C, 16 p.

Einstein, H. A., 1950, The bed-load function for sediment transportation in open channel flows: U.S. Dept. Agriculture Tech. Bull. 1026, 70 p. [1951].

Einstein, H. A., and Barbarossa, N. L., 1952, River channel roughness: Am. Soc. Civil Engineers Trans. paper 2528, v. 117, p. 1121–1132.

Einstein, H. A., and Chien, Ning, 1954, Second approximation to the solution of the suspended load theory: California Univ., Inst. Engineering Research, Missouri River Div. sediment ser. 3, 30 p.

——— 1955, Effects of heavy sediment concentration near the bed on velocity and sediment distribution: California Univ., Inst. Engineering Research, Missouri River Div. sediment ser. 8, 45 p.

Ismail, H. M., 1951, Turbulent transfer mechanism and suspended sediment in closed channels: Am. Soc. Civil Engineers Proc., separate no. 56, 26 p.

Keulegan, G. H., 1938, Laws of turbulent flow in open channels: U.S. Natl. Bur. Standards, Jour. Research, v. 21, no. 6, p. 707–741.

Liu, H. K., and Hwang, S. Y., 1959, Discharge formula for straight alluvial channels: Am. Soc. Civil Engineers Journ., v. 85, no. HY 11.

O'Brien, M. P., 1933, Review of the theory of turbulent flow and its relation to sediment transportation: Am. Geophys. Union Trans., v. 14, p. 487–491.

Richardson, E. V., Simons, D. B., and Posakony, G. J., 1961, Sonic depth sounder for laboratory and field use: U.S. Geol. Survey Circ. 450, 7 p.

Rouse, H., 1937, Modern conceptions of the mechanics of fluid turbulence: Am. Soc. Civil Engineers Trans., paper 1965, v. 102, p. 463–543.

Sayre, W. W., and Albertson, M. L., 1961, Roughness spacing in rigid open channels: Am. Soc. Civil Engineers Jour., v. 87, no. HY 3.

Simons, D. B., and Richardson, E. V., 1961, Forms of bed roughness in alluvial channels: Am. Soc. Civil Engineers Jour., v. 87, no. HY 3.

Simons, D. B., Richardson, E. V., and Haushild, W. L., 1963, The effects of fine sediment on the mechanics of flow: U.S. Geol. Survey Water-Supply Paper 1498–G.

U.S. Inter-Agency Report No. 4, 1941, Methods of analyzing sediment samples: St. Paul, Minn., U.S. Dept. Army.

U.S. Inter-Agency Report No. 12, 1957, Measurement and analysis of sediment loads in streams: Washington, U.S. Govt. Printing Office.

Vanoni, V. A., 1946, Transportation of suspended sediment by water: Am. Soc. Civil Engineers Trans., paper 2267, v. 111, p. 67–102.

Vanoni, V. A., and Brooks, N. H., 1957, Laboratory studies of the roughness and suspended load of alluvial streams: California Inst. Technology, sediment lab., rept. E–68, 99 p.

Vanoni, V. A., Brooks, N. H., and Kennedy, J. F., 1961, Lecture notes on sediment transportation and channel stability: California Inst. Technology Rept. KH–R–1.

O

A Preliminary Study of Sediment Transport Parameters Rio Puerco Near Bernardo New Mexico

By CARL F. NORDIN, JR.

SEDIMENT TRANSPORT IN ALLUVIAL CHANNELS

GEOLOGICAL SURVEY PROFESSIONAL PAPER 462-C

UNITED STATES GOVERNMENT PRINTING OFFICE, WASHINGTON : 1963

UNITED STATES DEPARTMENT OF THE INTERIOR

STEWART L. UDALL, *Secretary*

GEOLOGICAL SURVEY

Thomas B. Nolan, *Director*

For sale by the Superintendent of Documents, U.S. Government Printing Office
Washington, D.C. 20402

CONTENTS

	Page
Glossary of terms	III
Symbols	IV
Abstract	C1
Introduction	1
Purpose and scope	1
Previous investigations	1
Rio Puerco drainage basin and the study reach	2
Observed data	2
Velocity distributions	C7
Flow resistance	9
Concentration distributions	10
Channel bed	15
Extreme concentrations in ephemeral streams	19
Summary	20
References cited	21

ILLUSTRATIONS

	Page
FIGURE 1. Rio Puerco drainage basin	C3
2. Sketch map of study reach	4
3. Study reach, July 1961	4
4. Daily water discharge and concentration of suspended sediment, July-September 1961	5
5. Variation of velocity with distance above streambed	8
6, 7. Variation of concentration with $(D-y)/y$, station 200—6. August 19, 1961	10
7. September 11, 1961	11
8. Variation of concentration with $(D-y)/y$, station 170, September 20, 1961	11
9. Particle-size distribution from visual-accumulation-tube analysis	12
10. Variation of fall velocity with concentration	12
11. Z and Z' plotted against Z_1	13
12. Variation of apparent viscosity with temperature	14
FIGURE 13. General shape of viscosity curves for clay-water systems with various amounts of added base	C14
14. Section B, showing thickness of clay-impregnated layer of bed	15
15. Particle-size distribution of clay-impregnated layer of bed and of underlying sand	15
16. Cross sections defined from water-discharge measurements, and lateral distribution of bed material	16
17. Standing waves and antidunes in reach, September 11, 1961	17
18. Headcut in clay-armored bed	18
19. Section B on October 5, 1961	18
20. Study reach, October 5, 1961	18
21. Relation of transport rate of suspended sand per foot of width to unit discharge	19

TABLES

	Page
TABLE 1. Basic data	C5
2. Velocity distributions	5
3. Concentration distribution	6
4. Particle-size distribution of suspended sediment and bed material	6
5. Measured and computed exponents of sediment distribution	13
TABLE 6. Partial chemical analysis of native water	C14
7. Mineralogical composition of suspended sediment finer than 0.004 mm, September 11, 1961	14
8. Extreme sediment concentrations observed in ephemeral streams	20

GLOSSARY OF TERMS

Bed material. Material that makes up the channel bed.

Clay. Sediment finer than 0.004 millimeters (mm), regardless of mineralogical composition.

Concentration. Sediment concentration, except where specified otherwise, is the ratio of the dry weight of sediment to the weight of the water-sediment mixture, expressed in parts per million (ppm). In general, this definition of concentration may refer to any material, dissolved or suspended, in a stream.

Fine material. Material finer than 0.062 mm.

High concentrations. Arbitrarily taken as any concentration greater than 50,000 ppm.

Sand. "Sand" and "sand sizes" are used interchangeably to refer to sediment between 0.062 mm and 2.0 mm in size, regardless of mineralogical composition.

Sediment. Fragmental material that originates from weathering of rocks and is transported by, suspended in, or deposited by water.

Silt. Sediment between 0.004 mm and 0.062 mm in size.

SYMBOLS

		Units
a	Reference distance above the bed	ft
A	Unit horizontal area	ft^2
c	Concentration, in weight per unit volume	lb per ft^3
C	Concentration	ppm
C_v	Volume concentration	0
$C_c/\sqrt{g}$	Dimensionless Chezy coefficient	0
C_1	A constant	0
d	Median diameter	mm
d_{65}	Particle size for which 65 percent by weight is finer	mm
D	Depth at a vertical	ft
$\overline{D}$	Mean depth of flow at a cross section	ft
F	Froude number	0
g	Acceleration of gravity	fps^2
k	The coefficient of turbulent exchange	0
K_s	A length parameter	ft
m	Slope of the semilogarithmic plot of velocity versus depth above the streambed	fps
n	Manning's resistance coefficient	$ft^{1/6}$
P_f	Power to overcome friction	ft-lb per sec
P_s	Power to support the sediment	ft-lb per sec
P_s'	Power added by the sediment	ft-lb per sec
q	Discharge per foot of width	ft^3 per sec per ft
q_s	Transport rate of observed suspended sand	tons per day per ft
R	Hydraulic radius	ft
S	Water-surface slope	ft per ft
V	Velocity at a point	fps
$\overline{V}$	Mean velocity in a cross section	fps
V_*	Shear velocity	fps
y	Distance above the streambed	ft
Z	Computed exponent for the vertical distribution of suspended sediment	0
Z_1	Observed exponent for the vertical distribution of suspended sediment	0
β	Angle of inclination between the streambed and the horizontal	degrees
γ	Specific weight of water	lb per ft^3
γ_s	Specific weight of sediment	lb per ft^3
ϵ_m	Momentum transfer coefficient	0
ϵ_s	Sediment transfer coefficient	0
μ	Coefficient of viscosity	centipoise
ω	Fall velocity	fps

A PRELIMINARY STUDY OF SEDIMENT TRANSPORT PARAMETERS, RIO PUERCO NEAR BERNARDO, NEW MEXICO

By Carl F. Nordin, Jr.

ABSTRACT

Preliminary findings of a study of sediment transport in streams with high concentrations of suspended fine sediment indicate that for the Rio Puerco near Bernardo, N. Mex., the velocity varies logarithmically with depth, and the concentration distribution for several size classes of sand may be described by a conventional distribution equation if the fall velocity of the sand is corrected for the influence of the fine sediment. A corrected fall velocity, empirically defined for a temperature of 24° C and for concentrations of as much as about 150,000 parts per million, is given.

Through the period of the study, the channel of the Rio Puerco changed rapidly. The bed material varied from cohesive fine material to coarse sand. At the beginning of the study, the sand bed of the channel was impregnated with clay, and the clay-impregnated layer acted as an effective "armoring" which persisted for several weeks, forming a cohesive boundary for the flow and limiting the availability of sand for transport. For the last several observations, a "headcut" in the armored layer had progressed upstream into the study reach. The influence of the headcut was reflected in an increase in the water-surface slopes and in the concentrations of suspended sand.

Flow resistance, as measured by Manning's n, was approximately constant and was independent of the condition of the bed (cohesive or noncohesive) and of the average size distribution of the bed material.

Some observations of extreme sediment concentration are cited, and some of the problems involved in attempting to explain or to predict sediment transport rates for extreme conditions are discussed briefly.

The rapid changes in the channel geometry and in the characteristics of the bed material, and the extreme sediment concentrations that were observed, reflect conditions which, in general, are not described adequately by conventional sediment transport relations.

Observations in this report point out the extreme complexity of the natural processes operating in the Rio Puerco watershed and indicate the need for a better understanding of the factors controlling the flow and the sediment transport in ephemeral streams.

INTRODUCTION

Arid and semiarid regions are characterized by spectacular erosion features that have developed over short periods of time. Along with the erosion features, and equally spectacular, are the vast quantities of sediments delivered by the ephemeral streams to the major watercourses. Suspended-sediment loads in streams have been observed for many years, and something of the magnitude of the loads carried by the streams in arid or semiarid environments is known. However, there is little or no information on the mechanics of flow in streams carrying extreme concentrations of fine suspended material, and there exist no suitable methods for estimating the rates of sediment transport or for describing the flow and sediment characteristics which control the rates of transport.

This report presents preliminary findings of a study of sediment transport in streams with high concentrations of fine suspended sediment.

PURPOSE AND SCOPE

The purpose of this study was to investigate some aspects of the sediment-transport parameters and the mechanics of flow in streams transporting high concentrations of suspended fine material. Field observations were conducted on a reach of the Rio Puerco near Bernardo, N. Mex. The data obtained were supplemented by existing records of the Rio Puerco and other streams where applicable.

Specifically, the investigation included a study of the following: (a) Vertical-velocity distributions; (b) flow resistance; (c) vertical suspended-sediment concentration distributions; (d) channel-bed material and its effect on sediment-transport rates and related flow phenomena; and (e) extreme sediment concentrations.

PREVIOUS INVESTIGATIONS

The Rio Puerco in New Mexico is a notorious example of accelerated erosion, and several references to the channel and to the watershed are found in the literature. Bryan (1928, 1940) discussed some of the historical evidence of erosion in the Rio Puerco, and Leopold [1] presented some aspects of the erosion problem

[1] Leopold, L. B., 1950, The erosion problem of Southwestern United States: Ph. D. Dissertation, Harvard University.

over a wide area of the Southwest, including the Rio Puerco basin. Several reports deal with observations of other streams in semiarid environments, and many of the conclusions drawn probably apply to the Rio Puerco. Leopold and Miller (1956) indicated that certain hydraulic factors such as width, depth, velocity, and suspended-sediment load are related to the discharge as simple power functions. Schumm (1960, 1961) related the shape of alluvial channels (the width to depth ratio) to the types of sediment in the bed and banks and suggested that the relation between the channel shape and the weighted mean percent silt-clay can be used as a criterion for channel stability in ephemeral streams.

These and many other studies provide considerable insight into the nature of erosion and channel morphology, but none of the references deals specifically with the mechanics of sediment transport. Haushild (oral communication, 1960) and Simons and others (1963) used high concentrations of bentonite and kaolin as fine sediments in a series of flume experiments. They found that the fine material had a definite effect on the viscosity and specific weight of the fluid. Changes in the fall velocities of the bed material, caused by the variations in the fluid properties, influenced the form of bed roughness, the flow resistance, and the sediment transport. Earlier studies of transportation of fine sediments were given by Hsia [2] and Kalinske and Hsia (1945), who related the concentration of fine sediment to the composition of the bed, the ratio of fall velocity to shear velocity, and the shear velocity Reyonold's number. Some limited information on velocity and concentration distributions for field conditions was discussed by Nordin and Dempster (1963).

RIO PUERCO DRAINAGE BASIN AND THE STUDY REACH

The Rio Puerco drains approximately 6,200 square miles in central New Mexico (fig. 1). The drainage basin is bounded on the east by the Rio Grande drainage basin, on the west by the Continental Divide, on the north by the Jemez Mountains, and on the south by the Ladrone Mountains. Altitudes in the basin range from 4,700 feet above mean sea level near the confluence with the Rio Grande to about 10,000 feet near the headwaters. Rainfall varies roughly with altitude. The average annual rainfall ranges from 20 inches or more in the headwaters to about 10 inches over a major part of the basin (Dorroh, 1946).

In the past, some irrigated agriculture was practiced in the Rio Puerco valley. In more recent times, the major land use has been for grazing cattle and sheep. Over most of the watershed, vegetation is sparse, consisting mostly of pinon, juniper, and rough range grasses.

Large quantities of readily erodible sediments are available over most of the watershed. Observed suspended-sediment samples for the Rio Puerco near Bernardo contain, on the average, more than 50 percent clay-sized material. Clays derived from weathered shales, primarily the Chinle Formation of Triassic age and the Mancos Shale of Cretaceous age, represent the bulk of the sediment load carried by the Rio Puerco. At times the Rio Puerco also carries large quantities of sand, of which there is an abundant supply generally available for transport. Deposits of fine wind-blown sands are present over much of the watershed, but the Santa Fe Formation of middle(?) Miocene to Pleistocene(?) age is exposed in many places along the lower 50 or 60 miles of the Rio Puerco and probably serves as a source for much of the sand transported by the stream. The bed material of the active channel of the Rio Puerco, from the Chico Arroyo to the confluence with the Rio Grande, is composed primarily of fine sand with thin layers of clay. Core drilling in the channel at the Rio Puerco near Bernardo, N. Mex., shows alternate layers of fine sand and clay to a depth of about 70 feet and layers of sand and coarse gravel to greater depths.

The major tributaries to the Rio Puerco, the site of the U.S. Geological Survey gaging station near Bernardo, and the location of the study reach are shown in figure 1. Streamflow and suspended-sediment records for the Rio Puerco near Bernardo are published annually in Geological Survey Water-Supply Papers covering the hydrologic division, Part 8, Western Gulf of Mexico Basins.

The study reach for the observations presented in this report is approximately one-quarter of a mile downstream from the gaging station on the Rio Puerco near Bernardo, N. Mex. Figure 2 is a sketch map of the study reach, and figure 3 shows the reach as it appeared in July 1961. Section B is the site of the permanent cable installed for stream gaging and is approximately midway between the two bridges, which are about 1,900 feet apart.

OBSERVED DATA

Field observations and sampling included the following: Measuring water discharge, water-surface slope, water temperature, and water velocities at several points in one or more verticals in the section; collecting bed- and suspended-material samples; and taking photographs of the reach.

[2] Hsia, C. H., 1943, A study of transportation of fine sediments by flowing water: Ph. D. Dissertation, Iowa State University.

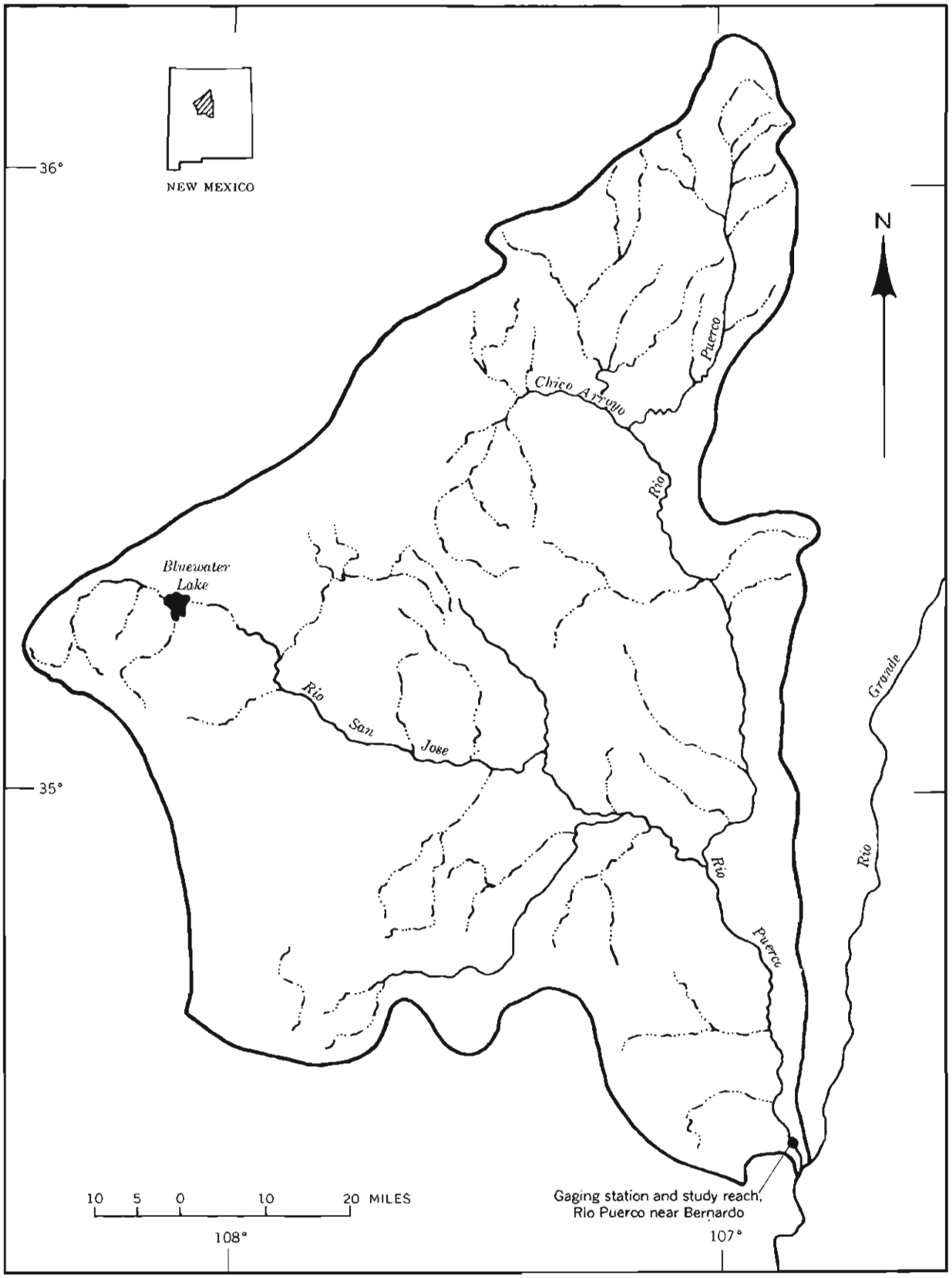

FIGURE 1.—The Rio Puerco drainage basin, showing the location of the study reach.

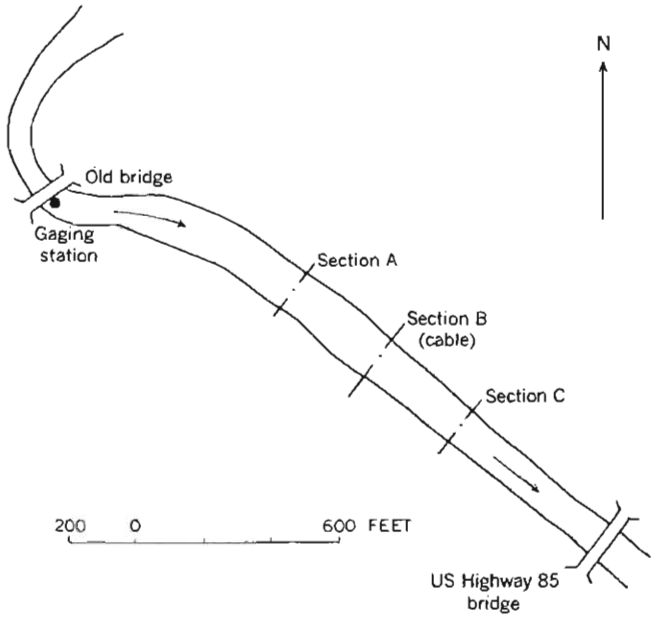

FIGURE 2.—Sketch map of the study reach.

Velocities at points in the verticals were measured with a Price current meter, and water discharge was computed. Water-surface slopes were determined by staff gages at sections A, B, and C, referred to the datum of mean sea level. Bed material was sampled with a BM–54 bed-material sampler, which collects material from the top 1 or 2 inches of the bed. Suspended sediment was sampled with a US P–46 point-integrating sampler or with a modified US DH–48 hand sampler. These samplers collect material to within about 0.3 to 0.5 foot from the streambed.

Suspended-sediment samples were collected at several points in one or more verticals in the cross section to define vertical sediment concentration distributions. Depth-integrated samples collected at equal centroids of flow or depth-integrated samples collected at a series of equally spaced verticals of the cross section were analyzed to determine average concentrations and particle-size distributions of the suspended sediment in the sampled zone.

Particle-size distributions of bed material and of suspended sediments were determined by the pipette method for sizes smaller than 0.062 millimeter (Kilmer and Alexander, 1949) and by the visual-accumulation method for sand sizes (U.S. Inter-Agency Committee on Water Resources, 1957a).

Basic data for the hydraulic characteristics of the reach for the several observations in 1961 are given in table 1. Tables 2 and 3 show point velocity measurements and concentration distributions for various size classes of the point sediment samples, respectively, in 1961. All observations were at section B, and the stations shown in tables 2 and 3 correspond to the stationing of the permanent cable. Table 4 gives the average particle-size distributions for samples of suspended sediment and of bed material.

Water discharges and mean daily concentrations for July through September 1961 are shown in figure 4. Typically, the flow rose rapidly over the dry bed from runoff of short duration that resulted from high-intensity storms occurring upstream from the study reach. Discharge measurements and samples were difficult to obtain on rising stages because of the debris carried by the flow. Observations and sampling for the data in tables 1 through 4 were conducted during periods of receding flow.

A

B

FIGURE 3.—The study reach, July 1961. *A*, View upstream from section B; *B*, view downstream from section B.

TABLE 1.—*Basic data*

[Water surface altitudes are referred to the datum of mean sea level]

Date	Q (cfs)	T (°F)	b (ft)	$\overline{D}$ (ft)	$\overline{V}$ (fps)	S (ft per ft)	Water surface altitude	$V_* = \sqrt{gDS}$ (fps)	$C_c/\sqrt{g} = \overline{V}/\sqrt{g\overline{D}S}$	n (ft$^{1/6}$)	F
July 10	403	72	82.0	1.71	2.88	0.000385	4,730.76	0.145	19.9	0.0144	0.39
Aug. 18	31.4	82	24.0	.74	1.76	.00073	----------	.132	13.3	.0180	.36
Do	636	75	90.0	2.08	3.40	.00049	4,731.30	.181	18.8	.0159	.42
Aug. 19	2,380	74	119	4.47	4.46	.00024	4,734.60	.192	23.2	.0140	.37
Aug. 30	5.46	79	16.0	.29	1.14	.00105	----------	.099	11.5	.0185	.37
Sept. 11	1,110	66	91	2.08	5.87	.00122	4,731.81	.286	20.5	.0144	.72
Sept. 20	1,430	63	89	2.48	6.48	.00148	4,731.49	.344	18.9	.0162	.73

TABLE 2.—*Velocity distributions*

Date	Station	D (ft)	y (ft)	V (fps)	y (ft)	V (fps)	y (ft)	V (fps)	y (ft)	V (fps)	y (ft)	V (fps)
July 10	170	2.6	0.3	2.92	0.7	3.28	1.1	3.80	1.6	3.97	2.2	3.97
	170	2.5	.3	2.86	.7	3.43	1.2	3.72	1.7	3.97	2.1	3.97
Aug. 18	170	3.6	.5	3.20	1.0	3.88	2.0	4.25	3.0	4.54	------	------
	185	2.6	.5	3.43	1.1	3.97	1.6	4.15	2.1	4.15	------	------
Aug. 19	170	5.8	.5	3.80	1.0	4.25	2.2	4.84	3.4	5.18	4.6	5.18
	200	4.8	.5	4.45	.8	4.48	1.8	4.69	2.8	4.89	3.8	5.12
Sept. 11	155	2.6	.5	4.86	1.1	5.74	1.6	6.38	2.1	6.85	------	------
	170	3.1	.6	5.80	1.1	6.85	1.6	7.23	2.1	8.18	2.6	8.02
	185	3.0	.5	5.33	1.0	5.96	1.5	6.99	2.0	7.46	2.5	7.59
Sept. 20	155	2.5	.5	4.90	1.0	5.95	1.5	6.76	2.0	7.14	------	------
	170	3.6	.5	7.38	1.6	9.12	2.6	9.79	------	------	------	------
	185	3.8	.5	6.83	1.4	7.75	2.5	9.66	3.2	9.79	------	------

The reach of the Rio Puerco near Bernardo has been steadily aggrading for a number of years. At the beginning of the observations in the summer of 1961, the sand bed of the channel was impregnated with clay to a depth of about 0.6 foot. This clay armoring of the bed persisted through the observations of July 10 and August 18 and 19, 1961, and was reflected in extremely low concentrations of suspended sands for these dates (table 4). For the observations on September 11 and 20, at least a part of the bed was sand, and the concentrations of suspended sands were much higher.

Because the bed material varied from cohesive fine material to coarse sand with a median diameter of 0.5 mm, the results discussed below may not be generally applicable to all streams carrying high concentrations of suspended material. Nonetheless, differences in the characteristics of flow and of sediment transport for the different bed conditions lead to some significant conclusions that should prove useful to understanding the mechanics of flow and the sediment transport in similar streams.

In the following discussion of the results of this investigation it is assumed that the flow is uniform for

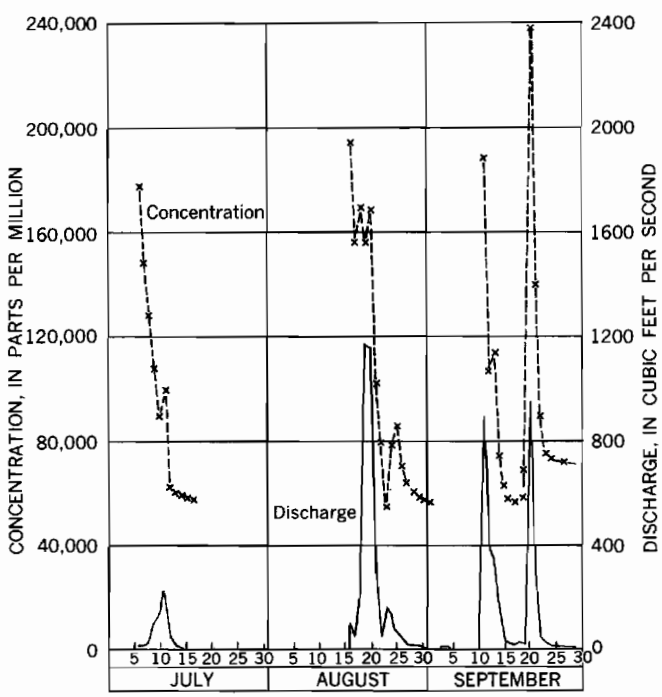

FIGURE 4.—Daily water discharge and concentration of suspended sediment, July–September 1961.

TABLE 3.—*Concentration distribution*

Date	Station	D (ft)	Y (ft)	$\frac{D-y}{y}$	Concentration in parts per million, for indicated size class, in millimeters									
					<0.002	0.002–0.004	0.004–0.008	0.008–0.016	0.016–0.031	0.031–0.062	0.062–0.125	0.125–0.25	0.25–0.50	Total
July 10	170	2.6	0.3	7.67	47,000	4,310	10,900	5,590	495	495	608	1,220	57	70,660
			.7	2.71	41,300	8,810	11,100	5,160	1,170	688	323	248	----------	68,810
			1.1	1.36	41,000	9,030	10,100	5,270	1,570	889	287	191	----------	68,360
			1.6	.625	41,800	8,600	9,850	5,090	1,970	475	48	20	----------	67,890
			2.2	.182	47,700	4,670	8,120	4,540	1,620	677	230	95	----------	67,690
Do	170	2.5	.3	7.33	41,500	7,530	8,340	5,560	2,170	1,360	502	841	----------	67,800
			.7	2.57	41,600	10,300	7,760	4,380	928	663	332	298	----------	66,320
			1.2	1.08	41,600	8,610	9,330	4,500	1,060	596	265	192	----------	66,160
			1.7	.471	40,800	8,620	8,420	4,770	1,500	784	215	137	----------	65,280
			2.1	.190	40,500	9,240	9,240	4,580	1,110	524	203	118	----------	65,520
Aug. 18	185	2.6	.5	4.20	95,400	15,700	11,700	26,300	24,000	3,920	410	344	36	178,200
			1.1	1.36	93,300	14,600	13,900	31,500	21,400	2,670	357	357	18	178,500
			1.6	.625	98,100	10,300	19,200	25,800	19,200	4,630	391	355	18	177,500
			2.1	.238	91,500	13,400	20,500	20,600	23,100	8,370	268	250	18	178,400
Aug. 19	170	5.8	.5	10.6	73,400	6,070	10,800	19,500	13,200	4,880	2,080	1,620	424	132,400
			1.0	4.80	68,600	17,000	7,200	15,900	12,600	6,160	1,930	1,400	197	131,100
			2.2	1.64	63,900	16,100	13,900	14,100	14,500	4,980	1,880	1,340	158	131,400
			3.4	.706	68,600	13,400	14,800	12,800	13,500	4,580	1,960	1,200	105	130,900
			4.6	.261	70,200	11,400	11,700	15,700	14,400	4,720	2,010	903	----------	130,800
Do	200	4.8	.5	8.60	66,800	8,980	15,800	13,600	16,000	7,390	1,950	1,330	119	131,800
			.8	5.00	66,300	10,400	13,000	13,800	16,900	6,630	1,780	1,210	52	130,200
			1.8	1.67	66,500	13,100	13,100	14,100	14,300	6,810	1,750	1,200	92	130,800
			2.8	.714	71,400	7,730	11,800	14,700	16,100	6,420	1,760	1,080	26	131,200
			3.8	.263	66,400	6,050	11,600	13,500	17,400	8,320	1,730	993	13	125,700
Sept. 11	200	2.0	.3	5.67	61,700	7,990	10,200	13,300	21,600	21,600	22,500	10,200	1,020	170,300
			.6	2.33	62,500	6,720	8,360	11,600	20,000	26,400	21,100	6,800	580	163,600
			1.0	1.00	59,000	8,860	9,020	12,300	18,000	28,000	22,000	6,430	426	164,000
			1.5	.333	63,000	11,100	4,350	12,400	21,700	22,400	20,500	5,590	97	161,000
Sept. 20	170	3.4	.4	7.50	55,900	16,300	8,750	13,900	34,700	34,300	50,300	27,200	1,700	243,100
			1.0	2.40	55,400	4,920	5,410	38,600	10,100	41,800	56,800	30,700	2,210	245,700
			2.2	.545	70,200	14,600	8,320	13,200	22,600	40,700	45,000	16,100	231	236,000
			3.0	.133	75,300	11,400	6,050	16,400	22,000	40,500	39,400	13,000	----------	223,700
Do	185	3.3	.4	7.25	64,800	7,480	11,900	14,400	24,800	39,500	52,600	36,600	5,930	258,000
			1.3	1.54	63,900	8,260	10,200	17,700	23,300	41,800	51,700	24,300	1,700	242,600
			2.1	.571	51,400	16,600	8,320	17,100	24,700	45,500	46,300	19,200	926	231,400
			2.7	.222	82,100	9,680	1,580	17,100	25,900	32,000	38,300	17,600	902	225,500

TABLE 4.—*Particle-size distribution of suspended sediment and bed material*

[Methods of analysis: P, pipette; W, in distilled water; C, chemically dispersed; M, mechanically dispersed; V, visual-accumulation tube]

Date	Type of sample	Water discharge (cfs)	Concentration sample (ppm)	Percent finer than indicated size, in millimeters												Methods of analysis
				0.002	0.004	0.008	0.0156	0.0312	0.0625	0.125	0.250	0.500	1.00	2.00	4.00	
July 19	Suspended	403	75,800	63.0	73.4	87.7	98.7	99.2	99.4	99.8	99.9	100	------	------	------	VPWCM
Aug. 18	do	636	178,000	50.8	61.7	71.0	84.4	96.7	99.6	99.8	100	------	------	------	------	VPWCM
Aug. 19	do	2,380	132,000	52.0	59.2	66.8	80.5	92.5	97.3	99.1	100	------	------	------	------	VPWCM
Sept. 11	do	1,110	175,000	33.6	38.5	41.1	49.9	60.5	75.5	93.8	99.8	100	------	------	------	VPWCM
Sept. 20	do	1,430	240,000	26.6	30.3	35.1	42.3	51.8	64.9	88.6	99.6	100	------	------	------	VPWCM
July 10	Bed material	403	----------	24.2	28.4	34.4	39.6	45.3	53.3	70.8	92.3	99.8	100	------	------	VPWCM
Aug. 18	do	636	----------	------	------	------	------	------	84.8	88.7	96.9	99.7	100	------	------	V
Aug. 19	do	2,380	----------	------	------	------	------	------	65.6	69.3	81.1	98.2	100	------	------	V
Sept. 11	do	1,110	----------	21.9	25.7	27.4	31.6	36.2	44.8	55.0	80.5	95.1	99.7	100	------	VPWCM
Sept. 20	do	1,430	----------	11.6	14.1	16.4	20.4	24.2	29.5	43.0	68.7	85.9	97.8	99.6	99.9	VPWCM

the time of the observations; that the water-surface slope equals the slope of the energy gradient through the reach; and that the hydraulic radius, R, approximately equals the mean depth of flow, $\overline{D}$.

VELOCITY DISTRIBUTIONS

Plots of velocity, V, against the distance, y, from the streambed for the various points in the verticals (fig. 5) indicate that the velocity is proportional to the logarithm of the depth. The figure suggests that the velocity distribution perhaps can be described by some form of the von Karman-Prandtl logarithmic velocity equation.

The logarithmic velocity equation, as given by Kuelegan (1938) for two-dimensional open-channel flow over a rigid wholly rough boundary, is

$$\frac{V}{V_*}=\frac{2.303}{k}\log\frac{y}{K_s}+C_1, \tag{1}$$

where

y=the distance from the streambed, in feet;
V=the velocity at the distance y from the streambed, in feet per second;
V_*=the shear velocity=$\sqrt{gRS}$, in feet per second;
k=the dimensionless coefficient of turbulent exchange;
K_s=a length parameter, describing the roughness elements on the bed, in feet;
C_1=a dimensionless constant;
R=the hydraulic radius, in feet;
S=the slope of the energy gradient, in feet per foot; and
g=the acceleration due to gravity, in feet per second squared.

For a sand-grain-type roughness, the length parameter, K_s, assumes the value of the representative size of the sand. For uniform sands, the representative size may be taken as the median diameter, d; whereas for naturally worn river sediments, the representative size is more closely given by the diameter for which 65 percent by weight of the mixture is finer, d_{65} (Einstein, 1950).

In general, equation 1 does not adequately describe the velocity distributions for flow over an alluvial bed. The values of K_s and C_1 which are found applicable for flow over a rigid boundary with a sand-grain roughness, are not applicable for flow over a mobile boundary where there is moving sediment, even though the channel bed be plane and free from irregularities. A recent study of vertical velocity distribution for flow in the Rio Grande showed that for flow over a plane bed, if the constant C_1 is assumed equal to the value 8.5 given by Kuelegan, the length parameter, K_s, has an average value of about 400 times d_{65} (Nordin and Dempster, 1963). On the other hand, if there are dunes and major bed configurations in the channel, the velocity is not proportional to the shear velocity, $\sqrt{gRS}$, but to some values less than the shear velocity (Einstein, 1950).

Regardless of the values which K_s and C_1 may assume, if a form of equation 1 applies for the velocity distributions in the individual verticals, it is possible to investigate the values of the von Karman coefficient of turbulent exchange from the observed vertical velocity distributions. Values of k can be computed from equation 1 as

$$\frac{V_1-V_2}{\log y_1-\log y_2}=\frac{2.303\ V_*}{k}=m, \tag{2}$$

where V_1 and V_2 are the velocities at distances y_1 and y_2, respectively, and m is the slope of the velocity profile, in feet per second, and is equal to the change in velocity for one log cycle of depth; thus,

$$k=\frac{2.303\ V_*}{m}. \tag{3}$$

Values of k were computed for each of the verticals plotted in figure 5 by measuring the slope, m, of the line fitted by eye through the plotted points and by assuming the value of V_* to be equal to $\sqrt{gDS}$, where D is the depth at the vertical. Values of m and k, so computed, are shown in figure 5.

Some of the velocity profiles are not well defined. The velocity profile for station 185 on September 20 was influenced by violent antidunes in the section and probably is not suited to the determination of k. The k value of 0.617 for station 200 on August 19 was probably due to three-dimensional flow effects or to secondary circulation. Sayre and Albertson (1961) reported k values ranging from 0.34 to 2.77, as determined by the velocity-profile method for clear-water flow over isolated roughness baffles. They attributed the large variation in k to three-dimensional flow effects and to large-scale vortices. Nordin and Dempster (1963) showed a similar large variation in k for flow over a dune bed in the Rio Grande, where k ranged from 0.35 to 1.2 and was generally greater than 0.4.

The values of k found in the Rio Puerco appear to be consistent with the values reported by other investigators (Vanoni and Nomicus, 1960; Nordin and Dempster, 1963). For those dates when the channel bed was armored with clay, the values of k varied from 0.32 to 0.62 and averaged 0.38; whereas for the observations when the bed was partly covered with sand and large quantities of sand were carried in suspension, the values of k varied from 0.22 to 0.31 and averaged 0.25.

Ismail (1951) suggested that sediment dampens the turbulence and reduces the momentum transfer, which

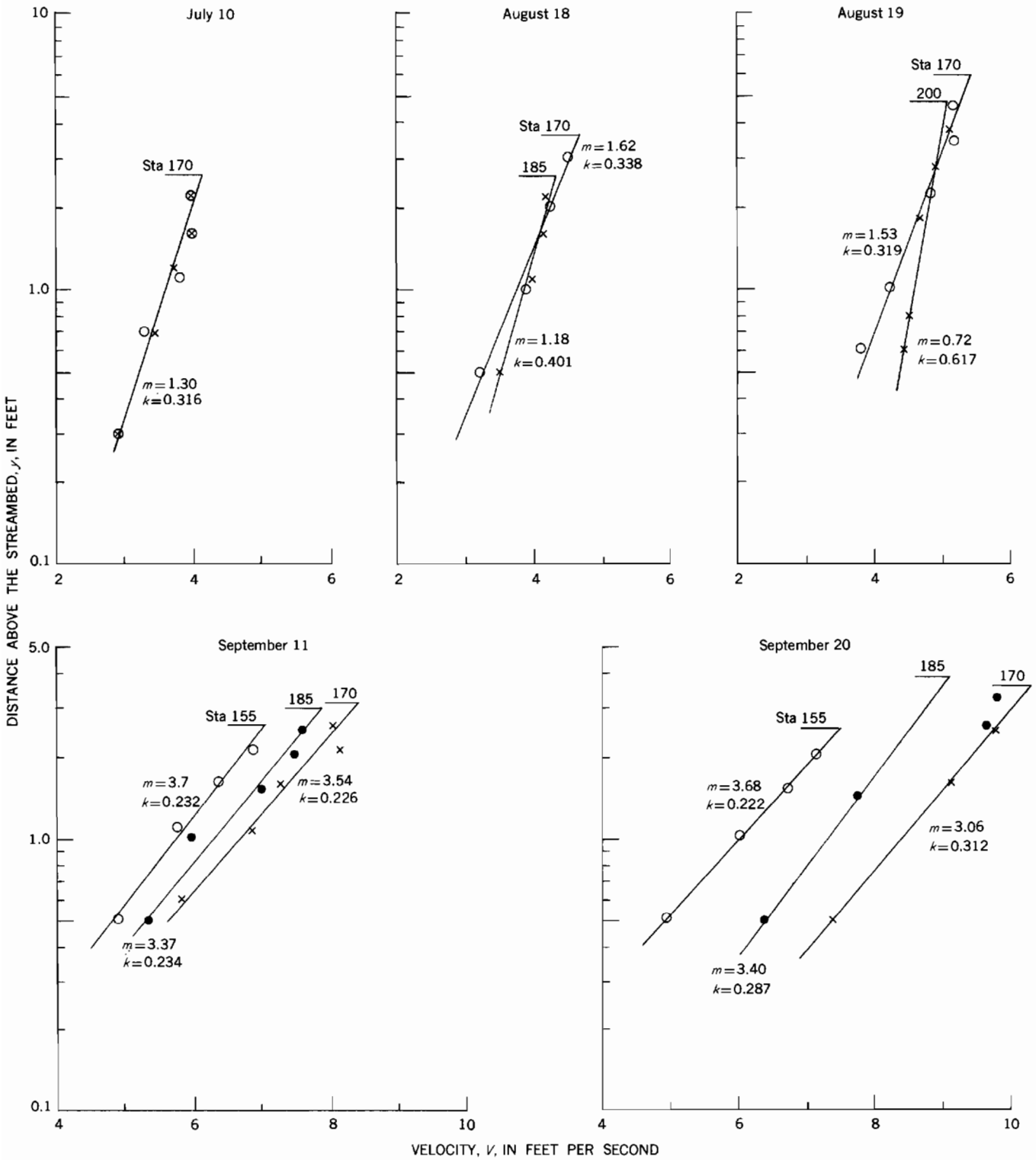

FIGURE 5.—Variation of velocity with the distance above the streambed.

results in a reduction in k. Einstein and Chien (1954) and Vanoni and Nomicus (1960) correlated the reduction in k with the ratio of energy required to support the sediment to the energy dissipated in overcoming friction. According to Vanoni and Nomicus, the power, P_s, to support the sediment in a water prism with unit horizontal area, A, and depth, D, equal to the stream depth is

$$P_s=\frac{\gamma_s-\gamma}{\gamma_s}Ac\omega D, \tag{4}$$

in which γ and γ_s are the specific weights of water and sediment, respectively; c is the mean concentration over the depth, in weight per unit volume; and ω is the settling velocity of the sediment. The power P_f to overcome the friction of the prism of water is

$$P_f=A\gamma DVS. \tag{5}$$

The ratio of the two powers is

$$\frac{P_s}{P_f}=\frac{(\gamma_s-\gamma)c\omega}{\gamma_s\gamma VS}. \tag{6}$$

The value of k was found to decrease with increasing values of the ratio P_s/P_f (Einstein and Chien, 1954).

The values of the ratio P_s/P_f were not computed for the data given in this report for two reasons. First, it is extremely difficult to determine what fall velocity should be used in equation 4 when high concentrations of fine material are present in the stream, due to the variable viscosity and mass density of the stream fluid; and second, equation 6 is not a good index to the reduction in k in streams transporting high concentrations of fine material, because the equation does not account for the energy added by the sediment.

According to Bagnold (1956), the sediment contributes to the total tractive force on the bed by an amount equal to the tangential component along the bed of the submerged weight of the sediment. In form analogous to equation 4, the power contributed by the sediment can be expressed as

$$P_s'=\frac{\gamma_s-\gamma}{\gamma_s}AcVD\ \mathrm{Sin}\ \beta, \tag{7}$$

where β is the postive angle of inclination between the bed and the horizontal. For the small angles usually found in natural channels, Sin β may be assumed equal to the slope, S. The ratio of the power to support the sediment to the power contributed by the sediment (equation 4 divided by equation 7) is given by

$$\frac{P_s}{P_s'}=\frac{\omega}{VS}. \tag{8}$$

Thus, the power added by the sediment to the flow will be greater than the power extracted from the flow in supporting the sediment when ω is less than the product VS. For the August 18 observation, the product $VS=3.40\times0.00049=0.00167$ fps (feet per second), and the median diameter of the suspended material is less than 0.002 mm (millimeter). The fall velocity from Stokes' equation for a sphere with a diameter of 0.002 mm and a specific gravity of 2.65 falling in distilled water at a temperature of 75° F is about 1.28×10^{-5} fps. The fall velocity of a similar particle in natural stream conditions would be even less. Thus, the energy added by the sediment is about 130 times as great as the energy required to support the sediment.

Equation 6 probably is not a good measure of the reduction in k where the energy added by the sediment is equal to or greater than the energy required to support the sediment.

If equation 8 is approximately correct, it can be seen that the concentration of fine sediment can be increased indefinitely; that is, there is no upper limit to the concentration which may be found in natural streams transporting fine materials other than the static limit imposed by some upper limiting concentration at which the mixture turns into a mudflow.

FLOW RESISTANCE

The overall resistance to flow, as measured by Manning's n and by the dimensionless Chezy coefficient $C_c/\sqrt{g}$, was determined for each of the observations in table 1. Excluding the two lowest discharges (August 18, 30), the flow resistance was remarkably constant. Values of Manning's n ranged from 0.0140 to 0.0162 and averaged 0.0150. The maximum deviation from the average value was +8 percent.

For the low discharges of August 18 and 30, values of Manning's n were about 0.018. The greater flow resistance may be attributed, in part, to sinuosity effects in the low flow channel.

Recent (1962) studies of flow resistance for the Rio Grande near Bernalillo, N. Mex., indicate that values of Manning's n vary from 0.035 to 0.012, depending upon the configuration of the channel bed. The average value of n is about 0.030 for a dune bed and 0.015 for a plane bed. The median diameter of the bed material for these observations was 0.29 mm.

The flow resistance for the Rio Puerco was comparable to the flow resistance over a plane sand bed for the Rio Grande. In general, bed configuration does not influence the flow resistance for the Rio Puerco except at low stages; most of the flows for discharges greater than

about 300 cfs (cubic feet per second) are over a plane bed.

It is significant that the resistance coefficients for the Rio Puerco do not seem to be controlled by the condition of the channel bed or by the size distribtuion of the bed material. There was no appreciable difference between the flow resistance over the clay-armored bed and the flow resistance over the sand bed.

CONCENTRATION DISTRIBUTIONS

The equation for sediment suspension was introduced by O'Brian (1933) in the form of a standard diffusion equation:

$$\omega C = \epsilon_s \frac{dc}{dy}, \tag{9}$$

where $\epsilon_s dC/dy$ equals the rate of upward transfer of suspended sediment through turbulent exchange. Rouse (1937) showed that equation 9 could be integrated to yield an equation for the distribution of the relative concentration of the suspended sediment as

$$\frac{C_y}{C_a} = \left(\frac{D-y}{y}\,\frac{a}{D-a}\right)^Z, \tag{10}$$

where

C_y = the concentration of a grain size at the distance y above the bed, in parts per million;
C_a = the concentration of a grain size at reference level a above the bed, in parts per million; and
Z = the theoretical exponent of the distribution equation given by

$$Z = \frac{\omega}{kV_*}. \tag{11}$$

In the derivation of equations 10 and 11, it was assumed that the transfer coefficient for the sediment ϵ_s equals the momentum transfer coefficient ϵ_m.

Equation 10 plotted logarithmically is a straight line with a slope Z. If values of the observed concentration C_y at the depth y are plotted against the values of $(D-y)/y$ on a logarithmic scale, the slope of the line through the plotted points equals Z_1, the observed exponent of suspended-sediment distribution. Typical concentration distributions for some of the size classes given in table 3 are shown plotted in figures 6 through 8. In general, the slope, Z_1, of the line which was fitted by eye to the plotted points is not well defined.

Values of the observed exponent Z_1 usually do not agree with the values of Z, the computed exponent from equation 11. One reason for the difference is that the fall velocity, ω, used to compute Z is usually taken as the terminal fall velocity of a particle falling alone in quiescent distilled water of temperature equal to the stream temperature, whereas the fall velocity in the actual stream may assume a value of a completely different order of magnitude.

It is impossible to determine the fall velocity of a sediment particle in the natural condition of a stream, but it is possible to determine some of the effects of the concentrations of fine sediment upon the fall velocity of the sand-size particles. Simons and others (1963) determined apparent viscosities of suspensions of varying concentrations of bentonite and kaolin in water and computed fall velocities based upon the mass densities

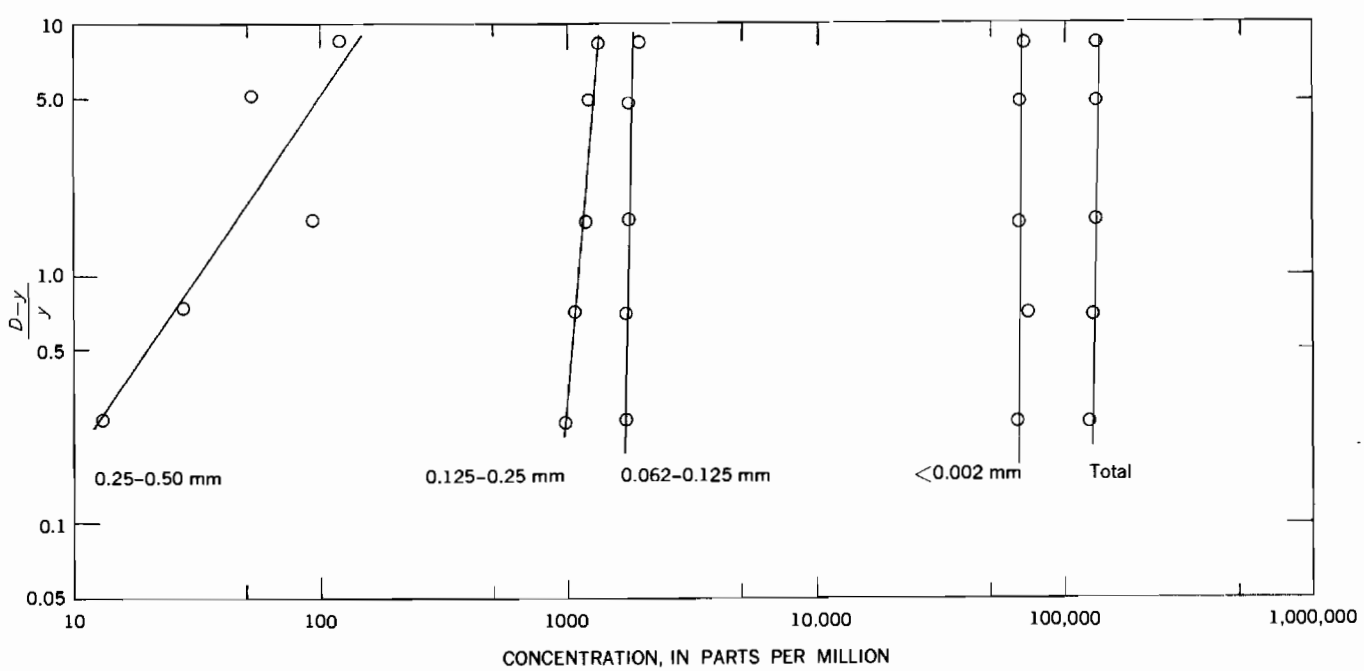

FIGURE 6.—Variation of concentration with $(D-y)/y$, station 200, August 19, 1961.

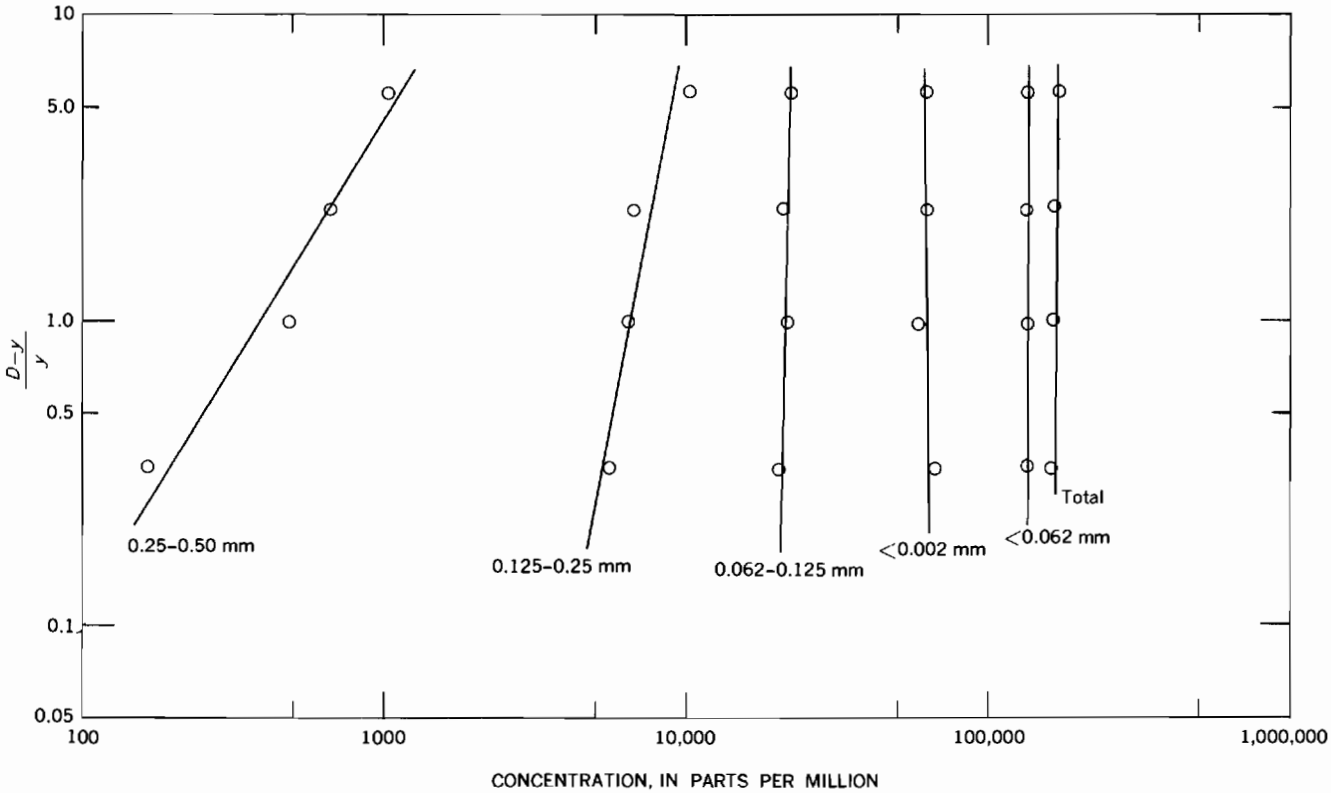

FIGURE 7.—Variation of concentration with $(D-y)/y$, station 200, September 11, 1961.

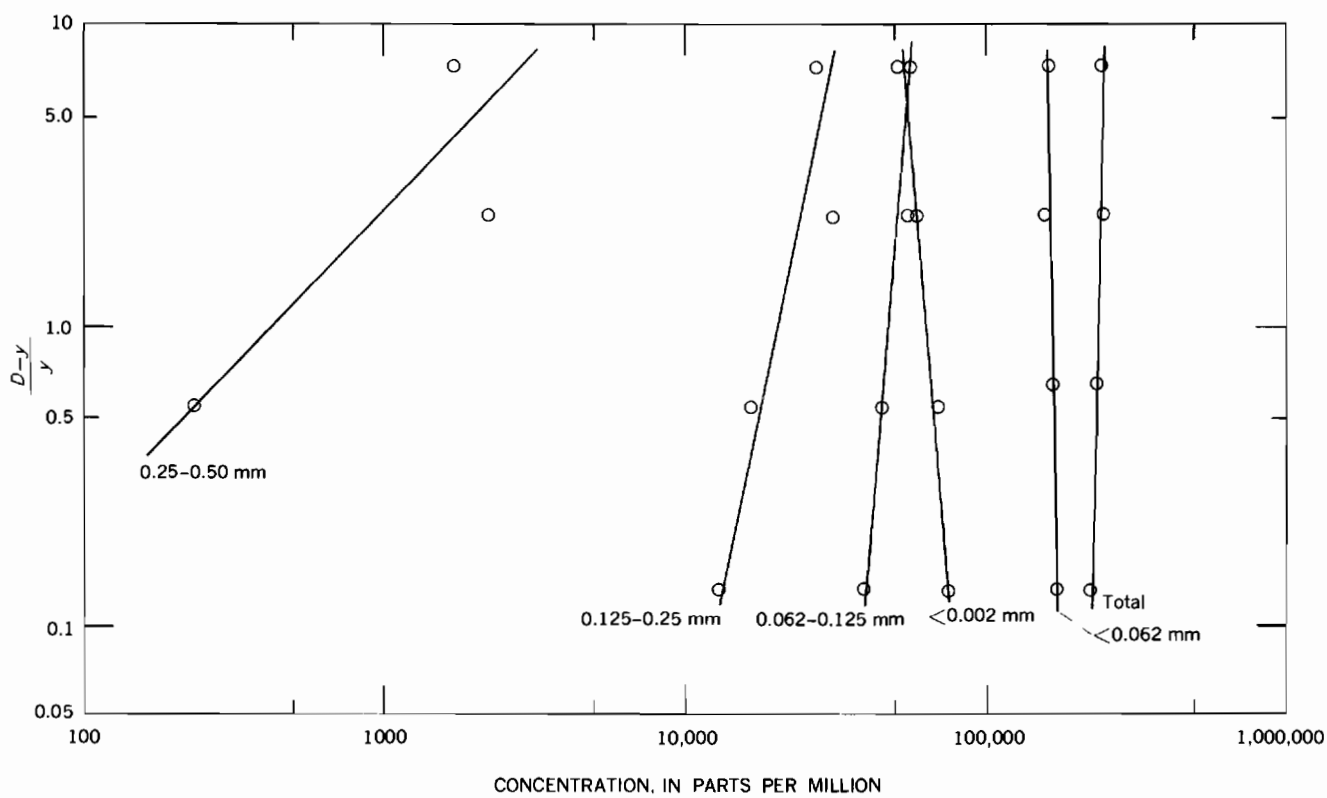

FIGURE 8.—Variation of concentration with $(D-y)/y$, station 170, September 20, 1961.

and the apparent viscosities of the fluids, using theoretical considerations and empirical relations given in Inter-Agency Committee on Water Resources (1957b). The computed fall velocities compared favorably with fall velocities determined by analyzing a sand of known distribution in the visual-accumulation tube, using suspensions of known concentrations of fine material as a sedimentation fluid.

The determination of the effects of concentrations of suspensions of fine sediment upon fall velocities using the visual-accumulation tube is simple. Figure 9 shows the particle-size distribution of a sample of sand from the bed of the Rio Puerco analyzed in distilled water (curve *A*) and in a suspension of fine sediment (curve *B*). The median diameter in distilled water is 0.33 mm, which has a standard fall velocity of 4.9 cm per sec (centimeters per second) at 24° C. The median diameter of the sample in the native water is 0.16 mm, which has a standard fall velocity of about 1.84 cm per sec. If values of fall velocity determined in this manner are plotted along the ordinate against concentrations of fine sediment in the sedimentation fluid, plotted on the abscissa, the plotted points define a trend which is indicative of the effects of concentrations of fine material upon fall velocity.

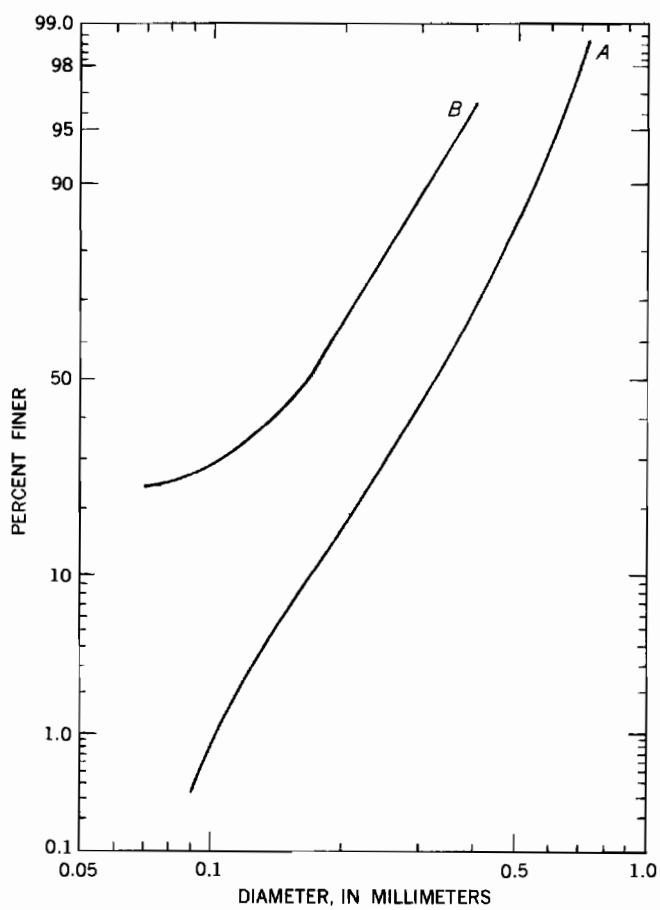

FIGURE 9.—Particle-size distributions from visual-accumulation-tube analysis in distilled water (curve *A*) and in native water with 150,000 ppm suspended sediment finer than 0.053 mm (curve *B*).

Figure 10 shows the trends defined by the method described above for the geometric mean of several size classes of sands. The sedimentation fluids used were (a) suspensions of fine material (<0.053 mm) from the Rio Puerco in native water, mechanically dispersed; and (b) suspensions in distilled water, mechanically and chemically dispersed. The ratio of the weight of the dispersing agent (sodium hexametaphosphate) to the weight of the fine sediment was 1 to 100. Some flocculation of the clays occurred in the native water. The flocculation did not have any major effects on the size distributions for low concentrations of fine material, but at concentrations of about 100,000 ppm or greater the flocculation of the clay appeared to cause a clogging of the sand grains in the visual-accumulation tube. Several of the points in figure 8 with extremely low fall velocities are the results from analysis where the clogging occurred. No weight was given these points in drawing the trend lines in the figure. The fall velocity defined by figure 10 will be designated ω'.

Values of Z', the sediment distribution exponent computed from equation 11 using ω' from figure 10, show better agreement with Z_1 than do the values Z com-

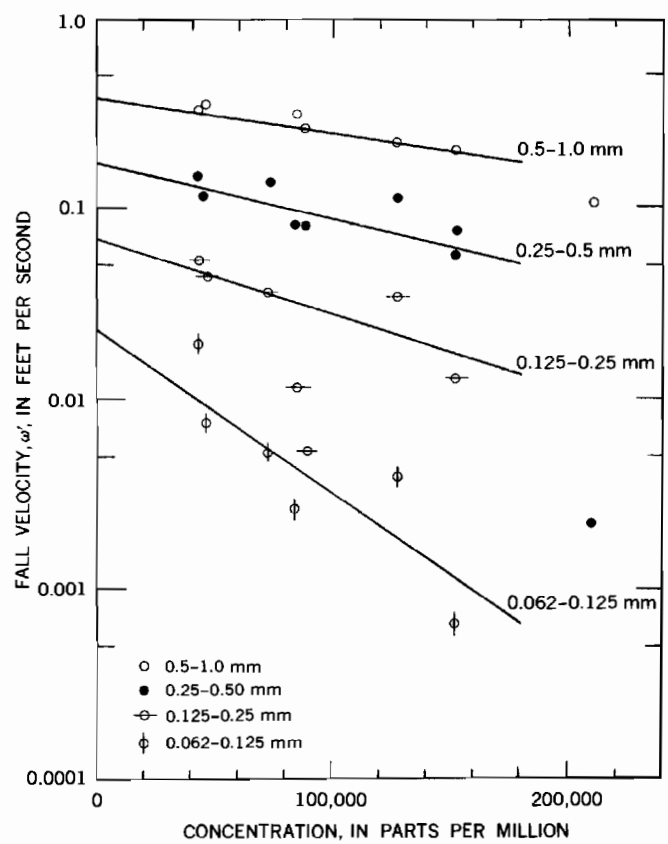

FIGURE 10.—Variation of fall velocity with concentration.

puted using the standard fall velocities, ω. Computations of values Z and Z' for given dates in 1961 are given in table 5, and values of Z and Z' are plotted against Z_1 in figure 11.

As might be expected, there is considerable scatter in the relation of Z' to Z_1. Part of this scatter may be attributed to variations in the stream temperature, which ranged from 17° C to 24° C. The relation of fall velocity to concentration was defined for only one temperature, 24° C, and was applied to all the Z values regardless of the temperature of the stream.

The effect of temperature on the fall velocities for a given sand size and concentration of fine material was not defined from the data in this investigation. However, something of the magnitude of the temperature effects may be indicated. Figure 12 shows the variation of the apparent viscosity with temperature of dispersed fine sediments in native water for the Rio Puerco near Bernardo, N. Mex., for a range of temperature from 2° C to 40° C at a constant concentration of 127,000 ppm. The apparent viscosities were determined with a Stormer Viscometer. Simons and others (1963) found that for a given fine material dispersed in distilled water, the ratio of the viscosity of the dispersion to the viscosity of water was independent of temperature. Therefore, some of the scatter in figures 10 and 12 probably is due to variations in viscosity of the dispersions other than the variations caused by concentration and temperature.

Other major factors which influence the viscosity of a clay-water system are the mineralogical composition of the clay, the nature and amount of adsorbed ions, and the electrolytes present in solution (Houwink, 1952).

Partial chemical analyses of the native water of the Rio Puerco for two of the observation dates in 1961 are given in table 6. The mineralogic composition of the suspended sediment finer than 0.004 mm for September 11, 1961, is shown in table 7. This information was furnished by Mr. V. C. Kennedy, U.S. Geological Survey, Denver, Colo. (oral communication, 1962). The cation exchange capacity for this sample was not available for this report. Without knowing the exchange capacity, it is impossible to predict the effects of the chemical constituents in the native water upon the properties of the suspension.

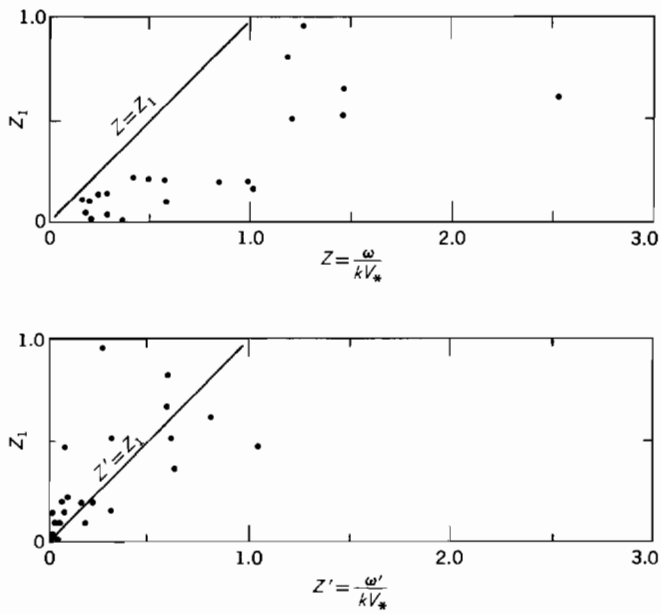

FIGURE 11.—Z and Z' plotted against Z_1.

Because illite and montmorillonite plus mixed-layer clay constitute more than 50 percent of the clay-sized material, it is assumed that the exchange capacity is high and that the chemical constituents of the native water have considerable effect upon the properties of the suspension.

The general shape of the viscosity curves for clay-water systems with various amounts of added base is shown qualitatively in figure 13. Where both monovalent and divalent ions are present (table 6), the general shape of the viscosity curve would probably fall somewhere between the extremes shown in figure 13.

TABLE 5.—*Measured and computed exponents of sediment distribution*

Date	Station	D (ft)	$V_*=\sqrt{gDS}$ (fps)	k	T (°C)	ω, in feet per second			ω', in feet per second			Z_1			$Z=\omega/kV_*$			$Z'=\omega'/kV_*$		
						0.062 -0.125 (mm)	0.125 -0.25 (mm)	0.250 -0.50 (mm)	0.062 -1.25 (mm)	0.125 -0.25 (mm)	0.250 -0.50 (mm)	0.062 -0.125 (mm)	0.125 -0.25 (mm)	0.250 -0.50 (mm)	0.062 -0.125 (mm)	0.125 -0.25 (mm)	0.250 -0.50 (mm)	0.062 -0.125 (mm)	0.125 -0.25 (mm)	0.250 -0.50 (mm)
July 10	170	2.6	0.179	0.317	22	0.0226	0.0669	--------	0.005	0.034	--------	0.48	0.82	--------	0.400	1.18	--------	0.088	0.600	--------
	170	2.5	.176	.316	22	.0226	.0669	--------	.005	.034	--------	.22	.51	--------	.406	1.20	--------	.090	.612	--------
Aug. 18	185	2.6	.205	.401	24	.0233	.0699	0.174	.00066	.014	0.052	.14	.20	0.36	.283	.837	2.12	.008	.170	0.63
Aug. 19	170	5.8	.212	.319	23	.0230	.0684	.172	.0017	.021	.070	0	.16	.47	.340	1.01	2.54	.025	.311	1.04
	200	4.8	.192	.617	23	.0230	.0684	.172	.0017	.021	.070	.02	.10	.67	.195	.580	1.46	.014	.178	.593
Sept. 11	200	2.0	.280	.23	19	.0207	.0633	.163	.0007	.014	.052	.03	.20	.62	.321	.983	2.53	.011	.217	.807
Sept. 20	170	3.4	.402	.312	17	.0203	.0623	.159	.0002	.0077	.034	.10	.21	.96	.162	.498	1.27	.002	.062	.272
	185	3.3	.383	.287	17	.0203	.0623	.159	.0002	.0077	.034	.10	.20	.52	.185	.566	1.45	.002	.070	.309

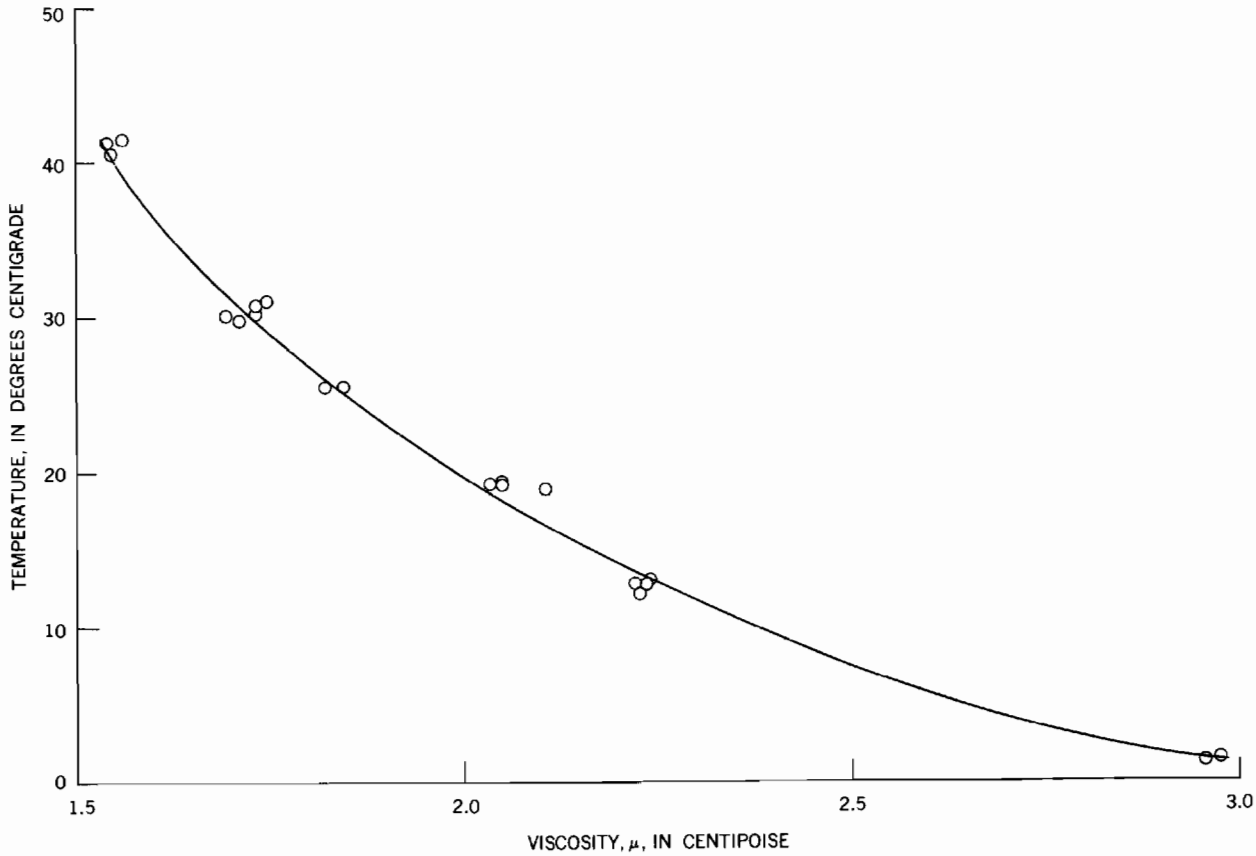

FIGURE 12.—Variation of apparent viscosity with temperature for dispersed fine sediment in native water, Rio Puerco near Bernardo, N. Mex.

TABLE 6.—*Partial chemical analysis of native water*

Date	Specific conductance (micromhos at 25°C)	pH	Concentration (parts per million)					
			Total	Ca	Mg	Na	K	Na+K
July 10	3,050	7.2	2,200	198	36	473	15	-------
Sept. 11	1,730	7.3	1,270	158	17	------	------	228

TABLE 7.—*Mineralogical composition of suspended sediment finer than 0.004 mm, September 11, 1961*

Material	*Percent*
Amorphous material	2–3
Kaolinite (hydromica)	25–30
Illite	10–15
Montmorillonite plus mixed-layer clay	40–45
Quartz	9–12
Calcite	2–3

Previous records show appreciable variations in the concentrations of the chemical constituents in the Rio Puerco flow. The physical properties of the fine sediments—such as the color, size distribution, and plasticity—are known to vary, depending upon the source of the sediment. It may be assumed that the mineralogical composition of the material finer than 0.004 mm also varies. Obviously, on the Rio Puerco the clay-water systems become extremely complex, and the viscosities of the dispersions cannot be predicted with any degree of certainty. It is generally conceded that the effects of the factors influencing the viscosity of heterogeneous fluids containing ionized particles are beyond explanation at the present time (Houwink, 1952).

So far as sediment transport is concerned, the effects of fine material upon the fall velocities and concentration distributions of sand-sized particles must be defined from empirical relations, such as those in figures 10

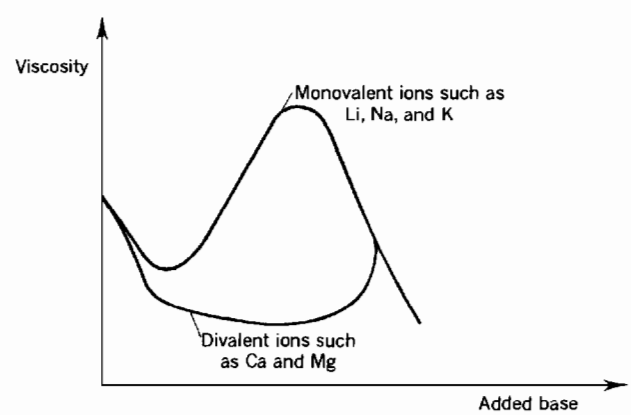

FIGURE 13.—General shape of the viscosity curves for clay-water systems with various amounts of added base. From Simons and others (1963).

and 12. As shown by figure 11, these empirically defined relations cannot be expected to yield accurate results.

From a practical viewpoint, however, it is probably not necessary to determine accurately the concentration distributions in streams such as the Rio Puerco, because the total concentration distribution is so nearly uniform through a vertical that samples taken anywhere in the vertical give a reasonable representation of the average concentration and particle-size distribution of the sediment transported by the stream. From figures 6 through 8 and table 3, it can be seen that in almost all instances the slope of the line through the points representing total concentrations is not much different from the slope of the line through the points for the very finest fraction. (Some of the fine fractions show a reverse concentration gradient; that is, the concentration appears to be greater near the surface than near the bed. This is probably due to errors inherent in the sampling and laboratory procedures.) Also, the total concentration distribution depends to some extent upon the concentrations of sands in the flow; as will be shown in the next section, the concentration of the sands is unpredictable over a considerable range of conditions.

CHANNEL BED

The characteristics of the channel-bed material effect both the flow and the sediment transport.

When this investigation began in July 1961, the sand bed of the channel was impregnated with clay to a depth of about 0.6 foot (fig. 14). Analyses of core samples for particle-size distribution showed the clay-armored layer to have a median particle diameter of 0.067 mm and to contain about 50 percent sand, 23 percent silt, and 27 percent clay. The underlying sand contained 10 percent fine material and had a median particle diameter of 0.20 mm (fig. 15).

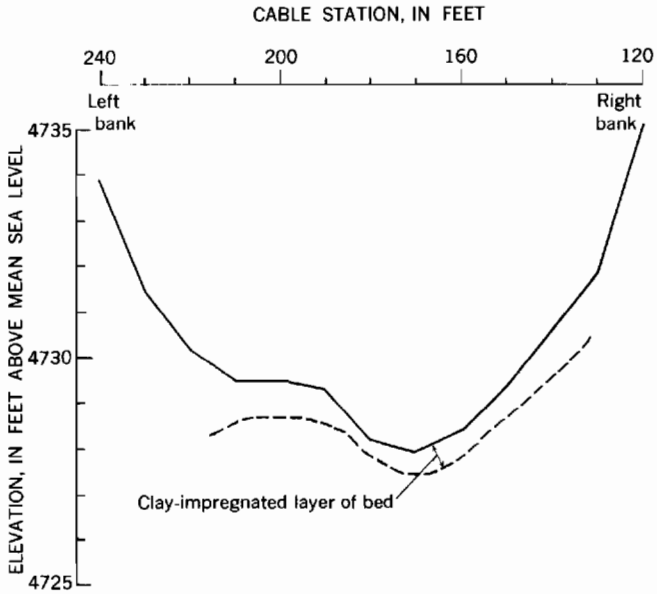

FIGURE 14.—Section B, showing the thickness of the clay-impregnated layer of the bed.

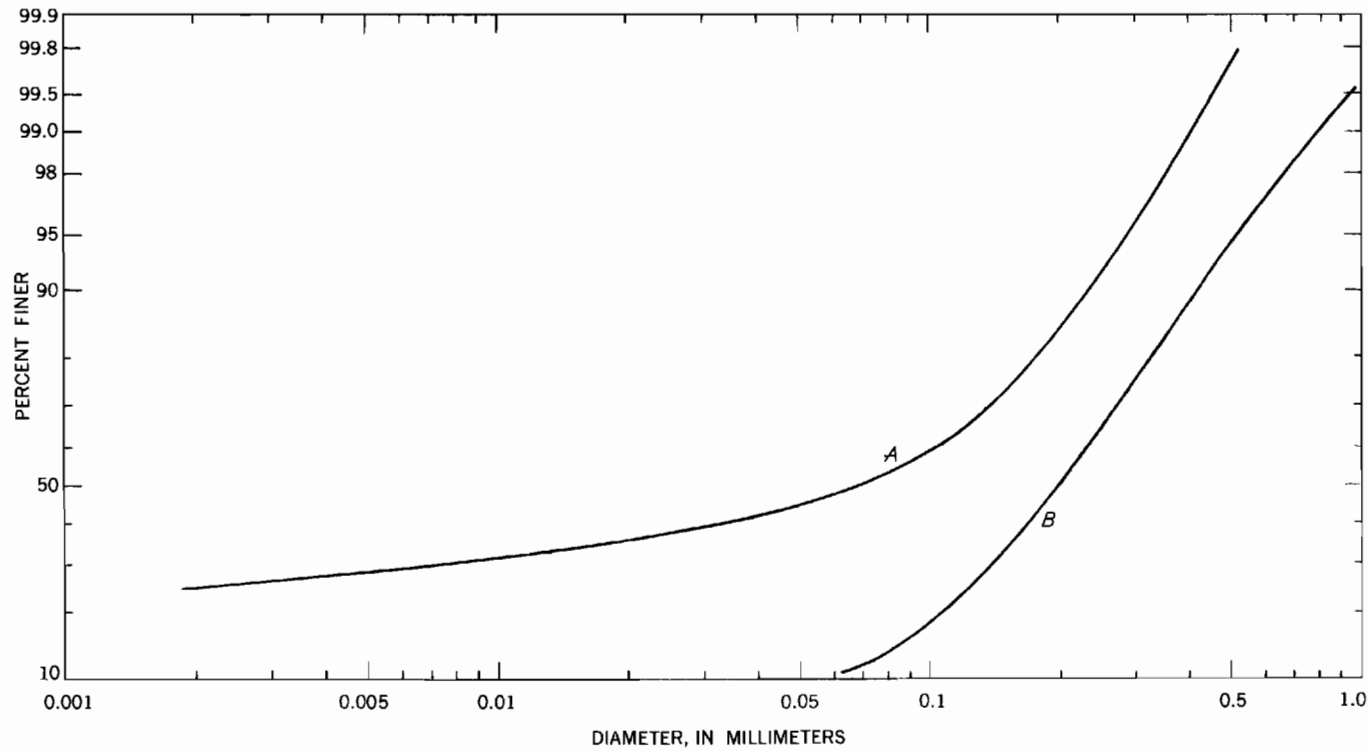

FIGURE 15.—Particle-size distribution of the clay-impregnated layer of the bed (curve A) and of the underlying sand (curve B).

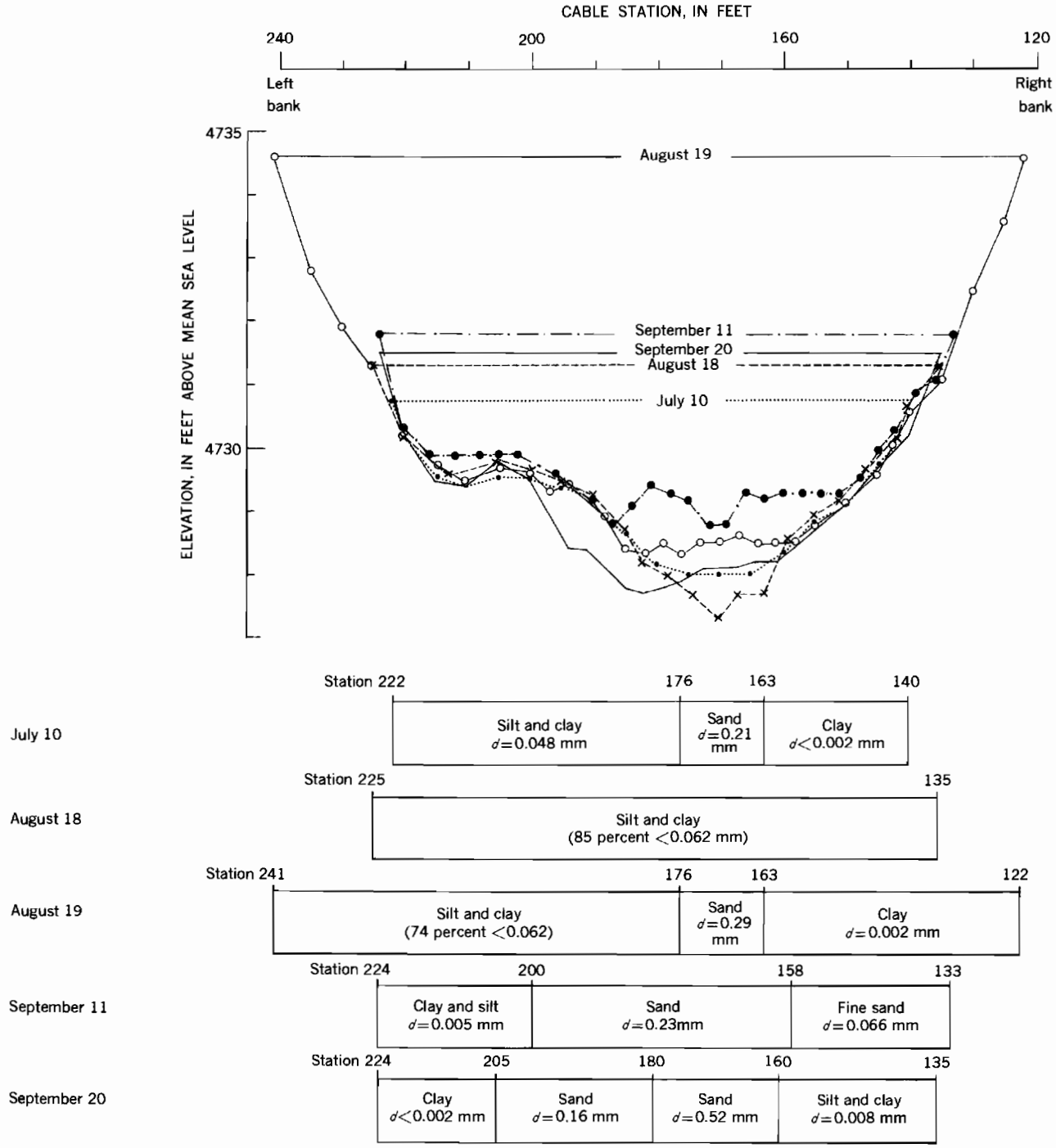

FIGURE 16.—Cross sections defined from water-discharge measurements, and lateral distribution of bed material, 1961.

The conditions which caused the bed to armor are not known. Probably, the armoring was the result of a combination of (a) the deposition of sand, silt, and clay during receding flows; and (b) the infiltration of flow into the channel bed, carrying clay into the pore spaces between the sand grains. The clay served as a matrix to bind the top few inches of the bed when the material dried.

Streamflow records show that the July and August flows originated above the confluence of the Rio Puerco and the Chico Arroyo. From the extremely low concentrations of suspended sand in these flows (table 4), it is concluded that the channel bed was armored through the entire 100-mile reach. Thus, although there are vast quantities of sand in the Rio Puerto watershed, under some conditions this sand is not available for transport.

Figure 16 shows the cross sections of the channel defined from the water-discharge measurements. The bar graphs plotted below the cross sections give an indication of the bed material across the wetted perimeter at the time of the observations. The graphs were constructed from the size analyses of the individual samples of bed material collected with the BM–54 sampler. The stations listed at the top of each bar graph indicate the approximate boundaries of the different types of bed material. The graphs show, for example, that on July 10, 1961, sand with a median particle diameter of 0.21 mm was present on the bed of the channel between stations 163 and 176, whereas on August 18, the entire wetted perimeter (station 135 to station 225) was covered with silt and clay. The average size distribution of the bed material is given in table 4. Of special interest are the wide variations in the size distributions of the bed material and the presence of the coarse sand (d=0.52 mm) on September 20.

Trains of standing waves were present through the reach during both of the September observations (fig. 17); on September 20, violently breaking antidunes were noted. The coarse sand was found on the bed in the area of the channel where trains of these waves were forming, breaking, and reforming at regular intervals of about 2 to 3 minutes. Standing waves were not observed to form over the clay-impregnated bed.

During July through September, the period of these observations, the channel of the Rio Puerco was undergoing relatively rapid changes. A "headcut" in the clay armoring of the bed, commencing at the confluence of the Rio Puerco and the Rio Grande, had progressed upstream by August 19 to the bridge at U.S. Highway 85. On August 30, it was about 50 yards downstream from the cable (fig. 18). There was no evidence from the cross sections in figure 15 to indicate that the headcut had moved upstream from section B on September

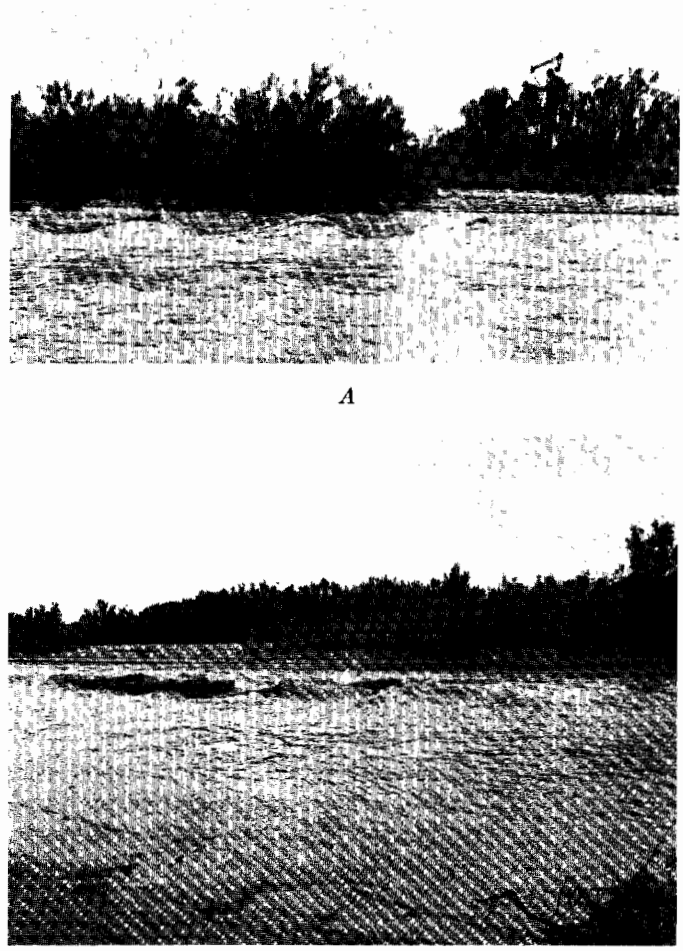

A

B

FIGURE 17.—Standing waves and antidunes in the reach, September 11, 1961.

11 or 20. Probably, the headcut was upstream from section B, and the cut channel had refilled with sand. There was no discontinuity in the water-surface profile to indicate the presence of the headcut, because at discharges greater than about 300 cfs, the plunge pool would drown out. Figure 19 shows the cross section of the channel measured under the cable on October 5, 1961. On this date the headcut was upstream from the old Highway 85 bridge. In the channel above the headcut the bed was still armored with clay; in the cut channel the bed material was composed of sand with a median diameter of 0.35 mm. The core samples taken prior to the headcut showed the material at the same elevation to have a median diameter of about 0.2 mm, hence there was an appreciable change in the bed material as the headcut moved upstream.

The presence of the headcut in the study reach is reflected in the increased water-surface slopes for the September observations. The cut channel through the reach was uniform in cross section, averaging 25 feet wide and 3 feet deep (fig. 20). Changes in the channel

Scour and Fill in Sand-Bed Streams

By BRUCE R. COLBY

SEDIMENT TRANSPORT IN ALLUVIAL CHANNELS

GEOLOGICAL SURVEY PROFESSIONAL PAPER 462-D

UNITED STATES GOVERNMENT PRINTING OFFICE, WASHINGTON : 1964

UNITED STATES DEPARTMENT OF THE INTERIOR

STEWART L. UDALL, *Secretary*

GEOLOGICAL SURVEY

Thomas B. Nolan, *Director*

For sale by the Superintendent of Documents, U.S. Government Printing Office
Washington, D.C. 20402

CONTENTS

	Page
Definitions	IV
Abstract	D1
Introduction	1
Determinations of scour and fill	2
Photography	2
Cross-section soundings	2
Stage-discharge relations	2
Sonic soundings	2
Probing	3
Plastic ribbons	3
Log chains	3
Interpreting observations of scour and fill	3
General principles of scour and fill	5
Quantity of sands being transported	6
Some previous statements or uses of the principles	7
Discharge of sands as a function of flow characteristics	8
The simple continuity equation	8
Applications of the principles to assumed channel reaches	D9
Channel downstream from a reservoir	10
Straight, uniform channel	10
Uniform slope and roughness	12
Changing slope or roughness	12
Constriction in a straight, generally uniform channel	14
Winding streams	21
Scour and fill in natural streams	21
A generally stable sand-bed stream	21
Narrow section of a natural sand-bed stream	24
A pool-and-riffle stream	25
Streamflow, sediment concentration, and changes in bed elevation	25
Application of principles of scour and fill	30
Conclusions	31
References	32

ILLUSTRATIONS

		Page
FIGURE	1. Schematic diagram of instantaneous bed positions at six points in a stream cross section	D4
	2. Approximate volume of moving sands per unit area of streambed for 0.30-millimeter median diameter of bed material and 60° F water temperature	7
	3. Approximate discharge of sands for 0.30-millimeter median diameter of bed material and 60° F water temperature	8
	4. Properties of assumed cross section	9
	5. Streamflow and discharge of sands at the downstream end of an assumed 1,000-foot channel reach immediately downstream from a dam that traps all sands in the flow	11
	6, 7. Streamflow, discharge of sands, and accumulated sands in an assumed 5,000-foot reach—	
	6. Straight, uniform channel	13
	7. Straight channel that is uniform in bed material and cross section but has a gradually decreasing slope toward the downstream end	15
	8. Depths of computed scour at narrow section of an assumed 1,000-foot reach of straight channel	19
	9. Schematic profile of bed position at and near a narrow section of an assumed straight sand-bed channel after a short period of constant flow	19
	10–13. Changes in average gage height of the streambed of the Elkhorn River near Waterloo, Nebr.—	
	10. During a period of high flow in 1951	22
	11. During a period of high flow in 1952	22
	12. May 18–July 19, 1951	23
	13. April 1–October 23, 1952	24
	14. Comparison of scour and fill computed from changes in bed position at two cableway sections on the Elkhorn River near Waterloo, Nebr	25
	15. Streamflow and changes in average bed position of Missouri River near Yankton, S. Dak., March–September 1941	25
	16. Streamflow, measured sediment concentrations, and changes of average bed position at Lees Ferry and Grand Canyon, Ariz., April 1–August 31, 1955	26
	17, 18. Changes of average bed position at Lees Ferry and near Grand Canyon, Ariz.—	
	17. October–December 1957	27
	18. April–July 1959	28
	19. Variable relation of concentration of measured sands to flow of the Colorado River near Grand Canyon, Ariz	30

TABLES

	Page
TABLE 1. Differences between two types of concentration of transported sands at a vertical	D6
2. Volumes of sand removed from a 1,000-foot reach of channel downstream from a dam at different constant rates of steamflow through the standard cross section	10
3. Fill in an assumed 5,000-foot reach of straight channel of the standard cross section if velocities at a given depth are 20 percent lower at the downstream end of the reach than at the upstream end	14
4. Computed initial rates of scour between cross sections A and B at different flows for which the depths of flow above the flat beds are assumed to be equal at the two sections	16
5. Average scour at section B after five constant flows have established equilibrium bed positions	D17
6. Computed scour at cross section where bottom width is 66 feet in channel whose uncontracted bottom width is 84 feet	20
7. Computed average scour or fill, by months, during 1955 water year in 88-mile reach from Lees Ferry to Grand Canyon, Ariz	30

DEFINITIONS

Antidunes.—Roughly symmetrical sand waves that are about in phase with similar water waves. Definition includes as antidunes roughly symmetrical sand waves that may exist below quiet and symmetrical standing waves on water surface.

Bars.—Extensive raised areas or ridges, larger than dunes in same flow, on bed of stream whose bottom shifts readily, at least at high flow.

Bed elevation.—Vertical position of surface of streambed above arbitrary datum. For flow over sand bed, streambed is lowest position at which sand grains are generally moving at a particular instant. Perhaps sand grains shift somewhat, but without moving far, below streambed.

Bed material.—Sediment of particle sizes found in appreciable quantity in streambed. Term is based on particle size rather than on mode of transportation or location in cross section.

Dunes.—Somewhat irregularly spaced mounds of loose sand whose upstream faces are usually gently inclined as compared with their much steeper downstream faces.

Fill.—Net deposition of sediment on stream boundary. Fill may be measured in volume of sediment added to a channel reach, in average depth of sediment accumulation over an area, in average change of depth at a cross section, or in change of depth at a point.

Fine sediment.—Term used in this paper for sediment finer than 0.062 mm.

Flat bed.—Term applied in this paper to general configuration of beds of assumed channels. Does not imply absence of dunes, antidunes, or bars.

Measured concentration of sediment or of sands.—Concentration based on depth-integrated sediment samples which generally are obtained by sampling flow from water surface to within 0.3 or 0.4 ft of streambed.

Measured discharge of sediment or discharge of sands.—Discharge that is usually determined directly from streamflow and depth-integrated sediment samples. Depth integrated samples obtained by sampling flow from water surface to within 0.3 to 0.4 ft of streambed.

Plane bed.—Bed that is free of dunes and antidunes and, consequently, has low resistance to flow. Usually is smoother and firmer than bed of sand-bed streams of other configurations.

Pool-and-riffle stream.—Stream characterized by alternate pools and riffles.

Sand.—Sediment particles that have diameters between 0.062 and 2.0 mm.

Sand-bed stream.—Reach of stream whose bed consists almost entirely of cohesionless shifting sand and whose channel is not confined by walls of rough rock or other material that would cause unusually high turbulence throughout much of flow.

Scour.—Net removal of sediment from stream boundary by action of fluid flow. Scour may be measured in volume of sediment removed from a channel reach, in average depth of sediment removal from an area, in average change of depth at a cross section, or in change of depth at a point.

Unmeasured discharge of sands.—Difference between total discharge of sands and measured discharge of sands at a cross section.

SEDIMENT TRANSPORT IN ALLUVIAL CHANNELS

SCOUR AND FILL IN SAND-BED STREAMS

By Bruce R. Colby

ABSTRACT

The surface of a sand bed of a stream rises when more sand is deposited on it than is removed from it and falls when more sand is removed from it than is deposited on it. The average elevation of the surface is constant whenever the volume of sand being deposited equals the volume of sand being removed. Hence, two basic principles generally are required to explain or to understand scour and fill in sand-bed channels. One principle is continuity of sediment discharge along a stream reach—that is, for a sand-bed stream, a balance between the volume of sand-size particles deposited on and removed from a sand bed. The other principle is that a relation exists between discharge of sands and characteristics of flow and available sands. If no such relation were to exist, the difference between the discharges of sands into and out of a channel reach would be wholly indeterminate except by measurement.

Although the basic principles of scour and fill are not new, they are frequently disregarded or misunderstood, partly because many observations of scour and fill in streams have been misinterpreted. These misinterpretations are due largely to the common assumptions that scour or fill at a point is representative, both in quantity and in timing, of average scour or fill at a cross section and that average scour or fill at a cross section is representative of scour or fill in a long reach of channel.

The principles of scour and fill when applied to assumed channels define general patterns of streambed changes for certain types of channel. These principles indicate fairly definite limits on the rate of net scour or net fill over long reaches of channel.

Observed changes in bed elevation, defined by streamflow measurements on the Elkhorn River at Waterloo, Nebr., the Missouri River near Yankton, S. Dak., and the Colorado River at Lees Ferry and near Grand Canyon, Ariz., show, respectively, the different general patterns of scour and fill in a stream that has a generally stable sand bed, in a stream at a laterally constricted cross section, and in a pool-and-riffle stream. These patterns are explainable in terms of the basic principles of scour and fill, although scour and fill in a pool-and-riffle stream may be difficult to compute theoretically.

Conclusions indicated by the study, but not universally accepted, include the following:

1. At any instant, the quantity of moving sand, even in deep and swift flows, is usually equivalent to an average depth of deposit of only a few hundredths of a foot on the streambed.
2. In a straight sand-bed channel that has uniform cross section, slope, roughness, and bed material, the streambed does not either scour or fill appreciably during the passage of a flood.
3. In a straight channel having uniform cross section but varying slope or roughness along the channel, fill during a rising stage is usually followed by fill on the falling stage, and scour during a rising stage is usually followed by scour on the falling stage.
4. If a change in roughness or in streamflow requires a change in the depth of flow, the depth generally adjusts through a change in elevation of the water surface and not through a change in elevation of the streambed.

INTRODUCTION

Sand on the bed of a stream usually shifts readily, and unless the velocity of flow near the bed is very low, some sand grains are moving at every instant. If the velocity near a sand bed is high, many grains move from a particular area during each short period of time and are replaced by many other grains. Because of the continual shifting of individual grains, the average elevation of the sand bed of a stream frequently is assumed to be very unstable.

The assumption of instability seems to be supported by observations that are commonly made by stream gagers, among others, who, when wading on a sand bed where velocities are high, feel the sand wash out around and under their feet. Also, cross-sectional areas of a series of streamflow measurements that are made while a flood wave was passing a measuring section generally show scour during high and rising stages and fill during falling and low stages. When the series of measurements is plotted against gage height, the slope of the average relation may indicate that the flow increased more rapidly with stage than it would have for a channel having rigid boundaries. Thus, on the basis of general experience, many stream gagers and hydraulic engineers assume that the average elevation of a streambed fluctuates widely from time to time, especially during periods of high and rapidly changing flow. The limitations imposed on changes of the average elevation of the bed by continuity of quantity of the bed material along the stream are frequently overlooked.

The purpose of this paper is to show in reasonably simple and practical terms the general principles that

govern scour and fill in sand-bed streams at cross sections that are free from obstructions such as piers or pilings. These principles are not new, but they are sometimes disregarded or misapplied. In particular, the application of the principle of continuity is stressed.

Determinations of scour and fill and possible misinterpretations of them are discussed first; then the principles of scour and fill are explained; and, finally, the principles are applied to some assumed channel reaches and are illustrated by the behavior of a few types of natural streams.

Some unpublished information on concentrations and particle sizes of sediment and on elevations of the streambed of the Colorado River at Lees Ferry and near Grand Canyon, Ariz., was furnished by J. M. Stow, district chemist, Albuquerque, N. Mex.

DETERMINATIONS OF SCOUR AND FILL

Several direct or indirect methods for determining scour and fill are sometimes used in flumes or in natural streams. A few of these methods are mentioned briefly, and some possibly misleading interpretations of results of the methods are pointed out.

PHOTOGRAPHY

The general shape and movements of sand-bed features that are formed by flows in a flume can often be best shown by photographs. For example, the topography of a sand bed can be shown by a photograph taken after the water has been drained from the flume, profiles of dunes or antidunes can be photographed through observation ports of flumes during runs, and the changing features of a sand bed can often be well shown by moving pictures that are taken while water is flowing in a flume. Ordinarily, however, photographic observations cannot be made satisfactorily of the sand beds in field streams.

CROSS-SECTION SOUNDINGS

Soundings by either mechanical or sonic methods at several or many verticals of a cross section provide a direct measure of the average position of the streambed at a particular time. Thus, cross-section soundings made periodically furnish reasonably good determinations, by difference, of the average scour or fill at a cross section. However, even in a fairly uniform channel, the changes in average bed elevation may differ from one cross section to another. Much present information on scour and fill in stream channels is based on cross-section soundings at bridges or cableways where streamflow measurements are made, but, unfortunately, streamflow measurements are usually made at narrower-than-average channel sections of sand-bed streams. As will be shown later, in the sections entitled "Constriction in a straight, generally uniform channel" and "Narrow section of a natural sand-bed stream," the changes in average bed elevation at narrow cross sections are likely to be much greater than those at nearby cross sections of the same stream. Hence, although scour and fill can generally be determined with reasonable accuracy at streamflow-measuring sections, the interpretation of the determined scour and fill may be, and often is, misleading.

Even though streamflow measurements are made occasionally at wide cross sections, scour and fill information based on soundings for these measurements can seldom be interpreted correctly unless amounts of scour and fill are determined for the whole width between banks rather than for only the width of the water surface. Water-surface width may vary greatly with time and, for some wide sections of sand-bed streams, may even be less at high flows than at some much lower flows. Therefore, scour and fill generally should be determined for shifting cross sections by defining periodically the position of the surfaces of temporarily unsubmerged parts of the cross section at the same times that the position of the submerged streambed is defined. Of course, determinations for the whole width between banks are made regularly at few, if any, streamflow-measuring sections of wide sand-bed streams.

STAGE-DISCHARGE RELATIONS

Major changes in the bed configuration of sand-bed streams may cause large changes in resistance to flow (Vanoni and Brooks, 1957; Brooks, 1958; Liu and Hwang, 1961; Simons, Richardson, and Haushild, 1962). If a sand bed is in the form of dunes at low flow and in the form of a plane or antidune bed at high flow, the stage-discharge relation may show a large increase in flow for a small increase in stage, according to Einstein and Chien (in Brooks, 1958, p. 556–557, figs. 12, 14), a two-part stage-discharge relationship (Dawdy, 1961), or even a discontinuity (Colby, 1960). This large increase in flow for a small increase in stage has sometimes erroneously been assumed to be an indirect measure of scour of the streambed rather than a measure of decrease in resistance to flow.

SONIC SOUNDINGS

Sonic sounders, although they have not yet been used extensively by the U.S. Geological Survey, would provide much more dependable information on scour and fill at a point in many streams than is commonly obtained by using most other methods for determining stream-bed position. These instruments can be used to

record not only the time and the elevation of the bed when it is at its lowest position at a point but also to define a graph of bed position at a point against time. Sonic sounders also can be used to establish profiles or cross sections of the streambed. Measurements made using the sounders should prove helpful in interpreting correctly observations of scour and fill made using other less informative procedures.

PROBING

The depth of maximum scour during a stream rise sometimes can be determined at points in a cross section or a stream reach by probing with steel rods or soil tubes after the flow has receded. Unless the properties of the recently deposited fill differ appreciably from those of the material that was not moved during the rise, the maximum depth of scour may not be discernible at some points. Even though the maximum depth of scour at each of several points in the cross section can be determined satisfactorily, it rarely occurs simultaneously at all the points. Hence, the interpretation of the maximum depth of scour as determined by probing and of the observed fill above the maximum depth of scour may be questionable, as is the interpretation of other determinations of maximum scour at a point at some unknown time during a flood.

PLASTIC RIBBONS

Maximum scour at points in an ephemeral stream can be determined after a flood by observation of plastic ribbons that had been inserted vertically into the bed of a stream before the flood (Essex, Terry, and Culbertson, written communication, 1954). If enough ribbons at a cross section can be dug out after the flood, the points at which the ribbons bend from vertical to horizontal will define the maximum depth of scour across the section. However, the ribbons may be difficult to recover after a flood, and the time of maximum scour at each point is unknown.

LOG CHAINS

Light log chains have been used in some northern Mississippi streams by the Agricultural Research Service, U.S. Department of Agriculture, to show maximum depths of scour. Each chain was attached to a ring that was slipped over the top of a steel angle that had been driven into the streambed. A pin kept the ring from coming off the top of the angle, but the ring could slide down the angle easily if scour removed the sand below the ring and the chain. The chain was initially laid at or just below the surface of the bed and was extended horizontally downstream from the angle. The position of the chain usually could be determined easily at low flow or no flow whenever knowledge of the depth of maximum scour prior to a selected time was needed. Probably the observed positions of a chain indicated the maximum depth of scour fairly accurately, although the steel angle and the chain may have affected the scour a little and the chain may have tended to settle slightly into a loose sand bed during periods of flow. Of course, the exact time of the maximum scour was not known, and the maximum scour at all points along a chain may not have occurred at the same time. Also, the maximum scour at two or more chains at the same cross section may have occurred at different times.

INTERPRETING OBSERVATIONS OF SCOUR AND FILL

Three general problems are involved in interpreting some observations of scour and fill. The first problem is whether or not an average position of the streambed at a cross section can satisfactorily be based on a few observations at the section. The second problem is whether or not an average bed position at a cross section can be determined from observations of maximum instantaneous depths of scour. The third problem is whether or not average or typical changes in elevation of the sand bed in a stream reach can be determined from observed changes in average position of the streambed at one or a few cross sections. These problems prevent the behavior of shifting streambeds from being easily determined and understood from the usual observations available for natural streams.

A few observations are inadequate to determine the average position of a shifting streambed at cross sections where the bed position fluctuates widely. Such sections include those on the San Juan River near Bluff, Utah, on the Colorado River at Grand Canyon, Ariz., on the Rio Grande near Bernalillo, N. Mex. (Leopold and Maddock, 1953, figs. 22, 24, 26), and on the Elkhorn River near Waterloo, Nebr. (Beckman and Furness, 1962, figs. 8, 9). For beds as unstable at individual points as those at the above sections, many measurements obviously are required to define accurately the bed position or changes in the position even for a single cross section. Stream gagers usually make soundings at 20 or more points in most cross sections to be reasonably sure of defining satisfactorily the cross section and the velocity distribution. Changes in bed elevation probably should be based also on measurements at about 20 or more points for most cross sections. If only a few soundings at a cross section are available for a given time, the average bed position based on these soundings should be considered to be inexact unless a study has been made to find if fewer than 20 points are likely to define accurately a bed position for the section.

The second problem, that of determining an average bed position at a cross section from observations of maximum instantaneous depths of scour, is usually difficult and frequently cannot be solved satisfactorily. Suppose that the minimum elevations at 20 points in a cross section of a straight, uniform reach were determined after a flood from the positions of plastic ribbons or log chains that had been installed before the flood. At comparatively low flows at the beginning of the flood, the assumed bed was covered with sand dunes; at high flows the bed was a combination of plane bed near the banks and antidune bed along the middle of the channel. A schematic diagram (fig. 1) for 6 of the 20 points gives a general idea of the difference between the scour that is indicated by the ribbons or chains and the actual lowest average position of the bed at the cross section. As will be shown later, the average position of the streambed in a straight, uniform channel that has uniform bed material usually remains nearly constant during the passage of a flood. This stability of the average bed position was assumed at each point when the schematic diagram was prepared.

Even though the average position of the streambed remains almost constant during the passage of a flood, the maximum scour at each point is roughly 1 foot in figure 1. Thus, an entirely fictitious average scour at sometime during the passage of the flood and an equally fictitious average fill during the recession of the flood (a fairly uniform and even bed with ripples usually is left when the flow ceases or becomes very low in a straight, uniform channel) seem to be indicated by the observed minimum elevations of the streambed. Also, if the average position of the streambed is virtually constant at a cross section, the stability of the average

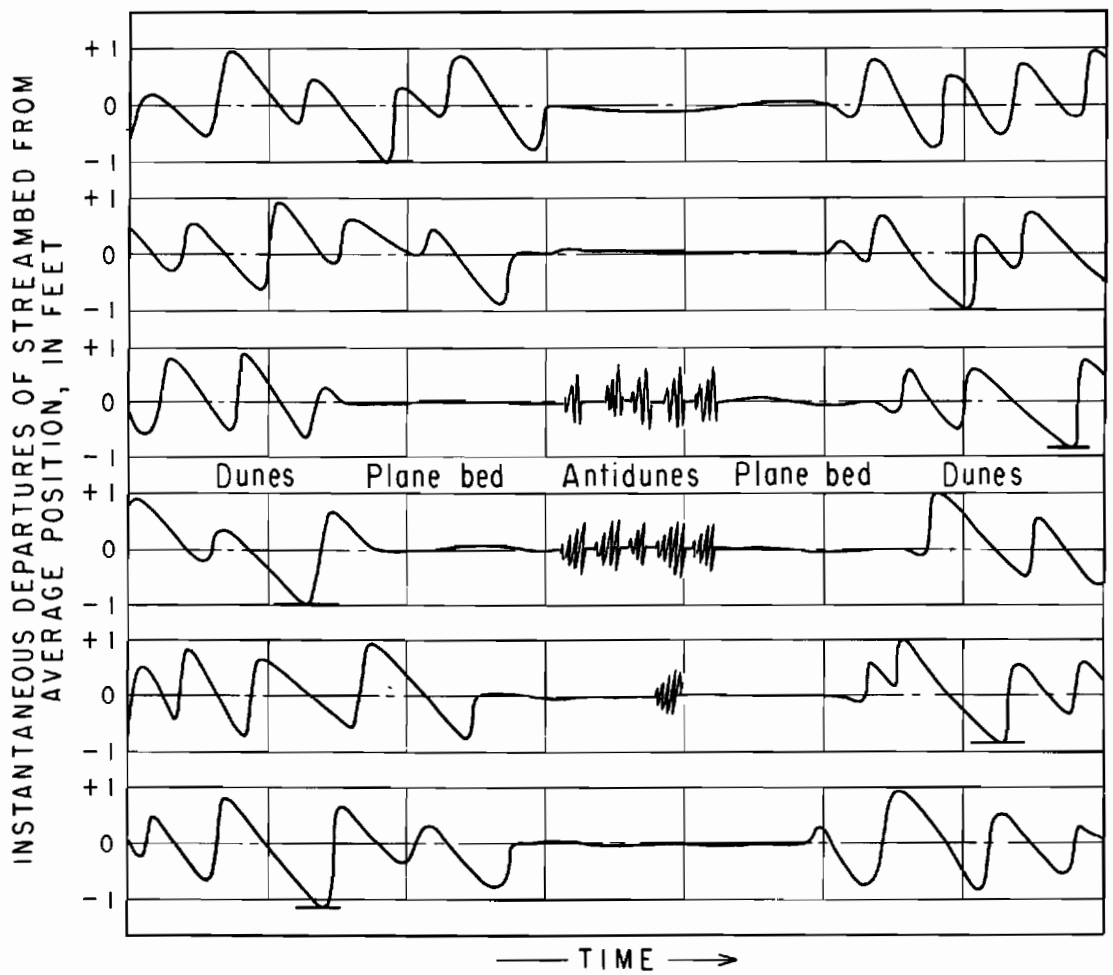

FIGURE 1.—Schematic diagram of instantaneous bed positions at six points in a stream cross section. Time of changes not to scale.

position might not be shown when the bed was rough unless observations were made at many points in the cross section (Beckman and Furness, 1962, p. 12 and figs. 8, 9). For the assumed fairly stable time-averaged elevation at each point, the maximum point scour does not occur at the highest flow. In fact, the least amount of point scour would be indicated at the peak flow at points where the highest flow was over a plane bed. According to the schematic diagram (fig. 1), the maximum point scour does not occur at the peak flow even at a point where the highest flow is over antidunes; it occurs when the bed is the roughest, which is usually when the bed has the largest dunes. In general, the largest dunes are formed at about the deepest flows at which dunes exist. Dunes may exist at the peak flow if the velocity is slow enough in relation to the depth, bed material, water temperature, and concentration of fine sediment; but for many sand-bed streams, at least part of the cross section will have a plane or an antidune bed at the highest flows.

If the assumed cross section had been at a narrow segment of a straight channel, the average bed position at the cross section generally would have been lower at high flows than at low flows. Hence, the observed maximum scour at individual points might have occurred when the bed was plane, if a plane bed existed at the highest flows at the point, or when antidunes were forming and breaking, if antidunes existed at the highest flows. However, the problem is further complicated because the average maximum scour for a narrow section usually occurs after the peak flow.

Sometimes an adjustment might be applied to approximate the average position of the streambed from observations of instantaneous maximum scour at a point. If the streambed at a point was known to be at its lowest position when the bed was covered with dunes, a very rough adjustment to the observed maximum scour might be made by adding an approximation of half of the probable dune height to the observed lowest position at the point. If the bed at a point was known to be plane throughout the passage of the flood (an unusual condition), the observed maximum instantaneous scour may require no adjustment. If the bed position at the point was known to be lowest when the flow was over antidunes, the observed position at maximum scour might be increased by approximately half of the probable maximum amplitude of the antidunes on the bed. Obviously, adjustments such as these, if they can be made at all, are usually inaccurate; but they may at least indicate the probable inaccuracies in the maximum observed point scour during a flood.

The third problem, that of determining average or typical changes in bed elevation for reaches of a stream from changes at a cross section, requires a consideration of the general principles of scour and fill and the application of these principles to different types of channel. This problem will be considered at length in the following sections. In general, it will be shown that alternate scour and fill at a cross section usually indicate that the observed scour and fill are not representative of a long reach of channel even though based on accurate soundings at many points in the cross section. Therefore, alternate scour and fill at a cross section may lead to an incorrect assumption of changes in average bed position in a reach of channel in much the same way that alternate scour and fill at a point may incorrectly be interpreted to mean that the average position of the bed changed at the cross section.

Also, some observed changes in the average bed elevation at a cross section may not be representative or significant even at the cross section. A log or a pile of driftwood at a section or immediately upstream from if may affect the cross-sectional area at least occasionally. A field stream may shift its alinement somewhat from time to time, and a change in alinement may be associated with changes in the shape and size of the cross section at a given flow. Sometimes a narrow and deep channel may form, at least temporarily, in a sand-bed stream (Lane and Borland, 1954, p. 1088–1089). Sandbars may shift on the streambed and cause somewhat unrepresentative short-time changes in cross-sectional area. Therefore, some observed variations in average bed position at a cross section may be due to chance rather than be directly related to changes in flow or in the available sediment.

GENERAL PRINCIPLES OF SCOUR AND FILL

Two simple principles can be used to explain scour and fill in sand-bed streams. One principle is that a relation exists between the discharge of bed material, which is sediment of sizes found in appreciable quantity in the streambed, and the characteristics of the flow and available sediment. Without such a relation, the discharge of sands into or out of a reach of sand-bed channel would be wholly indeterminate except by measurement. The other principle is continuity of the sediment discharge along a stream reach. Each principle is obviously applicable even though some details of its use may be obscure or questionable.

Simple logic indicates that the discharge of sediment of particle sizes that are readily available in the streambed must, for a steady state, be limited by the characteristics of the flow and sediment. If the sediment discharge were not so limited, the available sediment would not remain in the bed. Also, the reproducibility of sediment discharges in flume investigations at steady

711-563 O—64——2

flow suggests a relation of sediment discharge to the characteristics of the flow and sediment.

Although steady flow is rare in natural streams, an approximate relation of discharge of sands in sand-bed streams to mean velocity, width, depth, median particle size of the bed sands, and viscosity or apparent viscosity exists in natural streams (Colby, 1964). If the effects of all the characteristics of the flow and sediment could be accurately evaluated and if all experimental error could be removed, a good relationship could certainly be defined between the discharge of sands and these characteristics for naturally changing rates of flow as well as for constant flows.

Continuity as applied to scour or fill of a channel reach requires that the difference between the discharge of sediment into and out of the reach be balanced by a gain or loss of accumulated sediment within the reach. If fine sediment accumulates within a reach during a period of time, the inflow of fine sediment must have exceeded the outflow of fine sediment during the time. However, in general, the silt and clay that enter a sand-bed reach also leave the reach; so the principle of continuity need be applied to the sands only. Hence, the concentrations of fine sediment in sand-bed streams are usually not directly related to scour and fill. Of course, inflow or outflow of sands or of sediment of all sizes may occur either at the ends of the reach or through tributaries or diversions along the reach. Also, a change in the quantity of sediment in a stream reach may result in a change either in the average elevation of the streambed or in the quantity of sediment that is moving above the streambed. (The weight per unit volume of the sediment in the streambed is assumed to remain unchanged.)

The principles of scour and fill are more easily stated and applied if the quantity of sand being transported can be shown to be negligible. Persons aware of the low concentrations of sands in natural streams may already realize that the amount of sands being transported can usually be disregarded in the application of the principle of continuity. Others may want some rough approximation of the amount of sands being moved at different combinations of depth and velocity.

QUANTITY OF SANDS BEING TRANSPORTED

The depth of all sands in transit, if instantaneously deposited, could be computed from the product of a concentration by weight; the depth of flow; and the ratio, by weight, of a cubic foot of water-sediment mixture to a cubic foot of deposited sands. Unfortunately, the type of concentration c_1 that is needed for such a computation is seldom available, because it is the ratio, by weight, of the sediment to the water-sediment mixture above a particular area of the bed. In contrast, the concentration c_2 that is usually determined from sediment samples is a weight ratio of the discharged sediment to the discharged water-sediment mixture. In terms of sampling at a vertical, the first concentration (c_1) would be obtained if an equal volume of water-sediment mixture could be collected from each small equal increment of depth, including the bed layer, and if all the equal volumes could be mixed and sampled. The second concentration (c_2) would be obtained if the volume from each small equal increment of depth could be collected in proportion to the flow velocity through the increment and if all the volumes could be mixed and sampled. Because the concentration of sands is greatest where the velocity is slowest in the vertical, the first concentration is larger than the second.

For sediment as coarse as sands, the difference between the two types of concentration is large and variable (table 1). Six computations of the ratio of $c_1 : c_2$ ranged from 1.2 to 2.6 and averaged 1.7. Of course, the computations on which information in table 1 is based require extensions, usually inexact, of velocity and concentration of sands from points of observation in the flow to the streambed. However, the inaccuracy is not objectionable for estimating the depth of all sands in transit, if instantaneously deposited from a flow, because the maximum indicated depth of deposit for the flows and concentrations in table 1 is less than 0.01 foot.

TABLE 1.—*Differences between two types of concentration of transported sands at a vertical*

Selected vertical	Date	Median size of bed material (mm)	Flow		Concentration of sands (ppm)		Ratio $c_1:c_2$
			Depth (ft)	Velocity (fps)	c_1	c_2	
Assumed flow		0.25	5.00	3.5	1,330	980	1.4
Barton and Lin (1955), run 22		.18	.76	3.2	2,870	1,090	2.6
Mississippi River at St. Louis, Mo	June 7, 1954	.3	33.5	5.8	292	242	1.2
Do	April 24, 1956	.3	27.0	4.0	344	185	1.9
Do	May 5, 1956	.3	32.8	4.1	161	97	1.7
Do	May 13, 1959	.45	36.8	5.0	159	100	1.6

Approximate depths of average deposits (fig. 2) that might result from the instantaneous settling of moving sands in a reach can be based on a graph by Colby (1964, fig. 21). The graph shows approximate c_2 concentrations of sands for a wide range of mean velocities and depths, a median grain-size diameter of 0.30 millimeter for the bed sands, and a water temperature of 60°F. These c_2 concentrations were determined from an analysis of many available records of the discharge of sands in flumes and in field streams. They should be increased somewhat (Colby, 1964, fig. 24) for high concentrations of fine sediment in the flow. The c_2 concentrations from the graph were doubled (table 1) to obtain approximate c_1 concentrations. A weight of 85 lb per cu ft (pounds per cubic foot) was assumed for the deposited sands; and the approximate volume of moving sand per unit area of the streambed was computed from the product of the c_1 concentration, the depth of flow, and the ratio of 62.4 lb per cu ft to 85 lb per cu ft. The indicated depths of average deposits (fig. 2) are only a few hundredths of a foot, even for deep and fast flows; for many flows the indicated depth is less than 0.01 foot. These amounts of moving sand are so small that they can usually be disregarded in studies of scour and fill.

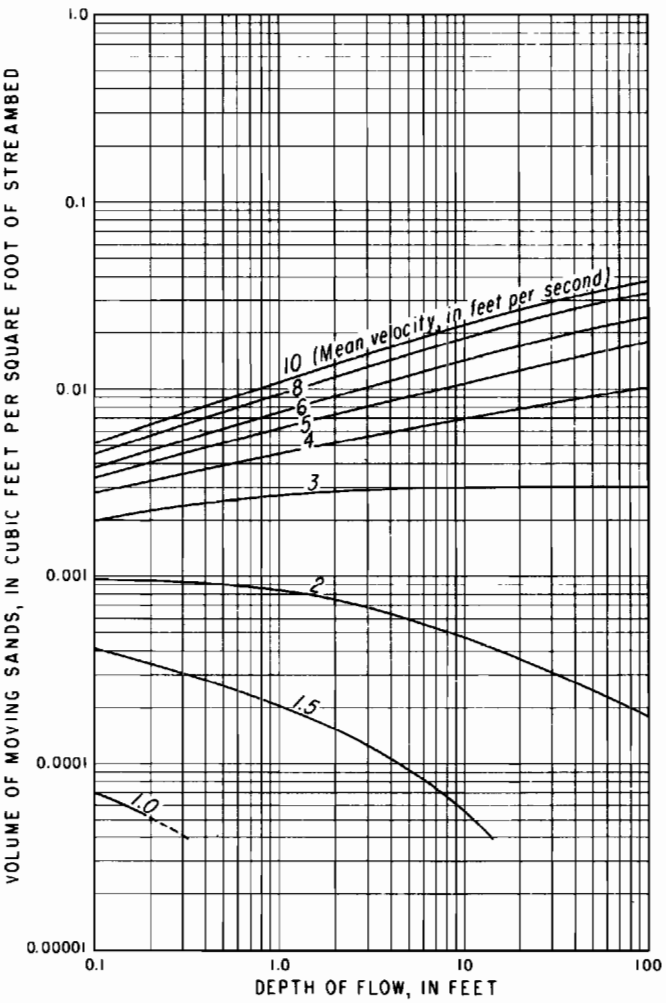

FIGURE 2.—Approximate volume of moving sands per unit area of streambed for 0.30-millimeter median diameter of bed material and 60° F water temperature. Assumed weight per unit volume of sands is 85 lb per cu ft.

SOME PREVIOUS STATEMENTS OR USES OF THE PRINCIPLES

Straub (1934) computed scour for constant flow at a laterally contracted cross section from his form of the Du Boys equation and from the principle of continuity of the bedload discharge. He concluded that observed amounts of scour at narrower-than-average cross sections of a stream probably were not representative of long reaches of a river.

In 1948, the scour and fill in the Missouri River at bridge cross sections where streamflow measurements had been made were reported to be greater than the scour and fill away from the bridges (B. R. Colby and R. E. Oltman, written communication). The conclusion was based on continuity of the sediment discharge and on relatively smaller fluctuations in the stage-discharge relation than in the average elevation of the streambed at the bridge sections.

In 1952, Billy Mitchell and A. J. Harrison, in separately discussing a paper by Leopold and Maddock (1952, p. 172, 173, 176), noted the significance of continuity of the sediment sizes in the streambed. Unfortunately, Mr. Harrison's brief and excellent statement of the principles of scour and fill apparently received little attention, perhaps because it differed from the ideas presented by the authors of the paper.

E. M. Laursen (1952) stated well the fundamental principles of scour and fill. He applied the principles more fully to scour by jets and to scour around bridge piers and abutments than to general scour or fill in a channel reach.

Lane and Borland (1954) studied scour and fill, particularly in the middle Rio Grande, and concluded that the streambed did not generally degrade appreciably during floods although scour was pronounced at some narrow sections. In spite of this excellent paper by Lane and Borland and the statements of principles by Straub, Mitchell, and Harrison, the inherent stability of the average elevation of sand beds, especially in reasonably uniform channels, is still largely unrecognized.

In 1959, John Fisher Kennedy (oral communication) pointed out the stringent limitations imposed on scour and fill in a uniform channel by the principle of continuity and the principle of a relation between the discharge of bed material and the characteristics of the flow and available sediment. His reasoning was almost

exactly the same as that previously used by the present writer in unpublished reports.

In 1960, the stability of a sand bed during rises was emphasized in a study of the stage-discharge relationship for Pigeon Roost Creek (Colby, 1960, p. 13–15). The reasons given for the stability of the average elevation of the sand bed had been arrived at independently, but they closely paralleled those given years earlier by Mitchell and Harrison (in Leopold and Maddock, 1952, p. 176).

The concepts and principles applied by the preceding workers were generally consistent, but they differ from the idea (Leopold and Maddock, 1952, 1953; Brooks, 1958, p. 553–555) that an imposed sediment load affects the resistance to flow and hence the depth of flow for a given rate of flow. According to this idea, scour or fill results from an attempt of the stream to adjust its depth of flow to a changing sediment discharge. Information on large amounts of scour and fill at the measuring section on the Colorado River near Grand Canyon, Ariz., was given in support of this idea. On the other hand, Einstein and Chien (in Brooks, 1958, p. 558) stated that the cited information did not support the idea that changes in the elevation of the streambed at the measuring section were due to changing resistance to flow. The scour and fill and the effect of changing roughness on depth at this measuring section will be examined in more detail under the heading "A pool-and-riffle stream."

DISCHARGE OF SANDS AS A FUNCTION OF FLOW CHARACTERISTICS

The discharge of sands can be roughly computed for different flows and bed-material sizes according to the procedure suggested by Einstein (1950) or according to any other of several equations or procedures that are available for determining the discharge of sands in a sand-bed stream. In this paper, approximate discharges of sands in sand-bed streams are based on relations that were obtained from an analysis of the total discharge of sands in field and laboratory streams (Colby, 1964). The relations do not apply unless the streambed consists almost entirely of nearly cohesionless sand and unless the banks are not excessively rough as rock walls might be. The relation for low concentrations of fine sediment, a water temperature of 60° F, and a median particle size of bed sands of 0.30 millimeter is given in figure 3. For the stated conditions, the discharge of sands per foot of width is determined according to figure 3 by mean velocity and depth of flow. (Relations for other median particle sizes and approximate adjustments for changes in water temperature and for the effects of high concentrations of fine sediment are also given in Colby, 1964.)

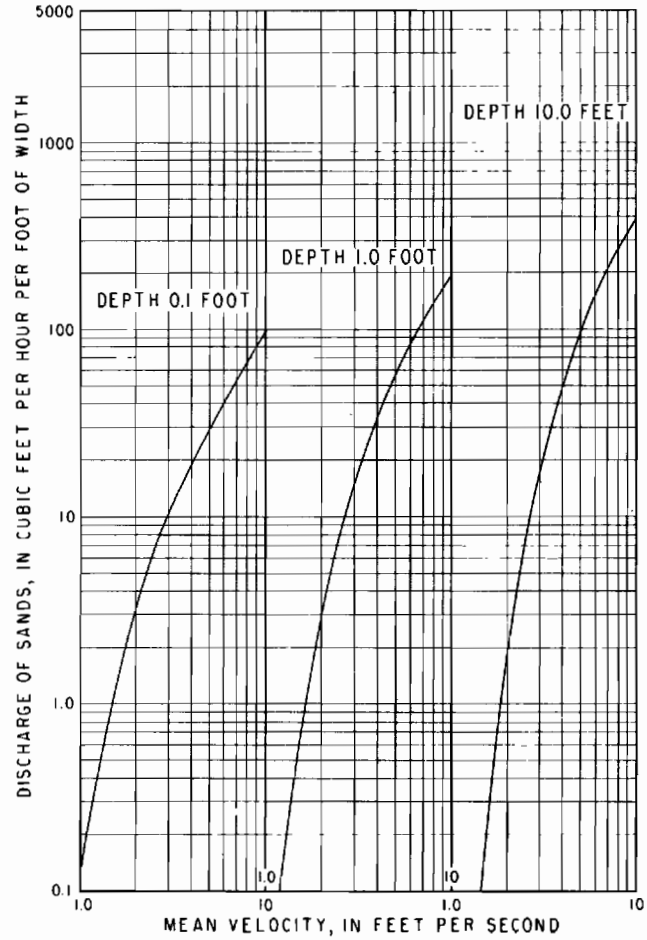

FIGURE 3.—Approximate discharge of sands for 0.30-millimeter median diameter of bed material and 60° F water temperature. Assumed weight per unit volume of sands is 85 lb per cu ft.

THE SIMPLE CONTINUITY EQUATION

The continuity equation for a reach of channel below the highest water-surface position that is to be considered can be written

$$Q_s' = \Delta S + Q_s''$$

or

$$\Delta S = Q_s' - Q_s'' \qquad (1)$$

in which

Q_s' is the quantity of sediment that enters the stream reach during a period,

Q_s'' is the quantity of sediment that leaves the reach during the period, and

ΔS is the quantity of sediment that accumulates (or erodes if ΔS is negative) during the period within the reach and below the highest position of the water surface.

The equation is obviously true for any time period, whether the sediment is transported in the main channel, in tributaries, or in diversions or whether the sediment enters or leaves through the action of wind or human agencies.

The three quantities of equation 1 usually can be used more conveniently for computations of scour and fill

if they are expressed in terms of equivalent volumes of deposit rather than in terms of weight. The equivalent volume of deposit is the weight of sediment divided by a known or assumed weight per unit volume of deposited sediment. The weight per unit volume can generally be approximated accurately enough for sands, but it is questionable for silt and clay or for mixtures of clay, silt, and sand.

Assume that the average elevation of the streambed would remain constant if no net weight of sediment were added nor taken away during the period to which equation 1 is applied and that the amount of sands being transported at any instant is so small that changes in the amount during a computation period can be disregarded. Equation 1 for computing the depth D, in feet, of average fill on the sand bed of a stream reach during a period then becomes

$$D=\frac{\Delta S}{A}$$

$$=\frac{Q_s'-Q_s''}{A}, \qquad (2)$$

in which A is the area, in square feet, of the bed of the channel reach if the sediment quantities are in cubic feet for the period. The quantity of silt and clay being transported has not been shown to be negligible, and the weight per unit volume of fine sediment may be questionable; therefore, equation 2 should be limited to flows over sand beds. However, Q_s' and Q_s'' can generally, but not always, be volumes either of sediment of all sizes or of only sands, because the difference will usually be almost entirely a difference in volume of sands.

APPLICATIONS OF THE PRINCIPLES TO ASSUMED CHANNEL REACHES

Although the general principles are broadly applicable, discussions of scour and fill in assumed channel reaches will, for convenience, be limited to reaches without diversions or tributary inflows of water or sediment. Also, only flows within the channel banks will be considered. Because changes in the amount of sands being transported must be small (fig. 2), they usually will be disregarded.

Two extremes must be avoided if the principles and applications of scour and fill in the assumed channels are to be reasonably well understood. One extreme is a tendency to become enmeshed in questionable details and minor effects so that general and significant relations are obscured; the other is a tendency to oversimplify and hence to eliminate some significant effects.

The following assumptions, unless otherwise noted, will apply for all the computations in the assumed channels:

1. The bed material is cohesionless sand whose median diameter is 0.30 millimeter, and the sand is uniform along the reach.
2. The water temperature is 60° F.
3. The combined concentrations of silt and clay do not exceed 10,000 ppm (parts per million).
4. The standard cross section has a flat bottom 84 feet wide and 45° bank slopes (fig. 4). (The term "flat" applies to general configuration and, as used in this report, does not imply an absence of dunes and antidunes.)
5. The stage-discharge relation (stage is measured above the flat bed) for a straight reach is assumed to be that shown in figure 4.
6. For this stage-discharge relation, the velocity-discharge relation must also be that shown in figure 4 for the standard cross section.
7. The discharges of sands for different combinations of depth and mean velocity in a straight or nearly straight channel are assumed to be as defined by figure 3.

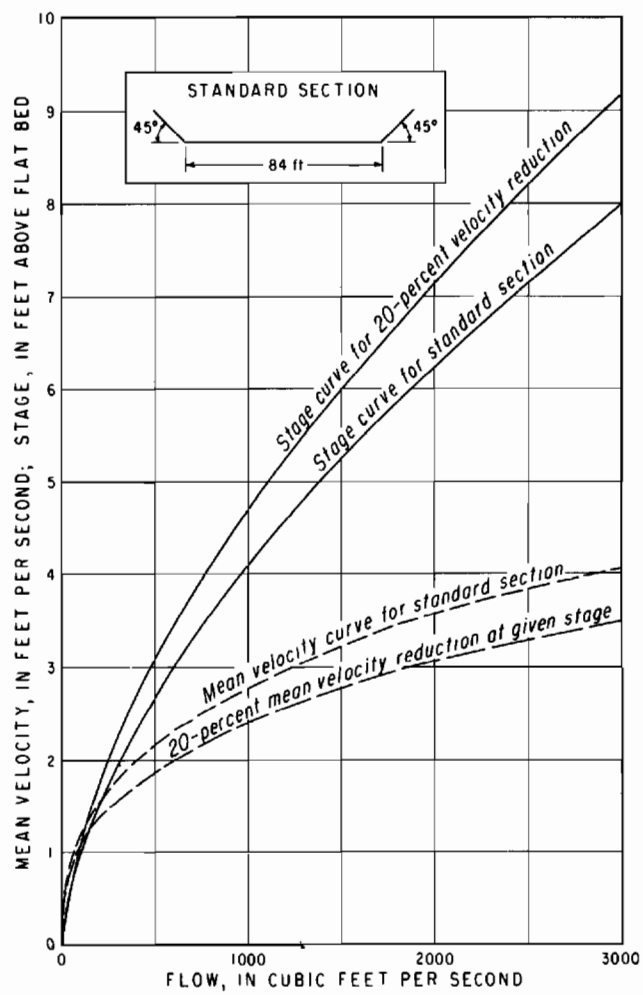

FIGURE 4.—Properties of assumed cross section.

CHANNEL DOWNSTREAM FROM A RESERVOIR

If all the sediment is removed from a flow in a reservoir, equation 1 for a reach of channel immediately downstream from the reservoir reduces to

$$\Delta S = -Q_s'', \tag{3}$$

and the quantity of scour in the reach is known if the sediment outflow Q_s'' is known or can be computed for the downstream end of the reach. The conversion of weight to volume might be based on the weight per unit volume of deposited sands (a weight that can be reasonably accurately estimated) if the discharged sediment is entirely sands. If the discharged sediment contains appreciable quantities of silt and clay and the size distribution is approximately that of the material in place before it was scoured out, the weight per unit volume of the material before it was scoured away can be used to convert from weight to volume. Even though the quantity of sediment discharged from the reach has not been measured, the discharge of sands from the reach can be computed from such a relationship as that in figure 3. However, figure 3 is based on an assumed weight of 85 lb per cu ft for sands and on the assumption that the flow has had time to pick up its equilibrium load of sands. If a cubic foot of material before it was removed by scour contained, for example, only 55 pounds of sand and no great amount of selective sorting of particle sizes took place within the reach, the volumes from figure 3 should be increased in the ratio of 85:55 for computing quantities of scour.

Sometimes the amount of sediment released from a reservoir is known, and then this amount of sediment inflow to the reach can be subtracted from a measured or computed outflow of sediment from the reach to compute scour.

For a computation of the volume of scour, assume that the standard cross section exists in a fairly straight and uniform reach of channel at a point 1,000 feet downstream from a reservoir where all the sand is removed from the streamflow. If this distance is sufficiently long to permit the streamflow to pick up its equilibrium load of sands, the discharges of sands at the downstream end of the reach should, according to figure 3, be those given in table 2 for different constant rates of flow. If all the material scoured from the channel was sand and the weight per unit volume of sand in place was 85 lb per cu ft, the volumes in column 6 of table 2 would indicate the volume of scour directly. Perhaps only 60 percent of the eroded material was sands, and the weight per unit volume of the material in place before it was removed by the flow was 80 lb per cu ft. Then if the amount of selective sorting within the reach was not appreciable, the volumes of scour for this material could be computed from the volumes in column 6 of table 2 by multiplying by 85/48 or 1.77.

TABLE 2.—*Volumes of sand removed from a 1,000-foot reach of channel downstream from a dam at different constant rates of streamflow through the standard cross section*

Streamflow (cfs)	Depth of flow above the flat bed (ft)	Mean velocity (fps)	Width at water surface (ft)	Discharge of sands (cu ft per hr)		
				Per foot of width (assumed 85 lb per cu ft)	For the total width	
					Assumed 85 lb per cu ft	Assumed 48 lb per cu ft
(1)	(2)	(3)	(4)	(5)	(6)	(7)
100	0.97	1.21	86.0	0.11	9.5	17
500	2.68	2.15	89.4	3.7	330	580
1,000	4.10	2.76	92.2	11.5	1,060	1,880
2,000	6.20	3.58	96.4	31.5	3,030	5,360
3,000	8.00	4.08	100.0	52	5,200	9,200

The computed amounts of scour are for a 1,000-foot reach, but they would be very unequally distributed along the reach. Most of the scour probably would take place within the first 100 or 200 feet below the dam.

If the hydrograph of figure 5 represents flow through the standard cross section 1,000 feet downstream from the dam, the velocities and depths can be determined from the curves of figure 4 for many times during the period of flow. These velocities and depths and figure 3 can then be used to compute the discharges of sands at frequent enough times to determine a graph (fig. 5) of discharge of sands during the period of flow. A cumulative curve of the volume and average depth of sands removed from the reach (fig. 5) can then be drawn from this graph. Of course, the volumes indicated by the curve are for 85 pounds of sands per cubic foot and should be increased if less than this weight of sands is removed for each cubic foot of sediment that is scoured from the reach. The average depth of sands removed is based on the 1,000-foot length of reach and on the maximum water-surface width of 100 feet.

STRAIGHT, UNIFORM CHANNEL

The reason for constancy of the average elevation of the sand bed of a uniform channel should be clear from the principles of scour and fill. (The channel is assumed to be uniform in slope, bed material, and resistance to flow at a given depth and velocity as well as uniform in cross section.) For such a channel, the relation between a particular flow and the depth and mean velocity of that flow is the same at each end of a reach. If the reach is not excessively long nor the volume of flow very small in comparison to the size of the channel, the hydrograph of flow at the downstream end of the reach will lag somewhat but will otherwise differ only a little from the hydrograph of flow at the upper end of the reach. Hence, the graph of discharge of sands from the reach will also lag a little as compared with

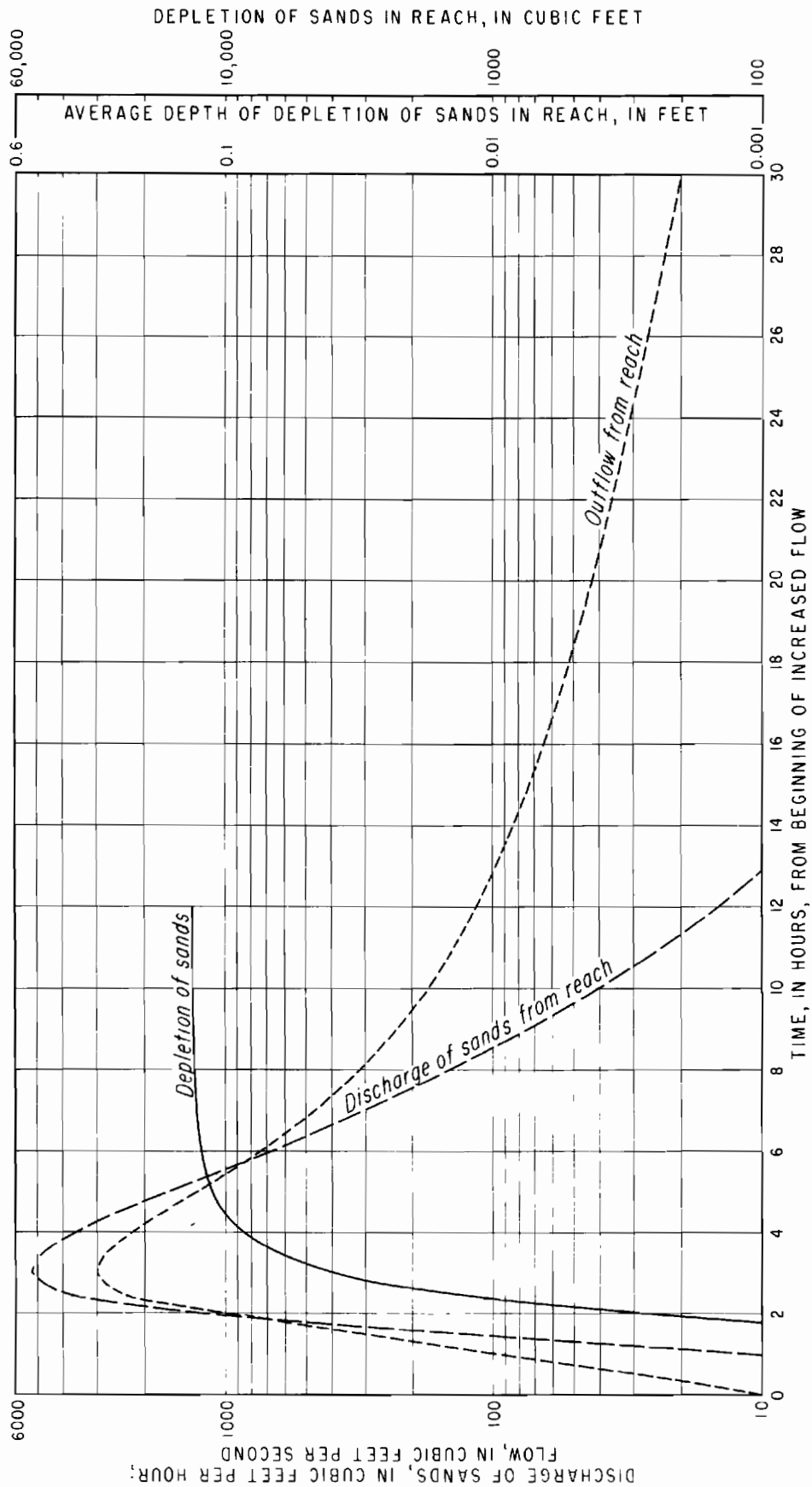

FIGURE 5.—Streamflow and discharge of sands at the downstream end of an assumed 1,000-foot channel reach immediately downstream from a dam that traps all sands in the flow.

the graph of discharge of sands into the reach, but these graphs will be otherwise about the same. Therefore, the discharges of sands into and out of the reach must be about equal during a runoff event, and the average elevation of the sand bed in the uniform channel should be about the same after a flood as before the flood. If an allowance for the lag is made in the hydrographs of flow and in the graphs of discharge of sands, the inflows and outflows of sands must be about equal during intervals of time during a flood and the average elevation of the sand bed must remain about constant within the reach throughout the flood.

Perhaps an even simpler concept of the reason for constancy of the average elevation of a sand bed in a uniform channel can be based on consideration of volumes of water within short segments of length as these segments of flow pass along the channel. If the mean velocity and average depth of each segment of flow do not change as the flow moves through a reach of channel, the sand-transporting ability of each segment does not change either, and the segments of flow neither pick up nor drop appreciable net amounts of sands. Hence, the average elevation of the sand bed does not change as the flow passes over the bed.

UNIFORM SLOPE AND ROUGHNESS

For illustrative computations, assume a straight reach of uniform channel that has at all sections the stage-discharge relation (fig. 4) for the standard cross section and the relation of streamflow to discharge of sands that is shown in figure 3. Constant flows of 100; 500; 1,000; 2,000; and 3,000 cfs (cubic feet per second) would be accompanied by discharges of sands of about 9.5; 330; 1,060; 3,030; and 5,200 cubic feet of sands per hour (table 2, column 6) at each end of the reach. Because the discharges of sands into and from the reach are equal for any constant rate of flow, the sand bed on the average neither scours nor fills within the reach.

If the hydrograph of streamflow and the graph of discharge of sands (fig. 5) are assumed to apply at the upstream end of a 5,000-foot reach of the same assumed straight, uniform channel, the hydrograph of outflow at the downstream end of the reach would be about as shown in figure 6. The relation between flow and discharge of sands (fig. 5) can then be used with the hydrograph of outflow to compute a graph of discharge of sands from the reach. Differences between the discharges of sands into and out of the reach were accumulated by short intervals of time to define the accumulation-of-sands curve (fig. 6). According to equation 1, this curve represents the accumulation of sands within the 5,000-foot reach from the beginning of the increased flow to any time covered by the curve. This accumulation may be either within the flow or on the streambed. If the accumulation of sands within the reach were distributed evenly over the area that is submerged at peak flow, 1,000 cubic feet of sands would be equivalent to an average depth of accumulation, including the accumulation in the flow, of 0.002 foot (fig. 6). If the accumulation of sands within the reach were distributed evenly over the flat part of the streambed, an area 84 feet by 5,000, the computed average depths of cumulative deposit would be increased in the ratio of 100 : 84. Even though the 84-foot width is used, the maximum accumulation of sands represents an average depth of less than 0.01 foot during the total time shown in the assumed hydrograph of flow. The accumulation of sands is greatest when the outflow of sands becomes equal to the inflow of sands.

CHANGING SLOPE OR ROUGHNESS

For the next computations, assume that the reach is the same but that the slope of the channel gradually decreases through the downstream part of the reach. The assumed change in slope begins far enough downstream so that the stage-discharge relation is not affected at the upstream end of the 5,000-foot reach, but the mean velocity at a given depth is exactly 20 percent less at the downstream end of the reach than at the upstream cross section. This assumed velocity reduction is significantly less than a 20-percent velocity reduction at a particular flow. (See fig. 4.)

Volumes and depths of fill in the assumed reach can be computed readily. Discharges of sands into the reach at constant rates of flow of 100; 500; 1,000; 2,000; and 3,000 cfs can be taken from column 6 of table 2. The discharges of sands from the reach can be computed from the properties of the flow at the downstream end of the reach. A curve of relation between flow and depth at the downstream end of the reach was drawn in figure 4 by reducing the flows for the upstream end by 20 percent for each of enough stages to define the stage-discharge curve for the downstream end of the reach. The stages directly determine the cross-sectional areas from the standard cross section (fig. 4) and hence the mean velocities for different flows at the downstream end of the reach. The mean velocities and the depths of flow can then be used to determine the discharges of sands per foot of width from figure 3. These discharges of sands multiplied by the water-surface widths are the total discharges of sands from the reach. At each of the five constant rates of flow, the computed differences between discharges of sands into and out of the reach gives, according to equation 1, the rate of accumulation of sands (expressed in terms of volume) within the 5,000-foot reach. (See table 3.) The volume of sand accumulation can also be expressed as an average depth of fill on the total submerged area, which is

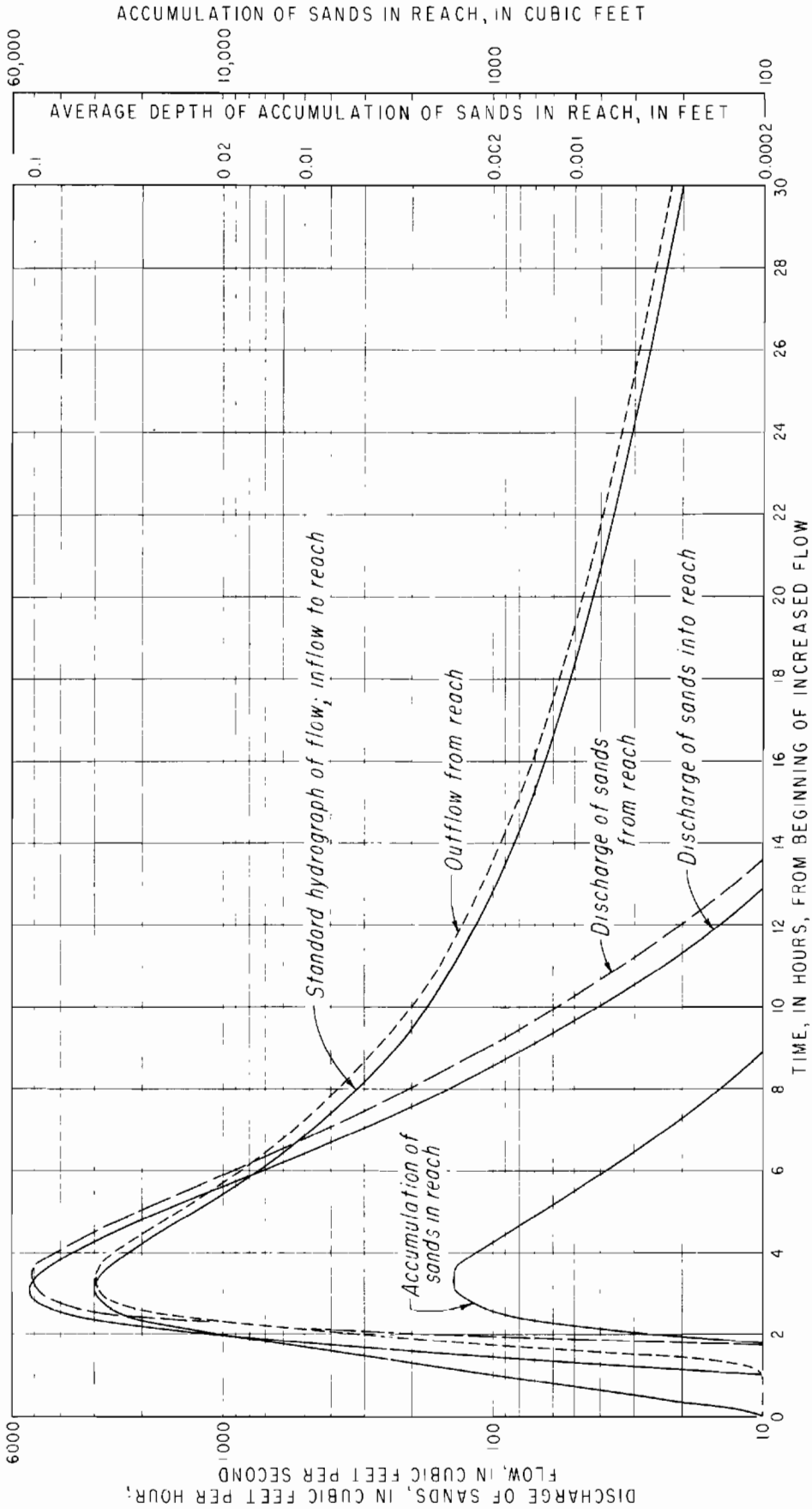

FIGURE 6.—Streamflow, discharge of sands, and accumulated sands in an assumed 5,000-foot reach of straight, uniform channel. The channel is uniform in bed material (median diameter 0.30 mm), slope, and cross section.

TABLE 3.—*Fill in an assumed 5,000-foot reach of straight channel of the standard cross section if velocities at a given depth are 20 percent lower at the downstream end of the reach than at the upstream end*

Streamflow (cfs)	Discharge of sands (cu ft per hr)			Average depth of fill (ft per hr)	
	Upstream end (table 2)	Downstream end	Difference	On horizontal submerged area	On flat-bed area (420,000 sq ft)
100	9.5	1.5	8.0	0.00002	0.00002
500	330	150	180	.00040	.00043
1,000	1,060	600	460	.00099	.0011
2,000	3,030	1,830	1,200	.0025	.0029
3,000	5,200	3,350	1,850	.0037	.0044

the product of the length of the reach and the average of the surface widths at the ends of the reach, or on the area of the flat bed of the reach, which is 5,000 feet by 84 feet. Of course, the volume of fill is greater for the larger constant flows, but a smaller percentage of the incoming sands remains in the reach at the larger flows.

The fill in the same assumed channel reach of 5,000 feet was computed for the inflow that is represented by the hydrograph of figure 5. The computed approximate hydrograph of flow at the downstream end of the reach, where the slope is flatter, is shown in figure 7. The depths and velocities at many times during the flow were computed for the downstream cross section, and these depths and velocities were then used with figure 3 to compute a graph of discharge of sands at the downstream end of the reach through the period of flow. The curve of volume of sand accumulation (fig. 7) within the reach was determined from the differences between the inflow and the outflow of sands during short increments of time. This cumulative curve is also shown as depth of average deposit on figure 7. Similar sediment accumulation would be caused if the velocity at the downstream end of the reach was reduced 20 percent for a given depth of flow by increased resistance such as might result from growth of small willows in the channel. In a straight, uniform channel, a change of slope or of roughness that causes fill while the flow is decreasing can also be expected to cause fill while the flow is increasing.

Of course, large amounts of fill over a long period of time are inconsistent with the maintenance of a uniform channel. A uniform channel was assumed to simplify the study of the principles of scour and fill as much as possible.

Obviously, an assumed increase in slope or decrease of roughness toward the downstream end of a 5,000-foot reach of uniform channel of the standard cross section would result in computed scour during periods of both increasing and decreasing flow. Also, the amount of the scour in the reach would, except for the usually small effect of the change in the hydrograph of flow as the water passes through the reach, be about the same as the amount of fill shown in figure 7, if the hydrographs of flow and the graphs of discharge of sands were assumed to apply at the opposite ends of the reach—that is, if the 20-percent lower velocities for a given depth existed at the upstream end of the reach rather than at the downstream end.

CONSTRICTION IN A STRAIGHT, GENERALLY UNIFORM CHANNEL

Consider, next, the scour and fill at a narrower-than-average cross section in a long straight reach that has the standard cross section (fig. 4) except at the contraction. At a cross section A in the uniform channel upstream from the narrow section, the relations of depth and mean velocity to flow are assumed to be those shown in figure 4, and the discharges of sands are assumed to be given by the curves in figure 3. Also, these relations and figure 3 are assumed to apply at a cross section C that is downstream from the narrow section and 1,000 feet downstream from section A. A suitable distance downstream from section A, the width of the channel slowly and smoothly decreases to an assumed bottom width of either 75 or 66 feet (9 or 18 ft less than the bottom width at section A). The bottom widths of 75 or 66 feet are assumed to be constant for a short distance before the channel gradually widens to the standard cross section and bottom width of 84 feet. The channel banks are assumed to have a 45° slope throughout the reach. Some computations of scour and fill will be based on a cross section B that is 200 feet downstream from section A and in the narrow section. Because the transitions are slow and smooth and because section B is in a short reach of straight channel, the relationship of mean velocity to turbulence at section B will be assumed to be normal for a sand-bed reach at the computed depths and velocities. Hence, figure 3 will be assumed to apply at section B as well as at sections A and C.

If sections A and C are far enough upstream and downstream from the narrow reach, the net scour and fill between these sections would be the same as for a straight, uniform 1,000-foot reach. At constant flow, neither net scour nor net fill would occur in the reach. If the flow indicated by the hydrograph of figure 5 passes through the reach, the net accumulation of sands (expressed in terms of volume) within the reach would be about one-fifth as much as that for the 5,000-foot reach (fig. 6), but the average net depth of accumulation of sands in the reach would be about the same as that for the 5,000-foot reach. The average elevation of the streambed in the 1,000-foot reach would be about the same after the flow has passed through the reach as before the flow arrived.

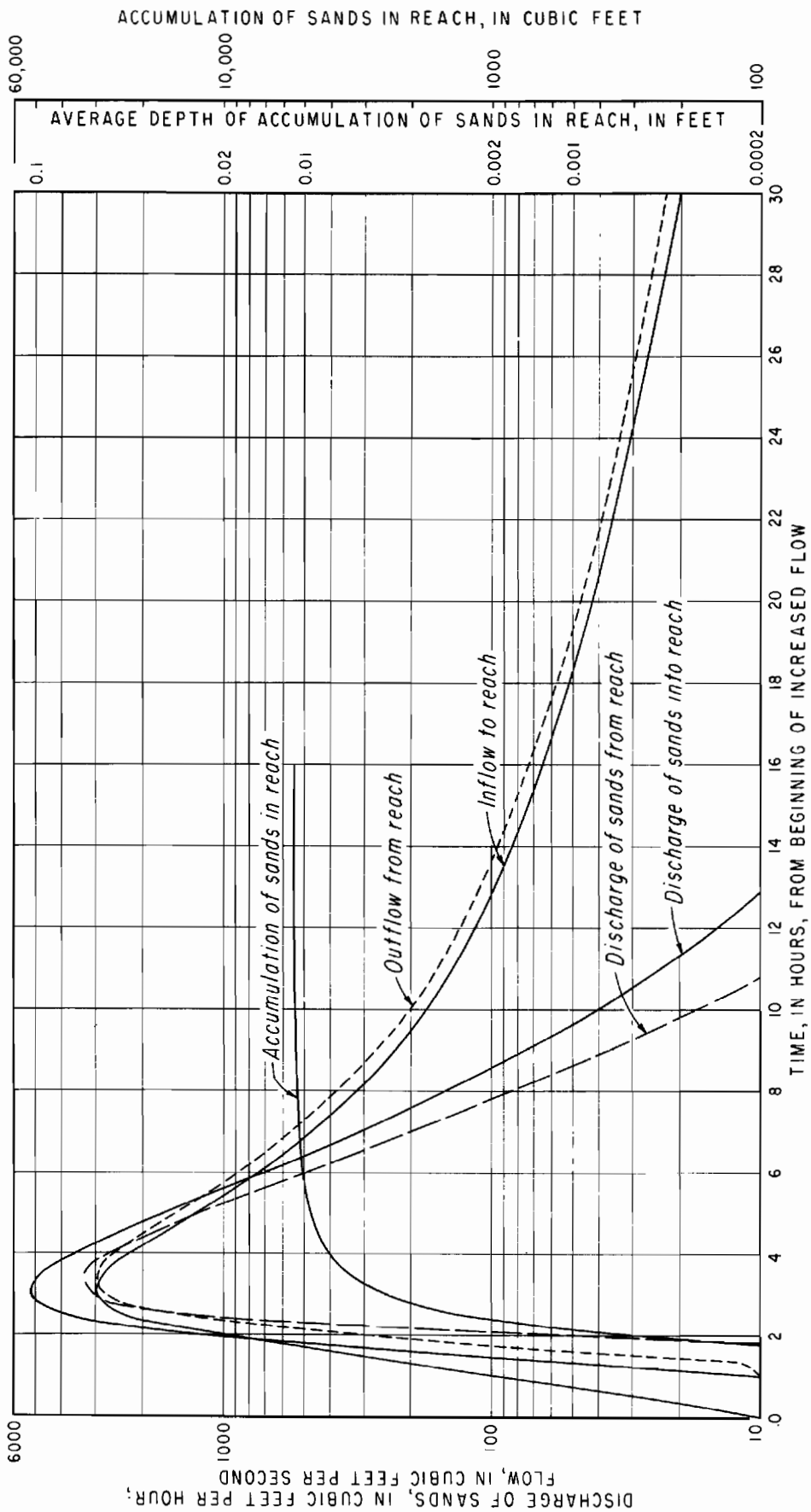

FIGURE 7.—Streamflow, discharge of sands, and accumulated sands in an assumed 5,000-foot reach of straight channel that is uniform in bed material (median diameter 0.30 mm) and cross section but has a gradually decreasing slope toward the downstream end. Mean velocities at a given depth of flow are 20 percent lower at the downstream end of the reach than at the upstream end.

Two types of information were computed for five different rates of constant flow. One type is the initial rate of volume of net scour in the reach between sections A and B. This initial rate of net scour is numerically equal to the initial volume rate of net fill in the reach between sections B and C. The initial rate of scour or of fill, respectively, means the difference between the discharges of sands from and into or into and from the reach, provided that the discharges of sands are based on positions of the streambed before these positions are changed by the flow. Thus, if a streambed is generally flat (although ripples, dunes, bars, or antidunes may cause local irregularities) before flow begins, the initial rate of scour in a reach between a wide and a narrow cross section is the difference between the discharges of sands at the narrow section and at the wide section before the streambed scoured noticeably at the narrow section. The significance of the initial rate of scour or fill is that it represents a maximum rate of removal or accumulation of sands in the reach for a particular rate of streamflow. The second type of information is the approximate depth of average scour to be expected at section B after flow has continued at the constant rates until an equilibrium cross section or bed position has been reached at section B.

The computed initial rates of scour in the 200-foot reach between section A and section B (table 4) are based on the assumptions that the sand that is removed from the channel bed weighs 85 lb per cu ft and that the depths of flow at sections A and B are equal at the beginning of each flow at a constant rate. The steps in the computation of the initial scour are shown in table 4 and are rather obvious. The discharges of sands (table 2, column 6) at the constant rates of flow had already been computed for sections such as A and C. The depths of flow (table 2, column 2) and the geometry of section B determine the surface widths and the cross-sectional areas of section B. The streamflow divided by the area gives the mean velocity, and the mean velocity and the depth define the discharges of sands per foot of width in figure 3. The rate of initial scour in the reach between section A and B is the difference in discharges of sands at the ends of the reach. The net average depth of scour per hour is obtained by dividing the volume of scour by the product of the length of the reach and an effective bottom width of the reach. The effective bottom widths were assumed to be 78 and 72 feet for the two different reductions in bottom width. Of course, the scour at section B probably would be at least twice the net average depth of scour and may well be somewhat more than twice the average.

A precise effective width of channel subject to scour, fortunately, is not necessary for computing approximate average depths of scour in the reach for different flows and reductions in channel width. In the computations for table 4, only the flat bed of the channel was assumed to be subject to scour. For a rough computation, both the depth of scour and the reduction in channel width can be assumed to vary directly with distance from section A. Under these assumptions, the effective width of flat bed subject to scour in the reach would be $W_1-2(W_1-W_2)/3$ or 78 and 72 feet, respectively, for the reductions of 9 and 18 feet in channel width. (W_1 and W_2 are the bottom widths at sections A and B.) The

TABLE 4.—*Computed initial rates of scour between cross sections A and B at different flows for which the depths of flow above the flat* R *beds are assumed to be equal at the two sections*

[Net average depth of scour between sections is based on product of length of reach (200 ft) and effective bottom widths of 78 ft for 9-ft contraction and 72 ft for 18-ft contraction]

Streamflow (cfs)	Section A	Section B, bed not scoured by flow					Scour between sections or difference in discharges of sands (rounded)	
	Discharge of sands (cu ft per hr)	Depth of flow above the flat bed (ft)	Area (sq ft)	Mean velocity (fps)	Surface width (ft)	Discharge of sands (cu ft per hr)	Cu ft per hr	Ft of net average scour per hr
Bottom width 9 ft less at section B than at section A								
100	9. 5	0. 97	73. 7	1. 36	77. 0	20	10	0. 0006
500	330	2. 68	208	2. 40	80. 4	506	180	. 012
1, 000	1, 060	4. 10	325	3. 08	83. 2	1, 500	440	. 028
2, 000	3, 030	6. 20	504	3. 97	87. 4	3, 760	730	. 047
3, 000	5, 200	8. 00	664	4. 52	91. 0	6, 280	1, 080	. 069
Bottom width 18 ft less at section B than at section A								
100	9. 5	0. 97	64. 9	1. 54	68. 0	41	31	0. 002
500	330	2. 68	184	2. 72	71. 4	770	440	. 031
1, 000	1, 060	4. 10	288	3. 47	74. 2	2, 150	1, 090	. 076
2, 000	3, 030	6. 20	448	4. 46	78. 4	4, 940	1, 910	. 133
3, 000	5, 200	8. 00	592	5. 07	82. 0	7, 870	2, 670	. 185

effective width can be multiplied by the length of the reach and by the average depth of scour to obtain the volume of scour under the stated assumptions. This effective width is less than the average bottom width because the depth of scour increases as the width decreases. Of course, the net average depth of scour would be a little less if the width of water surface had been used rather than the width of the flat bed.

The 18-foot decrease of bottom width, which represents roughly a 20-percent decrease in area, produced initial rates of scour between sections A and B that were about 2.5–3.0 times the rates of scour that were caused by the 9-foot decrease in bottom width, which represents roughly a 10-percent decrease in area. (See table 4.)

Of course, the initial rates of scour would begin to decrease immediately because the scour would reduce the mean velocity at section B and hence decrease the difference in discharges of sands between sections B and A. The equilibrium bed positions at section B, the positions for which the discharges of sands at sections A and B are equal, were computed for the same decreases in bottom width and the same five constant flows that were used in the computation (table 4) of initial rates of scour.

The computation of average depth of scour at equilibrium bed position at section B is indicated in table 5 and begins with the assumption that the discharges of sands are to be the same at sections A and B. The discharge of sands at each constant rate of flow is taken from column 6 of table 2 and is divided by the surface width at section B (the water-surface slope is assumed to be the same as though the width were not contracted) to obtain the equilibrium discharges of sands per foot of width at section B. The difference in discharges of sands per foot of width at sections B and A requires an increase in mean velocity from section A to section B, an increase that can be approximated from figure 3, and the mean velocity at section B is computed from that at section A (table 2, column 3) by adding this increase. The flow is divided by the mean velocity to obtain the cross-sectional area necessary to discharge the flow. If the banks are considered to remain stable at section B and all scour is assumed to occur at the flat bed, the average depth of flow above the flat bed can be computed from the geometry of section B. The difference between this depth of flow and the depth of flow above the flat bed at section A (table 2, column 4) is the indicated average depth of scour of the flat bed at section B.

The computations of average depth of scour at equilibrium indicate at least three significant points. One is that at the narrow section the depths of scour, like the initial rates of scour between sections, increase fairly rapidly as the flow increases. A second point is that at a given flow the depth of scour is about directly proportional to the reduction in width. A third point is that the length of the reach does not influence the computations, and hence the equilibrium depth of average scour at the narrow section is independent of the length of reach between the sections unless the reach is so short and the change in cross section and streamlines so abrupt that the depths and mean velocities cannot be satisfactorily determined or that the relations of figure 3 do not apply.

The standard hydrograph of flow and the graph of discharge of sands (fig. 5) were assumed at section A and also at section C except for a few minutes lag

TABLE 5.—*Average scour at section B after five constant flows have established equilibrium bed positions*

Streamflow (cfs)	Section A	Section B		Difference between sections A and B		Section B			
	Discharge of sands (cu ft per hr)	Surface width (ft)	Discharge of sands (cu ft per hr per ft of width)	Discharge of sands (cu ft per hr per ft of width)	Mean velocity (fps)	Mean velocity (fps)	Cross sectional area (sq ft)	Depth of flow above the flat bed (ft)	Average scour of flat bed (ft)
Bottom width 9 ft less at section A than at section B									
100	9. 5	77. 0	0. 123	0. 013	0. 01	1. 22	82	1. 08	0. 11
500	330	80. 4	4. 10	. 40	. 05	2. 20	227	2. 93	. 25
1, 000	1, 060	83. 2	12. 7	1. 2	. 06	2. 82	355	4. 50	. 40
2, 000	3, 030	87. 4	34. 6	3. 1	. 09	3. 67	545	6. 75	. 55
3, 000	5, 200	91. 0	57. 2	5. 2	. 11	4. 19	717	8. 70	. 70
Bottom width 18 ft less at section A than at section B									
100	9. 5	68. 0	0. 14	0. 03	0. 03	1. 24	81	1. 20	0. 23
500	330	71. 4	4. 60	. 9	. 10	2. 25	222	3. 25	. 57
1, 000	1, 060	74. 2	14. 3	2. 8	. 14	2. 90	345	4. 99	. 89
2, 000	3, 030	78. 4	38. 6	7. 1	. 19	3. 77	530	7. 46	1. 26
3, 000	5, 200	82. 0	63. 4	11. 4	. 25	4. 33	693	9. 56	1. 56

for the passage of the flow through the 1,000-foot reach; scour was computed at section B for reductions in bottom width of 9 and 18 feet. At the beginning of the standard hydrograph, the depth of the low flow was assumed to be the same at all three cross sections. Computations were made for 20-minute intervals before the peak discharge at section A and for 30-minute or longer intervals after the peak. No time lag was applied for the 200-foot reach between sections A and B, and scour was assumed to be limited to the flat bed. The average depth of scour in the reach was based on effective bottom widths of 72 and 78 feet for the two different reductions in bottom width, and the depth of scour at section B was assumed to be double the average depth of scour for the reach.

The same type of computation was made for each successive time interval. The depths and streamflows at section B at the beginning and at the end of the first time interval and the channel geometry were used to compute the cross-sectional areas and the velocities at section B at the beginning and end of the interval. From the depths, velocities, and widths at section B, the discharges of sands at the beginning and end of the time interval were computed from figure 3. The difference between the discharges of sands from and into the reach during the interval was used to compute the volume of scour and the average depth of scour in the 200-foot reach. This average depth was then doubled to obtain an assumed, but perhaps somewhat too small, depth of scour at section B. Next, a similar computation was made for the second time interval except that the discharge of sands at section B at the beginning of this time interval did not have to be computed unless the computed scour at the end of the first interval was large enough to require a recomputation of the discharge of sands. The same procedure was followed for each successive interval except that as the scour became appreciable, the amount of scour at the end of the interval at section B was estimated in advance. A recomputation was necessary only if the computed scour differed significantly from the estimated scour. The details of the computations for the reduction of 18 feet in bottom width are shown in table 6.

The cumulative depths of computed scour at section B (fig. 8), although inexact, indicate qualitatively the general behavior of scour and fill at a contracted section during the passage of an assumed variable flow. The average elevation of the bed at the narrow section is lowest an appreciable time after the peak of the flow when the discharge of sands at the narrow section has decreased until it exactly equals the discharge of sands upstream from the narrow section. The depths of scour are roughly in proportion to the percentage reductions of bottom width. Also, much of the scour is not replaced by fill during the recession of this particular hydrograph of flow. In general, the recession side of a hydrograph of flow is long; and in many sand-bed streams, even low flows transport appreciable quantities of sands; hence, soon after a flood has passed, the streambed at a narrow section may have filled as much as it scoured during the earlier part of the flood. Narrow cross sections of a sand-bed stream are likely to be characterized by alternate scour and fill with the passage of each flood, but the actual amounts of scour and fill depend partly on the form and size of the hydrograph of flow and partly on the initial position of the streambed.

The maximum computed depth of scour at the narrow section is roughly 40 percent of the equilibrium depth of scour for the peak flow of 3,000 cfs (table 5). The figure of 40 percent, as well as the amount of fill after the flow has passed and the time between the peak of the flow and the maximum depth of scour, is largely a function of the shape, size, and duration of the hydrograph of flow and of the graph of sands.

Although little scour or fill occurs at representative cross sections such as A and C of the assumed uniform channel, a pattern of alternate scour and fill is characteristic at a narrow section. (Of course, the scour and fill that are discussed here are based on an average bed elevation across a channel; such very local irregularities as sand dunes are assumed to be smoothed out in the computation of the average bed elevation at a cross section.) Because most information on scour or fill has been obtained at streamflow measuring sections, which are usually at narrower-than-average parts of the channel or at structures that constrict the flow laterally, the untypical alternation of scour and fill is often thought to be representative for sand-bed streams (Lane and Borland, 1954). On the other hand, a sand bed whose average elevation is stable during periods when the flow changes greatly indicates uniformity of width of flow and of available bed sand with distance along the channel.

The principles of scour and fill apply, of course, to the reach between sections B and C. If this 800-foot reach is long enough for normal flow and discharge of sands to become reestablished in the straight, uniform channel, the discharge of sands at section C differs from that at section A only by a few minutes lag. Slight adjustment can be made for this lag, or it can be disregarded. In simple terms and with reasonable accuracy, any net volumes of sands that were removed from the reach between sections A and B can be considered to be balanced by equal volumes of net deposit in the reach between sections B and C. This broad relation exists in spite of the facts that the bed at section

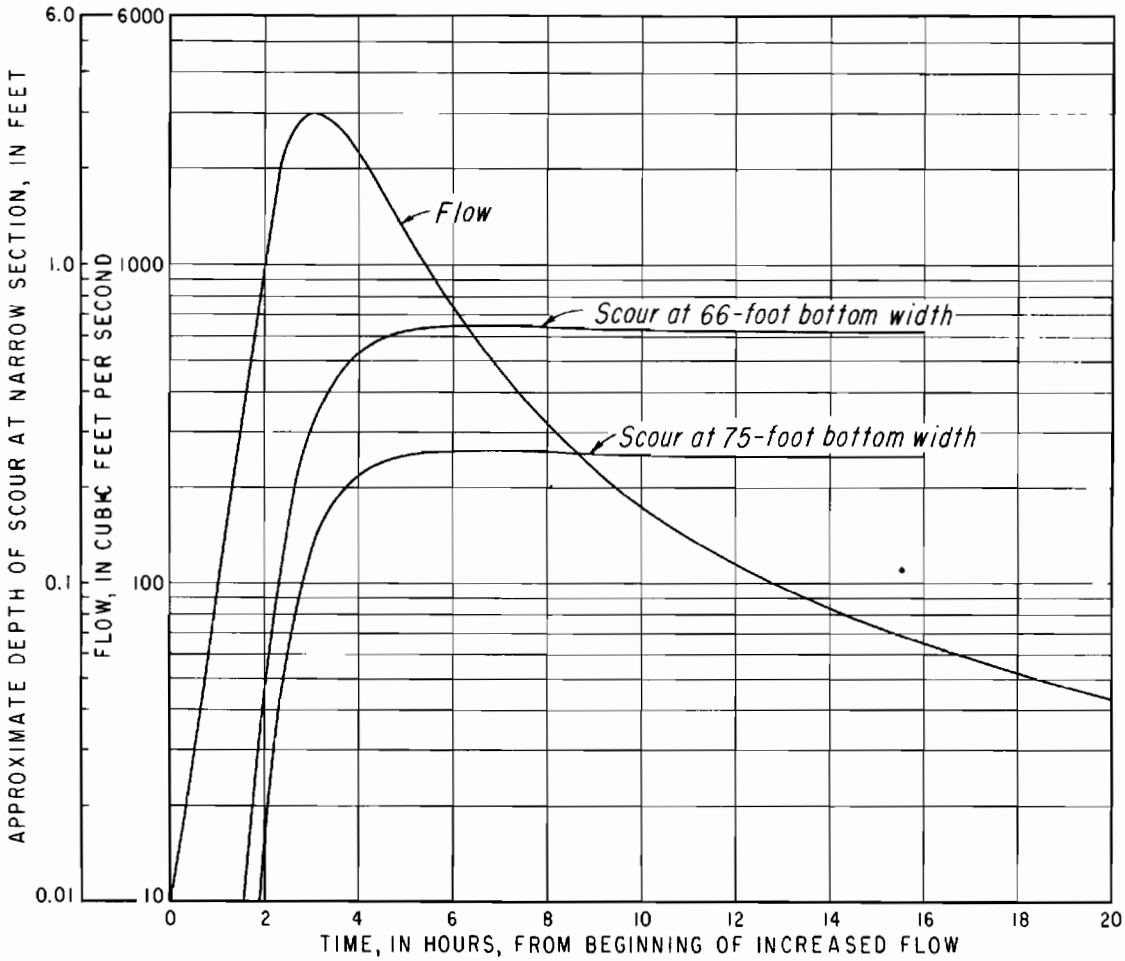

FIGURE 8.—Depths of computed scour at narrow section of an assumed 1,000-foot reach of straight channel.

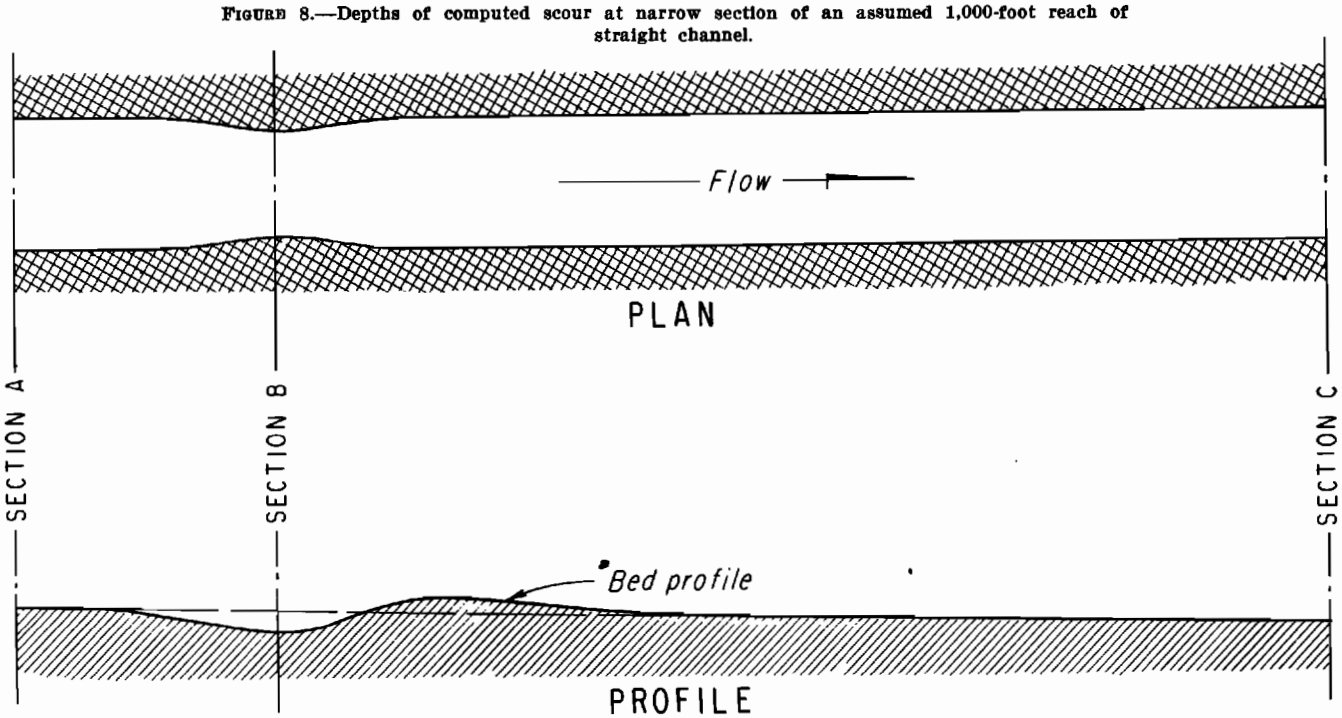

FIGURE 9.—Schematic profile of bed position at and near a narrow section of an assumed straight sand-bed channel after a short period of constant flow.

TABLE 6.—*Computed scour at cross section where bottom width is 66 feet in channel whose uncontracted bottom width is 84 feet*

Column 1: Time from beginning of increased flow.
Column 2: Flow from hydrograph on figure 5.
Column 3: Depth, or stage, above flat bed from figure 4.
Column 4: Mean velocity from figure 4.
Column 5: Discharge of sands per foot of width from figure 3.
Column 6: Surface width of wide section is bottom width of 84 feet plus twice the depth.
Column 7: Discharge of sands per foot of width times the surface width.
Column 8: Surface width of narrow section is bottom width of 66 feet plus twice the depth at the wide section or the surface width at the wide section minus 18 feet.
Column 9: Bottom width of 66 feet plus the depth at the wide section.
Column 10: The average width from column 9 minus the computed scour from column 22. For a first trial, the computed scour is estimated.
Column 11: The same depth as given in column 3 for the wide section.
Column 12: The depth from column 11 plus the computed scour from column 22.
Column 13: The product of the average width from column 10 and the depth from column 12.
Column 14: The velocity is obtained by dividing the flow from column 2 by the area from column 13.
Column 15: The discharge of sands per foot of width from figure 3 for the depth from column 12 and the mean velocity from column 14.
Column 16: The discharge of sands from column 15 multiplied by the surface width from column 8.
Column 17: The difference in discharge of sands from column 16 and from column 7.
Column 18: Graphically estimated difference in discharge at a time halfway between the times given in column 1. (Figures used only for rapidly increasing or high flows.)
Column 19: Volume removed from reach during period that ended at the time given in column 1. Volume is equal to the product of the length of period in hours and the average difference in discharge of sands in cubic feet per hour, based on figures in columns 17 and 18.
Column 20: Cumulative volume of sands removed from reach.
Column 21: Average depth of scour in reach is computed from the cumulative volume from column 20 divided by the product of the 200-foot length of the reach and an estimated average bottom width of 72 feet.
Column 22: The average depth of scour in the reach, from column 21, multiplied by 2. This assumes a straight-line variation of the scour from zero at the upper and wide end of the reach to a maximum at the narrow section.

Time (hr)	Upstream section, 84-foot bottom width						Downstream section, 66-foot bottom width									Difference in discharges of sands between sections				Depth of scour	
								Average width		Depth above flat bed											
	Flow (cfs)	Depth above flat bed (ft)	Mean velocity (fps)	Discharge of sands per foot of width (cu ft per hr)	Surface width (ft)	Discharge of sands through section (cu ft per hr)	Surface width (ft)	No scour (ft)	Scoured (ft)	No scour (ft)	Scoured (ft)	Area of scoured section (sq ft)	Mean velocity (fps)	Discharge of sands per foot of width (cu ft per hr)	Discharge of sands through section (cu ft per hr)	At stated time (cu ft per hr)	Estimate between times (cu ft per hr)	During period (cu ft)	Cumulative (cu ft)	Average in 200-ft reach (ft)	Estimated at narrow section (ft)
(1)	(2)	(3)	(4)	(5)	(6)	(7)	(8)	(9)	(10)	(11)	(12)	(13)	(14)	(15)	(16)	(17)	(18)	(19)	(20)	(21)	(22)
0:00	10	0.22	0.54	--------	84.4	--------	66.4	66.2	------	0.22	------	14.6	0.68	--------	--------	--------	--------	--------	--------	--------	--------
0:20	20	.35	.68	--------	84.7	--------	66.7	66.4	66.4	.35	0.35	23.2	.86	--------	--------	--------	--------	--------	--------	--------	--------
0:40	44	.58	.90	--------	85.2	--------	67.2	66.6	66.6	.58	.58	38.6	1.14	0.07	5	5	--------	0.4	0.4	0.00003	0.00006
1:00	100	.97	1.21	0.11	85.9	9.5	67.9	67.0	67.0	.97	.97	65.0	1.54	.60	41	31	12	5	5	.00035	.0007
1:20	210	1.56	1.59	.72	87.1	63	69.1	67.6	67.6	1.56	1.56	105	2.00	2.55	176	113	70	24	29	.002	.004
1:40	460	2.53	2.10	3.3	89.1	294	71.1	68.5	68.5	2.53	2.54	174	2.64	9.5	675	381	200	74	103	.007	.014
2:00	1,000	4.10	2.76	11.5	92.2	1,060	74.2	70.1	70.1	4.10	4.14	290	3.45	28	2,080	1,020	610	218	321	.022	.044
2:20	2,000	6.20	3.58	31.5	96.4	3,030	78.4	72.2	72.1	6.20	6.31	456	4.38	65	5,100	2,070	1,500	507	828	.057	.11
2:40	2,700	7.50	3.93	47	99.0	4,630	81.0	73.5	73.3	7.50	7.71	565	4.78	83	6,720	2,090	2,080	693	1,521	.106	.21
3:00	3,000	8.00	4.08	52	100.0	5,200	82.0	74.0	73.7	8.00	8.31	612	4.90	88	7,210	2,010	2,050	683	2,204	.153	.31
3:30	2,800	7.70	4.00	48	99.4	4,770	81.4	73.7	73.3	7.70	8.13	596	4.70	79	6,430	1,660	1,860	924	3,128	.217	.43
4:00	2,230	6.70	3.70	37	97.4	3,600	79.4	72.7	72.2	6.70	7.23	521	4.28	60	4,760	1,160	1,410	705	3,833	.265	.53
4:30	1,700	5.70	3.40	27	95.4	2,570	77.4	71.7	71.1	5.70	6.29	448	3.80	41	3,170	600	840	430	4,263	.297	.59
5:00	1,280	4.80	3.00	16.5	93.6	1,550	75.6	70.8	70.2	4.80	5.43	381	3.36	25	1,890	340	--------	235	4,498	.312	.62
5:30	960	4.00	2.75	11.5	92.0	1,060	74.0	70.0	69.4	4.00	4.64	322	2.98	15.7	1,160	100	--------	110	4,608	.320	.64
6:00	740	3.40	2.50	7.6	90.8	690	72.8	69.4	68.8	3.40	4.04	278	2.66	9.7	706	16	--------	29	4,637	.322	.64
7:00	470	2.60	2.12	3.4	89.2	304	71.2	68.6	68.0	2.60	3.24	220	2.14	3.7	264	−40	--------	−12	4,625	.321	.64
8:00	320	2.00	1.85	1.7	88.0	150	70.0	68.0	67.4	2.00	2.64	178	1.80	1.45	102	−48	--------	−44	4,581	.318	.64
9:00	230	1.63	1.63	.86	87.3	75	69.3	67.6	67.0	1.63	2.26	151	1.52	.57	40	−35	--------	−42	4,539	.315	.63
10:00	175	1.36	1.50	.50	86.7	43+	68.7	67.4	66.8	1.36	1.99	134	1.31	.21	14	−29	--------	−32	4,507	.313	.63
11:00	140	1.20	1.37	.27	86.4	23	68.4	67.2	66.6	1.20	1.82	121	1.16	.08	5	−18	--------	−24	4,483	.311	.62
12:00	115	1.06	1.28	.17	86.1	15−	68.1	67.1	66.5	1.06	1.68	112	1.03	.022	2	−13	--------	−16	4,467	.310	.62
14:00	84	.86	1.14	.07	85.7	6.0	67.7	66.9	66.3	.86	1.48	98	.86	--------	--------	−6	--------	−19	4,448	.308	.62
16:00	65	.74	1.03	.02	85.5	1.7	67.5	66.7	66.1	.74	1.36	90	.72	--------	--------	−1.7	--------	−8	4,440	.308	.62
18:00	52	.64	.96	--------	85.3	--------	67.3	66.6	66.0	.64	1.26	83	.63	--------	--------	--------	--------	--------	4,440	.308	.62
20:00	43	.56	.90	--------	85.1	--------	67.1	66.6	66.0	.56	1.18	77.8	.55	--------	--------	--------	--------	--------	4,440	.308	.62
24:00	31	.46	.80	--------	84.9	--------	66.9	66.5	65.9	.46	1.08	71.2	.44	--------	--------	--------	--------	--------	4,440	.308	.62
30:00	20	.35	.68	--------	84.7	--------	66.7	66.4	65.8	.35	.97	63.8	.31	--------	--------	--------	--------	--------	4,440	.308	.62
36:00	13	.26	.58	--------	84.5	--------	66.5	66.3	65.7	.26	.88	57.8	.22	--------	--------	--------	--------	--------	4,440	.308	.62
42:00	10	.22	.54	--------	84.4	--------	66.4	66.2	65.6	.22	.84	55.1	.18	--------	--------	--------	--------	--------	4,440	.308	.62

Note.—The computed scour from column 22 was first needed in the computations for columns 10 and 12. At that point in the computations, the scour is estimated and the computations of the computed scour are completed. If the estimated scour and the computed scour do not agree very closely, the computations from column 10 to column 22 are repeated with either the first computed scour or an estimate that is based on the first computed scour.

B generally scours when the reach from A to B scours and the bed at section C generally shows little net scour or net fill. Therefore, the volume of fill in the reach between sections B and C must roughly balance both the volume of scour in the upstream end of the reach between sections B and C and the volume of scour in the reach between sections A and B. If the reach downstream from the narrow section is longer than the reach upstream from the section, the net average depths of fill in the downstream reach must be less than the net average depths of scour in the upstream reach. The bed profile for a constant flow must have the general shape indicated in figure 9. Obviously, the reach between sections B and C must be long, or the flow and discharge of sands at its downstream end may be affected appreciably by the contraction and expansion of the flow.

WINDING STREAMS

The discharge of sands at bends of a sand-bed stream may be significantly different from that indicated by figure 3 because the turbulence for a given depth, mean velocity, water temperature, and bed material may be different from the turbulence in a straight reach of channel. Although a relation may exist between the discharge of sands at a bend and the characteristics of flow and sediment, the relation would be complex and has not yet been defined. Hence, one of the principles of scour and fill cannot now be used at a stream bend; but the principle of continuity does, of course, apply. Also, both principles can be applied at reasonably straight reaches of channel between bends provided that these reaches are long enough for the flow to entrain about its equilibrium discharge of sands. Thus, in some ways a channel reach containing a bend is like a straight channel reach that contains a narrow section.

The amount of scour and fill at a bend may be difficult to determine, but the net volume of scour or fill within a reach that includes the bend can be computed if the difference in sediment discharges at the ends of the reach can be measured or computed. A general restriction on the scour of sands from a long reach of winding channel is, of course, imposed by the total discharge of sands at any cross section. Thus, the total discharge of sands should be about 13,000 cubic feet (fig. 5) or about 130 cubic feet per foot of surface width at maximum stage for the standard cross section in a fairly straight reach of channel (0.30-mm median diameter of the bed sediment) and for the hydrograph of flow and the discharge of sands that are given in figure 5. In a reach of channel 1 mile long that has no inflow of sands, the indicated average depth of net scour during the passage of the flow would be only 0.02–0.03 foot. For five constant rates of flow, the discharges of sand per hour per foot of width of the standard cross section would be approximately the same as those given in table 2, column 5. At the highest of the constant flows, 3,000 cfs, the indicated net scour would be about 0.01 foot per hour for a reach 1 mile long having no inflow of sand. Volumes of discharge of sand, in cubic feet per hour per foot of width, are given in figure 3 for many combinations of depth and mean velocity in sand-bed channels and for water temperatures of 60° F, bed sediment of 0.30-millimeter median diameter, and low concentrations of fine sediment. These volumes of sand can be converted to net scour, in feet per hour, of the sand bed of uniform-width channels by subtracting the inflow of sands per foot of width and dividing the difference by the length of the channel reach, in feet. Of course, if a channel reach cannot be considered to have about a uniform width, the volumes of sand per foot of width per hour at different flows can be multiplied by the channel width at the downstream end of the reach, any inflow of sands per hour can be subtracted, and the difference can be divided by the area of the bed of the reach to obtain a net depth of average scour, in feet per hour. Obviously, large depths of scour or fill in a winding channel like those in a straight channel usually are not typical of long reaches of streams.

SCOUR AND FILL IN NATURAL STREAMS

Most natural streams differ considerably from the assumed channels for which computations of scour and fill have been made for this report. The comparatively few streams that have continuous sand beds usually have somewhat variable widths, uneven lateral distributions of depth and velocity, and some change in particle size with distance along the channel. Many natural streams are pool-and-riffle streams and have mean velocities, widths, depths, and particle sizes that change widely and rapidly with distance along the channel. Although the pools may have sand beds much or all of the time, the pool-and-riffle streams as a whole are not really sand-bed streams.

The differences in pattern of scour and fill will be shown for only three natural streams.

A GENERALLY STABLE SAND-BED STREAM

Changes of bed position in a generally stable sand-bed stream have been defined by many streamflow measurements or cross-section soundings under two cableways over the Elkhorn River near Waterloo, Nebr. (Beckman and Furness, 1962, table 2). The general stability of the sand bed implies few, if any, large changes in bed elevation for a stream reach of appreciable length. This stability exists in spite of frequent and rapid changes in bed elevation at individual points and even appreciable changes in average bed elevation

at entire cross sections (Beckman and Furness, 1962, p. 12). The average bed positions at the two cableways, which are about 1,670 feet apart, were usually determined at about the same time. The width of the water surface at the upstream cableway varied, partly with stage and partly with time, from 224 to 283 feet over a period of 2 or 3 years. Usually the width was at least 245 feet; therefore, this width was used in computing changes in the bed elevation. Changes in bed elevation outside of this width were disregarded. The width of the water surface at the downstream cableway was usually 285–290 feet, although some widths were a little outside of this range. Because the range in width was small, the changes in bed elevation at the downstream cableway were based on the reported area and width at the time of each measurement. The width of the channel at the upper cableway was probably significantly less than the average width for the reach of channel, and the width of channel at the lower cableway was probably about average for the reach near the cableways.

The cableways are in a reach of channel whose bed is composed almost entirely of shifting sand that had a median diameter of about 0.24 millimeter in 1952 when many of the observations were made. The bed shifts readily. Driftwood occasionally lodges on or near the cableways and somewhat distorts the streambed and the pattern of the flow. Also, scour and fill at the upstream end of the reach may be affected somewhat by the shifting shape and elevation of a large sand bar a few hundred feet upstream from the upper cableway and by sometimes active erosion of the right bank about opposite the bar. Computed average changes of 0.1 or 0.2 foot in elevation of the wide and shifting streambed at either cableway section may be practically meaningless as measures of scour or fill in the reach.

As Beckman and Furness (1962, p. 12) concluded earlier, no clearcut relationship is apparent between flow or changes in flow and net scour or fill (figs. 10–13). Of course, the position of the streambed generally changes faster at high flow than at low flow, but the direction of the change is not consistent from one cableway section to the other. The change in average bed elevation at the downstream cableway was determined from consecutive cross-section soundings for 34 times when the difference in flow between the times of the soundings was 5 percent or more. Of the 11 times when the flow increased 5 percent or more, the computed bed elevation increased 3 times at the upstream cableway and 8 times at the downstream cableway. If only changes greater than 0.20 foot are considered, the computed bed elevation increased one time out of eight at the upstream cableway and five times out of five at the downstream cableway. Of the 23 times when the flow decreased 5 percent or more, the computed bed elevation increased 16 times at the upstream cableway and 9 times at the downstream cableway. If only changes greater than 0.20 foot are considered, the computed bed elevation for decreases of flow increased 12 times out of 15 at the upstream cableway and 3 times out of 7 at the downstream cableway. Thus, whether all changes of the bed elevation or only those greater than 0.20 foot are considered, the tendency is for the slightly narrower upstream cross section to scour on increasing flow and to fill on decreasing flow, as narrow sections are gen-

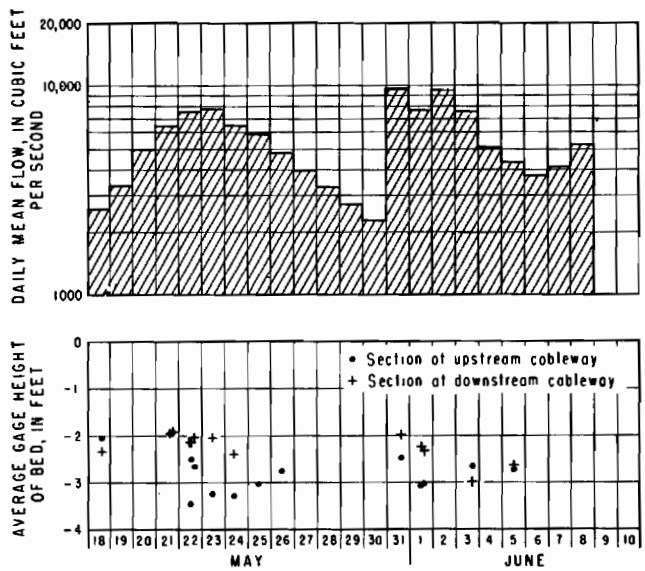

FIGURE 10.—Changes in average gage height of the streambed of the Elkhorn River near Waterloo, Nebr., during a period of high flow in 1951.

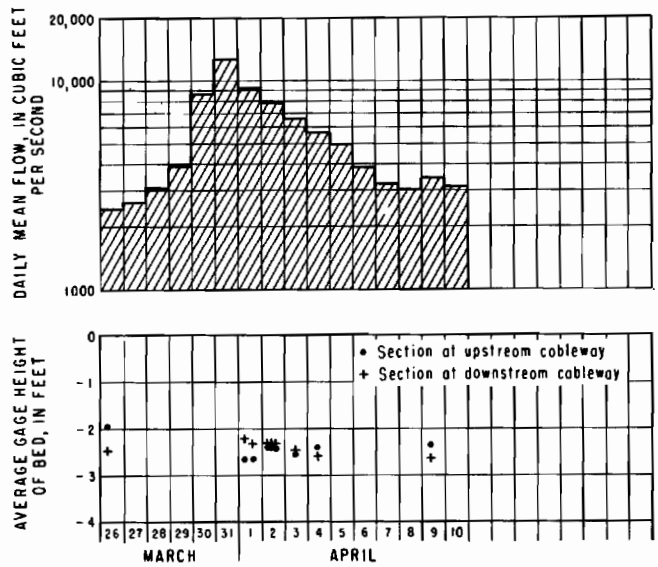

FIGURE 11.—Changes in average gage height of the streambed of the Elkhorn River near Waterloo, Nebr., during a period of high flow in 1952.

erally likely to do. The wider downstream cross section shows a slight tendency to fill on increasing flow and to scour on decreasing flow, but this tendency may not be significant.

The lack of agreement between the computed net scour and net fill at the two cableways is clear from a graph of change in bed elevation at one cableway (fig. 14) against change in bed elevation at the other. Of 42 comparisons, the computed change in average bed position at the downstream cableway was in the same direction as that at the upper cableway 22 times, and once a large fill at the upper cableway was accompanied by no change at the lower cableway. A reasonable conclusion from figure 14 seems to be that the two cross sections do not show any significant tendency to scour or to fill at the same time. Hence, measured scour or fill at either cross section is unlikely to represent average scour or fill along a channel reach near the cableways. Also, the lack of consistency indicates that net scour or fill is not governed directly by changes either in flow or in sediment concentration, because the rate of flow and the concentration of sediment are nearly the same at the two cross sections. The upstream cross section does show somewhat greater amounts of net scour and fill, as a narrower section is likely to, than the downstream section. At the downstream section, changes of the average bed position seem to be nearly random, as they should be for a uniform sand-bed

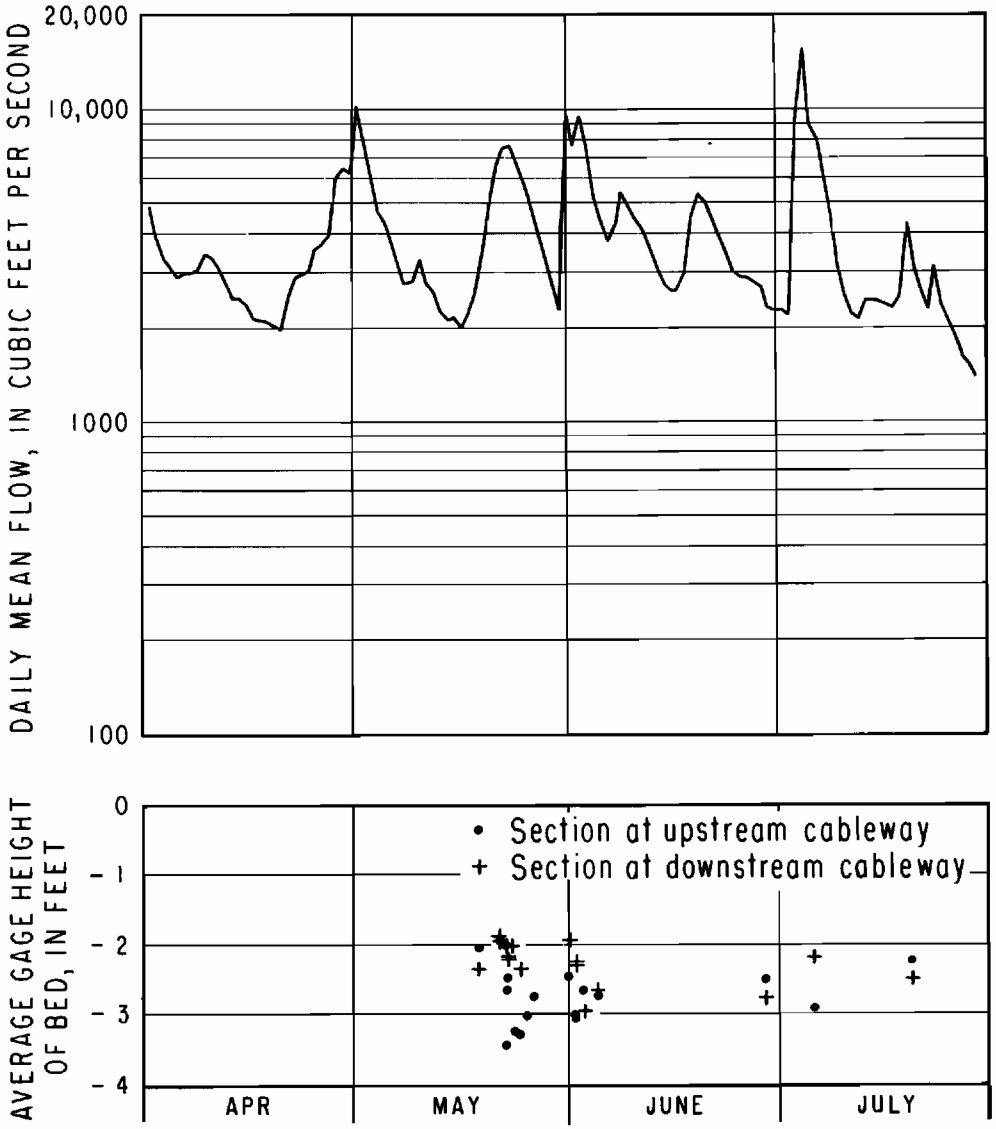

FIGURE 12.—Changes in average gage height of the streambed of the Elkhorn River near Waterloo, Nebr., May 18–July 19, 1951.

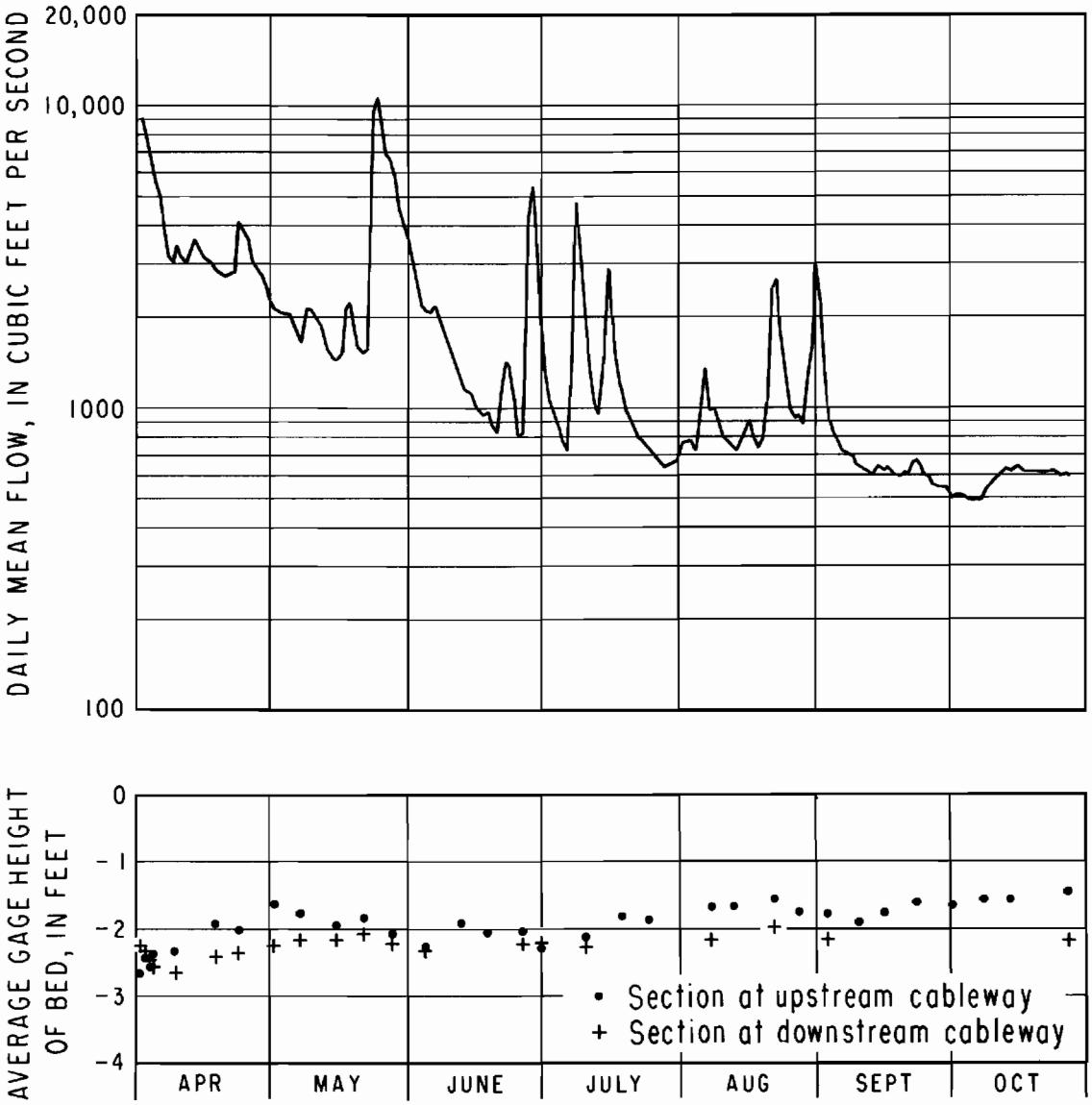

FIGURE 13.—Changes in average gage height of the streambed of the Elkhorn River near Waterloo, Nebr., April 1–October 23, 1952.

channel, except, of course, that the bed position changes faster at high flows than at low flows.

The general behavior of the streambed at the downstream cableway on the Elkhorn River near Waterloo is probably similar to that of the Colorado River at the site of Imperial Dam before the dam was constructed. At that site, too, measurements at a cableway at a laterally unconstricted section showed fluctuations of the streambed but no appreciable net scour or fill even during a high flow (Lane and Borland, 1954, p. 1075).

NARROW SECTION OF A NATURAL SAND-BED STREAM

Streamflow measurements made from a bridge over the Missouri River near Yankton, S. Dak., during 1941 show scour and fill (B. R. Colby and R. E. Oltman, written communication) that may occur at a cross section where the flow of a sand-bed stream is laterally constricted (fig. 15). Measurements were not made at or near all peak flows, but the available measurements show clearly that the streambed usually was lower than its average position whenever the flow was high. After the high flow ended, the streambed filled again to about the original position. The alternation of scour and fill is typical behavior at a narrow cross section of a sand-bed stream. A somewhat similar pattern of scour and fill was shown by the computations for the narrow section in the assumed uniform channel. The amounts of net scour or fill at this narrow cross section are not, however, representative for the reaches upstream and downstream from the measuring section.

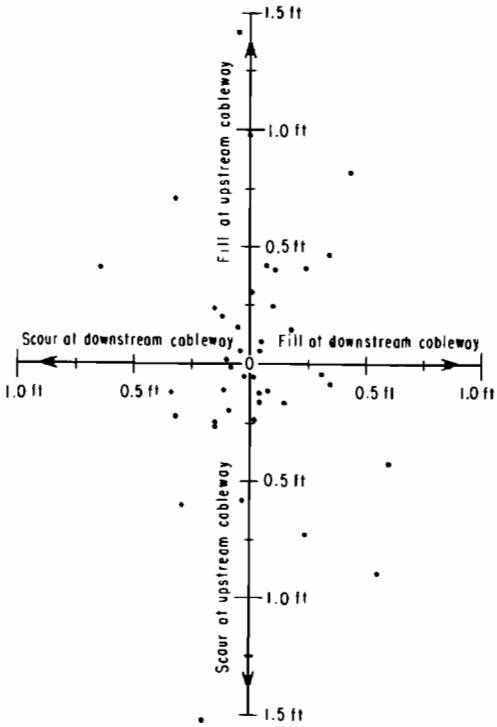

FIGURE 14.—Comparison of scour and fill computed from changes in bed position at two cableway sections on the Elkhorn River near Waterloo, Nebr.

A POOL-AND-RIFFLE STREAM

Although pool-and-riffle streams are not strictly sand-bed streams, they are discussed here because data from such streams have sometimes been used as indications of the scour and fill to be expected at sections of sand-bed streams.

A pool-and-riffle stream is one in which the water-surface slope alternates between long and comparatively level reaches (the pools) and short and comparatively steep segments (the riffles). Such a stream may have a sand bed throughout most pools, but its riffles normally have beds of material that is coarser than sand. The presence of the coarser bed material indicates that the quantity of available sand at the riffles is less than the stream can transport at the riffles. The mean velocity in a pool-and-riffle stream varies widely from one cross section to another along the channel, whereas continuity of the discharge of bed material and the abundant availability of sands prevent large changes in mean velocity from one section to another along a sand-bed stream.

STREAMFLOW, SEDIMENT CONCENTRATION, AND CHANGES IN BED ELEVATION

Leopold and Maddock (1952, 1953) and Brooks (1958) attempted to explain scour and fill at the streamflow-measuring section on the Colorado River near Grand Canyon, Ariz., on the basis of an assumed tendency for the depth of flow to adjust itself to changes

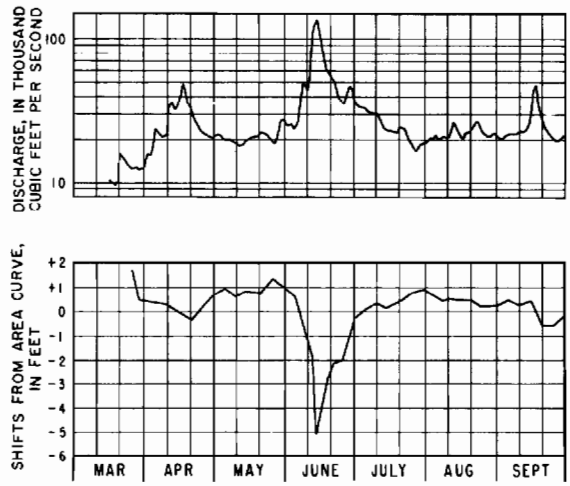

FIGURE 15.—Streamflow and changes in average bed position of the Missouri River near Yankton, S. Dak., March–September 1941. After Colby and Oltman (written communication, 1948).

in resistance to flow, changes that resulted from, or at least accompanied, changes in measured sediment concentration. These writers assumed that the pattern of scour and fill at the streamflow-measuring section of this pool-and-riffle stream was typical of a long reach of channel. Brooks' assumption (1958, p. 545) of constant water-surface slope implies a representative relation for a long reach. Actually, the slope in a pool may vary widely if the bed elevation changes appreciably. The assumptions seem to be questionable for at least four reasons, one of which is that the measuring section is at a cross section that is probably narrower than average for the pool, and hence untypically large amounts of alternate scour and fill are to be expected. Also, Einstein and Chien (in Brooks, 1958, p. 558) pointed out that according to the reasoning of Lane and Borland (1954), a change in bed elevation at this measuring section was "* * * a transient change of the local river bed during a flood." They further stated that "It should not be interpreted as an adjustment of river regimen in response to the change of independent variables imposed on the channel by the watershed."

A second reason for questioning the assumptions is that scour and fill may be inconsistent at two cross sections even though the flows and the suspended-sediment concentrations are about the same at both sections. The inconsistency of scour and fill at the two cableways on the Elkhorn River near Waterloo, Nebr., was clearly shown in figure 14. Similar inconsistency of scour and fill also exists between the measuring sections on the Colorado River at Lees Ferry and near Grand Canyon, Ariz., for periods of high flow in 1955, 1957, and 1959 (figs. 16–18). Not only are the patterns of scour and fill dissimilar from one measuring section to the other

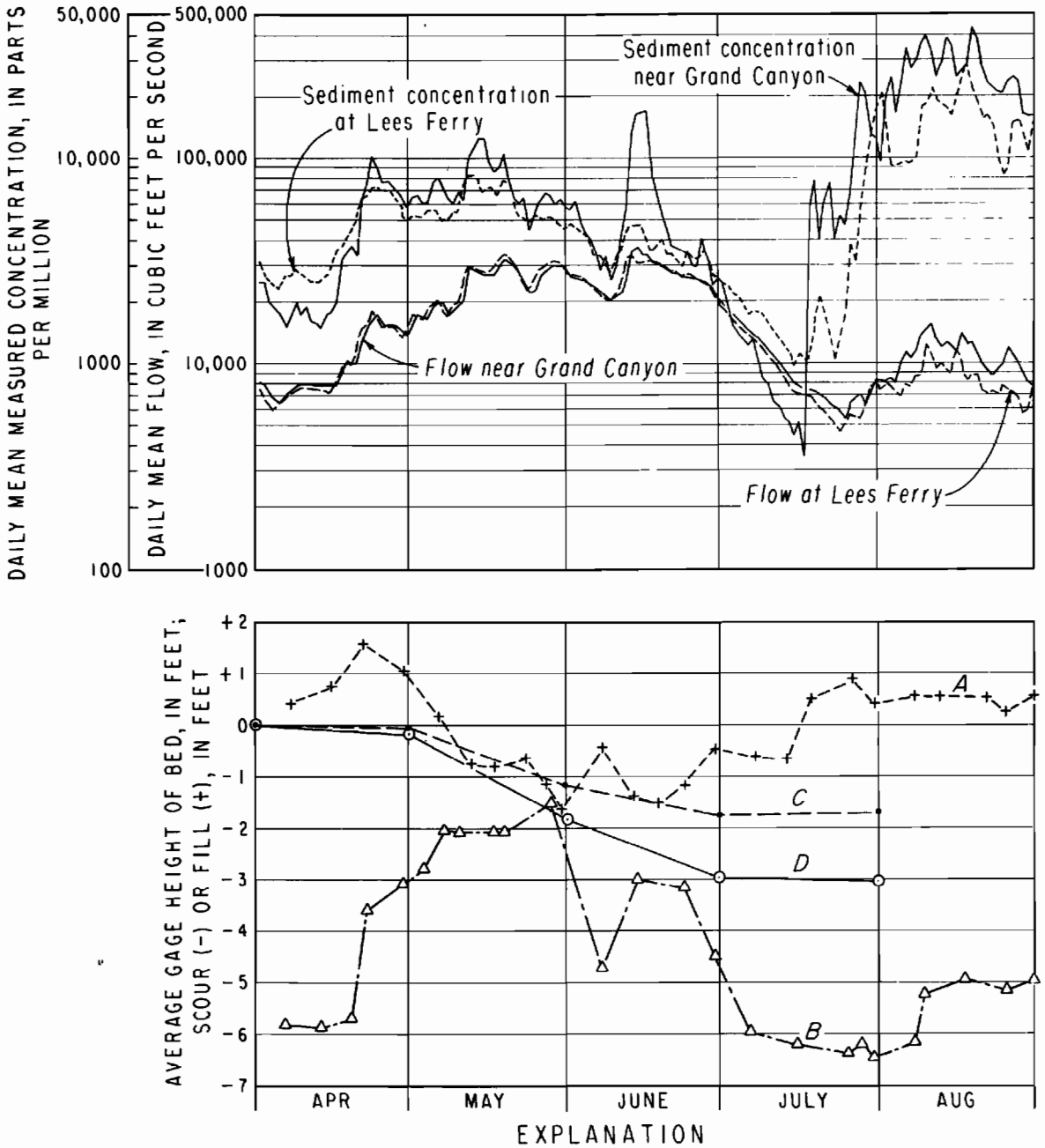

EXPLANATION

Average gage height of bed—

A, at Lees Ferry

B, near Grand Canyon

Cumulative computed monthly change in average bed position from Grand Canyon to Lees Ferry—

C, based on difference between discharge of sands at Lees Ferry and Grand Canyon

D, based on discharge of sands at Grand Canyon (assumed no inflow of sand to reach)

FIGURE 16.—Streamflow, measured sediment concentrations, and changes of average bed position at Lees Ferry and near Grand Canyon, Ariz., April 1–August 31, 1955.

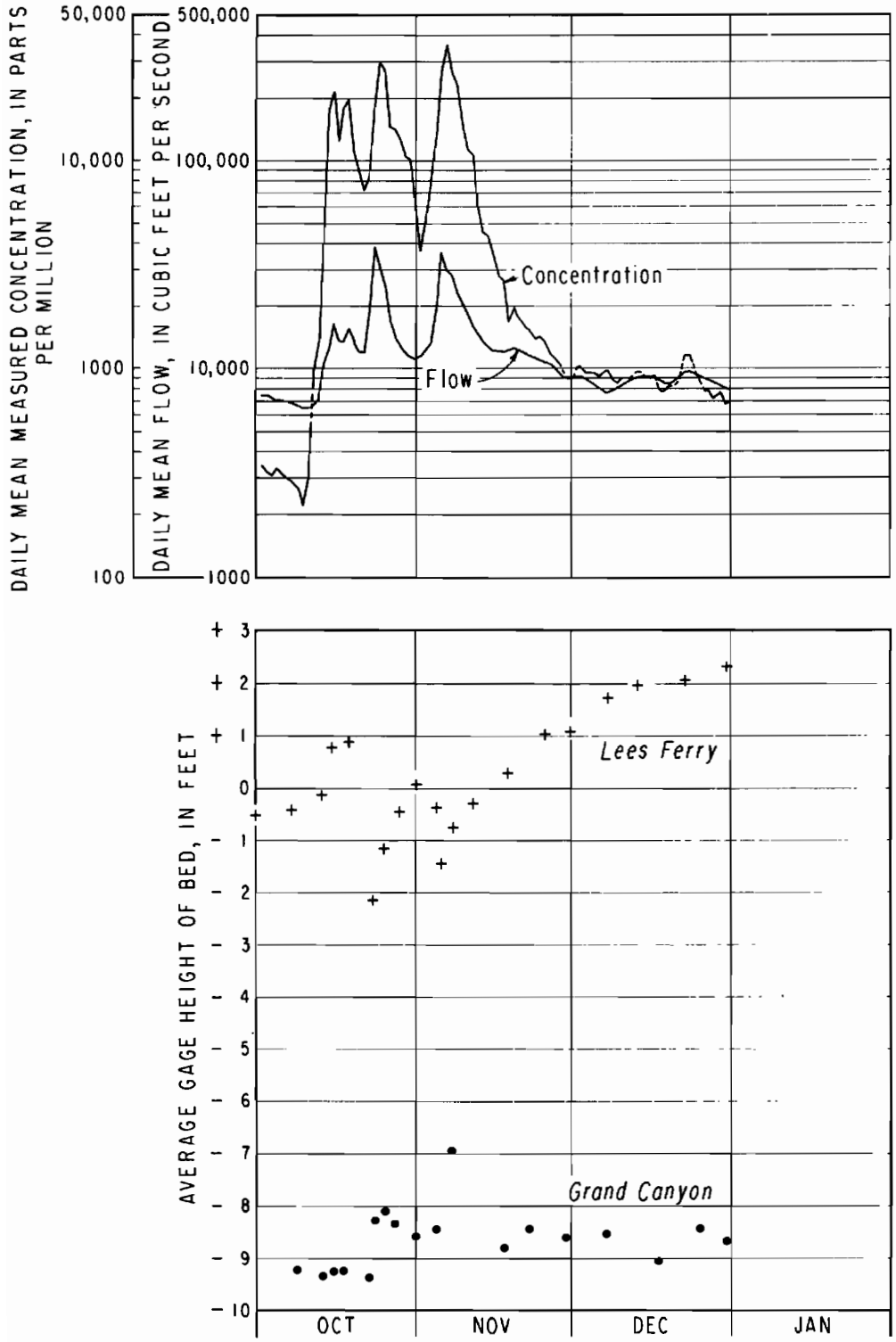

FIGURE 17.—Changes of average bed position at Lees Ferry and near Grand Canyon, Ariz., October–December 1957. Concentration and flow near Grand Canyon.

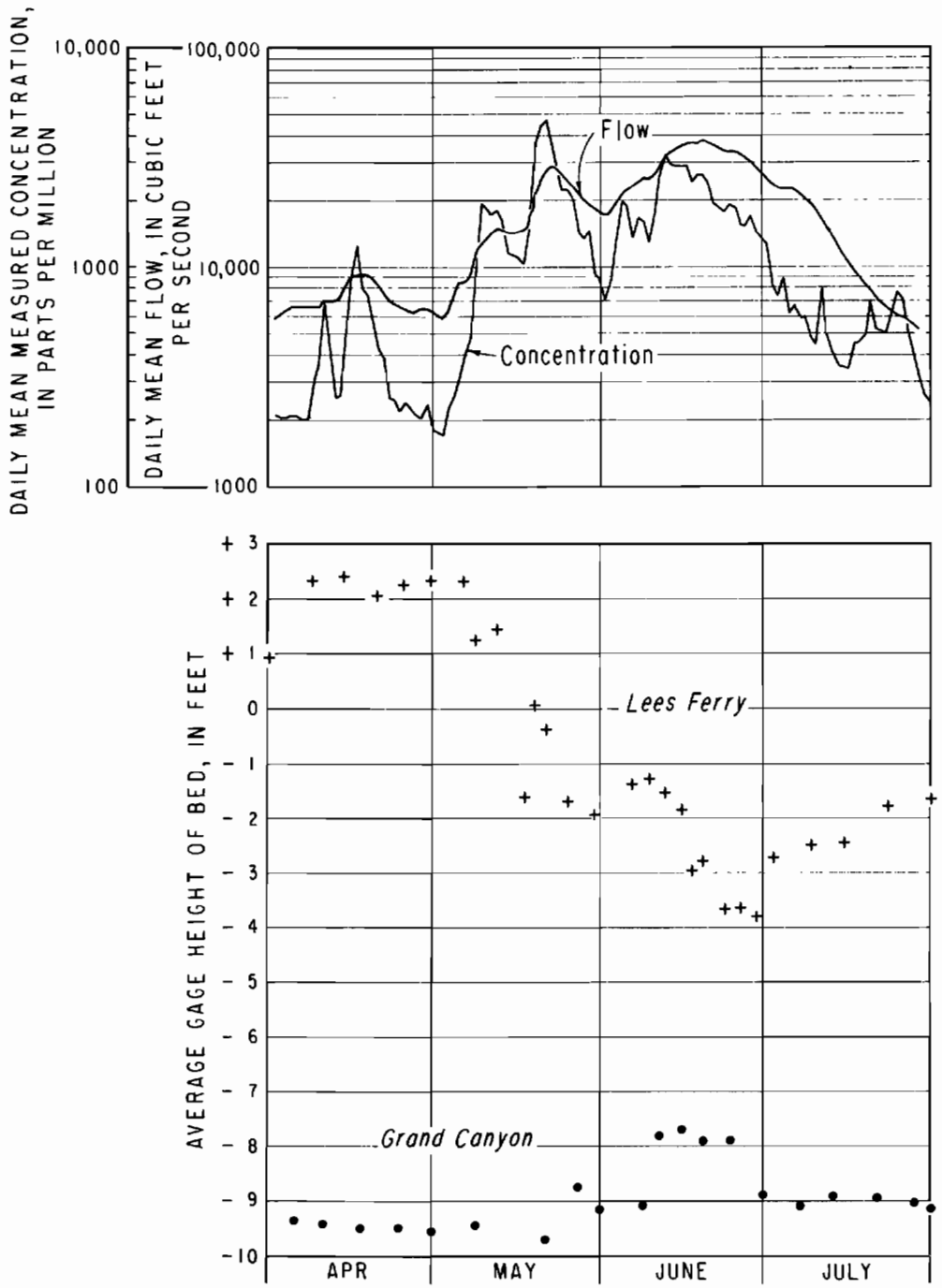

FIGURE 18.—Changes of average bed position at Lees Ferry and near Grand Canyon, Ariz., April–July 1959. Concentration and flow near Grand Canyon.

but also from one period of high flow to another at either measuring section, particularly the measuring section near Grand Canyon. The flow and the measured concentration of sediment are given (fig. 16) for both sections for the high flow in 1955, when they probably differed more than in 1957 and 1959. Obviously, neither the flow nor the measured concentration is a satisfactory guide to scour or fill at some cross sections.

A third reason for questioning the assumptions is that changes in resistance to flow in a pool usually do not cause large changes in depth of flow at a measuring section that is only a comparatively short distance upstream from a riffle. Suppose that the energy loss is 0.20 foot between a measuring section and the beginning of a fairly stable riffle downstream. This riffle is assumed to determine a stage-discharge relation that is

independent of changes in roughness in the upstream pool. Now, if at a particular streamflow the Chezy C for this reach of channel between the measuring section and the beginning of the riffle was to be decreased 50 percent or to be doubled, the energy loss through the reach would be about 0.80 or 0.05 foot, respectively. The indicated change in depth at the measuring section would be about 0.60 or 0.15 foot. Even for the large assumed changes in resistance to flow through the reach, only those rather small changes in depths would be required. Experimentally, the small effect of changes in resistance to flow on depth at the Grand Canyon measuring section is shown by the agreement (Leopold and Maddock, 1953, fig. 23) between the stage-discharge relations for the same flows at different times regardless of whether the stage was rising or falling. (The gage is at the measuring section.)

The change in depth because of a given change in resistance depends on distance upstream from the riffle. If a pool extended far enough upstream along a uniform channel, the depth effect at the head of the pool would approach the depth effect in a long uniform channel. In such a channel, a change in resistance to flow along the channel results in a change in depth because the slope of the energy gradient in the uniform channel (uniform resistance is, of course, assumed along the channel) must be nearly constant at all steady flows. If the channel is wide and the width is constant as the depth changes in the channel, a decrease of 50 percent in Chezy C requires an increase in depth of about 60 percent. This adjustment of depth in a uniform sand-bed channel is the sort of effect that Brooks (1958) found in his flume investigations.

A fourth reason for questioning the assumptions, rather an obvious one even without the preceding discussion, is that any adjustment required in depth of flow by changes in roughness, flow, or energy gradient will generally appear as a difference in elevation or slope of the water surface rather than in elevation of the streambed. In other words, if the water surface is not somehow fixed in position, it can adjust readily in response to changes in flow, roughness, or energy gradient; but the streambed adjusts only as sediment accumulates or erodes. Thus, a useful general guide is that changes in bed elevation should be explained on the basis of the principles of scour and fill whereas changes in depth of flow that result mainly from changes in water-surface elevation should be explained in terms of changes in rate of flow, energy gradient, or resistance to flow.

Depth adjustments resulting from changes in water-surface elevation may be correctly called adjustments in cross section of flow but not adjustments of the stream channel. Also, in a channel of uniform roughness and cross section, the adjustment in the water surface, at least at constant flow, will usually be an adjustment in elevation rather than in water-surface slope. On the other hand, in a pool upstream from a riffle that controls the stage-discharge relation, the adjustment in the water surface will usually be mainly in slope rather than in elevation.

Briefly summarized, scour and fill at the streamflow-measuring section on the Colorado River near Grand Canyon represent local changes that are untypical of long reaches of channel; neither concentration nor flow is generally a satisfactory guide to scour and fill at the Grand Canyon or Lees Ferry sections; changes in resistance in a pool cause little depth change immediately upstream from a riffle that controls the stage-discharge relationship; and when adjustment of depth is required by change in flow, roughness, or energy gradient, the adjustment is usually in water-surface elevation rather than in bed elevation.

The variability of the relation between discharge of bed material and flow in sand-bed streams should be noted before any attempt is made to apply the principles of scour and fill to a pool-and-riffle stream such as the Colorado River between Lees Ferry and Grand Canyon. If neither the banks of a pool nor the riffle at the downstream end of the pool shifts appreciably, any major change in the average elevation of the streambed of the pool must cause an appreciable change in the mean velocity through the pool for a given rate of flow. For an abundant supply of bed material of a given particle size, even a small change in mean velocity usually causes a significant change in discharge of sands (fig. 3). Hence, the relation between discharge of bed material and flow usually changes, sometimes widely, if the mean velocity at a particular flow is changed because of scour or fill in a pool. Furthermore, the scour that might reduce the mean velocity at a particular flow is usually accompanied by an increase in particle size of the bed material in the pool and, perhaps, by a decrease in the proportion of the streambed that is covered with sand. Thus, when the elevation of the streambed is low in a pool, three factors—the velocity decrease, the particle-size increase, and the decrease of sands on the bed—tend to decrease the discharge of sands for a given flow. Of course, factors other than these also affect somewhat the relation between measured discharge of sands and flow.

The large overall effect of the difference in elevation of the streambed at the measuring section near Grand Canyon and in upstream measuring sections probably caused the large difference (figs. 16, 17) in measured discharge of sands between 1955 and the fall of 1957 for given flows (fig. 19). The long-continued high flows during the summer of 1957 scoured the bed of the pool at the measuring section near Grand Canyon and prob-

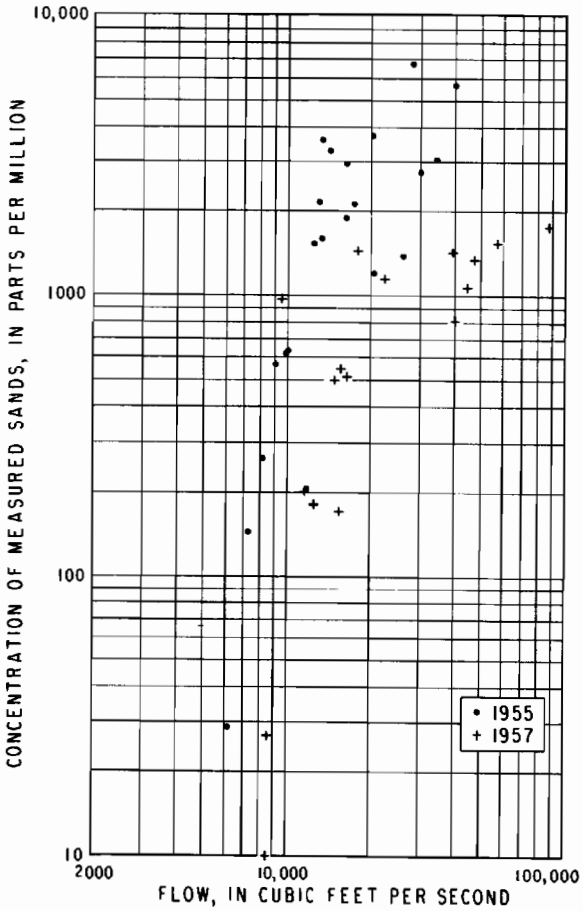

FIGURE 19.—Variable relation of concentration of measured sands to flow of the Colorado River near Grand Canyon, Ariz.

ably also scoured the beds of many pools upstream. These pools could not refill except as sediment, presumably nearly all sands, was trapped in them. Also, flows high enough to bring in appreciable quantities of sand may also be high enough to carry much of the incoming sand through the pools. Hence, during periods of high flow in the fall of 1957 and the summer of 1959, the deeply scoured pool near Grand Canyon filled very little even though the flows and the sediment concentrations were moderately high (figs. 17, 18).

APPLICATION OF PRINCIPLES OF SCOUR AND FILL

The principle of a relation between discharge of sands and characteristics of the flow and available sands applies to a pool-and-riffle stream, but the relation existing at a particular time may be impossible to determine. In such a stream, the quantity and particle size of the available sediment generally change with time, as the particle size of the bed material did in the Colorado River near Grand Canyon (U.S. Geological Survey, 1961, p. 168) in 1956, and with distance along the stream. Because of changing configuration within a short distance and perhaps because of unusually rough walls, the mean velocity is not so good a measure of discharge of sands in a pool-and-riffle stream as it is in a sand-bed stream where turbulence and mean velocity are closely related for a particular roughness and depth of flow. Hence, an equilibrium relation such as that given between discharge of sands and parameters of flow in figure 3 for sand-bed streams can seldom be established for permanent use at a section of a pool-and-riffle stream. In general, neither theoretical nor empirical relations can be used to compute the discharge of sands at many cross sections of pool-and-riffle streams; the discharge of sands at these sections often must be based at least in part on sediment sampling of the suspended sands.

In a pool-and-riffle stream the principle of continuity applies directly, the same as it does in sand-bed streams. This statement does not mean that the bed-material discharges are about the same from one cross section to

TABLE 7.—*Computed average scour or fill by months during 1955 water year in 88-mile reach from Lees Ferry to Grand Canyon, Ariz.*

[Assumed average width of reach, 400 ft; assumed weight of sands, 85 lb per cu ft]

Month (1)	Computed total discharge of sands near Grand Canyon (1,000 tons) (2)	Average scour in reach, based on column 2 (ft) (3)	Computed total discharge of sands at Lees Ferry (1,000 tons) (4)	Difference in discharge of sands from columns 4 and 2 (1,000 tons) (5)	Average scour (−) or fill (+) in reach, based on column 5 (ft) (6)
October	370	−0.05	700	+330	+0.04
November	22	−.003	240	+220	+.03
December	9	−.001	150	+140	+.02
January	4	−.0005	110	+110	+.01
February	6	−.0008	98	+92	+.01
March	790	−.10	1,040	+250	+.03
April	1,470	−.19	1,220	−250	−.03
May	13,500	−1.71	4,700	−8,800	−1.11
June	9,340	−1.18	4,810	−4,530	−.57
July	500	−.06	940	+440	+.06
August	660	−.08	690	+30	+.004
September	33	−.004	120	+90	+.01
Water year		−3.38			−1.50

another along the stream but only that equation 1 applies.

Continuity of bed-material discharge limits the average scour in the 88-mile reach of the Colorado River between the measuring sections at Lees Ferry and near Grand Canyon, Ariz. Daily discharges of sands were computed roughly for the 1955 water year from records of flow, measured concentration of suspended sediment, and size distributions of the measured suspended sediment for Lees Ferry and for Grand Canyon (U.S. Geological Survey, 1959, p. 135–137, 153–156). These daily discharges were added by months and were increased by 20 percent for unmeasured discharge of sands. The estimate of 20 percent was an average of seven computations of unmeasured sediment discharge for the measuring section at Grand Canyon. The seven computed unmeasured sediment discharges varied from 12 to 28 percent of the measured discharge of sands without any definite trend of the percentage with flow. If only the discharge of sands near Grand Canyon is considered—that is, no inflow of sands to the reach is assumed—the computed monthly scour (table 7, column 3) shows an average depth for the 88-mile reach of less than 0.01 foot for each of 5 months of the 1955 water year. The computed average depth of scour is 1.71 feet during May and 1.18 feet during June and totals 3.38 feet for the water year. If scour and fill in the reach are based on the difference in discharges of sands at the ends of the reach (table 7, column 6), average fill of 0.06 foot or less is shown for each of the first 6 and the last 3 months of the 1955 water year. Computed average scour totals 1.71 feet for the combined months of April, May, and June; and the net average scour for the water year is 1.50 feet. Of course, computed amounts of fill would be increased and computed amounts of scour would be decreased if the discharge of sands into the reach from the Paria and the Little Colorado Rivers and from other tributaries was known and could be included in the computations. Cumulative scour from April 1 to July 31 is shown in figure 16 and is based on the computed figures of scour from columns 3 and 6 of table 7.

The same sort of limitation that was imposed on scour and fill by continuity of bed-material discharge during the 1955 water year also applies in general. If the total discharge of sands into the 88-mile reach were known for any month or year, a limit could be established for the volume of sands that might be deposited within the reach for the month or year. If both the total discharge of sands into and out of the reach were known for any period of appreciable length, the volume of scour or fill could be reasonably closely determined for the period. Usually, such a determination would be more accurate than an estimate of volume of scour for a reach from observations of change in bed elevation at one or two cross sections along the reach.

CONCLUSIONS

Observations of scour and fill in field streams that have sand beds are frequently misinterpreted for several reasons. The position of the streambed may be defined at too few points to determine a satisfactory average elevation at a cross section or at too few cross sections to establish an accurate average bed elevation for a channel reach. Many available observations at points represent approximately the lowest positions of the bed at some unknown time during a flood. This time may have been when dunes were largest and the flow was fairly low. Also, when the bed was lowest at one point, it may have been much higher at several nearby points. Thus, many observations of scour and of subsequent fill tend to represent maximum amounts at points rather than average amounts for a cross section or an area. Also, changes in average bed elevation at narrow cross sections are almost always greater than changes at representative cross sections of channel reaches, and many streamflow-measuring sections are narrower than the average width of the nearby channel.

The sand being transported even in deep and swift flows would amount to an average depth of deposit of only a few hundredths of a foot if it could all be instantaneously deposited on the streambed.

Two principles are helpful in understanding scour and fill in sand-bed streams. One is the principle of continuity of volume of the bed material along a stream reach. This principle indicates that changes in elevation of an area of sand bed result from a difference in the rates at which sand reaches and leaves the area. The second principle is that a relation exists between the discharge of sands and the characteristics of flow and available sands.

These two principles indicate that the average bed elevation in a reach of uniform sand-bed channel is usually fairly stable during the passage of a flood because the discharge of sands into the upper end of the reach tends to be about balanced by the discharge of sands from the lower end of the reach.

A straight channel of uniform cross section may either scour or fill during rising flow because of a change in bed slope or in resistance to flow along the channel. In such a channel, scour while flow is increasing is usually followed by scour while the flow is decreasing, and fill while flow is increasing also is usually followed by fill while flow is decreasing.

Because the characteristics, especially mean velocity, of a flow are different at a narrow cross section in a sand-bed channel than at more representative cross sections, the amounts of scour and fill at a narrow cross

section are unrepresentative of a channel reach. The amounts usually are larger than the average for the reach; to some extent, scour tends to accompany high or increasing flows whereas fill tends to accompany low or falling flows.

In spite of usually small and somewhat random changes in the characteristics of the streambed, the sand bed of the Elkhorn River near Waterloo, Nebr., showed general stability on the basis of many determinations of bed elevation at two cableways. At the upstream cableway, where the width was a little less than at the downstream cableway, the streambed seemed to have a slight tendency to lower during increasing flow and to rise during decreasing flow; but the streambed showed no significant tendency to change in the same direction at the downstream cableway as at the upstream cableway.

Streamflow measurements on the Missouri River near Yankton, S. Dak., showed that the streambed at the laterally constricted measuring section usually was much lower at high flow than at low flow, a pattern of bed change that characterizes many narrow cross sections in sand-bed streams.

Although the Colorado River is a pool-and-riffle stream rather than a sand-bed stream, many of its pools have sand beds. Measurements during three periods of high flow showed that the pattern of scour and fill as related to flow at Lees Ferry was different from that near Grand Canyon, Ariz., and that the pattern was inconsistent from one period to another near Grand Canyon. Changes in bed elevation at the measuring section near Grand Canyon and in upstream pools changed the relations of discharge of sands to flow and to measured sediment concentration.

Neither flow nor measured sediment concentration showed any clearcut relation to the diverse patterns of scour and fill for the Elkhorn River near Waterloo, a sand-bed stream, or for the Colorado River, a pool-and-riffle stream, at Lees Ferry or near Grand Canyon. Because bed changes at one cross section were inconsistent with those at another section on the same stream, observed scour and fill at a cross section are, at least sometimes, poor indications of scour and fill in a channel reach.

When a change in depth of flow is required because the resistance, slope, or streamflow changes, the water surface rather than the streambed adjusts to the new depth of flow. A useful general guide is that changes in bed elevation should be explained on the basis of the principles of scour and fill whereas changes in depth of flow that result mainly from changes in water-surface elevation should be explained in terms of changes in rate of flow, energy gradient, or resistance to flow.

In a pool, changes in depth of flow caused by changes in resistance to flow in the pool are usually small and decrease with nearness to a downstream riffle.

REFERENCES

Barton, J. R., and Lin, Pin-Nam, 1955, A study of the sediment transport in alluvial channels: Colorado State Univ., Fort Collins, Colo., Dept. Civil Eng. pub. 55JRB2, 43 p., 21 figs.

Beckman, E. W., and Furness, L. W., 1962, Flow characteristics, Elkhorn River, Waterloo, Nebraska: U.S. Geol. Survey Water-Supply Paper 1498–B, 34 p.

Brooks, N. H., 1958, Mechanics of streams with movable beds of fine sand: Am. Soc. Civil Engineers Trans., v. 123, p. 526–594.

Colby, B. R., 1960, Discontinuous rating curves for Pigeon Roost and Cuffawa Creeks in northern Mississippi: U.S. Dept. Agriculture, Agr. Research Service pub. ARS41–36, 31 p.

——— 1964, Sand discharge and mean-velocity relationships in sandbed streams: U.S. Geol. Survey Prof. Paper 462–A (in press).

Dawdy, D. R., 1961, Depth-discharge relations of alluvial streams—discontinuous rating curves: U.S. Geol. Survey Water-Supply Paper 1498–C, 16 p.

Einstein, H. A., 1950, The bed-load function for sediment transportation in open channel flows: U.S. Dept. Agriculture Research Bull. 1026, 70 p.

Lane, E. W., and Borland, W. M., 1954, River-bed scour during floods: Am. Soc. Civil Engineers Trans., v. 119, p. 1069–1089.

Laursen, E. M., 1952, Observations on the nature of scour: Iowa State Univ., Proc. 5th Hydraulic Conf., Studies in Eng., Bull. 34, p. 179–197 [1953].

Leopold, L. B., and Maddock, Thomas, Jr., 1952, Relation of suspended-sediment concentration to channel scour and fill: Iowa State Univ., Proc. 5th Hydraulic Conf., Studies in Eng., Bull. 34, p. 159–178 [1953].

——— 1953, The hydraulic geometry of stream channels and some physiographic implications: U.S. Geol. Survey Prof. Paper 252, 57 p.

Liu, Hsin-Kuan, and Hwang, Shoi-Yean, 1961, Discharge formula for straight alluvial channels: Am. Soc. Civil Engineers Trans., v. 125, p. 1787–1857.

Simons, D. B., Richardson, E. V., and Haushild, W. L., 1962, Depth-discharge relations in alluvial channels: Am. Soc. Civil Engineers Proc., v. 88, HY 5, p. 57–72.

Straub, L. G., 1934, Effect of channel-contraction works upon regimen of movable bed-streams: Am. Geophys. Union Trans., pt. 2, p. 454–463.

U.S. Geological Survey, 1959, Quality of surface waters of the United States, 1955: U.S. Geol. Survey Water-Supply Paper 1403, pt. 9–14.

——— 1961, Quality of surface waters of the United States, 1957: U.S. Geol. Survey Water-Supply Paper 1523, pt. 9–14.

Vanoni, V. A., and Brooks, N. H., 1957, Laboratory studies of the roughness and suspended load of alluvial streams: Pasadena, Calif., California Inst. Tech. Sedimentation Lab. Rept. E–68, 121 p.

○

An Analysis of Some Storm-Period Variables Affecting Stream Sediment Transport

By H. P. GUY

SEDIMENT TRANSPORT IN ALLUVIAL CHANNELS

GEOLOGICAL SURVEY PROFESSIONAL PAPER 462-E

UNITED STATES GOVERNMENT PRINTING OFFICE, WASHINGTON : 1964

UNITED STATES DEPARTMENT OF THE INTERIOR

STEWART L. UDALL, *Secretary*

GEOLOGICAL SURVEY

Thomas B. Nolan, *Director*

For sale by the Superintendent of Documents, U.S. Government Printing Office
Washington, D.C. 20402

CONTENTS

	Page
Abstract	E1
Introduction	1
Scope of work and available information	2
Theory of sediment yield and transport	3
Fine sediment	3
Splash, sheet, and rill erosion	3
Environmental factors	3
Coarse sediment	5
Effect of velocity	5
Effect of particle size	5
Storm characteristics	6
The runoff hydrograph	6
Seasonal characteristics	8
Precipitation	8
Infiltration	8
Runoff	9
A graphical search for variables	12
The storm event technique	12
Water-sediment discharge relations	12
Compilation of data	14
Surface runoff	15
Season	15
Ground-water runoff	17
A graphical search for variables—Continued	
Peakedness	E20
Rainfall	20
Trend	21
Concentration as a dependent variable	21
Summary of graphical search	22
The model and transformation of variables	24
Computation results	25
The means and standard deviations	26
Simple correlations	27
Multiple regression equations for Hazel River	27
Comparison of streams	29
Effects of dependent variables	29
Effects of independent variables	30
Variation among basins	31
Examples of application	32
Range of specific variables	32
Comparison of locations	32
Extrapolation to other streams	33
Summary	37
Recommendations	39
References	39
Appendix—multiple regression equations	42

ILLUSTRATIONS

		Page
FIGURE	1. Chart of the principal factors affecting erosion and transport of sediment from the land surface	E4
	2. Components of a streamflow hydrograph	7
	3. Seasonal probability of an intense 6-hour rainfall for the central Atlantic coast area	9
	4. Wischmeier's erosion index for the area of the United States east of 105° W	10
	5. Seasonal distribution of erosion index values at four locations in the Atlantic coast area	10
	6. Seasonal distribution of surface and total runoff for Rock Creek at Sherrill Drive, Northwest Branch Anacostia River near Colesville, Md., and precipitation for the Washington Metropolitan area	11
	7. Effect of hysteresis and progressive lag on water-sediment discharge relations	13
	8. Daily mean water and sediment discharge for two storm events for Hazel River at Rixeyville, Va	14
	9. Relation of sediment to water discharge for storm events, Hazel River at Rixeyville, Va	17
	10, 11. Variation of sediment discharge.	
	10. With time of year	18
	11. With mean air temperature for time of year of given storm events	18
	12. Magnitude and recession of ground-water runoff for Hazel River at Rixeyville, Va	19
	13–16. Variation of sediment discharge with—	
	13. Ground-water runoff	20
	14. Peakedness index	21
	15. Rainfall quantity	22
	16. Rainfall intensity	23
	17. Variation of unadjusted and seasonal adjusted departure ratios with time	24
	18. Relation of sediment concentration to water discharge for storm events, Hazel River at Rixeyville, Va	25
	19, 20. Test of selected models against observed data for—	
	19. Shenandoah River	34
	20. Potomac River	35
	21, 22. Comparison of the modified formula for—	
	21. James River at Buchanan with the observed data for the Shenandoah and Potomac Rivers	36
	22. Brandywine Creek with the observed data for the Shenandoah and Potomac Rivers	37

TABLES

Page

TABLE 1. Daily suspended-sediment records to September 1960 for streams draining to the Atlantic Ocean from the United States ---- E2
2. Computation of storm surface runoff and sediment discharge ---- 15
3. Water, sediment, and related factors for storm events of the Hazel River at Rixeyville, Va ---- 16
4. Sediment records used for correlation and multiple regression analysis ---- 23
5. Means and standard deviations of variables used in multiple regression analysis, by streams ---- 26
6. Simple correlation coefficients and their significance, by streams ---- 28
7. A matrix of variables showing the average direction and significance of simple correlations ---- 29
8. Regression coefficients and standard error of estimate of principle regression equations, by streams ---- 30
9. The regression equations, by streams, for 1, 2, or 3 independent variables ---- 32
10. Measured data for extrapolation of models to other streams ---- 33

AN ANALYSIS OF SOME STORM-PERIOD VARIABLES AFFECTING STREAM SEDIMENT TRANSPORT

By H. P. Guy

ABSTRACT

This study of the effect of some natural factors on storm-period fluvial-sediment transport is a part of the development of techniques for utilization of sediment reconnaissance data. In more general terms, this report presents a study of the time and space variation of sediment transport in streams.

A review of the theory of sediment yield and transport indicates that for most streams the bulk of the suspended sediment transport occurs during the relatively brief storm periods when the drainage basin collects and routes precipitation excess to a specific site. Therefore, a description of the quantity of sediment moved during the storm runoff periods at a stream location must be based principally on the active and passive forces of erosion.

The investigation of these forces was accomplished by using a combination of graphical and analytical multiple correlation techniques. Graphical correlation was employed on data for seven stream locations in the Atlantic coast area; first, to determine which climatic, hydrologic, and sedimentologic variables might be used; second, to determine the required transformation of data; and third, to note any unusual elements of data or wild points for specific variables. An analytical method using the general multiple regression model on the electronic computer was then employed to develop and indicate the accuracy of optimum equations for predicting sediment movement with surface runoff. Several combinations of variables for each stream location were used to show the effect of interdependence among the variables.

In regard to a choice of the dependent variable for defining sediment variation, the mean concentration of sediment in streamflow was found to be somewhat superior to sediment discharge due to the high degree of intercorrelation between water discharge and sediment discharge.

Some of the storm-to-storm variation of sediment concentration in streamflow was found to be associated with storm magnitude, the time during a period of record, the season of the year, the antecedent condition of the basin, and the storm intensity. The sediment moving in streams tends to increase with measures of storm magnitude such as surface runoff quantity or rainfall quantity. An apparent trend of decreasing sediment with time was indicated for the records of all seven locations, but was statistically significant only for the locations on the Brandywine Creek and the James River basins. With respect to seasonal change, sediment concentration tends to increase as mean air temperature increases. With respect to antecedent condition, sediment concentration tends to decrease as ground-water runoff increases. Ground-water runoff is generally high during the cool season for the Atlantic coast area; therefore, intercorrelation with mean air temperature reduces the importance of this variable. Sediment concentration was found to increase with storm intensity. The measures of storm intensity used were peakedness index, peak flow, and rainfall intensity; however, only peakedness index was tested for all streams.

The standard error of estimate of the dependent variable (the storm-period sediment concentration) ranged from 0.14 to 0.30 log units for most combinations of the independent or causative variables mentioned above. The range of this error was greater among the different streams than among the different combinations of variables for a given stream. This is attributed to variance of hydrologic and environmental factors that are not evaluated by the data, or possibly by the effect of some measurement errors in the basic data.

Three of the regression formulas derived in the above analysis were tested for extrapolation to other areas using observed data from the Shenandoah and Potomac Rivers. The results showed that these formulas can and must be modified to give a satisfactory comparison with the observed data.

INTRODUCTION

The development of methods for more effective use, and understanding, of available and future fluvial-sediment data is considered to be the principal objective of this study. Sediment stations on streams are widely scattered or nonexistent in many areas because of (1) the high cost of sediment-measuring programs, (2) inadequate interpretation of the data, and (3) rather poor recognition of the need for sediment knowledge. Knowledge of stream-sediment conditions is so meager in many places that effective fluvial-sediment measurement programs cannot be designed satisfactorily without first making some reconnaissance measurements. Kind and intensity of such required reconnaissance observations must be based on knowledge of sediment conditions in distant as well as nearby streams and of the applicable techniques for interpreting the data. The study should also advance progress toward development of a "universal equation" for computing the magnitude of stream sediment transport by application of observations to specific variables.

Sediment transport in a stream depends on such a great variety of circumstances that it is not considered practical to define fixed laws that would indicate the rate and amount of such sediment transport in the stream at any specific location. More specifically, the effects of widely varying climate, vegetation, and soils cause sediment conditions in streams to vary widely in time and space. Therefore, the task of describing and interpreting the yield, character, transport, and deposition of fluvial sediment seems almost insurmountable. In the past the most common method for describing fluvial sediment has been to collect a body of seemingly basic data representing the conditions of the problem requiring solution. Nearly all these data have been interpreted only so far as required for solution of the problem at hand, leaving the broader implications untouched. These programs have resulted in the basic data being widely scattered or even nonexistent in most parts of the country. This widely scattered information, however, could be a reservoir of data that if properly interpreted would increase general knowledge of fluvial sediment characteristics.

Therefore, the purpose of the project was to develop principles and methods for better understanding and use of sediment data. Experience has shown that it is not practical to describe sediment conditions in time and space with a comprehensive sampling program involving vast quantities of basic-sediment data. It may be practical, however, to use a limited amount of basic data and a program of data analysis and interpretation based on knowledge from adjacent areas. It is expected that the principles and methods will indicate the kind of measurements of environmental factors that can reasonably be obtained for interpretation of the sediment data.

The author acknowledges with warm appreciation the helpful suggestions and criticisms from colleagues who assisted in the formulation of the project, provided technical guidance, and read an early draft of the manuscript. Particular thanks are extended to W. F. White, W. B. Langbein, R. B. Vice, P. C. Benedict, B. R. Colby, B. C. Colby, and D. W. Hubbell. Messrs. F. J. Keller and H. E. Reeder assisted in assembly of data and correlation of variables for the Scantic and James River basins, respectively.

SCOPE OF WORK AND AVAILABLE INFORMATION

The scope of the work involved to meet the objective of developing principles and methods for better understanding and use of sediment data is limited to a considerable extent by the availability of sediment and environmental data. Hence, it is necessary to determine what correlative, mathematical, and "intuitive" techniques can be developed to give substance and understanding to this limited supply of available data.

The analysis of the available data for this report is limited to the Atlantic coast area. The bulk of the sediment data consists of daily mean concentration and daily suspended-sediment discharge at 39 sites in several river basins as indicated by the records listed in table 1. These records of sediment data were determined from the results of depth-integrated samples mostly taken at a single fixed stream vertical and adjusted, if necessary, by use of more complete definition of concentration in the stream cross section. Samples generally were taken once per day, except during periods of rapidly changing water discharge or sediment concentration. During these changing conditions the aim was to make several observations per day. When sufficient samples could not be obtained during the changing conditions to define the nature of concentration variation during the storm-runoff event, simple statistical methods were used to arrive at a computed or estimated value of the concentration.

TABLE 1.—*Daily suspended-sediment records to September 1960 for streams draining to the Atlantic Ocean from the United States*

[Dates marked with an asterisk indicate record still in progress September 1960]

Stream and location	Drainage area (sq mi)	Month and year of record
Scantic River at Broad Brook, Conn	98.4	*11/52
Kayaderosseras Creek near West Milton, N.Y	90	3/53–7/55
Mohawk River at Cohoes, N.Y	3,456	1/54–6/59
Stoney Brook at Princeton, N.J	44.5	*1/56
Delaware River at Port Jervis, N.Y	3,076	2/57–9/58
Lehigh River at Walnutport, Pa	889	5/48–3/53
Delaware River at Trenton, N.J	6,780	*9/49
Schuylkill River at Port Carbon, Pa	27.1	2/49–6/51
Schuylkill River at Landingsville, Pa	133	9/47–3/53
Schuylkill River at Auburn, Pa	160	9/47–6/51
Schuylkill River at Berne, Pa	355	*9/47
Schuylkill River at Pottstown, Pa	1,147	3/48–9/51
Little Schuylkill River at South Tamaqua, Pa	69.4	4/50–4/53
Little Schuylkill River at Drehersville, Pa	122	9/47–6/51
Perkiomen Creek at Gratersford, Pa	279	4/48–3/53
Schuylkill River at Manayunk, Philadelphia, Pa	1,893	*10/47
Brandywine Creek at Wilmington, Del	314	*12/46
Corey Creek near Mainesburg, Pa	12.2	*5/54
Elk Run near Mainesburg, Pa	10.2	*5/54
Susquehanna River at Towanda, Pa	7,797	1/51–7/54
North Bald Eagle Creek at Milesburg, Pa	265	12/55–3/58
Bald Eagle Creek at Blanchard, Pa	339	12/55–3/58
Marsh Creek at Blanchard, Pa	44.1	11/55–3/58
Juniata River at Newport, Pa	3,354	1/51
Bixler Run near Loysville, Pa	15.0	*2/54
Swatara Creek at Harper Tavern, Pa	333	*5/59
Shenandoah River at Front Royal, Va	1,638	4/53–9/56
North Fork Shenandoah River near Strausburg, Va	772	10/55–9/56
Hazel River at Rixeyville, Va	286	10/51–9/55
Rappahannock River at Remington, Va	616	*4/51
Rapidan River near Culpepper, Va	465	5/51–9/56
James River at Buchanan, Va	2,084	5/51–9/56
James River at Scottsville, Va	4,571	12/50–9/56
Roanoke River at Altavista, Va	1,802	2/53–9/56
Roanoke River at Randolph, Va	3,000	1/54–6/57
Dan River at Paces, Va	2,550	1/54–6/57
Tar River at Tarboro, N.C	2,140	*1/58
Yadkin River at Yadkin College, N.C	2,280	*1/51
South Yadkin River near Mocksville, N.C	313	*1/58

The variation found in sediment conditions, among sites and with time, indicates that most records of less than 4 years do not define the sedimentologic conditions of the stream within acceptable limits. This is caused

by the highly variable meteorologic and cultural patterns acting on the drainage basin which affects the sediment transported in the surface runoff. Thus when sediment data are collected only for a few storms in one season, the results are considered to be reconnaissance information.

Table 1 shows that most of the data for the Atlantic coast area are from a few States; thus, further indicating the need for developing techniques to extend available sediment data. Furthermore, even though Pennsylvania has the greatest number of station-years of record, the data represents only a small percentage of the drainage area in this particular State. Also, the special sediment studies in the Schuylkill River basin are demonstrative of the fact that stations on large drainage basins do not give information as to the various conditions in that particular basin. On the other hand, the small area stations represent only some of the environmental conditions. The overall result is that, although the 39 stations listed in table 1 seem to represent a lot of information, the deficiency of sediment knowledge is still very great.

The development of the principles and methods used in this report is based on aspects of hydrology and sedimentology discussed in the following sections, entitled "Theory of sediment yield and transport" and "Storm characteristics."

THEORY OF SEDIMENT YIELD AND TRANSPORT

The two principal components of natural streamflow for eroding and transporting sediment are the surface or overland flow resulting from precipitation excess and the base flow from springs and other ground-water seepage. The sedimentological aspects of these segments of hydrology stem from the erosion and transportation capacity of the overland flow as it makes its way to stream channels by way of sheet and rill flow and (or) from the transporting and bank-eroding power of high streamflow which may be derived from large quantities of ground-water flow.

Overland runoff, as determined from precipitation excess, is the most active agent causing erosion and sediment transport. Thus rainfall intensity and infiltration capacity at the land surface are important factors affecting the amount of sediment movement. Both these factors are known to vary greatly with time and location within a drainage basin. The precipitation generally ranges from a light drizzle during the cool season to a heavy downpour during the warm summer months. The infiltration ranges from zero through impermeable surfaces to several inches per hour through a forest floor with good duff and a very permeable subsoil.

FINE SEDIMENT

SPLASH, SHEET, AND RILL EROSION

On land surfaces of erodible sediment, the kinetic energy of the raindrops causes a large amount of splashing of the soil and water and, hence, transport of fine sediment in two ways. First, is the net movement in a downslope direction by gravity and (or) in the leeward direction by wind as it is briefly airborne. Second, is that the impact of rainfall and dispersion of soil particles cause a sealing of the soil surface thereby reducing the infiltration. The reduced infiltration increases the amount of precipitation excess that must make its way to stream channels carrying its load of eroded sediment. This movement of flow over the land before collecting in the rills is called sheet flow. The reduced infiltration is effective in increasing the amount of flow in the rills and stream channels and thereby the erosive power in these channels is also increased.

The way in which sheet flow differs from rill and channel flow in eroding and transporting sediment is considerable. Sheet flow moves rather slowly owing to the small amount of tractive force (small depth) and owing to the large amount of resistance (relative roughness) offered by the land surface. The rill and channel flow, on the other hand, is confined to a small area of resistance; and with its relatively great depths and hence large tractive force or gravity potential, the energy of flow concentrated in a small area can be sufficient to move sand, gravel, or even boulders. Sheet flow therefore erodes and transports fine-grained sediment, the silts and clays, whereas the rill and other types of concentrated channel flow will carry all the fine-grained load derived from this sheet flow in addition to both fine and coarse sediments that may be eroded from the bed and walls of the channels.

Thus, it is evident that the quantity of fine sediment moved by the stream at a given time is nearly equal to that released by the environmental factors causing erosion within the drainage basin; whereas, the quantity of the various coarser sizes in transport is closely related to the magnitude of the fluid forces. For coarse material, Lane (1955) reported that if the supply is not equal to the carrying capacity through a stream reach, the stream will aggrade or degrade to establish approximate equilibrium between capacity and discharge of coarse sediment within the reach.

ENVIRONMENTAL FACTORS

Only small and generally unrelated segments of the relation of environmental factors to fluvial sediment have been studied by hydrologists and sedimentologists because of the diversity of climatic conditions, geographic areas, and segmented problem-solving objec-

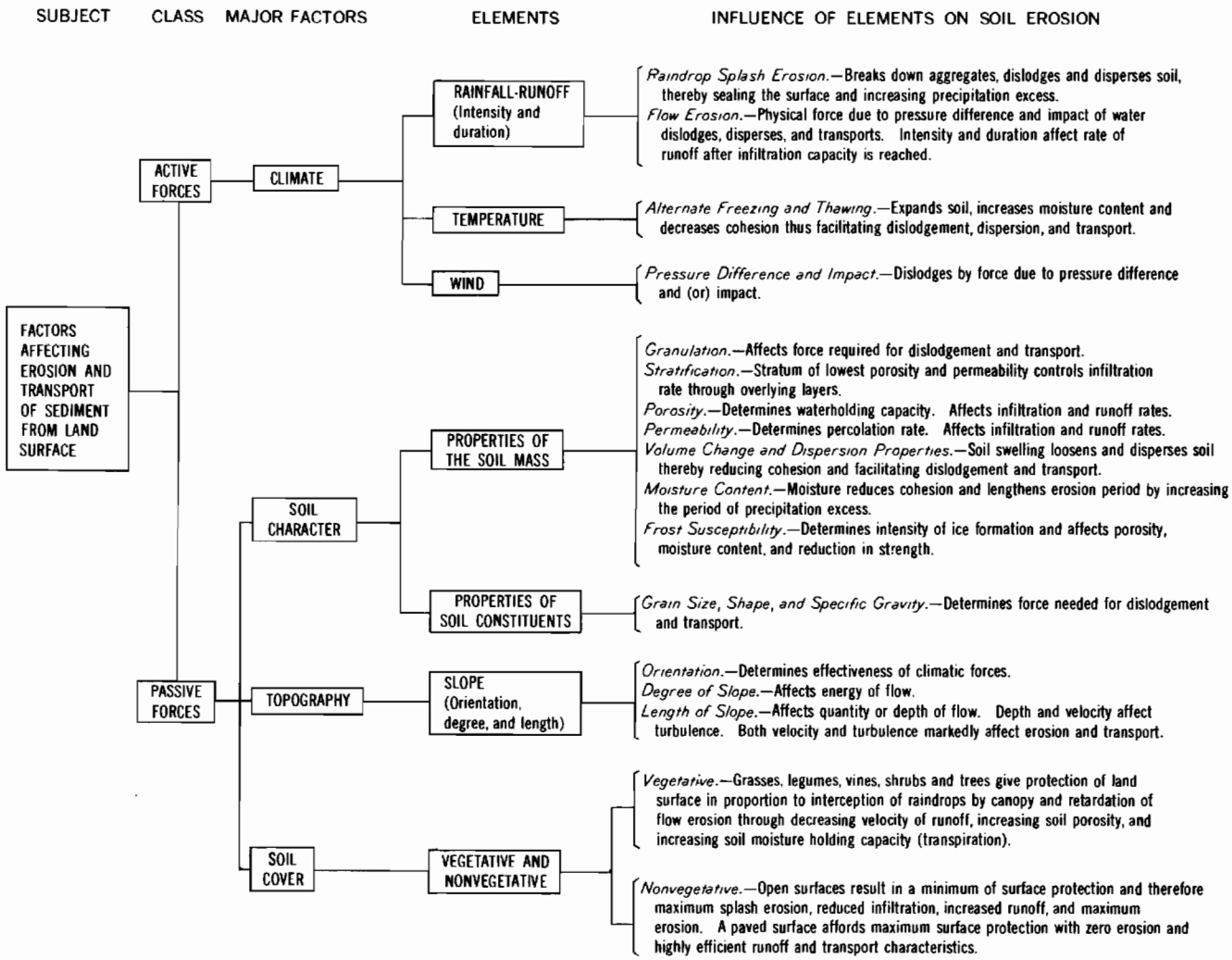

FIGURE 1.—Chart of the principal factors affecting erosion and transport of sediment from the land surface. Modified from Johnson (1961).

tives. Interpretation of this relation, using limited data for some specific climatic and drainage basin characteristics are reported by Glymph (1954), Maner (1958), Langbein and Schumm (1958), and Stall and Bartelli (1959). The sum of these and other works compose a meager knowledge of the total relation of environment to fluvial sediment.

Sayre, Guy, and Chamberlain (1962) listed five factors affecting the supply of sediment moved into and through a stream channel and, most applicable, the fine material contributed from the drainage area. This list, which follows, expands on the broad terms of climate and physical characteristics:

1. The nature, amount, and intensity of precipitation.
2. The orientation, degree, and length of slopes.
3. The geology and soil types.
4. The land use.
5. The condition and density of the channel system.

They noted also that these factors can operate either, or both, to resist or to advance the rate of erosion and transport. Precipitation, for example, if occurring at a low intensity and at ideal intervals, may advance the growth of vegetation and thereby the resisting force. Precipitation, if intense and following a drought, or occurring on an area without vegetative cover, is likely to cause a large amount of erosion. Because of the large variance and interrelation associated with the preceding list of factors, the definition of erosion and transport in drainage areas is difficult to attain.

One important factor resulting from the integrated effect of the above five factors is that the sediment yield of a large basin is generally found to be less than the sum of its subbasins. For example, the yield from a drainage area of 5 square miles generally ranges from 400 to 4,000 tons per square mile; whereas, for 500 square miles the range is 100 to 2,000 tons per square mile (Glymph, 1951). Though the deviation of yield

for a given size of basin is very great, the trend implies that sediment yield decreases as drainage area increases. For streams in equilibrium and having a fixed base level at the mouth, this loss of sediment in a stream system may be temporary. On the other hand, if the oceans are gradually rising with respect to the stream system, or a system of manmade base levels is imposed, the loss of sediment may be accounted for by the aggradation of the streams. Such sediment loss or aggradation also occurs when accelerated erosion in a drainage basin supplies more sediment than can be transported by the channel system. An index of the phenomenon of decreasing sediment in the downstream direction may at some future time be evaluated through some index of the condition and density of the channel system.

The interrelations of the active and passive forces that influence erosion are summarized in figure 1, as modified from Johnson (1961). Climate is considered the important active force as determined by rainfall, temperature, and wind. The important passive forces are the soil character (properties of soil mass and constituents), the topography (orientation, degree of slope, and length of slope), and the soil cover (vegetative and nonvegetative). Each of the active and passive forces are further described by refined factors in the illustration. For example, rainfall has a double action—first is that of falling raindrops as described in a preceding paragraph and second is that of flowing water, which in broad terms is of either laminar or turbulent flow. The type of flow is a function of the velocity and depth of the water and the roughness of the surface over which it flows. Erosion and transport of sediment are negligible under the condition of laminar flow but, as the water from such laminar flow collects in rivulets and larger channels, the resulting energy of flow with increased scale and intensity of turbulence can be sufficient to carry heavy loads of sediment, especially fine particles. The important passive forces, therefore, tend to alter the depth and velocity patterns of overland or surface flow by keeping the flow spread thinly or by increasing the resistance to flow.

COARSE SEDIMENT

EFFECT OF VELOCITY

B. R. Colby (written communication) showed that the discharge of sand in a sand-bed stream is closely related to the mean velocity of flow for rivers of a wide range of sizes. Many investigators had previously used the supposedly logical parameter of stage or depth as the independent variable for determining sand transport. The fallacy of the depth-transport concept is that the relation between velocity and depth has been demonstrated by Dawdy (1961) to be poorly defined both for an individual stream and among streams. Colby (1961) illustrated the complexity of the depth-transport concept by showing that the transport decreases with increasing depth at low velocity (less than about 3 fps (feet per second) and increases with increasing depth at high velocity.

Einstein (1950) treated the beginning of movement and the pickup of the sand grains from the bed as a probability for the individual grains to move. Thus a specific critical velocity is probably arbitrary and inexact as a measure of bed movement because of the arrangement of the grains on the bed and on local variations of velocity. At a velocity greater than the so-called critical value, movement in a very thin layer occurs by rolling, sliding, or skipping along the bed.

Sand swept up from the bed of a natural stream or suspended in a stream may be supported and transported downstream a considerable distance by the vertical components of currents in turbulent flow. The magnitude of these currents is largely a function of the horizontal velocity, the bed roughness, and the distance above the streambed. Hence, the suspended load of sand in a stream vertical can be considered to be associated with the mean velocity of flow.

EFFECT OF PARTICLE SIZE

The settling rate of a particle is a measure of its resistance to transport. Fine sediment particles in a dispersed state having a slow settling rate are easily carried in complete suspension by the fluid forces in natural streams, and, hence, have a tendency to move out of the drainage basin with the flow in which they are suspended. In contrast, coarse sediment particles with a fast settling rate may move by suspension for only short distances, or more probably, by rolling and bounding along the streambed. The smaller of these coarse particles move at a faster mean velocity than do the larger particles. The largest particles in a given stream would be transported only a short distance in a given period of movement and then only when the stream is experiencing a great flood. The coarse sediments on or near a streambed are being continuously sorted by the selective transport capacities of the stream.

Equilibrium of the concentration gradient of suspended sediment at a stream vertical requires that particles settling through a plane be balanced with a net upward movement of particles through this plane from a zone of heavier concentration. Particle fall velocity is then considered to be an indication of the rate of change of sediment concentration with distance above the streambed for a given scale and intensity of turbulence. An increase in turbulence, considered to

716-824 O—64——2

mean an increase in the vertical movements of flow, causes more uniformity of concentration for a specific size of sediment with respect to distance above the bed. Therefore, high values of velocity and (or) low values of particle size tend toward a uniform vertical concentration of sediment. If mean velocity is an indication of the scale and intensity of turbulence and the vertical variation of sediment concentration, then the discharge of coarse sediment is related to both stream velocity and particle size.

Colby (1961) showed that for a given mean velocity and a roughly equal bed roughness, a stream at a section of shallow depth will result in greater turbulence and hence contain a higher concentration of suspended coarse particles in a vertical than will be found in a deep section of the stream. Averaged over a long period of time, the sediment transported at the two sections, even though several hundred feet apart, is likely to be equal. With a substantial change of flow characteristics, such as greater depth and velocity, the transport through the two sections may temporarily be different, causing aggradation or degradation of the streambed.

The laboratory studies by Simons, Richardson, and Haushild (1962) showed inconclusive results regarding the effect of increasing concentration of fine material on the transport of coarse sediment. The data support the conclusion, however, that if bed roughness were the same, increasing fine sediment concentration will increase the transport of coarse sediment because the mean velocity of flow may be increased and the fall velocity of sediment particles may be decreased due to changes in the apparent viscosity and density of the suspending fluid.

Water temperature is an important environmental factor affecting the transport of sediment through its effect on viscosity of the fluid and the resulting changes in the fall velocity of the particles and changes in the turbulence of the streamflow. The effect of change in water temperature on particle fall velocity is greatest for fine sediment because these sizes settle more nearly in accordance with Stokes' law. For example, particles in a size class of 0.016–0.062 mm have a fall velocity of about 0.0017 fps at 32°F and 0.0038 fps at 90°F; whereas, particles in a class of 1.00–2.00 mm have a fall velocity of 0.59 fps at 32°F and 0.74 fps at 90°F (Hubbell and Matejka, 1959). Temperature change, however, does not affect the transport of fine material (less than 0.062 mm) because it is limited by the amount supplied to the stream system; that is, the stream will readily carry all available fine sediment at either a high or a low temperature. The temperature effect is probably most important for fine and medium sizes of sand.

STORM CHARACTERISTICS

Precipitation is undoubtedly one of the most important and yet most complex factors associated with the erosion and transport of fluvial sediment. A wealth of data concerning precipitation characteristics has been obtained by the U.S. Weather Bureau since 1891. The basic precipitation data, daily quantity for nonrecording gages and hourly quantity for recording gages, is published in "Climatological data" by the Bureau. This data has been recorded for 40 to 50 years. The density of the gages in the Atlantic coast area averages about 2.5 per 1,000 square miles for the nonrecording gages and 0.9 per 1,000 square miles for the recording gages. This seemingly large number of gages gives a fair representation of precipitation over large river basins, especially for storms of large aereal extent but are very inadequate when correlation with small basins is necessary, especially for the small convection storms.

Wischmeier and Smith (1958), in a correlation of rainfall characteristics with erosion and soil loss data, showed that an index consisting of the product of rainfall energy and the maximum 30-minute intensity of the storm is the most important measurable precipitation variable to explain storm-to-storm variation of soil loss from field plots. This concept is based on the fact that large fast-falling raindrops with a large amount of kinetic energy will cause much splash erosion, thereby sealing the surface and increasing the amount of surface runoff. The maximum 30-minute intensity is also proportional to both the total quantity of rainfall and the average intensity.

THE RUNOFF HYDROGRAPH

Storm runoff is defined as the part of total runoff derived from storm rainfall or rapid snowmelt which reaches an observation point within a relatively short period of time. The time of runoff depends on the drainage basin characteristics, especially that of area, and requires only a few minutes for areas of a few acres but 5–12 days for drainage areas of 10,000 square miles. The ground water runoff or base flow part of a streamflow hydrograph lags the causative precipitation by a distinguishably longer period of time than does the surface runoff. Oftentimes, storm runoff may include subsurface ground-water flow which has infiltrated the surface of the ground but causes an increase in ground-water flow to the surface channel sufficiently soon to be classed as storm runoff. Such rapid transit of the subsurface storm flow results from the relatively short underground path through perched water tables, through flowing saturated zones, or through semichannels beneath the surface. The true

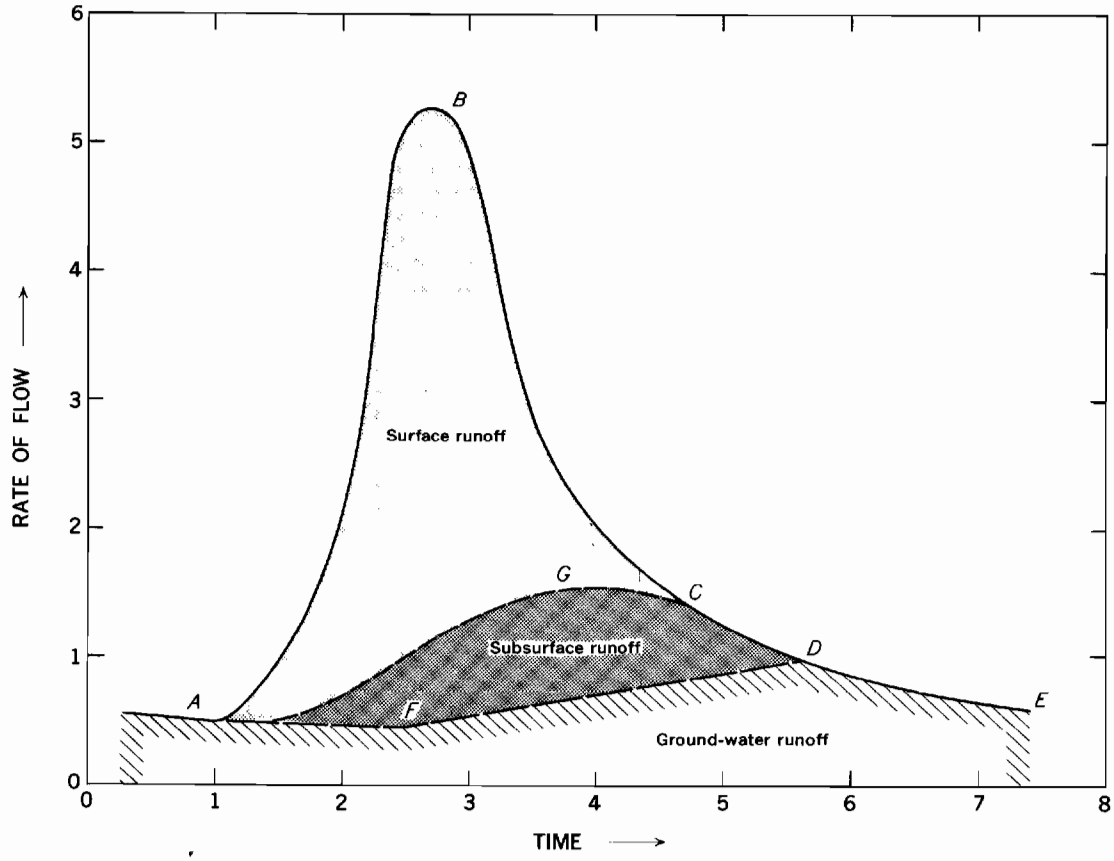

FIGURE 2.—Components of a streamflow hydrograph.

surface runoff, or that amount of precipitation in excess of infiltration and surface storage, reaches a surface channel with its path on and above the ground surface. Except for ephemeral streams and small plots or fields, the physical measurement of these separate components of flow is practically impossible.

Attempts to separate storm runoff into the components of surface and underground runoff are made primarily through empirical analysis of runoff hydrographs. The general concepts of such an analysis are illustrated by figure 2, showing a typical hydrograph where *ABCDE* represents the total runoff, where *AFDE* represents the amount of ground-water runoff, and where *AGC* is the estimated division line between true surface runoff and subsurface runoff. The area between curves *AGC* and *AFD* represents the volume of subsurface flow effected by the storm. The division line *AGC*, separating the surface and underground runoff, is of greatest significance in this study since the amount of sediment erosion in the upland areas should logically be directly related to only the amount of surface runoff. The transport rate of the coarser sizes of sediment in the stream channels is affected by the total flow.

Since water discharge generally varies directly with gage height at a given stream site, it is feasible to use the trace of the gage-height recorder instead of plotting the water discharge against time to separate the components of surface and underground runoff. In fact, more sensitive results are possible by use of the gage-height chart because the line represents nearly instantaneous conditions, whereas most discharge data are averages for discrete elements of time. The writer has not found it convenient, however, to obtain and use the gage-height records in most instances.

The most convenient hydrographic data source for investigating records of considerable length is the series of Water-Supply Papers, "Surface Water Supply of the U.S.," which give the mean flow for each day of all streams gaged. With the exception of the low-yield storms, the author has also found that a tabular system using these daily values is quite adequate to separate the components of surface and underground runoff. Fortunately, the errors involved in estimating the volume of underground runoff are generally small in comparison with the volume of total surface runoff. For low-yield storms, where the amount of underground flow is more significant relative to the total flow, the number of days involved in the hydrograph will be fewer and hence the chance of significant cumulative error will be less.

SEASONAL CHARACTERISTICS

PRECIPITATION

The air always contains some water vapor, but rain or snow occurs only a small part of the time. Precipitation requires, in addition to moist air, and atmospheric disturbance in the air mass through lifting of large volumes of warm moist air to higher altitudes where it is cooled to a temperature below the dew point. Although the lifting is the decisive factor, strong convergence is also necessary to produce heavy precipitation. On the basis of the meteorological phenomena that cause and accompany precipitation, the causative storms may be divided into three types, namely, cyclonic, convectional, and orographic.

The contrast of the large land and water masses of the earth causes differential heating from the sun and therefore a great impetus for circulation of air. For example, in the winter the landmass cools more rapidly and may be covered with snow which reflects much of the sun's heat rather than absorbing it. High pressure cells of cold then push the polar front toward the south in North America. Low pressure cells of warm air are formed over adjacent ocean areas at this time. In the summer this situation is reversed.

Cyclonic storms are atmospheric waves, formed along the polar front by the interaction of the cold and warm airmasses. The general circulation pattern caused by the earth's rotation, or the terrestrial winds, pushes these storms from west to east in the latitude of the United States. Such cyclonic storms are characterized by a warm moist air sector on the south side which, being lighter than the existing cool air it meets, rides up over the wedge of cool heavy air. This causes condensation and a broad belt of rather low-intensity and long-duration precipitation when a warm front is experienced and a belt of rather high-intensity and short-duration precipitation when a cold front is experienced. The cold front moves more rapidly and has a steeper gradient of cold air than does the warm front.

The convectional type of storm is caused by uneven heating over a relatively small area and occurs only in areas of the large low pressure cells of warm air. For example, convection may be triggered by excessive heating of the air over a city when the streets and roofs are warmer than the surrounding countryside. The ascending warm air expands and cools as it rises, and if sufficient moisture is present, precipitation is formed. Such storms affect a relatively small area and at times cause heavy downpours; however, when the conditions of high temperature and moisture are present, the result is generally one of numerous cells of precipitation. The multiplicity of such convection cells and their movement with the larger patterns of circulation tend to cause precipitation over relatively large areas, although the amount at points within the area may be highly variable.

Orographic precipitation occurs wherever mountain ranges, highlands, or ridges rise above the surrounding country in the path of the moisture-bearing airmasses. An example of this is found on the southwesterly slope of the Appalachian Mountains to which the moisture-laden air is brought by tropical maritime airmasses from the ocean. As a result of the way warm moist air moves from the Atlantic Ocean with the terrestrial air movements and due to the relatively small change in altitude of the terrain, the orographic precipitation is not an important factor in producing storm runoff in the rivers draining the Atlantic coast area States.

It is evident that most of the above types of storms would vary considerably with the months and seasons of the year by the general northward and southward migrations of the planetary wind systems and by variations in convectional activity. Although the annual distribution of precipitation, by months, is rather uniform in the Eastern United States, the winter precipitation is mainly of cyclonic origin resulting from the interaction of moist tropical air from the south and dry polar air from the north. In summer, precipitation is mainly of the convectional and frontal thunderstorm variety. The total quantity of precipitation on an annual basis tends to increase in a southerly direction.

The statistics of storm precipitation are summarized by the U.S. Weather Bureau's Technical Paper 40 (1961). The maximum total amount of rainfall to be expected in a given length of time, at a given location, and for a given return period can be determined. The durations of rainfall are for ½, 1, 2, 3, 6, 12, and 24 hours. The return periods are for 1, 2, 5, 10, 25, 50, and 100 years. The publication also gives the seasonal probability of intense 1-, 6-, and 24-hour rainfalls for eight subareas of the United States east of 105°W. Figure 3 shows a chart from this reference for the seasonal variation of the 6-hour storms in the central Atlantic coast area. This illustration shows, for example, that a storm of an intensity likely to occur on an annual basis has a probability of 1 percent of happening in January and 23 percent of happening in August. This and other charts show that storms of greater intensity and return period are also likely to occur in July and August.

INFILTRATION

In addition to precipitation variation, seasonal variation in infiltration capacity is also an important cause of seasonal variation in stormrunoff. The effects

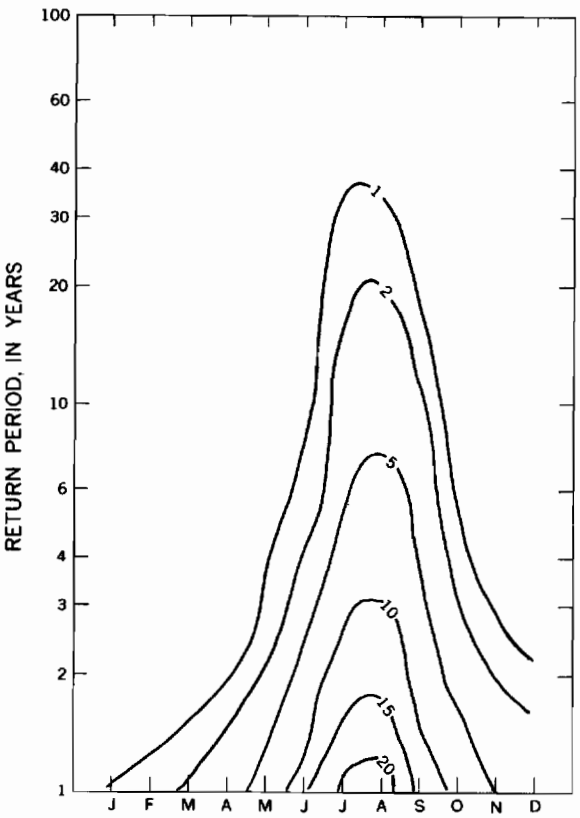

FIGURE 3.—Seasonal probability in percent of an intense 6-hour rainfall for the central Atlantic coast area. (After U.S. Dept. of Commerce, 1961.)

of season and temperature on infiltration were discussed by the author (1951), as follows:

* * * While resembling the mean temperature curve, the season infiltration capacity curves have a more marked rise in the spring and a more rapid recession in the fall. With respect to actual water temperature, sprinkling from a height of about six feet with water ranging from 40° to 110°F showed no significant differences of infiltration rates. Free, Browning, and Musgrave (1940) found that the contribution of temperature * * * was not a dominant factor in a study of 68 soils. There must then be other factors which largely over-balance the effect of change in viscosity due to change of water temperature. Water at the higher temperatures may cause swelling in the soil which will oppose the effects of decreased viscosity.

—and—

Since changes in water temperature cannot account for seasonal infiltration changes, it is believed that biologic factors are the principal causes. These include soil fungae, earth worms, ants, and beetles. The activity of these biota is largely dependent upon proper moisture conditions which may account for some of the increased variability of infiltration capacity under mid-summer conditions as compared to other seasons of the year.

The rate of storm infiltration would be at a minimum if the soil were frozen. In drainage areas of the central Atlantic area States, soil freezing may occur in varying degrees during part of the year. Topsoil in a wooded area having a good layer of duff and snow cover is protected against freezing at very cold temperatures. The areal extent, depth, and duration of freezing, however, do increase in a northerly direction.

Seasonal variation in infiltration is also a product of several changes in land use during a year. Under agricultural use, the state of cultivation is likely to cause a high infiltration rate under a firmly aggregated soil with a cloddy surface condition and a low rate under a fine-textured soil with an easily dispersed surface condition. The varying condition of the vegetative cover during the season is a critical element in reducing the impact of the raindrop and hence splashing and sealing of the soil pores. Other activities of man and animals tend to compact the soil surface or disrupt vegetative cover in varying amounts during the season.

RUNOFF

The runoff characteristics of a storm depend on the integrated precipitation and infiltration characteristics over a drainage basin and the routing of the resulting precipitation excess to the site on the stream in question. Splash, sheet, and rill erosion, with subsequent transport of fine sediment, is dominant for storms having a great deal of surface or overland runoff. Channel erosion, with subsequent transport of the coarser material found lining the channels, is dominant for storms carrying a great deal of underground runoff. Movement of the coarse material is largely a function of stream hydraulic and roughness characteristics and is therefore more readily correlated with the stage of the stream. This is not so for the fine material since its movement at a stream site is determined largely by erosion of the land surface and the routing with waterflow.

A study of stream sediment movement then should have close correlation with the geographic and seasonal distribution of rainfall erosion potential as determined by Wischmeier (1962). For a specific storm, the most applicable erosion potential was found to be the product of two rainstorm parameters; the kinetic energy of the rainfall in hundreds of foot-tons per acre times the maximum 30-minute intensity in inches per hour. The average of these values for the storms during the year is called the annual erosion index where all factors contributing to soil erosion other than rainfall are held constant. The index is directly proportional to- or closely approximates, the annual soil loss from open cultivated areas. Figure 4 shows a map of the mean annual erosion index for the area of the United States east of 105° W. The approximate seasonal values of the erosion index are shown in figure 5 for central Vermont, central Pennsylvania, central North Carolina, and central Georgia. The increase in magnitude and peakedness of the seasonal indexes from north to south

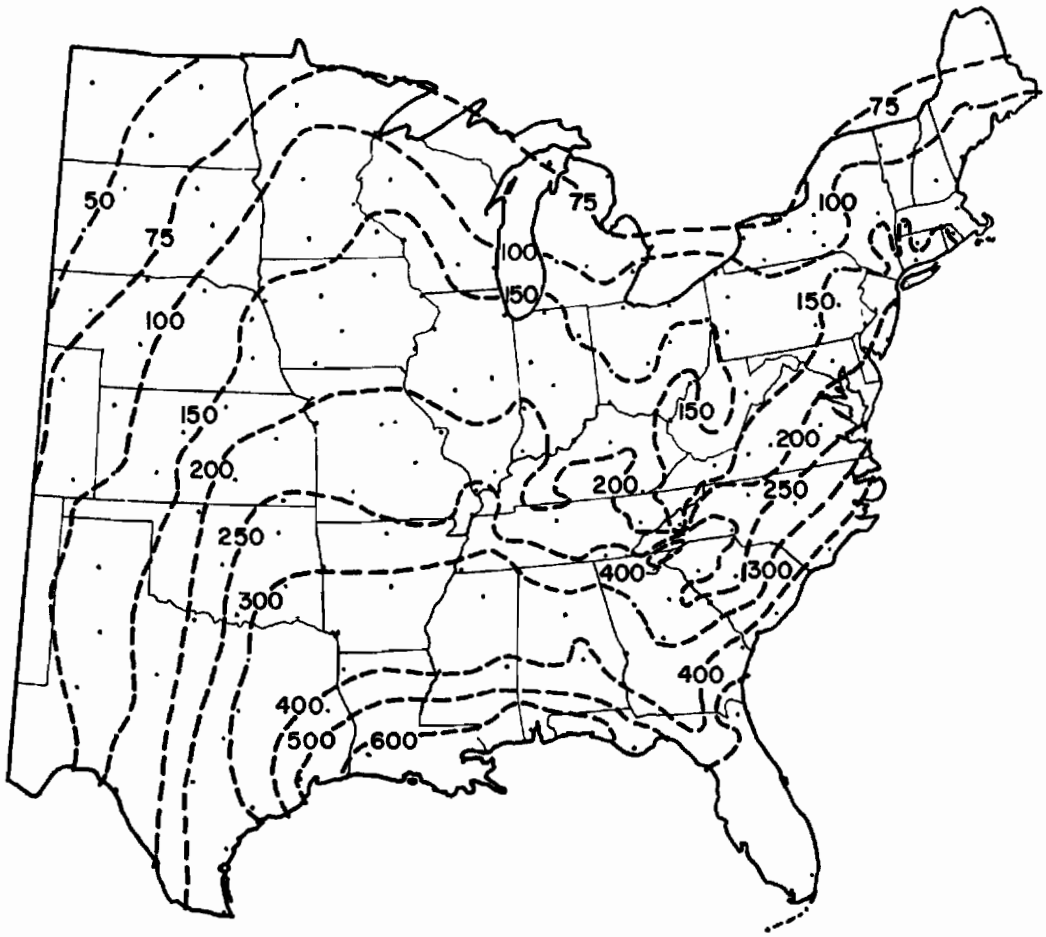

FIGURE 4.—Mean annual values of Wischmeier's erosion index for the area of the United States east of 105° W.

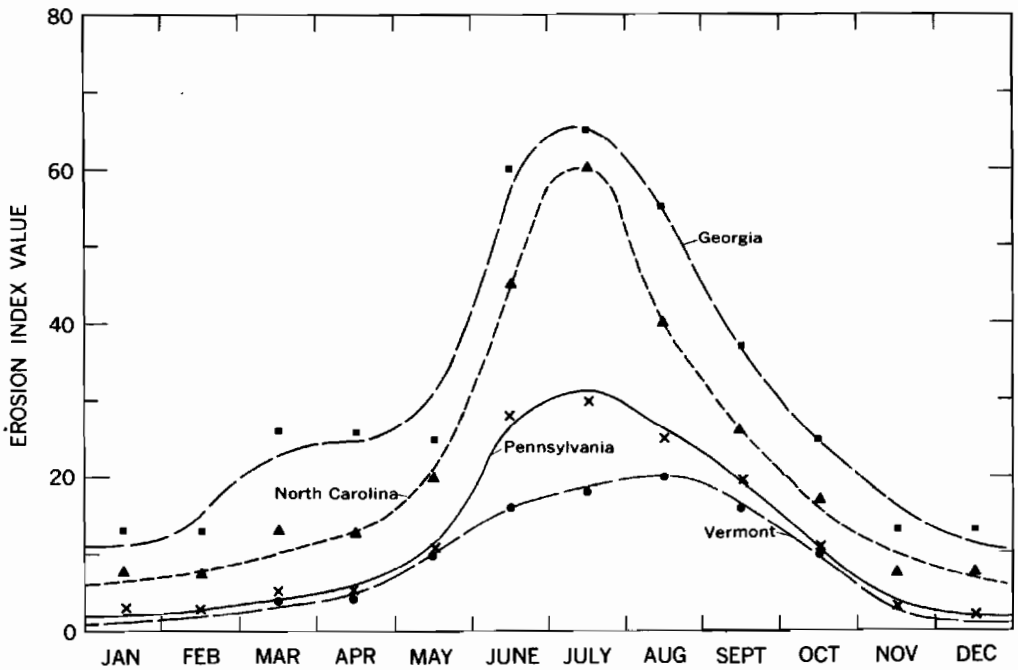

FIGURE 5.—Seasonal distribution of erosion index values at four locations in the Atlantic coast area.

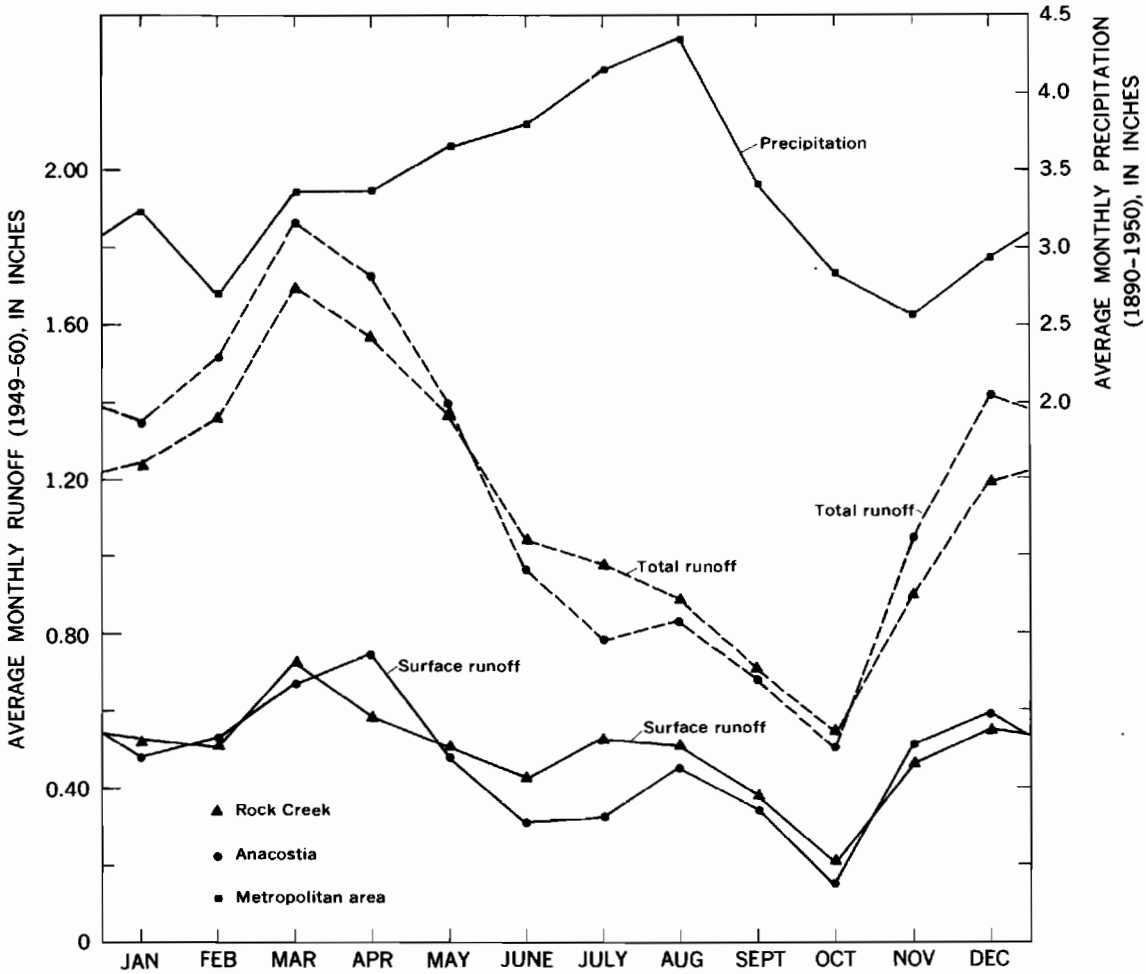

FIGURE 6.—Seasonal distribution of surface and total runoff for Rock Creek at Sherrill Drive, Northwest Branch Anacostia River near Colesville, Md., and precipitation for the Washington Metropolitan area.

in the Atlantic coast area indicates the need for giving greater attention to the passive forces in the south than in the north. The seasonal effect of the erosion index of the important active forces (rainfall parameters) must be integrated with the seasonal effect of the passive forces such as the changes in soil properties and cover if the relative amount of sediment transport in streams is to be evaluated.

Information in the literature on the seasonal variation of surface or overland runoff in streams is lacking. Therefore, the storm-by-storm surface runoff of Rock Creek at Washington, D.C., and the Northwest Branch Anacostia River near Colesville, Md., was computed for the years 1949–60. The land use in these basins, though adjacent to each other, is quite different in that the Anacostia is largely rural in character; whereas Rock Creek is about ⅓ rural, ⅓ urban, and ⅓ in various stages of becoming urban. Figure 6 shows the variation of the monthly average surface runoff as well as the total flow for this 12-year period of flow. The same chart also shows the monthly average precipitation to 1950 for a 60-year period.

As expected, the proportion of surface runoff to total runoff was somewhat greater for Rock Creek than for the Anacostia River due to the greater amount of impervious surface in the Rock Creek basin. The effect of impervious surface is also shown by the fact that Rock Creek has the greatest flow (both surface and total) during the warm season, whereas the Anacostia has the greatest total flow during the cool or low intensity precipitation season. Greater losses by evapotranspiration during the warm season are likely in the Anacostia basin. The seasonal effect of evapotranspiration is very evident when the decreasing total flow of May, June, and July is contrasted with increasing precipitation of these months. The reverse occurs in the fall when the mean flow (both surface and total) increases nearly 100 percent from October to November while precipitation decreases somewhat.

A GRAPHICAL SEARCH FOR VARIABLES

THE STORM EVENT TECHNIQUE

The task of selecting useful correlative, mathematical, and "intuitive" techniques to explain the storm-to-storm variation of sediment moved by a stream is made difficult by the complexity of hydrologic and sedimentologic conditions resulting from the active and passive forces of erosion and from the streamflow characteristics which route the sediment through the channel system. Readily available hydrologic and sedimentologic data, however, will be assembled and tested by correlative techniques. The investigations are limited to the Atlantic coast area and to streams selected from those listed in table 1.

The graphical technique is used to search for suitable variables to explain the nature and cause of sediment discharge variation. Mathematical analysis was avoided at this searching stage because it is more cumbersome to use, and the variance of individual bits of data would be obscured. The graphical technique of multiple correlation using the method of deviations is most adaptable to the "trial and error" and "intuitive" methods for selecting optimum measures for reducing the data scatter and for determining the type of conversions necessary for normalization of the data. In other words, graphical regression is less restrictive than analytical regression in that the model need not be completely specified in advance.

WATER-SEDIMENT DISCHARGE RELATIONS

Of all the data available for streams in the Atlantic coast area, the principle bivariate system for a specific stream location is generally considered to be that of the relation of sediment discharge to water discharge. The sediment-water discharge relation has been used by several investigators to solve specific problems. Campbell and Bauder (1940) used it for comparing discharges in the Red River Basin of Oklahoma and Texas; Miller (1951) for extrapolation of records for the San Juan River of Utah using flow-duration curves, and Leopold and Maddock (1953) for describing the interrelations of measured sediment with other hydraulic variables. One of the most comprehensive reports summarizing the applications of the sediment-water discharge curves is that of Colby (1956).

The sediment-water curves used by these investigators were derived from instantaneous, mean daily, mean monthly, or mean yearly sediment and water discharge data. There are four severe limitations to the curves derived by the instantaneous approach: (1) The sample data may be biased with respect to either time or water discharge because generally measurements are made more frequently at times of high flow and high concentration of sediment, especially during the recession of the runoff hydrograph, than at other times. (2) The sediment concentration of instantaneous samples for a given stream tends to fluctuate about a mean value due to variation in the amount of fine material eroded and transported from upstream tributaries and due to changes in suspension of coarse material at the sampling vertical. (3) The sediment load for small drainage areas is generally, and for large streams is often, much greater for a given water discharge during the rising leg of a storm hydrograph than for the falling leg. (4) Under conditions of relatively high base flow and sediment originating at a considerable distance upstream, it has repeatedly been found that the sediment movement lags behind the flood wave so that the peak sediment concentration may occur after the flood crest.

Figure 7 illustrates the third and fourth concepts. Data from Leopold and Maddock (1953) showed the hysteresis effect for the San Juan River and illustrated that the sediment load for a water discharge of 5,000 cfs (cubic feet per second) is 10 times greater on the rising leg than on the falling leg of the hydrograph. The effect of the progressive lag of sediment movement with respect to the downstream movement of the flood wave is demonstrated by data from Heidel (1956) for the Bighorn River at Manderson and Kane, Wyo.

Water-sediment discharge data plotted from mean daily data, although very convenient because most data are published in this form, have some of the shortcomings exhibited by the instantaneous data; especially the previously mentioned concepts three and four. The small scale variations of concept two are averaged during the 24-hour period, but the 24-hour division of the hydrograph is random, causing undefinable scatter in the relation due to concepts three and four. If the instantaneous or mean daily data were used, the effects of rainfall and possibly other weather and hydrologic conditions would be difficult to evaluate for correlation with sediment discharge due to the complexity of routing their effects downstream to the measuring site.

Monthly and especially yearly plotting cannot be effectively used for lack of sufficient record; at least they would not be effective for making predictions due to the higher standard error of estimate resulting from the small number of points. Each monthly or yearly discharge would be a composite of several hydrologic events, the integrated effect of which would be difficult to ascertain.

On the basis of the above considerations, the storm event is the most logical unit of data to fulfill the objectives of this study. The storm event unit (1) will not bias the curve with untimely data, (2) will average out the instantaneous fluctuations, and (3) will integrate the overall variations of sediment-water conditions over the hydrograph. One important advantage of using

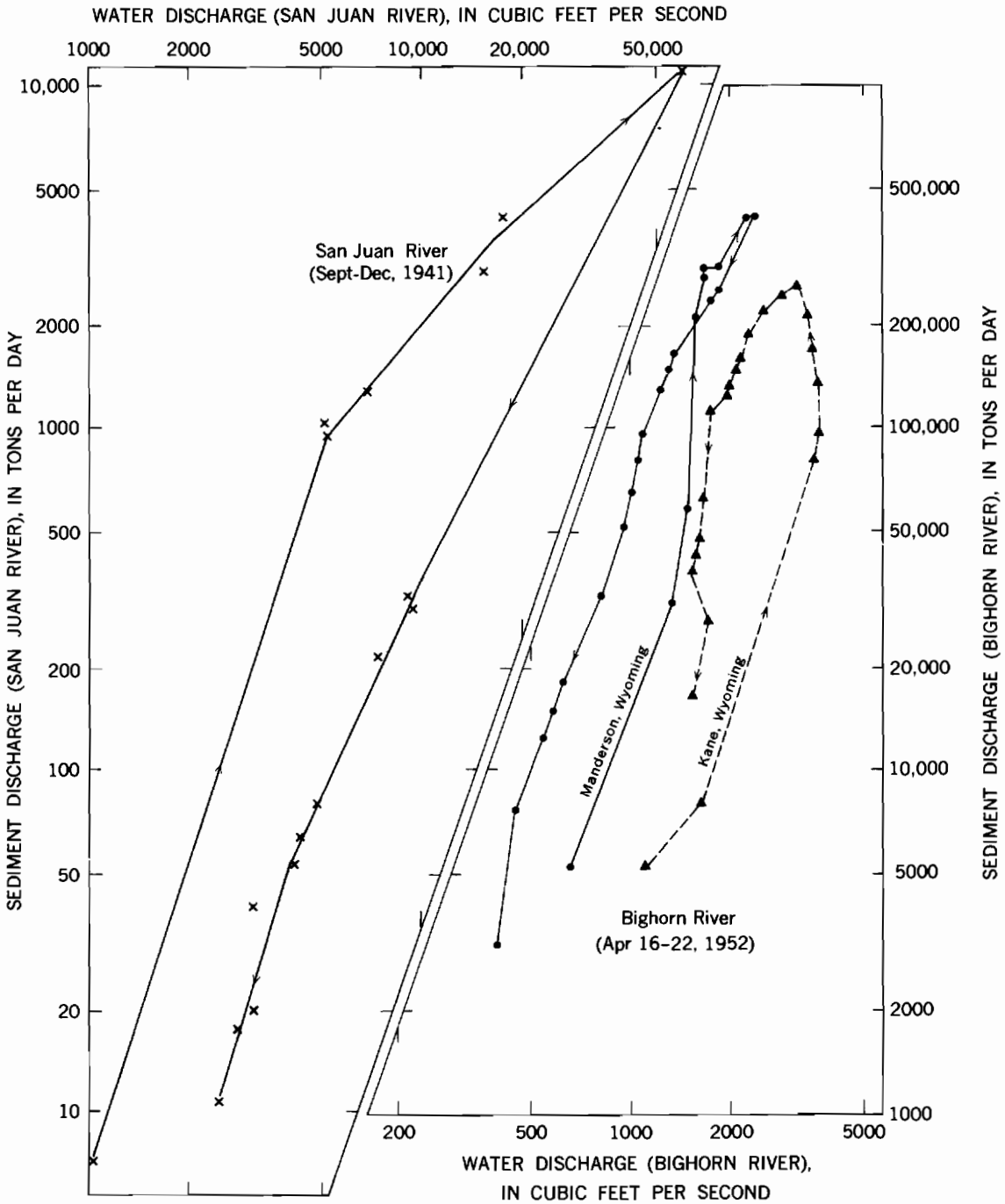

FIGURE 7.—Illustration of variation in water-sediment discharge relations. Effect of hysteresis for the San Juan River. Effect of progressive lag for the Bighorn River.

the storm event unit, especially when only surface runoff is used, is that adjacent storm events are less likely to be related serially than are adjacent instantaneous or daily sediment data. Another advantage is that certain weather and hydrologic conditions can be evaluated for correlation with the sediment-water discharge relation. The two principal disadvantages of the storm event technique are that (1) data are published on the instantaneous, daily, or monthly basis and (2) the sequence of weather may be such that the discharge from different storms may overlap each other in some instances. In the Atlantic coast area, a 3- or 4-year record will generally yield a sufficient number of storm events to adequately define the necessary correlations; whereas, if daily or instantaneous values were used only a sampling of the total data would probably be used to avoid an unwieldy volume of data.

716-824 O—64——3

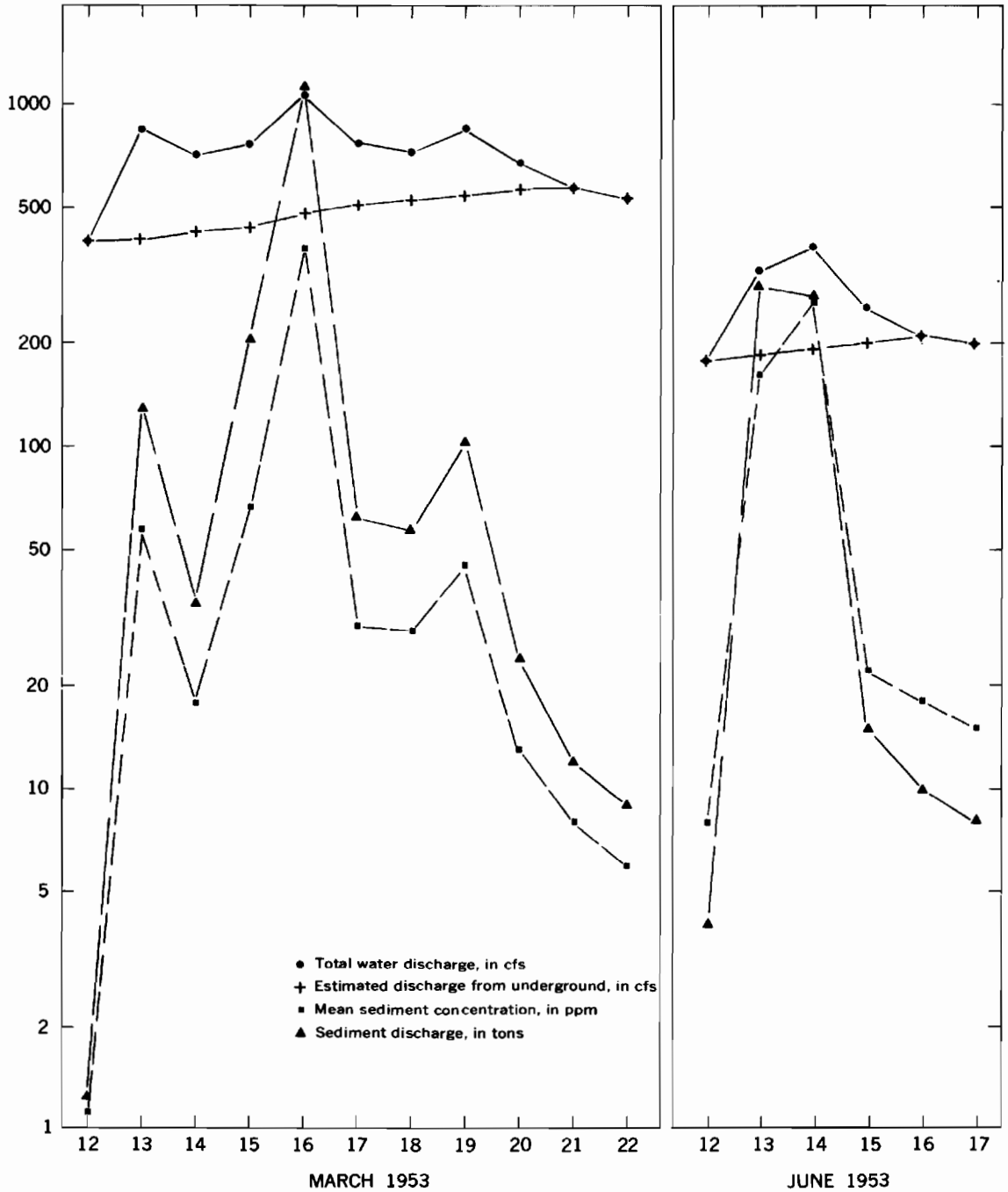

FIGURE 8.—Graphs of daily mean water and sediment discharge for storm events of March 13–20 and June 13–15, 1953, Hazel River at Rixeyville, Va.

COMPILATION OF DATA

Any statistical evaluation of the variation of sediment concentration in streamflow should be conducted so that the principal cause of the variation will be considered first. A reasonably convenient measure of the important storm volume variable is that of the surface runoff past a stream site for a specific storm. Records from the Hazel River at Rixeyville, Va., will be used to illustrate how data are extracted for the storm event technique. Table 2 shows the results for the two storms, March 13–20 and June 13–15, 1953. Graphs of the daily mean total water and estimated underground runoff, or the combined subsurface and groundwater runoff, are plotted with daily mean sediment concentration and daily sediment discharge in figure 8. Computations for the surface runoff and sediment discharge for other storm events were made directly on the tables of published data to eliminate the need for

copying the data to tables or plotting hydrographs. Estimated daily values of underground runoff were used that would result in a rounded figure of the net surface runoff for each day, see table 2. Also, as shown in table 2, the sediment discharge for the storm event is the rounded total of all days having net surface waterflow. Mention should be made of the fact that the standard procedures used to obtain the published data omit from consideration the sediment moving near the streambed.

TABLE 2.—*Computation of storm surface runoff and sediment discharge*

[Illustration from record of Hazel River at Rixeyville, Va.]

Date	Total runoff (cfs)	Estimated underground runoff (cfs)	Net surface runoff (cfs)	Sediment discharge (tons)
1953				
March 12	397	397	0	1
13	845	405	440	130
14	712	422	290	35
15	769	439	330	207
16	1,060	480	580	1,170
			2,500	1,790
17	769	509	260	62
18	731	531	200	57
19	845	555	290	103
20	676	566	110	24
21	578	578	0	12
June 12	178	178	0	4
13	326	186	140	296
14	382	192	190	273
			380	580
15	252	202	50	15
16	210	210	0	10

The water, sediment, and related factors for 75 storm events for the Hazel River from October 1951 to September 1955 are listed in table 3. The basic data for each storm event are described by column numbers as follows:

1. The consecutive number of months during the period of record M_t, beginning with May 1951.
2. The net surface runoff Q_w in cfs-days.
3. The sediment discharge Q_s in tons.
4. The water-discharge-weighted storm event concentration of sediment, $C=\frac{370.4Q_s}{Q_w}$ in ppm (parts per million).
5. The ground-water runoff at the beginning of the storm event, Q_b in cfs.
6. The long-term mean air temperature for the given time of year, T_a in °F.
7. The peak rate of water discharge, less the base flow, P_n in cfs.
8. A peakedness index indicating a measure of storm intensity, $P_i=\frac{P_n}{Q_w}$.
9. The aerial mean precipitation for the basin, R_a in inches, as computed by the Thiessen method.
10. The aerial mean precipitation intensity for the basin, R_i in inches per hour, as computed by the Thiessen method using the hourly data given from recording gages in or near the basin and using only the periods of rainfall for which 0.05 inch or more in a given hour was recorded.

SURFACE RUNOFF

In the search for an explanation of the variation of sediment discharge, the water and sediment discharge data for the Hazel River at Rixeyville, Va. (table 3, columns 2 and 3), were used to plot a sediment transport relation. The data were plotted (fig. 9) with separate symbols for the cool and warm seasons to determine if there is a difference in transport with change of season. The transport curve, which appears to be a straight line on a log–log graph, was drawn approximately through the means of groups of storm events subdivided on the basis of several approximately equal logarithmic intervals of the volumes of water discharge. The division of the data into the two seasons shows three things: first, that the warm season storms have a greater range of water discharge volume; second, that the number of warm season storms greatly exceeds the number of the cool season storms on the side of the higher sediment discharge, and vice versa; and third, at small volumes of water discharge the division is very pronounced, but at large volumes of water discharge the storms for each season are dispersed on both sides of the line.

To visualize how the sediment concentration varies among the storm events, lines of equal concentration for 100, 200, 500, and 1,000 ppm were drawn on the graph. At a small volume of water discharge, for example 500 cfs-days, the concentration lines show that the data scatters from 100 ppm to nearly 1,000 ppm; but, at a large volume of water discharge, for example 10,000 cfs-days, the scatter is less and ranges from about 300 ppm to about 800 ppm.

SEASON

The previously mentioned implications regarding the variation of sediment discharge with season require further testing. The ratio of the observed sediment discharge to that indicated by the transport curve is shown in column 11 of table 3 for each storm. These ratios, when considered as a group, are a measure of the departures or deviations of sediment discharge about the transport curve independent of water discharge or storm size. A plotting of these ratios against their respective time of year (fig. 10) results in a mean curve that varies with time of year, ranging from about 0.50 in February and March to about 1.75 in June and July. The plot also shows again the great diversity in sediment yield of the storms larger than 3,000 cfs-days and their occurrence with all seasons.

TABLE 3.—*Water, sediment, and related factors for storm events of the Hazel River at Rixeyville, Va.*

Date of collection	Time in months M_t (1)	Surface runoff Q_w (2)	Sediment discharge Q_s (3)	Sediment concentration C (4)	Base flow Q_b (5)	Mean air temp. T_a (6)	Peak water discharge P_n (7)	Peakedness index P_i (8)	Mean rainfall quantity R_q (9)	Mean rainfall intensity R_i (10)	Ratio to transport curve (11)
1951											
Nov. 7–10	7	810	510	233	75	48	520	0.64	1.84	0.212	0.66
Dec. 5–9	8	2,230	2,820	469	75	39	2,000	.90	1.94	.270	1.08
Dec. 21–25	8	2,420	1,810	277	190	36	1,250	.52	1.10	.138	.67
1952											
Jan. 5–8	9	960	160	62	270	35	380	.40	.67	.089	.17
Jan. 10–12	9	750	300	148	320	35	520	.69	.82	.091	.43
Jan. 22–24	9	600	170	105	235	35	530	.88	.75	.131	.32
Jan. 27–31	9	1,010	360	132	380	35	700	.69	.85	.075	.36
Feb. 3–9	10	5,250	7,270	512	425	36	3,500	.67	1.79	.152	1.09
Feb. 17–19	10	730	220	111	325	37	520	.71	.99	.099	.33
Mar. 11–17	11	7,630	14,500	704	300	44	4,400	.59	1.66	.133	1.42
Mar. 19–22	11	1,920	1,640	316	490	46	950	.49	.94	.088	.67
Mar. 23–29	11	800	270	125	580	47	300	.38	.86	.084	.36
Apr. 5–9	12	1,100	360	121	465	52	450	.41	.57	.102	.33
Apr. 14–18	12	1,640	1,470	332	430	55	600	.37	1.80	.106	.85
Apr. 24–May 4	12	11,060	6,520	218	430	59	3,500	.31	4.19	.077	.41
May 11–15	13	950	450	175	440	64	600	.63	1.48	.137	.49
May 25–27	13	370	180	180	330	68	250	.68	.90	.166	.57
May 30–June 2	13	430	140	120	325	69	270	.63	.99	.139	.38
June 15–16	14	140	180	476	150	73	160	1.14	.29	.050	1.79
June 22–26	14	1,090	2,330	792	115	74	700	.64	1.44	.193	2.16
June 27–July 2	14	470	860	677	140	75	190	.40	2.44	.432	2.10
July 8–11	15	1,470	1,620	408	110	76	610	.42	2.58	.171	1.07
July 17–18	15	250	360	533	110	76	280	1.12	.26	.143	1.80
Aug. 2–3	16	410	630	569	60	76	450	1.10	1.97	.723	1.80
Aug. 6–11	16	2,700	2,700	370	90	75	2,100	.78	3.08	.226	.89
Aug. 16–17	16	90	60	246	135	72	110	1.22	.77	.430	1.00
Sept. 1–5	17	2,360	4,430	694	90	69	1,900	.80	4.39	.259	1.70
Nov. 15–17	19	300	40	49	80	45	220	.73	.83	.152	.17
Nov. 20–27	19	14,650	20,880	528	115	43	6,200	.42	5.77	.168	.97
Dec. 11–14	20	1,430	1,560	403	330	37	1,000	.70	1.20	.157	1.05
1953											
Jan. 1–4	21	570	130	84	300	35	300	.53	.37	.100	.25
Jan. 8–16	21	4,090	3,470	314	360	35	1,400	.34	1.78	.081	.70
Jan. 24–28	21	2,110	1,880	329	440	35	1,100	.52	1.04	.119	.82
Feb. 15–17	22	670	83	46	270	37	430	.64	.60	.078	.13
Feb. 21–24	22	930	450	179	375	38	500	.54	.45	.103	.50
Mar. 13–20	23	2,500	1,790	265	390	46	800	.32	1.64	.102	.64
Mar. 24–Apr. 1	23	8,720	6,580	279	500	48	2,300	.26	2.77	.189	.55
Apr. 12–17	24	1,870	1,350	267	400	55	800	.43	1.20	.103	.68
May 4–10	25	800	700	324	380	62	300	.38	1.40	.251	.91
May 14–19	25	3,720	7,540	853	310	65	2,200	.59	1.96	.251	1.67
May 20–24	25	1,310	650	183	370	66	750	.57	.82	.113	.49
May 31–June 2	25	510	520	377	280	69	350	.69	.96	.133	1.16
June 13–15	26	380	580	565	175	73	240	.63	.70	.176	1.81
June 22–23	26	360	840	863	150	74	370	1.03	.44	.100	2.80
Aug. 17–19	28	510	510	370	30	73	510	1.00	2.00	.253	1.13
Oct. 28–31	30	290	133	81	30	52	180	.62	2.29	.167	.57
Nov. 23–25	31	290	77	98	45	42	180	.62	1.34	.231	.32
Dec. 7–9	32	490	280	211	105	38	370	.76	1.50	.151	.65
Dec. 13–16	32	1,080	1,200	333	100	37	700	.65	1.38	.104	.84
1954											
Feb. 21–24	34	580	155	99	100	38	490	.84	.80	.132	.30
Mar. 1–8	35	5,240	9,250	652	150	42	2,000	.38	2.88	.256	1.27
Apr. 16–21	36	1,750	450	95	160	56	720	.41	1.83	.113	.24
Apr. 24–30	36	1,750	4,090	866	260	58	600	.34	1.59	.137	1.93
May 3–6	37	700	1,630	861	240	61	400	.57	.98	.104	2.09
May 28–31	37	980	2,200	830	165	69	600	.61	.56	.370	2.32
June 10–13	38	470	750	590	105	72	200	.43	.68	.168	1.83
June 14–15	38	380	570	555	120	72	320	.84	.92	.625	1.78
June 16–21	38	680	530	288	130	73	280	.41	.65	.051	.78
Aug. 20–22	40	100	20	74	10	72	120	1.20	1.08	.063	.30
Aug. 30–31	40	190	100	195	14	70	200	1.05	.98	.090	.69
Oct. 15–18	42	3,210	10,400	1,200	6	56	2,900	.90	6.35	.374	2.85
Nov. 19–22	43	1,030	420	151	80	44	670	.65	1.65	.095	.42
Dec. 14–17	44	1,090	1,130	247	110	36	1,100	.65	1.52	.074	.63
1955											
Dec. 29–Jan. 2	44	1,590	1,230	286	150	35	1,100	.69	1.24	.109	.74
Feb. 6–10	46	1,220	550	167	110	36	800	.66	1.06	.074	.45
Mar. 5–13	47	4,480	3,290	264	220	43	1,400	.31	2.34	.144	.60
Mar. 21–28	47	2,530	1,080	158	255	48	990	.39	1.15	.095	.38
May 22–24	49	220	55	93	150	67	200	.91	.78	.128	.32
June 8–10	50	750	300	148	72	71	430	.57	1.33	.144	.43
June 11–15	50	1,110	550	184	145	72	560	.50	.80	.127	.50
June 19–21	50	260	150	214	140	73	160	.62	.66	.120	.73
July 9–12	51	260	140	199	57	76	220	.85	1.00	.223	.68
Aug. 8–9	52	460	920	740	35	75	540	1.17	1.47	.278	2.30
Aug. 12–16	52	5,610	7,900	522	65	74	4,400	.78	4.33	.251	1.10
Aug. 17–25	52	34,460	41,010	441	225	72	28,700	.83	8.07	.248	.71

The model for analytical computation requires that a numerical linear measure of the seasonal factor be obtained. Assignment of arbitrary numbers to months of the year is not adequate. Since seasonal variation is a result of climate, some measure of climatic variation should logically be suitable. A seasonal curve of the mean monthly air temperature has been found to vary closely with the seasonal variation of sediment dis-

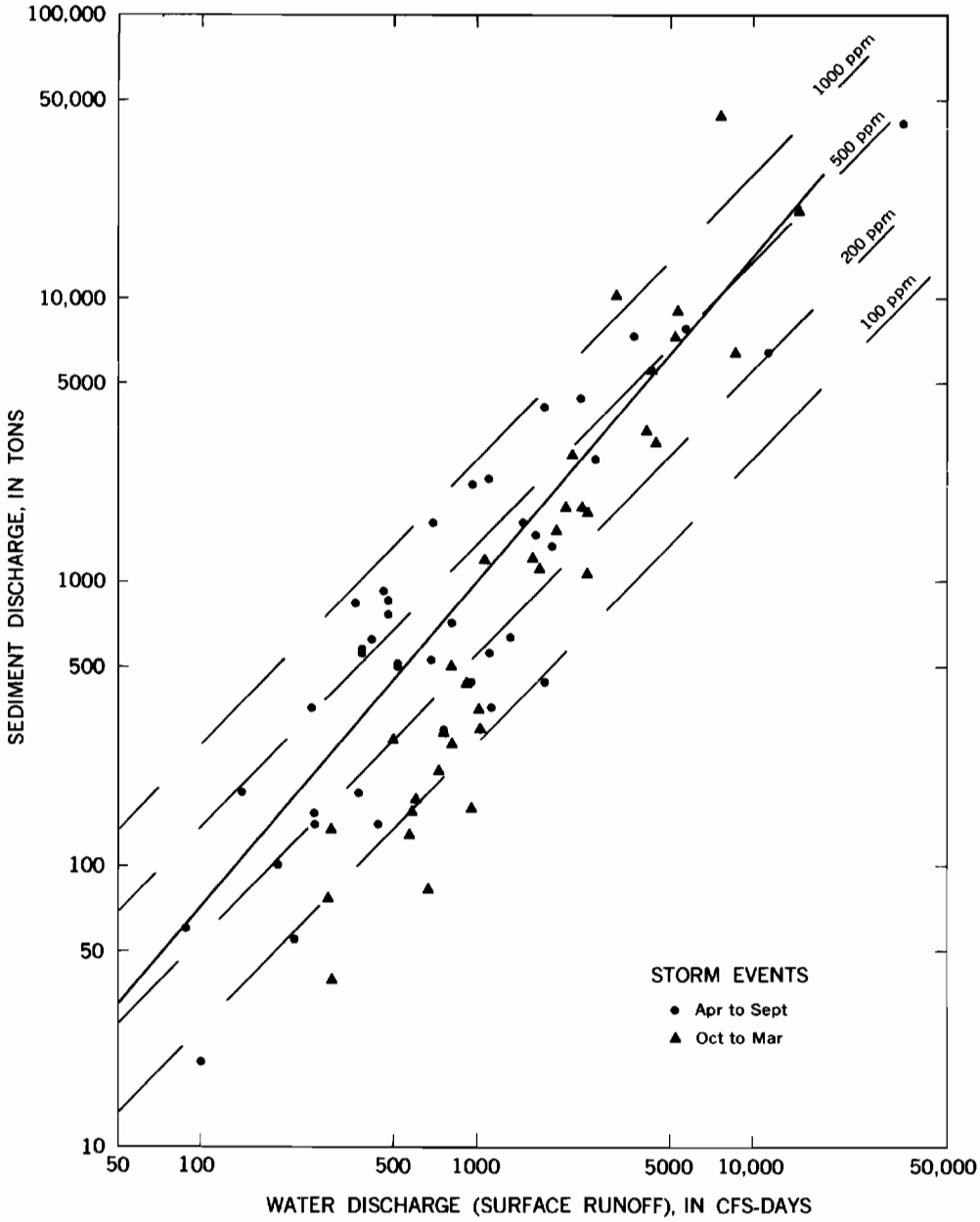

FIGURE 9.—Relation of mean sediment concentration and discharge to water discharge for cold and warm season storm events, Hazel River at Rixeyville, Va.

charge. Figure 11 shows a plotting of the mean air temperature (column 6, table 3) for the date of the specific storms against the same departure ratios or measure of sediment discharge variation. The mean linear regression ranges from a ratio of 0.43 at 35° to 1.45 at 75°. The extremes of the scatter in the plot tend to be parallel to the regression.

GROUND-WATER RUNOFF

Because the amount of runoff and erosion from a drainage basin probably depends on the length of time since the last storm and the condition of the basin with respect to "wetness" and vegetative cover, it is necessary that some measure of the antecedent condition of the basin be used. A reliable determination of the traditional antecedent precipitation index is difficult to obtain for a complete drainage basin. The rate of ground-water runoff of a stream prior to a storm is assumed to be related to the time since the previous storm and the "wetness" of the basin. It has already been noted that the base flow increases during the course of a storm and decreases following the runoff event. Thus, the amount of the ground-water flow at any time will be a function of the length of time and

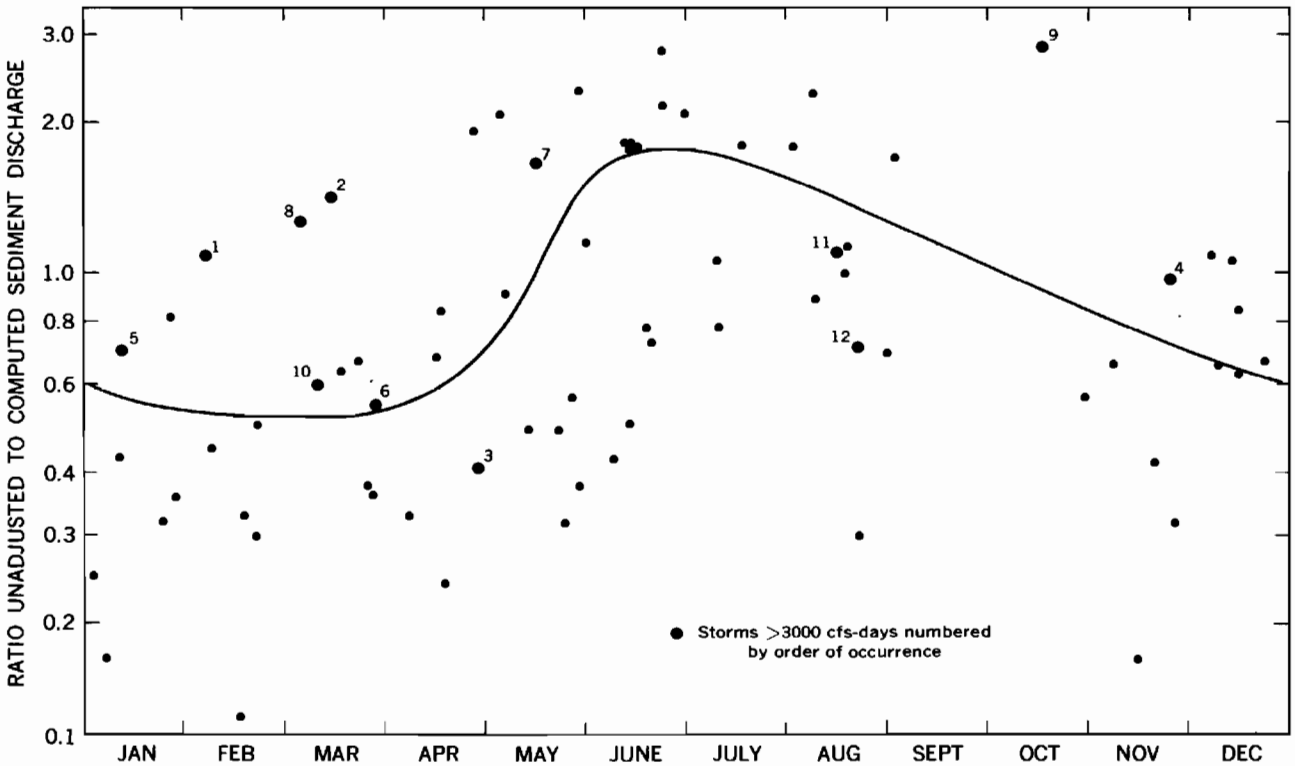

FIGURE 10.—Variation of unadjusted departure ratio or sediment discharge for a given storm size with time of year.

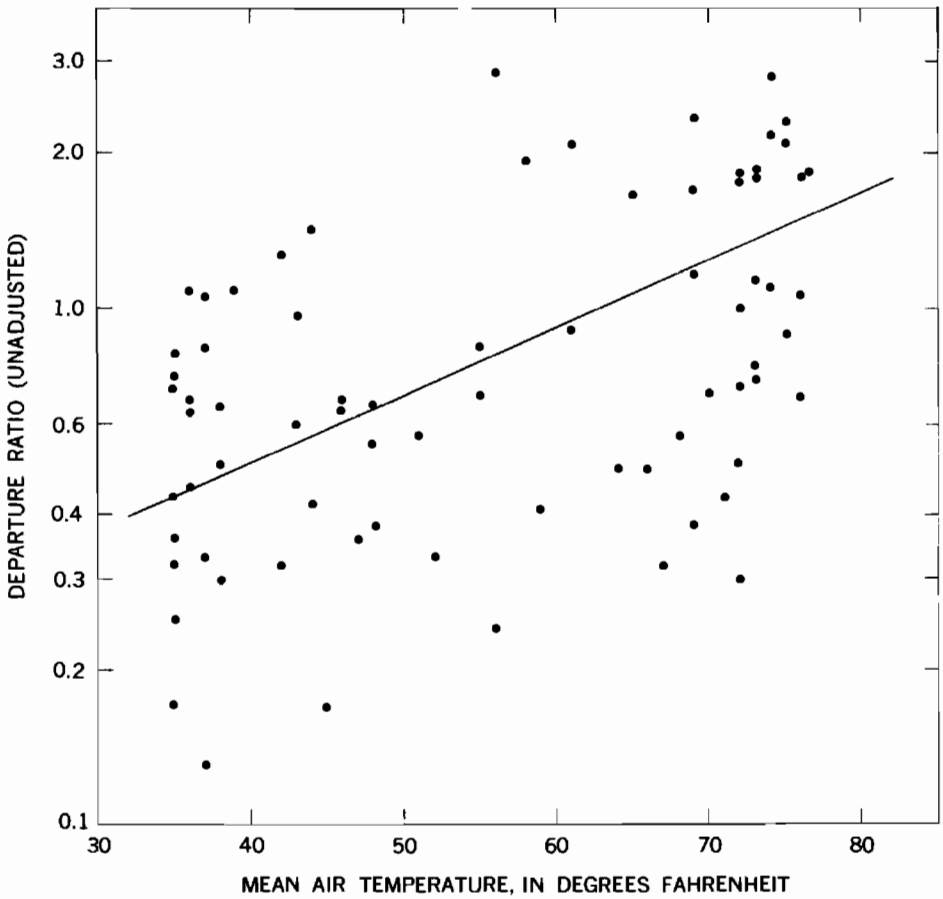

FIGURE 11.—Variation of unadjusted departure ratio or sediment discharge for a given storm size with mean air temperature for time of year of given storm events.

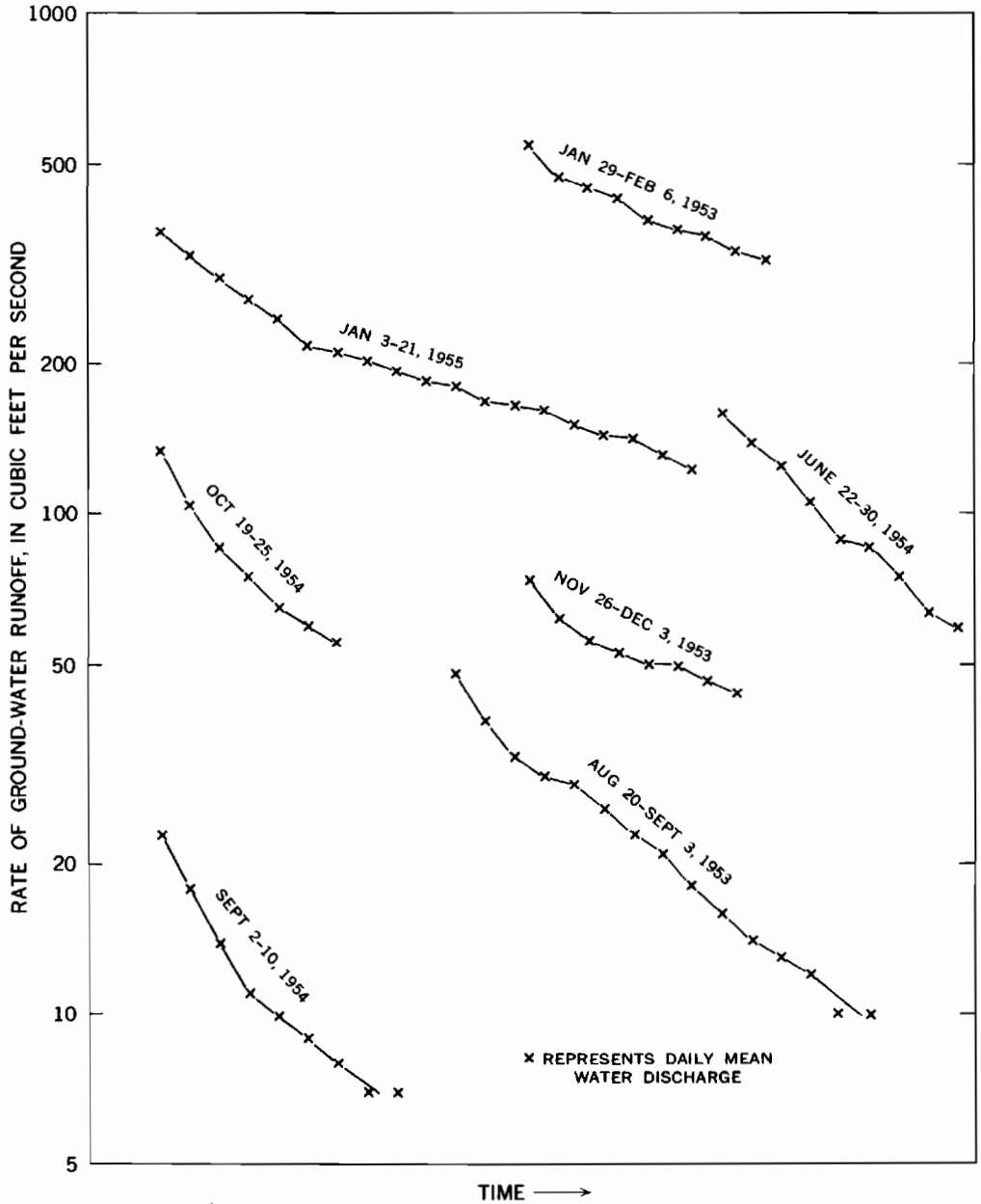

FIGURE 12.—Illustrations of the magnitude and recession of ground-water runoff for Hazel River at Rixeyville, Va.

amount of flow immediately after passage of surface runoff. Figure 12 illustrates several ground-water recession curves for the Hazel River. The recession of flow tends to be steeper and of generally lower magnitude during the warm season than during the cool season, thus again reflecting the seasonal changes of evapotranspiration.

To determine if ground-water runoff, as a measure of antecedent conditions in the basin, is effective in explaining variation in sediment discharge, the departure ratios or measure of sediment discharge variation were plotted (fig. 13) against a logarithmic expression of the base flow (columns 11 and 5, table 3). Again, there are several factors other than ground-water runoff causing a wide variation in the departure ratios, but the trend of the data indicates decreasing sediment concentration with increasing ground-water runoff. As noted from figure 12, the high rate of ground-water runoff generally occurs during the cool season when other factors causing sediment erosion are at a minimum. Further study of ground-water runoff as a variable affecting sediment variation is indicated.

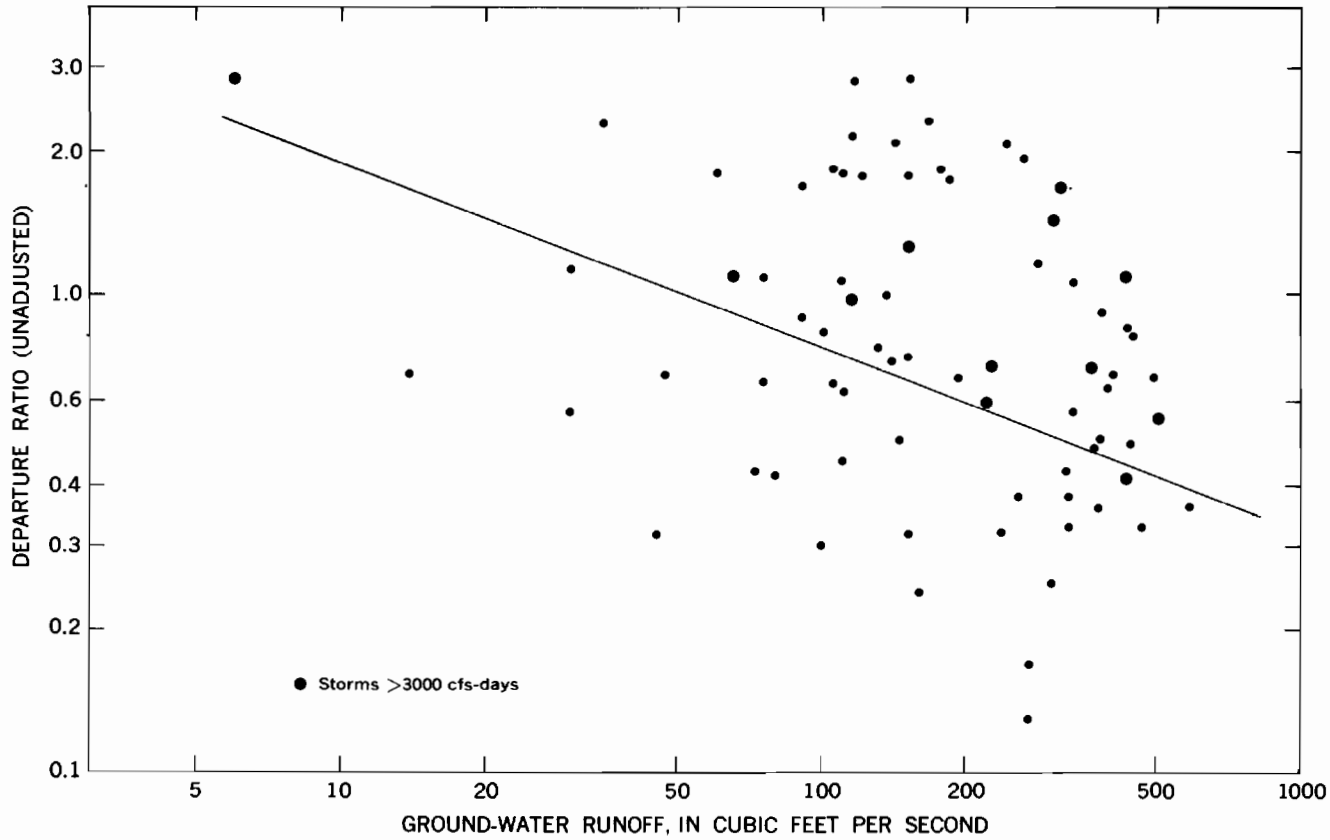

FIGURE 13.—Variation of unadjusted departure ratio or sediment discharge for a given storm size with ground-water runoff.

PEAKEDNESS

Measures of storm intensity should help to explain some of the storm-to-storm variation in the sediment transport relation of figure 9. The intensity of the storm is assumed to affect the rate of erosion and transport. One measure of storm intensity that can readily be obtained from the data at hand, other than rainfall intensity, is the peakedness of the runoff hydrograph. A peakedness index P_i, defined as a ratio of the peak rate of water discharge to the storm runoff volume for the event, is used in these analyses. The underground runoff was also subtracted from the peak flow because this underground runoff varies considerably with season and from storm to storm.

Figure 14 illustrates the relation of the unadjusted departure ratios to the peakedness indexes for the Hazel River data. The plotted data are from columns 11 and 8 of table 3. The general increase of the departure ratio with increase of peakedness index indicates that further study of this factor is desirable.

RAINFALL

Measurement and publication of rainfall data on a daily and hourly basis for a network of stations make it possible to compute by the Thiessen method the storm rainfall quantity and intensity on a particular drainage basin. See page E15 for further definition of the rainfall quantity and intensity factors. The results of such computations may, at times, poorly, represent the actual conditions over the basin due to the variation of the aerial distribution of the precipitation patterns with respect to the small sampling of the event. This is especially true for the thunderstorms that occur during the warm season. The applicability of such data also tends to decrease with decreasing size of drainage area. A small basin of 300 square miles, for example, may not contain a daily gage within its boundaries. There is even a much less chance of such a basin containing a recording rain gage.

In an attempt to use these precipitation data to help explain the variation of sediment discharge for the Hazel River, figures 15 and 16 were plotted to show the relation of the rainfall quantity (R_q) and rainfall intensity (R_i), respectively, to the first departure ratio. The apparent correlation of R_q with the departure ratios is poor, partly due to the error in measuring R_q, partly due to several factors affecting the variation in sediment discharge which cannot be observed, but mostly due to the fact that there is much intercorrelation between R_q and the quantity of runoff already

accounted for in deriving the departure ratio. The poor correlation of R_t with the departure ratios is due to the same factors, probably more so in regard to measurement error of R_t and less so in regard to intercorrelation with quantity of runoff. The poor showing of the simple correlation of these precipitation factors with sediment data for the Hazel River does not preclude their application in a system of multiple regression analysis.

TREND

Several of the active and passive factors affecting soil erosion and transport indicated in figure 1 may sufficiently change during the course of a sediment record so that the average storm-to-storm sediment yield may gradually change. Such changes can be detected and evaluated by correlating time or the month M_t from the beginning of the record as an independent variable with the departure ratios. This would then show the variation of the storms and the general trend during the period of record. Data for the Hazel River are shown in figure 17 for both the unadjusted and the seasonally adjusted departure ratios. The unadjusted ratios, plotted on the upper part of the illustration, indicate a somewhat sinuous relation reflecting the seasonal variation as already shown by figures 10 and 11. Such scattering makes the definition of trend of sediment yield more difficult to determine. The bottom part of figure 17 shows a more compact plotting of the sediment variation (nearer to 1.00) owing to the removal of the average seasonal variation. The scatter of the ratios throughout the period of record for the Hazel River for either type of plotting, however, is such that increasing or decreasing trend of sediment yield is not apparent.

CONCENTRATION AS A DEPENDENT VARIABLE

In a multiple regression equation, the regression coefficients are called partial regression coefficients. Each coefficient shows the effect on the dependent variable as a result of a unit change in the particular independent variable, while the other independent variables are held constant.

Sediment discharge, used as the dependent variable in the preceding discussions, is defined as the product of the sediment concentration in the stream, the quantity of water discharge, and a constant. This, then, makes sediment discharge highly interrelated with water discharge, and thus the true independent variable, or sediment concentration, cannot be evaluated in terms of a unit change of water discharge. In other words, sediment discharge will always correlate well with water discharge. For example, a log-log plot of water-sediment discharge data for 10 storms having a wide range of water discharge but each having identical

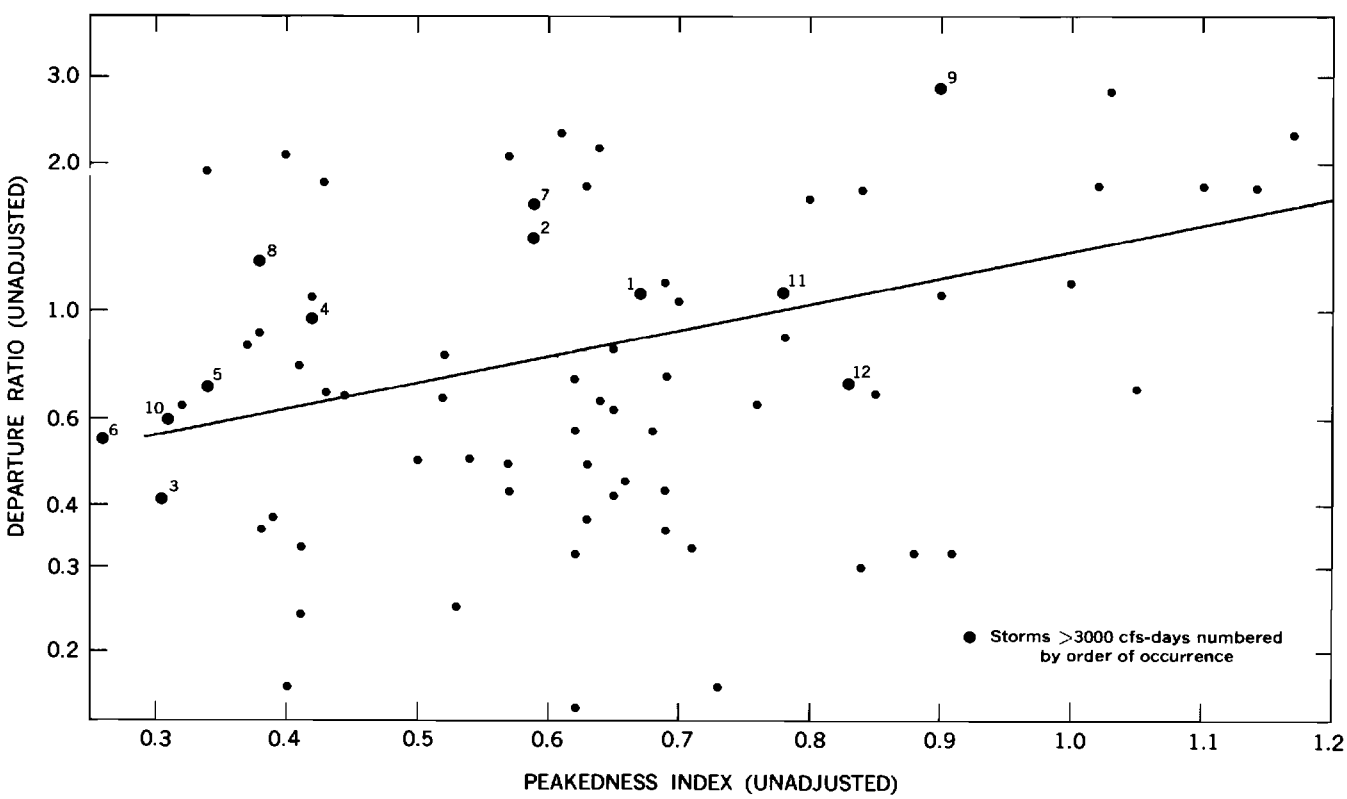

FIGURE 14.—Variation of unadjusted departure ratio or sediment discharge for a given storm size with peakedness index.

716-824 O—64——4

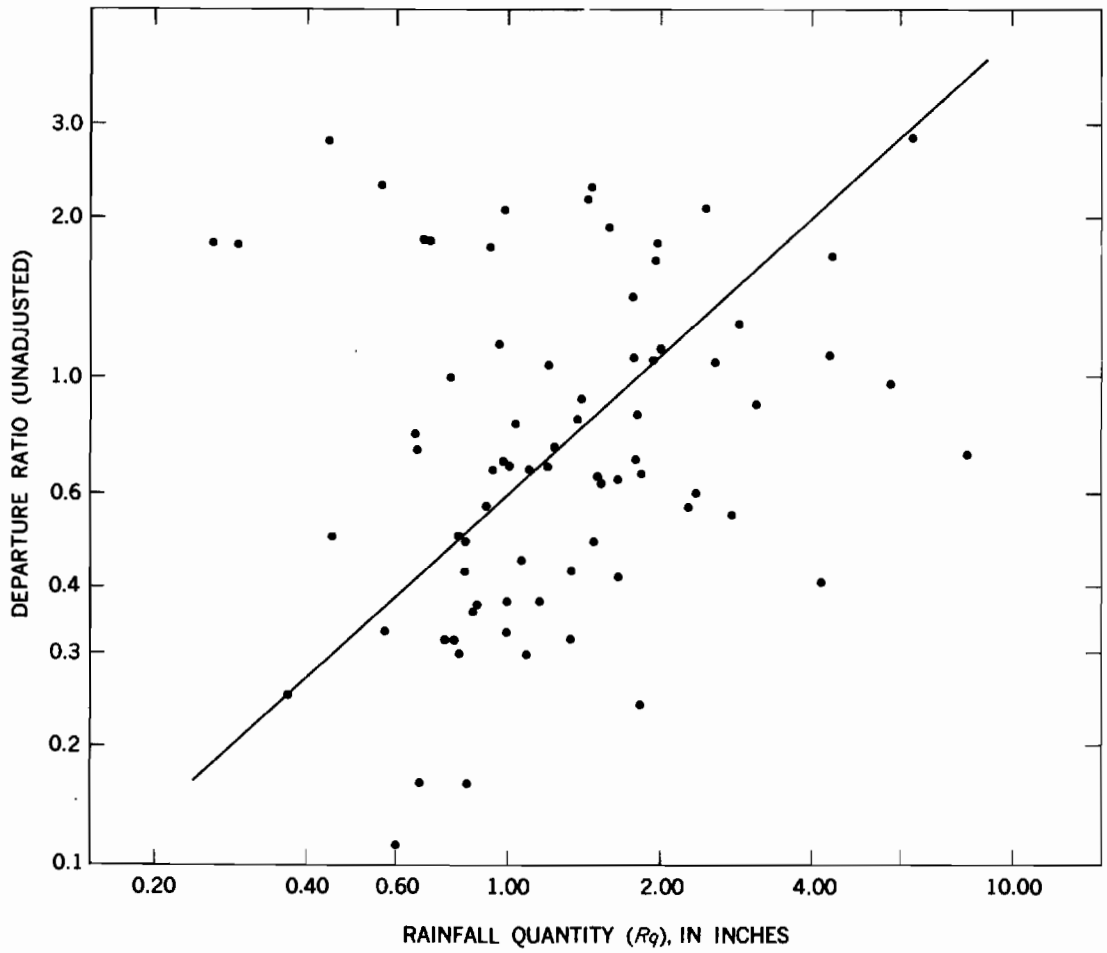

FIGURE 15.—Variation of unadjusted departure ratio or sediment discharge for a given storm size with rainfall quantity.

concentration will result in a perfect and, at first glance, an important correlation with a regression slope of one. On the other hand, if the concentration for these same storms were plotted against water discharge, the correlation and slope of regression would be zero.

Figure 18 shows the relation of mean storm sediment concentration to water discharge for the Hazel River data. The illustration can be compared directly with the sediment-water discharge plotting of figure 9. The apparent correlation between water discharge and concentration is not as good as that between water discharge and sediment discharge. The appraisal of concentration variation (fig. 18) as a dependent variable, however, for a given water discharge is readily visualized, whereas to obtain such an appraisal of concentration from the sediment discharge (fig. 9), it would be necessary to divide the sediment discharge by respective values of water discharge.

The impact of the nature of the storm-to-storm variation is also more apparent when concentration is used. This variation tends to be masked by the intercorrelation effect when sediment discharge is used. For example in figure 18, it is much easier to visualize the need for and to delineate separate curves for the cool and warm seasons than it is in figure 9. It is further readily apparent from figure 18 that the transport curve of figure 9, transposed into concentration terms, was drawn too high at the lower values of water discharge.

SUMMARY OF GRAPHICAL SEARCH

Limitations on time for search of useful variables did not permit the investigation of many conceivable measures or to find the optimum mathematical expression of the variables used. For example, several measures of antecedent conditions may be determined, some based on precipitation quantity and time, some based on ground-water runoff and time, and some based on a measure of moisture deficiency in the basin. Also, measures of the seasonal variation may be tied to climatic factors other than air temperature such as precipitation quantity and intensity in some combination with air temperature, some measure of plant growth and residue, or to Wischmeier's erosion index.

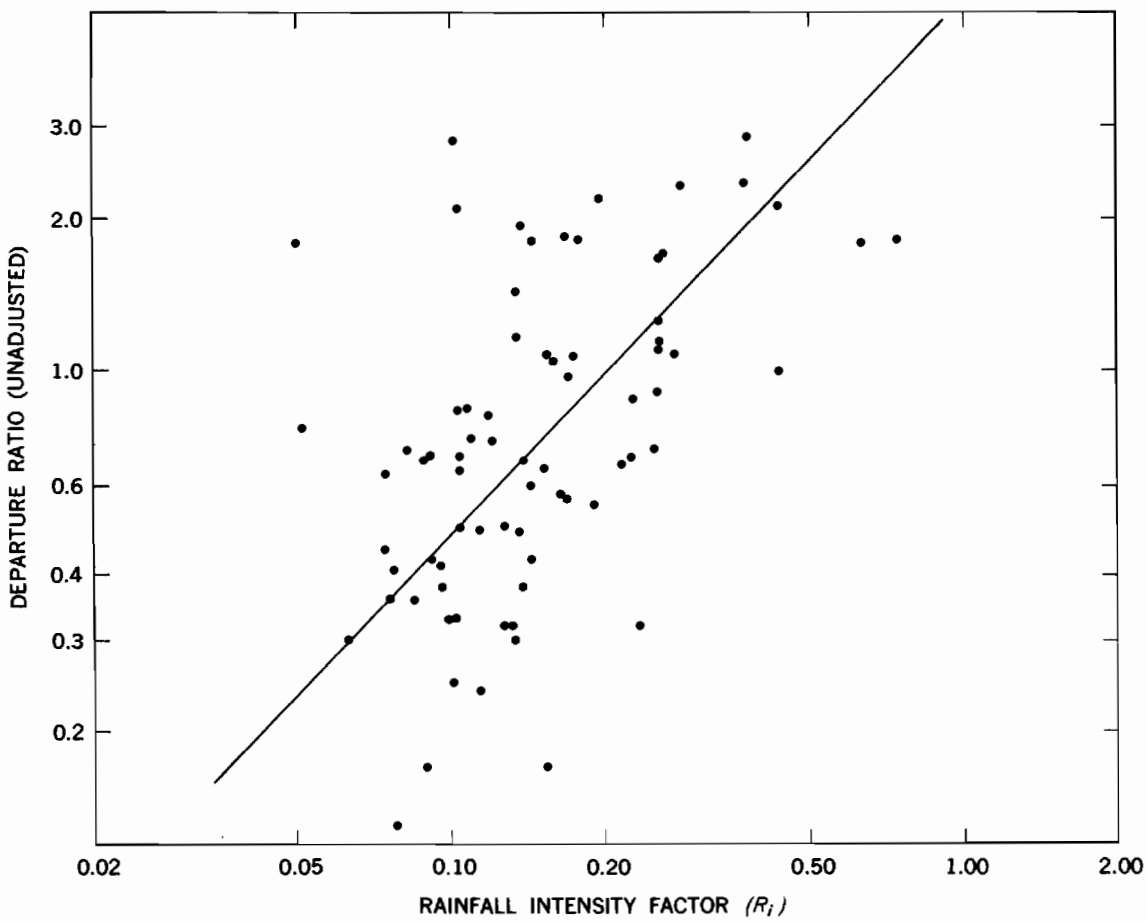

FIGURE 16.—Variation of unadjusted departure ratio or sediment discharge for a given storm size with rainfall intensity factor.

The graphical phase of the analysis for the sediment records of seven river basins in the Atlantic coast area as listed in table 4, involved plotting or correlating data for each of the 65–138 storm events on 10–25 graphs per basin. Much of this was done before the availability of the computer program and involved trial plots with variables that were noneffective, with other transformations of variables, and with checking on the effect of intercorrelation among the independent variables.

TABLE 4.—*Sediment records used for correlation and multiple regression analysis*

Stream and location	Drainage area (sq mi)	Period of record used	Number of storm events
1. Scantic River at Broad Brook, Conn.	98.4	Dec. 1952–Sept. 1958	65
2. Brandywine Creek at Wilmington, Del.	314	Dec. 1946–Sept. 1956	138
3. Hazel River at Rixeyville, Va	286	Oct. 1951–Sept. 1956	75
4. Rappahannock River at Remington, Va.	616	May 1951–Sept. 1958	82
5. Rapidan River near Culpepper, Va.	465	May 1951–Sept. 1956	85
6. James River at Buchanan, Va	2,084	do	65
7. James River at Scottsville, Va	4,571	do	67

This graphical search for variables that may be useful in explaining the variation of sediment discharge from storm to storm indicates that:

1. The month during the period of record (M_t) may be used to measure the trend of change with time.
2. The quantity of surface runoff per storm (Q_w) may be used to indicate the magnitude and (or) intensity of erosion and transport. Precipitation quantity (R_q), though difficult to evaluate, may also be used to indicate storm magnitude.
3. The long-term mean air temperature (T_a) for a given time of year can be used as a linear substitute for seasonal changes.
4. The ground-water runoff of the stream immediately prior to storm runoff (Q_b) may be used as a measure of antecedent conditions.
5. The ratio of the peak rate of flow on the storm hydrograph to storm runoff volume (P_t) can be used as a measure of storm intensity which probably affects intensity of erosion and transport. Precipitation intensity (R_i), though difficult to evaluate, may also be used for this purpose.

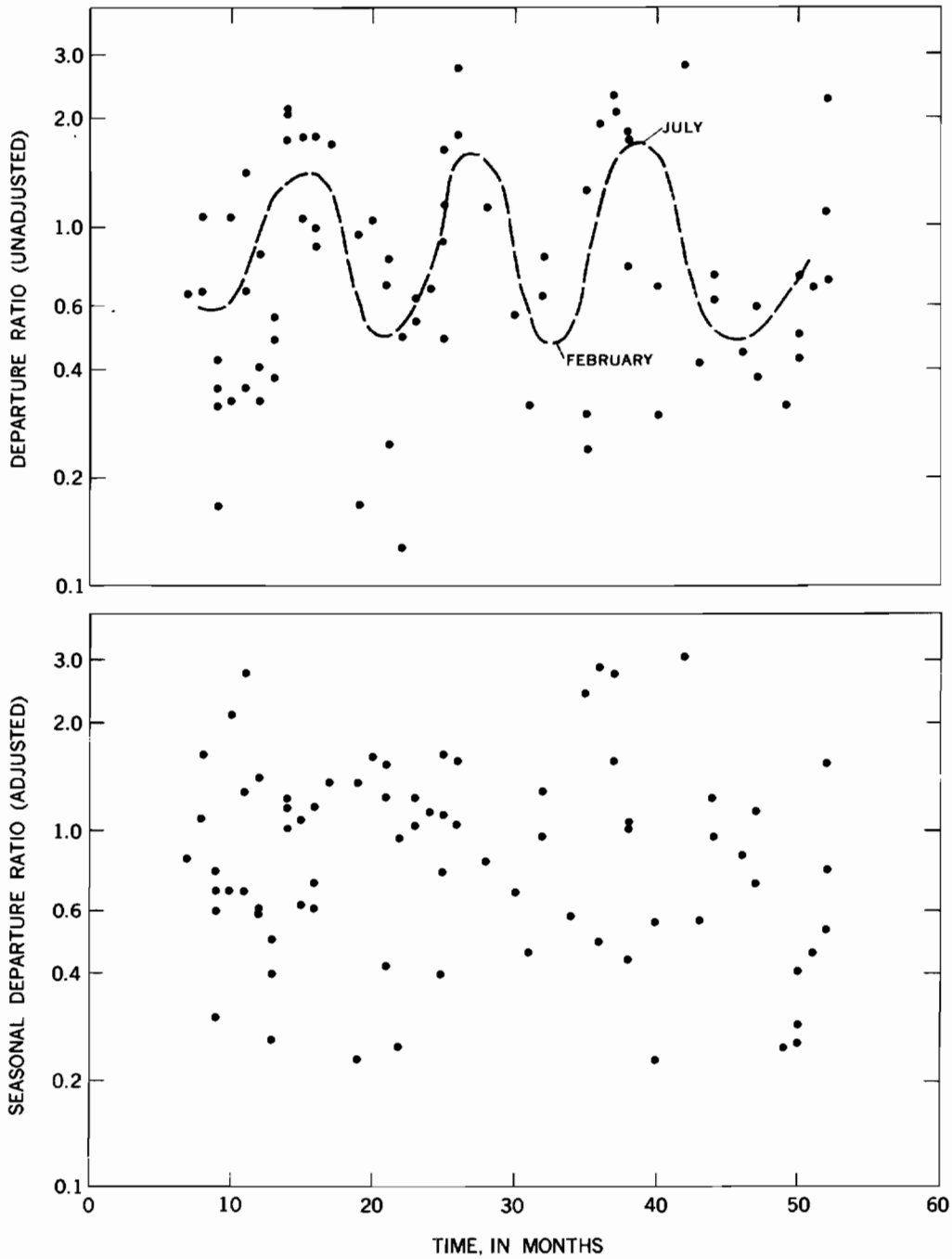

FIGURE 17.—Variation of unadjusted and seasonal adjusted departure ratios with time.

THE MODEL AND TRANSFORMATION OF VARIABLES

Owing to the multiplicity and intercorrelative effects of the variables, it is apparent that the graphical approach to solution or evaluation of the cause of storm-to-storm sediment variation would be difficult and to some degree indeterminate. Also, a rigorous definition of the significance of the regressions found by the graphical approach would not be attainable.

The total effect of all the advantages and disadvantages of the graphical and analytical methods listed by Riggs and others (written communication) is that a combination of the two methods must be used for this problem. Simple graphical correlation must be used to define the appropriate model, to determine the required transformation of the data, and to bring attention to wild points. The analytical method can then be used to obtain the best estimate of the

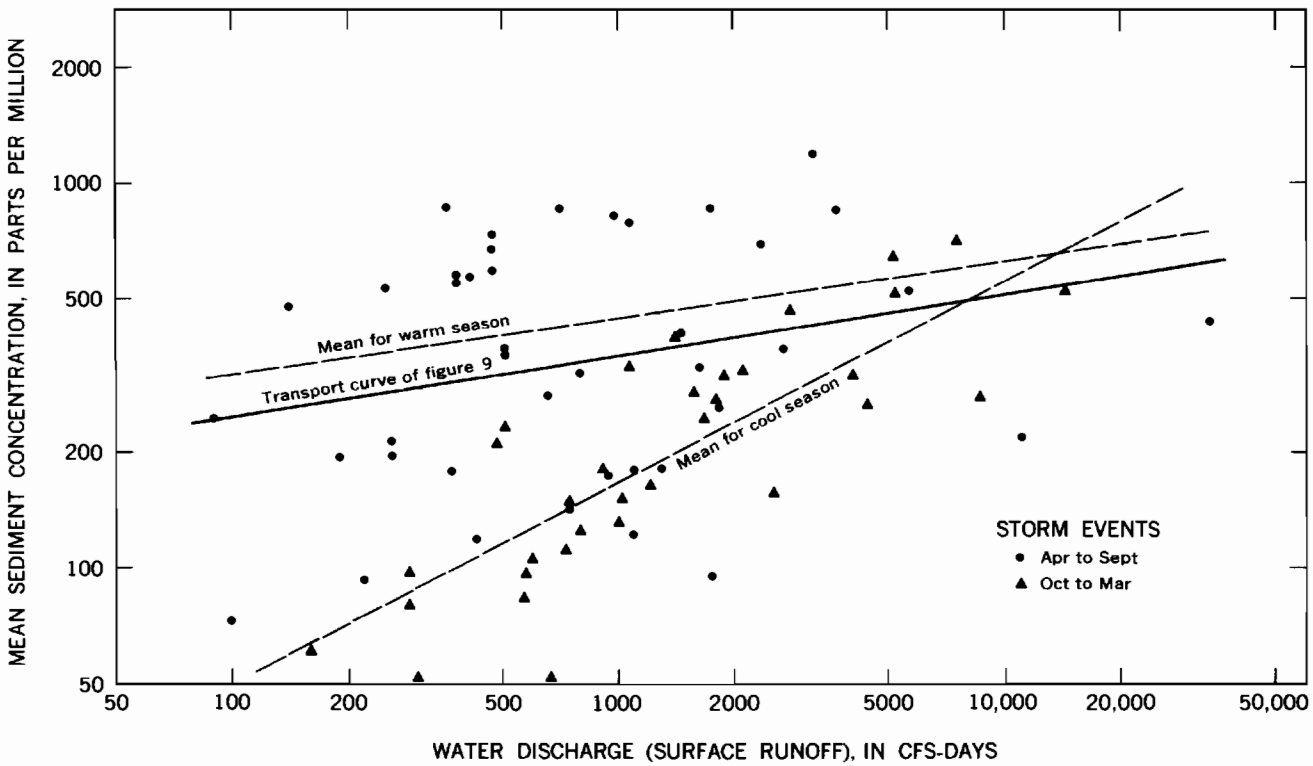

FIGURE 18.—Relation of mean sediment concentration to water discharge for cold and warm season storm events for Hazel River at Rixeyville, Va.

equation coefficients and their significance and the standard error of estimate of the equation. The procedure for making the analytical computations are outlined in most textbooks on statistical methods, such as: Dixon and Massey (1957), Ezekiel and Fox (1959), and Snedecor (1956). The results of the analytical method are unique for the model and sample used and can be presented in a concise manner. Before completion of the multiple regression program for the electronic computer, the "hand" analytical procedure was found to be cumbersome and time-consuming even when as few as two or three independent variables were used. With use of the computer, up to 50 variables may be assimilated and multiple regressions computed from many combinations of the available variables.

Based on the generalized form of the regression model,

$$Y=b_o+b_1x_1+b_2x_2+\ .\ .\ .\ +b_nx_n,$$

the most frequently used models of the basic data for the computer program are as follows:

$$\text{Log } Q_s=b_o+b_1 \log Q_w+b_2M_t+b_3T_a+b_4 \log Q_b+b_5P_i$$
$$\text{Log } C=b_o+b_1 \log Q_w+b_2M_t+b_3T_a+b_4 \log Q_b+b_5P_i$$
$$\text{Log } C=b_o+b_1 \log Q_w+b_2M_t+b_3T_a +b_4 \log Q_b+b_5 \log R_q+b_6 \log R_i$$
$$\text{Log } C=b_o+b_1 \log Q_w+b_2M_t+b_3T_a+b_4 \log Q_b+b_5 \log P_n$$
$$\text{Log } C=b_o+b_1M_t+b_2T_a+b_3 \log Q_b+b_4 \log R_q+b_5 \log R_i$$

Where Y is the dependent variable, $x_1\ .\ .\ .\ x_n$ are independent variables, $b_o\ .\ .\ .\ b_n$ are constants, and the other symbols are defined on page E15. These combinations of variables are sufficient to define differences due to use of sediment discharge in place of concentration for the dependent variable, and more important to indicate the magnitude of the effects due to measurable factors for storm size, time trend, seasonal variation, antecedent conditions, and storm intensity.

Multiple regression analysis on the electronic computer is programmed so that all variables may either be converted to logarithms or left in the presented form. The above models show that nearly half are arithmetic and the remainder are logarithmic. Therefore, conversion must be done manually for the variables Q_s, C, Q_w, Q_b, P_n, R_q, and R_i. Data for all variables had to be given for a specific observation or storm event. Therefore, some estimates of missing data were made, and in a few instances, the entire observation was omitted. To simplify the logarithmic expression of R_q and R_i, these data were multiplied by 10 and 100, respectively, before conversion.

COMPUTATION RESULTS

The electronic computer program for multiple regression analysis provided options for print-out of the many statistics normally found by longhand computation. The opportunity to check on the approximate

accuracy of the original data, some of the internal computations made by the computer, and the statistics summarizing the results and their significance is provided in the print-out of the following:

1. The original data.
2. The arithmetic mean and standard deviation for all variables.
3. The simple correlation coefficients between all pairs of original variables and the t-test for significance.
4. The partial correlation coefficients and test of significance.
5. The multiple regression coefficient and test of significance.
6. The regression weights, their standard error, and test of significance.
7. The regression coefficients, $b_1, \ldots, b_n$.
8. The regression equation constant, b_o.
9. The predicted values of the dependent variable and the residuals between the observed and computed dependent variable.
10. The sums of squares of residuals and standard error of estimate of the dependent variable.

The first three of these items deal with the mass of original data or all variables and observations; whereas, the remaining seven deal with only the variables chosen for a specific multiple regression analysis. Usually, analyses are made of several combinations of the total number of available variables.

The use of a specific variable that is not important or effective in a given multiple regression analysis may increase the standard error of estimate of the dependent variable for an equation. Therefore, one important option on the computer program allows the machine, after completing items 4–10, to automatically reject the variable having the least significant regression weight (item 6) and then to repeat items 4–10 using the new set of variables. This is repeated down to a single independent variable. For example, if seven independent variables were selected for analysis, then the first equation would contain all seven variables, the second equation would contain the six most significant variables of the first equation. The optimum regression equation from a given combination is one with a combination of variables yielding a minimum standard error of estimate.

THE MEANS AND STANDARD DEVIATIONS

The statistics for the mean and standard deviation are listed in table 5 for 10 variables and each of the 7

TABLE 5.—*Means and standard deviations of variables used in multiple regression analysis, by streams*

	Mean concentration (log C)	Sediment discharge (log Q_s)	Water discharge (log Q_w)	Time trend (M_t)	Mean air temp. (T_a)	Ground-water runoff (log Q_b)	Peakedness index (P_i)	Peak flow (log P_n)	Rainfall quantity (log $10R_q$)	Rainfall intensity (log $100R_i$)
Scantic River near Broad Brook, Conn.										
Mean	2.203	----------	2.531	34.02	39.40	2.156	0.852	----------	1.142	1.100
Standard deviation	.154	----------	.385	21.88	13.03	.261	.052	----------	.312	.186
Brandywine Creek at Wilmington, Del.										
Mean	2.519	3.114	3.161	59.75	50.93	2.560	1.383	3.239	1.160	1.234
Standard deviation	.284	.578	.376	32.83	16.53	.232	.511	.382	.226	.310
Hazel River at Rixeyville, Va.										
Mean	2.426	2.887	3.016	26.56	55.63	2.190	0.650	2.807	1.099	1.162
Standard deviation	.335	.672	.501	14.07	15.50	.403	.239	.436	.297	.234
Rappahannock River at Remington, Va.										
Mean	2.543	----------	3.354	28.90	56.79	2.474	0.691	----------	1.120	1.176
Standard deviation	.280	----------	.502	17.76	15.71	.394	.228	----------	.273	.259
Rapidan River near Culpeper, Va.										
Mean	2.540	----------	3.234	28.07	55.40	2.444	0.636	----------	1.159	1.171
Standard deviation	.338	----------	.496	18.05	15.22	.351	.185	----------	.271	.238
James River at Buchanan, Va.										
Mean	2.076	----------	4.144	30.71	53.43	3.171	0.415	3.747	----------	----------
Standard deviation	.323	----------	.505	17.02	13.52	.286	.114	.463	----------	----------
James River near Scottsville, Va.										
Mean	2.367	----------	4.372	28.37	55.36	3.431	0.399	3.959	----------	----------
Standard deviation	.285	----------	.516	18.07	14.63	.309	.118	.472	----------	----------

streams used in the analysis. These statistics are useful for comparing the average characteristics among the streams used in the analysis. For example, the mean air temperature T_a for the time of the storms used is 39.4° for the Scantic River compared with 50.9° for the Brandywine Creek, and 56.8° for the Rappahannock River. The standard deviation measures the central tendency of the data or the degree of scatter; for example, the deviation of log C (concentration) on the Scantic is 0.154 log units, or ± 14 ppm, from the mean of 160 ppm compared to the deviation of 0.335 log units, or ± 22 ppm, from the mean of 266 ppm for the Hazel River.

SIMPLE CORRELATIONS

The independent variables in a regression are generally related to each other as well as to the dependent variable. The interrelation of the independent variables causes the partial coefficients in a multiple regression equation to be different from the simple regression coefficients. In the section, "Summary of graphical search," it was shown that a great deal of this intercorrelation among the variables existed. The simple correlation coefficients among the variables for each of the streams are given in table 6. The significance of each coefficient is indicated where the t-test shows a confidence level of 90 percent or greater.

The data in table 6 shows that several general correlations may be listed:

1. That the mean concentration of sediment for a large number of storm runoff events tends to increase with water discharge, air temperature, peak flow, rainfall quantity, and rainfall intensity.
2. That the sediment discharge tends to increase with water discharge, peak flow, rainfall quantity, and rainfall intensity and decreases with the peakedness index.
3. That the volume of water discharge per storm event tends to increase with ground-water runoff, peak flow, and rainfall quantity and decrease with air temperature and peakedness index.
4. That the ground-water runoff tends to increase with peak flow and decrease with time during the period of record, air temperature, peakedness index, rainfall quantity, and rainfall intensity.
5. That peak flow tends to increase with rainfall quantity.
6. That rainfall quantity tends to increase with rainfall intensity.

Several of these correlations among the variables may not hold for all records as indicated by table 6. A matrix of the variables is shown in table 7 summarizing the data of table 6. The relative values of the coefficients are not shown, but the signs and degree of significance substantiate and further evaluate the above generalizations.

On the two stations where sediment discharge was used in the analysis (Brandywine Creek and Hazel River), the simple correlation coefficients (table 6) are respectively +0.91 and +0.88 to the effect that sediment discharge will increase with water discharge. Concentration also increases for these stations with water discharge as shown by the highly significant coefficients of +0.53 and +0.32. The difference in magnitude of the correlation coefficients is due to the fact that the sediment discharge is the product of water discharge, concentration, and a constant. Water discharge correlates well with rainfall quantity, peakedness index, and peak flow; therefore, these elements correlate better with sediment discharge than with concentration due to the intercorrelation between water discharge and sediment discharge.

MULTIPLE REGRESSION EQUATIONS FOR HAZEL RIVER

Data for all 10 variables shown in table 3 were used for the multiple regression analysis for the Hazel River. A detailed comparison between the dependent variables C and Q_s was considered important. For each of these dependent variables, the multiple regression equations for the following combinations of independent variables were determined:

1. Log Q_w, M_t, T_a, log Q_b, P_t, log $10R_q$
2. Log Q_w, M_t, T_a, log Q_b, log $10R_q$, log $100R_t$
3. M_t, T_a, log Q_b, P_t, log $10R_q$
4. Log Q_w, M_t, T_a, log Q_b, P_t
5. Log Q_w, M_t, T_a, log Q_b, log P_n
6. Log Q_w, M_t, T_a, log Q_b, log $100R_t$

By use of the option to repeat the analysis on a given combination after rejection of the least significant variable, these 6 combinations resulted in a total of 32 multiple regression equations for each dependent variable. The 64 equations for the Hazel River from these combinations are shown in the appendix in which each of the above combinations are listed by a separate roman numeral.

Numerals I–VI in the appendix are for the combinations using log C as the dependent variable and VII–XII are for combinations using log Q_s. Evaluation of the relative merits of these dependent variables can be made by comparing the resulting regression coefficients, their significance, and most particularly, the standard error of estimate of the regression equations. Each equation for log C has a lower standard error of estimate than the corresponding equation for log Q_s. The use of log C instead of log Q_s results in a more uniform significance of the regression coefficients.

TABLE 6.—*Simple correlation coefficients and their significance, by streams*

	Mean concentration (log C)	Sediment discharge (log Q_s)	Water discharge (log Q_w)	Time trend (M_t)	Mean air temp. (T_a)	Groundwater runoff (log Q_b)	Peakedness index (P_i)	Peak flow (log P_n)	Rainfall quantity (log $10R_q$)	Rainfall intensity (log $100R_i$)
Mean storm concentration, log C										
Scantic			[1]+0.202	−0.116	+0.130	[2]+0.384	[3]+0.258		−0.038	−0.043
Brandywine		[2]+0.832	[2]+.531	[1]−.142	+.118	−.093	+.000	[3]+0.258	[2]+.456	[2]+.261
Hazel		[2]+.704	[2]+.316	+.058	[2]+.378	−.077	+.078	[2]+.400	[2]+.334	[2]+.470
Rappahannock			[1]+.190	−.052	[2]+.376	−.029	+.065		[3]+.255	[2]+.349
Rapidan			[2]+.380	−.135	[3]+.273	−.020	−.006		[2]+.294	[1]+.204
James, Buchanan			[3]+.309	−.187	+.167	[3]−.274	+.095	[2]+.361		
James, Scottsville			[2]+.647	−.043	−.143	+.190	−.078	[2]+.704		
Sediment discharge, log Q_s										
Brandywine	[2]+0.832		[2]+0.910	−0.075	−0.134	+0.016	[2]−0.367	[2]+0.818	[2]+0.706	+0.045
Hazel	[2]+.704		[2]+.880	+.009	−.056	+.179	[2]−.354	[2]+.881	[2]+.678	[3]+.256
Water discharge, log Q_w										
Scantic	[1]+0.202			−0.176	+0.159	+0.745	−0.115		[2]+0.655	[3]+0.292
Brandywine	[2]+.531	[2]+0.910		−.019	[2]−.228	+.098	[2]−.559	[2]+0.818	[2]+.744	−.121
Hazel	[2]+.316	[2]+.880		−.030	[2]−.318	[2]+.338	[2]−.524	[3]+.949	[2]+.665	+.025
Rappahannock	[1]+.190			+.038	[2]−.294	[2]+.377	[2]−.560		[2]+.660	−.123
Rapidan	[2]+.380			−.113	[3]−.272	[1]+.193	[2]−.548		[2]+.638	−.118
James, Buchanan	[3]+.309			+.040	[2]−.540	[2]+.338	[2]−.468	[2]+.973		
James, Scottsville	[2]+.647			+.065	[2]−.521	[2]+.549	[2]−.506	[2]+.976		
Time trend, M_t										
Scantic	−0.116		−0.176		+0.064	[3]−0.249	−0.131		−0.160	−0.034
Brandywine	[1]−.142	−0.075	−.019		+.044	[1]−.146	+.065	+0.136	−.002	−.082
Hazel	+.053	+.009	−.030		[3]+.256	[2]−.437	+.106	−.011	+.120	+.053
Rappahannock	−.052		+.038		+.161	[2]−.420	−.052		+.180	−.028
Rapidan	−.135		−.113		+.146	[2]−.499	+.117		[1]+.195	−.010
James, Buchanan	−.187		+.040		+.036	[3]−.251	[1]−.215	−.015		
James, Scottsville	−.043		+.065		+.001	−.165	+.141	+.111		
Mean air temperature, T_a										
Scantic	+0.130		+0.159	+0.064		+0.189	+0.097		[2]+0.366	[2]+0.367
Brandywine	+.118	−0.134	[2]−.288	+.445		[2]−.230	[2]+.337	[3]−0.170	+.134	[2]+.597
Hazel	[2]+.378	−.056	[2]−.318	[3]+.256		[2]−.317	[2]+.344	[3]−.238	+.021	[2]+.376
Rappahannock	[2]+.376		[2]−.294	+.161		[2]−.311	[2]+.292		+.130	[2]+.518
Rapidan	[3]+.273		[3]−.272	+.146		[2]−.309	[2]+.330		+.145	[2]+.501
James, Buchanan	+.167		[2]−.540	+.036		[2]−.436	[1]+.239	[2]−.538		
James, Scottsville	−.143		[2]−.521	+.001		[2]−.466	[2]+.426	[2]−.471		
Groundwater runoff at beginning of storm, log Q_b										
Scantic	[2]+0.384		+0.745	[3]−0.249	+0.189		+0.131		−0.108	[3]−0.280
Brandywine	−.093	+0.016	+.098	[1]−.146	[2]−.230		[2]−.263	−0.002	[2]−.256	[2]−.256
Hazel	−.077	+.179	[2]+.338	[2]−.437	[2]−.317		[2]−.576	+.182	[3]−.234	[2]−.308
Rappahannock	−.029		[2]+.377	[2]−.420	[2]−.311		[2]−.536		[3]−.223	[2]−.362
Rapidan	−.020		[1]+.193	[2]−.499	[2]−.309		[2]−.313		[2]−.335	[2]−.412
James, Buchanan	[3]−.274		[2]+.338	[3]−.251	[2]−.436		+.028	[2]+.376		
James, Scottsville	+.190		[2]+.549	−.165	[2]−.466		[2]−.367	[2]+.510		
Peakedness index, P_i										
Scantic	[3]+0.258		−0.115	−0.131	+0.097	+0.131			−0.048	−0.072
Brandywine	+.000	[2]−0.367	[2]−.559	+.065	[2]+.337	[2]−.263		[3]−0.192	[2]−.374	[2]+.339
Hazel	+.078	[2]−.354	[2]−.524	+.106	[2]+.344	[2]−.576		[3]−.259	−.171	[3]+.246
Rappahannock	+.065		[2]−.560	−.052	[2]+.292	[2]−.536			[1]−.197	+.124
Rapidan	−.006		[2]−.548	+.117	[2]+.330	[2]−.313			−.164	+.164
James, Buchanan	+.095		[2]−.468	[1]−.215	+.239	+.028		[3]−.256		
James, Scottsville	−.078		[2]−.506	+.141	[2]+.436	[2]−.367		[2]−.315		
Peakedness, log P_n										
Brandywine	[2]+0.581	[2]+0.818	[2]+0.818	[2]+0.136	−0.170	−0.002	[3]−0.192		[2]+0.609	[3]+0.008
Hazel	[2]+.400	[2]+.881	[2]+.949	−.011	[3]−.238	+.182	[3]−.259		[2]+.714	+.149
James, Buchanan	[2]+.361		[2]+.973	−.015	[2]−.538	[2]+.386	[3]−.256			
James, Scottsville	[2]+.704		[2]+.976	+.111	[2]−.471	[2]+.510	[2]−.315			
Rainfall quantity, log $10R_q$										
Scantic	−0.038		[2]+0.655	−0.160	[2]+0.366	−0.108	−0.048			[2]+0.546
Brandywine	[2]+.456	[2]+0.706	[2]+.744	−.002	+.134	[2]−.256	[2]−.374	[2]+0.609		[1]+.163
Hazel	[2]+.334	[2]+.678	[2]+.665	+.120	+.021	[3]−.234	−.171	[2]+.714		[2]+.404
Rappahannock	[2]+.255		[2]+.660	+.180	+.130	[3]−.223	[1]−.197			[3]+.284
Rapidan	[2]+.294		[2]+.638	[1]+.195	+.145	[2]−.335	−.164			[2]+.292
Rainfall intensity, log $100R_i$										
Scantic	−0.043		[3]+0.292	−0.034	[2]+0.367	[3]−0.280	−0.072		[2]+0.546	
Brandywine	[2]+.261	+0.045	−.121	+.082	[2]+.597	[2]−.265	[2]+.339	+0.008	[1]+.163	
Hazel	[2]+.470	[3]+.256	+.025	+.053	[2]+.376	[2]−.308	[3]+.246	+.149	[2]+.404	
Rappahannock	[2]+.349		−.123	+.028	[2]+.518	[2]−.362	+.124		[3]+.284	
Rapidan	[1]+.204		−.118	−.010	[2]+.501	[2]−.412	+.164		[2]+.292	

[1] Poorly significant (90 percent level).
[2] Highly significant (99 percent level).
[3] Significant (95 percent level).

TABLE 7.—*A matrix of variables showing the average direction and significance of simple correlations*

[+ or − is used when two-thirds or more of records show the respective sign. ± is used when more than one-third of records show both signs]

	Log C	Log Q_s	Log Q_w	M_t	T_a	Log Q_b	P_i	Log P	Log $10R_q$	Log $100R_i$
Log C	------	[1]+	[2]+	−	[3]+	−	+	[1]+	[2]+	[2]+
Log Q_s	[1]+	------	[1]+	±	−	+	[1]−	[1]+	[1]+	[3]+
Log Q_w	[2]+	[1]+	------	±	[1]−	[3]+	[1]−	[1]+	[1]+	±
M_t	−	±	±	------	+	[2]−	±	±	±	±
T_a	[3]+	−	[1]−	+	------	[1]−	[1]+	[1]−	+	[1]+
Log Q_b	−	+	[3]+	[2]−	[1]−	------	[1]−	[3]+	[2]−	[1]−
P_i	+	[1]−	[1]−	±	[1]+	[2]−	------	[2]−	−	+
Log P	[1]+	[1]+	[1]+	±	[1]−	[3]+	[2]−	------	[1]+	+
Log $10R_q$	[2]+	[1]+	[1]+	±	+	[3]−	−	[1]+	------	[2]+
Log $100R_i$	[2]+	[3]+	±	±	[1]+	[1]−	+	+	[2]+	------

[1] Highly significant (99 percent level).
[2] Significant (95 percent level).
[3] Poorly significant (90 percent level). Where no footnote is shown, correlation is not significant

The nonuniformity of significance for log Q_s is caused by the very high degree of simple correlation between log Q_s and log Q_w which results in log Q_w assuming more than its share of significance from the total regression.

In the instance when log $10R_q$ is used instead of log Q_w (compare combinations III and IV with X and XI), the minimum standard error is found to be 0.295 and 0.444, respectively, for log C and log Q_s. In other words, if log Q_s must be used, then it is essential that log Q_w be included as one of the independent variables; whereas, if log C is used, then the more uniform degree of intercorrelation among the independent variables results in a stronger equation. The use of log C instead of log Q_s also tends to increase the significance of P_i, log $10R_q$, and log $100R_i$ and tends to somewhat decrease the significance of log Q_b.

The usefulness of specific independent variables to predict sediment conditions in a stream is based on their statistical significance and numerical value in the equation. When log C is used as the dependent variable, the following observations from the appendix for the Hazel River data seem pertinent.

1. The measure of ground-water flow for antecedent conditions log Q_b is not effective. Only some equations in II and III, for example, rate as high as very poorly significant.
2. The coefficients for M_t or time trend are all negative, indicating the possibility of decreasing sediment during the period of record; however, it is not significant for any equation.
3. Runoff volume or log Q_w is a better measure of storm volume than is rainfall quantity or log $10R_q$ (contrast I–2 with III–1 and the respective S_e of 0.270 and 0.297).
4. Net peak flow log P_n is only a slightly better measure for a storm intensity factor than is peakedness index P_i (contrast IV and V).
5. Due to a large amount of intercorrelation, use of log P_n makes log Q_w insignificant (see V).
6. When only two independent variables are used, log P_n and T_a yield better results than log Q_w and T_a (contrast V–4 and I–5).
7. Log $100R_i$ is the best measure of storm intensity when contrasted with the measures of peakedness P_i and log P_n.

As a result of the characteristic intercorrelation among variables and their expected variation for different drainage basins, the conclusions noted above for the Hazel River cannot be rigorously applied to other streams. On the basis of hydrologic and sedimentologic theory, however, these conclusions are logical and should, within limits, find general application.

COMPARISON OF STREAMS

The two principal objectives of this analysis were to define the effect of specific measurable independent variables on the variation of sediment in streamflow for specific locations and to determine how these effects change from basin to basin. As in the above analysis of the Hazel River, the regression coefficients, their significance, and the standard error of estimate for the equations will be compared to show these effects for seven locations in the Atlantic coast area.

The regression equations and their standard error of estimate and the significance of coefficients for several combinations of variables for the seven locations are given in the appendix. The constants or regression coefficients and their significance for two or more combinations of variables for each of the seven locations are shown in table 8. Equations were chosen for this table which demonstrated a minimum standard error of estimate and yet used the principal combination of available and applicable variables.

EFFECTS OF DEPENDENT VARIABLES

The results of comparing the dependent variable log Q_s (sediment discharge) with the dependent variable log C (concentration) for the Hazel River were not conclusive in some respects. Therefore, a similar comparison was made for the Brandywine Creek. The two most important conclusions determined from the Brandywine data, which are similar to those determined for the Hazel River, are (1) that the standard error of estimate is less for log C than for log Q_s but not appreciably so, and (2) that the very high significance of log Q_w (water discharge) when log Q_s is used causes a tendency for the remaining independent variables to lose significance.

TABLE 8.—*Regression coefficients and standard error of estimate of principal regression equations, by streams*

	Equation constant [1]	Water discharge (log Q_w)	Time trend (M_t)	Mean air temperature (T_a)	Ground-water runoff (log Q_b)	Peakedness index (P_i)	Peak flow (log P_a)	Rainfall quantity (log 10 R_q)	Rainfall intensity (log 100 R_i)	Standard error of estimate (± S_e in log units)
Scantic River at Broad Brook, Conn.										
Surface runoff	+1.551	[2] +0.143			[2] +0.117	[2] +0.037		[2] −0.113		0.138
	+1.492	[2] +.135		+0.00112	[2] +.196			[2] −.149	+0.068	.143
Total runoff	+.031	[4] +.503	−0.00102		[2] −.206	[4] +1.205				.177
	+.034	[4] +.423	+.00120		[3] −.148	[4] +1.159		[2] +.121		.178
	+.241	[4] +.460	[3] +.00157		[2] −.239				[2] +.290	.198
Brandywine at Wilmington, Del.										
Log C	+0.886	[4] +0.644	[5] −0.00155	[2] +0.00385	[2] −0.195			[2] −0.365	[5] +0.338	0.215
	+1.039	[2] +.325	[4] −.00199	[4] +.00554	[2] −.183		[4] +0.333	[6] −.274		.211
	+.406	[4] +.719	[5] −.00150	[4] +.00484	[6] −.124	[4] +0.196		[6] −.232		.208
Log Q_s	−1.634	[4] +1.633	[2] −.00142	[2] +.00365	[2] −.199			[2] −.345	[5] +.328	.216
	−1.494	[4] +1.310	[5] −.00187	[4] +.00526	[2] −.185		[4] +.336	[3] −.262		.212
	−2.095	[4] +1.705	[2] −.00137	[5] +.00462	[3] −.131	[4] +.189		[3] −.225		.210
Hazel River at Rixeyville, Va.										
Log C	+0.642	[4] +0.513	−0.00256	[4] +0.00970	[2] −0.178			[2] −0.421	[4] +0.533	0.255
	+.791	−.098	−.00200	[4] +.01083	−.021		[6] +0.509			.269
	+.586	[4] +.397	−.00242	[4] +.01101	−.040	[3] +0.278				.270
	+.660	[4] +.474	−.00289	[4] +.01153	−.105	[3] +.258			+.149	.270
Log Q_s	−1.644	[4] +1.406	−.00254	[4] +.00837	[2] −.184			−.252	[5] +.493	.265
	−1.401	[4] +1.029	−.00269	[4] +.01005	−.119		+.341			.278
	−1.464	[4] +1.355	−.00308	[4] +.01025	[2] −.144	+.143				.280
	−1.456	[4] +1.363	−.00313	[4] +.01030	−.151	+.141			−.016	.282
Rappahannock River at Remington, Va.										
	+1.328	[2] +0.323	[3] −0.00276	[4] +0.00925	−0.092	+0.154		−0.171		0.247
	+1.395	[5] +.325	[3] −.00278	[4] +.00804	−.117			−.257	[6] +0.221	.245
Rapidan River near Culpeper, Va.										
	+0.768	[4] +0.529	[3] −0.00284	[4] +0.00959	−0.121	[6] +0.395		[3] −0.300		0.280
	+1.141	[4] +.449	−.00268	[4] +.00947	−.126			[3] −.283	+0.113	.287
James River at Buchanan										
	+0.960	[5] +0.532	[5] −0.00530	[5] +0.00777	[4] −0.556	[4] +1.019				0.230
	+1.783	[6] +.486	[5] −.00621	[5] +.00807	[4] −.572		[4] +1.027			.229
James River at Scottsville										
	+0.211	[4] +0.560	[2] −0.00297	[3] +0.00286	[2] −0.196	[5] +0.770				0.194
	+.832	[3] −.359	[2] −.00322	[3] +.00290	[6] −.184		[4] +0.926			.186
Equations of minimum S_e										
Scantic	+1.551	[2] +0.143			[2] +0.177	[2] +0.037		[3] −0.113		0.138
Brandywine	+.406	[4] +.719	[5] −0.00150	[4] +0.00484	[3] −.124	[4] +.196		[3] −.232		.208
Hazel	+.642	[4] +.513	−.00256	[4] +.00970	[3] −.178			[2] −.421	[4] +0.533	.255
Rappahannock	+1.333	[5] +.187	[3] −.00211	[5] +.00711					[6] +.204	.244
Rapidan	+.355	[4] +.524		[4] +.00970		[2] +.429		[6] −.275		.281
James, Buchanan	+.960	[5] +.532	[5] −.00530	[5] +.00777	[4] −.566	[4] +1.019				.203
James, Scottsville	+.211	[4] +.560	[2] −.00297	[3] +.00286	[2] −.196	[5] +.770				.194

[1] The dependent variable is log C except where noted for Brandywine Creek and Hazel River.
[2] Significant (95 percent level).
[3] Very poorly significant (80 percent level).
[4] Very highly significant (99.9 percent level).
[5] Highly significant (99 percent level).
[6] Poorly significant (90 percent level).

EFFECTS OF INDEPENDENT VARIABLES

The effects of selected independent variables on variation of sediment discharge can be determined by study of the coefficients and their relative significance as given in table 8 and the appendix. Again, it is noted that variation of coefficients for a specific variable at a specific stream location is largely due to the effect of intercorrelation among the independent variables. An outstanding example of this is shown by the difference in the first two equations for the Brandywine Creek in table 8. The first equation used rainfall intensity and the second equation uses peak flow as a measure of storm intensity. The first equation has a highly significant coefficient for log Q_w of +0.644, and the second equation has a less significant coefficient for this variable of +0.325. The difference is attributed

to a highly significant coefficient of +0.333 for log P_n in the second equation and to the fact that peak flow has a very strong simple correlation with the quantity of water discharge for a storm period.

The significant regression coefficients in table 8 are usually of the same variables that had significant simple correlation with sediment concentration. See the first section of table 6. Generally, the significance of a specific regression coefficient is improved over that of the simple correlation due to the effects of the multiple regression in isolating the effects of a single variable. For example, the simple correlation coefficients of concentration with time trend for the Brandywine Creek is poorly significant (table 6); whereas, the regression coefficients for time trend (table 8) are all highly significant. In other instances the simple correlation coefficients are not significant at the level tested, but the regression coefficients are significant.

The regression coefficients tend to have the same sign as the simple correlation coefficients, especially so if they are significant. Exception to this is noted for rainfall quantity on the Brandywine Creek in which the simple correlation coefficient is positive and highly significant; whereas, the regression coefficients are negative and less than highly significant. Intercorrelation among the independent variables is the cause of this change of sign and significance.

Based on data used in this analysis and the equations derived therefrom, water discharge proves to be the most important independent variable for describing variation of sediment transport in streams. The tendency is strong for the mean concentration of sediment (on a storm event basis) to increase with increasing volume of water discharge. The least important independent variable is rainfall quantity. The poor results obtained from using rainfall quantity may be attributed to the poor measure of this statistic to represent the true rainfall quantity on a storm-to-storm basis and to its high degree of intercorrelation with quantity of runoff.

The importance of other independent variables range between that of water discharge and rainfall quantity. The regression coefficient for time during the period of record is negative for nearly all equations and is significant for equations for the Brandywine Creek and James River Basins. Thus, there is an important sediment concentration reduction with time for the two basins and the possibility of decreasing concentration in other basins. Sediment concentration increases significantly with mean air temperature or time of year for all streams except for the Scantic River and the James River at Scottsville, Va. The range for a 50° change of temperature varies from about 0.5 log unit of concentration for the Hazel River down to about 0.2 log unit for the Brandywine Creek. An increase in ground-water runoff tends to correlate with a decrease in sediment movement. The coefficients for ground-water runoff variable were not significant for the Hazel, Rappahannock, and Rapidan Rivers and generally not highly significant in other basins. Thus, the rate of ground-water flow as a measure of antecedent conditions is not as effective in explaining storm-to-storm sediment variation as expected.

The three measures of storm intensity: peakedness index, peak flow, and rainfall intensity, were not fully compared for all streams. Only peakedness index was determined for all streams. Sediment concentration of storm runoff in streams increases with each of these measures of storm intensity. Peakedness index resulted in a slightly lower standard error of estimate than peak flow for the Brandywine Creek, the Hazel River, and the two locations on the James River. Peakedness index is not considered significant for the Hazel River. Rainfall intensity was not significant for the Rapidan River. Measures of rainfall intensity were not available for testing in the James Basin. Comparison of rainfall intensity with the parameters based on peak flow, as a measure of the effect of storm intensity, shows that the relative standard error of estimate of the equations is not consistently higher or lower when rainfall intensity is used. The significance of the regression coefficients shown in table 8 indicate that either peakedness index or peak flow is a better measure of storm intensity than is rainfall intensity.

VARIATION AMONG BASINS

Differences in the regression coefficients for the independent variables among the several streams used in the analyses may indicate part of the difference in the characteristics of drainage basins to cause storm-to-storm variation in sediment movement. Table 8 shows that the standard error of estimate S_e varies some for a given basin depending on the combination of independent variables used in the regression. The variation of S_e for several combinations of variables at a given location, however, is small compared to that among basins.

The list of equations by basins for the single, double, and triple most significant independent variables (table 9) further demonstrates that even though S_e decreases somewhat as the number of variables is increased, there is a range of S_e among the basins. This is caused by either some error in the basic data or, more likely, the variance of hydrologic and environmental factors which cannot be evaluated at this time. Evidence from the list of equations of the effect of intercorrelation among the independent variables suggests that if one variable contained considerable

error it would be replaced by another variable of greater significance. When this takes place, or when all variables except one or two remain, however, the error of estimate is not materially changed.

TABLE 9.—*The regression equations, by streams, for 1, 2, or 3 independent variables*

One independent variable		
Scantic	Log C=1.714+0.227 log Q_b	S_e=0.144
Brandywine	Log C=1.255+.400 log Q_w	S_e= .242
Hazel	Log C=1.563+.308 log P_a	S_e= .311
	Log C=1.973+.0082 T_a	S_e= .312
Rappahannock	Log C=2.193+.0054 T_a	S_e= .267
Rapidan	Log C=1.702+.259 log Q_w	S_e= .315
James, Buchanan		
James, Scottsville	Log C=0.683+0.425 log P_a	S_e= .204
Two independent variables		
Scantic	Log C=1.719+0.2106 log Q_b+0.031 P_i	S_e=0.142
Brandywine	Log C=.349+.582 log Q_w+.239 P_i	S_e= .220
Hazel	Log C=.809+.324 log Q_w+.0115 T_a	S_e= .273
	Log C=.704+.399 log P_a+.0108 T_a	S_e= .265
	Log C=1.576+.368 log $10R_i$+.0080 T_a	S_e= .296
Rappahannock	Log C=1.280+.233 log Q_w+.0078 T_a	S_e= .246
Rapidan	Log C=.957+.335 log Q_w+.0091 T_a	S_e= .289
James, Buchanan	Log C=1.352+.203 log Q_w−.0038 M_t	S_e= .308
James, Scottsville	Log C=1.129−.211 log Q_b+.496 log P	S_e= .198
Three independent variables		
Scantic	Log C=1.532+0.082 log Q_w+0.200 log Q_b+0.035 P_i	S_e=0.139
Brandywine	Log C=.122+.606 log Q_w+.0038 T_a+.208 P_i	S_e= .313
Hazel	Log C=.462+.391 log Q_w+.0106 T_a+.304 P_i	S_e= .268
	Log C=.554+.291 log Q_w+.0086 T_a+.441 log $100R_i$	S_e= .260
	Log C=.719−.0018 M_t+.0112 T_a+.402 log P_a	S_e= .266
Rappahannock	Log C=1.373+.232 log Q_w−.0021 M_t+.0079 T_a	S_e= .240
Rapidan	Log C=1.035+.327 log Q_w−.0027 M_t+.0094 T_a	S_e= .286
James, Buchanan	Log C=.036+.373 log Q_w−.0043 M_t+.0117 T_a	S_e= .278
James, Scottsville	Log C=1.271−.0029 M_t−.262 log Q_b+.525 log P_a	S_e= .192

EXAMPLES OF APPLICATION

RANGE OF SPECIFIC VARIABLES

The multiple regression equations determined in this analysis consists of an equation constant and coefficients for each independent variable. Each independent variable may affect the dependent variable through its range of values depending on the magnitude of the coefficient. One of the equations determined for the James River at Buchanan, Va. (see table 8) will be used to demonstrate this effect.

$$\text{Log } C=0.960+0.532 \log Q_w-0.0053\ M_t+0.00777\ T_a -0.556 \log Q_b+1.019\ P_i.$$

The following realistic minimum and maximum values of the variables are applied:

Q_w=1,000 and 100,000 cfs-days; log Q_w=3.00 and 5.00

M_t=1 and 65 months

T_a=35° and 75°F

Q_b=316 and 3,160 cfs; log Q_b=2.5 and 3.5

P_i=0.19 and 0.64

$$\text{Log } C\text{ (max)}=+0.960+2.659-0.344+0.583-1.943+0.652$$
$$=+2.567\pm0.230 \text{ or } C=369 \text{ ppm ranging from 217 to 626 ppm.}$$

$$\text{Log } C\text{ (min)}=+0.960+1.594-0.005+0.272-1.388+0.194$$
$$=+1.627\pm0.230 \text{ or } C=42 \text{ ppm ranging from 25 to 72 ppm.}$$

The differences between the maximum and minimum factors for these equations are +1.065, −0.339, +0.311, −0.555, and +0.458 log units for Q_w, M_t, T_a, Q_b, and P_i, respectively. These differences are all greater than S_e or 0.230 log units, and therefore, further indicate that these factors all yield a significant change in the dependent variable.

COMPARISON OF LOCATIONS

For comparing the regression equations between locations, the mean values of the independent variables will be used (see table 5) to compute the value of the dependent variable. The simplest comparison can be made by use of the equations for one and three independent variables as given in table 9.

For the single variable on the Brandywine Creek:

$$\text{Log } C=+1.255+0.400 \log Q_w$$
$$=+1.255+0.400\times3.161$$
$$=+2.520\pm0.242$$

This is an average of 331 ppm or a range from 190 to 578 ppm.

For the Rapidan River:

$$\text{Log } C=+1.702+0.259 \log Q_w$$
$$=+1.702+0.259\times3.234$$
$$=+2.540\pm0.315$$

This is a mean of 347 ppm or a range from 168 to 716 ppm. The regression slope of log Q_w is 0.400 for the Brandywine and 0.259 for the Rapidan, yet the mean concentration is nearly the same, due somewhat to the higher mean of log Q_w for the Rapidan, but mostly due to the greater equation constant for the Rapidan.

For the three independent variables on the Brandywine Creek:

$$\text{Log } C=0.122+0.606 \log Q_w+0.0038\ T_a+0.208\ P_i$$
$$=0.122+0.606\times3.161+0.0038\times50.93+0.208\times1.383$$
$$=2.518\pm0.213$$

This is a mean of 329 ppm or a range from 202 to 538 ppm.

For the Hazel River:

$$\text{Log } C=+0.462+0.391 \log Q_w+0.0106\ T_a+0.304\ P_i$$
$$=+0.462+0.391\times3.016+0.0106\times55.63+0.304\times0.650$$
$$=+2.426\pm0.268$$

This is a mean of 267 ppm or a range from 144 to 494 ppm. Comparison of the latter more complicated equations with the single variable equations shows that the Brandywine has the greater Q_w and P_i factors and that the Hazel has the greatest equation constant and T_a factors but the totals differ by less than 0.1 log unit. Note that the range defined by the limits of S_e is considerably less when three variables instead of one are used.

EXTRAPOLATION TO OTHER STREAMS

In order to demonstrate the feasibility of applying the computed regression formulas to other streams, testing with observed data from some other locations is necessary. Observed data are available for 15 storms on the Shenandoah River at Front Royal, Va., (1,638 sq mi) and for 14 storms on the Potomac River at Point of Rocks, Md., (9,650 sq mi). The Shenandoah data were obtained during the same period, and the Potomac data were obtained 7 or 8 years later than the data from which the models were derived. The Potomac River data, in addition to a somewhat different time span, also represent a much larger and more diverse basin than that from which the models were derived. The data are listed in table 10. The following are equations from the appendix for testing these data:

1. III–3 from the Brandywine Creek,

$$\text{Log } C = +0.181 + 0.610 \log Q_w - 0.00139 M_t + 0.00390 T_a + 0.214 P_t - (0.208)$$

2. III–2 from the Rappahannock River,

$$\text{Log } C = +1.059 + 0.289 \log Q_w - 0.00190 M_t + 0.00760 T_a + 0.199 P_t - (0.239)$$

3. IV from the James River at Buchanan, Va.,

$$\text{Log } C = -0.649 + 0.454 \log Q_w - 0.00333 M_t + 0.01175 T_a + 0.769 P_t - (0.269).$$

TABLE 10.—*Measured data for extrapolation of models to other streams*

Observation No.	Log C	Log Q_w	M_t	T_a	P_t
Shenandoah River					
1	1.88	3.72	34	38	0.65
2	2.81	4.53	35	41	.59
3	2.04	3.63	35	49	.90
4	2.39	4.18	38	73	.25
5	2.99	4.49	42	58	.52
6	2.25	4.39	43	44	.32
7	2.35	4.27	44	37	.53
8	2.38	4.21	46	39	.39
9	2.66	4.59	47	46	.27
10	2.40	4.16	47	50	.47
11	1.97	3.94	48	58	.41
12	2.05	3.68	48	59	.48
13	2.49	4.45	50	72	.20
14	2.58	4.45	52	75	.56
15	2.97	5.16	52	74	.43
Potomac River					
1	2.68	4.65	102	62	0.59
2	2.23	4.58	105	37	.71
3	2.90	5.41	107	52	.38
4	2.61	5.31	108	53	.51
5	2.77	5.29	109	63	.64
6	2.30	4.87	109	69	.60
7	2.92	5.34	117	41	.47
8	2.65	5.24	117	42	.53
9	2.29	5.30	119	55	.40
10	2.34	5.10	119	57	.52
11	1.90	4.13	120	63	1.29
12	2.11	4.73	120	67	.54
13	2.38	3.99	121	72	1.08
14	2.22	4.28	125	55	.77

The computed sediment concentration derived for each storm and for each model was plotted against the observed concentration in figures 19 and 20 for the Shenandoah and Potomac Rivers, respectively. The results show that:

1. None of the applications are reasonably close to the line of agreement; and, therefore, it is extremely dangerous to extend specific formulas to other basins.
2. The size of the river basin determines the shift of the computed values from the observed values. The model from the smallest stream (Brandywine Creek) yields results that are about 0.6 log unit too large when the Shenandoah data are used and about 0.9 log unit too large when the Potomac data are used. Also, the data from the larger Potomac River basin yield computed values for the three formulas that average about 0.2 log unit greater than data from the Shenandoah.
3. The concentrations computed from the models do not increase as rapidly as the observed concentrations. The Brandywine formula is not as serious in this respect as are the Rappahannock and James River formulas.

Although a given formula apparently cannot be extrapolated to another stream, the hypothesis that the general model can be extrapolated is still open. Thus, assuming that the observed data for the Shenandoah and Potomac are statistically representative, trial and error modification of the James River and Brandywine Creek formulas was made to shift the computed concentration. Shifting the set of computed values up and down on the ordinate of figures 19 and 20 is accomplished by adjusting the equation constant. Change in the slope and scatter of the set is accomplished by shifting the emphasis on Q_w or P_t. Due to the proximity of the James River and Brandywine Creek basins to the Shenandoah and Potomac River basins, there is little justification for altering the factors for M_t and T_a.

To accommodate the conditions exhibited by the Shenandoah River data, the equation constant and the coefficients for log Q_w and P_t in the James River formula were changed by trial and error to a modified formula,

$$\text{Log } C = -0.600 + 0.600 \log Q_w - 0.00333 M_t + 0.01175 T_a + 0.200 P_t.$$

The James River formula was also changed to accommodate the Potomac River data to

$$\text{Log } C = -0.800 + 0.600 \log Q_w - 0.00333 M_t + 0.01175 T_a.$$

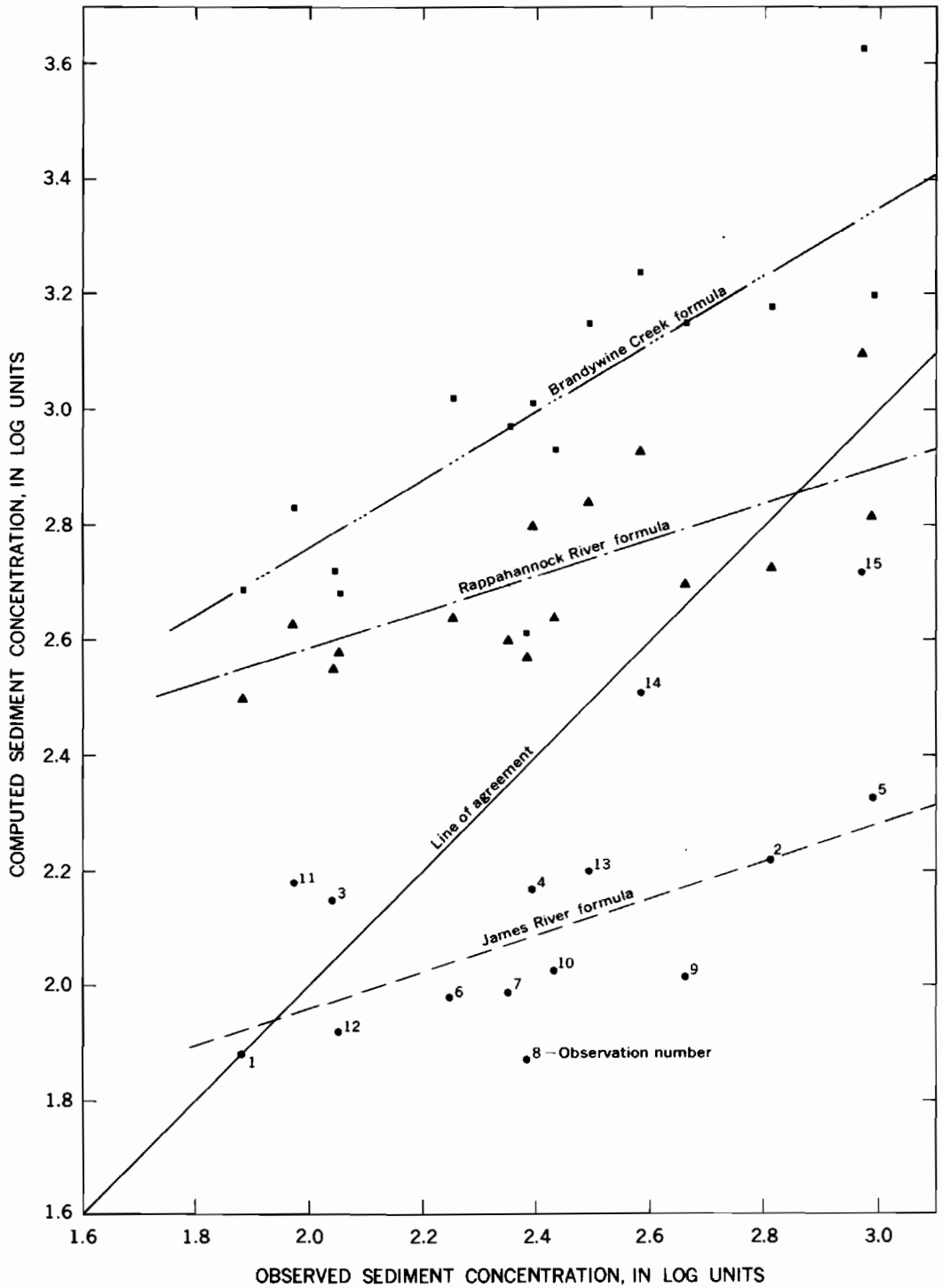

FIGURE 19.—Test of selected models against observed data for Shenandoah River.

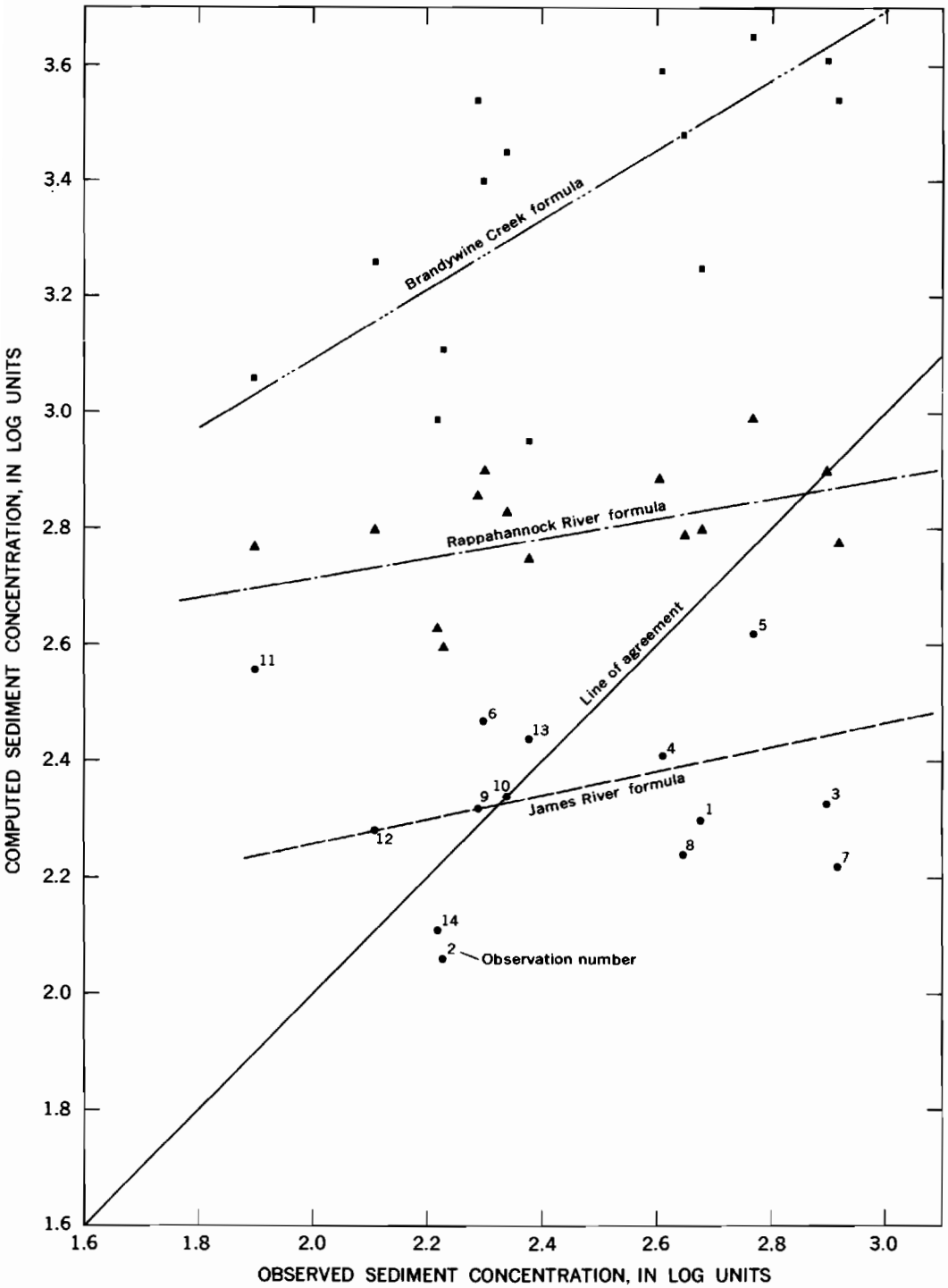

FIGURE 20.—Test of selected models against observed data for Potomac River.

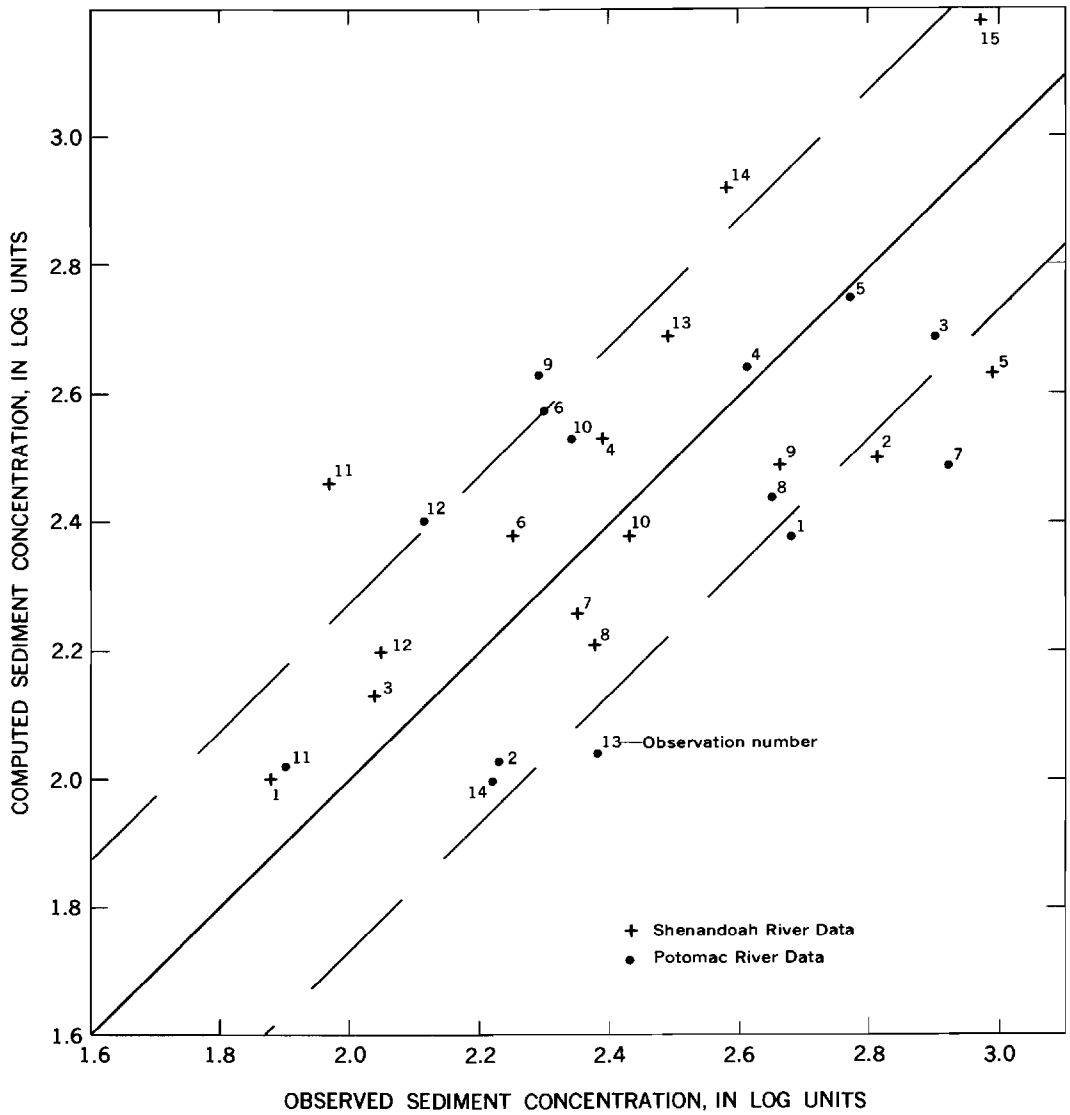

FIGURE 21.—Comparison of the modified formula for James River at Buchanan with the observed data for the Shenandoah and Potomac Rivers.

Figure 21 compares the computed sediment concentration from each modified formula with their respective observed sediment concentrations. The results of the comparison are reasonable in that the computed values are sufficiently close to the line of agreement so that all but 4 out of 15 for the Shenandoah River and all but 5 out of 14 points for the Potomac River are within the standard error of estimate (0.269 log units) defined by the original James River model.

In a like manner, the Brandywine Creek formula was changed to

$$\text{Log } C = -0.700 + 0.700 \log Q_w - 0.00139\, M_t + 0.00390\, T_a$$

to accommodate the Shenandoah River data; and to

$$\text{Log } C = -0.970 + 0.700 \log Q_w - 0.00139\, M_t + 0.00390\, T_a$$

to accommodate the Potomac River data. Comparison of the computed values from these modified formulas with the observed data (fig. 22) is within the standard error of estimate (0.208 log units) defined by the original Brandywine model.

The similarity of the two modified models is indicated by the similarity of the deviations from the line of agreement with respect to the individual storms. For example, in figures 21 and 22, note that observations 2 and 5 for the Shenandoah and 1 and 13 for the Potomac plot below the limits of one S_e.

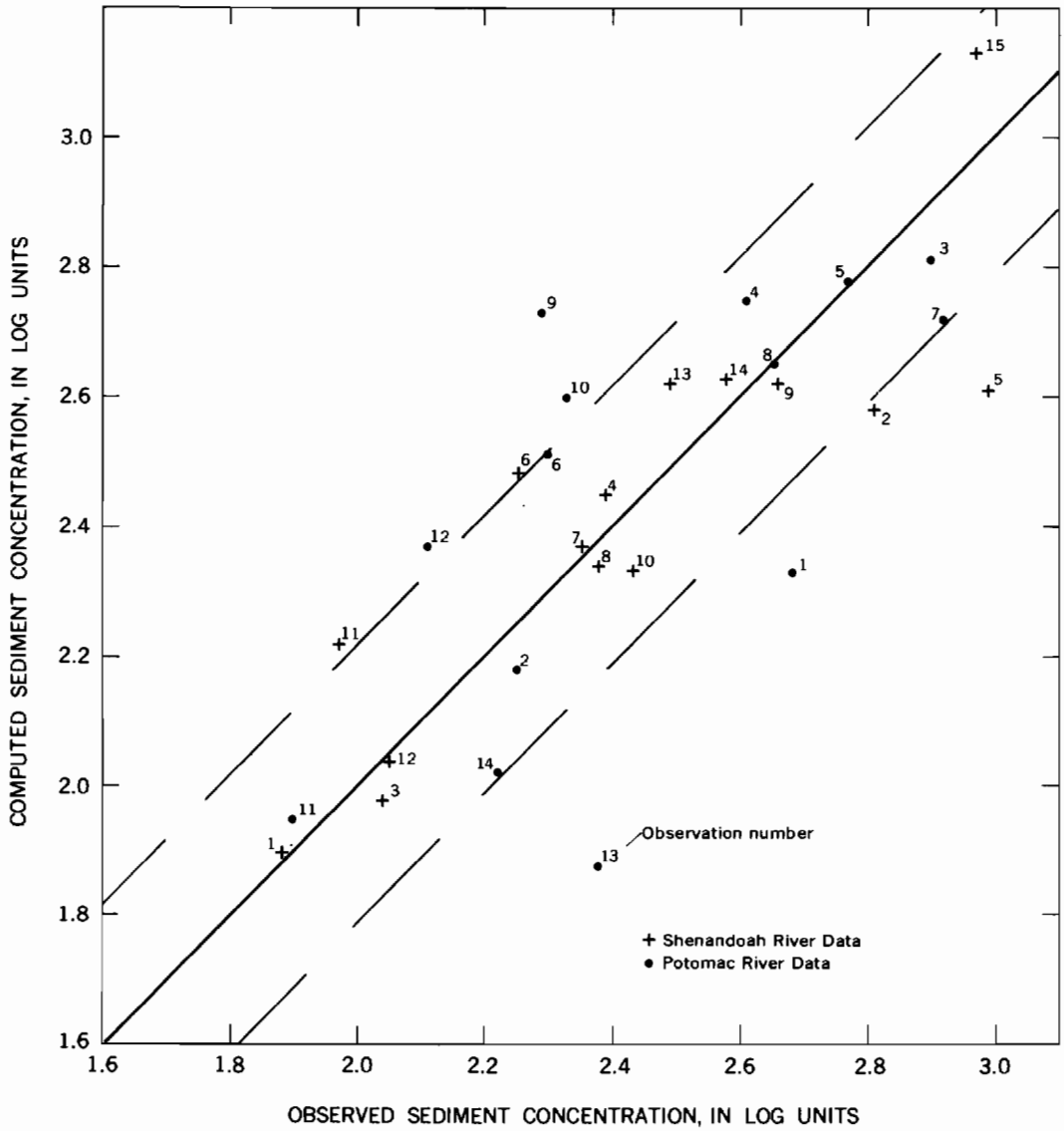

FIGURE 22.—Comparison of the modified formula for Brandywine Creek with the observed data for the Shenandoah and Potomac Rivers.

SUMMARY

The analysis of some storm period variables affecting stream sediment transport has involved a study of available sediment data to determine which hydrologic, physical, and biological factors cause sediment variation in time and space. The knowledge gained from this and other similar analyses can be used to interpret and extrapolate the small amount of information available from existing or reconnaissance sediment data.

A review of the theory of sediment yield and transport shows that most of the fine sediment (clay and silt sizes) eroded from a drainage basin is easily suspended by the stream turbulence and hence readily moved through the channel system; whereas, the coarser sediment (sands, gravels) are moved in accordance with the interaction of the stream energy on the particle and the settling rate of the particles. The amount of coarse sediment transported is generally much less than half the total sediment discharge. The coarse sediment discharge can be approximately determined by considering hydraulic factors; such considerations are beyond the scope of this report. The most important variables for consideration in the analysis involve the forces of erosion and transport as related to fine sediment.

These forces operate during or immediately following periods of substantial precipitation and runoff from the land surface, thus the adopted hydrologic unit for study in this report is the storm event. Subsurface and ground-water runoff are not important erodents

of the land surface; therefore, only the surface runoff part of the hydrograph is used.

Analysis of data to determine the cause of sediment variation was accomplished by a combination of graphical and analytical multiple regression methods. Graphical correlation was necessary to determine which variable to consider, to determine the required transformation of the data, and to note unusual elements of the relationship. Using the general regression model

$$Y=b_o+b_1x_1+b_2x_2+\ .\ .\ .\ +b_nx_n,$$

the analytical method was then used to obtain the best estimate of the equation coefficients and their significance and the standard error of the equation. The analysis was made using data for seven stream locations in the Atlantic coast area through a program developed for the Burroughs 220 computer.

The graphical search for variables useful to explain the variation of sediment concentration or discharge from storm to storm showed that:

1. The month during the period of record may be used to indicate the trend of change of time.
2. The quantity of surface runoff, expressed in log units, should be used as a measure of the magnitude and intensity of erosion and transport—precipitation quantity, also in log units, is not as effective.
3. The long-term mean air temperature for the time of year of the given storm can be used as a measure of seasonal change.
4. Ground-water runoff of the stream prior to storm runoff, expressed in log units, is a convenient measure of antecedent conditions.
5. The peakedness of the storm hydrograph can be used as a measure of storm intensity. Precipitation intensity, expressed in log units, is sometimes too difficult to evaluate and too inaccurately determined for an effective measure of storm intensity.

The computer program is designed to print out simple correlation coefficients and their significance. These indicate the degree of intercorrelation among the variables for a given set of storm-period data at a stream location. In general terms, the correlations show a tendency for:

1. The mean concentration of sediment in the storm runoff to increase with sediment discharge, water discharge, air temperature, peak flow, rainfall quantity, and rainfall intensity.
2. The quantity of sediment discharge to increase with water discharge, peak flow, rainfall quantity, and rainfall intensity, and to decrease with peakedness index.
3. The quantity of water discharge per storm event to increase with ground-water runoff, peak flow, and rainfall quantity, and to decrease with air temperature and peakedenss index.
4. The ground-water runoff to increase with peak flow and to decrease with time during the period of record, air temperature, peakedness index, rainfall quantity, and rainfall intensity.
5. The peak flow to increase with rainfall quantity.
6. The rainfall quantity to increase with rainfall intensity.

Comparison of log Q_s (sediment discharge) and log C (sediment concentration) for use as the dependent variable in the analytical computation of the multiple regression equation was completed for the Hazel River and Brandywine Creek. The two most important conclusions from this comparison are: (1) the standard error of estimate is less for log C than for log Q_s but not appreciably so; (2) when log Q_s is used, the very high degree of significance for log Q_w causes a decrease of significance for the remaining independent variables.

It was noted from the regression equations that variation of coefficients for a specific variable at a specific stream location, when different sets of variables are used, is largely due to the effects of intercorrelation among the variables. In regard to a measure of storm size, water discharge proves to be the most important independent variable for describing sediment variation, and rainfall quantity is generally the least important. The poor significance of rainfall quantity is probably due to the poor quality of available data and its high degree of intercorrelation with quantity of runoff and other hydrologic factors.

The regression coefficients for time during the period of record show a reduction of sediment concentration with time for nearly all sets of variables. This reduction is statistically significant for the locations on the Brandywine Creek and the James River basins.

The equations show that sediment concentration increases significantly with mean air temperature or time of the year for all streams except the Scantic and the James River at Scottsville.

Although the regression coefficients for ground-water runoff were not significant for the Hazel, Rappahannock, and Rapidan Rivers and not highly significant in other basins, the sediment concentration tends to decrease as ground-water runoff increases.

Of the three measures of storm intensity, only peakedness index was determined for all streams. Sediment in streams tends to increase with each of measures of storm intensity.

The standard error of estimate for the equations varies much more among the different streams than among the different combinations of variables for a given stream. This is caused by the variance of hydrologic and environmental factors not evaluated by the data used, or possibly by some error in the basic data. The standard error of estimate ranges from 0.14 to 0.30 of a log unit for most computed combinations of variables.

Three of the regression formulas were tested with observed data from 15 storm events on the Shenandoah River at Front Royal, Va., and from 14 storm events on the Potomac River at Point of Rocks, Md. The results indicated four points of interest: (1) None of the computed concentration values were consistently close to agreement with the observed values. (2) The relative size of the river basin determines the shift of the computed values from the observed values. (3) The ratio of the computed to the measured values decreases as the observed values increase. (4) The formulas can be modified to yield computed values in good agreement with the observed values.

RECOMMENDATIONS

Although the analysis of data for seven stream locations in the Atlantic coast area using several combinations of variables yields formulas for predicting sediment transport, it is apparent that extrapolation to basins of different sizes and locations is not practical at this stage.

Four areas of further study are apparent:

1. Continue the search for suitable independent variables and their proper transformation. This would further explain the storm-to-storm variation for specific stream locations.
2. Determine the effect of the number of storm events on the equation and its significance for at least three stream locations.
3. Reduce to dimensionless terms the data that is affected by drainage basin size. This would include such variables used in this study as sediment discharge Q_s, water discharge Q_w, ground-water runoff Q_b, and peak flow P_n.
4. Extend the work to other stream locations to encompass environments of considerably different climate, soil characteristics, topography, vegetative cover, drainage density, and drainage basin size. Measures of these characteristics on a stream location basis must be developed.

The results of such studies will help to advance progress toward development of a "universal equation" for computing stream sediment transport through application of specific observed variables.

REFERENCES

Campbell, F. B., and Bauder, H. A., 1940, A rating curve method for determining silt discharge of streams: Am. Geophys. Union Trans., part 2, p. 603–607.

Colby, B. R., 1956, Relationship of sediment discharge to streamflow: U.S. Geol. Survey open-file report, 170 p.

——— 1961, Effect of depth of flow on discharge of bed material: U.S. Geol. Survey Water-Supply Paper 1498–D.

Dawdy, D. R., 1961, Depth-discharge relations of alluvial streams—discontinuous rating curves. U.S. Geol. Survey Water-Supply Paper 1498–C, 16 p.

Dixon, Wilfred J., and Massey, Frank J., 1957, Introduction to statistical analysis: New York, McGraw-Hill, 2d ed.

Einstein, H. A., 1950, The bed-load function for sediment transport in open channels: U.S. Dept. Agriculture Tech. Bull. 1026, 70 p.

Ezekiel, Mordecai, and Fox, Karl A., 1959, Methods of correlation and regression analysis: New York, John Wiley and Sons, 3d ed.

Glymph, L. M., Jr., 1951, Relation of sedimentation to accelerated erosion in the Missouri River Basin: U.S. Dept. Agriculture, SCS–TP–102, p. 6.

——— 1954, Studies of sediment yields from watersheds: Assoc. Internac. d'Hydrol. Sci., U. Geophys. Internac., Assemblee Generale de Rome.

Guy, H. P., 1951, Level terrace design as affected by hydrologic factors: Unpublished thesis, Iowa State College, Ames, Iowa, p. 23–24.

Heidel, S. G., 1956, The progressive lag of sediment concentration with flood waves: Am. Geophys. Union Trans., v. 37, no. 1, p. 56.

Hubbell, D. W., and Matejka, D. Q., 1959, Investigations of sediment transportation Middle Loup River at Dunning, Nebraska: U.S. Geol. Survey Water-Supply Paper 1476, p. 72.

Johnson, A. W., 1961, Highway erosion control: Am. Soc. Agricultural Engineers Trans., v. 4, no. 1, p. 144–152.

Lane, E. W., 1955, The importance of fluvial morphology in hydraulic engineering: Am. Soc. Civil Engineers Proc., Vol. 81, Paper No. 475.

Langbein, W. B., and Schumm, S. A., 1958, Yield of sediment in relation to mean annual precipitation: Am. Geophys. Union Trans., 39, p. 1076–1084.

Leopold, L. B., and Maddock, Thomas, Jr., 1953, The hydraulic geometry of stream channels and some physiographic implications: U.S. Geol. Survey Prof. Paper 252, 57 p.

Maner, S. B., 1958, Factors affecting sediment delivery rates in the Red Hills physiographic area: Am. Geophys. Union Trans., 39, p. 669–675.

Miller, C. R., 1951, Analysis of flow-duration, sediment-rating curve method of computing sediment yield: U.S. Bur. of Reclamation Report, 15 p.

Rouse, Hunter, 1950, Engineering hydraulics: New York, John Wiley & Sons, p. 83–103.

Sayre, W. W., Guy, H. P., and Chamberlain, A. R., 1963, Uptake and transport of radionuclides by stream sediments: U.S. Geol. Survey Prof. Paper 433–A.

Simons, D. B., Richardson, E. V., and Haushild, W. L., 1962, Some properties of water-clay dispersions and their effects on flow: U.S. Geol. Survey Water-Supply Paper, 1498–G.

Snedecor, G. W., 1956, Statistical methods: Ames, Iowa, Iowa State College Press, 5th ed.

Stall, J. B., and Bartelli, L. J., 1959, Correlation of reservoir sedimentation and watershed factors, Springfield Plain, Ill.: Illinois State Water Survey, Report of Investigation 37.

U.S. Dept. of Commerce, 1961, Rainfall frequency atlas of the United States: Technical Paper No. 40, p. 113.

Wischmeier, W. H., 1962, Rainfall erosion potential: Agricultural Engineering, v. 43, no. 4, p. 212.

Wischmeier, W. H., and Smith, D. D., 1958, Rainfall energy and its relationship to soil loss: Amer. Geophys. Union Trans., v. 39, no. 2, p. 285.

APPENDIX

MULTIPLE REGRESSION EQUATIONS

This appendix contains regression equations for seven stream locations in the Atlantic coast area and for selected combinations of variables used in the analyses to show the effect of these variables in predicting sediment conditions on the basis of storm events. The relative value of each equation is indicated by the standard error of estimate of the dependent variable in terms of log units. This is shown in parentheses at the end of each equation. The significance of the regression coefficients is indicated by superscript as follows:

a. Very highly significant (99.9 percent level).
b. Highly significant (99 percent level).
c. Significant (95 percent level).
d. Poorly significant (90 percent level).
e. Very poorly significant (80 percent).

Where a superscript is not shown with a coefficient, the variable cannot be considered useful in explaining sediment variation. Such a variable, however, cannot be dropped from a specific equation without adjustment to coefficients of other variables.

SCANTIC RIVER NEAR BROAD BROOK, CONNECTICUT

Surface runoff—65 storm events

I. Log C is dependent variable

1. $\text{Log } C=1.548+0.151^{c} \log Q_w-0.00001\ M_t+0.00115\ T_a+0.163^{c} \log Q_b+0.036^{e}\ P_t-0.138^{e} \log 10\ R_q \quad S_e=0.140$
2. $\text{Log } C=1.547+0.151^{c} \log Q_w+0.00114\ T_a+0.163^{c} \log Q_b+0.036^{c}\ P_t-0.138^{d} \log 10\ R_q \quad S_e=0.138$
3. $\text{Log } C=1.551+0.143^{c} \log Q_w+0.177^{c} \log Q_b+0.037^{c}\ P_t-0.113^{e} \log 10\ R_q \quad S_e=0.138$
4. $\text{Log } C=1.532+0.082^{d} \log Q_w+0.200^{b} \log Q_b+0.035^{c}\ P_t \quad S_e=0.139$
5. $\text{Log } C=1.719+0.211^{b} \log Q_b+0.0314^{d}\ P_t \quad S_e=0.142$
6. $\text{Log } C=1.714+0.227^{b} \log Q_b \quad S_e=0.144$

II

1. $\text{Log } C=1.516+0.135^{c} \log Q_w-0.00021\ M_t+0.00121\ T_a+0.190^{c} \log Q_b-0.153^{d} \log 10\ R_q+0.065 \log 100\ R_t \quad S_e=0.144$
2. $\text{Log } C=1.492+0.135^{c} \log Q_w+0.00112\ T_a+0.196^{c} \log Q_b-0.149^{e} \log 10\ R_q+0.068 \log 100\ R_t \quad S_e=0.143$
3. $\text{Log } C=1.567+0.135^{c} \log Q_w+0.00138\ T_a+0.182^{c} \log Q_b-0.132^{e} \log R_q \quad S_e=0.142$
4. $\text{Log } C=1.572+0.125^{c} \log Q_w+0.200^{b} \log Q_b-0.102^{e} \log 10\ R_q \quad S_e=0.142$
5. $\text{Log } C=1.553+0.070^{e} \log Q_w+0.219^{b} \log Q_b \quad S_e=0.143$
6. $\text{Log } C=1.714+0.227^{b} \log Q_b \quad S_e=0.144$

Total runoff—65 storm events

III

1. $\text{Log } C=0.033+0.502^{a} \log Q_w-0.00100M_t+0.00019T_a-0.208^{d} \log Q_b+1.202^{a}P_t \quad S_e=0.179$
2. $\text{Log } C=0.031+0.503^{a} \log Q_w-0.00102M_t-0.206^{c} \log Q_b+1.205^{a}P_t \quad S_e=0.177$
3. $\text{Log } C=0.134+0.487^{a} \log Q_w-0.216^{c} \log Q_b+1.225^{a}P_t \quad S_e=0.177$
4. $\text{Log } C=0.090+0.398^{a} \log Q_w+1.387^{a}P_t \quad S_e=0.178$
5. $\text{Log } C=1.259+1.155^{a}P_t \quad S_e=0.213$

IV

1. $\text{Log } C=0.024+0.415^{a} \log Q_w+0.00131M_t-0.00104T_a-0.127 \log Q_b+1.171^{a}P_t+0.142^{e} \log 10R_q \quad S_e=0.178$
2. $\text{Log } C=0.034+0.423^{a} \log Q_w+0.00120M_t-0.148^{e} \log Q_b+1.159^{a}P_t+0.121^{e} \log 10R_q \quad S_e=0.177$
3. $\text{Log } C=0.154+0.412^{a} \log Q_w-0.166^{e} \log Q_b+1.187P_t+0.109 \log 10R_q \quad S_e=0.178$
4. $\text{Log } C=0.134+0.488^{a} \log Q_w-0.216^{c} \log Q_b+1.225^{a}P_t \quad S_e=0.178$
5. $\text{Log } C=1.259+1.155^{a}P_t$

V

1. $\text{Log } C=0.267+0.404^{b} \log Q_w+0.00181^{e}\ M_t-0.00138\ T_a-0.184^{e} \log Q_b+0.105 \log 10\ R_q+0.0256^{e} \log 100\ R_t \quad S_e=0.200$
2. $\text{Log } C=0.311+0.412^{b} \log Q_w+0.000165^{e}\ M_t-0.214^{d} \log Q_b+0.086 \log 10\ R_q+0.225^{e} \log 100\ R_t \quad S_e=0.199$
3. $\text{Log } C=0.241+0.460^{a} \log Q_w+0.00157^{e}\ M_t-0.239^{c} \log Q_b+0.290^{c} \log 100\ R_t \quad S_e=0.198$
4. $\text{Log } C=0.435+0.438^{a} \log Q-0.263^{c} \log Q_b+0.275^{d} \log 100\ R_t \quad S_e=0.200$
5. $\text{Log } C=0.768+0.481^{a} \log Q_w-0.341^{b} \log Q_b \quad S_e=0.204$
6. $\text{Log } C=0.527+0.327^{a} \log Q_w \quad S_e=0.217$

Total runoff—136 storm events

[Rainfall data not available]

VI

1. $\text{Log } C=0.549+0.695^{a} \log Q_w+0.00128\ M_t+0.00147\ T_a-0.318^{b} \log Q_b+1.42^{a}\ P_t \quad S_e=0.2387$
2. $\text{Log } C=-0.480+0.683^{a} \log Q_w+0.00132\ M_t-0.311^{b} \log Q_b+1.461^{a}\ P_t \quad S_e=0.239$
3. $\text{Log } C=-0.375+0.672^{a} \log Q_w-0.325^{b} \log Q_b+1.472^{a}\ P_t \quad S_e=0.239$
4. $\text{Log } C=-0.677+0.538^{a} \log Q_w+1.56^{a}\ P_t \quad S_e=0.247$
5. $\text{Log } C=0.558+0.285^{a} \log Q_w \quad S_e=0.279$

BRANDYWINE CREEK AT WILMINGTON, DELAWARE
Surface runoff—138 storm events

I

1. $\text{Log } C=0.886+0.644^{a} \log Q_w-0.00155^{b} M_t +0.00385^{c} T_a-0.195^{c} \log Q_b-0.365^{c} \log 10 R_q +0.338^{b} \log 100 R_t \quad S_e=0.215$
2. $\text{Log } C=0.450+0.559^{a} \log Q_w-0.00137^{c} M_t +0.0038^{c} T_a-0.208^{e} \log 10 R_q+0.368^{b} \log 100 R_t \quad S_e=0.218$
3. $\text{Log } C=0.611+0.452^{a} \log Q_w-0.00136^{c} M_t +0.00241^{d} T_a+0.353^{b} \log 100 R_t \quad S_e=0.219$
4. $\text{Log } C=0.674+0.429^{a} \log Q_w-0.00137 M_t +0.463^{a} \log 100 R_t \quad S_e=0.220$
5. $\text{Log } C=0.610+0.430^{a} \log Q_w+0.446^{a} \log 100 R_t \quad S_e=0.224$
6. $\text{Log C}=1.255+0.400^{a} \log Q_w \quad S_e=0.241$

II

1. $\text{Log C}=1.039+0.325^{c} \log Q_w-0.00199^{a} M_t +0.00554^{a} T_a-0.183^{c} \log Q_b+0.333^{a} \log P_n -0.274^{d} \log 10 R_q \quad S_e=0.211$
2. $\text{Log } C=1.029+0.166^{d} \log Q_w-0.00195^{a} M_t +0.00431^{a} T_a-0.109_{e} \log Q_b+0.352^{a} \log P_n \quad S_e=0.213$
3. $\text{Log } C=0.731+0.155^{d} \log Q_w-0.00186^{b} M_t +0.00462^{a} T_a+0.363^{a} \log P_n \quad S_e=0.213$
4. $\text{Log } C=0.859-0.00208^{a} M_t+0.00411^{a} T_a +0.486^{a} \log P_n \quad S_e=0.215$
5. $\text{Log } C=1.163-0.00194^{b} M_t+0.454^{a} \log P_n \quad S_e=0.224$
6. $\text{Log } C=1.120+0.432^{a} \log P_n \quad S_e=0.232$

III

1. $\text{Log C}=0.406+0.719^{a} \log Q_w-0.00150^{b}M_t +0.00484^{a}T_a-0.124^{e} \log \text{Q}_b+0.196^{a}\text{P}_1 =0.232^{e} \log 10 \text{R}_q \quad S_e=0.208$
2. $\text{Log } C=0.958+0.674^{a} \log Q_w-0.00139^{c} M_t +0.00457^{a} T_a+0.212^{a} P_t-0.127 \log 10 \text{R}_q \quad S_e=0.208$
3. $\text{Log } C=0.181+0.610^{a} \log Q_w-0.00139^{c} M_t +0.00390^{a} T_a+0.214^{a} P_t \quad S_e=0.208$
4. $\text{Log } C=0.121+0.606^{a} \log Q_w+0.00382^{b} T_a +0.208^{a} P_t \quad S_e=0.213$
5. $\text{Log } C=0.349+0.582^{a} \log Q_w+0.239^{a} P_t \quad S_e=0.220$
6. $\text{Log } C=1.255+0.400^{a} \log Q_w \quad S_e=0.241$

IV

1. $\text{Log } Q_s=-1.634+1.633^{a} \log Q_w-0.00142^{c} M_t +0.00365^{c} T_a-0.199^{c} \log Q_b-0.354^{c} \log 10 R_q+0.328_{b} \log 100 R_t \quad S_e=0.216$
2. $\text{Log } Q_s=-2.079+1.546^{a} \log Q_w-0.00123^{c} M_t +0.00317^{d} T_a-0.194^{e} \log 10 R_q+0.359^{b} \log 100 R_t \quad S_e=0.219$
3. $\text{Log } Q_s=-1.929+1.445^{a} \log Q_w-0.00123^{c} M_t +0.00227^{e} T_a+0.346^{b} \log 100 R_t \quad S_e=0.220$
4. $\text{Log } Q=-1.870+1.425^{a} \log Q_w-0.00123^{c} M_t +0.448^{a} \log 100 R_t \quad S_e=0.221$
5. $\text{Log } Q=-1.928+1.426^{a} \log Q_w+0.448^{a} \log 100 R_t \quad S_e=0.224$
6. $\text{Log } Q=-1.320+1.397^{a} \log Q_w \quad S_e=0.240$

V

1. $\text{Log } Q_s=-1.494+1.310^{a} \log Q_w-0.00187^{b} M_t +0.00526^{a} T_a-0.185^{c} \log Q_b+0.336^{a} \log P_n -0.262^{e} \log 10 R_q \quad S_e=0.212$
2. $\text{Log } Q_s=-1.504+1.158^{a} \log Q_w-0.00183^{b} M_t +0.00408^{a} T_a-0.144^{e} \log Q_b+0.355^{a} \log P_n \quad S_e=0.213$
3. $\text{Log } Q_s=-1.817+1.147^{a} \log Q_w-0.00174^{b} M_t +0.00441^{a} T_a +0.366^{a} \log P_n \quad S_e=0.214$
4. $\text{Log } Q_s=-1.884+1.205^{a} \log Q_w+0.00438^{a} T_a +0.298^{a} \log P_n \quad S_e=0.221$
5. $\text{Log } Q_s=-1.744+1.459^{a} \log Q_w+0.0049^{a} T_a \quad S_e=0.229$
6. $\text{Log } Q_s=-1.302+1.397^{a} \log Q_w \quad S_e=0.241$

VI

1. $\text{Log } Q_s=-2.095+1.705^{a} \log Q_w-0.00137^{c} M_t +0.00462^{b} T_a -0.131^{e} \log Q_b+0.189^{a} P_t -0.225^{e} \log 10 R_q \quad S_e=0.210$
2. $\text{Log } Q_s=-2.141+1.596^{a} \log Q_w-0.00131^{c} M_t +0.00358^{b} T_a -0.667 \log Q_b+0.200^{a} P_t \quad S_e=0.211$
3. $\text{Log } Q_s=-2.345+1.600^{a} \log Q_w-0.00125^{c} M_t +0.00374^{b} T_a +0.208^{a} P_t \quad S_e=0.211$
4. $\text{Log } Q_s=-2.399+1.597^{a} \log Q_w-0.00366^{b} M_t +0.202^{a} P_t \quad S_e=0.214$
5. $\text{Log } Q_s=-2.180+1.574^{a} \log Q_w+0.232^{a} P_t \quad S_e=0.221$
6. $\text{Log } Q_s=-1.302+1.397^{a} \log Q_w \quad S_e=0.241$

HAZEL RIVER NEAR RIXEYVILLE, VA.
Surface runoff—75 storm events

I

1. $\text{Log } C=+0.660+0.474^{a} \log Q_w-0.00289 M_t +0.00153^{a} T_a-0.105 \log Q_b +0.258^{e} P_t-0.149 \log 10 R_q \quad S_e=0.271$
2. $\text{Log } C=0.586+0.397^{a} \log Q_w-0.00242 M_t +0.01101^{a} T_a-0.040 \log Q_b+0.278^{e} P_t \quad S_e=0.270$
3. $\text{Log } C=0.470+0.396^{a} \log Q_w-0.00199 M_t +0.01104^{a} T_a+0.311^{d} P_t \quad S_e=0.268$
4. $\text{Log } C=0.462+0.391^{a} \log Q_w+0.01057^{a} T_a +0.304^{d} P_t \quad S_e=0.268$
5. $\text{Log } C=0.809+0.324^{a} \log Q_w +0.01148^{a} T_a \quad S_e=0.273$
6. $\text{Log } C=1.973+0.00815^{a} T_a \quad S_e=0.312$

II

1. $\text{Log } C = +0.642 + 0.513^{a} \log Q_w - 0.00256\, M_t + 0.00970^{a}\, T_a - 0.178^{e} \log Q_b - 0.421^{e} \log 10\, R_q + 0.533^{a} \log 100\, R_t$ $S_e = 0.255$
2. $\text{Log } C = +0.524 + 0.482^{a} \log Q_w + 0.00909^{a}\, T_a - 0.124 \log Q_b - 0.390^{e} \log 10\, R_q + 0.554^{a} \log 100\, R_t$ $S_e = 0.255$
3. $\text{Log } C = +0.362 + 0.394^{a} \log Q_w + 0.00918^{a}\, T_a - 0.251^{e} \log 10\, R_q + 0.551^{a} \log 100\, R_t$ $S_e = 0.256$
4. $\text{Log } C = 0.554 + 0.291^{a} \log Q_w + 0.00864^{a}\, T_a + 0.441^{b} \log 100\, R_t$ $S_e = 0.259$
5. $\text{Log } C = 0.809 + 0.324^{a} \log Q_w + 0.01148^{a}\, T_a$ $S_e = 0.273$
6. $\text{Log } C = 1.973 + 0.00815^{a}\, T_a$ $S_e = 0.312$

III

1. $\text{Log } C = +0.963 - 0.0045\, M_t + 0.00852^{a}\, T_a + 0.175^{e} \log Q_b + 0.188\, P_t + 0.452^{a} \log 10\, R_q$ $S_e = 0.297$
2. $\text{Log } C = +0.930 + 0.00845^{a}\, T_a + 0.183^{e} \log Q_b + 0.196\, P_t + 0.453^{a} \log 10\, R_q$ $S_e = 0.295$
3. $\text{Log } C = +1.236 + 0.00893^{a}\, T_a + 0.114 \log Q_b + 0.404^{a} \log 10\, R_q$ $S_e = 0.295$
4. $\text{Log } C = 1.576 + 0.00800^{a}\, T_a + 0.368^{b} \log 10\, R_q$ $S_e = 0.296$
5. $\text{Log } C = 1.973 + 0.00815^{a}\, T_a$ $S_e = 0.314$

IV

1. $\text{Log } C = 0.586 + 0.397^{a} \log Q_w - 0.00242\, M_t + 0.01101^{a}\, T_a - 0.040 \log Q_b + 0.278^{e}\, P_t$ $S_e = 0.270$
2. $\text{Log } C = 0.470 + 0.396^{a} \log Q_w - 0.00199\, M_t + 0.01104^{a}\, T_a + 0.311^{d}\, P_t$ $S_e = 0.268$
3. $\text{Log } C = 0.462 + 0.391^{a} \log Q_w + 0.01057^{a}\, T_a + 0.304^{d}\, P_t$ $S_e = 0.268$
4. $\text{Log } C = 0.809 + 0.324^{a} \log Q_w + 0.01148^{a}\, T_a$ $S_e = 0.273$
5. $\text{Log } C = 1.973 + 0.00815^{a}\, T_a$ $S_e = 0.312$

V

1. $\text{Log C} = +0.791 - 0.098 \log Q_w - 0.00200\, M_t + 0.01083^{a}\, T_a - 0.0214 \log Q_b + 0.509^{d} \log P_n$ $S_e = 0.269$
2. $\text{Log } C = +0.745 - 0.125 \log Q_w - 0.00176\, M_t + 0.01085^{a}\, T_a + 0.535^{c} \log P_n$ $S_e = 0.267$
3. $\text{Log } C = 0.719 - 0.00178\, M_t + 0.01125^{a}\, T_a + 0.402^{a} \log P_n$ $S_e = 0.266$
4. $\text{Log } C = 0.704 + 0.01082^{a}\, T_a + 0.399^{a} \log P_n$ $S_e = 0.265$
5. $\text{Log } C = +1.563 + 0.308^{a} \log P_n$ $S_e = 0.311$

VI

1. $\text{Log } C = +0.645 + 0.303^{a} \log Q_w - 0.00175\, M_t + 0.00902^{a}\, T_a - 0.034 \log Q_b + 0.419^{b} \log 100\, R_t$ $S_e = 0.262$
2. $\text{Log } C = +0.568 + 0.294^{a} \log Q_w - 0.00136\, M_t + 0.00901^{a}\, T_a + 0.436^{b} \log 100\, R_t$ $S_e = 0.260$
3. $\text{Log } C = +0.554 + 0.291^{a} \log Q_w + 0.00864^{a}\, T_a + 0.441^{b} \log 100\, R_t$ $S_e = 0.259$
4. $\text{Log } C = 0.809 + 0.324^{a} \log Q_w + 0.01148^{a}\, T_a$ $S_e = 0.273$
5. $\text{Log } C = 1.973 + 0.00815^{a}\, T_a$ $S_e = 0.312$

VII

1. $\text{Log } Q_s = -1.456 + 1.363^{a} \log Q_w - 0.00313\, M_t + 0.01030^{a}\, T_a - 0.151 \log Q_b + 0.141\, P_t - 0.016 \log 10\, R_q$ $S_e = 0.282$
2. $\text{Log } Q_s = -1.464 + 1.355^{a} \log Q_w - 0.00308\, M_t + 0.01025^{a}\, T_a - 0.144^{e} \log Q_b + 0.143\, P_t$ $S_e = 0.280$
3. $\text{Log } Q_s = -1.220 + 1.333^{a} \log Q_w - 0.00345^{e}\, M_t + 0.01052^{a}\, T_a - 0.186^{d} \log Q_b$ $S_e = 0.279$
4. $\text{Log } Q_s = -1.347 + 1.316^{a} \log Q_w + 0.00998^{a}\, T_a - 0.133_e \log Q_b$ $S_e = 0.280$
5. $\text{Log } Q_s = -1.597 + 1.288^{a} \log Q_w + 0.01078^{a}\, T_a$ $S_e = 0.283$
6. $\text{Log } Q_s = -0.677 + 1.182^{a} \log Q_w$ $S_e = 0.324$

VIII

1. $\text{Log } Q_s = -1.644 + 1.406^{a} \log Q_w - 0.00254\, M_t + 0.00837^{a}\, T_a - 0.184^{e} \log Q_b - 0.252 \log 10\, R_q + 0.493^{b} \log 100\, R_t$ $S_e = 0.265$
2. $\text{Log } Q_s = -1.761 + 1.375^{a} \log Q_w + 0.00778^{b}\, T_a - 0.130 \log Q_b - 0.221 \log 10\, \text{R}_q + 0.514^{b} \log 100\, R_t$ $S_e = 0.265$
3. $\text{Log } Q_s = -1.739 + 1.267^{a} \log Q_w + 0.00752^{b}\, T_a - 0.062 \log Q_b + 0.449^{b} \log 100\, R_t$ $S_e = 0.265$
4. $\text{Log } Q_s = -1.873 + 1.252^{a} \log Q_w + 0.00770^{b}\, T_a + 0.478^{b} \log 100\, R_t$ $S_e = 0.265$
5. $\text{Log } Q_s = -1.597 + 1.288^{a} \log Q_w + 0.01078^{a}\, T_a$ $S^{e} = 0.283$
6. $\text{Log } Q_s = -0.677 + 1.182^{a} \log Q_w$ $S_e = 0.324$

IX

1. $\text{Log } Q_s = -0.584 + 0.00390\, M_t + 0.00166\, T_a + 0.654^{b} \log Q_b - 0.059\, P_t + 1.713^{a} \log 10\, R_q$ $S_e = 0.450$
2. $\text{Log } Q_s = -0.686 + 0.00409\, M_t + 0.00149\, T_a + 0.678^{a} \log Q_b + 1.727^{a} \log 10\, R_q$ $S_e = 0.447$
3. $\text{Log } Q_s = -0.571 + 0.00434\, M_t + 0.662^{a} \log Q_b + 1.723 \log 10\, R_q$ $S_e = 0.444$
4. $\text{Log } Q_s = -0.317 + 0.597^{a} \log Q_b + 1.726^{a} \log 10\, R_q$ $S_e = 0.445$
5. $\text{Log } Q_s = +1.198 + 1.537^{a} \log R_q$ $S_e = 0.501$

X

1. $\text{Log } Q_s = -1.464 + 1.355^a \log Q_w - 0.00308\, M_t + 0.01025^a\, T_a - 0.144^e \log Q_b + 0.143\, P_t$ $S_e = 0.280$
2. $\text{Log } Q_s = -1.220 + 1.333^a \log Q_w - 0.00345^e\, M_t + 0.01052^a\, T_a - 0.186^d \log Q_b$ $S_e = 0.279$
3. $\text{Log } Q_s = -1.347 + 1.316^a \log Q_w + 0.00998^a\, T_a - 0.133^e \log Q_b$ $S_e = 0.280$
4. $\text{Log } Q_s = -1.597 + 1.288^a \log Q_w + 0.01078^a\, T_a$ $S_e = 0.283$
5. $\text{Log } Q_s = -0.677 + 1.182^a \log Q_w$ $S_e = 0.324$

XI

1. $\text{Log } Q_s = -1.401 + 1.029^a \log Q_w - 0.00269\, M_t + 0.01005^a\, T_a - 0.119 \log Q_b + 0.431 \log P_n$ $S_e = 0.278$
2. $\text{Log } Q_s = -1.528 + 0.961^a \log Q_w + 0.00957^a\, T_a - 0.067 \log Q_b + 0.403^e \log P_n$ $S_e = 0.278$
3. $\text{Log } Q_s = -1.668 + 0.878^a \log Q_w + 0.00981^a\, T_a + 0.485^e \log P_n$ $S_e = 0.277$
4. $\text{Log } Q_s = -1.597 + 1.288^a \log Q_w + 0.01078^a\, T_a$ $S_e = 0.283$
5. $\text{Log } Q_s = -0.677 + 1.182^a \log Q_w$ $S_e = 0.324$

XII

1. $\text{Log } Q_s = -1.642 + 1.280^a \log Q_w - 0.00205 M_t + 0.00797^b T_a - 0.098 \log Q_b + 0.425^b \log 100\, R_t$ $S_e = 0.266$
2. $\text{Log } Q = -1.739 + 1.267^a \log Q_w + 0.00752^b T_a - 0.062 \log Q_b + 0.449^b \log 100\, R_t$ $S_e = 0.265$
3. $\text{Log } Q = -1.873 + 1.252^a \log Q_w + 0.00770^b T_a + 0.478^b \log 100\, R_t$ $S_e = 0.265$
4. $\text{Log } Q = -1.597 + 1.288^a \log Q_w + 0.01078^a T_a$ $S_e = 0.283$
5. $\text{Log } Q = -0.677 + 1.182^a \log Q_w$ $S_e = 0.324$

RAPPAHANNOCK RIVER AT REMINGTON, VA.

Surface runoff—82 storm events

I

1. $\text{Log } C = 1.328 + 0.323^c \log Q_w - 0.00276^e M_t + 0.00925^a T_a - 0.092 \log Q_b + 0.154 P_t - 0.171 \log 10 R_q$ $S_e = 0.247$
2. $\text{Log } C = 1.130 + 0.270^b \log Q_w - 0.00202 M_t + 0.00890^a T_a + 0.207^e P_t - 0.0752 \log 10 R_q$ $S_e = 0.246$
3. $\text{Log } C = 1.202 + 0.235^a \log Q_w - 0.00215_e M_t + 0.00850^a T_a + 0.190^e P_t$ $S_e = 0.245$
4. $\text{Log } C = 1.462 + 0.191^b \log Q_w - 0.00229^e M_t + 0.00892^a T_a$ $S_e = 0.246$
5. $\text{Log } C = 1.448 + 0.184^b \log Q_w + 0.00843^a T_a$ $S_e = 0.248$
6. $\text{Log } C = 2.162 + 0.00671^a T_a$ $S_e = 0.263$

II

1. $\text{Log } C = 1.395 + 0.325^b \log Q_w - 0.00278^e M_t + 0.00804^a T_a - 0.117 \log Q_b - 0.257 \log 10 R_q + 0.221^d \log 100 R_t$ $S_e = 0.245$
2. $\text{Log } C = 1.230 + 0.238^b \log Q_w - 0.00189 M_t + 0.00753^a T_a - 0.126 \log 10 R_q + 0.240^d \log 100 R_t$ $S_e = 0.245$
3. $\text{Log } C = 1.333 + 0.187^b \log Q_w - 0.00211^e M_t + 0.00711^b T_a + 0.204^d \log 100 R_t$ $S_e = 0.244$
4. $\text{Log } C = 1.313 + 0.180^b \log Q_w + 0.00656^b T_a + 0.215^d \log 100 R_t$ $S_e = 0.246$
5. $\text{Log } C = 1.448 + 0.184^b \log Q_w + 0.00843^a\, T_a$ $S_e = 0.248$
6. $\text{Log } C = 2.162 + 0.00671^a T_a$ $S_e = 0.263$

Surface runoff—124 storm events

[Rainfall data not available]

III

1. $\text{Log } C = 0.826 + 0.286^a \log Q_w - 0.00182^b\, M_t + 0.00791^a\, T_a + 0.0734 \log Q_b + 0.252^d\, P_t$ $S_e = 0.239$
2. $\text{Log } C = 1.059 + 0.289^a \log Q_w - 0.00190^e\, M_t + 0.00760^a\, T_a + 0.199^e\, P_t$ $S_e = 0.239$
3. $\text{Log } C = 1.373 + 0.232^a \log Q_w - 0.00208^b\, M_t + 0.00792^a\, T_a$ $S_e = 0.240$
4. $\text{Log } C + 1.280 + 0.233^a \log Q_w + 0.00782^a\, T_a$ $S_e = 0.246$
5. $\text{Log } C = 2.193 + 0.00544^a\, T_a$ $S_e = 0.267$

I

RAPIDAN RIVER NEAR CULPEPER, VA.

Surface runoff—85 storm events

1. $\text{Log } C = 0.768 + 0.529^a \log Q_w - 0.00284^e\, M_t + 0.00958^a\, T_a - 0.121 \log Q_b + 0.395^d\, P_t - 0.300^e \log 10\, R_q$ $S_e = 0.280$
2. $\text{Log } C = 0.456 + 0.489^a \log Q_w - 0.00209\, M_t + 0.00962^a\, T_a + 0.421^c\, P_t - 0.208 \log 10\, R_q$ $S_e = 0.280$
3. $\text{Log } C = 0.355 + 0.524^a \log Q_w + 0.00970^a\, T_a + 0.429^c\, P_t - 0.275^d \log 10\, R_q$ $S_e = 0.281$
4. $\text{Log } C = 0.566 + 0.400^a \log Q_w + 0.00820^a\, T_a + 0.354^d P_t$ $S_e = 0.284$
5. $\text{Log } C = 0.957 + 0.335^d \log Q_w + 0.00904^a\, T_a$ $S_e = 0.287$
6. $\text{Log } C = 1.702 + 0.259^a \log Q_w$ $S_e = 0.315$

II

1. $\text{Log } C = 1.141 + 0.449^{a} \log Q_w - 0.00268\, M_t + 0.00947^{a}\, T_a - 0.126 \log Q_b - 0.283^{e} \log 10\, R_q \quad S_e = 0.287$
2. $\text{Log } C = 1.307 + 0.438^{a} \log Q_w - 0.00313^{e}\, M_t + 0.01008^{a}\, T_a - 0.149 \log Q_b - 0.249 \log 10\, R_q \quad S_e = 0.286$
3. $\text{Log } C = 0.960 + 0.380^{a} \log Q_w - 0.00222\, M_t + 0.01017^{a}\, T_a - 0.130 \log 10\, R_q \quad S_e = 0.287$
4. $\text{Log } C = 1.035 + 0.327^{a} \log Q_w - 0.00268^{e}\, M_t + 0.00944^{a}\, T_a \quad S_e = 0.286$
5. $\text{Log } C = 0.9568 + 0.335^{a} \log Q_w + 0.00904^{a}\, T_a \quad S_e = 0.287$
6. $\text{Log } C = 1.702 + 0.259^{a} \log Q_a \quad S_e = 0.315$

JAMES RIVER AT BUCHANAN, VA.
Surface runoff—65 storm events

[Computer option to discard least significant variable or each combination was not used]

I

$$\text{Log C} = +0.960 + 0.532^{b} \log Q_w - 0.00530^{b} M_t + 0.00777^{b}\, T_a - 0.556^{a} \log Q_b + 1.019^{a}\, P_t \quad S_e = 0.230$$

II

$$\text{Log C} = +1.783 - 0.486^{d} \log Q_w - 0.00521^{b}\, M_t + 0.00807^{b}\, T_a - 0.572^{a} \log Q_b + 1.027^{a} \log P_n \quad S_e = 0.229$$

III

$$\text{Log C} = +1.625 + 0.418^{a} \log Q_w - 0.00633^{b}\, M_t + 0.00826^{c}\, T_a - 0.482^{a} \log Q_b \quad S_e = 0.252$$

IV

$$\text{Log C} = -0.649 + 0.454^{a} \log Q_w - 0.00333^{d}\, M_t + 0.01175^{a}\, T_a + 0.769^{c}\, P_t \quad S_e = 0.269$$

V

$$\text{Log C} = +0.0359 + 0.373^{a} \log Q_w - 0.00434^{c} M_t + 0.01170^{a}\, T_a \quad S_e = 0.278$$

VI

$$\text{Log C} = +1.352 + 0.203^{b} \log Q_w - 0.00380^{d}\, M_t \quad S_e = 0.308$$

JAMES RIVER AT SCOTTSVILLE, VA.
Surface runoff—67 storm events

I

1. $\text{Log } C = +0.832 - 0.359^{e} \log Q_w - 0.00321^{c} M_t + 0.00290^{e} T_a - 0.184^{d} \log Q_b + 0.926^{a} \log P_n \quad S_e = 0.186$
2. $\text{Log } C = 1.245 - 0.446^{c} \log Q_w - 0.00333^{c} M_t - 0.217^{c} \log Q_b + 0.989^{a} \log P_n \quad S_e = 0.188$
3. $\text{Log } C = 1.271 - 0.00293^{c} M_t - 0.262^{b} \log Q_b + 0.525^{a} \log P_n \quad S_e = 0.192$
4. $\text{Log } C = 1.129 - 0.211^{c} \log Q_b + 0.496^{a} \log P_n \quad S_e = 0.198$
5. $\text{Log } C = 0.683 + 0.425^{a} \log P_n \quad S_e = 0.204$

II

1. $\text{Log } C = 0.211 + 0.560^{a} \log Q_w - 0.00297^{c}\, M_t + 0.00286^{e}\, T_a - 0.196^{c} \log Q_b + 0.770^{b}\, P_t \quad S_e = 0.194$
2. $\text{Log } C = 0.554 + 0.537^{a} \log Q_w - 0.00309^{c} M_t - 0.229^{c} \log Q_b + 0.846^{a}\, P_t \quad S_e = 0.196$
3. $\text{Log } C = 0.489 + 0.504^{a} \log Q_w - 0.182^{d} \log Q_b + 0.751^{b}\, P_t \quad S_e = 0.202$
4. $\text{Log } C = +0.074 + 0.451^{a} \log Q_w + 0.808^{b}\, P_t \quad S_e = 0.206$
5. $\text{Log } C = +0.806 + 0.357^{a} \log Q_w \quad S_e = 0.221$

U.S. GOVERNMENT PRINTING OFFICE: 1963 O—716-824

Sediment Transport in the Rio Grande New Mexico

By CARL F. NORDIN, JR., *and* JOSEPH P. BEVERAGE

SEDIMENT TRANSPORT IN ALLUVIAL CHANNELS

GEOLOGICAL SURVEY PROFESSIONAL PAPER 462-F

UNITED STATES GOVERNMENT PRINTING OFFICE, WASHINGTON : 1965

UNITED STATES DEPARTMENT OF THE INTERIOR

STEWART L. UDALL, *Secretary*

GEOLOGICAL SURVEY

Thomas B. Nolan, *Director*

For sale by the Superintendent of Documents, U.S. Government Printing Office
Washington, D.C. 20402 - Price 30 cents (paper cover)

CONTENTS

	Page
Glossary of terms	IV
List of symbols	IV
Abstract	F1
Introduction	1
Purpose and scope	1
Acknowledgments	2
Description of reach	2
Basic data	2
Flow characteristics and sediment concentration	5
Hydraulic variables	6
Transport relations	F11
Transport rates related to simple hydraulic variables	12
Transport parameters	17
Shear stress and effective shear stress	17
Bed-material characteristics	20
Temperature effects	20
Other considerations	22
Conclusions	22
References cited	35

ILLUSTRATIONS

	Page
FIGURE 1. Index map	F3
2. Channel profile	4
3. Graph showing average size distribution of bed material	4
4. Flow-duration curves	5
5–11. Graphs:	
5. Daily mean discharge and concentration, and water temperature, April through July, 1958, Rio Grande at Otowi Bridge	7
6. Daily mean discharge and concentration, and water temperature, Rio Grande near Bernalillo	8
7. Relation of slope to discharge, Otowi and Bernalillo	9
8. Hydraulic geometry-discharge relations, Otowi and Bernalillo	10
9. Shear-discharge relation, Otowi and Bernalillo	11
10. Discharge-$C/\sqrt{g}$ relation, Otowi and Bernalillo	11
11. Relation of median diameter of bed material to discharge, Otowi and Bernalillo	11
12. Particle-size histograms of bed material and suspended sediment, Rio Grande at Otowi Bridge, July 20, 1961	12
FIGURE 13–22. Graphs:	
13. Discharges of bed material coarser than 0.062 mm, 0.125 mm, and 0.250 mm, Rio Grade at Otowi Bridge	F13
14. Transport relations for Rio Grande at San Felipe	14
15. Relation of bed-material discharge to water discharge	15
16. Relation of unit bed-material discharge to unit water discharge	15
17. Relation of unit bed-material discharge to mean velocity	15
18. Relation of bed-material concentration to mean velocity	15
19. Relation of unit bed-material discharge to shear, Otowi and Bernalillo	17
20. Relation of unit bed-material discharge to effective shear, Otowi and Bernalillo	18
21. A dimensionless shear-transport relation, Otowi and Bernalillo	19
22. Systematic changes in bed material size distribution, 1958, Rio Grande at Otowi Bridge	21
23. Plot showing apparent effect of temperature on concentration, Rio Grande near Bernalillo	22

TABLES

TABLE 1–6. Basic hydraulic data and measured and computed sediment concentrations:
1. Rio Grande at Otowi Bridge, near San Ildefonso, N. Mex. — Page F23
2. Rio Grande at Cochiti, N. Mex. — 24
3. Rio Grande at San Felipe, N. Mex. — 25
4. Rio Grande near Bernalillo, N. Mex. — 26
5. Rio Grande at Albuquerque, N. Mex. — 27
6. Rio Grande near Belen, N. Mex. — 28

7–12. Particle-size analyses of bed material:
7. Rio Grande at Otowi Bridge, near San Ildefonso, N. Mex. — 28
8. Rio Grande at Cochiti, N. Mex. — 29

TABLE 7–12—Continued
9. Rio Grande at San Felipe, N. Mex. — Page F30
10. Rio Grande near Bernalillo, N. Mex. — 31
11. Rio Grande at Albuquerque, N. Mex. — 32
12. Rio Grande near Belen, N. Mex. — 33

13. Sources of published particle-size analyses of suspended sediment used in the modified Einstein calculations — 33
14. Previously unpublished particle-size analyses of suspended sediment used in the modified Einstein calculations — 34
15. Equations relating transport rates to simple hydraulic variables, with standard error of estimates in log units and percentages — 34

GLOSSARY OF TERMS

Bed material: The material composing the channel bed. For this study, bed material is considered all sediment coarser than 0.062 mm.

Bedload: Sediment that moves on or very near the streambed, in almost continuous contact with the bed. It moves by skipping, sliding, and rolling. Motion is derived from tractional and gravitational forces.

Concentration: The ratio of the dry weight of sediment to the weight of water sediment mixture of which it is part. Sediment concentration is commonly expressed in parts per million (ppm).

Fine material: All sediment finer than 0.062 mm; also called "wash load."

Sediment discharge: A time rate of movement of sediment passing a cross section; also called "sediment transport rate" or "sediment load." In this report, all sediment discharges are given in tons per day.

Suspended load: Sediment that is generally supported by turbulence and is transported at about the velocity of the water.

Total sediment load: All the sediment being moved by the stream, that is, suspended load and bedload.

Unit water discharge: Water discharge for unit width of a stream.

Unit bed-material discharge: Discharge of bed material (material coarser than 0.062 mm) per unit width of a stream.

SYMBOLS

		Unit
a	A coefficient	0
B	Width	ft
b	An exponent	0
C	Chezy discharge coefficient	ft$^{1/2}$ per sec
$c/\sqrt{g}$	Dimensionless Chezy coefficient	0
C_T	Bed-material concentration	0
D	Mean depth	ft
d	Median diameter of bed material	mm
d_{65}	Diameter of bed material for which 65 percent by weight, is finer	mm
g	Acceleration due to gravity, assumed constant and equal to 32.2	ft per sec^2
k_s	Representative grain roughness, d_{65}	ft
Q	Water discharge	ft^3 per sec
Q_T	Total bed-material discharge	tons per day
q	Unit water discharge	ft^3 per sec per ft
q_T	Unit bed-material discharge	tons per day per ft
S	Water-surface slope	0
S_e	Standard error of estimate	0
T	Water temperature	°F
U_*	Shear velocity, $\sqrt{gDS}$	ft per sec
U'_*	Shear velocity associated with the grain roughness	ft per sec
V	Mean velocity	ft per sec
X	An independent variable	0
x	A correction factor for transition from smooth to rough boundary	0
Y	A dependent variable	0
γ	Unit weight of water	lbs per ft^3
γ_s	Unit weight of sediment	lbs per ft^3
ρ	Density of the fluid	slugs per ft^3
ρ_s	Density of the sediment	slugs per ft^3
τ_0	Bed shear stress, γDS	lbs per ft^2
τ'	An effective shear, $\rho(U'_*)^2$	lbs per ft^2
ϕ_T	A dimensionless transport function	0
ψ'	A dimensionless shear parameter	0

SEDIMENT TRANSPORT IN THE RIO GRANDE, NEW MEXICO

By Carl F. Nordin, Jr., and Joseph P. Beverage

ABSTRACT

This report describes hydraulic data, observed and computed sediment concentrations, and size distributions of bed-material samples for 293 observations and presents the results of a series of investigations at six sediment stations on the Rio Grande in New Mexico.

The Rio Grande at Otowi Bridge, near San Ildefonso, N. Mex., the farthest upstream station, has a typical pool-and-riffle channel configuration, and the bed material consists of both sand and gravel. The Rio Grande at Cochiti and at San Felipe has a sand-gravel channel, but the marked controlling influence of riffles is lacking. The three downstream stations, near Bernalillo, at Albuquerque, and near Belen, have sand-bed channels. Slopes through the 110-mile reach range from about 12 feet per mile at Otowi to 4 feet per mile near Belen.

Transport rates of bed material computed by the modified Einstein method are related to the simple hydraulic variables, discharge, unit discharge, and velocity, for each of the stations. The sediment transport relations are found to vary systematically in a downstream direction, that is, with bed-material size, and to fall into two distinct groupings, one for the confined or partially confined sections and the other for the laterally unrestricted sections. Sediment transport rates are greater at the wide sections for higher discharges and greater at the narrow sections for the lower flows, probably because the wider sections have a tendency to aggrade and channelize at the lower flows.

Flow characteristics differ markedly for the pool-and-riffle channel at Otowi and the sand-bed channel near Bernalillo. At Otowi, the depth, slope, bed shear stress, resistance to flow, and the bed-material size all increase with increasing discharge. Near Bernalillo, slope and bed-material characteristics are approximately constant, flow resistance, which is dependent upon bed configuration, decreases with increasing discharge, and the range in bed shear stress, compared to Otowi, is very limited.

The mean velocities and sediment discharges for the two stations are comparable, in spite of the wide differences in flow characteristics. Sediment transport rates are found to relate reasonably well to "effective shear," a measure of the shear stress resisted by the grain roughness only. However, the variable size distribution of the bed material introduces considerable scatter for the Otowi relation. The scatter is reduced by converting the shear-transport relations to dimensionless form, similar to the parameters used by Einstein (1950, Bagnold (1956). and A. A. Bishop ("Sediment transport in alluvial channels: a critical examination of Einstein's theory: Colorado State Univ. Ph. D. thesis, 1961). Consideration of the curves developed by Bishop to predict total bed-material discharge and of the dimensionless relations for the Rio Grande indicate that to be generally applicable, the shear stress-transport functions probably should include additional parameters to explain the influence of temperature and the effects of flow depth. Systematic changes in bed-material characteristics for Otowi introduce changes in the sediment transport, independent of the hydraulics of the flow; a single simple parameter such as median diameter or a representative grain size is, therefore, not sufficient for characterization of the bimodal distribution of the bed material in the shear stress-transport functions.

The influence of temperature on sediment transport for the Rio Grande data is apparent, but a precise quantitative evaluation is impossible because the effects of temperature changes are not independent of the effects of interrelated changes in other variables.

INTRODUCTION

The sediment transported by natural streams often is an important factor in the design of reservoirs, conveyance channels, river rectification works, and related projects. To assist in understanding the complex phenomena of the mechanics of flow and sediment transport in alluvial channels and to provide basic data for the development of design methods and criteria, numerous laboratory and field studies have been undertaken. The Rio Grande in New Mexico has been the site of several investigations in sediment transport. This report presents the results of a series of investigations at six gaging stations on the middle Rio Grande in New Mexico.

PURPOSE AND SCOPE

The purpose of this report is to present observed sediment transport relations and to discuss some of the parameters describing the sediment and the flow which influence transport relations.

Sediment transport rates computed by the modified Einstein method (Colby and Hubbell, 1961) are given for 293 observations at the six gaging stations. The transport rates are related to simple hydraulic variables for each station, and the differences in the relations, from station to station, are discussed in terms of the bed-material size distributions and of the geometry of the cross sections.

The characteristics of flow and transport for a station with a pool-and-riffle channel configuration and for a sand-bed channel are compared, and the influence of bed-material size distribution and water temperature on sediment transport is considered briefly.

ACKNOWLEDGMENTS

The data presented for the period 1952–58 were collected as a part of a joint program between the U.S. Geological Survey and the U.S. Bureau of Reclamation.

This report was prepared under the supervision of J. M. Stow, district chemist, Albuquerque, N. Mex. W. L. Heckler, district engineer, Santa Fe, N. Mex., furnished the flow-duration curves and much of the basic hydraulic data from streamflow measurements.

DESCRIPTION OF THE REACH

Figure 1 is a location map of six gaging stations which are considered in this report. The stations, in downstream order, are:

Rio Grande at Otowi Bridge, near San Ildefonso
Rio Grande at Cochiti
Rio Grande at San Felipe
Rio Grande near Bernalillo
Rio Grande at Albuquerque
Rio Grande near Belen

From Otowi Bridge to Cochiti, through White Rock Canyon, the Rio Grande has a typical pool-and-riffle configuration. The riffles are composed of coarse gravel, cobbles, and boulders, and appear to be fairly stable and permanent features of the channel. Large cobbles and even boulders evidently move from the riffles during flood flows, but the relative shape and position of the riffles do not appear to change appreciably from year to year. At low discharges, the water-surface slope through the riffles is steep, the depth is shallow, and flow is supercritical. Because the riffles serve as controls, the water-surface slope through the pools may be very low, the depth is greater, and flow is subcritical. The bed material in the pools is sand at low flows and sand and gravel (a bimodal distribution) at high flows. At the Otowi station, the channel is confined, and the maximum width at the measuring section is about 150 feet.

Between Cochiti and San Felipe, the channel is braided between many bars and islands composed of coarse gravel and cobbles. As at Otowi, the bed is composed of sand at low discharges and of sand and gravel at higher flows. The cross section at Cochiti is relatively wide and unconfined; flow width varies upward to about 350 feet. At San Felipe, the channel is confined by a volcanic talus on the right bank and stable clay banks on the left; the maximum width at the measuring section is about 210 feet.

Downstream from the confluence of the Jemez River, the Rio Grande is a sand-bed stream. The Bernalillo station has a confined measuring section, and for all discharges more than about 2,000 cfs (cubic feet per second), the flow width is approximately constant at 270 feet.

During high flows, the discharge measurements and samples were obtained from highway bridges for the Rio Grande at Albuquerque and near Belen. However, except for local influence near the bridge piers, both of the sections are relatively unconfined, and flow widths range upward to about 400 feet at both sections.

A profile of the cannel from Otowi to Belen, a reach of about 110 miles, is shown in figure 2. Channel slopes range from 12 feet per mile near Otowi to about 4 feet per mile near Belen. The rate of change in slope with distance is nearly constant from Belen upstream to the Jemez River. From the Jemez River to White Rock Canyon, about 2 miles upstream from Cochiti, the slope increases rapidly. Through White Rock Canyon, the slope is nearly constant.

Nordin and Culbertson (1961) showed that the characteristics of the bed material in the middle Rio Grande change systematically with distance downstream from Otowi. This systematic variation is indicated by the average size distribution curves plotted in figure 3.

The behavior of the three downstream sections, which are sand-bed channels, and that of the three upstream sections, which are sand-gravel channels, differ significantly. These differences and some of their effects on the sediment-transport relations for the various sections will be discussed subsequently.

Three of the sections, Otowi, San Felipe, and Bernalillo, are confined or partially confined, but the other three stations are laterally unrestricted. The influence of width restrictions upon bed configuration and flow resistance has been demonstrated (Nordin, 1964), and sediment transport relations are also affected by lateral channel confinement, as will be shown.

BASIC DATA

The basic hydraulic data from water-discharge measurements and the water temperatures used in the modified Einstein calculations are given in tables 1–6. Also shown in the tables are the suspended-sediment concentrations from depth-integrated samples and computed total concentrations determined from modified Einstein calculations.

Tables 7–12 show the particle-size distribution of bed-material samples for each of the observations listed in tables 1–6. Most of the particle-size analyses of suspended-sediment samples used in the modified Einstein calculation have been previously published. Table 13 shows the sources in which these published data may be found. A few particle-size analyses not previously published are given in table 14.

Water-surface slopes were determined for many of the observations and are listed in tables 1–6. If water-

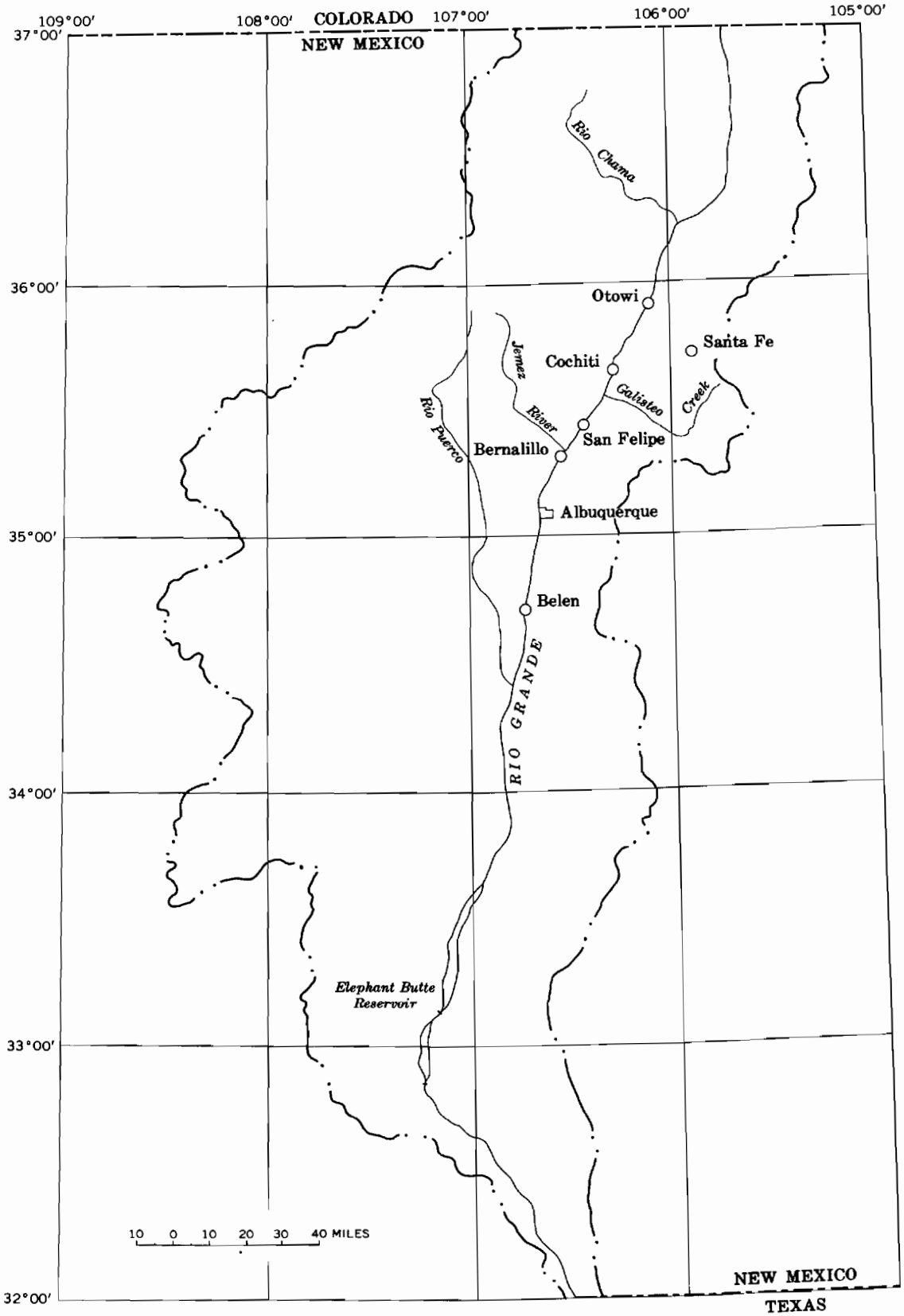

FIGURE 1.—Map showing part of the Rio Grande drainage basin. Adapted from U.S Geological Survey New Mexico base map, scale 1:500,000.

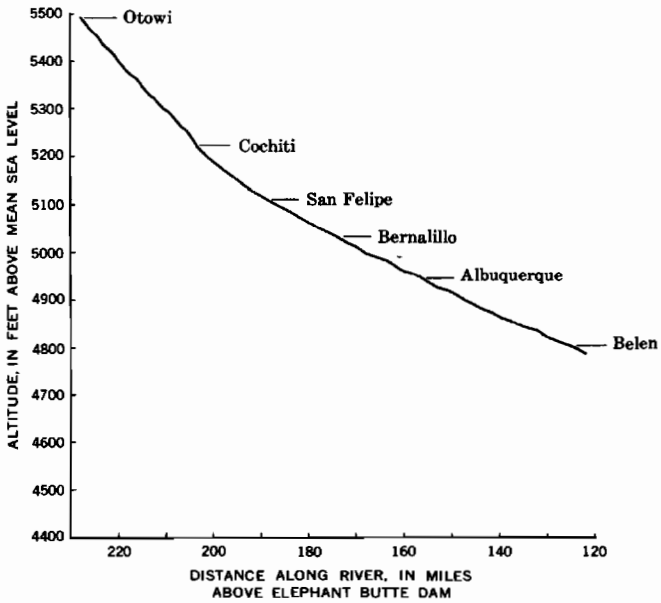

FIGURE 2.—Channel profile of the Rio Grande from Otowi Bridge to Belen.

surface slopes were not observed, the average water-surface slope or the average bed slope determined from Bureau of Reclamation aggradation-degradation studies are shown.

Streamflow records for the six stations are given in Part 8 of the Geological Survey Water-Supply Paper series "Surface-Water Supply of the United States." The station near Belen was discontinued in June 1957.

The stations at Otowi and near Bernalillo are daily sediment stations. Suspended-sediment loads for these stations and the results of miscellaneous observations at the other four stations are listed in Part 8 of the Water-Supply Paper series, "Quality of Surface Waters of the United States."

In addition to the Water-Supply Papers noted above and listed in table 13, the writers have drawn freely from data used or presented in previous studies of the Rio Grande (Culbertson and Dawdy, 1964; Nordin and Culbertson, 1961; Nordin and Dempster, 1963; Nordin, 1964).

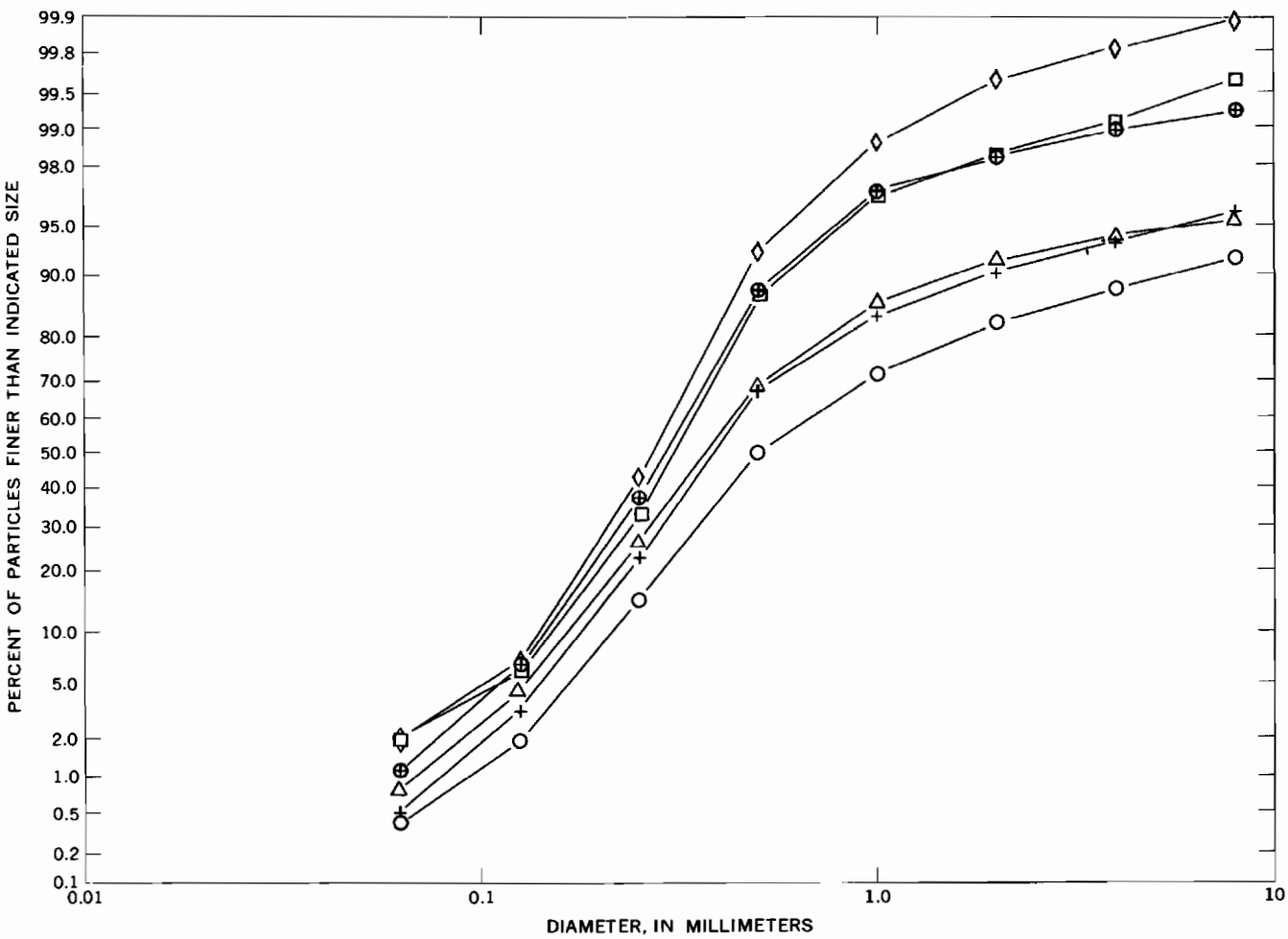

FIGURE 3.—Graph showing average size distribution of bed material. ○, Otowi; +, Cochiti; △, San Felipe; ⊕, Bernalillo; □, Albuquerque; ◇, Belen.

FLOW CHARACTERISTICS AND SEDIMENT CONCENTRATION

Flow in the Rio Grande is derived principally from snowmelt from the high mountains of northern New Mexico and southern Colorado. The spring runoff commences usually in March and persists for several months. El Vado Reservoir controls the flow of the Rio Chama and, within the limitations of the Rio Grande Compact, permits the regulation of continuous flow in the Rio Grande below Otowi during the irrigation season. Releases from El Vado Reservoir to downstream storage occasionally result in several months of sustained winter flow.

From Cochiti downstream, flow in the Rio Grande is depleted heavily by irrigation and by natural losses. Although the flow is generally perennial at Otowi and Cochiti, it is usually intermittent at Albuquerque and Belen. Flow-duration curves for the period of record through 1959 or 1960 (fig. 4) show clearly the influence of irrigation and natural losses during the lower discharges.

Although by far the greatest volume of flow in the Rio Grande is from spring runoff and reservoir releases, tributary inflow from summer storms of short duration and high intensity may contribute appreciable quantities of flow and large quantities of sediment. Galisteo Creek, entering the Rio Grande from the east about 8 miles downstream from the Cochiti station, is the largest tributary between Otowi and Belen and contributes heavy sediment loads to the Rio Grande. The Jemez River, joining the Rio Grande from the west about 8 miles north of the Bernalillo station, has been

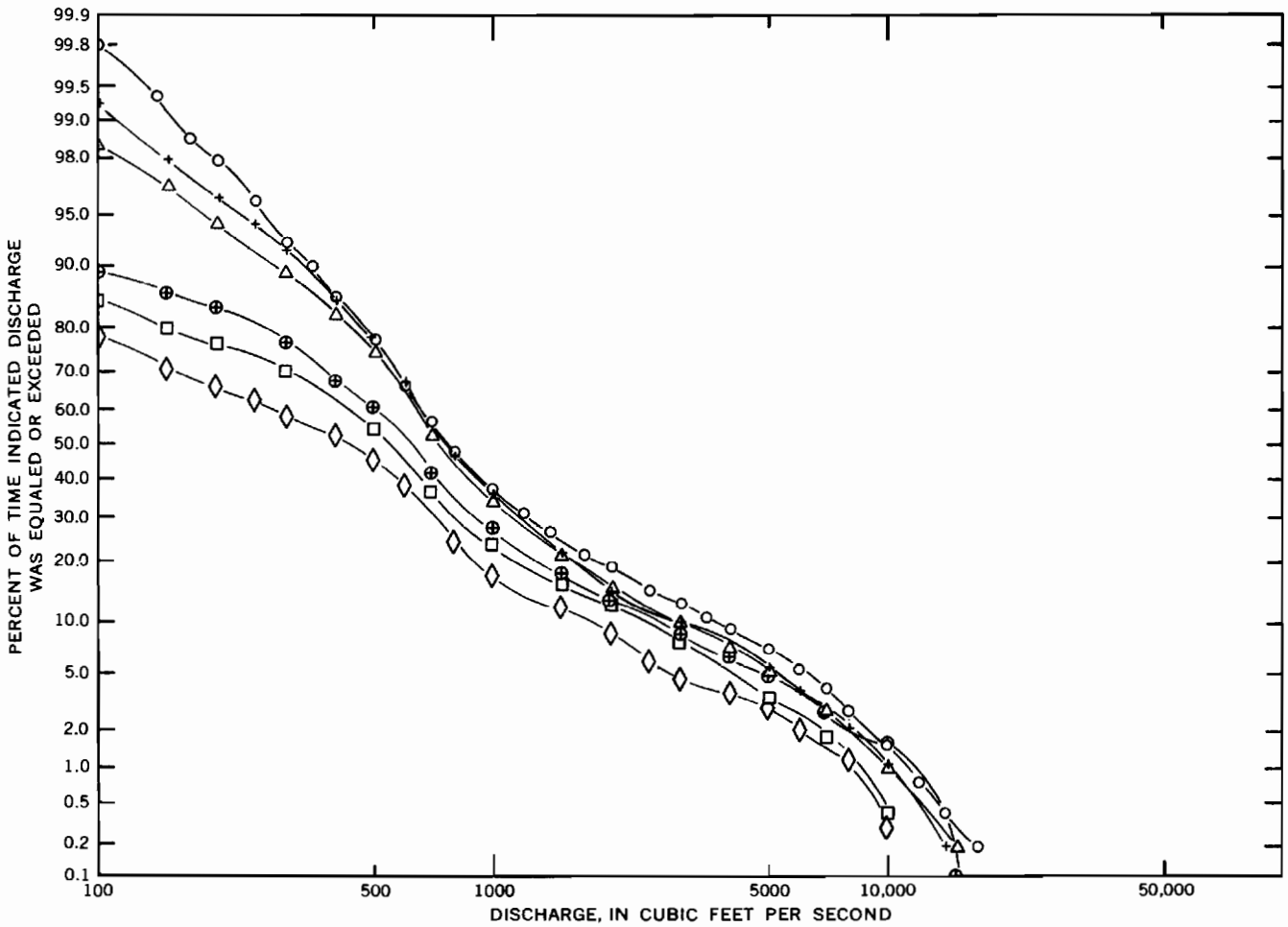

FIGURE 4.—Flow-duration curves for the period of record.

Station	Period of record
○ Otowi	1896–1905, 1910–14, 1919–59
+ Cochiti	1927–60
△ San Felipe	1928, 1931–60
⊕ Bernalillo	1942–59
□ Albuquerque	1943–60
◇ Belen	1943–56

753-190 O—65——2

regulated by the Jemez Canyon Reservoir since October 1953, hence inflow from this tributary did not influence appreciably the sediment transport relations presented herein.

Tributary runoff from "thunderstorm" rainfall imposed upon main-channel flow will create a sharp peak in both the flow and the concentration of suspended sediment. The instantaneous peak discharge from such storm runoff is often as great as or even greater than the peak discharge during spring runoff from snowmelt, but the duration is brief, persisting from a few hours to a few days. After the peak of the storm runoff passes a measuring section, both the discharge and the concentration attenuate with time, approaching the more or less stable condition which persisted before the inflow, provided, of course, that the main-channel flow is reasonably constant. The concentration attenuates much more slowly than the water discharge (Nordin, 1964). The time dependency of the concentration is noticeable in either the total concentration or in the concentration of any particular size class, but the rate of attenuation with time appears to vary directly with the size class of the suspended sediment.

Variations of daily mean water discharge, concentration, and water temperature for the Rio Grande at Otowi Bridge and Rio Grande near Bernalillo, New Mex., are shown in figures 5 and 6, respectively. The general shapes of the hydrographs and of the temperature and concentration curves for the two stations are similar, and during the spring runoff, as during storm runoff, the sediment concentration tends to decrease with time, independent of flow conditions. However, during spring runoff, changes in concentration are usually accompanied by changes in water temperature, whereas during a storm-runoff event in late summer or fall, changes in concentration may be independent of temperature changes.

The similarity in the discharge and concentration curves for the two stations suggests that the sediment transport relations for the stations should also be similar but some noticeable differences in the hydraulic variables of the two sections merit consideration.

HYDRAULIC VARIABLES

Pertinent hydraulic variables, so far as sediment transport is concerned, are the mean velocity (V), the mean depth (D), the product of depth and slope, or the shear stress on the bed (γDS), and the ratio of velocity to shear, which is a measure of the channel flow resistance. More specifically, the ratio of mean velocity (V) to shear velocity (U_*) may be taken as a measure of the overall channel roughness and is equal to Chezy's dimensionless coefficient $C/\sqrt{g}$.

Except for the bank friction, the overall channel roughness in a natural channel with a movable bed depends upon (1) the grain roughness and (2) the roughness due to bed configurations—the ripples, dunes, and bars which form on the bed. In general, only the part of the overall shear which is resisted by the grain roughness is effective in moving the bed material (Einstein, 1950; Laursen, 1958). Thus, the size distribution of the bed material, which determines the grain roughness, is a major factor in determining the effective shear stress. Strictly speaking, grain size cannot be classified as a hydraulic variable, but, because of the close relation of grain size to hydraulic factors, the size distribution of bed material will be considered in this section.

Some of the basic differences in behavior between the sand-bed channels of the Rio Grande and the channels that have a pool-and-riffle configuration and a bimodal distribution of bed material may be detected by considering the relations of simple hydraulic variables to discharge. For comparison, Otowi may be taken as a typical pool-and-riffle channel and Bernalillo as a typical sand-bed channel.

Figure 7 shows the observed water-surface slopes plotted against water discharges for Otowi and Bernalillo. The plotted points represent the data for 1958–62 from tables 1 and 4, excluding the June 24, 1958, observation at Otowi, which was not at the cable section, and the February 15, 1960, observation at Bernalillo, for which no slope was obtained. The slope at Bernalillo was approximately constant at about 0.0008, but the slope at Otowi increased with discharge and, for the range of discharge considered, varied by a factor of about 3.

Water-surface slopes at Otowi, plotted in figure 7, were measured over a relatively short reach, about 10 to 15 times the channel width, and are representative of the slopes through the pools, not the overall slope through a long reach. At low flows, the riffles serve as controls. At higher discharges, the controlling influence of the riffles is drowned out, and the water-surface slope approaches the natural topographic slope of the channel, about 12 feet per mile (0.0023).

At Bernalillo, the water-surface slope is about constant regardless of the length of reach considered, although the scatter about the average value is much greater when the slope is measured over shorter reaches.

Figure 8 shows mean velocity, depth, and width plotted against discharge, after the manner of Leopold and Maddock (1953). Lines were drawn through the plotted points, and the equations for the lines are shown on figure 8. The lines for Bernalillo were not extended below 2,000 cfs because there is an apparent break in

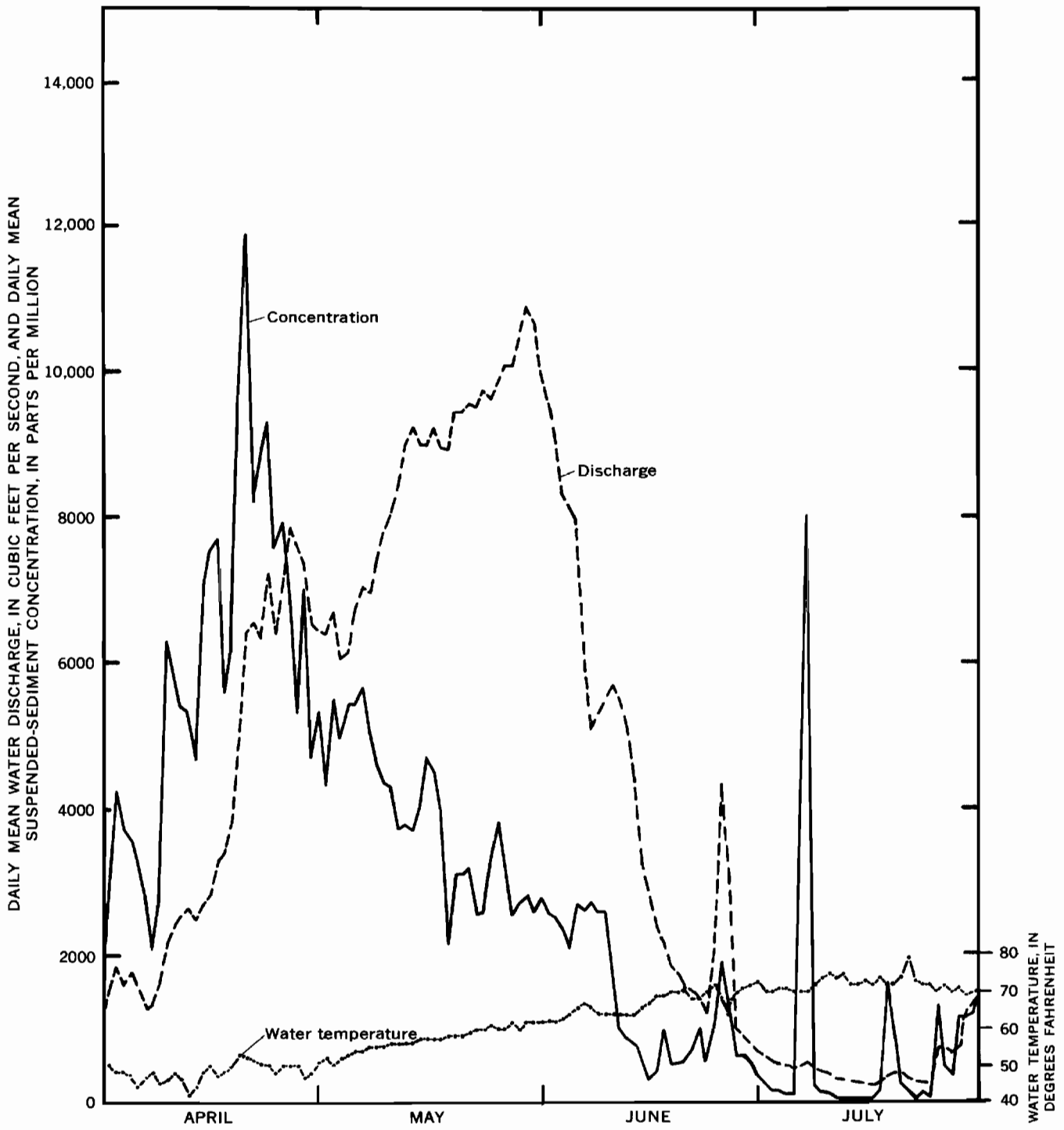

FIGURE 5.—Graph showing daily mean water discharge, daily mean suspended-sediment concentration, and water temperature, April through July, 1958, Rio Grande at Otowi Bridge, near San Ildefonso, N. Mex.

the relation at lower discharges when channelization occurs.

The exponents for the equations relating velocity to discharge are greater than the average exponents given by Leopold and Maddock (1953, p. 9) because, for the range of discharge considered, the measuring sections at both Otowi and Bernalillo are partially confined.

Figure 8 shows that the depth is greater and increases more rapidly with discharge at Otowi and that the range in velocity is about the same at both stations.

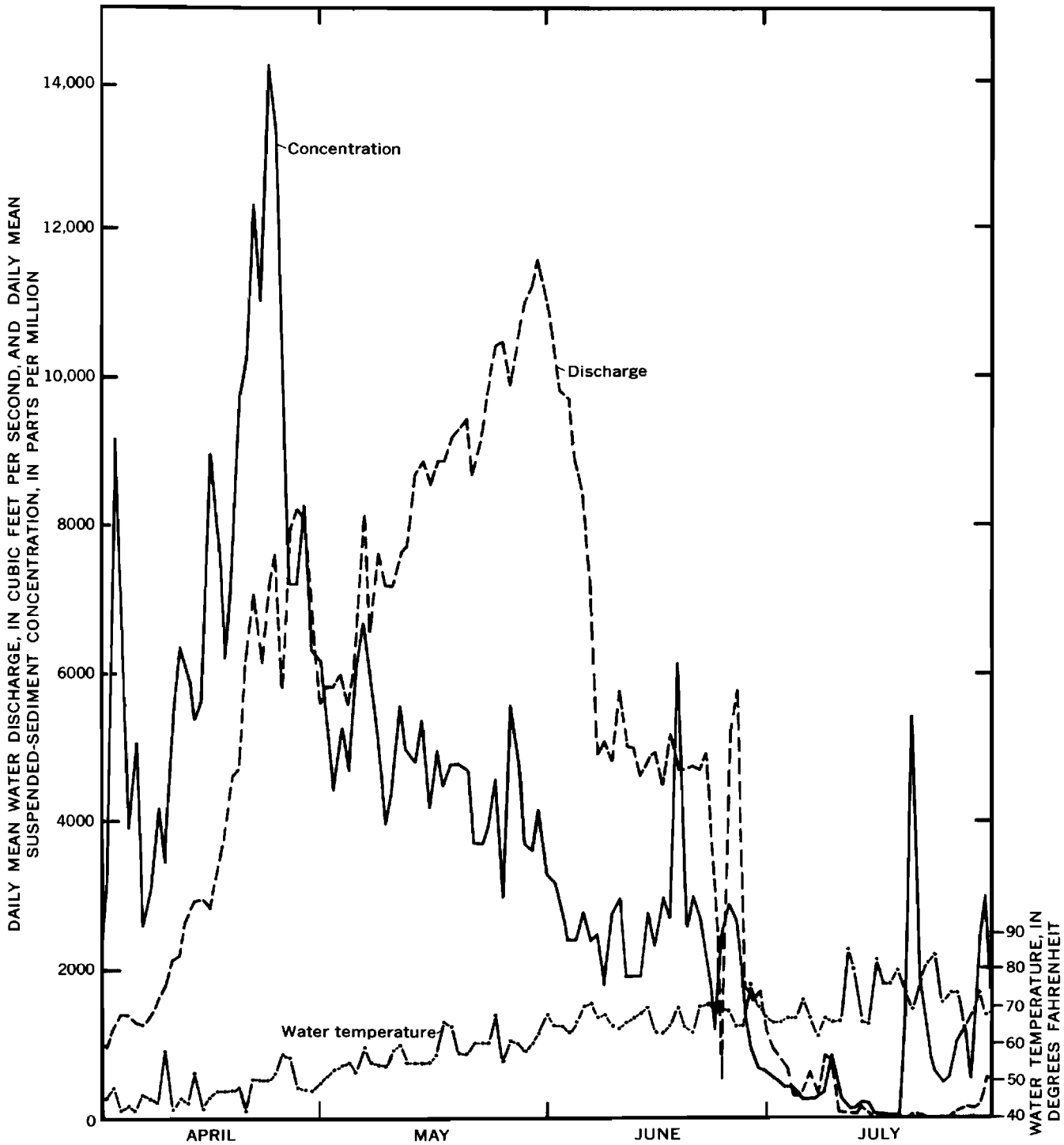

FIGURE 6—Graph showing daily mean water discharge, daily mean suspended-sediment concentration, and water temperature, April through July, 1958, Rio Grande near Bernalillo, N. Mex.

Because both depth and water-surface slope increase with discharge more rapidly at Otowi than at Bernalillo, it may be concluded that the relation of the velocity to the shear stress is different for the two stations. Figure 9 shows the bed shear stress ($\tau_0 = \gamma DS$) for Bernalillo and Otowi plotted against discharge. For the same range in velocities, the shear stress at Bernalillo varies from about 0.05 to 0.24, or by a factor of 5, while the shear stress at Otowi varies from about 0.03 to 1.50, by a factor of 50. Because shear stresses for

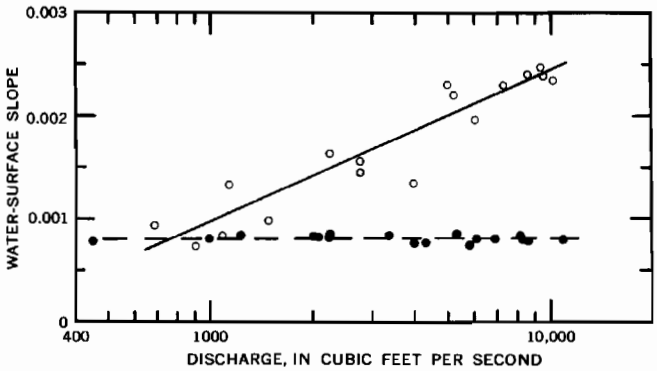

FIGURE 7.—Graph showing relation of water-surface slope to discharge for the Rio Grande at Otowi Bridge and near Bernalillo. (○, Otowi; ●, Bernalillo.)

Otowi were computed using local water-surface slopes through a pool, the range in shear stress is greater than if an average water-surface slope including both pools and riffles had been used.

These observations show the basic distinction between the hydraulics of the pool-and-riffle channels and of the sand-bed channels of the Rio Grande—the difference in the relation of flow resistance to discharge In the sand-bed channels, flow resistance is dependent mostly upon bed configuration. Flow may be classified conveniently into lower regime flow over a dune bed and upper regime flow over a plane bed (Culbertson and Dawdy, 1964). Between upper and lower regimes of flow is a transition region in which bed configurations and flow resistance vary widely. Lower regime flow is characterized by low sediment discharge and high flow resistance. Conversely, for upper regime flow, the sediment transport rate is high and the flow resistance is extremely low, dependent mostly upon grain roughness (Dawdy, 1961).

In pool-and-riffle channels, however, the flow resistance often increases with discharge, and the influence of the bed configuration at low flows appears to be completely overshadowed by the controlling influence of the riffles. A distinguishing feature of a pool-and-riffle channel is that at low discharges the energy dissipation is nonuniformly distributed along the channel and is concentrated at the riffles, whereas, at higher discharges, the distribution of energy dissipation approaches a more uniform condition along the channel.

Figure 10 shows the relation of $C/\sqrt{g}$ to discharge for Bernalillo and Otowi. The dashed lines show the approximate average values of $C/\sqrt{g}$ for lower and upper regime flow at Bernalillo; the solid line shows the trend of $C/\sqrt{g}$ values for Otowi. A $C/\sqrt{g}$ value of about 8 for the highest discharges at Otowi represents an extremely high flow resistance, greater than the resistance for flow over a well-defined dune bed.

The increase in the flow resistance with discharge at Otowi is due in part to the influence of bank roughness and in part to changes in the size distribution of the bed material which accompany the higher flows. The effects of the bank roughness may be accounted for, at least crudely, by the method outlined by Einstein (1942). The influence of the changing size distribution of the bed material requires additional consideration.

For most practical purposes, the particle-size distribution of the bed material for the sand-bed channels of the Rio Grande may be considered invariant and independent of discharge (Nordin and Culbertson, 1961). At Otowi, on the other hand, the size distribution of the bed material varies widely and erratically. The deviation of the median diameter about the average value from figure 3 is shown in figure 11, where median diameter (d) is plotted against water discharge.

As table 7 shows, the distribution of the bed material at Otowi sometimes is bimodal, and, although the dominant mode is composed of sand and the median diameter is usually in the sand size class (0.062–2.00 mm), the percentage of gravel is appreciable. The percentage of gravel in the bed material appears to vary roughly with discharge and also with time during a single runoff event. Antecedent conditions are probably important.

The size distributions of bed material in table 7, however, represent only material from the measuring section at Otowi—that is, from the pool. The material composing the riffles is much coarser, ranging in size from coarse gravel to boulders many feet in diameter.

At high flows, above 4,000 cfs, the overall flow resistance at Otowi is practically constant in spite of wide variations in the percentage of gravel in the bed material. Possibly, the flow resistance is independent of grain roughness at these higher discharges. However, the bed material generally becomes coarser with higher discharges, hence the grain roughness is at least partially responsible for the high flow resistance. The difficulties of obtaining representative samples of coarse gravel beds preclude adequate evaluation of a representative grain roughness.

For sand-gravel channels of the Rio Grande where riffle controls are lacking, the hydraulic behavior is between that of a sand-bed channel and that of a pool-and-riffle channel. Cochiti and San Felipe, for example, have the characteristics of sand-bed channels at discharges below about 2,000 cfs. The bed configuration is dunes, the size distribution of the bed material and the water-surface slope vary conservatively, and the flow resistance, which depends mostly upon bed configuration, decreases with discharge. At flows above 2,000 cfs, the bed material becomes coarser and flow resistance increases with discharge.

An increase in the size of the bed material is not necessarily accompanied by a decrease in the bed

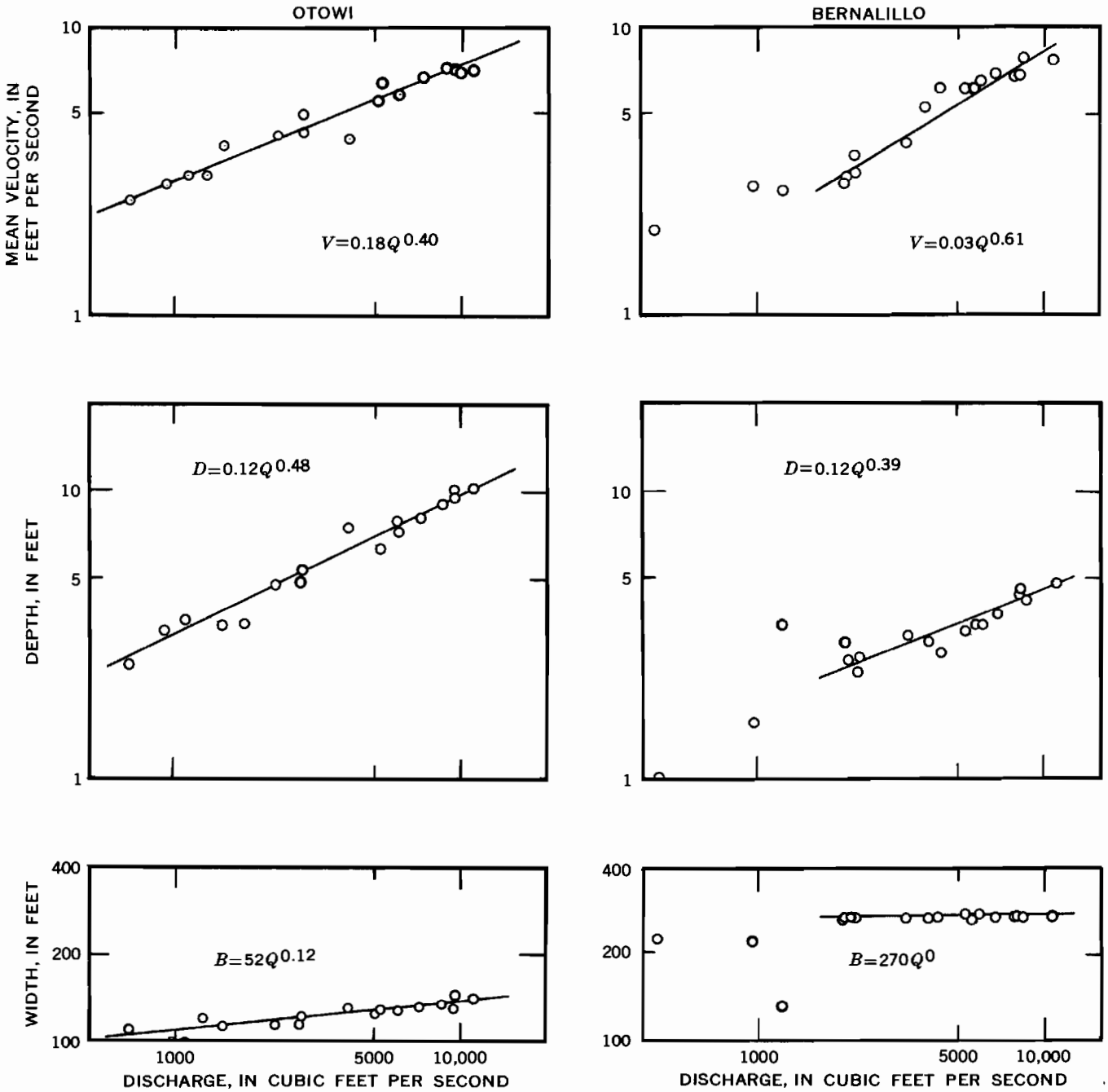

FIGURE 8.—Graph showing relation of width, depth, and velocity to discharge for the Rio Grande at Otowi Bridge and near Bernalillo.

elevation. The channel does not need to scour to the source of the coarser material; the gravel is actually transported into the reach from an upstream source, probably from the gravel bars and temporary islands which form at low and intermediate discharges.

Summarizing, for the sand-bed channels of the Rio Grande, the characteristics of the bed material and the water-surface slope are approximately constant. The flow resistance is dependent upon bed configuration and decreases with discharge until a plane bed occurs, whereupon the resistance, measured by $C/\sqrt{g}$, becomes approximately constant. At Otowi, where the channel has a pool-and-riffle configuration, the size of the bed material, the water-surface slope, and the flow resistance all increase with increasing discharge. The stations at Cochiti and San Felipe behave as sand-bed channels at lower flows, whereas, at higher flows, the size of the bed material and the flow resistance increase with discharge.

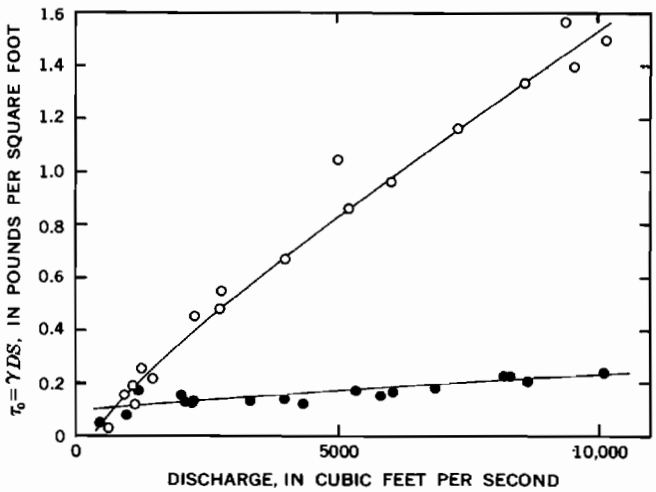

FIGURE 9.—Graph showing relation of bed shear stress (τ_0) to discharge for Rio Grande at Otowi Bridge and near Bernalillo. ○, Otowi; ●, Bernalillo.

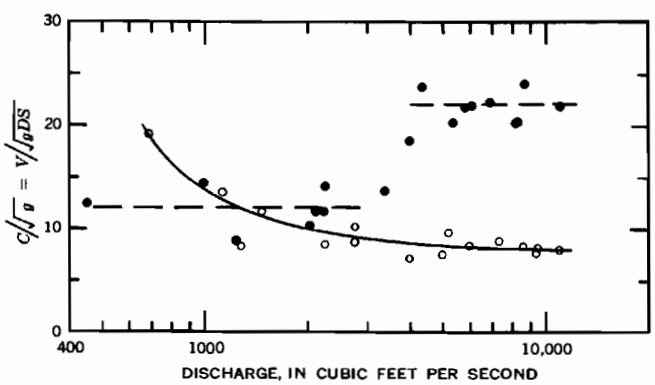

FIGURE 10.—Graph showing relation of $C/\sqrt{g}$ to discharge for the Rio Grande at Otowi Bridge and near Bernalillo. ○, Otowi; ●, Bernalillo.

TRANSPORT RELATIONS

The various components of the sediment load of streams, which is the total quantity of sediment being moved by a stream, can be defined in terms of (1) the method of movement and (2) the source. In defining the components by method of movement, a distinction is made between the suspended sediment, or suspended load, and the bedload. The suspended load is the sediment in suspension which is transported at about the velocity of the water. The bedload is the sediment that moves by sliding, rolling, or skipping on or very near the streambed.

In defining the sediment load by source, a distinction is made between the fine material, which is commonly called "wash load" (Einstein, 1950), and the coarse material, which is usually referred to as the "bed-material load." The bed-material load is that part of the sediment load of a stream which is composed of particle sizes found in appreciable quantities in the shifting portions of the streambed. The fine-sediment load is that part of the sediment load of a stream which

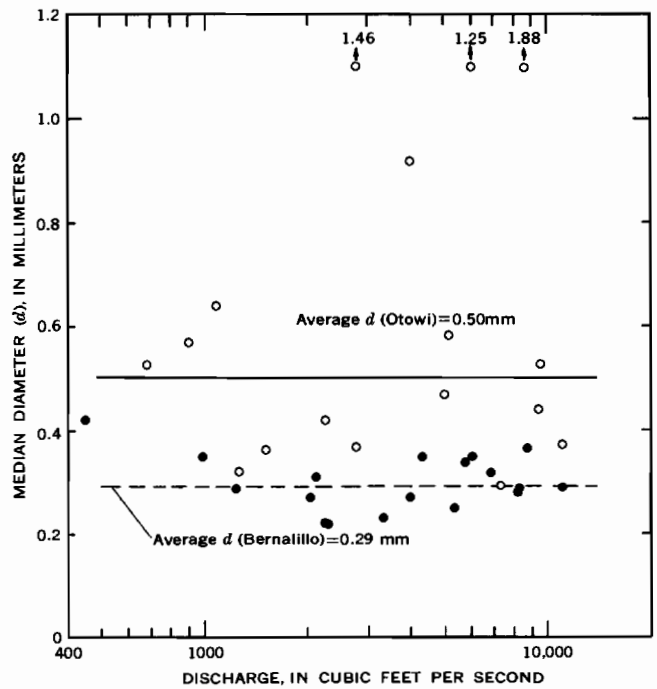

FIGURE 11.—Graph showing relation of median diameter of bed material to discharge for the Rio Grande at Otowi Bridge and near Bernalillo. ○, Otowi; ●, Bernalillo.

is composed of particle sizes finer than those generally found in shifting portions of the streambed.

As defined above, the only distinction between the fine-sediment load and the coarse-sediment load is one based upon the size distribution of the bed material. Such a definition gives little insight into the mechanics of sediment transport. Arbitrary definitions are therefore adopted which are based upon the properties of the two types of loads.

In general, the fine material is delivered to a channel by surface runoff, its transport rate is governed by the rate at which it is made available, and it is never transported at stream capacity, except in the upper limiting case of a mudflow. On the other hand, the transport rate of bed material moving past a given cross section in a stream presumably is governed solely by the ability of the flow to move the material. Bed material is always transported at the stream capacity, bacause any material in excess of stream capacity is immediately deposited and any deficit of material may be replenished by scouring the bed.

From a practical viewpoint, then, the bed material may be defined as that part of the sediment load for which a functional relation exists between the transport rate and the flow. The transport rate of fine material is not functionally related to the flow.

The distinction between the bed material and the fine material sometimes is quite obvious from histograms of the size distributions of bed-material samples and suspended-sediment samples, as shown in figure 12.

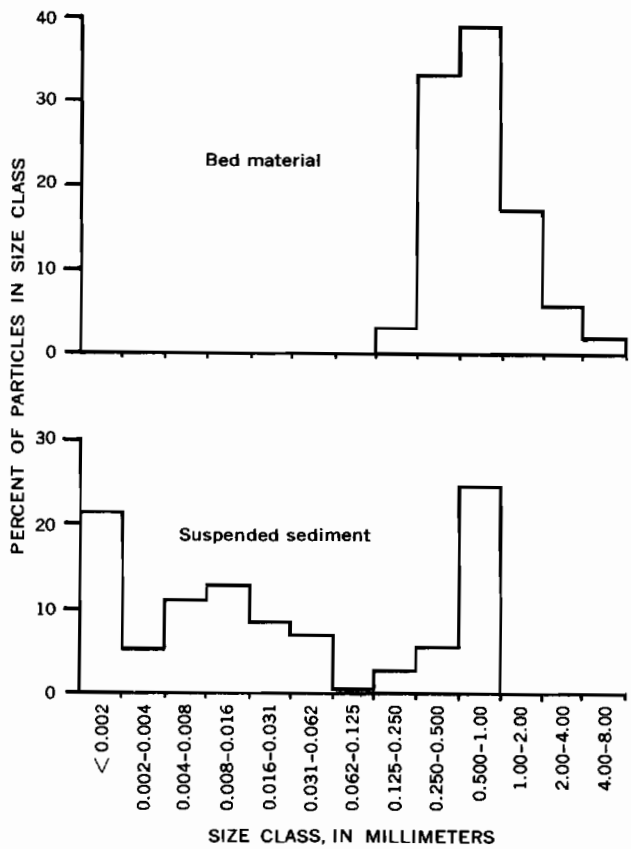

FIGURE 12.—Histograms of size distributions of bed material and suspended sediment for Rio Grande at Otowi Bridge, July 20, 1961.

Because none of the material finer than 0.062 mm is found in the bed material, it must be assumed that all material finer than this size is wash load. At other times, especially if large quantities of fine sand are transported, the distinction is not so simple. Material in the size class from 0.062 to 0.125 mm may behave as bed-material load at low flows and as wash load at higher flows, especially in the reaches that have pool-and-riffle channel configurations and in reaches in which extremely low discharges or periods of no flow occur. However, even though a functional relation between the flow and the discharge of finer sand sizes is not always readily apparent, observations show that decreases in the transport rates of these sand sizes are accompanied by decreases in the percentage of the same size classes in the composition of the bed material (Nordin and Beverage, 1964). These observations support the conclusions of Einstein and Chien (1953), who suggested that there is basically no difference in the interrelations of the flow, transport rate, and bed composition for the so-called wash load and the bed-material load, provided the composition of the surface layer of the bed is adequately defined. However, because it is virtually impossible, under most field conditions, to obtain adequate samples of the surface layer of the bed, the distinction between bed-material load and fine-material load must be maintained.

In this report, all material coarser than 0.062 mm is considered bed material. Of course, inclusion of the finer sand sizes may introduce some unexplained scatter in the transport relations, but the relation between the flow and the transport rate of material coarser than 0.062 mm is as well defined as are the relations for only the coarser fractions. Figure 13 is a plot of unit discharge (water discharge per foot of width) against unit bed-material discharge (bed-material discharge per foot of width) for transported materials (*A*) coarser than 0.062 mm, (*B*) coarser than 0.125 mm, and (*C*) coarser than 0.250 mm for the Rio Grande at Otowi Bridge. The lines shown were fitted by least squares. The standard errors of estimate were computed for each relation and are shown by the broken lines on the graph. The standard error is a measure of the relative scatter of the plotted points about the line of relation—that is, approximately two-thirds of the points fall within plus or minus one standard error, in log units.

The use of the 0.062-mm size as the break between bed material and fine material has the practical advantage of coinciding with the break between the sand sizes and the silt-clay sizes. Also, in general, material finer than 0.062 mm is uniformly distributed, vertically and laterally, in a cross section. Thus, a sample at any point in the cross section usually will give a representative picture of the transport rate of the fine material.

TRANSPORT RATES RELATED TO SIMPLE HYDRAULIC VARIABLES

For comparison purposes, transport rates can be related to hydraulic variables as simple power functions of the form

$$Y=aX^b. \qquad (1)$$

Station-to-station differences can be investigated in terms of the intercepts (a) and slopes (b) of the various relations. The formulas can be determined by fitting a straight line through logarithmic plots of the variables considered.

For this report, lines were fitted to the plotted points by the method of least squares. For some practical applications, lines fitted to the arithmetic averages of the dependent and independent variables for selected intervals of the independent variable might be more desirable (Colby 1956, 1957); however, group averages often yield curvilinear relations, which are difficult to compare, rather than the simple linear relation in terms of logarithms of equation 1.

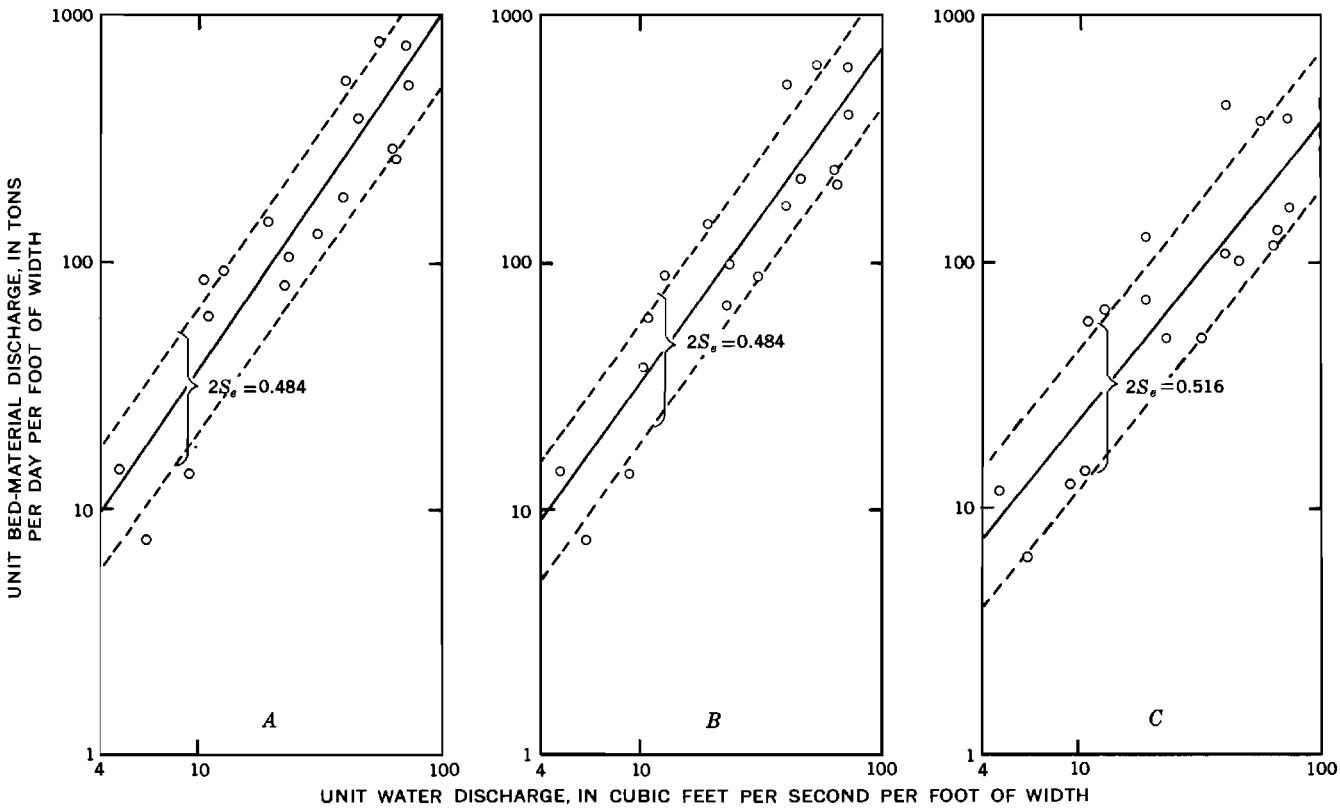

FIGURE 13.—Graphs showing unit bed-material transport rates for the Rio Grande at Otowi Bridge for material. *A* coarser than 0.062 mm; *B* coarser than 0.125 mm; and *C* coarser than 0.250 mm.

The relations for a given station are not directly comparable to the relations for another station unless the data for both stations cover the same periods of time, runoff events, and range of flow conditions. These qualifications are met only for Cochiti and San Felipe. For the other stations, especially Otowi and Belen, for which only a limited number of observations were available, the validity of the comparisons are open to question. In the following discussion, therefore, emphasis is given to the qualitative aspects of the relations.

From the data in tables 1–6, four types of transport equations were determined for each station; the following relations were defined: bed-material discharge (Q_T) to water discharge, (Q) (fig. 14*A*), unit bed-material (q_T) to unit water discharge (q) (fig. 14*B*), unit bed-material discharge to mean velocity (V) (fig. 14*C*), and (4) bed-material concentration (C_T) to mean velocity (fig. 14*D*).

The individual observations for each of these relations, together with the lines determined by the method of least squares, are plotted for the Rio Grande near San Felipe in figure 14. The amount of scatter about the lines is typical of such relations and gives a reasonable indication of the magnitude of errors which might be introduced if such relations are used to estimate transport rates.

Table 15 gives the equations for each of the relations for the six stations and the standard error of the estimate (S_e) in terms of log units and percentages (of the values given by the curve).

Logically, the relations, in terms of the standard errors, are better defined for the narrow confined sections than for the wider sections because both the simple hydraulic variables and the factors entering the total load calculations are more difficult to measure or sample accurately at the wider sections.

Figures 15–18 show the plotted lines for each of the computed relations in table 15. The lines are drawn through the approximate range for which they were defined.

Two important features of the curves are immediately apparent: (1) the slopes of the curves (the exponent b in eq. 1) tend to increase with distance downstream from Otowi and (2) the curves fall into two distinct groups, one group representing the confined sections at Otowi, San Felipe, and Bernalillo and the other group representing the unconfined sections at Cochiti, Albuquerque, and Belen.

Both of these characteristics of the curves might be expected, at least for some of the relations. The increasing exponent in a downstream direction may result from the decreasing bed-material size. For a

753-190 O—65——3

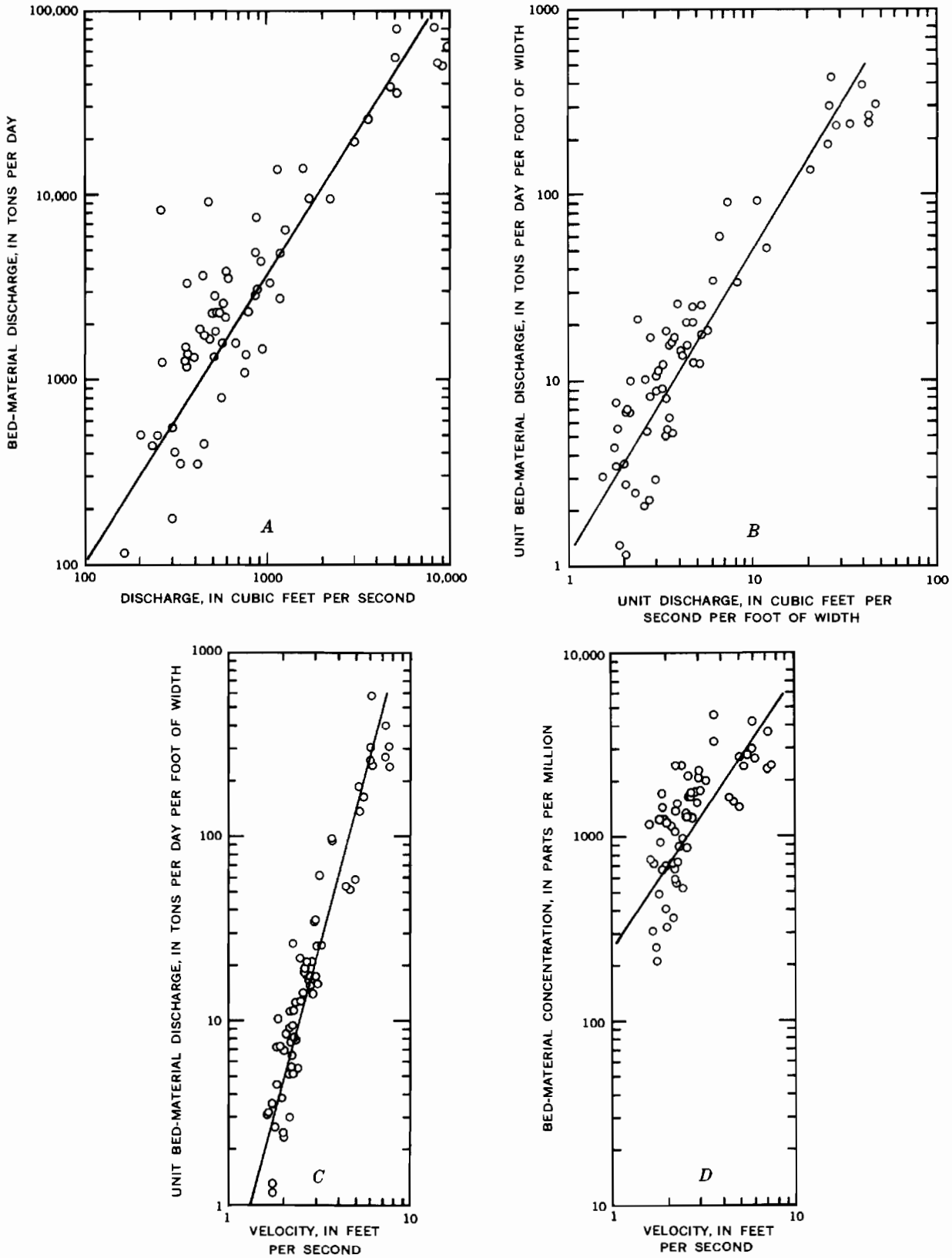

FIGURE 14.—Graph showing transport relations for Rio Grande at San Felipe, N. Mex.

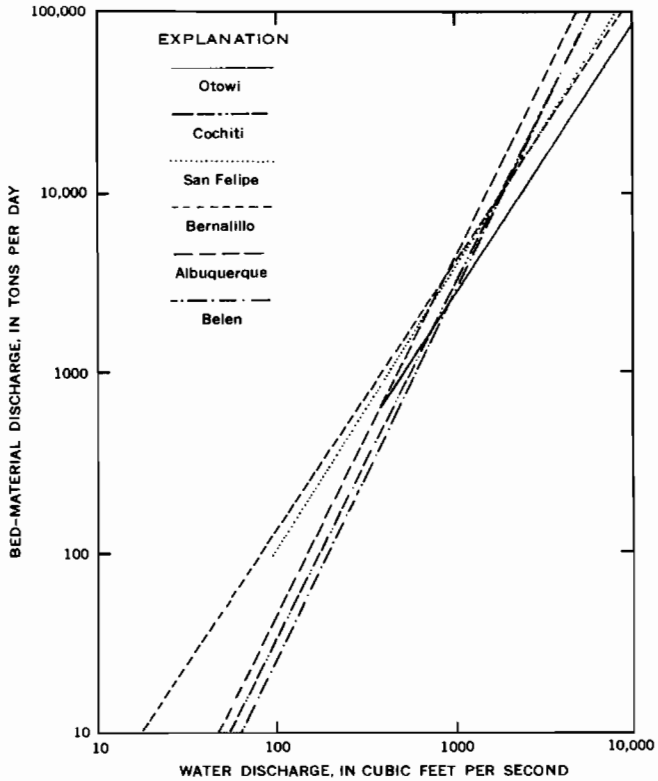

FIGURE 15.—Graph showing relation of bed-material discharge to water discharge.

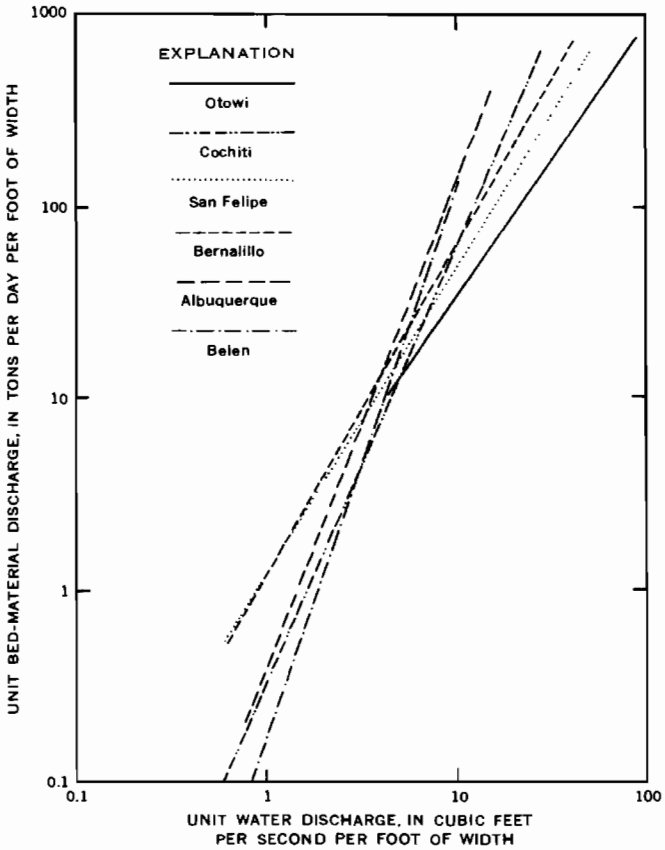

FIGURE 16.—Graph showing relation of unit bed-material discharge to unit water discharge.

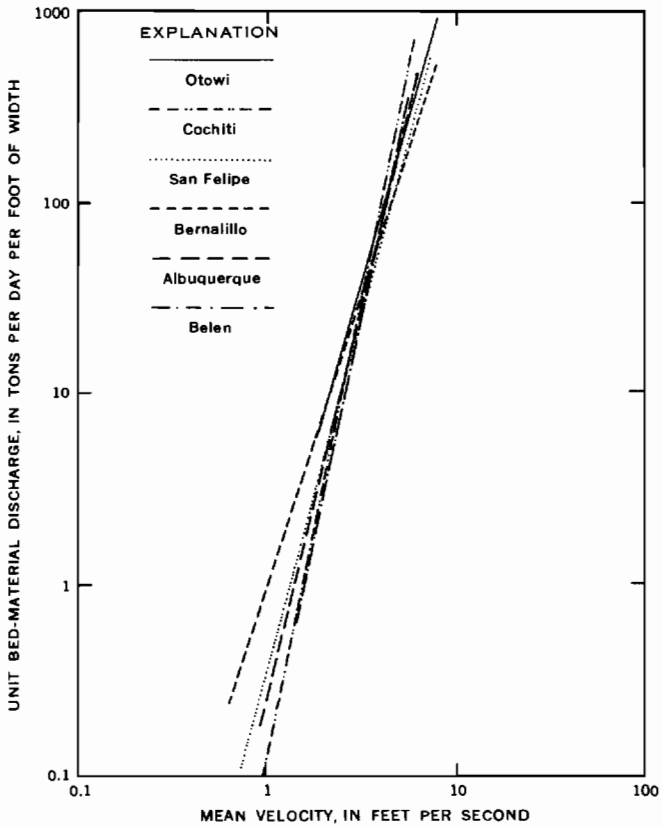

FIGURE 17.—Graph showing relation of unit bed-material discharge to mean velocity.

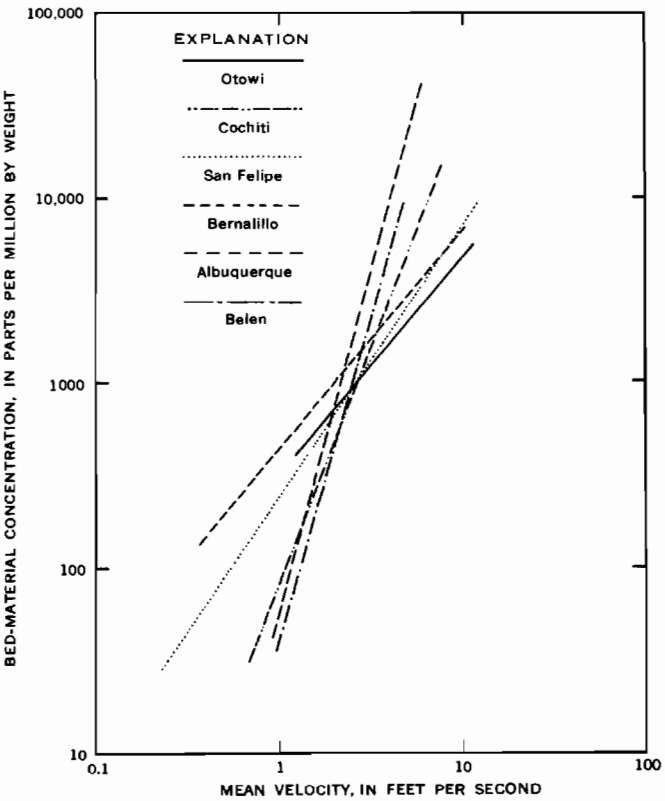

FIGURE 18.—Graph showing relation of bed-material concentration to mean velocity.

given increase in discharge, the percent increase in the transport of finer material is greater than the percent increase in the transport of coarser material. The groupings of the curves in terms of the confined and unconfined sections is logical for the relations involving mean velocity and unit water discharge because these two variables are closely interrelated with the ability of the flow to adjust its width. Velocity and depth will increase with increasing discharge more rapidly at sections of constant width than at sections where the width increases with discharge. Both the slopes and the intercepts of the curves involving unit discharge and velocity reflect the rate of change in velocity and depth with discharge.

The reason is not obvious for such marked differences between the confined and unconfined sections for the relations of total bed-material discharge (Q_T) to water discharge (Q). Figure 15 shows that for any discharge below 1,000 cfs, more sediment is transported at the narrow sections than at the wide sections. At discharges greater than about 4,000 cfs, the reverse is true; greater sediment loads are carried at the wider sections.

Figure 15 suggests that for any given period of time, say a spring runoff event, the pattern of scour and fill throughout the length of the reach will depend partly upon the nature of the cross section of the channel. During floods, scour occurs generally throughout a reach (Leopold and Wolman, 1956), and whereas the depth of scour will depend to a large extent upon local factors, greater volumes of material obviously should move from the wider sections than from the narrower sections if the trends shown in figure 15 are correct. Conversely, at low flows, greater volumes of material are moved through the narrow sections. At intermediate flows, shown by the converging lines in figure 15, the sediment-transport rates are about the same at all sections.

Observations of the Rio Grande near Bernalillo (Nordin, 1964) indicated that at low and intermediate flows, deposition and channelization occur concurrently with a decrease in width at the wider sections. These observations tend to confirm the general low-flow relations shown on figure 15.

Downstream from Cochiti, flow decreases in a downstream direction because of depletion by irrigation and channel losses from infiltration and evapotranspiration, and therefore, comparisons of the curves in figure 15 at equal discharges may be misleading. However, a comparison of transport rates from figures 4 and 15 at equal frequencies of discharge shows almost the same trends. At high flows, greater sediment loads are carried by the wide sections; at low flows, greater sediment loads are transported at the narrow sections.

The basic differences in the transport relations in figures 15–18 appear to be related directly to the nature of the cross sections—that is, to whether the channel is confined or laterally unrestricted. Even the plot of mean velocity and unit bed-material discharge (fig. 17), which is the most closely knit relation, indicates that the curves separate into groups for the confined and unconfined sections. This separation is a direct result of the effect of depth upon the transport of bed material, as shown by Colby (1961).

The most elemental relation, shown in figure 18, is the plot of mean velocity and bed-material concentration. Here, the influence of width restrictions and of concomitant depth effects are especially obvious. At the higher velocities, the effects of particle size are also readily apparent. For a given velocity, the higher concentrations are associated with the finer bed materials.

Bogardi (1961) furnished values of exponents for the concentration-velocity relations at six stations on the Danube River. The exponents given by Bogardi are of the same order of magnitude as those for the reach from Otowi to Bernalillo. His values, however, decreased from the upper station to the third station downstream and then remained constant. Bogardi found that, for any given velocity, the concentration increased in a downstream direction. This relation does not hold for the Rio Grande data shown in figure 18, except at the high velocities.

Any of the relations in figures 15–18 could be useful in practical applications. Curves such as those in figure 15 may be used in conjunction with a flow-duration curve to estimate long-term sediment yields (Miller, 1951). Relations based on unit discharge or mean velocity (figs. 16–18) are useful for estimating bed-material discharge at cross sections for which the curves were drawn or at similar cross sections (Colby, 1964).

The relations of mean velocity to unit bed-material discharge (fig. 17) appear the most logical type of sediment-transport curve to use for practical applications because the curves are about the same for all the stations, a point emphasized by Colby (1964). However, inasmuch as the curves have a relatively steep slope, any error in estimating mean velocity, width and depth being known, will introduce a larger percentage of error into the estimates of total bed-material discharge from the curves of figure 17 than is in estimates for any of the other transport relations shown.

The method of least squares is not always ideally suited for defining sediment-transport relations for practical applications, especially for the relations shown in table 15, because the data were not screened to eliminate unrepresentative sediment samples or concentrations which reflect the influence of tributary inflow.

The important features of the curves, however, are in the qualitative aspects of the relations. The sediment discharge apparently is greater at the wide sections at high flows and greater at the narrow sections at low flows. This difference is probably due to the tendency for the wide sections to aggrade and channelize at low flows. These differences in transport relations, which appear to reflect the characteristics of the cross sections, carry into the relations which are expressed on a unit width basis. Thus, the transport rates related to simple hydraulic variables for a particular cross section, such as the V-q_T relations of figure 17, may require considerable adjustment to be applicable to other types of cross sections.

The transport relations in figures 15–18 are useful for qualitative comparisons, but no single simple hydraulic variable can be expected to describe adequately the complex processes of bed-material transport. In the following section, some of the more complex factors and parameters which influence sediment transport are considered.

TRANSPORT PARAMETERS

Many factors influence sediment transport, and the parameters which describe the sediment, the channel geometry and the flow may be expressed either in dimensional or dimensionless forms. Dimensionless parameters are especially useful in reducing to comparable terms systems with variables of different orders of magnitude. On the other hand, it is often desirable to investigate the very simplest relations because the more complex parameters sometimes mask the interrelations of the variables considered, especially in investigations of field data, where controls of the factors usually considered as independent variables are lacking.

For this report, consideration was given only to some of the hydraulic parameters through the simpler relations for the stations at Otowi and near Bernalillo. No attempt was made to analyze, in detail, all the basic data.

SHEAR STRESS AND EFFECTIVE SHEAR STRESS

The transport curves in figures 15–17 are remarkably similar for Otowi and Bernalillo, especially in view of the extreme differences in the flow characteristics for the two stations. In figure 19, the relations of the unit bed-material discharge to the bed shear stress ($\tau_0=\gamma DS$) show different trends for Bernalillo and Otowi (the plotted points are for the same data compared in the previous discussion of flow characteristics). The steep slope in the trend of points for Bernalillo is indicative of the narrow range in shear stress for which there

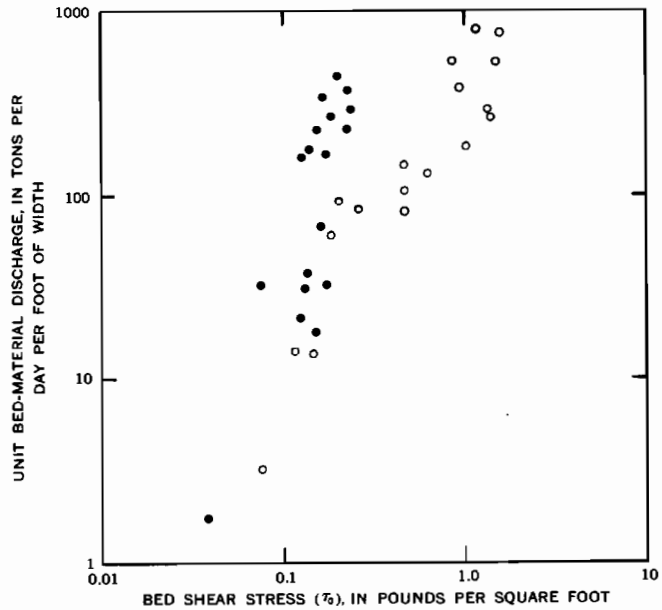

FIGURE 19.—Graph showing relation of unit bed-material discharge to bed shear stress for the Rio Grande at Otowi Bridge (○) and near Bernalillo (●).

exists a relatively wide range of velocity and sediment-transport rates. Such a trend (rapidly increasing bed-material discharge with respect to shear stress) is characteristic of shallow sand-bed streams in which the velocity-depth relation is controlled mostly by the bed configuration of the channel. For Otowi, the points follow the Bernallilo trend up to transport rates (q_T) of about 100 tons per day per foot of width; then there is a break in the trend for the higher transport rates. The break in the relation corresponds roughly with the flow conditions during which the controlling influences of the riffles is drowned out and during which the bed material begins to exhibit a marked bimodal distribution.

As mentioned previously, in the discussion of hydraulic variables, however, only the shear stress resisted by the grain roughness is effective in transporting sediment.

The concept of an effective shear stress or shear velocity has been utilized in transport relations by Meyer-Peter and Muller (1948), Einstein (1950), Colby and Hembree (1955), Laursen (1958), and perhaps others. The effective shear stress may be considered the bed shear stress which would yield the observed mean velocity if the flow resistance were due only to grain roughness. Effective shear stress may be estimated by selecting a representative grain size as a characteristic roughness length and introducing this grain size into some velocity-shear stress-roughness relation.

For this report, only one method of estimating effective shear was considered, the equation given by

Colby and Hembree (1955, equation E, p. 83) as

$$U'_* = \frac{V}{5.75 \log_{10} (12.27Dx/k_s)} \tag{2}$$

where U'_* = the shear velocity with respect to the particles,

x = a correction factor for the transition from smooth to rough boundary, and

k_s = the representative grain roughness, taken as d_{65}, the diameter of bed material for which 65 percent by weight is finer.

The parameter x is given as a function of shear velocity (U'_*), the grain roughness (k_s), and the kinematic viscosity of the fluid.

Assuming that equation 2 applies to the flow, U'_* is the shear velocity which would produce the observed mean velocity for flow with mean depth D and grain roughness k_s. The effective shear stress may be computed as $\tau' = \rho(U'_*)^2$.

When transport rates are plotted against effective shear stress (fig. 20), the reason for the similarity in transport relations at the two stations is readily apparent—the range in effective shear stress at the two stations is about the same. Although both depth and slope increase more rapidly at Otowi than at Bernalillo, the increase in flow resistance at Otowi offsets the increase in bed shear stress (γDS); hence the mean velocity is about the same as the mean velocity at Bernalillo for comparable discharges. Depth is greater and increases more rapidly with discharge at Otowi, but the bed material also becomes coarser with discharge, and the logarithm of the ratio D/k_s changes very little. The adjustments in the relations of velocity, depth, slope, and flow resistance for Bernalillo and Otowi are completely dissimilar; yet, so far as transport relations are concerned, the end results are about the same.

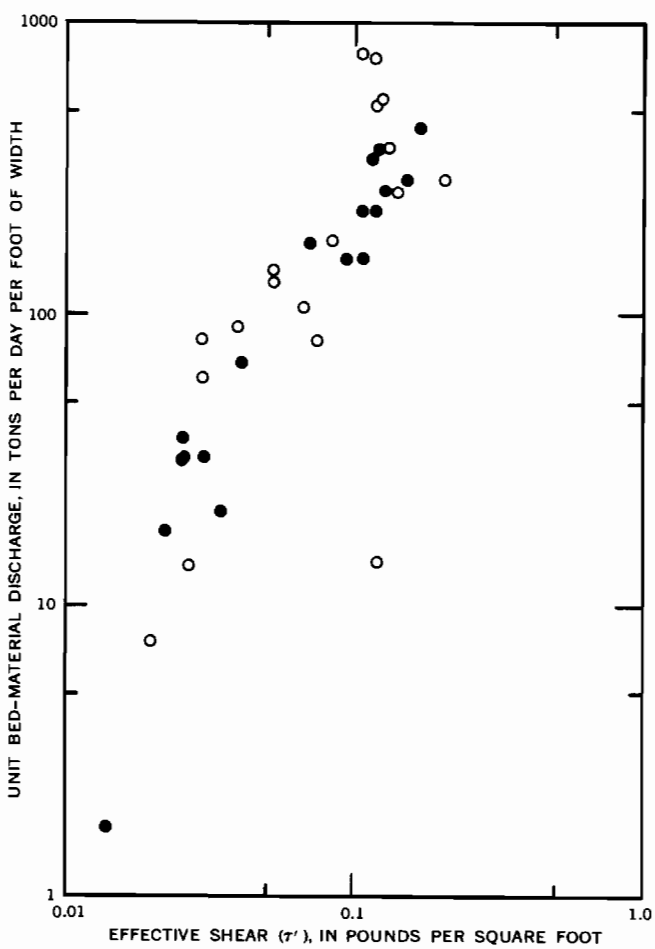

FIGURE 20.—Graph showing relation of unit bed-material discharge to effective shear stress for the Rio Grande at Otowi Bridge (O) and near Bernalillo (●).

There are still some erratic points in figure 20 for Otowi which might be expected to relate in some way to the variable size distribution of the bed material. Some of the scatter can be reduced by converting figure 20 to the form of a dimensionless shear stress-transport relation, as shown in figure 21. In this figure, abscissa values become

$$\frac{\tau'}{(\gamma_s - \gamma)d} \tag{3}$$

and the ordinate values are

$$\phi_T = \frac{q_T}{d^{3/2}\rho_s g^{3/2}\left(\frac{\rho_s - \rho}{\rho_s}\right)^{1/2}} \tag{4}$$

where ρ_s = the density of the sediment, assumed equal to 5.14 slugs per cubic foot,

ρ = the density of the fluid, 1.94 slugs per cubic foot,

g = acceleration due to gravity, 32.2 feet per second squared,

d = the median diameter of the bed material, in feet,

$\gamma = \rho g$, and

$\gamma_s = \rho_s g$.

Equations 3 and 4 are very similar in form to Bagnold's dimensionless shear-transport relation (Bagnold, 1956, eq. 42), and to Einstein's $\psi' = \phi$ relation (Einstein, 1950, equations 11, 42). Equation 3 is analogous to $1/\psi'$. However, both Einstein and Bagnold used the bed-load discharge in equation 4 rather than the total bed-material discharge, and Bagnold employed the total bed shear, rather than an effective shear.

A. A. Bishop (Sediment transport an alluvial channels: a critical examination of Einstein's theory: Colorado State Univ. Ph. D. thesis, 1961) suggested

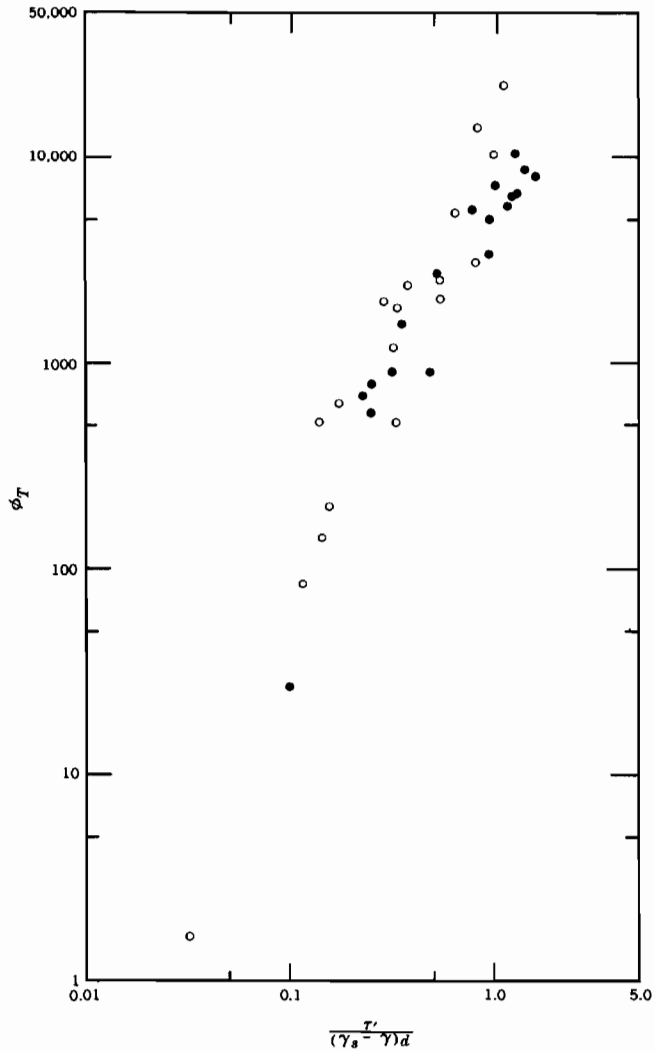

FIGURE 21.—Graph showing a dimensionless shear stress-transport relation for the Rio Grande at Otowi Bridge (○) and near Bernalillo (●).

that the total bed-material discharge (q_T) should be used in a dimensionless shear-transport relation similar to figure 21, and he proceeded to develop a family of curves from flume data for various sizes of bed material. The shear parameter ψ' is not directly comparable to equation 3 because different velocity equations were used to define the effective shear stresses, but a qualitative comparison shows that several differences exist between the relations in figure 21 and Bishop's curves. First, Bishop's curves show unrealistically high transport rates for the fine bed material at the higher effective shear stress values (low ψ' values); and second, for a given shear intensity (ψ') Bishop's curves show greater ϕ_T values for the finer sand than for the coarser material, whereas for figure 21, the reverse is true. The transport function ϕ_T is generally greater for Otowi than for Bernalillo.

The high transport rates in Bishop's relations may be attributable to the influence of standing waves and antidunes present in the flume at the high effective shears. Antidunes and standing waves are often observed in the Rio Grande but, because standing waves seldom occupy the full width of a natural channel, their influence on bed-material transport is usually local and transient (Nordin, 1964).

The trends of the plotted points in figure 21 suggest that Bishop is perhaps correct in attempting to develop a shear-transport relation in which the total bed-material transport rate rather than the bedload only is employed in the transport function. However, if Bishop's curves are applicable to the Rio Grande data, the Otowi points should fall below the Bernalillo points.

A consideration of equations 3 and 4 or of Bishop's $\Psi'=\phi_T$ curves shows two major shortcomings in the effective shear stress-transport relations. First, there is no direct consideration of temperature, which may have considerable influence on sediment transport through its direct effect on particle-fall velocity and its indirect effect on bed form (Straub and others, 1958; Kennedy, 1961); second, for any given value of effective shear stress, the bed-material discharge increases with increasing depth (Colby, 1961). To be generally applicable, the shear-transport relations of equations 3 and 4 should contain some correction for the effects of temperature and depth. Laursen (1958) gives the ratio of shear velocity to fall velocity as a major factor in determining both the bed-load concentration and the total bed-material concentration, and it seems likely that some form of this ratio should be introduced in the shear-transport parameters of figure 21. The ratio is a measure of the relative concentration distribution of suspended sediment and is commonly used in sediment transport relations.

This consideration of effective shear stress and transport for Otowi and Bernalillo leads to several important conclusions. The relations of velocity, shear, and roughness at the two stations are completely dissimilar, but the effects are compensating. At Otowi, the depth, bed shear stress, and roughness increase rapidly with discharge, whereas at Bernalillo, the depth and bed shear stress increase slowly and flow resistance decreases with increasing discharge. As a result, the velocity and effective shear at the two stations are about the same and the sediment transport relations are similar.

Either effective shear stress or mean velocity may be considered major parameters in sediment transport, as pointed out by Colby (1964). More specifically, the dimensionless transport function of equation 3, which is actually a measure of the ratio of the effective shear stress at the bed to the resistance of the topmost layer of the bed (Bagnold, 1956), would seem to be more suitable than the effective shear stress only.

Probably, the total bed-material transport may be considered a function of some shear-stress parameter as suggested by Bishop and as indicated by figure 21. However, some factors apparently would have to be introduced to explain the effect of temperature and depth.

No attempt was made to determine the most suitable method of estimating effective shear stress, to assess the grain size which should be used in equations 2, 3, and 4, or to introduce any corrections for the influence of temperature and depth in equations 3 and 4. These are questions which certainly deserve further study, but because total transport rates cannot generally be measured directly in the field, they are more suited to controlled laboratory investigations than to field studies. Actually, the lack of precision with which unit bed-material discharge (q_T) may be determined in the Rio Grande precludes any precise definition of the transport function (ϕ_T).

It might be pointed out that plotting the bed-material discharge (q_T) against effective shear stress in figures 20 and 21 is not exactly accurate, because the effective shear stress, or rather, the effective shear velocity from equation 2, is used to compute q_T in the modified Einstein method. However, Nordin (1964) has also pointed out that the total transport rate of bed material given by the modified Einstein method is dependent mostly upon the concentrations of bed material from suspended-sediment samples and that for a given cross section, excluding very shallow depths, the computed transport rates of material coarser than 0.062 mm bear a nearly constant ratio to the measured transport rates. Thus, the same qualitative conclusions could be drawn from figures 20 and 21, even if only the measured bed-material discharge had been considered.

BED-MATERIAL CHARACTERISTICS

For most sand-bed channels, the characteristics of the bed material change slightly with discharge or with time, and the bed-material characteristics to be used in transport parameters may often be expressed in terms of the median diameter or of some representative grain size. Even for some of the more complicated transport formulas, it is usually sufficient to specify only the median diameter and some simple gradation coefficient, or, as in the Meyer-Peter and Muller (1948) transport relations, an effective diameter which is weighted in terms of the percentage of each size class considered. For sand-gravel channels, however, in which the bed material exhibits a bimodal distribution and in which the distribution changes with time and discharge, such a simple representation of the bed-material characteristics does not seem adequate. Furthermore, it is difficult to relate, except in a general qualitative manner, the observed changes in the bed-material distribution to the observed changes in the transport relations. For example, from the data in table 1, the concentration of the bed material for Otowi decreases with time for the first five observations in 1958, but the temperature, velocity, depth, water-surface slope, and flow resistance change only a little. This apparent lack of a definable relationship between hydraulic variables and sediment transport was also obvious in figures 20 and 21.

The changes with time of the transport rates shown in table 1 must be directly related to the systematic changes with time of the characteristics of the bed material, shown in figure 22. Obviously, the median diameter and some simple gradation coefficient are not sufficient to describe the distributions in figure 22.

The lowest mean bed elevation (Culbertson and Dawdy, 1964) was for the second observation, on May 12, 1958. For the next three observations, the bed elevation increased somewhat—an indication that the coarse material was being transported into the reach from an upstream source and that some sort of selective transport process was depleting the material in the size range from about 0.5 mm to 2.0 mm. Field observations indicate that at low flows, sand is stored in the pools of pool-and-riffle channels. At higher flows, this sand is swept into suspension or otherwise moved from the pools, and some concurrent scour reduces the bed elevation, whereas the coarser gravel appears to move more or less continuously, independent of the bed elevation—that is, independent of channel scour. These observations explain, in part, why some of the cross sections of the Rio Grande exhibit the characteristics of sand-bed channels at low flows and of sand-gravel channels at high flows (Nordin and Culbertson, 1961). However, the problems of determining what causes systematic changes in bed-material characteristics in sand-gravel and pool-and-riffle channels, of describing methods to predict these changes, and of evaluating parameters to represent adequately the characteristics of the bed material in transport relations remain to be solved.

TEMPERATURE EFFECTS

The influence of temperature on sediment transport has been well documented by Straub and others (1958) and by Kennedy (1961), who have shown that a 50°F decrease in temperature will approximately triple the transport rate of bed material, other factors constant.

Figures 5 and 6 show that, for the Rio Grande, an increase in temperature accompanies a decrease in concentration during the spring-runoff event. The

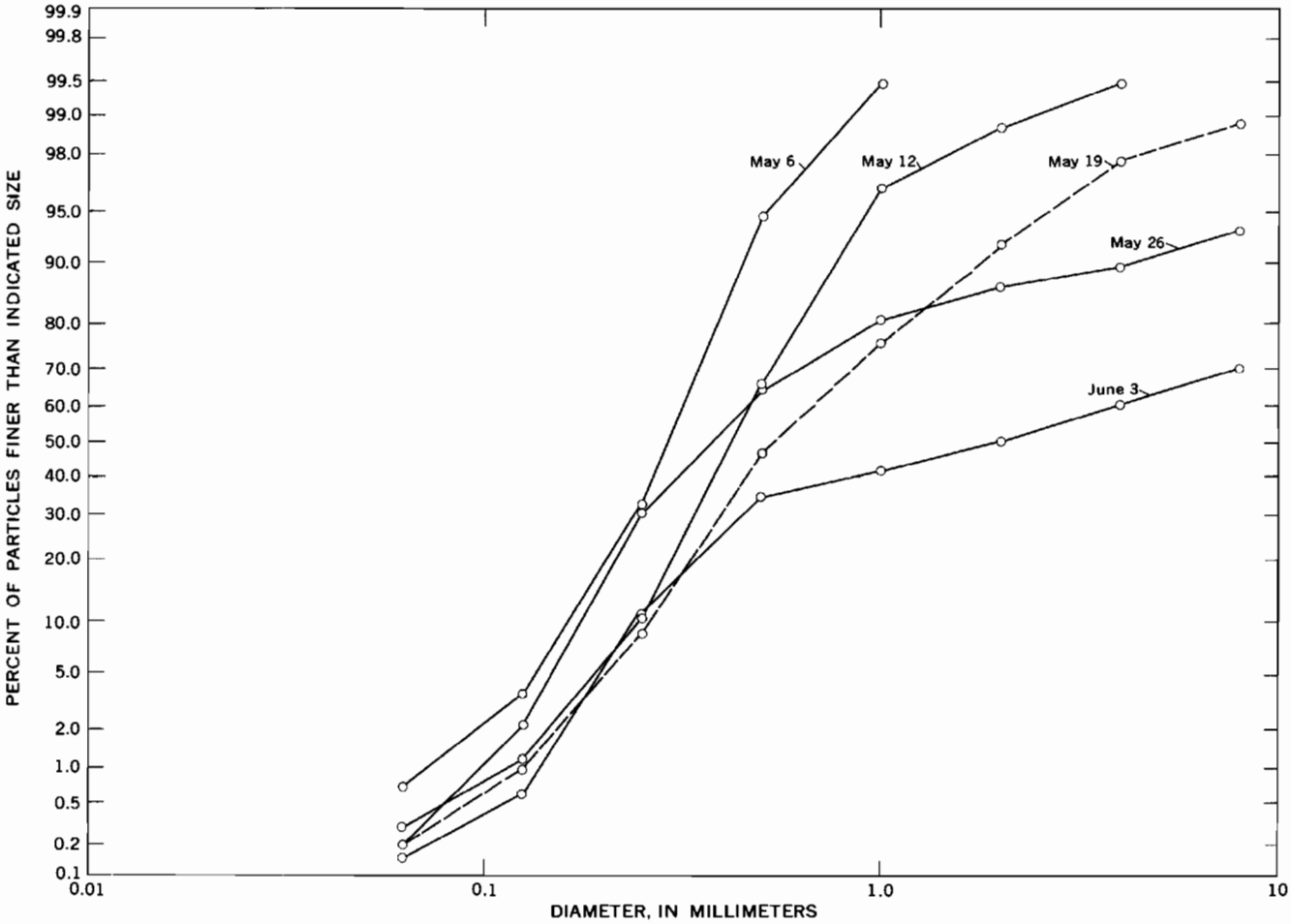

FIGURE 22.—Graph showing systematic changes in bed-material size distribution between May 6 and June 3, 1958, Rio Grande at Otowi Bridge.

decreasing concentration reflects changes in both the wash load and the bed-material load. Generally the bed-material concentration decreases less rapidly than the fine-material concentration.

Straub and others (1958) found that at a constant discharge, a decrease in temperature caused an increase in the slope, whereas the velocity and depth remained about constant. In a natural sand-bed channel, slope usually varies conservatively; hence a change in temperature for a given discharge results in a change in the velocity-depth relation. During a rising stage, a high bed-material discharge is accompanied by a high velocity, low depth, low flow resistance, and low water temperature. During receding stages, a lower bed-material discharge is accompanied by a low velocity, greater depth, greater flow resistance, and higher water temperature. In pool-and-riffle channels, temperature effects may be further complicated by changes in bed-material characteristics and by variations in slope with discharge.

Figure 23 shows the ratio of the computed bed-material concentration to the concentration from the velocity-concentration curve for Bernalillo (fig. 18) plotted against water temperature. Except in the four highest points, which were influenced by tributary inflow and are considered unrepresentative, the tendency for low ratios to accompany high water temperatures is apparent, but the relation is too poorly defined to yield a quantitative evaluation of the temperature effects.

Temperature effects would probably be more apparent if ratios were plotted from the q-q_T curves in figure 16 because, as noted previously, for a given water discharge, low temperatures usually accompany high sediment discharges, high velocities, and low depths. On the other hand, temperature effects on the V-C_T relations or on the V-q_T relations are complicated by the fact that temperature is not independent of flow resistance—that is, of the velocity-depth relation for a given cross section and a given water discharge.

Temperature is generally considered a factor of importance in sediment transport relations, but a precise quantitative evaluation of temperature effects is not possible, at least insofar as this investigation is

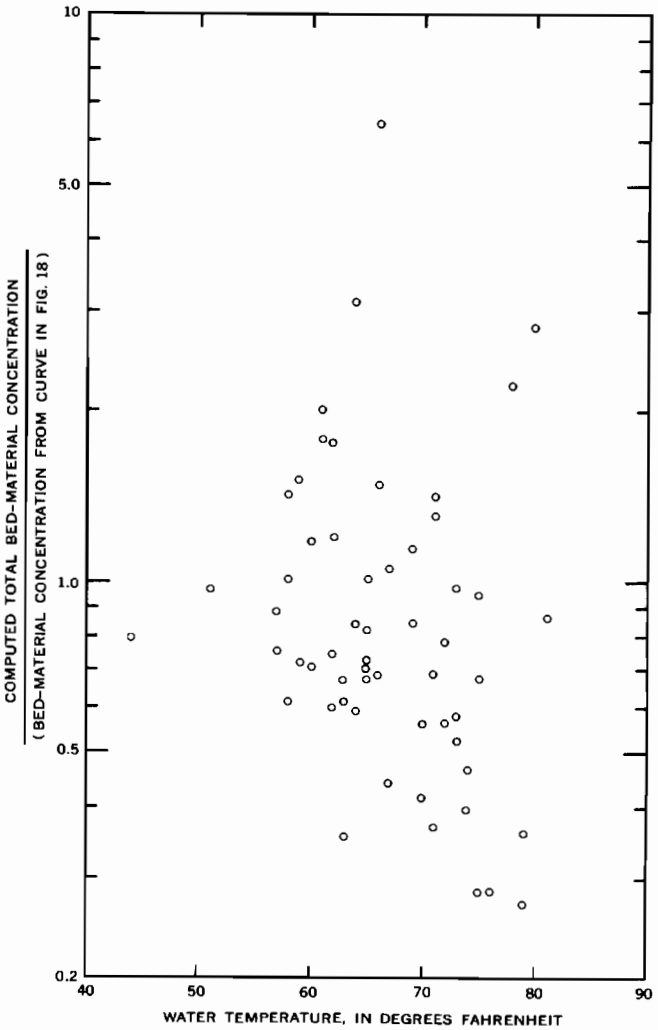

FIGURE 23.—Plot showing apparent effect of temperature on concentration, Rio Grande near Bernalillo, N. Mex.

concerned, for the Rio Grande data because the effects of temperature changes cannot be isolated from the effects of apparently interrelated changes in other variables.

OTHER CONSIDERATIONS

Many variables which influence sediment transport were not considered in this report. Studies of some of these factors, for the Rio Grande, have been presented elsewhere. Culbertson and Dawdy (1964) discussed depth-discharge discontinuities, and described the influence of changes in bed configuration and flow regime on sediment transport. Nordin and Dempster (1963) investigated vertical distributions of velocity and suspended-sediment concentration, and Nordin (1963) evaluated the influence of high concentrations of fine sediments on the relative concentration distribution of suspended sands.

Colby (1961, 1964) investigated many of these factors for a wide range of flow conditions, and developed several graphical relations to be used as a basis for the practical computations of bed-material discharge (Colby, 1964).

So far as the writers know, this report presents the first detailed information on the flow characteristics and transport relations for reaches of the Rio Grande with pool-and-riffle channel configurations and bimodal distributions of bed material. Additional studies in this area are highly desirable.

Finally, this investigation was of a single southwestern stream with a limited range of flow conditions. The findings of this study are probably not applicable to other flow conditions, especially to streams of great depth.

CONCLUSIONS

Bed-material discharge, computed by the modified Einstein method, is related to simple hydraulic variables for observations at six sediment stations through a 110-mile reach of the Rio Grande in New Mexico. Transport relations vary in a downstream direction, or with decreasing particle size, and fall into two distinct groups, one group representing the confined sections and the other representing sections without lateral restrictions. At low flows, greater sediment loads are transported at the narrow sections, while at high flows, greater loads are carried at the wide sections. This difference reflects the tendency for the wide sections to aggrade and channelize at low flows.

Flow characteristics at Otowi, which is the farthest upstream station and which has a pool-and-riffle channel configuration and a bimodal distribution of bed material, differ markedly from the flow characteristics at Bernalillo, which has a sand-bed channel. At Otowi, the depth, water-surface slope, bed shear stress, resistance to flow, and bed-material size increase with increasing water discharge. Near Bernalillo, water-surface slope and bed-material characteristics are approximately constant, flow resistance decreases with discharge, and the range in bed shear stress, compared to that at Otowi, is very limited.

The mean velocity and bed-material discharge for the two stations are comparable, and sediment-transport rates relate reasonably well to effective shear. However, the variable size distribution of bed material introduces considerable scatter in the relation for Otowi. Converting the shear-transport relations to a dimensionless form, in which the shear parameter is a measure of the ratio of the effective shear to the resistance of the topmost layer of the bed, reduces much of the scatter. This relation is very similar to the curves developed by A. A. Bishop (Sediment transport in alluvial channels: a critical examination of Einstein's theory, Colorado State Univ. Ph. D. thesis, 1961) to predict total bed-material

discharge. A qualitative comparison of the Rio Grande relations with Bishop's curves indicates that, to be generally applicable, the dimensionless shear-transport relations for predicting total bed-material transport should probably include parameters to explain the effects of temperature and flow depth.

In addition, systematic changes in bed-material characteristics at Otowi appear to be related to changes in transport which are independent of flow variables. Changes in the bed material may be caused by some selective transport process which depletes material in the size range from about 0.5 to 2.0 mm. A single representative grain size in the shear-transport relations probably does not adequately represent the complex bimodal size distribution of sand-gravel channels.

A consideration of water-temperature effects indicates that high bed-material discharge is associated with low temperatures. However, a quantitative evaluation of the influence of temperature was impossible because the effects of temperature changes are not independent of the effects of changes in flow resistance and in the velocity-depth relations.

TABLE 1.—*Basic hydraulic data with measured and computed sediment concentrations, Rio Grande at Otowi Bridge, near San Ildefonso, N. Mex.*

Date	Time	Q (cfs)	B (ft)	V (ft per sec)	D (ft)	S	T (°F)	Measured concentration of suspended load, ppm		Computed total concentration, ppm	
								All sizes	>0.062 mm	All sizes	>0.062 mm
1958											
May 6	1720	7,320	132	6.84	8.11	0.00230	59	7,440	4,960	7,790	5,310
May 12	1245	9,340	130	7.02	10.23	.00246	58	5,020	2,920	6,030	3,920
May 19	1720	9,490	145	6.98	9.38	[1].00240	62	2,390	834	3,050	1,500
May 26	1240	10,100	140	7.08	10.21	.00235	61	2,990	2,140	3,540	2,700
June 3	1015	8,590	135	7.10	8.96	.00240	62	1,720	1,240	2,190	1,710
June 9	1045	5,210	129	6.44	6.27	.00220	60	3,180	2,810	5,350	5,190
June 12	1040	5,000	125	5.56	7.19	.00231	62	1,110	942	1,860	1,690
June 17	0920	2,240	113	4.23	4.69	.00163	67	1,860	1,770	2,780	2,690
June 24	1030	1,130	234	3.35	1.44	.00131	72	316	262	1,150	1,100
1959											
Aug. 8	1145	1,270	120	3.04	3.47	----------	73	24,000	2,210	24,700	2,910
1961											
Apr. 25	1310	2,780	121	4.34	5.30	.00144	52	1,350	819	1,830	1,300
May 2	1415	4,000	128	4.10	7.63	.00133	57	2,480	1,180	2,840	1,540
May 17	1145	2,750	115	5.03	4.75	.00159	56	1,120	829	1,910	1,620
June 21	1440	908	97	2.82	3.32	.00072	76	284	146	689	551
July 20	1245	1,090	98	3.08	3.61	.00081	74	3,590	1,210	4,380	2,000
1962											
Apr. 19	1350	6,000	130	5.88	7.85	.00196	59	4,240	2,500	4,800	3,060
May 31	1350	1,460	112	3.87	3.37	.00098	59	1,660	1,540	2,740	2,620
July 2	1345	684	109	2.50	2.51	.00092	78	203	159	488	445

[1] Estimated.

TABLE 2.—*Basic hydraulic data with measured and computed sediment concentrations, Rio Grande at Cochiti, N. Mex.*

Date	Time	Q (cfs)	B (ft)	V (ft per sec)	D (ft)	S	T (°F)	Measured concentration of suspended load (ppm)		Computed total concentration (ppm)	
								All sizes	>0.062 mm	All sizes	>0.062 mm
1954											
Mar. 10	1200	416	208	1.70	1.17	[1] 0.00129	54	83	45	217	178
Mar. 23	1200	309	177	1.74	1.01	[1] .00129	51	57	11	90	43
Apr. 7	1135	541	288	1.91	.98	[1] .00129	58	290	32	400	135
Apr. 20	1135	709	300	1.94	1.22	[1] .00129	58	581	105	765	273
May 4	1000	1,170	300	2.26	1.73	[1] .00129	63	1,780	392	2,430	1,030
May 20	1210	1,590	284	2.97	1.89	[1] .00129	67	2,000	800	2,630	1,400
June 1	1150	881	300	2.19	1.34	[1] .00129	67	425	191	711	469
June 14	1045	667	204	1.89	1.73	[1] .00129	65	298	179	434	314
July 12	1150	784	295	2.14	1.24	[1] .00129	77	1,270	152	1,660	499
Aug. 10	1145	264	172	1.50	1.02	[1] .00129	73	750	352	878	472
Aug. 24	1125	252	175	1.50	.96	[1] .00129	70	2,920	29	3,080	149
Sept. 8	1105	500	178	1.87	1.50	[1] .00129	70	3,130	31	3,530	639
Sept. 23	1205	67.8	77.0	.97	.91	[1] .00129	71	118	37	212	129
Oct. 5	1245	144	88.0	1.38	1.18	[1] .00129	72	186	41	239	92
Oct. 19	1205	294	100	1.84	1.60	[1] .00129	58	182	107	351	276
Nov. 17	1330	347	115	2.03	1.49	[1] .00129	49	637	382	1,140	877
Dec. 15	1340	327	115	1.98	1.43	[1] .00129	38	362	261	1,390	1,290
Dec. 29	1510	464	124	2.27	1.65	[1] .00129	36	561	381	2,030	1,850
1955											
Jan. 11	1455	464	126	2.16	1.71	[1] .00129	37	1,030	865	1,970	1,800
Jan. 26	1515	468	128	2.14	1.71	[1] .00129	36	792	420	1,580	1,200
Feb. 9	1540	503	130	2.18	1.78	[1] .00129	40	670	436	1,620	1,390
Feb. 23	1445	517	124	2.28	1.83	[1] .00129	38	422	118	907	598
Mar. 8	1410	529	133	2.29	1.74	[1] .00129	49	540	173	1,700	1,330
Mar. 22	1500	414	120	2.17	1.59	[1] .00129	49	300	81	766	543
Apr. 6	1450	154	95.0	1.50	1.08	[1] .00129	53	66	7	99	39
Apr. 19	1310	272	114	1.84	1.30	[1] .00129	58	261	44	595	374
May 17	1530	1,040	280	2.45	1.52	[1] .00129	60	2,320	1,210	3,350	2,220
June 14	1045	514	164	1.80	1.74	[1] .00129	75	189	112	301	222
June 29	1205	262	90.0	1.66	1.76	[1] .00129	72	28	9	65	46
July 11	1315	420	100	2.16	1.94	[1] .00129	75	222	73	396	244
July 25	1425	161	86.0	1.32	1.42	[1] .00129	81	621	6	644	24
Aug. 8	1425	883	271	2.68	1.22	[1] .00129	76	15,700	628	16,900	1,410
Sept. 6	1150	1,150	279	2.84	1.46	[1] .00129	71	3,340	1,740	4,270	2,600
Sept. 19	1410	232	89.0	1.77	1.47	[1] .00129	74	623	137	734	234
Oct. 3	1500	205	90.0	1.65	1.38	[1] .00129	70	924	388	1,130	585
Oct. 18	1320	171	84.0	1.51	1.20	[1] .00129	63	170	126	295	248
Nov. 2	1400	173	92.0	1.59	1.18	[1] .00129	52	192	156	381	344
Nov. 15	1250	352	135	2.03	1.28	[1] .00129	42	1,160	974	1,890	1,700
Nov. 28	1150	385	104	2.77	1.34	[1] .00129	40	748	568	1,540	1,360
Dec. 14	1130	484	114	3.36	1.26	[1] .00129	36	947	701	2,250	2,000
Dec. 27	1100	558	125	3.15	1.42	[1] .00129	39	999	739	2,000	1,740
1956											
Jan. 24	1130	555	130	2.64	1.62	[1] .00129	41	895	770	1,690	1,560
Feb. 7	1140	583	140	2.67	1.56	[1] .00129	37	1,260	995	2,120	1,850
Feb. 22	1030	478	130	2.21	1.66	[1] .00129	42	3,170	2,880	3,630	3,350
Mar. 7	1220	938	259	2.28	1.59	[1] .00129	43	3,630	1,780	7,840	5,990
Apr. 3	1420	964	300	2.23	1.44	[1] .00129	47	5,000	3,750	5,750	4,470
Apr. 18	1430	919	241	2.63	1.45	[1] .00129	52	5,030	4,070	5,970	5,000
May 2	1530	1,250	281	2.73	1.63	[1] .00129	59	2,200	1,210	2,950	1,930
May 15	1315	556	256	2.31	.94	[1] .00129	59	939	639	1,940	1,640
May 29	1145	943	233	3.09	1.31	[1] .00129	66	969	669	2,040	1,730
June 12	1345	711	264	2.18	1.23	[1] .00129	73	1,060	901	1,370	1,210
June 26	1115	64.6	52.5	.88	1.40	[1] .00129	77	36	15	40	19
July 10	1200	34.7	61.0	.63	.90	[1] .00129	80	30	2	31	2
1957											
May 16	1600	3,470	283	4.81	2.55	[1] .00129	54	2,550	1,890	3,600	2,920
May 29	1500	3,350	287	4.65	2.51	[1] .00129	62	2,770	2,240	4,170	3,630
June 12	1700	5,520	297	5.61	3.31	[1] .00129	62	5,410	4,330	6,310	5,210
June 26	1740	4,800	291	5.27	3.13	[1] .00129	67	3,940	3,390	5,300	4,740
1958											
May 7	1210	7,960	308	6.58	3.93	[1] .00129	55	6,090	3,330	6,980	4,220
May 12	1550	8,900	328	6.64	4.09	.00120	58	4,550	2,700	6,030	4,160
May 20	1205	8,920	316	6.51	4.34	.00120	58	3,110	1,980	3,810	2,680
May 26	1630	9,810	335	6.67	4.39	.00127	61	3,110	2,100	3,490	2,480
June 3	1315	8,680	295	6.07	4.85	.00127	63	3,110	2,580	3,670	3,140
June 9	1340	4,990	297	4.62	3.64	.00123	62	7,670	7,170	11,200	10,700
June 12	1240	5,060	298	4.22	4.03	.00113	63	8,840	8,740	11,500	11,400
June 17	1205	2,040	285	3.20	2.24	.00118	70	5,240	5,050	7,410	7,230
June 24	1340	1,000	263	2.23	1.71	.00118	75	247	140	663	556
1961											
Apr. 26	1050	2,090	285	3.36	2.18	.00134	52	1,210	713	2,130	1,630
May 2	1155	3,680	288	4.54	2.82	.00137	57	2,370	1,040	3,150	1,820
May 18	1150	2,620	281	3.90	2.39	.00137	59	2,750	2,450	3,600	3,300
June 22	1110	674	280	2.25	1.09	.00128	76	153	30	491	304

[1] Average bed slope from aggradation-degradation studies.

TABLE 3.—*Basic hydraulic data with measured and computed sediment concentrations, Rio Grande at San Felipe, N. Mex.*

Date	Time	Q (cfs)	B (ft)	V (ft per sec)	D (ft)	S	T (°F)	Measured concentration of suspended load (ppm)		Computed total concentration (ppm)	
								All sizes	>0.062 mm	All sizes	>0.062 mm
1954											
Mar. 10	1445	457	153	2.17	1.38	[1] 0.00150	56	250	115	507	367
Mar. 23	1525	414	153	2.00	1.35	[1] .00150	53	308	166	464	320
Apr. 7	1500	562	153	2.42	1.52	[1] .00150	62	405	162	778	529
Apr. 20	1510	762	212	2.22	1.62	[1] .00150	64	790	245	1,230	667
May 4	1335	1,170	225	2.58	2.02	[1] .00150	64	1,770	425	2,260	879
May 20	1515	1,710	276	3.00	2.07	[1] .00150	74	2,010	764	3,340	2,090
June 1	1515	919	266	2.21	1.56	[1] .00150	71	513	262	857	596
June 14	1445	755	223	2.25	1.51	[1] .00150	68	339	197	699	553
July 12	1510	787	262	2.19	1.37	[1] .00150	81	1,560	468	2,230	1,120
Aug. 13	1330	330	145	1.98	1.15	[1] .90150	76	13,500	351	13,600	405
Aug. 24	1525	361	198	2.20	.83	[1] .00150	73	12,200	488	13,700	1,550
Sept. 8	1400	563	176	2.23	1.43	[1] .00150	73	4,220	591	4,780	1,080
Sept. 23	1505	169	90	1.75	1.07	[1] .00150	69	263	68	456	256
Oct. 5	1520	294	150	1.81	1.08	[1] .00150	74	639	198	950	496
Oct. 19	1445	305	150	1.96	1.04	[1] .00150	60	865	372	1,200	681
Nov. 3	1305	252	166	1.64	.93	[1] .00150	52	656	407	1,010	748
Nov. 17	1120	360	172	1.83	1.15	[1] .00150	44	1,280	858	1,690	1,260
Nov. 30	1025	369	172	2.02	1.06	[1] .00150	41	849	577	1,470	1,190
Dec. 15	1100	358	172	1.95	1.07	[1] .00150	34	954	725	1,540	1,280
Dec. 30	1450	386	75	2.80	1.84	[1] .00150	32	1,030	834	1,460	1,260
1955											
Jan. 11	1205	485	174	2.19	1.27	[1] .00150	36	926	630	1,420	1,120
Feb. 28	1555	515	169	2.27	1.34	[1] .00150	47	726	421	1,680	1,360
Mar. 7	1430	581	178	2.33	1.40	[1] .00150	48	935	552	1,820	1,420
Mar. 22	1120	480	178	2.18	1.24	[1] .00150	42	670	315	1,090	722
May 3	1155	446	176	1.67	1.52	[1] .00150	59	636	134	824	311
May 17	1050	1,180	143	2.97	2.78	[1] .00150	57	2,370	1,040	2,870	1,530
June 2	1245	1,580	146	3.69	2.93	[1] .00150	70	3,080	2,130	4,260	3,290
June 29	1500	309	151	1.77	1.16	[1] .90150	76	444	89	579	213
July 11	1010	453	174	1.90	1.37	[1] .00150	71	1,550	1,320	1,690	1,450
July 25	1005	366	155	2.44	.97	[1] .00150	71	38,300	1,150	41,100	3,410
Aug. 9	1405	862	128	3.13	2.15	[1] .00150	84	35,700	2,140	37,000	3,350
Sept. 6	1430	1,140	152	3.69	2.03	[1] .00150	74	5,670	3,800	6,500	4,580
Sept. 19	1145	264	146	1.62	1.12	[1] .00150	70	631	442	1,370	1,180
Oct. 4	1500	206	116	1.84	.97	[1] .00150	73	1,170	573	1,540	924
Oct. 19	1430	235	130	1.73	1.05	[1] .00150	64	712	278	1,160	719
Nov. 2	1115	273	124	1.88	1.17	[1] .00150	44	2,040	1,530	2,210	1,700
Nov. 14	1435	372	126	2.21	1.33	[1] .00150	52	1,510	846	2,100	1,380
Nov. 28	1500	426	111	2.70	1.42	[1] .00150	44	1,440	893	2,250	1,680
Dec. 14	1515	497	111	2.70	1.66	[1] .00150	40	1,480	1,080	2,140	1,730
Dec. 27	1335	615	115	3.03	1.77	[1] .00150	40	1,510	1,030	2,280	1,780
1956											
Jan. 10	1510	571	157	2.79	1.31	[1] .00150	43	1,100	781	2,010	1,670
Jan. 24	1440	523	150	2.78	1.25	[1] .00150	43	938	732	1,890	1,660
Feb. 7	1415	605	213	3.00	.95	[1] .00150	40	1,200	792	2,680	2,260
Feb. 22	1345	478	118	2.58	1.57	[1] .00150	47	867	685	1,490	1,300
Mar. 6	1405	863	258	2.61	1.28	[1] .00150	47	3,870	1,160	4,900	2,110
Mar. 21	1045	508	105	2.47	1.96	[1] .00150	51	916	522	1,380	981
Apr. 4	1425	892	215	2.84	1.46	[1] .00150	51	1,650	528	2,370	1,230
Apr. 19	1030	929	214	2.88	1.50	[1] .00150	50	1,780	890	2,660	1,750
May 2	1020	1,250	263	3.23	1.47	[1] .00150	58	2,170	1,020	3,190	2,000
May 15	1615	599	150	2.25	1.77	[1] .00150	66	2,550	2,170	2,820	2,430
May 29	1420	888	202	2.57	1.71	[1] .00150	70	1,190	702	1,830	1,320
June 12	1630	667	197	2.34	1.45	[1] .00150	76	641	397	1,130	876
July 10	1415	104	142	.85	.86	[1] .00150	80	84	3	86	5
July 24	1345	256	108	1.94	1.22	[1] .00150	80	608	91	1,200	671
1957											
May 15	1430	3,580	140	5.19	4.93	[1] .00150	57	3,360	2,180	3,900	2,710
May 28	1320	3,010	144	5.25	3.98	[1] .00150	61	2,250	1,780	2,890	2,410
June 13	1100	5,160	150	6.18	5.57	[1] .00150	64	2,670	1,900	3,400	2,620
June 28	1400	4,760	149	5.96	5.36	[1] .00150	73	2,160	1,620	3,580	3,030
1958											
May 12	1720	8,200	205	7.10	5.56	.00176	59	4,410	2,780	5,330	3,700
May 21	1250	9,140	210	7.43	5.86	.00180	65	2,790	1,670	3,140	2,020
May 26	1335	9,720	209	7.53	6.17	.00193	67	2,580	1,550	3,490	2,460
June 3	1630	8,590	200	7.16	6.00	.00168	67	2,430	1,610	3,130	2,310
June 9	1700	5,120	188	6.06	4.49	.00151	66	6,300	5,780	8,390	7,880
June 12	1710	5,010	187	5.99	4.47	.00151	66	2,740	2,400	4,510	4,170
June 17	1345	2,200	182	4.44	2.73	.00091	75	1,100	898	1,820	1,620
June 24	1600	1,020	181	2.60	2.17	.00100	80	577	418	1,390	1,230
1961											
Apr. 26	1350	2,200	177	4.60	2.70	.00115	57	1,360	797	2,100	1,540
May 2	1535	3,580	163	5.49	4.00	.00126	62	2,890	1,480	4,150	2,740
May 18	1110	2,510	168	4.99	3.10	.00108	62	1,040	685	1,800	1,450
June 22	1440	680	162	2.31	1.76	.00197	76	519	371	877	729

[1] Average bed slope from aggradation-degradation studies.

TABLE 4.—*Basic hydraulic data with measured and computed sediment concentrations, Rio Grande near Bernalillo, N. Mex.*

Date	Time	Q (cfs)	B (ft)	V (ft per sec)	D (ft)	S	T (°F)	Measured concentration of suspended load (ppm)		Computed total concentration (ppm)	
								All sizes	>0.062 mm	All sizes	>0.062 mm
1952											
Apr 25	----------	2,730	272	4.06	2.46	0.00089	58	3,320	1,860	4,640	3,130
May 12	----------	6,490	272	6.57	3.63	.00084	62	3,160	2,120	5,390	4,330
June 17	----------	6,140	272	5.96	3.79	.00083	70	1,990	1,550	2,590	2,150
June 20	----------	4,830	272	5.09	3.49	.00079	72	1,690	1,320	2,710	2,340
June 26	----------	2,760	269	3.71	2.76	.00076	70	1,040	853	1,700	1,520
July 24	----------	2,060	270	2.84	2.69	.00080	75	2,490	872	2,860	1,260
1953											
Apr. 29	----------	1,540	270	2.65	2.15	[1].00086	57	2,450	735	3,190	1,470
May 5	----------	551	265	1.66	1.25	[1].00086	63	554	288	809	544
June 1	----------	2,570	270	3.58	2.66	.00093	65	2,530	835	3,400	1,710
June 2	----------	2,150	270	3.11	2.56	[1].00086	71	2,010	724	2,750	1,460
June 4	----------	2,090	270	3.12	2.48	.00083	62	1.600	672	2,220	1,290
June 17	----------	1,340	268	2.34	2.14	.00086	69	1,060	615	1,640	1,200
1956											
Apr. 2	1520	759	237	2.23	1.44	[1].00086	47	3,560	2,140	4,030	2,570
Apr. 14	1235	610	262	1.98	1.18	[1].00086	51	1,840	589	2,390	1,100
Apr. 16	1615	623	266	1.91	1.23	[1].00086	62	2,360	920	2,790	1,310
Apr. 21	1410	741	280	2.05	1.29	[1].00086	65	2,100	672	2,700	1,230
Apr. 23	1505	653	255	1.94	1.32	[1].00086	64	3,330	2,060	4,510	3,210
May 1	1430	920	274	2.37	1.42	[1].00086	61	3,890	2,100	4,710	2,880
May 5	1330	1,000	266	2.51	1.50	[1].00086	69	2,600	1,010	3,450	1,810
May 12	1305	986	263	2.90	1.29	[1].00086	66	1,120	549	1,900	1,310
May 14	1415	395	244	1.44	1 12	[1].00086	61	2,040	857	2,520	1,310
May 18	1320	199	79.0	1.70	1.48	[1].00086	75	319	128	452	261
May 22	1325	98.4	89.0	1.40	.79	[1].00086	71	199	105	347	262
May 26	1330	564	262	2.01	1.07	[1].00086	71	1,720	688	2,600	1,520
May 29	1115	573	171	1.97	1.70	[1].00086	66	4,410	3,700	7,950	7,240
June 2	1630	496	260	1.85	1.03	[1].00086	75	926	444	1,490	985
June 4	1120	493	214	1.76	1.31	[1].00086	72	1,010	465	1,320	759
June 8	1200	612	294	1.89	1.10	[1].00086	78	2,090	1,250	3,240	2,370
June 12	1050	479	160	1.76	1.70	[1].00086	73	718	323	970	562
June 15	1230	186	46.0	2.09	1.94	[1].00086	80	3,820	2,250	5,040	3,460
June 29	1245	270	180	1.62	.93	[1].00086	81	3,350	402	3,750	741
Aug. 24	1040	17.6	29.0	1.17	.52	[1].00086	79	855	68	1,000	200
Sept. 7	1140	81.2	108	1.30	.58	[1].00086	76	1,000	60	1,140	183
1957											
Apr. 29	1500	1,580	275	3.73	1.54	[1].00086	59	3,680	2,240	5,460	4,160
May 13	1800	4,150	271	5.00	3.06	[1].00086	58	6,320	4,040	8,140	5,830
May 16	1800	3,080	272	5.17	2.19	[1].00086	60	4,460	3,120	6,430	5,050
May 27	1555	2,850	271	4.31	2.44	[1] 00086	64	2,540	1,730	3,640	2,810
June 11	1600	5,160	271	5.86	3.25	[1].00086	65	3,570	2,610	5,120	4,140
June 24	1630	4,570	271	5.56	3.03	[1].00086	73	1,900	1,290	3,080	2,460
1958											
May 8	1035	6,860	270	6.91	3.68	.00080	58	4,420	2,480	5,860	3,930
May 13	1035	8,320	271	6.88	4.46	.00080	60	4,740	3,180	6,050	4,500
May 21	1530	8,680	270	7.82	4.11	.00079	67	3,400	2,240	6,240	5,080
May 27	1130	10,100	273	7.71	4.80	.00080	74	3,040	2,070	3,920	2,940
June 4	1145	8,160	272	6.92	4.34	.00083	67	2,580	1,880	3,510	2,800
June 10	1015	5,800	270	6.27	3.43	.00074	65	3,480	2,850	4,570	3,950
June 13	1030	4,340	266	6.10	2.67	.00076	63	2,080	1,710	3,990	3,610
June 18	0945	4,000	267	5.06	2.96	.00076	67	5,980	2,930	7,460	4,390
June 25	1110	6,040	273	6.50	3.40	.00080	73	5,410	3,950	7,240	5,760
1960											
Feb. 15	1430	602	128	2.55	1.84	[1].00086	44	1,430	940	1,760	1,270
Apr. 6	1320	2,100	269	3.04	2.56	.00083	59	1,900	950	2,430	1,480
May 24	1220	1,240	133	2.71	3.44	.00083	65	1,200	768	1,720	1,280
June 22	0950	2,030	268	2.89	2.93	.00082	74	781	523	1,170	894
1961											
Apr. 27	1230	2,230	267	3.16	2.64	.00083	57	1,790	1,150	2,290	1,640
May 3	1430	3,360	270	3.99	3.12	.00083	66	2,670	1,320	3,400	2,040
May 11	1120	2,260	268	3.62	2.33	.00085	63	1,250	755	1,310	934
1962											
Apr. 30	1315	5,340	276	6.01	3.22	.00086	64	4,360	2,000	5,250	3,160
June 1	1430	987	223	2.88	1.54	.00080	71	1,720	1,490	2,960	2,730
June 25	1245	453	227	2.00	1.00	.00079	79	185	73	410	315

[1] Average of observed water-surface slopes.

TABLE 5.—*Basic hydraulic data with measured and computed sediment concentrations, Rio Grande at Albuquerque, N. Mex.*

Date	Time	Q (cfs)	B (ft)	V (ft per sec)	D (ft)	S[1]	T (°F)	Measured concentration of suspended load (ppm)		Computed total concentration (ppm)	
								All sizes	>0.062 mm	All sizes	>0.062 mm
1954											
Mar. 8	0930	268	77.0	1.99	1.75	0.00110	44	659	165	967	466
Mar. 11	1010	101	84.0	.99	1.21	.00110	49	588	6	598	6
Mar. 26	1045	670	333	1.83	1.10	.00110	47	2,890	578	3,420	1,060
Apr. 6	1150	386	338	1.63	.70	.00110	57	2,520	227	3,060	729
Apr. 8	1010	128	96.0	1.16	1.15	.00110	51	572	29	613	63
Apr. 19	1110	721	362	1.90	1.05	.00110	62	2,220	577	2,540	851
Apr. 22	1010	429	136	2.03	1.55	.00110	58	1,250	325	1,480	539
May 3	1330	1,420	332	2.72	1.57	.00110	65	3,780	643	4,670	1,450
May 6	1030	635	340	1.69	1.10	.00110	63	1,320	264	1,650	572
May 17	1620	1,420	333	2.61	1.63	.00110	67	3,190	510	3,770	1,060
May 21	1045	1,300	350	2.15	1.73	.00110	67	2,450	588	2,930	1,040
June 2	1025	388	115	1.63	2.07	.00110	67	523	120	612	204
June 4	1100	318	130	1.89	1.29	.00110	67	510	168	766	415
June 14	1000	427	135	1.89	1.67	.00110	67	635	254	958	574
June 18	1035	68.8	55.0	1.64	.76	.00110	61	307	227	732	651
July 12	1025	623	172	2.00	1.52	.00110	81	5,970	239	6,510	700
July 27	1000	172	96.0	1.31	1.36	.00110	82	2,970	89	3,080	149
Aug. 10	0900	236	103	1.69	1.36	.00110	70	9,370	94	9,510	94
Aug. 24	1545	1,040	246	3.18	1.33	.00110	75	56,300	1,130	58,800	2,900
Sept. 7	1030	366	128	1.98	1.45	.00110	71	19,600	784	21,700	2,640
Oct. 4	1630	71.9	31.5	1.67	1.37	.00110	78	2,390	96	2,600	274
Oct. 18	1440	81.0	58.0	1.52	.92	.00110	64	1,830	55	2,070	252
Nov. 2	1610	23.9	26.0	1.30	.71	.00110	57	525	32	601	99
Nov. 16	1125	247	154	1.87	.86	.00110	48	1,780	142	2,170	509
Dec. 13	1430	348	178	1.71	1.14	.00110	42	1,560	218	1,880	505
1955											
Jan. 10	1305	444	236	1.92	.98	.00110	37	1,720	413	2,350	996
Jan. 24	1150	242	135	1.70	1.05	.00110	34	893	277	1,230	594
Feb. 25	0925	558	355	1.86	.85	.00110	35	2,030	731	3,060	1,730
Mar. 7	1350	395	155	1.88	1.35	.00110	50	1,260	164	1,520	406
Mar. 22	1315	293	159	1.60	1.15	.00110	47	947	104	1,130	268
Apr. 4	0950	132	87.0	1.37	1.11	.00110	45	672	27	710	53
May 2	1420	281	98.0	2.01	1.43	.00110	58	1,630	244	2,050	637
May 31	1120	902	400	1.88	1.20	.00110	63	1,800	468	2,210	831
June 13	1400	205	96.0	1.40	1.52	.00110	60	1,070	749	1,140	816
June 27	1220	73.7	78.0	1.40	.67	.00110	61	211	34	327	140
July 11	1345	143	110	1.13	1.15	.00110	72	351	42	414	97
July 25	1330	265	97.0	1.80	1.52	.00110	72	14,600	584	15,100	1,070
Aug. 11	1400	2,520	327	3.91	1.97	.00110	76	49,800	3,980	51,800	5,820
Aug. 23	1130	1,380	325	3.45	1.23	.00110	75	39,800	1,190	42,300	3,080
Sept. 6	1215	791	327	1.67	1.45	.00110	73	3,960	990	5,930	2,920
Sept. 19	1510	51.0	71.0	1.21	.59	.00110	67	107	5	155	53
Oct. 4	1445	101	110	1.39	.66	.00110	68	1,420	28	1,560	143
Dec. 1	1430	406	155	2.01	1.30	.00110	49	1,310	236	1,680	570
Dec. 12	1450	430	133	2.04	1.59	.00110	42	1,900	513	2,230	807
Dec. 27	1430	602	169	1.92	1.85	.00110	48	2,680	858	3,060	1,210
1956											
Jan. 9	1545	582	149	2.24	1.74	.00110	48	2,210	597	2,720	1,060
Jan. 23	1555	605	166	2.63	1.39	.00110	43	1,910	707	2,900	1,650
Feb. 7	1545	676	186	2.59	1.40	.00110	45	4,130	1,240	5,440	2,460
Feb. 20	1600	570	224	1.93	1.32	.00110	50	3,090	1,050	3,850	1,420
July 20	1200	3,750	332	4.08	2.77	.00110	70	62,300	3,740	67,700	6,820
1957											
May 14	1515	4,030	320	4.17	3.02	.00110	62	9,490	6,260	10,800	7,550
May 27	1210	3,040	320	3.96	2.40	.00110	65	3,910	2,740	4,930	3,730
June 10	1245	5,500	324	4.20	4.04	.00110	67	5,540	3,930	6,610	4,990
June 24	1545	5,050	325	3.37	4.62	.00110	75	8,490	7,470	9,500	8,470

[1] Average bed slope from aggradation-degradation studies.

TABLE 6.—*Basic hydraulic data with measured and computed sediment concentrations, Rio Grande near Belen, N. Mex.*

Date	Time	Q (cfs)	B (ft)	V (ft per sec)	D (ft)	S[1]	T (°F)	Measured concentration of suspended load (ppm)		Computed total concentration (ppm)	
								All sizes	>0.062 mm	All sizes	>0.062 mm
1954											
Mar. 22	1405	94.4	82.0	1.09	1.05	0.00069	55	248	15	260	24
Apr. 6	1510	213	104	1.61	1.27	.00069	64	702	63	832	176
May 5	1810	404	265	1.66	.92	.00069	77	1,080	119	1,340	371
June 2	1410	188	150	1.11	1.13	.00069	71	217	4	229	11
June 14	1345	143	53.0	1.16	2.32	.00069	68	320	144	394	199
June 28	1430	74.4	45.0	1.58	1.04	.00069	75	149	34	245	128
July 12	1515	47.9	66.0	1.06	.68	.00069	78	123	27	162	63
Aug. 10	1345	108	72.0	1.58	.95	.00069	79	14,100	141	15,400	1,270
Sept. 21	1520	37.4	39.0	1.23	.77	.00069	74	68	7	98	35
Oct. 19	1625	86.4	61.0	1.05	1.35	.00069	63	1,400	28	1,440	48
Nov. 16	1510	164	65.0	1.72	1.46	.00069	53	1,460	15	1,540	81
1955											
Jan. 12	1235	543	204	1.74	1.53	.00069	38	1,750	262	2,010	497
Jan. 25	1210	316	117	2.00	1.35	.00069	40	1,240	223	1,590	558
Feb. 9	1350	454	208	1.54	1.42	.00069	41	1,380	262	1,680	549
Feb. 24	1445	382	161	1.78	1.33	.00069	45	1,120	224	1,470	557
Mar. 9	1635	184	86.0	1.63	1.31	.00069	57	676	88	827	229
Mar. 25	1600	103	98.0	1.32	.80	.00069	60	277	24	334	87
May 20	1625	459	272	1.57	1.08	.00069	73	2,190	153	2,500	407
Aug. 9	1145	651	207	2.54	1.24	.00069	76	23,900	478	25,200	1,350
Aug. 23	1520	1,180	258	2.93	1.56	.00069	79	27,100	542	28,400	1,500
1957											
May 15	1500	3,790	390	3.79	2.56	.00069	61	7,960	3,580	9,320	4,890
May 27	1230	2,950	395	3.50	2.14	.00069	64	5,210	2,240	6,390	3,350
June 24	1410	4,200	395	4.16	2.56	.00069	75	3,200	1,730	4,330	2,820

[1] Average bed slope from aggradation-degradation studies.

TABLE 7.—*Particle-size analyses of bed material, Rio Grande at Otowi Bridge, near San Ildefonso, N. Mex.*

[Method of analysis: S, sieve; V, visual accumulation tube]

Date	Sampling points	Water temperature (°F)	Percent finer than indicated size, in millimeters										Method of analysis
			0.062	0.125	0.250	0.500	1.000	2.000	4.000	8.000	16.00	32.00	
1958													
May 6	1	59	0.7	3.8	33.2	94.8	99.5	100	----------	----------	----------	----------	S
May 12	1	58	.3	1.2	10.3	66.3	96.6	98.8	99.5	100	----------	----------	S
May 19	2	62	.2	1.0	8.9	47.5	76.3	92.1	97.8	98.9	100	----------	S
May 26	1	61	.2	2.2	30.9	64.8	80.9	86.8	89.9	93.7	100	----------	S
June 3	3	62	.1	.6	11.2	34.5	42.1	50.6	61.2	70.6	89.5	100	S
June 9	3	60	1.1	5.0	16.3	45.7	66.6	85.8	96.8	99.2	100	----------	S
June 12	3	62	.1	.5	9.8	54.7	74.3	81.3	84.9	88.7	100	----------	S
June 17	3	61	2.2	8.4	30.5	57.0	74.5	87.8	94.9	98.1	99.5	100	S
June 24 [1]	3	72	.1	.4	4.1	26.8	36.6	39.8	42.3	47.1	54.1	72.2	S
1959													
Aug. 8	5	73	1.5	8.7	34.9	76.0	92.1	96.9	98.6	100	----------	----------	S
1961													
Apr. 25	5	52	0	.1	3.1	15.7	40.5	57.9	72.1	85.2	95.8	100	S
May 2	5	57	.1	.2	3.5	21.2	54.0	75.7	89.2	96.0	99.2	100	S
May 17	4	56	.1	.3	23.0	71.7	85.7	96.5	99.6	99.9	100	----------	V
June 21	6	76	----------	.2	4.4	43.7	73.5	83.5	89.2	93.5	95.6	100	S
July 20	5	74	.2	.4	3.2	35.8	74.0	91.2	97.3	99.7	100	----------	S
1962													
Apr. 19	6	59	.4	1.1	6.8	25.8	46.2	58.2	67.1	75.6	87.4	100	S
May 31	6	59	.1	.2	23.8	72.1	87.7	92.9	95.9	98.5	99.5	100	S
July 2	6	78	.1	.1	5.9	46.8	80.4	92.8	97.3	98.8	99.4	100	S

[1] 100 percent <64mm.

TABLE 8.—*Particle-size analyses of bed material, Rio Grande at Cochiti, N. Mex.*

[Method of analysis: S, seive; V, visual accumulation tube]

Date	Sampling points	Water temperature (°F)	Percent finer than indicated size, in millimeters										Method of analysis
			0.062	0.125	0.250	0.500	1.000	2.000	4.000	8.000	16.00	32.00	
1954													
Mar. 10	3	54	0.0	0.1	6.1	55.9	86.3	96.8	99.3	99.9	100	----------	S
Mar. 23	3	51	.0	.1	12.3	40.2	70.8	87.7	96.4	99.4	100	----------	S
Apr. 7	3	58	.1	.3	3.4	19.8	36.5	45.6	52.1	61.2	82.0	100	S
Apr. 20	3	58	.5	2.1	9.0	26.2	43.3	54.0	61.1	69.8	85.9	100	S
May 4	3	63	.2	1.2	9.4	40.3	75.6	90.4	95.9	98.8	100	----------	S
May 20	3	67	.4	4.1	35.2	69.8	81.0	88.5	93.4	96.0	99.0	100	S
June 1	3	67	.4	4.4	34.5	76.3	85.8	92.1	96.4	98.9	100	----------	S
June 14	3	65	.2	3.4	32.9	65.4	71.4	78.9	87.3	95.1	99.5	100	S
July 12	3	77	.5	3.1	47.1	94.3	96.5	97.8	98.6	99.4	100	----------	S
Aug. 10	3	73	.5	2.7	31.5	93.3	96.2	97.4	98.2	98.9	100	----------	S
Aug. 24	3	70	2.2	9.2	39.9	96.3	98.6	99.2	99.4	99.8	100	----------	S
Sept. 8	3	70	1.5	3.8	28.9	88.9	96.0	98.5	99.5	100	----------	----------	S
Sept. 23	3	71	4.9	19.8	36.6	89.4	94.6	97.2	98.8	100	----------	----------	S
Oct. 5	3	72	.4	2.1	15.8	82.0	91.7	96.6	99.0	99.9	100	----------	S
Oct. 19	3	58	2.3	11.9	24.3	92.3	98.2	98.9	99.6	100	----------	----------	S
Nov. 17	3	49	.3	2.2	14.2	86.5	97.6	99.2	99.7	100	----------	----------	S
Dec. 15	3	38	.2	.7	7.2	73.8	96.7	98.5	99.5	100	----------	----------	S
Dec. 29	3	36	.1	.4	4.6	77.6	94.3	99.3	99.8	100	----------	----------	S
1955													
Jan. 11	3	37	.0	.7	6.9	79.1	97.1	99.2	99.8	100	----------	----------	S
Jan. 26	3	36	.0	1.0	7.3	87.6	96.3	97.6	98.5	99.7	100	----------	S
1955													
Feb. 9	3	40	.1	1.0	6.7	78.7	95.7	98.3	99.3	100	----------	----------	S
Feb. 23	2	38	.2	.8	4.0	55.7	85.2	89.8	94.6	99.0	100	----------	S
Mar. 8	3	49	.0	.2	3.4	50.2	86.4	95.6	98.1	99.2	100	----------	S
Mar. 22	3	49	.1	.2	3.0	36.1	76.7	90.0	95.9	99.2	100	----------	S
Apr. 6	3	53	.1	.2	2.1	39.4	76.5	91.0	96.7	99.2	100	----------	S
Apr. 19	3	58	.1	.6	3.6	47.2	85.0	96.3	99.1	99.8	100	----------	S
May 17	3	60	.3	2.5	10.3	35.3	67.8	88.4	95.9	98.8	100	----------	S
June 14	1	75	.2	2.3	36.7	84.4	93.0	97.7	99.1	99.7	100	----------	S
June 29	2	72	.1	2.3	42.4	89.7	97.4	99.2	99.8	100	----------	----------	S
July 11	1	75	.2	4.3	72.8	99.1	99.8	100	----------	----------	----------	----------	S
July 25	4	81	.2	.8	19.3	66.8	85.4	96.2	98.9	99.6	99.9	100	S
Aug. 8 [1]	3	76	2.2	5.2	24.1	63.7	74.1	82.7	87.0	89.0	91.2	93.0	S
Sept. 6	2	71	1.2	7.2	25.4	81.0	89.4	92.9	95.2	97.4	99.3	100	S
Sept. 19	3	74	.8	4.3	16.5	53.1	78.0	88.5	94.3	97.1	100	----------	S
Oct. 3	3	70	.6	6.3	28.4	71.7	84.5	88.6	91.3	93.7	97.8	100	S
Oct. 18	3	63	1.2	8.4	52.4	78.2	85.7	91.9	97.1	99.5	100	----------	S
Nov. 2	3	52	.4	5.3	51.3	92.8	99.0	99.4	99.8	100	----------	----------	S
Nov. 15	3	42	.3	2.3	20.4	64.2	84.7	92.4	97.2	99.1	100	----------	S
Nov. 28	3	40	.3	3.4	27.8	96.5	99.4	99.7	99.8	100	----------	----------	S
Dec. 14	3	36	.2	2.7	19.3	93.9	98.0	99.3	99.8	100	----------	----------	S
Dec. 27	3	39	.2	3.2	18.3	79.9	99.1	100	----------	----------	----------	----------	S
1956													
Jan. 24	3	41	.0	1.6	16.0	76.8	95.8	98.8	99.3	99.5	100	----------	S
Feb. 7	3	37	.2	1.6	17.7	65.1	82.2	89.0	94.3	97.1	99.0	100	S
Feb. 22	3	42	.1	2.0	23.6	74.9	93.3	97.5	99.1	99.9	100	----------	S
Mar. 7	3	43	.1	1.3	10.3	52.4	85.6	95.0	97.6	98.8	99.7	100	S
Apr. 3	3	47	.2	1.1	6.9	58.1	81.6	92.4	97.4	99.6	100	----------	S
Apr. 18	3	52	.5	3.4	35.8	75.3	91.0	95.7	98.2	99.5	100	----------	S
May 2	3	59	.8	7.2	49.1	63.9	76.5	85.5	91.2	94.8	99.6	100	S
May 15	3	59	.2	3.1	44.8	88.5	93.8	95.1	97.6	98.5	99.2	100	S
May 29	3	66	.4	3.1	27.9	65.6	79.9	89.7	95.3	97.9	99.8	100	S
June 12	3	73	.5	6.4	37.9	66.2	77.8	85.4	93.4	98.0	100	----------	S
June 26	3	77	2.0	13.8	48.4	82.0	94.8	98.2	99.6	99.9	100	----------	S
July 10	3	80	.5	7.9	23.3	90.8	98.2	99.3	99.8	100	----------	----------	S
1957													
May 16	3	54	.8	5.8	50.4	94.2	99.6	99.9	100	----------	----------	----------	S
May 29	3	62	.2	1.5	21.5	85.5	99.1	99.7	99.9	100	----------	----------	S
June 12	3	62	4	1.8	23.0	68.5	91.9	96.8	98.8	99.5	100	----------	S
June 26	2	67	.3	1.5	18.5	90.6	99.4	99.7	99.8	100	----------	----------	S
1958													
May 7	3	55	.4	2.7	25.4	64.2	72.0	77.7	82.7	86.6	93.4	100	S
May 12	3	58	.4	2.3	17.0	59.7	69.9	77.0	83.2	88.9	96.5	100	S
May 20 [1]	6	58	.6	3.7	23.9	45.2	57.1	62.7	69.1	74.5	78.1	83.8	S
May 26	3	61	2.6	15.9	43.4	63.7	66.4	66.7	66.8	66.8	100	----------	S
June 3	3	63	.1	.7	10.3	44.2	57.4	66.4	72.4	78.9	85.5	100	S
June 9	3	62	.1	1.0	11.6	42.8	66.9	79.6	87.5	94.4	96.9	100	S
June 12	3	63	.1	.6	8.7	39.8	66.0	80.8	84.6	87.4	90.0	100	S
June 17	3	70	.2	1.1	12.7	54.5	81.1	92.7	95.3	98.2	99.3	100	S
June 24	3	75	.1	.5	8.0	38.2	59.9	75.2	83.6	90.1	96.2	100	S
1961													
Apr. 26	6	52	.1	.9	34.0	73.0	90.0	95.3	97.8	99.0	99.8	100	S
May 2	6	57	.2	1.6	23.1	56.6	79.4	89.4	93.0	95.6	98.6	100	S
May 18	6	59	.1	.5	22.3	60.7	73.1	80.1	86.1	91.7	96.6	100	S
June 22 [1]	6	76	.2	.8	11.3	34.3	49.2	55.2	59.6	66.6	79.7	98.5	S

[1] 100 percent <64mm.

TABLE 9.—*Particle-size analyses of bed material, Rio Grande at San Felipe, N. Mex.*

Date	Sampling points	Water temperature (°F)	Percent finer than indicated size, in millimeters										Method of analysis
			0.062	0.125	0.250	0.500	1.000	2.000	4.000	8.000	16.00	32.00	
1954													
Mar. 10	3	56	0.1	0.6	19.2	71.7	93.0	98.5	99.6	100	----------	----------	S
Mar. 23	3	53	.2	.9	14.8	45.6	61.4	68.7	74.1	81.0	91.6	100	S
Apr. 7	3	62	.1	.9	19.5	71.5	84.0	89.3	91.0	93.3	95.7	100	S
Apr. 20	3	64	.2	1.0	11.7	76.2	98.4	99.6	99.8	99.8	100	----------	S
May 4	3	64	.2	1.2	13.8	48.5	78.9	95.3	98.8	99.7	100	----------	S
May 20	3	74	.2	.8	6.3	50.0	84.2	93.3	96.0	98.3	100	----------	S
June 1	3	71	.2	2.3	25.8	77.4	93.2	97.3	98.8	99.4	100	----------	S
June 14	3	68	.1	1.0	19.7	70.5	94.0	98.1	99.1	99.8	100	----------	S
July 12	3	81	.2	1.9	27.9	84.3	96.9	99.1	99.6	99.8	100	----------	S
Aug. 13	3	76	2.0	5.5	13.9	57.0	85.3	94.3	97.9	99.2	100	----------	S
Aug. 24	3	73	12.7	33.3	73.1	90.2	97.0	99.3	99.9	100	----------	----------	S
Sept. 8	3	73	.9	4.4	16.8	57.5	89.8	98.3	99.6	100	----------	----------	S
Sept. 23	3	69	.4	1.8	14.6	75.6	94.9	98.4	99.5	99.9	100	----------	S
Oct. 5	3	74	.4	2.1	12.7	62.6	84.3	94.3	98.4	99.8	100	----------	S
Oct. 19	3	60	.7	5.5	24.2	53.1	84.8	95.7	98.5	99.9	100	----------	S
Nov. 3	3	52	1.2	8.8	51.2	70.5	86.3	95.0	98.8	100	----------	----------	S
Nov. 17	3	44	.7	6.3	30.3	80.6	94.8	98.5	99.2	99.8	100	----------	S
Nov. 30	3	41	.4	2.9	17.2	72.8	91.0	97.1	99.2	99.9	100	----------	S
Dec. 15	3	34	2.1	11.0	41.8	79.2	93.9	97.7	98.8	99.4	100	----------	S
Dec. 30	3	32	.2	2.2	23.5	80.0	93.0	98.7	99.8	99.9	100	----------	S
1955													
Jan. 11	3	36	.8	5.2	31.2	59.9	78.1	89.1	94.0	97.3	99.5	100	S
Feb. 28	3	47	.2	1.1	12.9	76.5	94.8	97.4	98.1	98.6	98.8	100	S
Mar. 7	3	48	.1	1.4	14.5	86.5	98.7	99.4	99.7	100	----------	----------	S
Mar. 22	3	42	.7	6.4	40.4	73.8	91.3	95.7	97.2	98.5	100	----------	S
May 3	3	59	.9	2.3	11.7	46.5	73.4	87.4	94.8	98.6	100	----------	S
May 17	2	57	.7	3.9	21.2	67.0	85.5	91.9	94.5	97.2	98.6	100	S
June 2	2	70	1.0	8.4	39.6	98.0	99.6	99.8	99.9	100	----------	----------	S
June 29	3	76	.1	1.7	13.8	67.3	94.6	98.5	99.5	99.9	100	----------	S
July 11	3	71	.4	2.9	15.3	59.7	83.2	93.6	98.2	99.7	100	----------	S
July 25	3	71	.6	2.1	14.8	68.9	90.3	94.2	95.6	97.6	100	----------	S
Aug. 9	3	84	1.0	5.4	22.5	55.8	74.9	85.9	91.5	94.7	97.5	100	S
Sept. 6	3	74	1.0	6.0	29.0	68.7	85.3	91.6	93.8	95.6	96.6	100	S
Sept. 19	3	70	.4	3.0	21.9	77.5	93.7	97.7	99.2	99.9	100	----------	S
Oct. 4	3	73	.7	2.2	7.1	44.6	94.3	98.6	99.5	99.9	100	----------	S
Oct. 19	3	64	.6	3.0	10.8	47.1	92.6	98.5	99.5	99.9	100	----------	S
Nov. 2	3	44	1.4	6.1	25.2	75.1	94.9	98.8	99.7	100	----------	----------	S
Nov. 14	3	52	.7	7.7	33.2	93.0	98.1	99.0	99.4	99.8	100	----------	S
Nov. 28	3	44	1.5	7.7	36.1	87.3	98.2	99.3	99.6	99.9	100	----------	S
Dec. 14	3	40	.2	2.3	11.9	62.8	91.7	97.6	98.6	99.2	100	----------	S
Dec. 27	3	40	.8	5.4	29.5	76.0	96.0	98.7	98.9	99.1	100	----------	S
1956													
Jan. 10	3	43	.5	5.1	40.2	86.5	97.4	99.0	99.6	99.8	100	----------	S
Jan. 24	3	43	4.4	23.8	65.5	91.4	94.0	94.4	94.5	94.7	95.2	100	S
Feb. 7	3	40	1.6	13.9	63.9	98.2	99.9	99.9	99.9	100	----------	----------	S
Feb. 22	3	47	.4	4.2	32.3	79.4	96.8	99.2	99.6	99.8	100	----------	S
Mar. 6	3	47	.8	4.8	17.7	50.6	58.0	60.0	62.5	68.7	84.3	100	S
Mar. 21	3	51	.6	5.7	55.3	96.9	99.3	99.9	100	----------	----------	----------	S
Apr. 4	3	51	.9	5.1	28.8	67.1	93.1	98.4	99.3	100	----------	----------	S
Apr. 19	3	50	.4	3.6	30.1	88.1	98.2	99.1	99.5	99.7	100	----------	S
May 2	3	58	1.5	8.4	40.1	78.4	82.2	83.0	84.4	87.4	96.3	100	S
May 15	3	66	.4	3.7	24.1	68.9	83.5	92.7	97.7	99.4	100	----------	S
May 29 [1]	3	70	.4	2.9	18.1	70.7	88.6	91.9	92.8	93.3	93.6	94.5	S
June 12	3	76	.6	5.4	39.1	87.4	96.9	99.5	100	----------	----------	----------	S
July 10	3	80	1.1	5.1	29.5	81.8	95.3	98.3	99.4	99.9	100	----------	S
July 24	3	80	.1	.5	3.2	41.5	83.6	93.8	97.5	99.1	100	----------	S
1957													
May 15	3	57	.5	2.7	28.9	65.9	72.6	77.3	81.8	87.3	96.9	100	S
May 28	3	61	2.0	6.7	40.9	86.8	99.0	99.8	99.9	100	----------	----------	S
June 13	3	64	.2	1.8	31.2	65.3	71.5	77.7	84.4	89.8	94.7	100	S
June 28	3	73	.3	.7	6.2	34.6	65.4	82.5	89.5	93.6	97.2	100	S
1958													
May 12	3	59	2.6	6.1	13.4	23.8	33.6	39.6	46.9	55.8	59.5	100	S
May 21 [1]	2	65	.3	2.0	31.1	50.9	51.6	51.9	52.2	52.5	55.2	74.4	S
May 26	3	67	.2	.9	9.0	27.0	48.1	63.2	68.5	71.2	74.9	100	S
June 3	2	67	.1	1.0	9.6	44.9	66.6	76.4	83.9	92.0	100	----------	S
June 9	3	66	.1	.8	12.5	48.7	81.9	93.5	96.3	98.3	98.7	100	S
June 12	3	66	1.2	2.5	14.5	40.7	50.0	60.9	70.9	77.8	82.9	100	S
June 17	3	75	.3	2.1	21.9	59.2	80.2	90.2	93.2	94.5	95.9	100	S
June 24	3	80	.1	.8	9.3	47.3	65.2	66.9	67.5	69.6	74.4	100	S
1961													
Apr. 26	6	57	.4	3.4	58.2	94.0	99.9	100	----------	----------	----------	----------	S
May 2	6	62	.1	2.5	41.2	79.2	88.7	93.4	95.5	97.0	98.7	100	S
May 18	6	62	.1	5.4	54.8	82.7	86.0	90.6	94.7	97.3	98.9	100	S
June 22 [1]	6	76	.3	1.0	12.3	58.5	82.5	90.4	93.2	95.6	97.6	98.5	S

[1] 100 percent < 64 mm.

TABLE 10.—*Particle-size analyses of bed material, Rio Grande near Bernalillo, N. Mex.*

Date	Sampling points	Water temperature (°F)	Percent finer than indicated size, in millimeters										Method of analysis
			0.062	0.125	0.250	0.500	1.000	2.000	4.000	8.000	16.00	32.00	
1952													
Apr. 25	3	58	2.1	10.8	56.5	93.4	98.2	98.8	99.2	99.2	100	----------	S
May 12	3	62	.2	1.5	15.2	70.6	93.7	97.8	99.1	99.3	100	----------	S
June 17	3	70	.4	3.0	37.4	93.0	98.9	99.4	99.5	99.6	100	----------	S
June 20	3	72	.4	2.8	26.7	86.4	95.3	97.3	98.2	98.7	99.9	100	S
June 26	3	70	.3	2.8	32.7	87.4	97.7	99.2	99.6	100	----------	----------	S
July 24	3	75	1.0	5.6	45.5	86.9	98.2	99.5	99.7	100	----------	----------	S
1953													
Apr. 29	15	57	.5	3.2	28.3	86.5	98.0	99.1	99.5	99.8	100	----------	S
May 5	15	63	.7	5.4	41.1	82.3	95.8	98.5	99.4	99.8	100	----------	S
June 1	3	65	.6	3.5	25.7	86.7	98.5	99.3	99.6	99.9	100	----------	S
June 2	15	71	.7	4.0	27.7	86.5	97.8	99.0	99.4	100	----------	----------	S
June 4	3	62	.5	3.6	34.1	74.3	91.0	94.4	96.2	97.4	98.4	100	S
June 17	3	69	.3	2.8	30.7	87.7	95.6	97.3	98.2	98.8	99.7	100	S
1956													
Apr. 2	3	47	1.6	9.1	24.1	77.3	91.2	93.1	99.0	99.6	100	----------	S
Apr. 14	3	51	2.0	9.8	44.4	88.1	97.1	98.6	99.4	100	----------	----------	S
Apr. 16	3	62	.9	5.3	22.3	81.4	95.2	98.2	99.3	99.8	100	----------	S
Apr. 21	3	65	.9	4.9	31.5	90.1	96.9	98.8	99.5	99.9	100	----------	S
Apr. 23	3	64	1.1	6.3	30.5	90.6	97.8	98.9	99.5	99.8	100	----------	S
May 1	3	61	.9	4.9	32.4	99.1	99.9	100	----------	----------	----------	----------	S
May 5	3	69	4.5	17.3	51.1	90.3	98.6	99.2	99.5	100	----------	----------	S
May 12	3	66	1.2	7.0	43.3	91.0	97.4	99.2	99.7	99.9	100	----------	S
May 14	3	61	2.3	17.1	62.5	91.4	98.3	99.5	99.9	99.9	100	----------	S
May 18	3	75	.5	4.1	21.2	87.1	96.7	98.0	98.7	99.2	99.5	100	S
May 22	3	71	.4	4.7	28.9	88.1	97.7	99.1	99.6	99.9	100	----------	S
May 26	3	71	2.2	12.8	79.0	96.7	99.2	99.6	99.8	100	----------	----------	S
May 29	3	66	.6	2.9	19.0	88.3	98.5	99.4	99.9	100	----------	----------	S
June 2	3	75	5.9	19.8	58.2	92.4	98.9	99.6	99.8	99.9	100	----------	S
June 4	3	72	1.8	8.6	37.2	94.8	99.4	99.8	99.9	100	----------	----------	S
June 8	3	78	1.1	4.7	24.9	92.1	98.2	99.0	99.5	99.9	100	----------	S
June 12	3	73	8.6	30.5	39.8	79.2	96.5	98.8	99.5	99.9	100	----------	S
June 15	3	80	1.2	9.0	43.5	95.6	99.2	99.7	99.9	100	----------	----------	S
June 29	3	81	5.1	24.2	54.7	93.2	98.6	99.2	99.7	100	----------	----------	S
Aug. 24	3	79	.6	9.9	39.1	87.7	97.9	99.5	99.9	100	----------	----------	S
Sept. 7	3	76	.9	5.0	38.2	96.0	99.8	100	----------	----------	----------	----------	S
1957													
Apr. 29	3	59	1.2	7.3	28.1	82.7	94.3	96.7	97.8	98.6	100	----------	S
May 13	3	58	1.1	9.6	41.6	93.4	99.7	99.9	100	----------	----------	----------	S
May 16	3	60	.6	4.9	38.4	87.0	96.0	98.1	99.4	100	----------	----------	S
May 27	3	64	.5	6.2	46.4	93.1	99.6	100	----------	----------	----------	----------	S
June 11	3	65	.7	5.2	43.0	94.2	98.9	99.5	99.8	100	----------	----------	S
June 24	3	73	.6	4.9	48.9	98.4	100	----------	----------	----------	----------	----------	S
1958													
May 8	4	58	.7	3.2	34.2	77.9	91.4	94.5	95.7	96.3	96.6	100	S
May 13	3	60	.8	6.1	39.0	83.0	97.0	98.4	98.8	99.2	100	----------	S
May 21	3	67	.2	1.3	12.8	78.9	98.5	99.6	99.8	99.8	100	----------	S
May 27	3	74	.3	2.4	38.0	88.6	97.1	98.8	99.6	99.7	100	----------	S
June 4	3	67	.4	3.3	33.4	97.3	99.9	100	----------	----------	----------	----------	S
June 10	3	65	.2	2.2	20.9	86.1	94.6	96.7	97.7	98.6	100	----------	S
June 13	3	63	.3	2.4	22.4	78.0	93.9	97.9	98.9	99.7	100	----------	S
June 18	3	67	.9	7.3	45.2	80.5	94.8	98.1	99.1	99.6	100	----------	S
June 25	3	73	.3	1.4	16.1	83.1	98.1	99.2	99.4	99.7	100	----------	S
1960													
Feb. 15	4	44	1.2	7.5	34.1	77.8	92.2	95.2	96.5	96.6	100	----------	S
Apr. 6	[1] 18	59	.5	3.7	32.2	84.7	95.6	97.4	98.2	99.0	100	----------	S
May 24	[2] 9	65	.3	3.3	35.6	89.4	96.9	98.4	99.4	99.9	100	----------	S
June 22	[3] 12	74	.2	4.3	42.6	86.8	96.9	98.8	99.4	99.8	100	----------	S
1961													
Apr. 27	6	57	.4	9.8	61.1	97.4	99.6	100	----------	----------	----------	----------	V
May 3	6	66	.4	6.4	58.8	96.6	99.8	100	----------	----------	----------	----------	V
May 19	6	63	.2	4.1	67.2	97.8	99.9	100	----------	----------	----------	----------	V
1962													
Apr. 20 [4]	6	64	1.6	7.1	49.2	80.5	83.3	83.8	84.0	84.3	85.1	93.8	V
June 1	3	71	.2	.8	23.6	77.3	96.1	98.5	98.9	99.3	100	----------	V
June 25	5	79	.1	1.3	18.8	62.8	93.8	97.9	99.3	99.9	100	----------	V

[1] Average of samples from 5 sections in the reach.
[2] Average of samples from 3 sections in the reach.
[3] Average of samples from 4 sections in the reach.
[4] 100 percent <64mm.

TABLE 11.—*Particle-size analyses of bed material, Rio Grande at Albuquerque, N. Mex.*

Date	Sampling points	Water temperature (°F)	Percent finer than indicated size, in millimeters										Method of analysis
			0.062	0.125	0.250	0.500	1.000	2.000	4.000	8.000	16.00	32.00	
1954													
Mar. 8	3	44	0.1	.8	14.4	85.6	98.1	99.3	99.7	100	----------	----------	S
Mar. 11	3	49	.1	1.3	16.8	74.0	93.3	96.9	98.3	99.4	100	----------	S
Mar. 26	3	47	.2	2.2	37.5	88.5	96.9	98.5	99.0	99.8	100	----------	S
Apr. 6	3	57	.7	7.3	56.0	84.8	92.6	95.7	97.7	99.2	100	----------	S
Apr. 8	3	61	.3	3.4	43.5	89.1	97.9	99.4	99.9	100	----------	----------	S
Apr. 19	3	62	.3	3.1	31.4	87.6	97.6	98.9	99.5	99.8	100	----------	S
Apr. 22	3	58	.2	2.4	33.8	96.2	99.3	99.6	99.7	100	----------	----------	S
May 3	3	65	1.5	7.1	57.2	96.8	99.5	99.9	100	----------	----------	----------	S
May 6	3	63	.3	2.9	34.2	82.8	95.2	97.4	98.4	99.2	100	----------	S
May 17	5	67	.6	3.8	29.9	84.7	91.0	92.1	92.7	93.9	96.6	100	S
May 21	3	67	.4	2.4	28.6	80.2	95.0	97.6	98.5	99.4	100	----------	S
June 2	3	67	1.4	10.1	50.5	85.2	96.3	98.7	99.4	99.9	100	----------	S
June 4	3	67	.3	2.2	28.5	78.1	93.1	96.5	98.0	99.0	100	----------	S
June 14	3	67	.1	1.1	20.8	80.4	93.2	96.5	98.0	99.6	100	----------	S
June 18	3	61	.2	2.5	46.2	93.1	98.2	99.5	99.9	100	----------	----------	S
July 12	3	81	16.8	30.2	41.4	73.8	88.4	94.9	98.3	99.3	100	----------	S
July 27	3	82	1.2	6.3	43.1	83.9	92.8	94.6	96.2	98.4	100	----------	S
Aug. 10	3	70	.2	1.8	19.8	77.0	97.6	99.2	99.7	99.9	100	----------	S
Aug. 24	5	75	10.4	15.0	52.6	95.9	99.4	99.9	100	----------	----------	----------	S
Sept. 7	3	71	9.4	10.2	22.0	88.1	95.8	97.2	98.1	98.7	99.9	100	S
Oct. 4	3	78	.1	1.7	29.2	93.2	98.8	99.5	99.7	99.9	100	----------	S
Oct. 18	3	64	.2	1.2	14.3	75.9	95.7	98.3	99.2	99.8	100	----------	S
Nov. 2	3	57	.3	1.5	21.4	85.3	97.3	99.0	99.6	100	----------	----------	S
Nov. 16	3	48	.7	3.9	31.1	91.4	97.8	98.5	99.0	99.3	100	----------	S
Dec. 13	3	42	1.6	5.4	21.6	78.0	96.6	99.0	99.8	100	----------	----------	S
1955													
Jan. 10	3	37	1.8	9.2	56.0	87.1	96.2	98.8	99.7	100	----------	----------	S
Jan. 24	3	34	.9	5.1	37.9	93.0	98.2	98.9	99.3	99.9	100	----------	S
Feb. 25	3	35	.2	2.1	27.0	88.2	96.6	98.1	99.2	100	----------	----------	S
Mar. 7	3	50	.3	2.4	25.8	95.2	99.2	99.8	100	----------	----------	----------	S
Mar. 22	3	47	.7	5.6	46.1	92.7	97.8	98.8	99.5	100	----------	----------	S
Apr. 4	3	45	.2	1.5	16.8	91.2	99.1	99.6	99.9	100	----------	----------	S
May 2	3	58	.2	1.1	16.9	96.6	99.4	99.6	99.8	100	----------	----------	S
May 31	3	63	.6	3.0	38.5	92.6	98.4	99.5	99.8	100	----------	----------	S
June 13	3	60	.5	3.4	23.9	80.0	95.6	98.7	99.5	99.8	100	----------	S
June 27	3	61	1.3	2.9	39.6	88.6	97.4	99.4	99.8	100	----------	----------	S
July 11	3	72	25.5	32.7	57.9	95.4	98.2	99.5	99.9	100	----------	----------	S
July 25	3	72	1.9	4.9	28.6	91.8	98.6	99.3	99.6	99.9	100	----------	S
Aug. 11	3	76	2.6	8.9	38.8	89.2	96.6	98.6	99.5	99.9	100	----------	S
Aug. 23	2	75	3.1	12.0	49.9	96.0	98.7	99.4	99.8	100	----------	----------	S
Sept. 6	3	73	.6	2.5	14.4	64.9	90.3	95.6	97.6	99.0	100	----------	S
Sept. 19	3	67	.2	.7	5.4	61.4	94.8	96.4	99.3	99.8	100	----------	S
Oct. 4	3	68	.0	1.1	14.5	90.7	98.6	99.5	99.8	99.9	100	----------	S
Dec. 1	3	49	.6	2.3	18.0	91.9	98.7	99.1	99.3	99.6	100	----------	S
Dec. 12	3	42	1.4	4.6	31.0	77.2	92.6	97.0	99.0	99.8	100	----------	S
Dec. 27	3	48	1.3	5.1	35.8	81.1	97.7	99.0	99.4	99.6	100	----------	S
1956													
Jan. 9	3	48	1.1	4.2	29.8	93.5	99.7	99.9	99.9	100	----------	----------	S
Jan. 23	3	43	.5	2.4	22.7	96.7	99.7	99.9	100	----------	----------	----------	S
Feb. 7	3	45	.5	2.1	15.2	72.7	93.6	96.5	97.4	98.3	100	----------	S
Feb. 20	3	50	1.3	4.4	19.1	82.4	97.4	99.1	99.6	99.9	100	----------	S
July 20	3	70	3.3	9.7	42.7	92.5	97.9	99.3	99.9	100	----------	----------	S
1957													
May 14	3	62	2.8	11.7	40.1	85.0	95.8	97.1	98.0	98.8	99.4	100	S
May 27	3	65	4.2	24.4	73.1	95.6	99.3	99.9	100	----------	----------	----------	S
June 10	3	67	.6	4.2	28.0	74.7	87.9	92.2	95.4	98.0	100	----------	S
June 24	3	75	.6	4.6	29.9	93.5	99.1	99.8	100	----------	----------	----------	S

TABLE 12.—*Particle-size analyses of bed material, Rio Grande near Belen, N. Mex.*

[Methods of analysis: S, sieve; V, visual accumulation tube]

Date	Sampling points	Water temperature (°F)	Percent finer than indicated size, in millimeters										Method of analysis
			0.062	0.125	0.250	0.500	1.000	2.000	4.000	8.000	16.00	32.00	
1954													
Mar. 22	3	55	1.0	4.3	22.9	87.2	97.4	99.1	99.4	99.8	100	----------	S
Apr. 6	3	64	.2	2.0	35.1	87.7	99.4	99.9	99.9	100	----------	----------	S
May 5	3	77	.1	1.3	32.4	96.9	98.9	99.9	100	----------	----------	----------	S
June 2	3	71	.3	2.5	31.7	88.4	98.9	99.8	99.8	100	----------	----------	S
June 14	3	68	3.0	21.7	97.3	99.8	100	----------	----------	----------	----------	----------	S
June 28	3	75	.1	1.8	38.6	89.7	98.7	99.9	100	----------	----------	----------	S
July 12	3	78	.8	6.9	58.2	96.6	99.3	99.7	100	----------	----------	----------	S
Aug. 10	3	79	.6	5.8	47.9	91.5	98.6	99.7	100	----------	----------	----------	S
Sept. 21	3	74	.4	3.9	35.8	88.0	98.1	99.1	99.2	99.2	99.4	100	S
Oct. 19	3	63	1.1	6.3	37.4	89.2	98.6	99.6	99.9	100	----------	----------	S
Nov. 16	3	53	.3	2.8	31.2	88.9	97.1	98.8	99.5	100	----------	----------	S
1955													
Jan. 12	3	38	2.0	9.6	47.9	96.9	99.4	99.8	100	----------	----------	----------	S
Jan. 25	3	40	.1	1.3	20.5	90.2	98.1	99.4	99.8	100	----------	----------	S
Feb. 9	3	41	25.1	36.8	69.8	97.7	99.7	100	----------	----------	----------	----------	S
Feb. 24	3	45	.1	1.9	21.0	94.0	98.2	99.0	99.5	99.8	100	----------	S
Mar. 9	3	57	.2	3.4	41.6	93.0	99.1	99.8	100	----------	----------	----------	S
Mar. 25	3	60	.3	3.1	30.9	88.7	98.7	99.7	99.9	100	----------	----------	S
May 20	3	73	5.0	15.0	49.8	91.0	98.9	99.7	99.8	99.9	100	----------	S
Aug. 9	3	76	.2	1.1	32.4	92.2	98.2	99.3	99.8	100	----------	----------	S
Aug. 23	3	79	.8	4.0	28.9	98.2	99.8	99.9	100	----------	----------	----------	S
1957													
May 15	3	61	1.0	4.2	40.7	89.7	96.7	98.1	98.9	99.7	100	----------	S
May 27	3	64	1.3	5.2	48.1	93.1	99.6	99.9	100	----------	----------	----------	S
June 24	3	75	1.1	8.3	61.4	97.4	99.6	100	----------	----------	----------	----------	S

TABLE 13.—*Sources of published particle-size analyses of suspended sediment used in the modified Einstein calculations*

Sediment station	Water year	Source: USGS Water Supply Paper—
Rio Grande at Otowi Bridge near San Ildefonso, N. Mex.	1958	1573.
Rio Grande at Cochiti, N. Mex.	1954, 1955	1402, p. 515–517.
	1956	1452, p. 459–460.
	1957	1522, p. 486.
	1958	1573.
Rio Grande at San Felipe, N. Mex.	1954, 1955	1402, p. 517–518.
	1956	1452, p. 460–461.
	1957	1522, p. 487.
	1958	1573.
Rio Grande near Bernalillo, N. Mex.	1952	1498–H (Nordin, 1964).
	1956	1452, p. 365–366.
	1957	1522, p. 410.
	1958	1573.
Rio Grande at Albuquerque, N. Mex.	1954, 1955	1402, p. 523–525.
	1956	1452, p. 461–462.
	1957	1522, p. 488.
Rio Grande near Belen, N. Mex.	1954, 1955	1402, p. 530–531.
	1957	1522, p. 489.

TABLE 14.—*Previously unpublished particle-size analyses of suspended sediment used in the modified Einstein calculations*

[Method of analysis: P, pipette; S, sieve; W, in distilled water; C, chemically dispersed; V, visual accumulation tube]

Date	Time	Water discharge (cfs)	Water temperature (°F)	Suspended sediment: Concentration of sample (ppm)	Suspended sediment: Concentration of suspension analyzed (ppm)	Percent finer than indicated size, in millimeters: 0.002	0.004	0.016	0.062	0.125	0.250	0.500	1.000	2.000	Method of analysis
Rio Grande at Otowi Bridge, near San Ildefonso, N. Mex.															
1959															
Aug. 8	1300	1,270	73	24,000	3,980	----	54	77	91	97	99	100	------	------	VPWC
1961															
Apr. 25	1310	2,780	52	1,350	1,980	13	16	24	39	56	80	95	100	------	VPWC
May 2	1415	4,000	57	2,480	3,890	14	16	28	52	73	90	96	100	------	VPWC
May 17	1145	2,750	56	1,120	--------	----	----	----	26	36	67	92	100	------	V
June 21	1440	908	76	284	--------	----	----	----	48	52	65	96	99	100	S
July 20	1245	1,090	74	3,590	3,010	21	27	51	66	67	70	75	100	------	VPWC
1962															
Apr. 19	1350	6,040	59	4,240	4,510	10	13	19	41	70	91	98	100	------	VPWC
May 31	1350	1,460	59	1,660	--------	----	----	----	7	11	44	94	100	------	V
July 2	1345	684	78	203	--------	----	----	----	22	25	51	97	100	------	V
Rio Grande at Cochiti, N. Mex.															
1961															
Apr. 26	1050	2,090	52	1,210	--------	----	----	----	41	53	89	100	------	------	V
May 2	1155	3,680	57	2,730	3,530	16	18	31	56	68	91	99	100	------	VPWC
May 18	1150	2,620	59	2,750	1,920	3	4	6	11	16	36	73	96	100	VPWC
June 22	1110	674	76	153	--------	----	----	----	80	85	96	100	------	------	S
Rio Grande at San Felipe, N. Mex.															
1961															
Apr. 26	1350	2,220	57	1,360	2,310	13	16	25	41	53	87	100	------	------	WPVC
May 2	1535	3,580	62	2,890	2,710	15	17	28	49	59	82	98	100	------	VPWC
May 18	1110	2,510	62	1,040	--------	----	----	----	34	51	90	100	------	------	V
June 22	1140	680	76	519	--------	----	----	----	28	34	58	91	100	------	V
Rio Grande near Bernalillo, N. Mex.															
1953															
Apr. 29	--------	1,540	57	2,450	--------	----	----	----	70	83	96	100	------	------	V
May 5	--------	551	63	554	--------	----	----	----	48	73	98	100	------	------	V
June 1	--------	2,570	65	2,530	--------	----	----	----	67	87	100	------	------	------	V
June 2	--------	2,150	71	2,010	--------	----	----	----	64	84	97	100	------	------	V
June 4	--------	2,090	62	1,600	--------	----	----	----	58	80	99	100	------	------	V
June 17	--------	1,340	69	1,060	--------	----	----	----	42	64	93	100	------	------	V
1962															
Apr. 20	1315	5,340	64	4,360	3,510	12	16	24	54	77	97	100	------	------	VPWC
June 1	1430	987	71	1,720	--------	----	----	----	13	20	44	80	100	------	V
June 25	1245	453	79	453	--------	----	----	----	60	76	98	100	------	------	V

TABLE 15.—*Equations relating transport rates to simple hydraulic variables, with standard error of estimate in log units and percentages*

Station	Q vs Q_T: Equation	S_e: Log units	Percent +	Percent −	q vs q_T: Equation	S_e: Log units	Percent +	Percent −	V vs q_T: Equation	S_e: Log units	Percent +	Percent −	V vs C_T: Equation	S_e: Log units	Percent +	Percent −
Otowi	$Q_T=0.169Q^{1.43}$	0.228	69	41	$q_T=1.257q^{1.44}$	0.242	75	43	$q_T=0.605V^{3.48}$	0.255	80	44	$C_T=318V^{1.17}$	0.236	72	42
Cochiti	$Q_T=0.00361Q^{1.93}$	.433	171	63	$q_T=0.321q^{2.37}$	.498	215	68	$q_T=0.105V^{4.59}$	.370	134	57	$C_T=80.4V^{2.65}$	.514	226	69
San Felipe	$Q_T=0.0764Q^{1.56}$	.340	118	54	$q_T=1.186q^{1.63}$	.320	109	52	$q_T=0.359V^{3.60}$	.276	89	47	$C_T=250V^{1.46}$	.346	122	55
Bernalillo	$Q_T=0.137Q^{1.49}$	.258	81	45	$q_T=1.232q^{1.73}$	.175	50	33	$q_T=0.877V^{3.08}$	.286	93	48	$C_T=446V^{1.19}$	.260	82	45
Albuquerque	$Q_T=0.00435Q^{2.00}$	.376	138	58	$q_T=0.391q^{2.57}$	.374	136	58	$q_T=0.219V^{4.54}$	.313	106	51	$C_T=58.8V^{3.56}$	.554	258	72
Belen	$Q_T=0.00224Q^{2.03}$	.412	158	61	$q_T=0.165q^{2.91}$	.421	164	62	$q_T=0.104V^{3.13}$	.375	137	58	$C_T=41.3V^{3.54}$	.355	126	56

REFERENCES CITED

Bagnold, R. A., 1956, The flow of cohesionless grains in fluids: Royal Soc. (London) Philos. Trans., ser. A, v. 249, p. 235–297.

Bogardi, J. L., 1961, Some aspects of the application of the theory of sediment transportation to engineering problems: Jour. Geophys. Research, v. 66, No. 10, p. 3337–3346.

Colby, B. R., 1956, Relationship of sediment discharge to streamflow: U.S. Geol. Survey open-file rept., 170 p.

——— 1957, Relationship of unmeasured sediment discharge to mean velocity: Am. Geophys. Union Trans., v. 38, No. 5, p. 708–717.

——— 1961, Studies of flow in alluvial channels; effect of depth of flow on discharge of bed material: U.S. Geol. Survey Water-Supply Paper 1498–D, 12 p.

——— 1964, Sediment transport in alluvial channels: sand discharge and mean velocity relationships in sand-bed streams: U.S. Geol. Survey Prof. Paper 462–A, 47 p.

Colby, B. R., and Hembree, C. H., 1955, Computations of total sediment discharge, Niobrara River near Cody, Nebraska: U.S. Geol. Survey Water-Supply Paper 1357, 187 p.

Colby, B. R., and Hubbell, D. W., 1961, Simplified methods for computing total sediment discharge with the modified Einstein procedure: U.S. Geol. Survey Water-Supply Paper 1593, 17 p., 8 pl.

Culbertson, J. K., and Dawdy, D. R., 1964, A study of fluvial characteristics and hydraulic variables, middle Rio Grande New Mexico: U.S. Geol. Survey Water-Supply Paper 1498–F, 74 p.

Dawdy, D. R., 1961, Depth-discharge relations in alluvial streams-discontinuous rating curves: U.S. Geol. Survey Water-Supply Paper 1498–C, 16 p.

Einstein, H. A., 1942, Formulas for the transportation of bed load: Am. Soc. Civil Engineers Trans., v. 107, p. 561–597.

——— 1950, The bed-load function for sediment transportation in open channel flows: U.S. Dept. Agriculture Tech. Bull. 1026, 71 p.

Einstein, H. A., and Chien, Ning, 1953, Transport of sediment mixtures with large ranges of grain sizes: Univ. California Inst. of Eng. Research [Berkeley, Calif.], U.S. Army Corps of Engineers, Missouri River Division Sediment Ser. 2, 42 p.

Kennedy, J. F., 1961, Further laboratory studies of roughness and suspended load of alluvial streams: California Inst. of Technology [Pasadena, Calif.], W. M. Keck Laboratory of Hydraulics and Water Resources Rept. KH–R–3, 36 p.

Laursen, E. M., 1958, The total sediment load of streams: Am. Soc. Civil Engineers Proc., v. 84, No. HY 1, paper 1530, p. 1–35.

Leopold, L. B., and Maddock, T., Jr., 1953, The hydraulic geometry of stream channels and some physiographic implications: U.S. Geol. Survey Prof. Paper 252, 57 p.

Leopold, L. B., and Wolman, M. G., 1956, Floods in relation to the river channel: Internat. Assoc. of Hydrology [Dijon, France] Pub. 42, p. 85–98.

Meyer-Peter, E., and Muller, R., 1948, Formulas for bed-load transport: Internat. Assoc. for Hydraulic Structures Research, 2d mtg., Stockholm, 1948, p. 39–64.

Miller, C. R., 1951, Analysis of flow duration, sediment-rating curve method of computing sediment yield: U.S. Bur. Reclamation [Denver, Colo.], 15 p.

Nordin, C. F., Jr., 1963, A preliminary study of sediment transport parameters, Rio Puerco near Bernardo, New Mexico: U.S. Geol. Survey Prof. Paper 462–C, 21 p.

———, 1964, Aspects of flow resistance and sediment transport, Rio Grande near Bernalillo, New Mexico: U.S. Geol Survey Water-Supply Paper 1498–H, 41 p.

Nordin, C. F., Jr., and Beverage, J. P., 1964, Temporary storage of fine sediment in islands and point bars: U.S. Geol. Survey Prof. Paper 475–D, Art. 150, p. D138–D140.

Nordin, C. F., Jr., and Culbertson, J. K., 1961, Particle-size distribution of stream-bed material in the middle Rio Grande basin, New Mexico: U.S. Geol. Survey Prof. Paper 424–C, Art. 265, p. C323–C326.

Nordin, C. F., Jr., and Dempster, G. R., 1963, Vertical distribution of velocity and suspended-sediment concentration, Middle Rio Grande, New Mexico: U.S. Geol. Survey Prof. Paper 462–B, 20 p.

Straub, L. G., Anderson, A. G., and Flammer, G. H., 1958, Experiments on the influence of temperature on sediment load: Univ. California Inst. of Eng. Research [Berkeley, Calif.], Missouri River Division Sediment Series No. 10, 36 p.

U.S. GOVERNMENT PRINTING OFFICE: 1965 O—753-190

Effects of Water Temperature on the Discharge of Bed Material

By B. R. COLBY *and* C. H. SCOTT

SEDIMENT TRANSPORT IN ALLUVIAL CHANNELS

GEOLOGICAL SURVEY PROFESSIONAL PAPER 462-G

A study of the theoretical and observed effects of changes in water temperature on the transportation of bed material

UNITED STATES GOVERNMENT PRINTING OFFICE, WASHINGTON : 1965

UNITED STATES DEPARTMENT OF THE INTERIOR

STEWART L. UDALL, *Secretary*

GEOLOGICAL SURVEY

Thomas B. Nolan, *Director*

For sale by the Superintendent of Documents, U.S. Government Printing Office
Washington, D.C. 20402 - Price 25 cents (paper cover)

CONTENTS

	Page
Abstract	G1
Introduction	1
Temperature effects through viscosity changes	2
Effect on thickness of the laminar sublayer	2
Effect on vertical distribution of suspended sediment	3
Theoretical equation for vertical distribution	3
Relation of fall velocity to temperature	5
Computed temperature effects on bed-material discharge	5
Temperature effects through viscosity changes—Con.	
Effect on bed configuration	G7
Field streams	12
Flume flows	14
Overall temperature effects on bed-material discharge	17
Differences between flume flows and field streams	18
Roughly defined effect for field streams	19
Effect of concentration of fine sediment	22
Conclusions	24
References	25

ILLUSTRATIONS

	Page
FIGURE 1–9. Graphs showing—	
1. Specific weight and kinematic viscosity of distilled water	G2
2. Nomograph for ratio of mean velocity to $\sqrt{(RS)_m}$	4
3. Effect of a change in water temperature from 40° to 80° F on the fall velocity of quartz spheres of several sizes	5
4. Size distributions of bed sediments for computing temperature effects	6
5. Computed effect of water temperature on the relation of bed-material discharge to mean velocity	8
6–8. Computed sediment discharges by size ranges for a bed sediment:	
6. Median diameter, 0.20 mm	9
7. Median diameter, 0.40 mm	10
8. Median diameter, 0.60 mm	11
9. General variation of Manning's n with water temperature for Middle Loup River at Dunning, Nebr., section C_2	12
10. Longitudinal profiles of streambed at different water temperatures, Middle Loup River at Dunning, Nebr	13
11–19. Graphs showing—	
11, 12. Variation of Manning's n with streamflow and water temperature:	
11. Elkhorn River near Waterloo, Nebr	14
12. Mississippi River at St. Louis, Mo	15
13. Ratios of observed values of n to values of n from average curve of figure 12 plotted against water temperature	15
14. Differences in resistance to flow for pairs of flume runs at high and low water temperatures	16
15. Differences in bed-material concentration for pairs of flume runs at high and low water temperatures	17
16. Relation of bed-material discharge to mean velocity for Niobrara River near Cody, Nebr	20
17, 18. Approximate relative effect of water temperature on the relation between bed-material discharge and mean velocity:	
17. Niobrara River near Cody, Nebr	20
18. Three rivers	21
19. Approximate effect of water temperature and concentration of fine sediment on the relation of bed-material discharge to mean velocity	23

TABLE

	Page
TABLE 1. Measured and computed bed-material discharges for Middle Loup River at Dunning, Nebr	G21

EFFECTS OF WATER TEMPERATURE ON THE DISCHARGE OF BED MATERIAL

By B. R. Colby and C. H. Scott

ABSTRACT

Changes in water temperature and consequent changes in viscosity affect bed-material discharge (for this paper, the discharge of particles larger than 0.062 mm) in complex ways. These ways may be explained in terms of three separate effects. One effect is on the thickness of the laminar sublayer, and this effect is usually the smallest of the three. A second effect is on the vertical distribution of suspended bed material. It is a large effect that causes, according to several somewhat inexact computations, an approximate doubling of bed-material discharge if water temperatures are decreased from 80° to 40°F and if mean velocities, depths, and sizes of the bed sediments are the same for the two water temperatures. This second effect seems to be the most consistent and predictable of the three. The third effect is on the bed configuration and, hence, on the resistance to flow. It is a seemingly erratic and somewhat indeterminate effect that is sometimes large and sometimes small.

Temperature effects on bed-material discharge may be of several kinds, and they require careful classification if their different possible meanings are to be understandable.

Experimentally defined temperature effects on bed-material discharge usually require classification in terms of the flow characteristics that were kept constant, the variables that were involved in the analysis of the data, and the way in which the data were analyzed. These effects for flume flows may seem to be considerably different from those for field flows. Part of the difference is due to the shallow flows, variable energy gradients, wide range of bed configuration, and relative lateral and longitudinal uniformity of the flume flows as compared with field flows. Part is due to differences in the kinds of temperature effects that are generally defined. That is, in flume flows, the bed-material discharges may be measured at constant flow, constant depth, variable energy gradient, and two or more different water temperatures. The bed-material discharges may then be plotted against shear, and a temperature effect may be determined on the relation between bed-material discharge and shear. For flows at a cross section of a natural stream, the bed-material discharges per foot of width at approximately constant energy gradient may be plotted against mean velocity to define an average relation. The individual departures of observed bed-material discharges from the average relation may be plotted against water temperature to show any general effect of temperature in causing bed-material discharge to depart from the average relation. Such a general effect might be much different from the temperature effect on the relation between bed-material discharge and shear in flume flows.

Experimental defined temperature effects on the relation of bed-material discharge to mean velocity for three rivers indicate an average increase of about 75 percent in bed-material discharge for a decrease of water temperature from 80° to 40°F. This average increase together with some other experimental data and theoretical computations is the basis of a graph that is given to show the approximate temperature effect on the relation between bed-material discharge and mean velocity. The graph shows an increase in the percentage of this temperature effect with increase in depth of flow.

High concentrations of fine sediment increase the apparent viscosity of a water-sediment mixture. The addition of 20,000 parts per million of bentonite to distilled water has an effect on viscosity that is about the same as the effect on distilled water of a reduction in water temperature from 60° to 34°F (Simons, Richardson, and Haushild, 1963, fig. 6). The equivalence of a particular concentration of fine sediment to a particular temperature change and some observed bed-material discharges for the Rio Puerco in New Mexico largely define the given graph of approximate effect of high concentration of fine sediment on the relation of bed-material discharge to mean velocity.

Of course, effects of temperature or of concentrations of fine sediment on the relation of bed-material discharge to mean velocity are not directly applicable to the relation of bed-material discharge to any factor or variable other than mean velocity.

INTRODUCTION

A general increase of bed-material discharge with decrease in water temperature has been reported for the Missouri River (U.S. Congress, 1935, p. 1089–1092), the Colorado River (Lane, Carlson, and Hanson, 1949), the Middle Loup River (Hubbell and others, 1956, p. 54), and the Niobrara River (Colby, 1956, p. 31–32). However, some flume experimenters have reported a decrease and some an increase of bed-material discharge with decrease in water temperature (Hubbell and Al-Shaikh Ali, 1961).

The purposes of this paper are (1) to explain at least qualitatively three different temperature effects that are due to changes in viscosity of the water, (2) to indicate reasons why temperature effects for flume flows may seem inconsistent or somewhat contradictory, whereas temperature effects for field streams seem to be relatively consistent, and (3) to give a rough idea of the temperature effect on the relation between bed-material discharge per foot of stream width and mean velocity. Al-

though changes in water temperature may affect somewhat the discharge of fine sediment (silt and clay), most streamflows can transport at any temperature their supplied amounts of fine sediments. Hence, this paper deals mainly with temperature effects on bed-material discharge, which for this paper is defined as the discharge of particles larger than 0.062 mm. The paper is based on some field and flume studies and on theoretical computations of the temperature effect. It is not comprehensive enough to be much more than a reconnaissance report on the whole field of temperature effects on bed-material discharge.

First, three temperature effects are explained individually, and some idea of the general magnitude of each is given; next, overall temperature effects as reported for flume and field studies are discussed; and finally, an approximate quantitative effect of water temperature on the relation between bed-material discharge and mean velocity is given.

TEMPERATURE EFFECTS THROUGH VISCOSITY CHANGES

Both the specific weight (or the density) and the viscosity of a liquid change as the temperature changes. The change in specific weight of water is small (fig. 1) for the usual range of temperature in natural streams. The change in viscosity of water (fig. 1) is much greater than the change in specific weight. The effect on sediment discharge of changes in the specific weight of water is so small that it generally can be disregarded, but the effect on sediment discharge of changes in viscosity may be large enough to be very significant, especially for some particle sizes.

Viscosity changes that result from changes in water temperature have three effects on sediment discharge. The first to be discussed is the effect on the thickness of the laminar sublayer; the second, the effect on the fall velocity of suspended sediment and hence on the vertical distribution of suspended sediment in turbulent flow; and the third, the effect on the bed configuration.

EFFECT ON THICKNESS OF THE LAMINAR SUBLAYER

Changes in thickness of the laminar sublayer because of temperature changes are generally small but should not be completely disregarded. Like other temperature effects, the effect on bed-material discharge of changes in this thickness depends not only on the flow and the bed sediment but on the factors, other than temperature, that also control bed-material discharge or are correlated with bed-material discharge. This effect is complex and difficult to evaluate except in terms of some selected relations that may not be generally accepted. (No one relation or set of relations is generally accepted as satisfactory for computing either bedload discharge

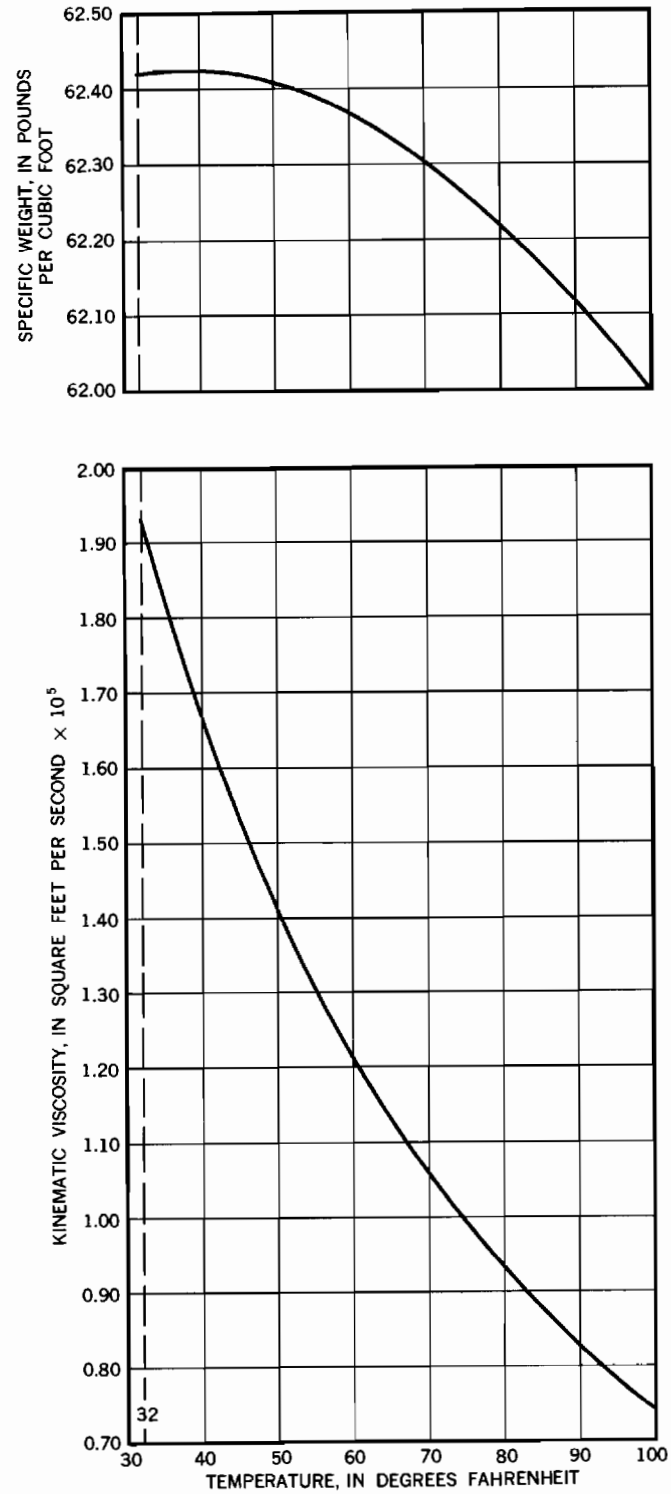

FIGURE 1.—Specific weight and kinematic viscosity of distilled water.

or bed-material discharge.) The effect is discussed here in terms of a particular relation of bedload discharge (the discharge of particles on or within a few particle diameters of the streambed) to mean velocity (Colby and Hubbell, 1961, pls. 1, 2). The relation involves $(RS)_m$, a quantity that has the physical dimensions of a

length and that is equal to the effective shear on the bed sediment divided by the specific weight of the water-sediment mixture. This relation was used for this paper in computing bed-material discharge at the same mean velocities, depths, and size distributions of bed sediments, but at different water temperatures. Of course, other relations may be preferred by many persons, but the one used here should give at least a rough idea of the possible changes in bedload discharge and bed-material discharge when the thickness of the laminar sublayer varies as a result of changes in water temperature.

A change in thickness of the laminar sublayer affects the relation between mean velocity $\bar{u}$ and effective shear on the bed sediment $\gamma_f(RS)_m$. This effective shear is the product of γ_f, the specific weight of water-sediment mixture, and $(RS)_m$, a quantity that is computed from known mean velocity and a mean-velocity equation. The quantity γ_f is approximately constant, and $(RS)_m$ is roughly equivalent to $R'S$, the product of the hydraulic radius with respect to the grains as used by Einstein (1950) and the energy gradient. For a hydraulically rough boundary, the ratio of $\bar{u}$ to $\sqrt{(RS)_m}$ or to $\gamma_f(RS)_m$ does not change as water temperature changes. Also, if $1{,}000\ k_s\bar{u}/(\nu\cdot 10^5)$ is less than about 5, the relative effect of a change in water temperature is less at high ratios of $\bar{u}$ to $\sqrt{(RS)_m}$ than at low ratios. (See fig. 2.) The amount and the direction of the temperature effect on the ratio are determined by the quantity $1{,}000\ k_s\bar{u}/(\nu\cdot 10^5)$, in which k_s is the diameter of bed sediment for which 65 percent by weight is finer and ν is the kinematic viscosity of water. Except for shallow depths and low mean velocities (the lower left corner on fig. 2), even an increase of temperature from 32° to 100°F changes the ratio of $\bar{u}$ to $\sqrt{(RS)_m}$ by only 10 percent or less. Figure 2 is based on an evaluation of fixed boundary roughness by Keulegan (1938) and in particular on his equation 38 for a rectangular channel of infinite width and on his figure 3.

The method given by Colby and Hubbell (1961) for computing bed-material discharge from mean velocity is based mainly on the procedure formulated by Einstein (1950). The method implies the assumptions that the relation of bedload discharge to $(RS)_m$ is independent of water temperature and that the bed-material discharge is proportional to the bedload discharge if the depth of flow and the relative vertical distribution of suspended sediment remain constant. If these two assumptions are correct, changes in thickness of the laminar sublayer because of temperature changes should not affect the relation between bed-material discharge and effective shear on the bed sediment. The changes should, however, affect somewhat the relation between bed-material discharge and mean velocity for a given depth unless the boundary is hydraulically rough. The effect of a particular temperature change on the relation between bed-material discharge and mean velocity should sometimes be in one direction and sometimes in the other. (See fig. 2.) Fortunately, it should be small enough to be insignificant in comparison to the larger effects of water temperature on the vertical distribution of suspended sediment and on the bed configuration.

EFFECT ON VERTICAL DISTRIBUTION OF SUSPENDED SEDIMENT

Basically, the vertical distribution of suspended sediment depends on a ratio between two quantities—the fall velocity of the sediment particles in a turbulent water-sediment mixture and the effective turbulence of the flow for suspending sediment. Neither quantity has a well-defined effect that can be expressed in simple and exact mathematical terms.

THEORETICAL EQUATION FOR VERTICAL DISTRIBUTION

The usual equation for the vertical distribution of suspended sediment of a single fall velocity or a narrow range of fall velocities in turbulent flow between a water surface and a streambed that are plane and parallel was given by Rouse (1937):

$$\frac{c_y}{c_a}=\left(\frac{d-y}{y}\,\frac{a}{d-a}\right)^z. \tag{1}$$

By definition

$$z=w/(ku_*) \tag{2}$$

in which

d	is the depth of flow;
a and y	are distances above the streambed;
c_a and c_y	are concentrations at distances a and y above the bed;
w	is the fall velocity of sediment particles of one size or of a representative particle from a narrow range of sizes;
k	is the turbulence constant; and
u_*	is the shear velocity and equals $\sqrt{gRS}$, which is the square root of the product of the gravity constant, the hydraulic radius, and the energy gradient.

According to equation 2, z is inversely proportional to the product of k, a measure of the rate of change of velocity with depth and hence a measure of turbulence, and u_*, a measure of shear on the streambed and hence, too, a measure of turbulence. Also, for a given turbulent flow, ku_* is constant and z varies directly with fall velocity according to equation 2. Unfortunately, equation 2 is rather inaccurate.

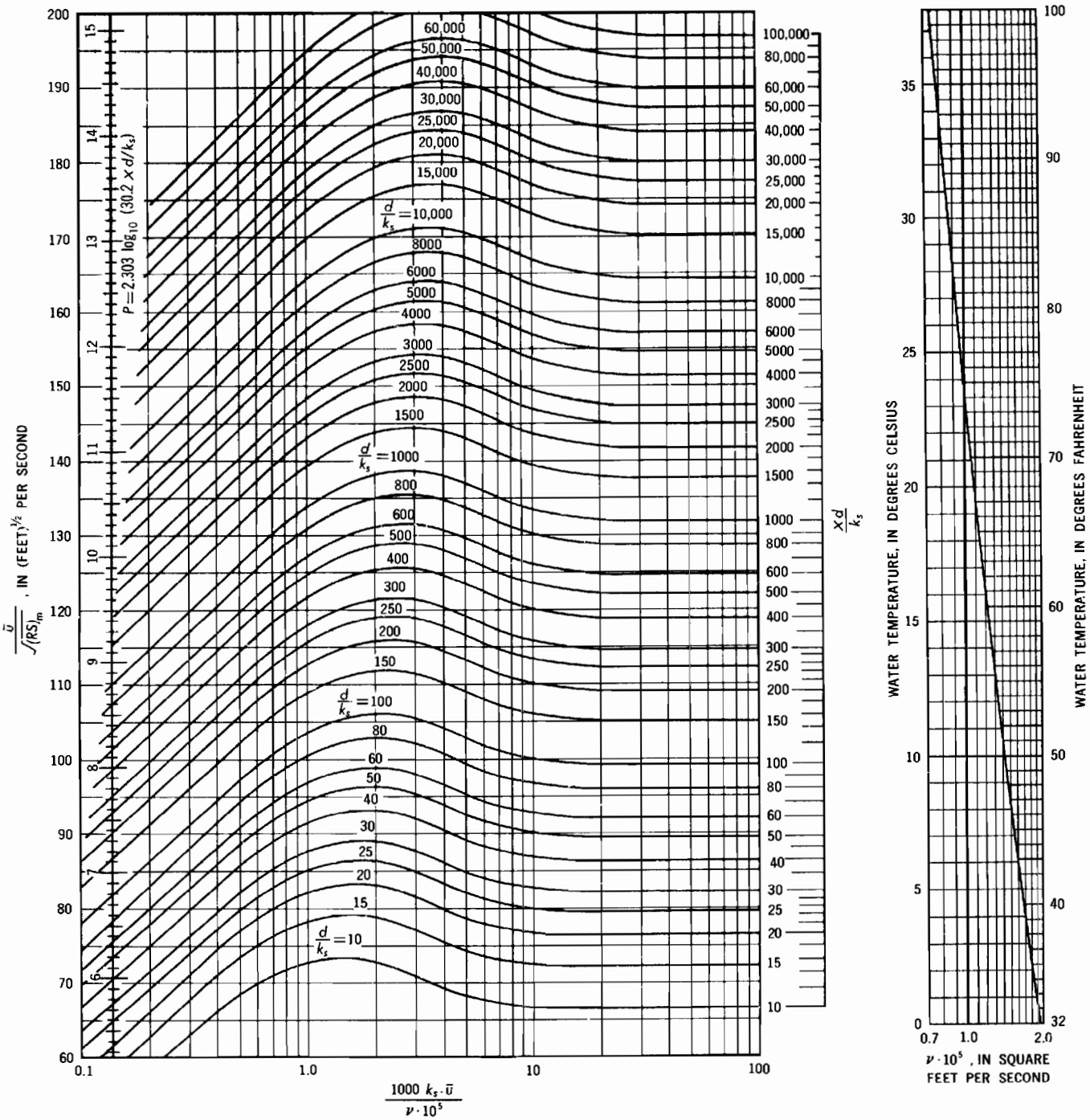

FIGURE 2.—Nomograph for ratio of mean velocity to $\sqrt{(RS)_m}$.

The quantity ku_* is an uncertain measure of turbulence. The turbulence constant k is commonly assumed to be about 0.40 for clear-water flow and to be somewhat lower for sediment-laden flows because of an effect of sediment on the vertical distribution of velocity (Einstein and Chien, 1954, fig. 12). For flow over dunes, the assumptions on which the turbulence constant k was originally based do not apply satisfactorily, and k as computed from a vertical-velocity curve varies widely as position of the vertical changes with respect to the crest of a dune. Hubbell and Matejka (1959, p. 71) found k's much higher than 0.40 for flows over sand dunes. Besides the uncertainty and variation of k, the use of u_* has also been questioned. Einstein (1950, p. 28, 59) used u_*', which may be much less than u_* for some flows, in the computation of z.

The numerator of the right-hand side of equation 2 may be about as uncertain as the denominator. Experimentally determined z's (often called z_1's) for different size ranges of sand within a given flow (Anderson, 1942) do not necessarily increase so rapidly as the 1.0 power of the fall velocity. Experimental z's for some streams increase as about the 0.7 power of fall velocities that are based on equations given by Rubey (1933, p. 332), according to Colby and Hembree (1955, p. 69–71) and Hubbell and Matejka (1959, p. 70–72). Of course, a defined relation between experimental z's for different particle sizes and fall velocities depends not only on the z's but also on the uncertain fall velocities that are assumed to apply. Particle sizes may be either sieve sizes or fall diameters. The effective fall velocities in a given turbulent flow are not known; the fall velocities used are based on laboratory experiments in relatively still water.

RELATION OF FALL VELOCITY TO TEMPERATURE

The temperature effect on the fall velocities of sediment particles is different for different sizes. The resistance to fall of a particle through a fluid is due mainly to viscous forces for particles that are small and that fall slowly and is due mainly to turbulent forces for particles that are fairly large and that fall rather rapidly. The fall velocities of sands (particles whose diameters are from 0.062 to 2.0 mm) in water are affected by both viscous and turbulent forces, but to different relative degrees for different particle sizes. Fall velocities of sediment particles have been discussed at length by Schulz, Wilde, and Albertson (1954) and by the U.S. Inter-Agency Committee on Water Resources (1957).

The variable effect of water temperature on the fall velocities of quartz spheres of different sizes in water is indicated on figure 3. The percentage effect for the change in temperature from 40° to 80°F is greatest for the quartz spheres in the size range of very fine sand and decreases progressively as the particle size and the fall velocity increase. The greatest absolute increase in fall velocity for the temperature change from 40° to 80° F is for quartz spheres whose median diameters are about 2 or 3 mm.

The percentage change in bed-material discharge that accompanies a particular temperature change is generally small for particles of 1 mm or larger. The fall of particles as large as 1 mm is resisted much more by the generation of turbulence, which does not vary appreciably with water temperature, than by viscous drag. The fall velocity of particles finer than sand is low no matter what the temperature may be, and a large percentage change in the low fall velocities may not affect the carrying ability of the stream for these sizes to a significant degree.

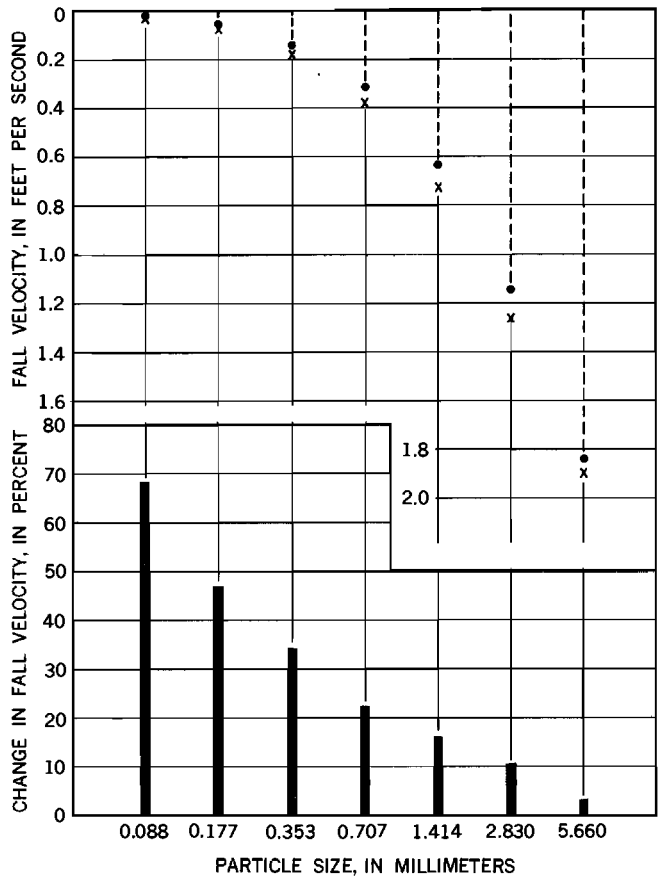

Explanation

X, 80°F ●, 40°F

Geometric mean size (mm)	Geometric mean size (ft)	Size range of spheres (mm)
0.088	0.00029	0.062–0.125
.177	.00058	.125– .250
.353	.00116	.250– .500
.707	.00232	.500–1.000
1.414	.00464	1.000–2.000
2.830	.00928	2.000–4.000
5.660	.01856	4.000–8.000

FIGURE 3.—Effect of a change in water temperature from 40° to 80°F on the fall velocity of quartz spheres of several sizes (U.S. Inter-Agency Comm. on Water Resources, 1957, table 2).

COMPUTED TEMPERATURE EFFECTS ON BED-MATERIAL DISCHARGE

The effect on bed-material discharge of changes in vertical distribution of suspended sediment can be roughly evaluated at stream verticals from a few computations of bed-material discharge at different water temperatures. These computations are based partly on theoretical and partly on empirical relations. Even though the computed bed-material discharges are inaccurate, perhaps largely because of inaccurate z's, the ratio between the computed bed-material discharge for one water temperature and that for another may be reasonably representative of actual temperature effects on bed-material discharges. The computed bed-material

discharges should at least indicate the general way in which the temperature effect, mainly due to changes in vertical distribution of suspended sediment, varies with changes in particle sizes, depths of flow, and mean velocities.

Computations were made for three size distributions of bed material (fig. 4), at mean velocities of 2, 5, and 10 feet per second, for depths of 1 (or 4) and 10 feet, and at water temperatures of 40°, 60°, and 80°F. In a general way, the computations were based on the procedure by Einstein (1950); however, the bedload discharge per foot of width, $i_B q_B$, was computed from a graph given by Colby and Hubbell (1961, pl. 2), and $\sqrt{(RS)_m}$ was taken from figure 2. The bed-material discharges, which include both bedload and suspended sediment of the appropriate particle sizes, were computed from $i_B q_B(PI_1+I_2+1)$; P is from figure 2, and I_1 and I_2, which is always a negative quantity, were taken from curves given by Einstein (1950, figs. 1 and 2). For mean velocities of 10 feet per second, a depth of 4 feet—rather than 1 foot—was used to avoid Froude numbers greater than 1.0. (The Froude number equals $\bar{u}/\sqrt{gd}$.)

The computations of bed-material discharge included the effects of water temperature on both the thickness of the laminar sublayer, through the use of figure 2, and the vertical distribution of suspended sediment, through the use of the I_1 and I_2 curves. Because of the uncertainty of equation 2, the z's that were used to determine I_1's and I_2's were computed from the simple and partly arbitrary equation

$$z=4.0\ w^{0.7} \tag{3}$$

The equation was based on an examination of experimental z's for the Niobrara River near Cody, Nebr., and for the Mississippi River near St. Louis, Mo.

The fall velocity w for equation 3 was based on a table given by the U.S. Inter-Agency Committee on Water Resources (1957, p. 26, table 2). Accurate fall velocities are not necessary for this equation because the computed temperature effect is based mainly on change in fall velocity rather than on absolute fall

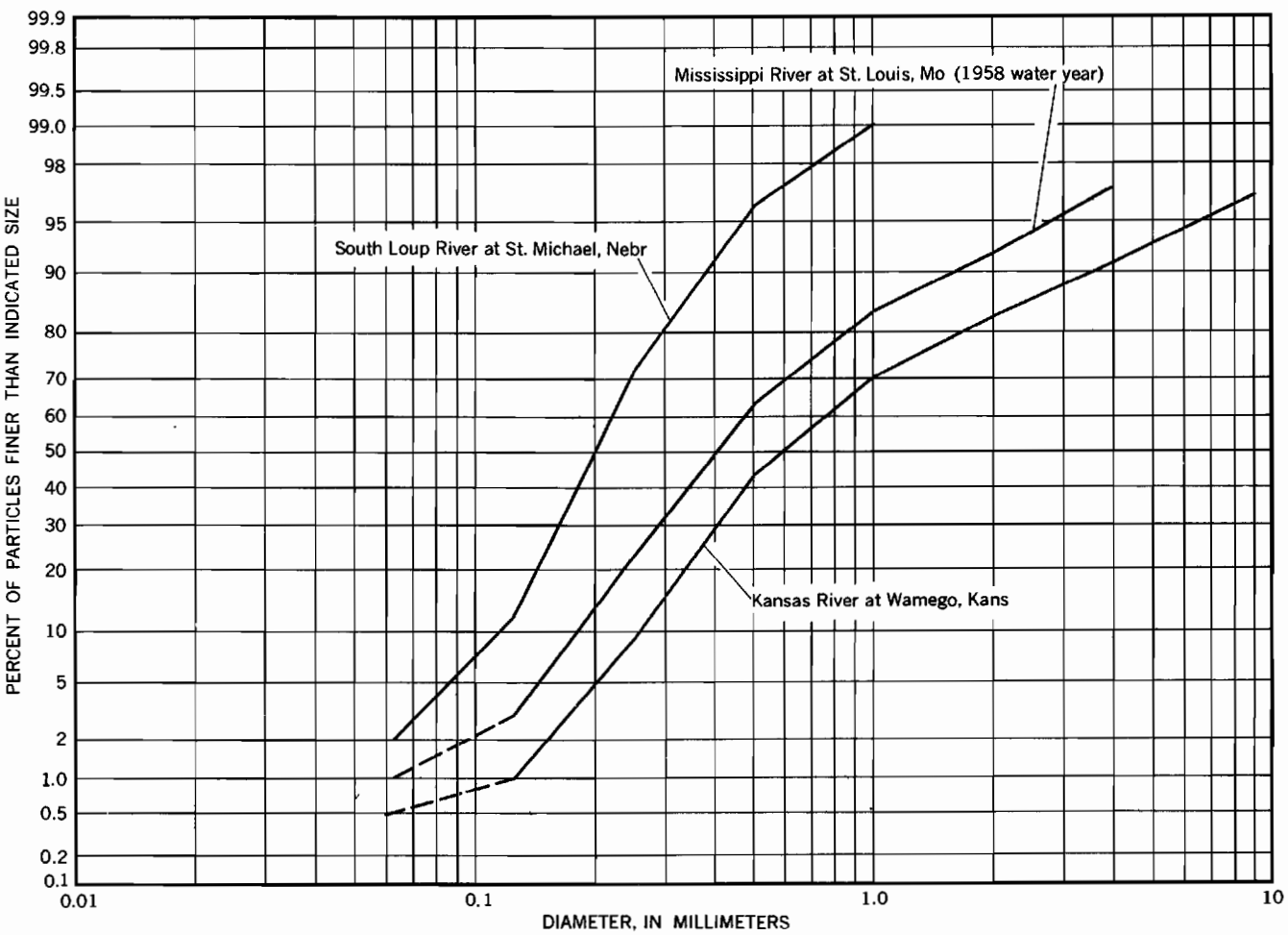

FIGURE 4.—Size distributions of bed sediments for computing temperature effects.

velocity. Similarly, the accuracy of equation 3 is not particularly significant because the computations are intended to indicate mainly a relative temperature effect on the discharge of bed material instead of absolute discharges of bed material.

The ratio of computed total discharge of bed material at 40°F to the computed total discharge of bed material at 80°F averaged roughly 2:1 (fig. 5). The ratio always increased as the depth of flow increased. The ratio tended to decrease, at least slightly, as either mean velocity or median particle size increased. The decrease in ratio may not be significant, however, except for the change in median size from 0.40 to 0.60 mm.

The relations of computed total discharge of bed material to depth are not necessarily straight lines on log-log paper, but straight lines should be satisfactory approximations on figure 5 for connecting computed points.

Although the computed total discharges of bed material are inexact, they probably are realistic enough to make the computed temperature effects reasonable approximations of actual temperature effects on bed-material discharges at a stream vertical. However, a further check was made to see if a large change in computed z's might give a much different indicated temperature effect.

The check was made by arbitrarily dividing the z's from equation 3 by 2.0 and then recomputing the total bed-material discharges for a depth of 10 feet, a mean velocity of 10 feet per second, the bed sediment whose median diameter is 0.40 mm, and water temperatures of 40°, 60°, and 80°F. Although the recomputed bed-material discharges were about seven to nine times the original bed-material discharges (fig. 5), the indicated temperature effect was reduced only about 25 percent. Thus, the recomputations indicate that large absolute errors in computing total bed-material discharges may not change greatly the indicated temperature effect.

The relative consistency of the temperature effect (fig. 5) may be misleading unless the computed bed-material discharges are shown for individual size ranges and for the water temperatures of 40° and 80°F. (See figs. 6–8.) The percentage temperature effect indicated by the computed bed-material discharges is largest for the size range from 0.125 to 0.25 mm. The percentage effects for the two size ranges from 0.062 to 0.125 mm and 0.25 to 0.50 mm are about equal, and they are next largest to the effect for the 0.125- to 0.25-mm-size range. The percentage temperature effect on bed-material discharge decreases markedly as the particle size increases above 0.50 mm and would be small if all bed material transported by a flow were larger than 0.50 mm. Especially for the two finer bed sediments (figs. 6 and 7), nearly all the computed bed-material discharges were of particles finer than 0.50 mm. For any one depth, the percentage temperature effect is reasonably constant for all the flows and bed sediments for which computations were made, but this relation may be due partly to the use of equation 3 for all flows. This effect generally increases as the depth of flow increases, particularly if the temperature effect is appreciable as it is for the fine sand.

The computed differences in bed-material discharge for different water temperatures were due mostly to changes in the vertical distribution of the suspended sediment rather than to changes in the thickness of the laminar sublayer. According to the computation procedure, only the bedload discharge is affected by changes in thickness of the laminar sublayer, and any percentage change in the bedload discharge will cause an equal percentage change in the bed-material discharge. The bedload discharge of all particle sizes for the 0.20-mm median diameter, at a depth of 1.0 foot and a mean velocity of 2.0 feet per second, was about 11 percent more at 40° than at 80°F. For this size of bed sediment and this assumed flow, the bedload discharges for two of the individual size ranges were about 20 percent more at 40° than at 80°F. For all other computations, the differences in bedload discharge for individual size ranges or for total bedload discharge were never more than a few percent for the change in temperature from 40° to 80°F. Some of these small changes in bedload discharge were plus and some were minus for the stated change in temperature. Minus changes in bed-material discharges, because of changes in the thickness of the laminar sublayer, exceeded the computed plus changes in vertical distribution of suspended sediment for the two coarsest size ranges of the 0.40-mm sand for a mean velocity of 5 feet per second. That is, the computed bed-material discharg increased rather than decreased for a change in temperature from 40° to 80°F. (See fig. 7.)

EFFECT ON BED CONFIGURATION

The sand bed in a laboratory channel may have several distinctive kinds of bed configurations and widely different resistances to flow (Simons and Richardson, 1961). The configurations are related to some measure of flow, and physical size of the bed sediment has a complex and sometimes large effect on bed configuration (Simons and Richardson, 1961, fig. 3; 1962, fig. 2). A change caused in the fall velocity of sediment of a given physical size by a change in viscosity probably affects bed configuration and resistance to flow in much the same way as a similar change in fall velocity caused by a change in physical size.

Because bed configuration is difficult to define quantitatively and to express mathematically especially for

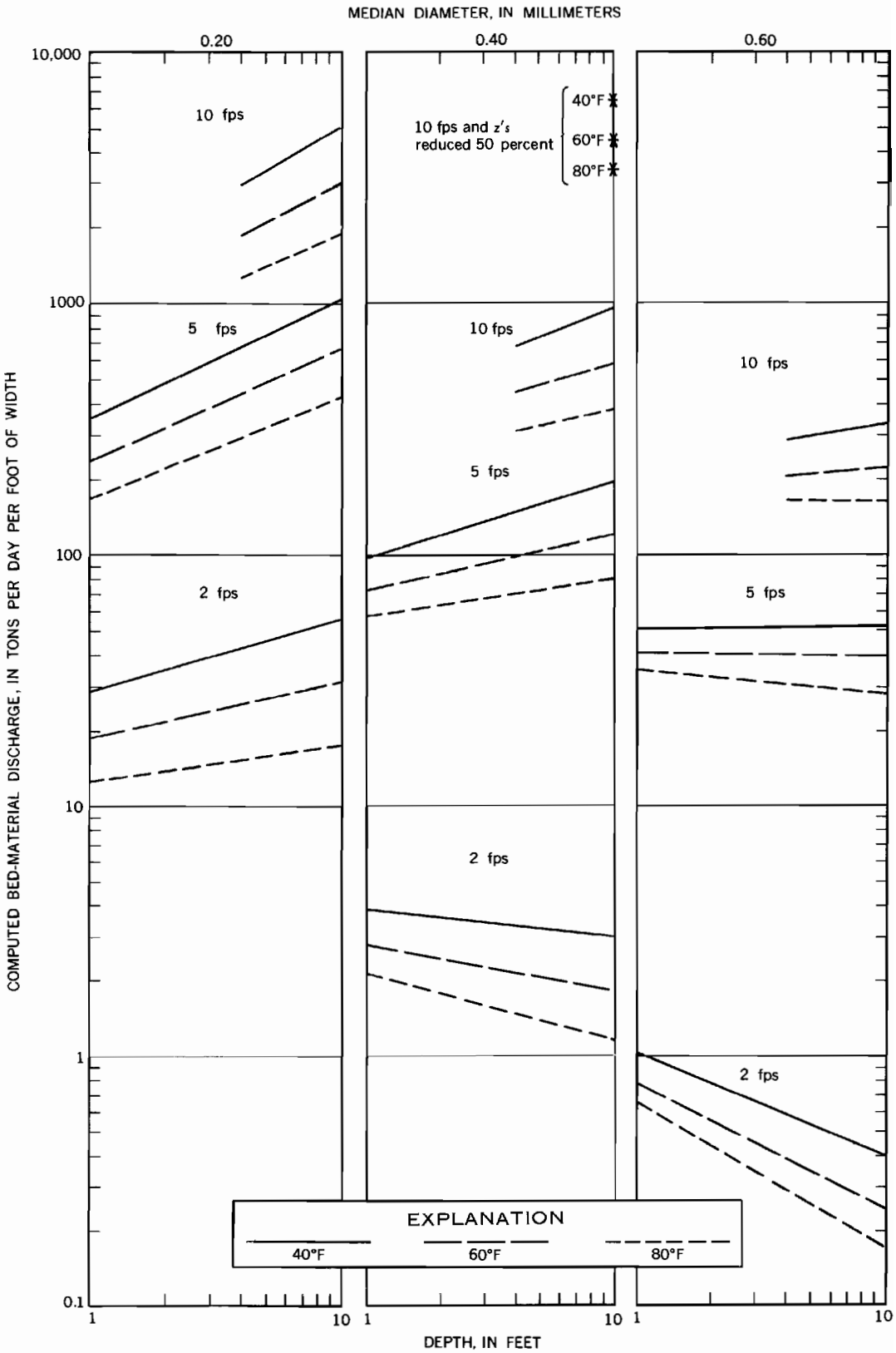

FIGURE 5.—Computed effect of water temperature on the relation of bed-material discharge to mean velocity.

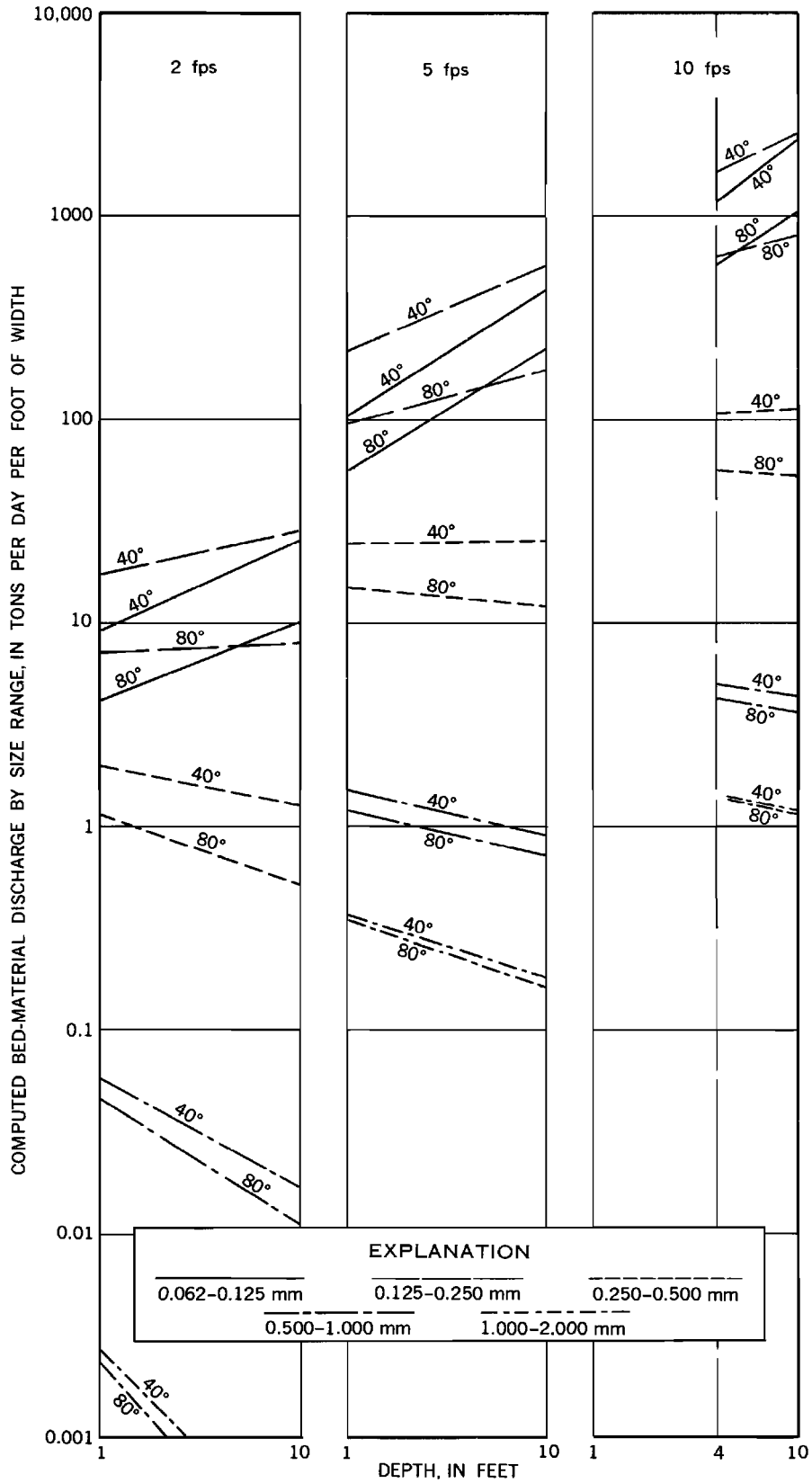

FIGURE 6.—Computed sediment discharges by size ranges for a bed sediment whose median diameter is 0.20 mm. Temperatures are on the Fahrenheit scale.

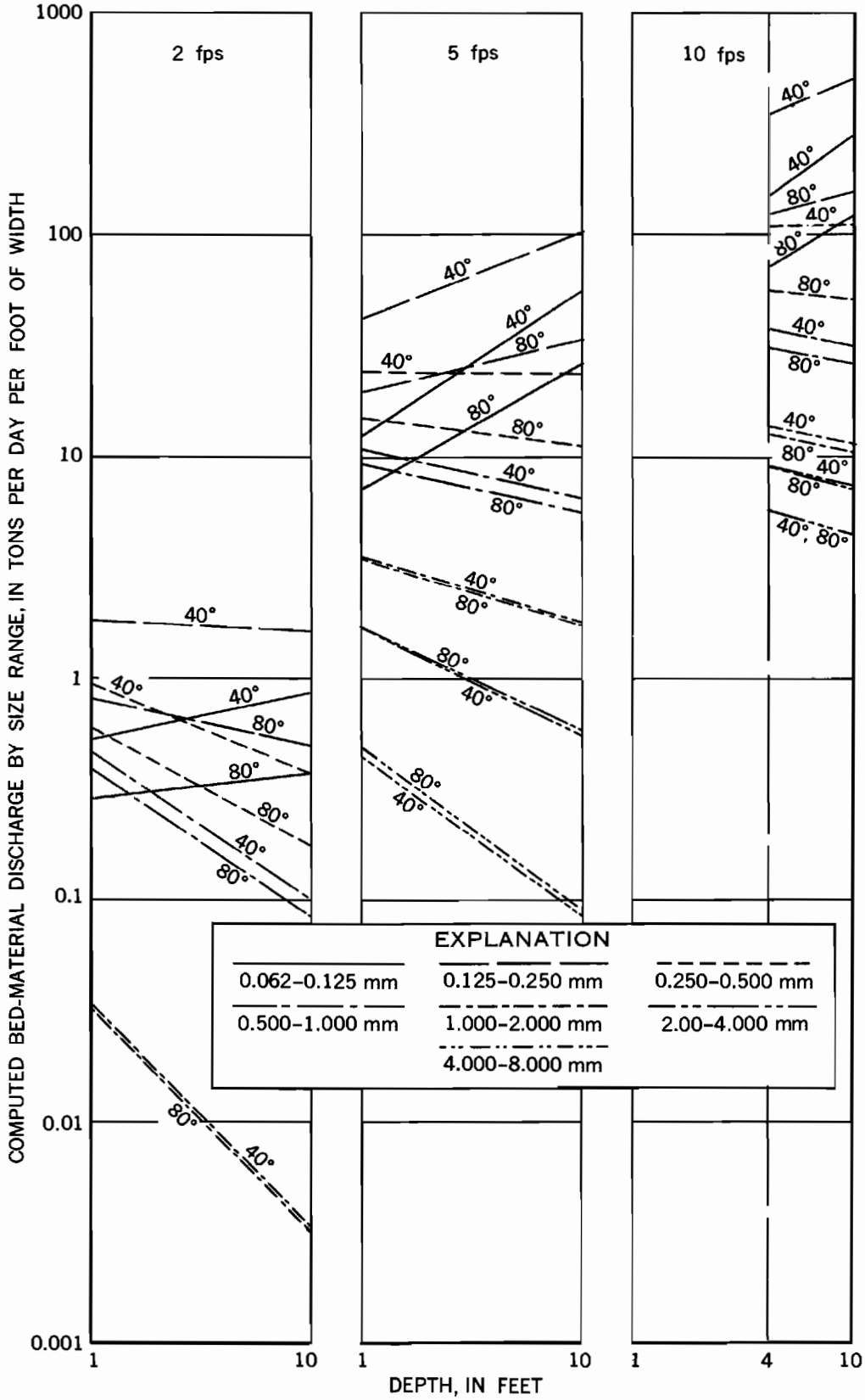

FIGURE 7.—Computed sediment discharges by size ranges for a bed sediment whose median diameter is 0.40 mm. Temperatures are on the Fahrenheit scale.

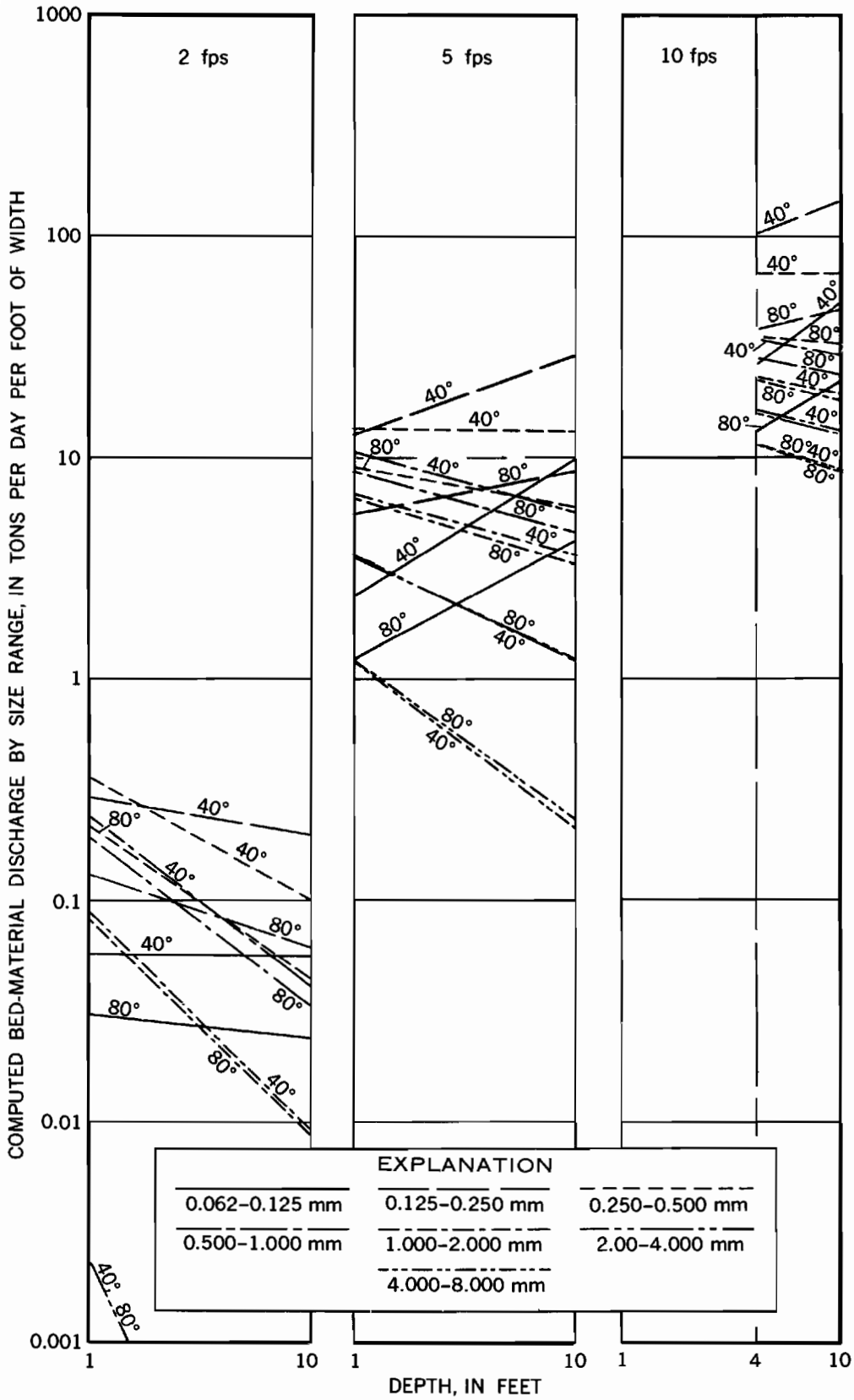

FIGURE 8.—Computed sediment discharges by size ranges for a bed sediment whose median diameter is 0.60 mm. Temperatures are on the Fahrenheit scale.

field streams, resistance to flow generally is used in this paper as an indication of bed configuration. The use of resistance to flow should be fairly satisfactory because of the comparatively large effect of bed configuration on resistance to flow (Vanoni and Brooks, 1957, p. 93–94), though sediment in the flow tends to decrease the resistance to flow for a given bed roughness (Vanoni and Brooks, 1957, p. 93–94). Furthermore, if the streambed is fairly smooth, the resistance to flow seems to vary as the median diameter of the bed sediment changes (Dawdy, 1961, p. C14).

Persons who study mainly flows in laboratory flumes are likely to have concepts of bed configuration somewhat different from those of persons who study mainly field flows. Part of the difference is due to differences in the methods of study and observation and part to differences in behavior of the streambed in small flumes and in field streams.

A worker with laboratory flumes may define a dune in terms of the dune shapes and the particle movements that he can readily see. On the other hand, the shape of the dunes and the movements of sediment particles over the dunes are difficult to observe in field streams, but the characteristic softness of the dunes and the general irregularity of a dune-covered streambed are well known to a worker with field streams. Such a worker is likely to define the dunes in terms of the observations that he has made of the softness and irregularity of the bed. A flume worker usually thinks in terms of a wide range of bed configurations from a plane bed without sediment movement to violent antidunes at a high Froude number, perhaps as high as 2.0. The field worker realizes that neither the plane bed without sediment movement nor the antidunes at Froude numbers as high as 2.0 have much field significance; he concentrates his attention on bed configurations that range from ripples to perhaps a narrow band of antidunes down the middle of a field stream whose cross section seldom has a Froude number that even approaches 1.0.

A significant difference in bed configurations in laboratory flumes to those in field streams is that the bed configurations in flumes are usually about uniform over the bed during most runs, whereas the bed configurations in field streams may differ greatly both laterally and longitudinally. Even though the entire bed of a field stream may be covered with dunes, the size of the dunes is likely to vary from place to place. The nonuniformity of bed configurations in field streams results mainly from variations of depth, average velocity at a vertical, and particle size from place to place in a channel reach. A change of flow with time may cause a certain change in bed configuration at one place but a different change at another place in a field stream. In general, the changes in bed configuration and in resistance to flow in field streams tend to average out to some degree over even short reaches and to be more gradual and less distinct and extreme than those in laboratory flumes.

FIELD STREAMS

The effects of temperature changes on bed configuration and on resistance to flow are difficult to determine for field streams. Flows usually fluctuate widely, sometimes during short periods of time, and changes in flow may cause changes in bed configuration. Large changes in water temperature usually occur gradually and over longe periods of time. Hence, the effects of such temperature changes are not so clearly indicated as they would be if the changes occurred rapidly and if variations in flow and possibly in size of the bed sediment were small during the temperature changes. Even fairly large changes in temperature probably sometimes cause little change in resistance to flow if, for example, the stream has ripples or sand dunes on the bed throughout the range of flow. Furthermore, many field sites where flow and resistance to flow are observed are a short distance upstream from a gravel bar or a riffle that is more effective than bed configuration in controlling depth and velocity of flow.

The Middle Loup River at Dunning, Nebr., which has unusually constant flow throughout most years, has generally lower Manning's n's when the water temperature is low than when the temperature is high (Hubbell and others, 1956, p. 54 and fig. 23). Although the computed n's scatter considerably from the average relation on figure 9, the trend is fairly clear. Hubbell and others (1956, p. 3, 5) also noted a general absence of sand dunes at some cross sections during the winter, when n's were commonly low.

Observations with an ultrasonic depth sounder confirm the change of bed roughness of the Middle Loup River at Dunning from summer to winter for approximately equal flows. (See fig. 10.) Three longitudinal

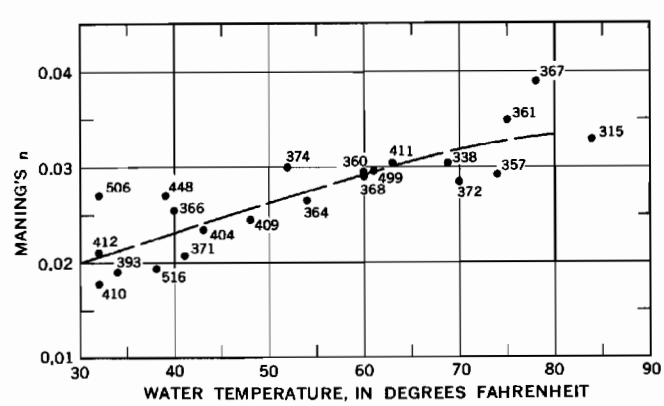

FIGURE 9.—General variation of Manning's n with water temperature for Middle Loup River at Dunning, Nebr., section C_2. Numbers beside points indicate flow, in cubic feet per second.

profiles were defined for a summer day and three for a winter day. Each profile was selected as at least roughly representative of the streambed for one-third of the width of the flow. Each profile for June 25 indicated dunes of about the same size as the dunes indicated by the other two profiles. The dunes extended throughout the lengths of the sounder runs. The bed on December 5 was definitely smoothest at the left profile and roughest at the right profile, but even the right profile was smoother than any of the three profiles for June 25. The bed configurations of figure 10 indicate major decreases in Manning's n from summer to winter and are considered to be representative for the flows and temperatures at which they were defined.

The ultrasonic sounder was described by Richardson, Simons, and Posakony (1961). The field use of the sounder in the Middle Loup River at Dunning, Nebr., was explained by D. W. Hubbell, C. H. Scott, and J. V. Skinner (written commun., 1960).

Some other streams show less consistent decreases in Manning's n with decrease in water temperature. Manning's n's given by Beckman and Furness (1962, table 2) for the Elkhorn River near Waterloo, Nebr. (fig. 11), show no clear-cut reduction in n as the temperature decreases at either low or high flows. However, the few n's for low temperatures average considerably lower than the n's for high temperatures at flows between 2,500 and 5,000 cfs (cubic feet per second). Somewhat

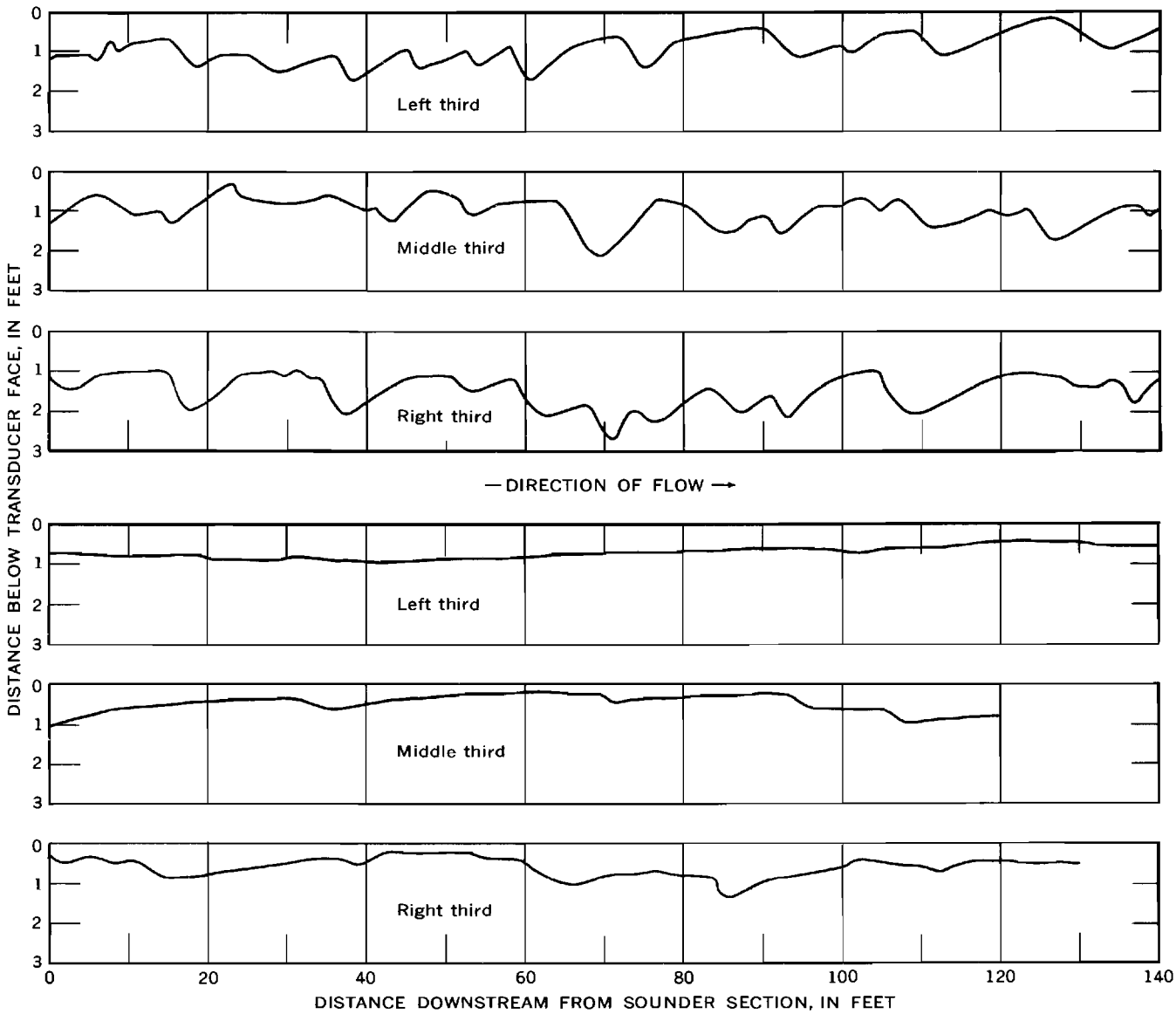

FIGURE 10.—Longitudinal profiles of streambed at different water temperatures, Middle Loup River at Dunning, Nebr. Upper set of graphs shows variations in streambed for June 25, 1959 (flow, 350 cfs; temperature, 83°F). Lower set of graphs shows variations in streambed for December 5, 1959 (flow, 360 cfs; temperature, 39°F).

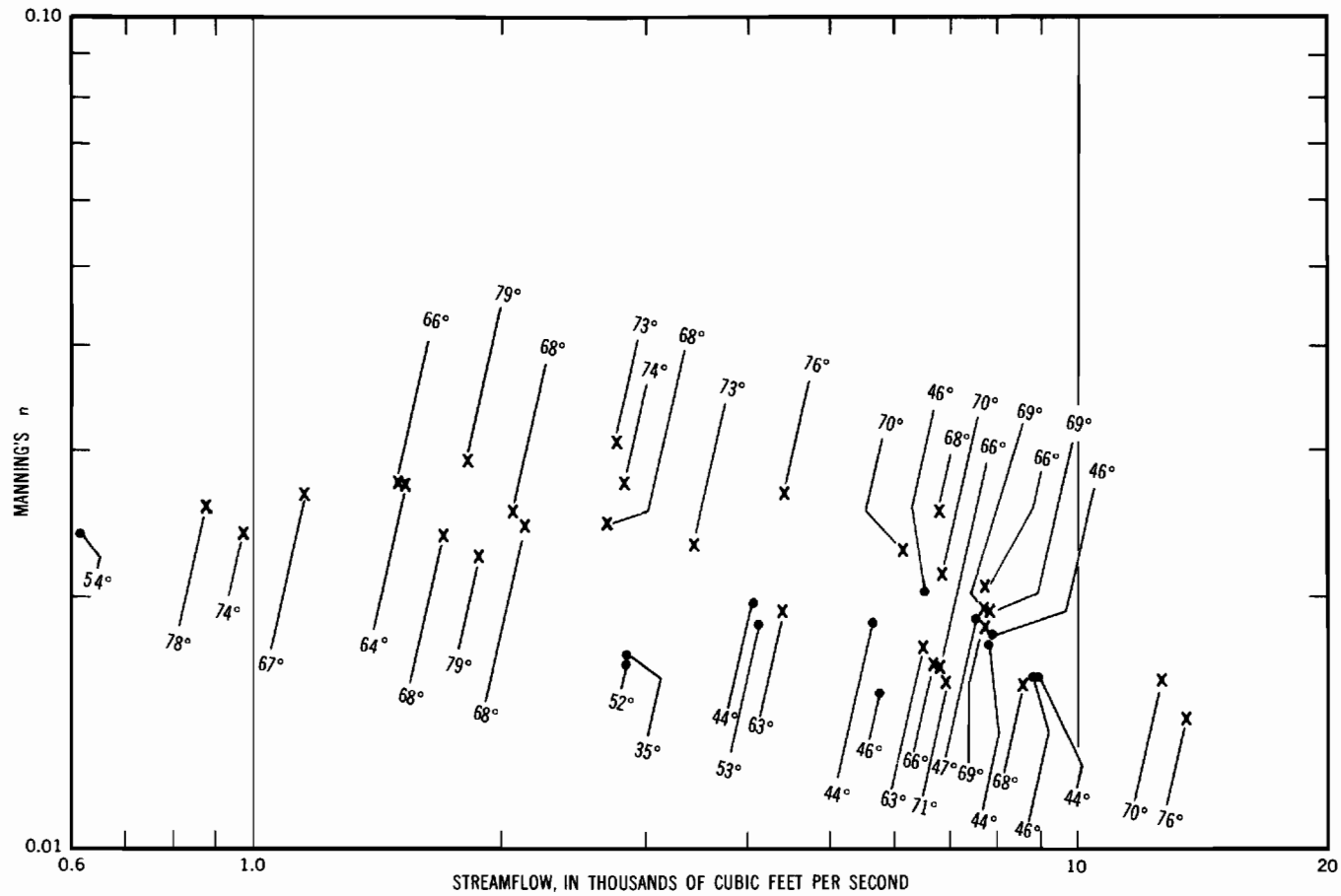

FIGURE 11.—Variation of Manning's n with streamflow and water temperature for Elkhorn River near Waterloo, Nebr. ×, 60°F and above; ●, below 60°F. (Data from Beckman and Furness, 1962, table 2.)

similarly, the n's given by Jordan (1965, table 2) for the Mississippi River at St. Louis, Mo., generally decrease as the flow increases (fig. 12); but, except perhaps for flows of more than 400,000 cfs, n's do not seem to vary significantly with temperature (fig. 13).

The n's for the three rivers probably indicate that water temperature has an appreciable effect on the resistance to flow only within certain ranges of flow, and these ranges are different for different streams. The flow of the Middle Loup River seems to be generally in the range for which a decrease in temperature may cause an appreciable decrease in n.

FLUME FLOWS

For some experiments in laboratory flumes, water temperature may have no consistent effect on resistance to flow (fig. 14). The data on which figure 14 is based were reported by Hubbell and Al-Shaikh Ali (1961, fig. 301.1) for a bed sediment whose median standard-fall diameter, as defined by the U.S. Inter-Agency Committee on Water Resources (1957, p. 13, 14), was 0.31 mm. Probably the information on figure 14 is insufficient to justify many conclusions except that of apparent inconsistency. Perhaps a tendency should be noted for a particularly high or a particularly low resistance to flow at either high or low temperatures to change toward more moderate resistances whether the temperature is increased or decreased, but the tendency may not be significant.

A set of flume experiments by Straub, Anderson, and Flammer (1958) was made to determine a temperature effect on bed-material discharge for bed sediment from the Missouri River. The stated median sieve diameter of the bed sediment was 0.163 mm, and runs were made at the same water discharge and at six different water temperatures. Depth of flow apparently depended on the volume of water in the experimental equipment. A 9-percent reduction in depth as the temperature decreased from 86° to 34°F was, of course, accompanied by a 10-percent increase in mean velocity. The combined effect of the increased velocity and the decreased temperature was insufficient to change the bed configuration appreciably under the conditions of the experiments. The resistance to flow did increase somewhat as the temperature decreased. The energy gradient was permitted to adjust freely.

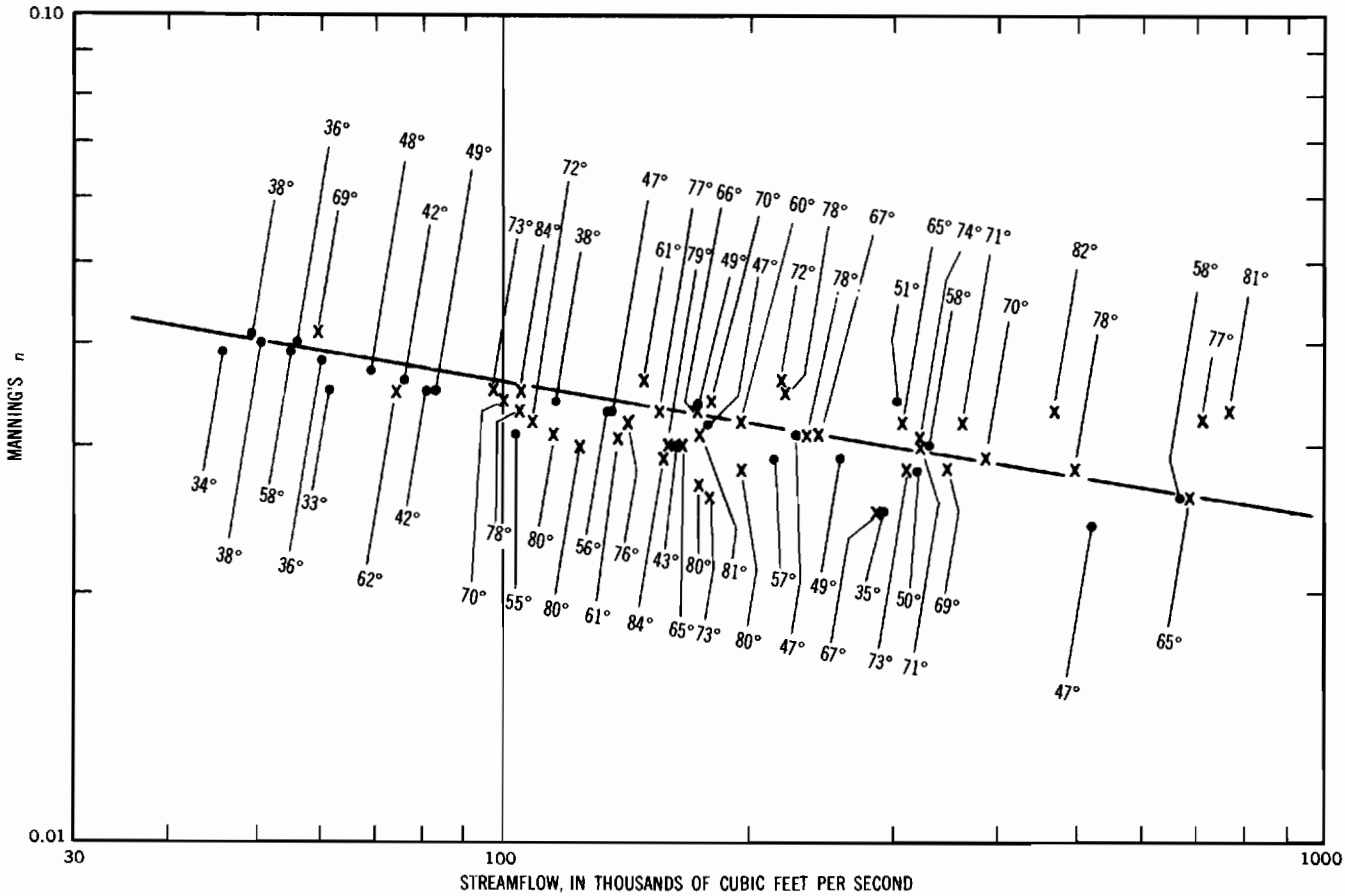

FIGURE 12.—Variation of Manning's n with streamflow and water temperature for Mississippi River at St. Louis, Mo. ×, 60°F and above; ●, below 60°F. (Data from Jordan, 1965, table 2.)

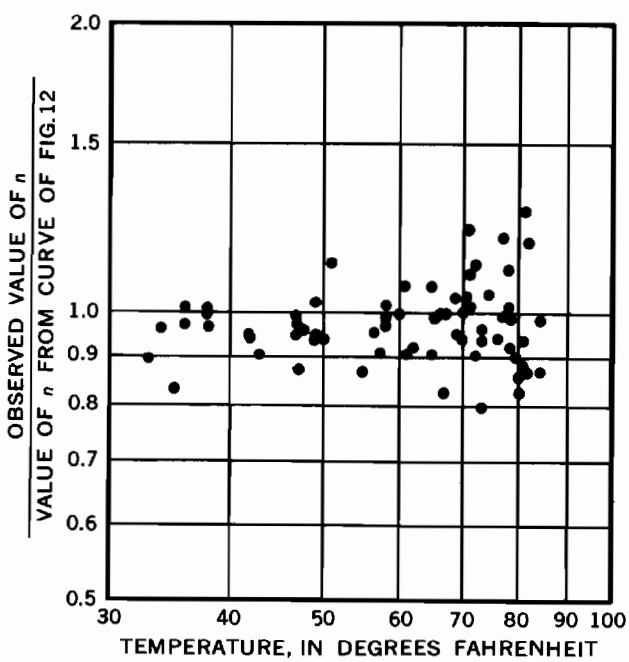

FIGURE 13.—Ratios of observed values of n to values of n from average curve of figure 12 plotted against water temperature.

In spite of the wide differences in resistance to flow (fig. 14), the observed changes in bed-material concentration reported by Hubbell and Al-Shaikh Ali (1961, fig. 301.1) were not particularly large (fig. 15). The greatest increase of concentration at low temperature over the concentration at high temperature was 73 percent, and the greatest decrease was 29 percent. The changes were much less than those for the Middle Loup River at Dunning, Nebr. (Hubbell and others, 1956, fig. 23), or those for the Missouri River bed sediment (Straub, Anderson, and Flammer, 1958, p. 8).

Presumably a main purpose of flume experiments should be to obtain information that may be applied to the behavior of field streams. In such streams, the temperature effects that usually have the most meaning are those at a cross section or within a short reach of stream. If the cross section is representative of a fairly long reach of the stream, the energy gradient, at least at steady flow, does not change appreciably as the temperature changes. That is, the energy gradient of a long reach of stream channel is generally constant over long periods of time. Hence, if a temperature

change could increase appreciably the energy gradient at one place along the reach, it would necessarily decrease the energy gradient at some other place. Therefore, flume studies of temperature effect on bed configuration and on bed-material discharge might be more meaningful for field streams if they were made at constant energy gradient.

If width and energy gradient are constant during a set of experiments with flume flows, the relations among other variables probably are more nearly restricted to the relations that exist in fairly uniform field channels. Any change in resistance to flow requires changes in both depth and mean velocity if the flow is constant. Any change in resistance to flow at either constant depth or at constant mean velocity requires a change in flow. If the bed configuration varies when water temperature varies, the change in bed configuration generally depends on which of the variables—flow, depth, or mean velocity—is kept constant. Perhaps fairly consistent temperature effects on bed configuration could be defined regardless of which of these three variables was kept constant while the temperature changed.

If energy gradient is fairly constant, a progressive increase in depth and flow may cause successively a plane bed without sediment movement, ripples, dunes, a transition phase, plane bed with sediment movement, standing waves, and antidunes to form on a sand bed

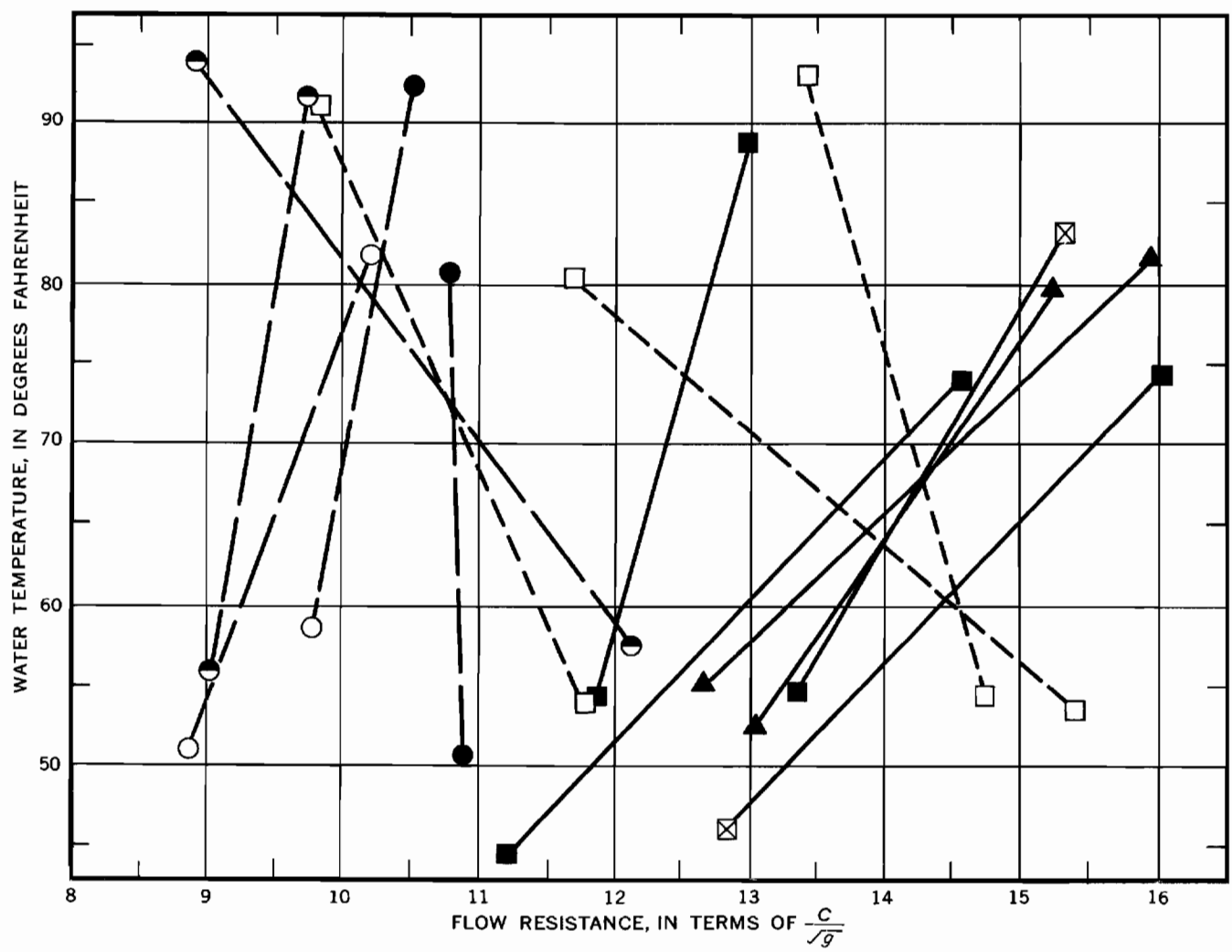

Bed form and flow regime

○, ripples
●, dunes with ripples superposed
◓, dunes
□, transition
⊠, plane
■, mild antidunes
▲, antidunes
Long-dash line indicates lower regime
Short-dash line indicates transition
Solid line indicates upper regime

FIGURE 14.—Differences in resistance to flow for pairs of flume runs at high and low water temperatures (after Hubbell and Al-Shaikh Ali, 1961, fig. 301.1).

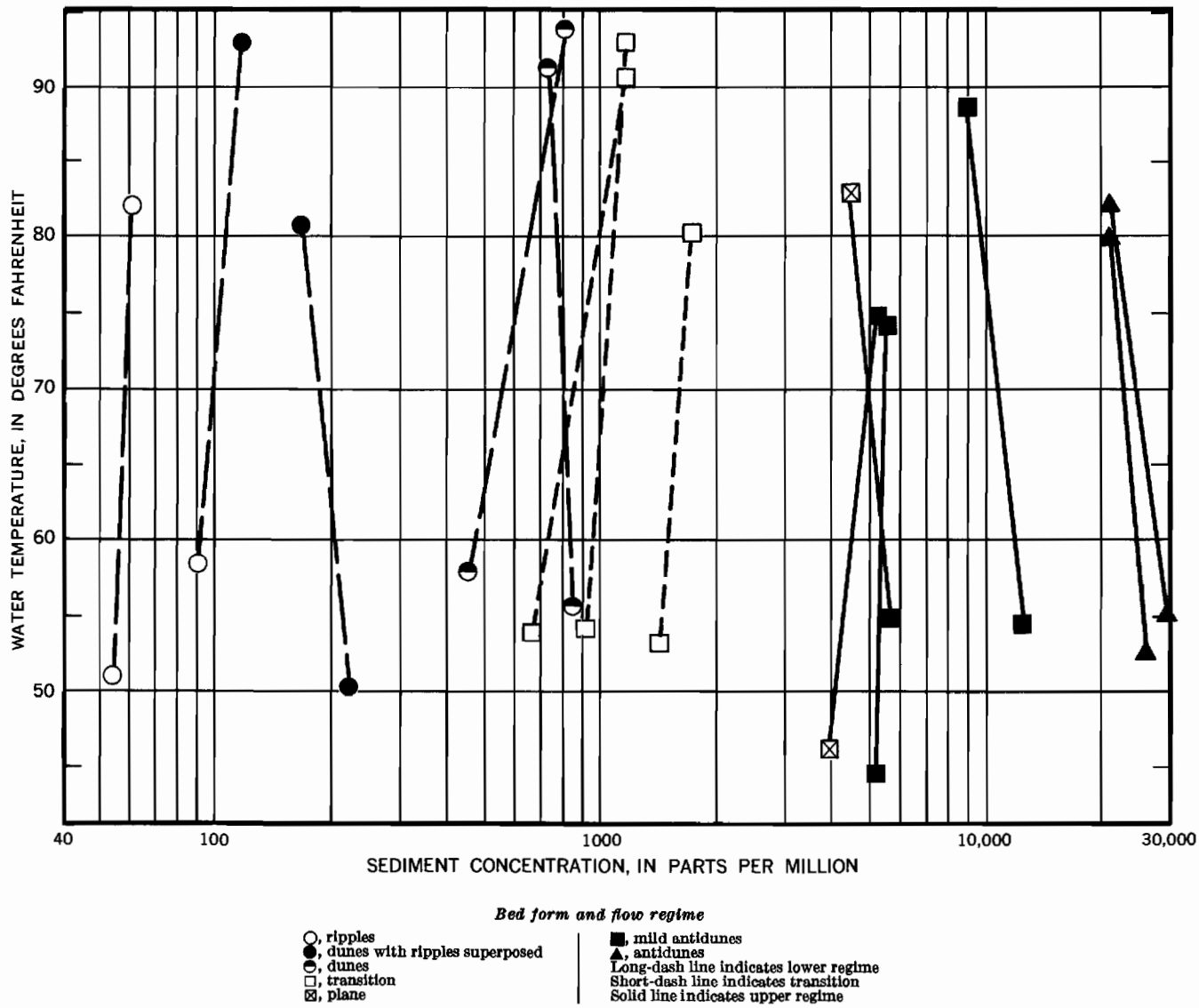

FIGURE 15.—Differences in bed-material concentration for pairs of flume runs at high and low water temperatures (after Hubbell and Al-Shaikh Ali, 1961, fig. 301.1).

(Simons and Richardson, 1960, p. 77). However, the change in flow would have to be very large to produce all these kinds of streambed at constant energy gradient. A small change in flow may have a much larger effect on bed configuration at some ranges of the progressive increase than at other ranges.

Experiments at constant energy gradient should show a reasonably understandable temperature effect on the succession of bed configurations as the flow increases. In general, a decrease of fall velocity because of a decrease in temperature should have much the same effect on bed configuration as an appropriate increase in flow at constant energy gradient. In other words, the effect produced on the bed configuration by a particular temperature change should be about reproducible by the proper change in flow at constant temperature.

OVERALL TEMPERATURE EFFECTS ON BED-MATERIAL DISCHARGE

In the preceding discussions, three temperature effects that changes in viscosity cause on flow and on bed-material discharge have been considered. These effects—on the thickness of the laminar sublayer, on the vertical distribution of suspended sediment, and on the bed configuration—are the ones that might be included in a theoretical computation of bed-material discharge. Although theoretically computed bed-material discharges are generally inaccurate, a study of these three effects provides a background for evaluating and

interpreting available field and laboratory information on the overall effect of water temperature on bed-material discharge.

Overall temperature effects, as the term is used here, are those that are based on experimentally determined bed-material discharges. They require careful classification mainly in relation to the other independent variables that were used as measures of bed-material discharge and to the manner in which the effects were determined rather than in relation to the theoretical temperature effects. Temperature, as compared to mean velocity or to shear, has a relatively minor effect on bed-material discharge, and the relation of bed-material discharge to factors that have major effects partly controls the residual temperature effect. For example, an experimentally defined temperature effect on bed-material discharge might be for a constant flow and mean velocity and a variable energy gradient, for a constant mean velocity and energy gradient and a variable flow, or for a constant flow and energy gradient and a variable mean velocity. A temperature effect might be obtained by a regression study that involved such other statistically independent variables as median particle size of the bed sediment, shear, and depth of flow. The effect on the relation between bed-material discharge and total shear might be considerably different from the effect on the relation between bed-material discharge and mean velocity; either of these effects usually is different for deep flows than for shallow flows, and for fine bed sediment than for coarse bed sediment. Briefly, any defined or definable overall temperature effect has little specific meaning unless it is carefully identified and clearly stated.

DIFFERENCES BETWEEN FLUME FLOWS AND FIELD STREAMS

Overall temperature effects for flows in laboratory flumes may appear to be considerably different from those for flows in field streams for at least five somewhat related reasons. These reasons are (1) the relative shallowness of flume flows, (2) the wide range of Froude number and of bed configuration for flume flows, (3) the general uniformity of bed configuration over the effective part of the flume bed at most times, (4) the variability of energy gradients for flume flows, and (5) the difference in types of data analysis for flume data and for field data. Because temperature effects are small as compared with some other effects on bed-material discharge, they usually are observed and defined for field streams at a cross section of a fairly uniform reach of channel in which the particle sizes of the bed sediment and the energy gradient remain fairly constant.

The relative shallowness of flume flows has considerable bearing on the observed temperature effects. In particular, the percentage effect, which is reasonably consistent, of water temperature on bed-material discharge because of changes in fall velocity and in vertical distribution of the suspended sediment is less in shallow flume flows than in deep field flows (fig. 5). In contrast, the highly variable effect of water temperature on bed configuration and on resistance to flow (fig. 14) is just as large and probably more noticeable in shallow flume flows than in deep field flows.

The wide range of Froude numbers and of bed configurations for flume flows leads to a strong emphasis on the variable effect of water temperature on bed configuration and on resistance to flow. In contrast, most canals and many large field streams that flow over beds of sand are in the dune range of flow nearly all the time. For example, the Mississippi River at St. Louis, Mo., seldom has a Froude number greater than about 0.20 for a cross section and probably always has dunes on at least part of its bed even at the highest flows. (Of course, the Froude number for the whole cross section is only a very rough guide to bed configuration, but a low Froude number does indicate a narrow range of possible bed configurations.) Thus, the range of bed configuration of the Mississippi River at St. Louis may be only from dunes everywhere to dunes on part of the streambed and washed out dunes or perhaps a plane bed on other parts of the bed. For this range, a decrease of water temperature at a particular flow should always tend to reduce the resistance to flow, if it causes any appreciable effect.

The general uniformity of the bed configuration from place to place in a flume flow provides a better chance for observing the effect of water temperature for distinctly different bed configurations than does the usually less uniform bed configuration of natural streams. In field streams, most observations of temperature effect are made for a bed that is partly or wholly covered with dunes. Overall temperature effects on bed-material discharge have probably never been clearly defined for a natural stream that had one consistent bed configuration, other than dunes, throughout a reach at both high and low temperatures. (A natural stream does not include canals or artificially improved stream channels.) Many field streams may also have bars or riffles of coarse sand or of gravel. The surfaces of these bars or riffles may not change configuration or resistance to flow appreciably as the temperature changes.

The variability of energy gradients for flume flows introduces a complicating factor that is largely avoided for field flows by studying temperature effects at one cross section or within one short reach. The same sort of complicating factor might be included in studies of the temperature effect for field streams if these studies

were attempted by comparing bed-material discharges from cross sections of different streams whose energy gradients differed greatly. Because energy gradients usually are permitted to vary widely in flume experiments, flow is not closely related to either mean velocity or depth alone. In field streams on the other hand, streamflow, mean velocity, and depth are likely to be closely interrelated except, perhaps, for a narrow range of discontinuity (Dawdy, 1961) if the reach has relatively uniform lateral and longitudinal distributions of velocity, depth, and particle size. Because of the interrelations, the temperature effect at a constant flow has a more definite meaning for a field stream than for a flume flow, and fewer variables may need to be included in an analysis of the temperature effect in a field stream.

Methods of analyzing temperature effects for flume studies may be much different from those for field studies. As noted above, somewhat different temperature effects are likely to be stressed and observed for flume flows than for field flows, and different data may be measured for the two types of flow. For example, energy gradient—or at least water-surface slope—is nearly always determined for flume flows, whereas it may not be determined at all or may be very inaccurate for field flows. On the other hand, mean velocity is nearly always known for field flows, but it is usually not determined directly for flume flows. Thus, workers with flume flows are inclined to base their analyses of data on such factors as shear or stream power that require a knowledge of energy gradient; workers with field flows are more likely to base their analyses on mean velocity or on discharge per foot of stream width. The use of mean velocity largely bypasses the rather indeterminate effect of water temperature on bed configuration. Flume workers, however, may reject mean velocity as a basic measure of bed-material discharge because it is a poor measure, according to A. A. Bishop (Sediment transport in alluvial channels: a critical examination of Einstein's theory: Colorado State Univ. Ph. D. thesis, 1961), at the high Froude numbers at which many flume experiments are run. Actually, few field streams have Froude numbers as high as 1.0 even for short periods of time.

Some difficulties in applying flume results to field streams are illustrated by the flume experiments for the Missouri River bed sediment (Straub, Anderson, and Flammer, 1958). Because the depth of flow was permitted to decrease 9 percent as the temperature decreased, the mean velocity at constant flow per unit width increased 10 percent. If both the energy gradient and the flow had been kept constant, the indicated increase in resistance to flow with decrease in temperature from 86° to 34°F would have required a decrease in mean velocity rather than an increase. Because bed-material discharge is likely to increase as perhaps the third power of the mean velocity at constant temperature, an appreciable part of the reported 200-percent increase in bed-material discharge may have been due to experimental conditions that were somewhat inconsistent with conditions at a representative cross section of a sand-bed stream.

The confirmation of the experimental temperature effect (Straub, Anderson, and Flammer, 1958, p. 10, 11, and fig. 16) for the Missouri River sediment through computations of suspended sediment by the Einstein procedure (1950) was based on z's somewhat inconsistent with observed z's for field streams. Generally, vertical distributions of suspended bed material in rivers (Einstein and Chien, 1954, fig. 1; Colby and Hembree, 1955, p. 69–77; Hubbell and Matejka, 1959, p. 70–72) show that z changes less rapidly than theoretical z's, which vary directly as the first power of the fall velocity. If Straub, Anderson, and Flammer had used z's that changed less rapidly than the first power of the fall velocity, the differences between the computed bed-material discharges would have been smaller for each temperature change.

Briefly, the overall temperature effect observed on bed-material discharge in flumes is generally due largely to changes in bed configuration and resistance to flow. On the other hand, the overall temperature effect on the relation between bed-material discharge and mean velocity in deep field streams is due mainly to changes in vertical distribution of the suspended bed material.

ROUGHLY DEFINED EFFECT FOR FIELD STREAMS

Even though the effect of water temperature on bed-material discharge cannot be defined accurately, a rough idea of the amount of the effect on bed-material discharges in field streams should be generally helpful. A first step in determining the effect is to decide which other factors should be included as measures of bed-material discharge. As already indicated, the effect of change in water temperature on bed configuration and on resistance to flow is not well known but seems to be erratic and to depend on the antecedent bed configuration, whereas the effect of water temperature on the relation of bed-material discharge to mean velocity (fig. 5) may be fairly consistent. Hence, mean velocity may be a suitable major factor to use as a dominant measure of bed-material discharge, and a defined temperature effect on the relation of bed-material discharge to mean velocity may be meaningful and helpful.

An average relation between bed-material discharge (equivalent to discharge of sands for this site) per foot of stream width and mean velocity shows a rapid in-

crease of bed-material discharge for the Niobrara River near Cody, Nebr., with increase in velocity. (See fig. 16.) The ratios of the individual bed-material discharges to the average bed-material discharges from the curve of figure 16 can be plotted against water temperature (fig. 17) to define a rough experimental effect of water temperature on the relation between bed-material discharge and mean velocity. Of course,

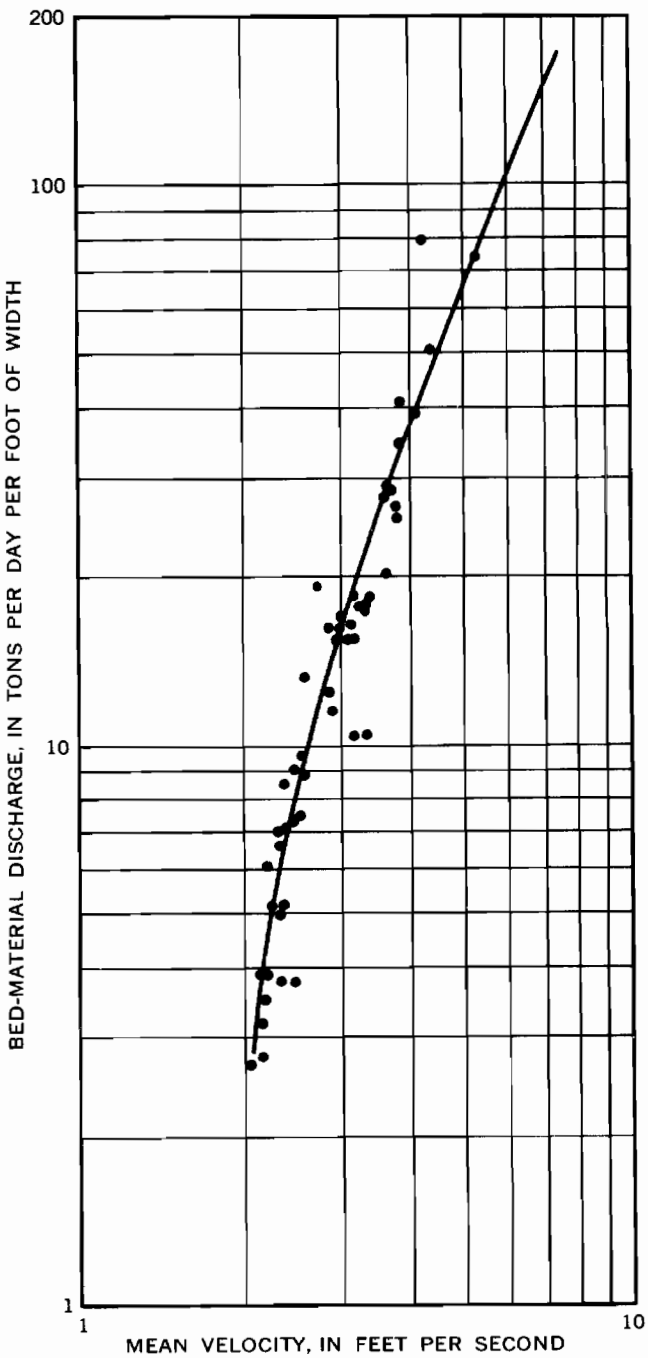

FIGURE 16.—Relation of bed-material discharge to mean velocity for Niobrara River near Cody, Nebr. (from Colby, 1964, fig. 7).

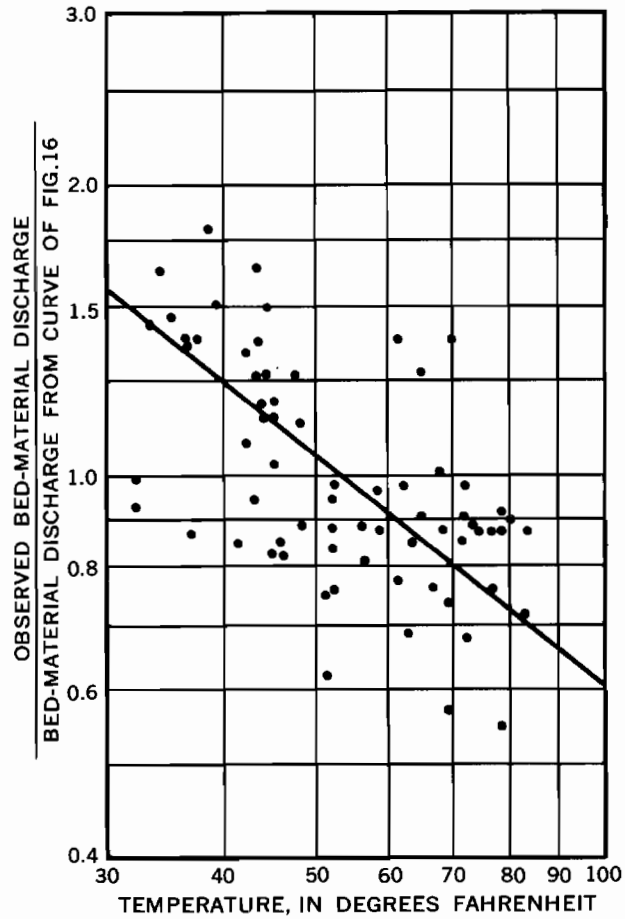

FIGURE 17.—Approximate relative effect of water temperature on the relation between bed-material discharge and mean velocity for Niobrara River near Cody, Nebr. (from Colby, 1964, fig. 22).

scatter of points from the curve of figure 17 is due partly to experimental error and to factors whose effects have not been eliminated. Hence, the effect of water temperature should be more consistent than figure 17 seems to indicate.

Temperature effects on the relation of bed-material discharge to mean velocity were similarly defined for the Middle Loup River at Dunning, Nebr., and for the Mississippi River at St. Louis, Mo. The three experimentally determined effects are surprisingly consistent (see the slopes of lines on fig. 18), perhaps partly by chance. They provide a rough idea of the probable temperature effect for field streams. The slopes of the lines on figure 18 indicate a change of bed-material discharge that is fairly consistent with the computed temperature effects of figure 5.

The relation of bed-material discharge to mean velocity for the Niobrara River (fig. 16) was based mainly on measurements that were made when the water was at least moderately warm. The streamflow and the depth generally increased as the mean velocity increased. The question might be raised whether the

relations shown by figures 16 and 17 can be applied to a stream such as the Middle Loup River at Dunning, Nebr., in which the size of the bed sediment is about the same as that for the Niobrara River at Cody but in which the sediment discharge and the resistance to flow may change rather widely without much change in streamflow (Hubbell and others, 1956, fig. 23).

Bed-material discharges computed from figures 16 and 17 (table 1) seem to explain adequately the increase of sediment discharge, mostly bed-material discharge, that accompanied a decrease in Manning's n, according to Hubbell and others (1956, fig. 23). The total bed-material discharges were computed from information given by Hubbell and others (1956, table 1) for section D at which substantially the total sediment discharge was measured. Water temperatures, mean velocities, and stream widths for computing bed-material discharges from figures 16 and 17 were also given by Hubbell and others (1956, tables 1 and 4).

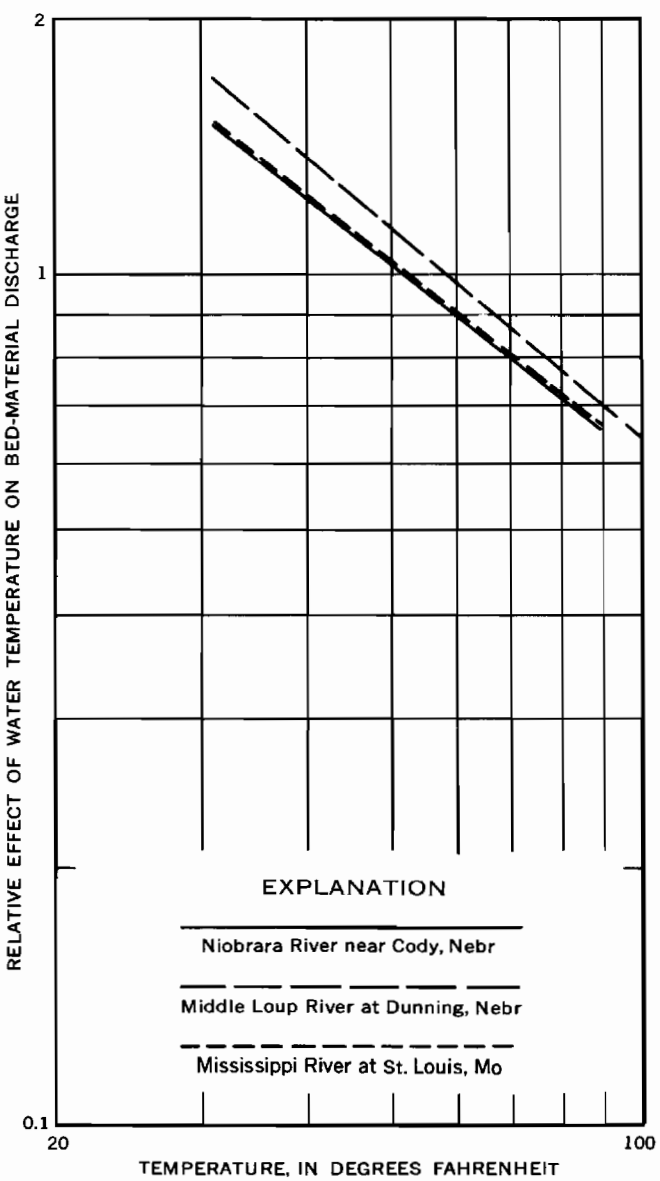

FIGURE 18.—Approximate relative effect of water temperature on the relation between bed-material discharge and mean velocity for three rivers (after Colby, 1964, fig. 23).

TABLE 1.—*Measured and computed bed-material discharges for Middle Loup River at Dunning, Nebr.*

[Basic data from Hubbell and others, 1956, tables 1 and 4]

Date	Section	Temperature (° F)	Bed-material discharge (tons per day)	
			Measured at section D [1]	Computed [2]
1955				
Nov. 24	B_1	38	2,550	2,300
Nov. 24	C_2	35	2,550	3,100
1956				
Jan. 7	C_2	32	2,850	3,400
Jan. 8	C_2	32	2,790	2,800
Mar. 7	C_2	39	2,970	2,800
Mar. 8	B_1	32	3,200	3,900
May 8	A	55	1,830	1,100
May 8	E	64	1,290	1,300

[1] Practically the entire sediment discharge is in suspension and can be measured at section D.
[2] Based on relations shown by figures 16 and 17 and on mean velocities, widths, and water temperatures for sections other than section D.

The generally satisfactory agreement (table 1) between bed-material discharges measured at section D and those computed for sections other than D from mean velocities, widths, water temperatures and figures 16 and 17 implies some significant findings. (The agreement for section A, May 8, 1956, is not good, but section A is more than a mile upstream from section D and is usually a poor section for either measuring or computing bed-material discharge.) One point is that figures 16 and 17 may be applicable to streams other than the ones for which they were defined. Another point is that the increase in bed-material discharge that accompanies a decrease in resistance at almost constant flow is explainable in terms of the effect of the increased mean velocity on the bed-material discharge. A consequent point is that the erratic and difficult-to-define temperature effect on bed configuration and resistance to flow (figs. 11, 12, and 14) probably can be avoided by using mean velocity as a measure of bed-material discharge.

If mean velocity is accepted as a logical major factor that correlates with bed-material discharge, an inexact but probably logical and practical graph can be defined for indicating the general effect of water temperature on the relation of bed-material discharge to mean velocity. The slopes of the curves of figure 18 can be used as experimental measures of the temperature effect for bed sediments whose median diameters are about 0.2 to 0.3 mm. Unfortunately, these curves were based on data (fig. 17) that were not sufficiently exact to define

a difference between the temperature effect at one depth and that at another. However, the probable relative effect of water temperature on the relation between bed-material discharge and mean velocity can be approximated for different depths from the curves of figure 5. Thus, information, partly theoretical and partly experimental, can be combined to define roughly the temperature effect that is indicated by the main graph of figure 19, a figure that was given by Colby (1964, fig. 24). Of course, the relation is not well defined and gives only an approximate idea of the effect that might be expected for different depths and water temperatures. The effect is defined for, and is directly applicable to, only those bed sediments whose median diameters are about 0.2 to 0.3 mm. The effect is on the relation between bed-material discharge and mean velocity. The temperature effect might be considerably different on, for example, the relation of bed-material discharge to total shear or to stream power. Hence, the temperature effect indicated on figure 19 should always be understood and designated as an effect of water temperature on the relation of bed-material discharge to mean velocity.

Of course, the temperature effect varies somewhat as the size distribution of the bed sediment changes even though the median diameter remains constant. It also varies as the depth or the mean velocity changes. A complete definition of the complex temperature effect on the relation of bed-material discharge to mean velocity obviously is not now possible. Even if a complete definition were possible, it probably would be very complicated, and its application for many flows might not appreciably improve the accuracy of computed bed-material discharge.

Because the effect of water temperature on the relation of bed-material discharge to mean velocity varies as the median particle size of the bed sediment changes, the effect indicated by the main graph of figure 19 should be decreased as the bed sediment sizes become either much smaller than 0.2 mm or much larger than 0.3 mm. (See figs. 5–8.) A very rough idea of the possible change in temperature effect with change in median diameter was given by Colby (1964, fig. 24) and is shown on the small graph of figure 19. The indicated decrease of the temperature effect as the median particle size of the bed sediment increases above 0.3 mm may be too rapid. The decrease depends considerably on the size distribution as well as on the median diameter and has not yet been experimentally defined. Of course, an adjustment coefficient of 1.20 from the main graph would become 1.16 (1.00+80 percent of 0.20) rather than 0.96 (80 percent of 1.20) for an 80-percent effect from the small graph. Thus, the effect on computed bed-material discharges of large errors in the small graph generally will be small as compared to other possible errors in computing bed-material discharge, except for very high concentrations of fine sediment.

EFFECT OF CONCENTRATION OF FINE SEDIMENT

The effect of high concentrations of fine sediment, particularly of some clays, is discussed briefly here for two reasons. First, this effect, like the temperature effect, seems to be mainly through an increase in the apparent viscosity of the water-sediment mixture (Simons, Richardson, and Haushild, 1963). Second, the effect of high concentrations of fine sediment may be much greater than the effect of water temperature and may obscure the effect of temperature in some field flows.

If the effect of the fine sediment on bed-material discharge is due almost wholly to the change that the fine sediment causes in the apparent viscosity of the water-sediment mixture, the effect should be similar to a change in water temperature. According to Simons, Richardson, and Haushild (1963), the addition to distilled water at 60°F of 2 percent or 20,000 ppm (parts per million) by weight of a commercial bentonite had the same effect on the apparent kinematic viscosity as a change in water temperature from 60° to 34°F. This general equivalence of concentration of bentonite to change in temperature was used by Colby (1964, fig. 24) as the basis for estimating the effect (fig. 19) of concentrations as high as 20,000 ppm of fine sediment that is mostly bentonite. Extensions of the effect to higher concentrations of fine sediment were based on rough proportioning from the lower concentrations and on some determinations of bed-material discharge, mostly determinations for the Rio Puerco near Bernardo, N. Mex. A given concentration of bentonite has a greater effect on apparent viscosity than the same concentration of kaolin (Simons, Richardson, and Haushild, 1963).

Recently, C. H. Scott (U.S. Geol. Survey unpub. data, 1964) measured the fall velocities of three small samples of sorted sands in distilled water and in dispersions of Wyoming bentonite in distilled water. The nominal diameters of the smallest and the largest of the sorted sands were 0.48 and 3.20 mm, and the maximum concentration of bentonite was 17,500 ppm. At this maximum concentration, the fall velocities of the 0.48- and 3.20-mm sands were about 39 and 5 percent less, respectively, than in clear distilled water. The 3.20-mm sand is large enough to have its fall controlled much more by turbulent forces than by viscous forces. The relatively small effect of the bentonite in suspension on the fall velocity of the coarse sand is consistent with the assumption that fine sediment probably af-

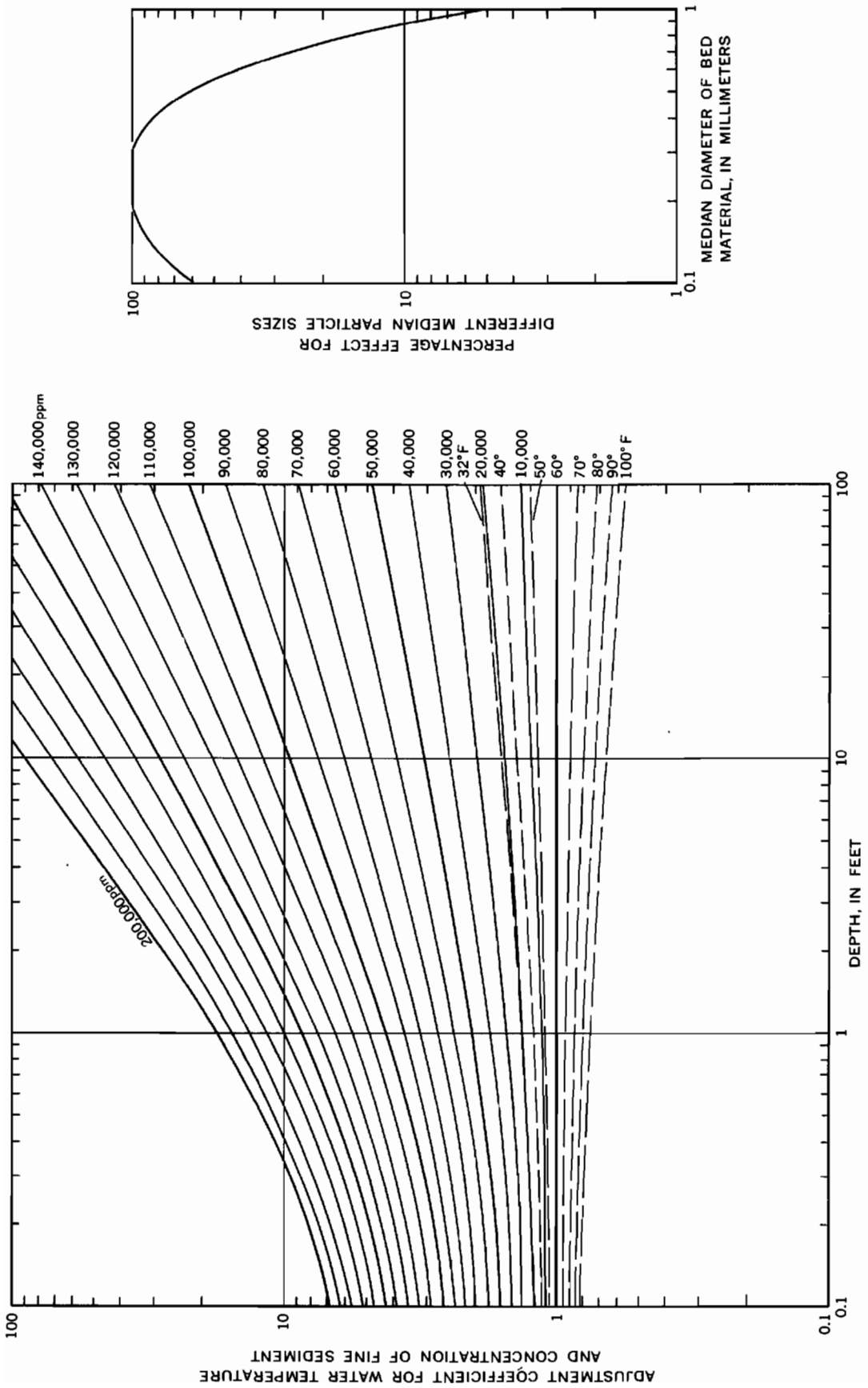

FIGURE 19.—Approximate effect of water temperature and concentration of fine sediment on the relation of bed-material discharge to mean velocity (from Colby, 1964, fig. 24).

fects fall velocity mainly by changing the apparent viscosity of the water-sediment mixture rather than by directly interfering with the settling of the course particles.

However, Scott found that the fall velocity of the 0.48-mm sand decreased much more rapidly with increasing concentration of bentonite than the fall velocity of the 0.47-mm sand that was used by Simons, Richardson, and Haushild (1963). The reasons for the difference in effects are not clear, but the difference may be due, at least partly, to differences between the commercial bentonites that were used in the dispersions. J. C. Mundorff (written commun., 1960) has shown that both concentration and characteristics of the suspended material have a significant effect on the fall velocities of sands and that, in general, bentonite has the most pronounced effect.

Of course, care should be used in interpreting laboratory experiments on the effects of bentonite or other fine sediment on the fall velocities of sands. Differences in the kinds and concentrations of dissolved solids in the water-sediment mixture, in the exchangeable ions on the clay particles, and in turbulence all may have appreciable effects on the relation of the concentration of fine sediment to the fall velocities of the sands.

Presumably, the small graph of figure 19 can be used in a similar manner for adjustments for the effect of fine sediments and for the effect of water temperature. Of course, the indicated effect of the concentration of fine sediment is an effect on the relation of bed-material discharge to mean velocity and should not be used directly as an effect on any other relation of bed-material discharge to a factor that controls bed-material discharge.

CONCLUSIONS

Changes in water temperature have at least three effects on bed-material discharge as the result of changes in the viscosity of the water.

One effect is on the thickness of the laminar sublayer. A change in this thickness affects the relation between mean velocity at a given depth and the effective shear on the bed sediment. For most flows, the change in the relation is only a few percent for usual temperatures in natural streams.

A second effect is on the vertical distribution of sediment concentration because of changes in fall velocity. Several computations of bed-material discharge for different depths, average velocities, median particle sizes, and water temperatures of 40°, 60°, and 80°F gave reasonably consistent temperature effects on bed-material discharges for a stream vertical. The computed bed-material discharges were roughly twice as large for the temperature of 40° as for the temperature of 80°. Effects of changes in the thickness of the laminar sublayer were included in the computations, but they were small as compared with the effects of changes in fall velocity. The computed temperature effect on bed-material discharge varied little as the velocity changed, but it did increase somewhat as the depth increased. The percentage effect differed widely from one size range to another and was small for particles coarser than 0.5 mm.

A third effect is on bed configuration and resistance to flow. It seems to be rather erratic, at least for flume flows, and presumably affects field flows significantly when the bed configuration is close to a critical point of change to another configuration. This poorly defined temperature effect on bed-material discharge can be largely eliminated by using mean velocity as a dominant measure of bed-material discharge for field streams.

A temperature effect is rather meaningless unless it is carefully defined and clearly designated. Not only are there the three general types of temperature effect mentioned above, but each type of analytical study and each set of experiments may define a different sort of temperature effect because different variables are kept constant or different variables are included in the study.

Temperature effects observed in flumes may be considerably different from those defined at a cross section of a field stream. As compared with field streams, flume flows generally are shallow, have energy gradients that are frequently adjusted, and may cover a wide range of Froude numbers and bed configurations, but the bed configuration at any one time is likely to be relatively uniform laterally and longitudinally. Furthermore, the type of analysis used for flume data may be different from that used for field data.

A temperature effect was roughly defined for field streams whose bed sediments have median diameters of about 0.2 to 0.3 mm. For each of three rivers, an average curve was prepared of bed-material discharge per foot of stream width against mean velocity. The indicated scatter of each bed-material discharge from the average curve was then plotted against water temperature to define experimentally an average effect of water temperature on the relation of bed-material discharge to mean velocity for the river. The three resultant curves of temperature effect and the computed increase of percentage temperature effect as the depth increases (fig. 5) were used as the principal bases for a graph of approximate temperature effect on the relation between bed-material discharge and mean velocity.

High concentrations of fine sediment may have an effect on the apparent viscosity of a water-sediment mixture that is generally similar to and may obscure

the effect of water temperature. A graph of probable effect of concentrations of fine sediment that is mostly bentonite was based partly on the graph for the temperature effect and partly on some bed-material discharges for the Rio Puerco in New Mexico. Although the graph is inexact, it indicates a possibly very large effect of high concentrations of fine sediment on the relation of bed-material discharge to mean velocity.

Only a general idea is given in this paper of the different temperature effects and of the quantitative effect of water temperature on the relation of bed-material discharge to mean velocity. Much further study is required before the many different and complex temperature effects can be defined satisfactorily.

REFERENCES

Anderson, A. G., 1942, Distribution of suspended sediment in a natural stream: Am. Geophys. Union Trans., 23d ann. mtg., pt. 2, p. 678–683.

Beckman, E. W., and Furness, L. W., 1962, Flow Characteristics of Elkhorn River near Waterloo, Nebraska: U.S. Geol. Survey Water-Supply Paper 1498–B, 34 p.

Colby, B. R., 1956, Relationship of sediment discharge to streamflow: U.S. Geol. Survey open-file report.

——— 1964, Discharge of sands and mean-velocity relationships in sand-bed streams: U.S. Geol. Survey Prof. Paper 462–A, 1964, 47 p.

Colby, B. R., and Hembree, C. H., 1955, Computations of total sediment discharge, Niobrara River near Cody, Nebraska: U.S. Geol. Survey Water-Supply Paper 1357, 187 p.

Colby, B. R. and Hubbell, D. W., 1961, Simplified methods for computing total sediment discharge with the modified Einstein procedure: U.S. Geol. Survey Water-Supply Paper 1593, 17 p.

Dawdy, D. R., 1961, Depth-discharge relations of alluvial streams—discontinuous rating curves: U.S. Geol. Survey Water-Supply Paper 1498–C, 16 p.

Einstein, H. A., 1950, The bed-load function for sediment transportation in open channel flows: U.S. Dept. Agriculture Tech. Bull. 1026, 70 p.

Einstein, H. A., and Chien, Ning, 1954, Second approximation to the solution of the suspended load theory: California Univ. Inst. Eng. Research, U.S. Army Corps of Engineers, Missouri River Div. Sediment Ser. 3, 30 p.

Hubbell, D. W., and Al-Shaikh Ali, K., 1961, Qualitative effects of temperature on flow phenomena in alluvial channels: U.S. Geol. Survey Prof. Paper 424–D, Art. 301, D21–D23.

Hubbell, D. W., and Matejka, D. Q., 1959, Investigations of sediment transportation, Middle Loup River at Dunning, Nebraska: U.S. Geol. Survey Water-Supply Paper 1476, 123 p.

Hubbell, D. W., Jordan, P. R., Culbertson, D. M., and Hembree, C. H., 1956, Progress report number 1, Investigations of some sedimentation characteristics of a sand-bed stream: U.S. Geol. Survey open-file report.

Jordan, P R., 1965, Fluvial sediment of the Mississippi River at St. Louis, Missouri: U.S. Geol. Survey Water-Supply Paper 1802 (in press).

Keulegan, G. H., 1938, Laws of turbulent flow in open channels: U.S. Natl. Bur. Standards Jour. Research, v. 21, p. 707–741.

Lane, E. W., Carlson, E. J., and Hanson, O. S., 1949, Low temperature increases sediment transportation in Colorado River: Civil Eng., v. 19, p. 619–620.

Richardson, E. V., Simons, D. B., and Posakony, G. J., 1961, Sonic depth sounder for laboratory and field use: U.S. Geol. Survey Circ. 450, 7 p.

Rouse, Hunter, 1937, Modern conceptions of the mechanics of fluid turbulence: Am. Soc. Civil Engineers Trans., v. 102, p. 463–543.

Rubey, W. W., 1933, Settling velocities of gravel, sand, and silt particles: Am. Jour. Sci., 5th ser., v. 25, no. 148, p. 332.

Schulz, E. F., Wilde, R. H., and Albertson, M. L., 1954, Influence of shape on the fall velocity of sedimentary particles: Colorado Agr. and Mech. Coll., U.S. Army Corps of Engineers, Missouri River Div. Sediment Ser. 5, 161 p.

Simons, D. B., and Richardson, E. V., 1960, Resistance to flow in alluvial channels: Am. Soc. Civil Engineers Proc., v. 86, no. HY5. p. 73–99.

——— 1961, Forms of bed roughness in alluvial channels: Am. Soc. Civil Engineers Proc., v. 87, no. HY3, p. 87–105.

——— 1962, The effect of bed roughness on depth-discharge relations in alluvial channels: U.S. Geol. Survey Water-Supply Paper 1498–E, 26 p.

Simons, D. B., Richardson, E. V., and Haushild, W. L., 1963, Some effects of fine sediment on flow phenomena: U.S. Geol. Survey Water-Supply Paper 1498–G, 47 p.

Straub, L. G., Anderson, A. G., and Flammer, G. H., 1958, Experiments on the influence of temperature on the sediment load: Minnesota Univ., U.S. Army Corps of Engineers, Missouri River Div. Sediment Ser. 10, 36 p.

U.S. Congress, 1935, Missouri River: U.S. 73d Cong., 2d sess., H. Doc. 238, p. 1089–1092.

U.S. Inter-Agency Committee on Water Resources, 1957, Some fundamentals of particle size analysis, *in* A study of methods used in measurement and analysis of sediment loads in streams: Rept. 12, 55 p., Washington, U.S. Govt. Printing Office.

Vanoni, V. A., and Brooks, N. H., 1957, Laboratory studies of the roughness and suspended load of alluvial streams: California Inst. Technology [Pasadena, Calif.], Sedimentation Lab. Rept. E–68, 121 p.

U.S. GOVERNMENT PRINTING OFFICE: 1965 O—756-940

Bedload Equation for Ripples and Dunes

By D. B. SIMONS, E. V. RICHARDSON, *and* C. F. NORDIN, JR.

SEDIMENT TRANSPORT IN ALLUVIAL CHANNELS

GEOLOGICAL SURVEY PROFESSIONAL PAPER 462-H

An examination of conditions under which bedload transport rates may be determined from the dimensions and speed of shifting bed forms

UNITED STATES GOVERNMENT PRINTING OFFICE, WASHINGTON : 1965

UNITED STATES DEPARTMENT OF THE INTERIOR

STEWART L. UDALL, *Secretary*

GEOLOGICAL SURVEY

Thomas B. Nolan, *Director*

For sale by the Superintendent of Documents, U.S. Government Printing Office
Washington, D.C. 20402 - Price 20 cents (paper cover)

CONTENTS

	Page
Symbols	IV
Abstract	H1
Introduction	1
Bedload Transport	H1
Conclusions	7
References cited	9

ILLUSTRATIONS

	Page
FIGURE 1. Definition sketch of dunes	H2
2. Comparison of computed bedload with observed bed-material load	3
3. Comparison of computed and observed bedload	4
FIGURES 4–7. Relation of—	
4. V_* to $(V-V_0)\frac{D}{h}$	H5
5. V_* to $\frac{V^3}{gD}$	6
6. h to $\frac{V-V_0}{V_0}\frac{g}{C^2}D$	7
7. q_T to $r_0V\left(\frac{V-V_0}{V_0}\right)$	8

TABLE

	Page
TABLE 1. Variables considered	H2

LIST OF SYMBOLS

C	Chezy coefficient
C_1	A constant
D	Mean depth
g	Accleration due to gravity
h	Average ripple or dune amplitude
K_1, K_2, K_3, K_4, K_5	Constants
q_b	Bedload, by volume or weight
q_T	Bed material load
S	Slope of the energy gradient
t	Time
V	Mean velocity
V_0	Noneroding mean velocity
V_s	Average velocity of ripples or dunes in the direction of flow
x	Distance parallel to the direction of flow
y	Elevation of the bed above an arbitrary horizontal datum
γ	Unit weight of the fluid
δ	A transformation, $\delta = x - V_s t$
τ_0	The shear stress at the bed
λ	Porosity of the sand bed
∂	Partial derivative

BEDLOAD EQUATION FOR RIPPLES AND DUNES

By D. B. Simons, E. V. Richardson and C. F. Nordin, Jr.

ABSTRACT

A simple bedload transport equation based on the mean forward velocity and mean height of ripples and dunes is applied to 101 observations from flume studies by using a recirculating flume and four different sands. Where average dune velocities and heights are determined accurately with sonic equipment, and where suspension of bed material is negligible, the computed and observed transport rates of bed material agree reasonably well. General guidelines for adapting the procedure to field applications are given.

INTRODUCTION

The bedload in most natural channels cannot be measured economically by presently available (1964) sampling techniques. However, where the size and shape of bed configurations—the sand waves or ripples and dunes which form on the channel bed—and the speed of shifting of the bed forms can be determined with reasonable accuracy, a simple relation based on the mean height and velocity of the sand waves can be used to determine bedload transport. It is the purpose of this paper to investigate the applicability and some of the limitations of such a relation.

The bedload equation presented herein was previously given by Richardson and others (1961), and presents no new ideas; in fact, the concept of determining bedload from the dimension and speed of the dunes and ridges in a channel dates from the 19th century (Hubbell, 1964). However, because of the recent technical advancements in electronic equipment (Richardson and others, 1961; Karaki and others, 1961) which is both portable and reliable and which permits rapid and accurate determination of bed configuration over large areas of a channel, it seems desirable to evaluate the applicability of the equation to the practical problem of determining bedload discharge.

BEDLOAD TRANSPORT

When the velocity of flow in an alluvial channel is low, the channel bed configuration is ripples or dunes, or both, and a part of the transported material moves as bedload, in almost continuous contact with the bed. The bedload moves up the face of a ripple or a dune to the crest; the coarser particles then avalanche down the slope to be deposited on the downstream face of the dune or in the trough, and the finer particles may be deposited on the faces of downstream dunes or swept temporarily into suspension. The ripples and dunes move downstream owing to erosion from their upstream face and deposition on their downstream face.

The differential equation of bedload transport for the ripple and dune bed configuration (see fig. 1) may be written

$$\frac{\partial y}{\partial t}+\frac{1}{(1-\lambda)}\frac{\partial q_b}{\partial x}=0. \tag{1}$$

Using the transformation

$$\delta=x-V_s t, \tag{2}$$

$$\frac{\partial y}{\partial t}=\frac{\partial y}{\partial \delta}\frac{\partial \delta}{\partial t}=-V_s dy/d\delta \tag{3}$$

and

$$\frac{\partial q_b}{\partial x}=\frac{\partial q_b}{\partial \delta}\frac{\partial \delta}{\partial x}=dq_b/d\delta. \tag{4}$$

Substituting these expressions in equation 1,

$$-V_s\frac{dy}{d\delta}+\frac{1}{(1-\lambda)}\frac{dq_b}{d\delta}=0. \tag{5}$$

Simplifying,

$$dq_b=(1-\lambda)V_s dy, \tag{6}$$

from which

$$q_b=(1-\lambda)V_s y+C_1. \tag{7}$$

Assuming that the dunes and ripples have triangular shapes, the final equation for bedload transport becomes

$$q_b=(1-\lambda)V_s h/2+C_1. \tag{8}$$

Values of q_b may be converted from volume to weight basis by multiplying equation 8 by the unit weight of the sediment.

In the above,

q_b=volume rate of bedload transport per unit width per unit of time,

λ=porosity of the sand bed,

V_s=average velocity of the ripples or dunes in the direction of flow,

h=average amplitude of the ripples or dunes,

y=elevation of the sand bed above an arbitrary horizontal datum,

x=distance parallel to the direction of flow,

t=time.

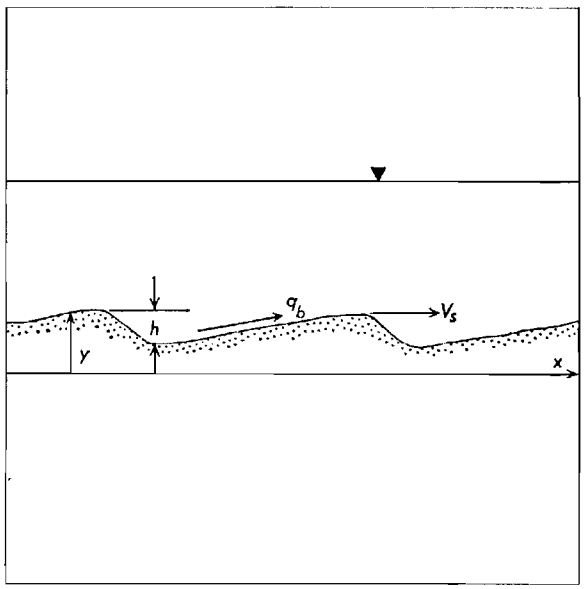

FIGURE 1.—Definition sketch of dunes.

The constant of integration (C_1) may be interpreted as that part of the bedload which does not enter into the propagation of dunes and ripples. Obviously, at the threshold of movement, $C_1=0$ and, so long as the bed is entirely covered with ripples and dunes, C_1 will remain equal to 0 (assuming that bedload is defined as the material that moves in almost continuous contact with the bed). But as the velocity of flow increases, the bed configuration changes from dunes through a transition region of multiple bed forms to a plane bed. For the plane bed condition, $h=0$ and $C_1=q_b$. For the transition region, C_1 is indeterminate.

Equation 8 was applied to 101 observations of equilibrium flows in an 8 foot-wide recirculating flume, where the average heights (h) and velocities (V_s) of the ripples and dunes were recorded (Simons and Richardson, 1961). Velocities and heights of dunes were determined by probing, by visual observation in the transparent wall of the flume, and by the use of the sonic depth sounder described by Karaki and others (1961). A description of the flume and of the general procedures used in collecting data has been presented (Simons and Richardson, 1962; Simons and others, 1961).

The bed-material median diameters, the number of observations for each bed material, and the range of unit discharge of water and of bed-material considered are summarized in table 1.

TABLE 1.—*Variables considered*

Median diameter, in millimeters	Observations	Range of discharge per foot of width of—	
		Water, in cubic feet per second	Bed material, in pounds per second
0.19	17	0.428–2.75	0.0000276–0.226
.28	32	.520–2.75	.0000069– .211
.46	31	.865–1.95	.000086 – .350
.93	21	.862–2.84	.00220 – .474

Figure 2 shows the computed bedload transport rate from equation 8 (q_b) plotted against the observed bed-material transport rate (q_T) for each of these observations. For the coarser material (the 0.93-mm median diameter sand), the agreement between the computed bedload and the observed bed-material load is excellent throughout the range of transport considered. The three points which deviate most from the equal line are for observations where the bed configurations were in a transition between dunes and a plane bed. Similarly, for the 0.46-mm sand, the agreement between computed bedload and observed bed-material load is reasonably good, except at the higher transport rates where an appreciable percentage of the bed-material load was in suspension, or where the bed was in a transition stage between a dune and a plane configuration.

For the finer sizes, the computed bedload is approximately equal to the observed bed-material load for the ripple-bed configurations. For the dune bed, the observed bed-material load is always greater than the computed bedload—a fact that indicates that a large part of the total transport was in suspension.

In figure 3, the bedload transport computed from equation 8 is plotted against observed bedload. This observed bedload was determined as the difference between the observed total bed-material load and the observed suspended load, for the 0.19- and the 0.28-mm sand. Suspended load was determined from the concentration of integrated samples collected to within about 0.1 foot from the bed. For the ripple-bed formation, the relation is not improved, probably because of inherent difficulties in obtaining representative suspended-sediment samples at the extremely low transport rates. For the dune-bed configuration, however, the relation of figure 3 is improved appreciably over that of figure 2. Again, the points which deviate most from the equal line are for bed conditions in transition between a dune and plane bed.

From figures 2 and 3, it is concluded that equation 8 is suitable for computing bedload transport rates for

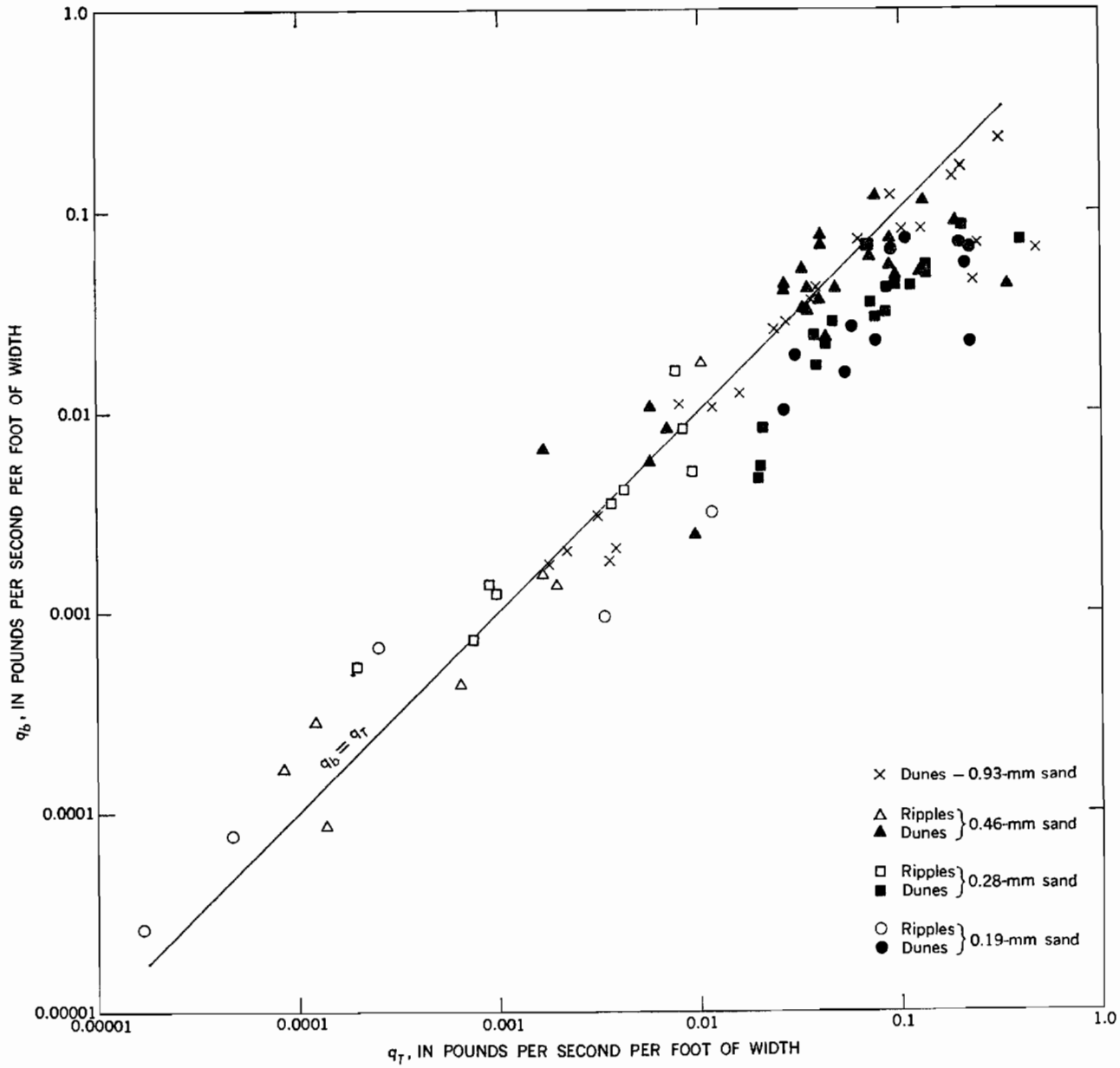

FIGURE 2.—Comparison of computed bedload (q_b) from equation 8 with observed bed-material load (q_T).

the entire range of conditions considered, excluding those observations when the bed configurations were in a transition from dune to plane bed. For the coarser material, where the suspended load was negligible, the equation may be used to estimate the total bed-material discharge, at least for shallow depths, that is, below approximately 3 feet. At greater flow depths, the suspended load perhaps would not be negligible.

Attempts have been made, notably by Russian investigators (Kondratév, 1962) to formulate relationships for estimating dune heights and dune velocities from the characteristics of the flow. Several empirical relations have been advanced. Znamenskaya (1962) proposed that V_s could be evaluated from the equation

$$V_s = K_1 \frac{D}{h}(V - V_0) \tag{9}$$

and Barekyan (1962) presented the following relations:

$$V_s = K_2 \frac{V_3}{gD} \tag{10}$$

$$h = K_3 D \frac{g}{C^2}\left(\frac{V - V_0}{V_0}\right). \tag{11}$$

In the above,

D=mean depth of flow,
V=mean velocity,
V_0=noneroding mean velocity,
g=acceleration due to gravity,
K_1, K_2, and K_3 are constants,
C=Chezy coefficient, $V/\sqrt{gDS}$,
S=slope of the energy gradient.

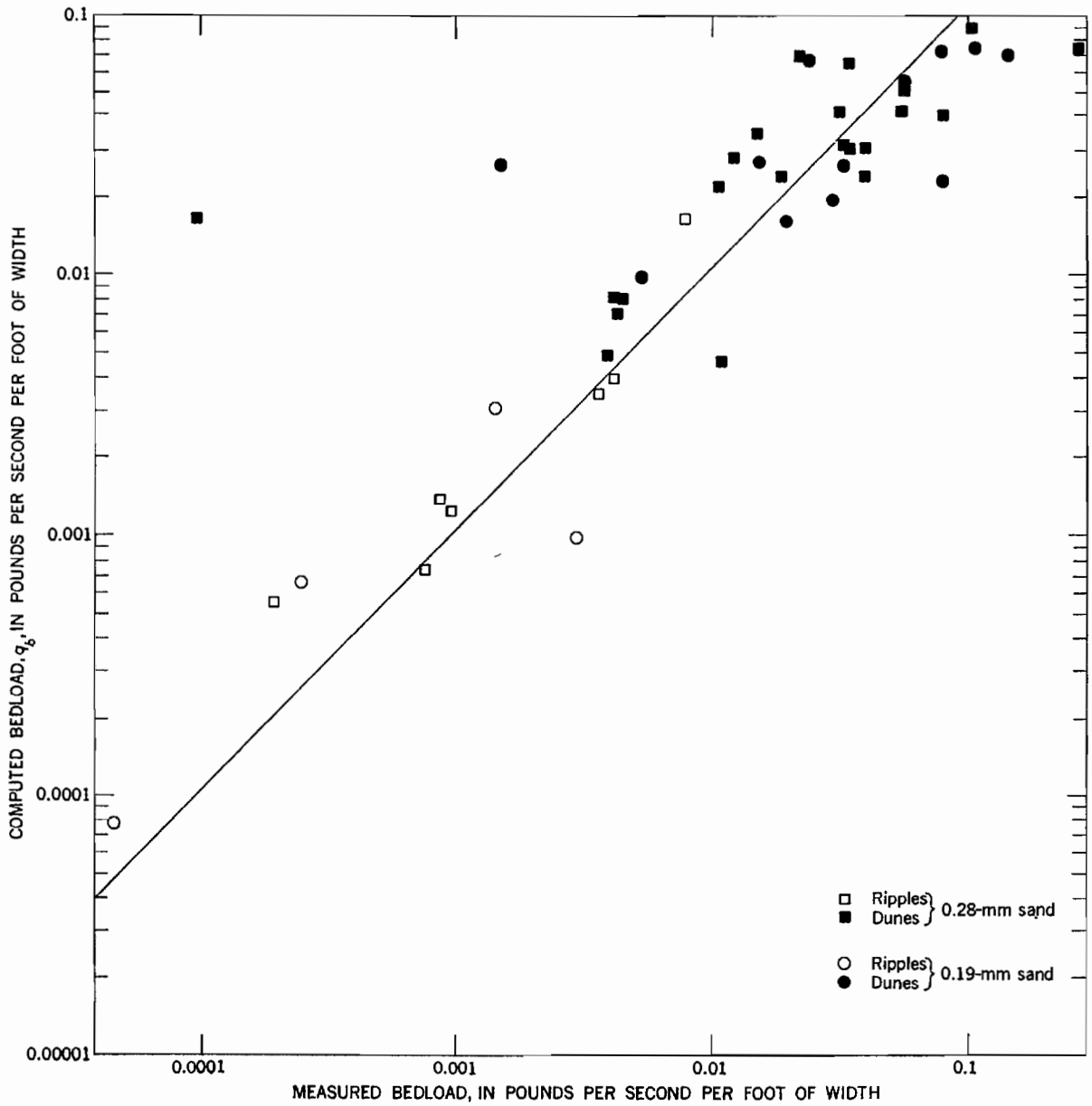

FIGURE 3.—Comparison of computed and observed bedload for the 0.19- and 0.28-mm sand.

When equations 8 and 9 are combined, the rate of bedload transport is found to be independent of dune height, and the transport relation of equation 8 simplifies to

$$q_b = K_4 D(V - V_0) \tag{12}$$

when K_4 is a constant. Equation 12 is quite similar to the expression for stream capacity used by G. K. Gilbert (1914).

The velocity of dune movement (V_s) is plotted against $\frac{D}{h}(V - V_0)$ in figure 4. The solid line in the figure is equation 9 with the constant K_1, as given by Znemenskaya. Figure 4 shows that equation 9 is unsuited to express dune velocities for the data considered, irrespective of the value of K. However, it should be noted that equation 9 was given for the speed of shifting of "meso-forms" (large-scale bars and ridges in natural channels), so the equation probably is not applicable to the ripples and dunes formed in laboratory flumes.

In figure 5, where V_s is plotted against $\frac{V^3}{gD}$, a trend line drawn through the plotted points could be represented by equation 10, but the constant K_2 is approximately 0.5, compared with 0.92 given by Barekyan, and the scatter of points about the line does not lend confidence to the relation.

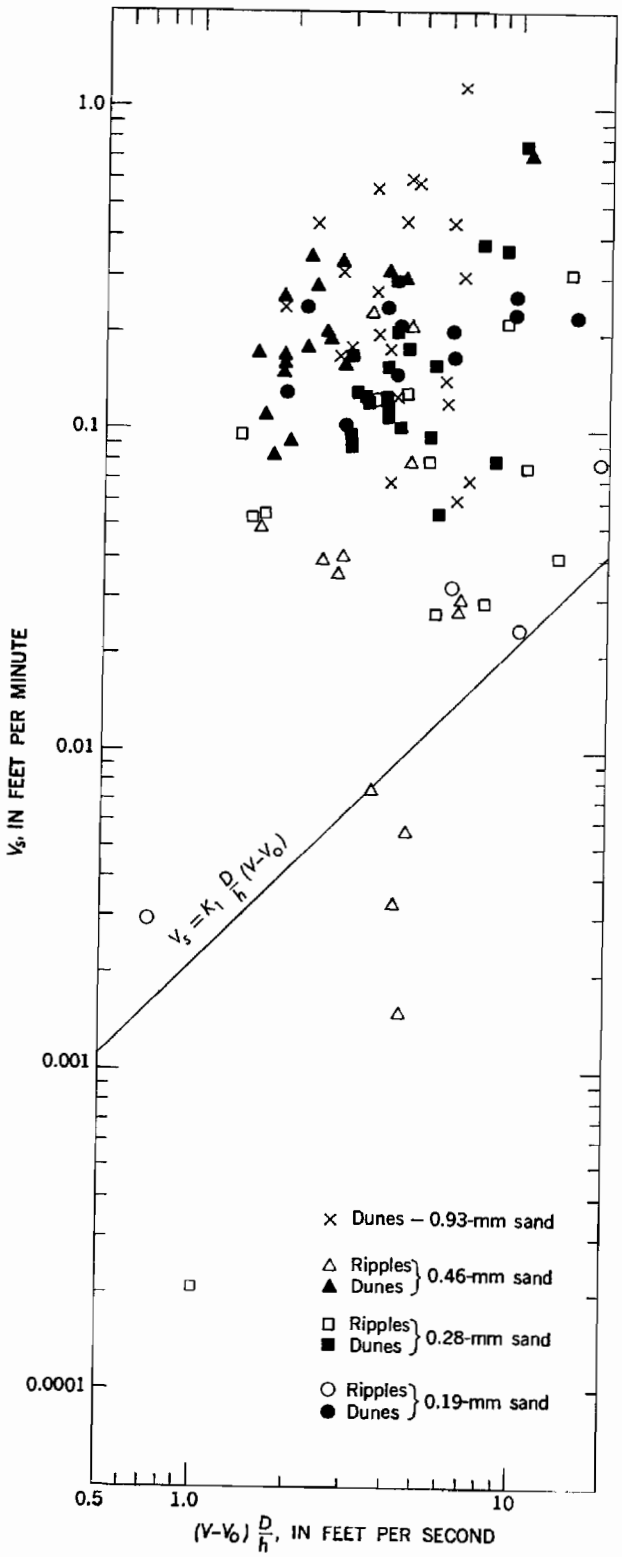

FIGURE 4.—Relation of V_s to $(V-V_0)\frac{D}{h}$.

The relation of equation 11 for dune height (h) shown in figure 6 is somewhat better defined than the relation for dune velocity in figure 5, and the constant $K_3=20.6$ has the same value as the constant given by Barekyan.

Combining equations 10 and 11 with equation 8 yields

$$q_b=K_5\tau_0 V\left(\frac{V-V_0}{V_0}\right) \tag{13}$$

in which

τ_0=shear stress at the bed (γDS)
γ=unit weight of the fluid,
K_5=a constant.

The product of shear stress and velocity, sometimes called "stream power," has been shown to be an important factor in sediment transport (Bagnold, 1960; Cook, 1936), but the correlation of transport to stream power is better for flow over a plane bed with antidunes and standing waves than for flow over a dune bed (Colby, 1964).

Values of q_T are plotted against $\tau_0 V\left(\frac{V-V_0}{V_0}\right)$ in figure 7. The constant K_5, defined from the trend line through the plotted points, is approximately 0.3. Equation 13 does not fit the data for the ripple-bed configuration, and the scatter of points is again too great to provide confidence in equations 10, 11, or 13. It must be concluded that equation 8 is best suited for determining bedload when the average values of V_s and h can be determined quite accurately, as with the sonic depth sounder. The relations for determining heights and velocities of bed forms from flow parameters (eqs. 9–11) do not appear to yield reliable results, especially for the ripples.

It is important to note the limitations of equation 8 and to recognize the factors which influence its accuracy. Critical assumptions in the application of equation 8 were: (1) that the ripples and dunes are triangular in shape, (2) that the ripples and dunes are two-dimensional—that is, the average V_s and h are assumed applicable across the entire width of the channel, and (3) that the porosity (γ) is constant.

Simons and others (1961) have indicated that the bed with a dune configuration is softer than the bed with ripples; this difference suggests that the porosity is not constant, even for a given bed material. However, the porosity probably varies within rather narrow limits for natural river sand, and the introduction of a constant value should not introduce errors of appreciable magnitude.

According to Simons and Richardson (1962), dunes of the coarser material are more angular than are dunes of finer material. The influence of the difference in the shapes of the dunes is reflected in figure 2, where the relation of computed to measured bedload is some-

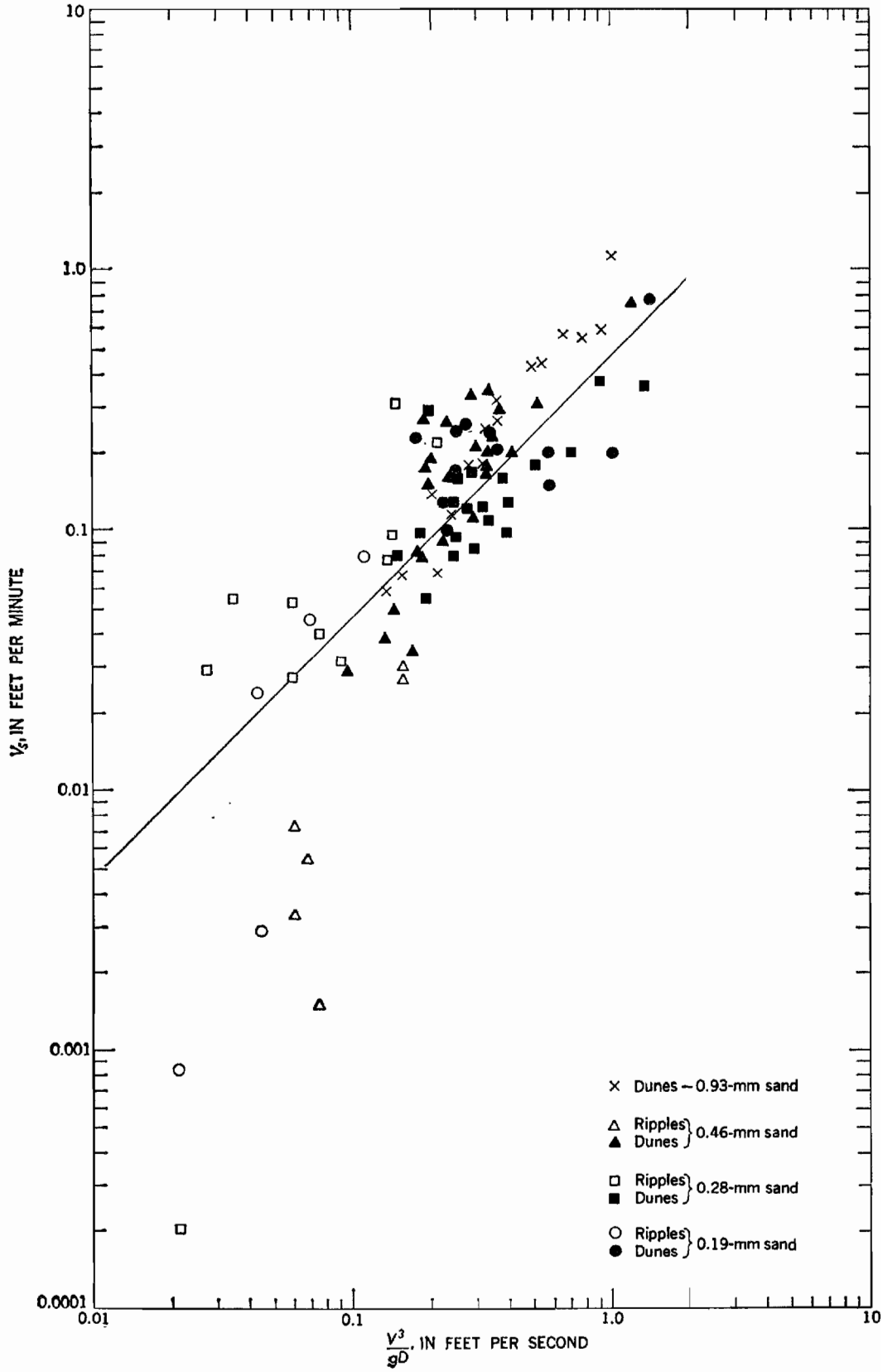

FIGURE 5.—Relation of V_s to $\frac{V^3}{gD}$.

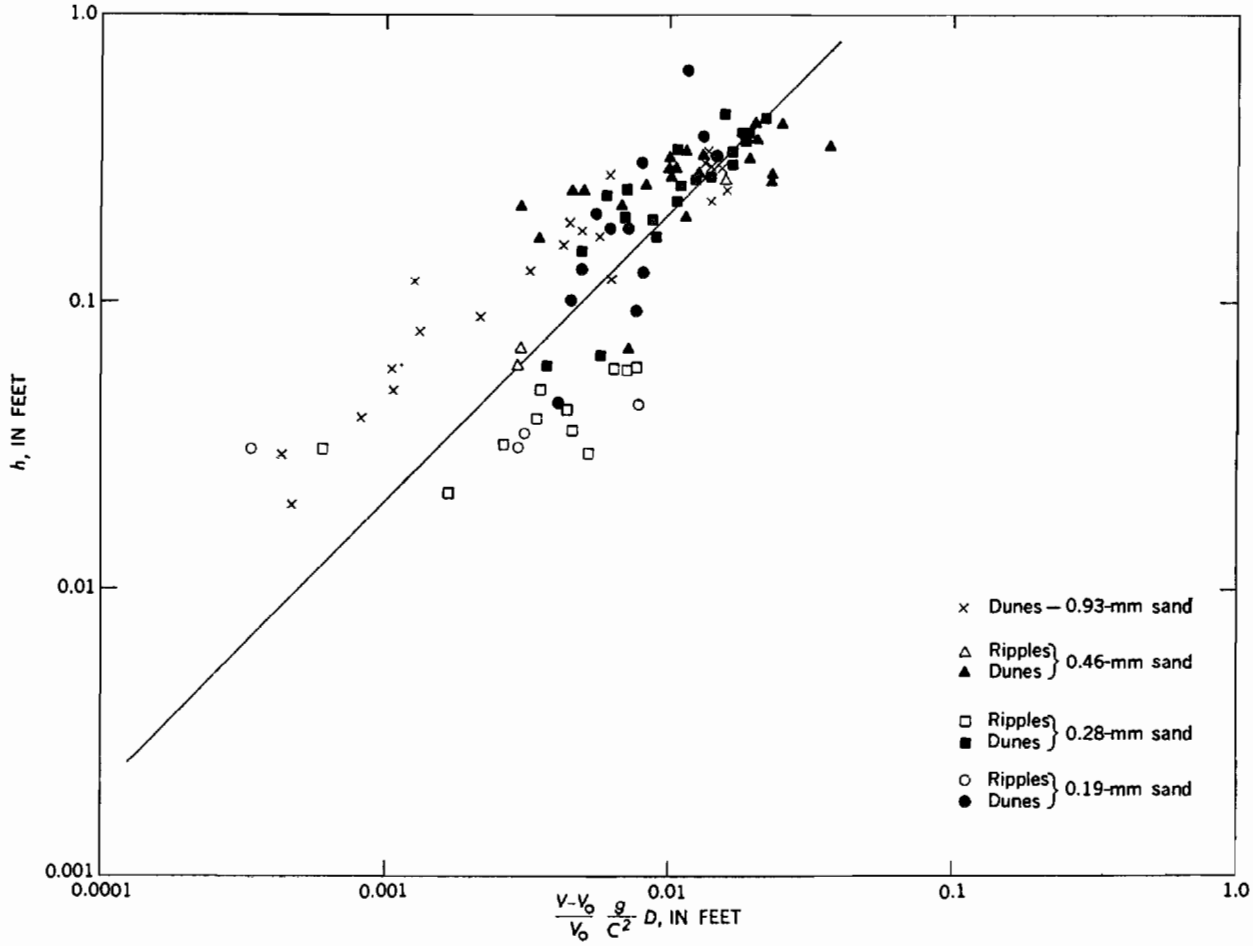

FIGURE 6.—Relation of h to $\frac{V-V_0}{V_0}\frac{g}{C^2}D$.

what better for the 0.93 mm sand than for the finer sizes of bed material.

Figures 2 and 3 show that the relation of computed to measured bedload is better for the dune formation than for ripples, probably because the dunes are more nearly two-dimensional. The equation does not give satisfactory results for bed configurations in a transition stage between dunes and a plane bed. The unsatisfactory results are due to changes in the shape of the dune, to three-dimensional flow and bed configurations, and to the fact that not all of the bedload is active in propagating dune movement. Where these conditions exist, estimates of bedload must be obtained by other methods, such as by sampling (Hubbell, 1964) or by computation. Unfortunately, neither current (1964) sampling techniques nor existing bedload equations yield satisfactory results.

CONCLUSIONS

Equation 8 should be useful in field applications when used in conjunction with a sonic depth sounder, which provides rapid and accurate determinations of bed configurations. Two proposed methods for estimating velocities of the bed forms from hydraulic characteristics were found to be inadequate. The analysis of flume data in this study gives some indications of the limitations of equation 8, and provides general guidelines for field applications. It is concluded that:

1. The equation is more suited for a dune-bed configuration than for ripples.
2. The equation will give more reliable results for coarse bed material than for fine material, because the dunes of coarse sand are more nearly triangular in shape than are the dunes of fine material.
3. The equation is applicable where average velocities and heights of the bed forms may be accurately determined and where the ripples or dunes cover the entire width of the channel. These conditions are probably met in straight, uniform channels of small width- to- depth ratios, where the flow is generally two-dimensional.

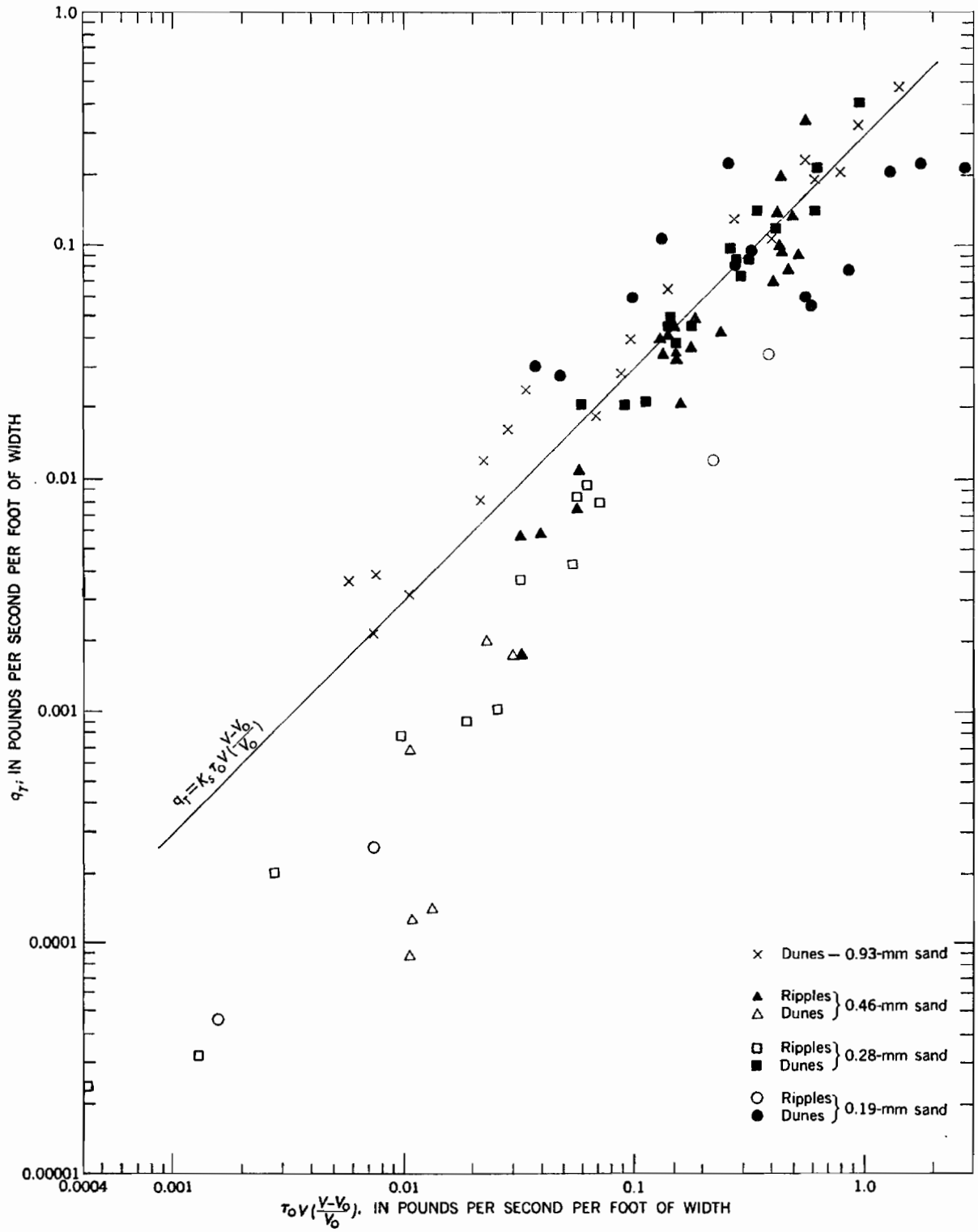

FIGURE 7.—Relation of q_T to $\tau_0 V\left(\frac{V-V_0}{V_0}\right)$.

4. Within the above limitations, the equation provides reasonably accurate values of bedload transport rates. For shallow flow over coarse material in dune formation, or for flow over fine sand in ripple formation, where suspension is negligible, equation 8 may be used to estimate total bed material transport.

REFERENCES CITED

Bagnold, R. A., 1960, Sediment discharge and stream power—a preliminary announcement: U.S. Geol. Survey Circ. 421, 23 p.

Barekyan, A., Sh., 1962, Discharge of channel forming sediments and elements of sand waves, *in* Soviet Hydrology: Selected Papers, Second Issue (Amer. Geophys. Union Russian Translations), p. 128–130.

Colby, B. R., 1964, Practical computations of bed-material discharge: Am. Soc. Civil Engineers Proc., v. 90, no. HY2, p. 217–246.

Cook, H. L., 1936, Outline of the energetics of stream-transportation of solids: Am. Geophys. Union Trans., pt. 21, p. 456–463.

Gilbert, G. K., 1914, Transportation of debris by running water: U.S. Geol. Survey Prof. Paper 86, 263 p.

Hubbell, D. W., 1964, Apparatus and techniques for measuring bedload: U.S. Geol. Survey Water-Supply Paper 1748, 74 p.

Kondratév, N. E., ed., 1959, River flow and river channel formation: Main Adm. Hydrometeorological Service Council of Ministers USSR (Selected chapters from Ruslovoi Protsess, translated by Y. Prushanoky) PST 471, U.S. Dept. Commerce, Office Tech. Services, 1962.

Karaki, S. S., Gray, E. E., and Collins, J., 1961, Dual channel stream monitor: Am. Soc. Civil Engineers Proc., v. 87, no. HY6, p. 1–16.

Richardson, E. V., Simons, D. B., and Posakony, G. J., 1961, Sonic depth sounder for laboratory and field use: U.S. Geol. Survey Circ. 450, 7 p.

Simons, D. B., and Richardson, E. V., 1961, Studies of flow in alluvial channels, basic data from flume experiments: Fort Collins, Colorado Univ. CER61EVR31.

——— 1962, Resistance to flow in alluvial channels: Am. Soc. Civil Engineers Trans., v. 127, pt. 1, p. 927–1006.

Simons, D. B., Richardson, E. V., and Albertson, M. L., 1961, Flume studies using medium sand (0.45 mm): U.S. Geol. Survey Water-Supply paper 1498–A.

Znamenskaya, H. S., 1962, Calculation of dimensions and speed of shifting channel formations, *in* Soviet Hydrology: Selected Papers, Second Issue (Amer. Geophys. Union Russian Translation), p. 111–116.

Summary of Alluvial Channel Data From Flume Experiments, 1956-61

By H. P. GUY, D. B. SIMONS, *and* E. V. RICHARDSON

SEDIMENT TRANSPORT IN ALLUVIAL CHANNELS

GEOLOGICAL SURVEY PROFESSIONAL PAPER 462-I

UNITED STATES GOVERNMENT PRINTING OFFICE, WASHINGTON:1966

UNITED STATES DEPARTMENT OF THE INTERIOR

STEWART L. UDALL, *Secretary*

GEOLOGICAL SURVEY

William T. Pecora, *Director*

Library of Congress catalog-care No. GS 66-219

For sale by the Superintendent of Documents, U.S. Government Printing Office
Washington, D.C. 20402 - Price 70 cents (paper cover)

CONTENTS

	Page
Glossary of terms	vi
Symbols	vii
English-metric conversion table	vii
Abstract	I 1
Introduction	1
Equipment and sands	2
Equipment	2
Sands	3
Operation procedure	3
Description of experimental variables and parameters	6
Water-surface slope	7
Depth of flow	7
Water discharge	7
Water temperature	8
Suspended-sediment concentration	8
Concentration of total-sediment discharge	8
Size gradation of sediment	8
Bed configuration	9
Mean velocity of flow	9
Velocity profile	9
Shear velocity	9
Bed-material discharge	9
Description of experimental variables and parameters—Continued	
Kinematic viscosity	I 10
Shear stress at bed	10
Reynolds number	10
Froude number	10
Resistance factors	10
Description of individual runs	10
Runs using 0.19-mm sand in 8-foot-wide flume	11
Runs using 0.27-mm sand in 8-foot-wide flume	21
Runs using 0.28-mm sand in 8-foot-wide flume	25
Runs using 0.45-mm sand in 8-foot-wide flume	31
Runs using 0.93-mm sand in 8-foot-wide flume	36
Runs using 0.32-mm sand in 2-foot-wide flume	44
Runs using 0.33-mm (uniform) sand in 2-foot-wide flume	47
Runs using 0.33-mm (graded) sand in 2-foot-wide flume	49
Runs using 0.47-mm sand in 8-foot-wide flume	52
Runs using 0.54-mm sand in 2-foot-wide flume	57
Basic data	61
References	96

ILLUSTRATIONS

		Page
FIGURE	1. Schematic diagram of 8-foot-wide flume	I 3
	2. Schematic diagram of 2-foot-wide flume	3
	3. Particle-size distribution curves for bed materials having median sizes of 0.19, 0.27, 0.28, 0.45, and 0.93 mm	4
	4. Particle-size distribution curves for bed materials having median sizes of 0.32, 0.33U, 0.33G, 0.47, and 0.54 mm	4
	5. Photographs of representative sand particles of bed materials used in the experiments	5
	6. Graph showing kinematic viscosity-temperature relation of aqueous dispersions of bentonite	10
	7–30. Photographs showing flow and bed conditions for runs using 0.19-mm sand:	
	7. Longitudinal upstream view of the flume bed showing ripples, run 2	11
	8. Transverse view of ripple formation at end of run 2	11
	9. Upstream view of ripples formed during run 25	12
	10. Transverse view of ripples formed during run 31	13
	11. Upstream view of ripple pattern on flume bed at end of run 23	13
	12. Upstream view of bed configuration at end of run 32	13
	13. Upstream view of ripple-dune pattern at end of run 8	14
	14. Downstream view of rippled-bed configuration through flow during run 3	14
	15. Upstream view of bed configuration at end of run 11	15
	16. Typical bed configuration at end of run 13	15
	17. Upstream view of bed configurations at end of run 14	15
	18. Upstream view of water surface during run 34	16
	19. Upstream view of water surface during run 12	16
	20. Bed configuration at end of run 12, viewed upstream	16
	21. Upstream view of ripples on low dunes characteristic of run 6	16
	22. Upstream view of water surface during run 6	17
	23. Upstream view of bed configuration at the end of run 7	17
	24. Upstream view of water surface showing standing waves during run 16	17

FIGURE 7–30. Photographs showing flow and bed conditions for runs using 0.19-mm sand—Continued — Page
25. Upstream view of water surface showing antidunes during run 18 — I 18
26. Side views of antidune flow during run 19 — 19
27. Upstream view of antidune wave pattern during run 21 — 19
28. Side view of breaking antidune during run 21 — 20
29. Upstream view of chute-and-pool flow conditions during run 36 — 20
30. Side views of chute-and-pool flow conditions during run 37 — 20
31–41. Photographs showing flow and bed conditions for runs using 0.27-mm sand:
31. Upstream view of ripples on the bed at the end of run 50 D — 21
32. Upstream view of ripples on the bed at the end of run 51 — 21
33. Upstream view of ripples on the bed at the end of run 52 — 22
34. Upstream view of the bed configuration at the end of run 53 — 22
35. Upstream view of bed configuration at the end of run 56 — 23
36. Upstream view of bed configuration at the end of run 55 — 23
37. Side view of the sliding face of a dune during run 43 — 23
38. Upstream view of water surface during run 58 — 24
39. Upstream view of bed configuration at the end of run 58 — 24
40. Downstream view of water-surface conditions during run 48 — 25
41. Downstream view of chute-and-pool flow during run 40 — 25
42–49. Photographs showing flow and bed conditions for runs using 0.28-mm sand:
42. Transverse view of rippled bed pattern at the end of run 9 — 26
43. Upstream view of rippled bed form at the end of run 4 — 26
44. Upstream view of the dune-bed configuration at the end of run 14 — 27
45. Upstream view of the dune-bed configuration at the end of run 20 — 27
46. Side view of avalanche face of a large dune formed during run 20 — 28
47. Upstream view of bed configuration at the end of run 34 — 29
48. Flow and bed conditions for run 25 — 30
49. Downstream view of antidune flow conditions during run 31 — 30
50. Sketch of chute-and-pool phenomenon — 31
51–58. Photographs showing flow and bed conditions for runs using 0.45-mm sand:
51. Transverse view of ripples formed during run 18 — 32
52. Upstream view of the dune-bed configuration at the end of run 21 — 33
53. Upstream view of the dune-bed configuration at the end of run 25 — 33
54. Upstream view of the dune-bed configuration formed during run 23 — 34
55. Flume conditions for run 27 — 35
56. Upstream views during and after run 36 — 35
57. Flow conditions during run 32 — 37
58. Upstream views of flow conditions for run 45 — 38
59–71. Photographs showing flow and bed conditions for runs using 0.93-mm sand:
59. Flume bed at end of run 14 — 39
60. Upstream view of plane bed at the end of run 32 — 39
61. Upstream view of dunes formed during run 16 — 39
62. Upstream view of the dune-bed condition at the end of run 35 — 40
63. Upstream view of low dunes on the flume bed at the end of run 33 — 40
64. Upstream view of the dune configuration at the end of run 10 — 40
65. Upstream view of dune-bed configuration formed during run 6 — 40
66. Upstream views of the flow conditions for run 11 — 41
67. Erosion of narrow dune trough during run 12 — 42
68. Upstream views of flow and bed conditions for run 13 — 42
69. Flow conditions for standing waves during run 2 — 43
70. Upstream views of flow conditions for run 4 — 43
71. Upstream views of flow conditions for runs 43 and 39 — 44
72–75. Photographs showing flow and bed conditions for runs using 0.32-mm sand:
72. Downstream view of dune-bed configuration formed during run 6 — 45
73. Side view of dunes and flow conditions during run 8 — 46
74. Side view of bed and flow during run 9 — 46
75. Side views of antidune flow conditions during run 15 — 47
76–79. Photographs showing flow and bed conditions for runs using 0.33-mm (uniform) sand:
76. Upstream view of rippled flume bed at the end of run 8 — 48
77. Flow and bed conditions for run 6 — 48
78. Side view of standing waves during run 2 — 49
79. Side view of breaking antidune during run 3 — 49

FIGURE 80–86. Photographs showing flow and bed conditions for runs using 0.33-mm (graded) sand: Page
80. Upstream view of ripples at the end of run 16 I 50
81. Upstream view of ripples formed during run 6 50
82. Upstream view of ripples formed during run 5 51
83. Upstream view of the dune-bed configuration at the end of run 1 51
84. Upstream view of the dune-bed configuration formed during run 9 51
85. Upstream view of the dune-bed configuration at the end of run 2 51
86. Upstream view of bed conditions at the end of run 12 52
87. Particle-size distribution of bentonite used in flume studies 52
88. Mineralogy of bentonite 53
89–100. Photographs showing flow and bed conditions for runs using 0.47-mm sand:
89. Side view of ripples and lenses of fine material during run 88 54
90. Upstream view of the bed configuration typical of runs 93, 92, and 91 54
91. Upstream views of water surface during runs 51 and 96 54
92. Upstream views contrasting dune shapes formed during runs 82 and 96 55
93. Upstream view of water surface during run 95 56
94. Upstream view of water surface during run 78 56
95. Upstream view of water surface during run 59 56
96. Upstream view of water surface during run 60 56
97. Upstream view of water surface typical of runs 64, 65, and 66 57
98. View of water surface typical of runs 81, 62, 67, and 79 57
99. Upstream views of standing waves and breaking antidunes during run 84 58
100. Downstream view of antidunes during run 98 58

TABLES

Page
TABLE 1. General information about the sands used in the experiments I 4
2–11. Experimental variables and parameters for:
2. 0.19-mm sand in 8-foot-wide flume 62
3. 0.27-mm sand in 8-foot-wide flume 64
4. 0.28-mm sand in 8-foot-wide flume 64
5. 0.45-mm sand in 8-foot-wide flume 66
6. 0.93-mm sand in 8-foot-wide flume 68
7. 0.32-mm sand in 2-foot-wide flume 70
8. 0.33-mm (uniform) sand in 2-foot-wide flume 72
9. 0.33-mm (graded) sand in 2-foot-wide flume 72
10. 0.47-mm sand in 8-foot-wide flume 74
11. 0.54-mm sand in 2-foot-wide flume 76
12–21. Velocity-profile data for:
12. 0.19-mm sand in 8-foot-wide flume 78
13. 0.27-mm sand in 8-foot-wide flume 80
14. 0.28-mm sand in 8-foot-wide flume 81
15. 0.45-mm sand in 8-foot-wide flume 83
16. 0.93-mm sand in 8-foot-wide flume 86
17. 0.32-mm sand in 2-foot-wide flume 89
18. 0.33-mm (uniform) sand in 2-foot-wide flume 90
19. 0.33-mm (graded) sand in 2-foot-wide flume 90
20. 0.47-mm sand in 8-foot-wide flume 91
21. 0.54-mm sand in 2-foot-wide flume 95

GLOSSARY OF TERMS

Alluvial channel. A channel whose bed is composed of noncohesive material that has been or can be transported by the flow.

Antidunes. Bed features that usually form in upstream-moving trains and are inphase with and strongly interact with gravity water-surface waves. The flow is in the upper flow regime; therefore, the water-surface waves have larger amplitudes than the antidunes. At higher Froude numbers, the surface waves usually grow until they become unstable and break in the upstream direction. The agitation accompanying breaking obliterates the antidunes, and the process of antidune initiation and growth is then repeated. At lower Froude numbers, the antidunes usually diminish in amplitude without the surface waves ever breaking.

Bar. A depositional feature whose length is of the same order as the channel width or greater, and whose maximum height is comparable to the mean depth of the generating flow. In longitudinal section, bars are approximately triangular, having very long gentle upstream slopes and short downstream slopes that are approximately the same as the angle of repose of the bed material. Alternate bars and point bars have transverse profiles that are triangular and taper from the bank to a point in the channel.

Bed material. The material of which a streambed is composed.

Clay. Sediment finer than 0.004 mm (millimeter), regardless of mineralogical composition.

Chute-and-pool flow. A flow condition that occurs where slopes are relatively steep and water-sediment discharges are relatively great, the channel consists of a series of pools, in which the flow is subcritical, connected by steep chutes, in which the flow is supercritical. A hydraulic jump forms at the downstream end of each chute, where the chute enters a pool. The chutes and pools may move slowly upstream.

Dunes. Bed features smaller than bars but larger than ripples that are out of phase with any water-surface gravity waves that accompany them. Dunes generally form at larger flow and sediment-transport rates than do ripples, but at smaller flow and transport rates than do antidunes; however, ripples often form on the upstream slopes of dunes at smaller rates of flow. In longitudinal profile, dunes are approximately triangular, having fairly gentle upstream slopes and downstream slopes that are approximately equal to the angle of repose of the bed material.

Fall diameter or standard fall diameter. The diameter of a sphere that has a specific gravity of 2.65 and the same terminal uniform settling velocity as the particle (any specific gravity) when each is allowed to settle alone in quiescent distilled water of infinite extent and at a temperature of 24°C.

Fine sediment. That part of the sediment discharge that consists of sediment so fine that it is about uniformly distributed in the vertical and is only an inappreciable fraction of the sediment on the streambed (referred to by some writers as wash load). Its upper size limit at a particular time and cross section is a function of the characteristics of the flow as well as of the characteristics of the sediment particles.

Flow regime. A range of flow conditions having somewhat similar resistance and sediment transport characteristics that produce similar bed forms.

Lower flow regime. Flow in sand channels which result in bed forms of ripples, ripples on dunes, and dunes.

Median diameter. Midpoint in the size distribution of a sediment, at which half the particles by weight are larger and half are smaller.

Plane bed. A bed form that has no irregularities larger in amplitude than a few grain diameters of the bed material. The plane bed in a sand channel that has movement of bed material occurs in the upper flow regime.

Ripples. Small triangular-shaped bed forms that have wave lengths of less than about 2 feet and heights of less than about 0.2 foot.

Sand. Sediment particles between 0.062 and 2.0 mm in diameter.

Sand waves. Crests and troughs (such as ripples, dunes, or symmetrical undulations) formed on the bed of an alluvial channel by the movement of the bed material.

Sediment. Fragmental material that originates from the disintegration of rocks and is transported by, suspended in, or deposited by water or air, or is accumulated in beds by other natural agencies.

Sediment concentration. The ratio of the dry weight of the sediment to the total weight of the water-sediment mixture, expressed in parts per million.

Sediment discharge. The amount of sediment that is moved by water past a section in a given length of time.

Silt. Sediment particles between 0.004 and 0.062 mm in diameter.

Suspended sediment. Sediment suspended in the flow by turbulent currents and (or) by colloidal suspension.

Standing waves. Virtually stationary waves that generally develop as a train. They are sometimes called nonbreaking antidunes.

Transition. A category for flows that mold bed forms ranging from those typical of the lower flow regime to those typical of the upper flow regime.

Upper flow regime. Flow in sand channels which results in bed forms of plane bed (with sediment movement), standing waves, and antidunes.

Velocity profile. Horizontal components of flow velocity in relation to depth at a vertical section over a point on the bed.

SYMBOLS

A	Area of flow cross section.	sq ft
B	Slope of semilogarithmic plot of velocity versus depth, above the bed.	fps per log unit
C	Velocity at a depth of 1.0 foot above bed.	fps
$C/\sqrt{g}$	Chezy coefficient of discharge; equal to V/V_*.	
C_f	Concentration of fine-sediment discharge.	ppm
C_s	Concentration of suspended-sediment discharge.	ppm
C_t	Concentration of bed material discharge.	ppm
D	Average depth of flow.	ft
d	Particle size in terms of fall diameter.	mm or ft
d_{16}	Particle size for which 16 percent of the sediment by weight is finer.	mm or ft
d_{50}	Median particle size of the sediment.	mm or ft
d_{84}	Particle size for which 84 percent of the sediment by weight is finer.	mm or ft
f	Darcy-Weisbach resistance coefficient; equal to $\frac{8gDS}{V^2}$.	
F	Froude number; equal to $\frac{V}{\sqrt{gD}}$.	
g	Acceleration of gravity (32.2 ft per sec per sec).	ft per sec per sec
n	Manning's resistance coefficient.	$ft^{1/6}$
Q	Discharge of water-sediment mixture.	Cu ft per sec
q_s	Discharge of suspended sediment.	lb per sec per ft
q_t	Discharge of bed material.	lb per sec per ft
R	Hydraulic radius.	ft
R	Reynolds number; equal to $\frac{VD}{\nu}$.	
S	Water-surface slope.	
T	Temperature.	°C
V	Average velocity based on continuity principal.	fps
V_*	Shear velocity; equal to $\sqrt{gDS}$ or $\sqrt{\tau_0/\rho}$.	fps
W	Width of flume.	ft
γ	Specific weight of water or water-sediment mixture.	lb per cu ft
μ	Dynamic viscosity.	lb-sec per sq ft
ν	Kinematic viscosity.	sq ft per sec
ρ	Mass density of water.	slug per cu ft
σ	A measure of sediment particle size gradation; equal to $\frac{1}{2}\left[\frac{d_{50}}{d_{16}}+\frac{d_{84}}{d_{50}}\right]$.	
τ	Shear stress or tractive force on bed; equal to γDS.	lb per sq ft
ω	Fall velocity of a particle.	ft per sec

ENGLISH-METRIC CONVERSION TABLE

Principal items	*English unit*	*Factor*	*Metric unit*
Depth of flow; Length and width of flume; Particle size; Hydraulic radius	ft	0.3048	m
		30.48	cm
		304.8	mm
Area of cross section	sq ft	929.0	sq cm
		.09290	sq m
Velocity of flow; Fall velocity of particles	ft per sec	0.3048	m per sec
		30.48	cm per sec
Velocity of bed configuration	ft per min	0.005080	m per sec
		.5080	cm per sec
		.01829	km per hr
Water discharge	cu ft per sec (cfs)	0.02832	cu m per sec
		2.832×10^4	cu cm per sec
Sediment discharge	lb per sec per ft	1.488	kg per sec per m
Acceleration of gravity	ft per sec per sec	0.3048	m per sec per sec
		30.48	cm per sec per sec
Shear stress	lb per sq ft	478.8	dynes per sq cm
		0.4882	g per sq cm
		4.882	kgm per sq m
Kinematic viscosity	sq ft per sec	929.0	sq cm per sec (Stokes)
Dynamic viscosity	lb sec per sq ft	0.04788	g per cm-sec (Poise)
		.4482	g-sec per sq cm
Specific weight	lb per cu ft	0.01602	g per cu cm
Mass density	slug per cu ft	0.5154	g per cu cm

SEDIMENT TRANSPORT IN ALLUVIAL CHANNELS

SUMMARY OF ALLUVIAL CHANNEL DATA FROM FLUME EXPERIMENTS, 1956–61

By H. P. Guy, D. B. Simons and E. V. Richardson

ABSTRACT

The primary purpose of this report is to summarize and make available to other investigators the results of the hydraulic and sediment data collected by D. B. Simons and E. V. Richardson in a unique series of experiments at Colorado State University between 1956 and 1961. The 339 equilibrium runs were made in 2- and 8-foot-wide recirculating flumes for 10 sets of conditions to determine the effects of size of the bed material, temperature of the flow, and fine sediment in the flow on the hydraulic and transport variables. The investigations for each set cover flow phenomena ranging from a plane bed and no sediment movement to violent antidunes.

INTRODUCTION

As a part of the research program of the Water Resources Division of the U.S. Geological Survey, a project was organized in September 1956 to study the mechanics of water and sediment movement in alluvial channels. Answers to questions on resistance to flow and sediment transport rates were sought at this time. The solutions to resistance and transport problems are complicated by the multitude of variables and parameters involved and by the complex interdependence of the variables.

The objective of the experiments was to obtain mean values of the resistance and transport variables and parameters for a large range of conditions most commonly found in natural streams and artificial channels. The large quantity of data required for a general solution to the problem was considered best obtained by use of recirculating flumes which *tend to simulate* conditions of uniform flow and sediment transport in an infinitely long channel. The recirculating-flume data are indirectly comparable to those for most streams where the water discharge, the imposed sediment discharge, and water temperature change considerably during the period of storm runoff. Such recirculating flume data are very comparable to data for regulated streams and canals fed by ground water or man-made storage facilities and to data for streams in which the water discharge changes slowly.

This report is a compilation of the data for 10 sets of conditions, or for a total of 339 equilibrium runs in recirculating flumes. The investigations for each set covered flow phenomena ranging from a plane bed and no movement of sediment to the antidunes first described by Gilbert (1914). The general procedure of recirculating the water-sediment mixture aided in obtaining the equilibrium conditions, because the roughness elements which resisted the flow were formed by the flow and the respective sediment-movement characteristics. In the experiments used for this compilation, the form of the bed was changed from plane without sediment movement, to ripples, to dunes, to transitional, to plane with sediment movement, and to antidunes by altering flow conditions. For a set of runs with a specific sand and flume, discharge and slope were the principal controllable variants for altering flow conditions. Depth, velocity, fluid resistance, sediment discharge, and, to some extent, slope changed with time until equilibrium was reached.

The scheme of presentation in the report is to:

1. Describe the equipment and sands.
2. Describe the procedure of operation.
3. Describe the data obtained.
4. Describe the characteristics of the individual runs.
5. Tabulate the mean values of the basic data for each run.
6. Tabulate the velocity-profile data for the runs having such data.

The project was under the general supervision of L. B. Leopold, Chief Hydrologist, Water Resources Division, with technical guidance from P. C. Benedict, R. W. Carter, and others from the Geological Survey.

The principal investigators were D. B. Simons, project chief, and E. V. Richardson. Technical guidance was also received from faculty members, especially from M. L. Albertson, at Colorado State University, where the project was located. The principal investigators were assisted in various phases of the work by W. L. Haushild, D. W. Hubbell, and R. K. Fahnestock, of the Geological Survey, and by H. J. Morel-Seytoux, R. J. Garde, A. A. Bishop, K. Al-Shaikh Ali, Niwat Daranandana, and H. C. Hilbrand, graduate students in Civil Engineering. The report was compiled after careful review of the original notes assembled during the laboratory work.

The data contained in this report have been used in several U.S. Geological Survey reports, professional societies' publications, and graduate student theses. A partial list of these papers, exclusive of those given as references, follows:

Bishop, A. A., 1961, Sediment transport in alluvial channels, a critical examination of Einstein's theory: Fort Collins, Colo., Colorado State Univ., Dept. Civil Eng., Ph.D. dissertation.

Chang, F. M., 1962, An investigation of total sediment discharge in alluvial channels: Fort Collins, Colo., Colorado State Univ., Dept. Civil Eng., Ph. D. dissertation.

Chang, F. M., Simons, D. B., and Richardson, E. V., 1965, Total bed-material discharge in alluvial channels: U.S. Geol. Survey Water-Supply Paper 1498–I, 23 p.

Daranandana, N., 1962, A preliminary study of the effect of graduation of bed material on flow phenomena in alluvial channels: Fort Collins, Colo., Colorado State Univ., Dept. Civil Eng., Ph. D. dissertation.

Garde, R. J., 1959, Total sediment transport in alluvial channels: Fort Collins, Colo., Colorado State Univ., Dept. Civil Eng., Ph. D. dissertation.

Haushild, W. L., 1960, The effect of fine sediment on the mechanics of flow in alluvial channels: Fort Collins, Colo., Colorado State Univ., Dept. Civil Eng., M.S. thesis.

Haushild, W. L., Simons, D. B., and Richardson, E. V., 1961, The significance of the fall velocity and effective fall diameter of bed materials: U.S. Geol. Survey Prof. Paper 424–D, p. 17–20.

Hubbell, D. W., and Ali, Al-Shaikh, K., 1961, Qualitative effects of temperature on flow phenomena in alluvial channels: U.S. Geol. Survey Prof. Paper 424–D, p. 21–23.

Richardson, E. V., 1960, Sediment transport in alluvial channels (examination of Bagnold's 1956 hypothesis): Fort Collins, Colo., Colorado State Univ., Dept. Civil Eng., M. S. thesis.

——— 1965, Resistance to flow in sand channels: Fort Collins, Colo., Colorado State Univ., Dept. Civil Eng., Ph. D. dissertation.

Richardson, E. V., Simons, D. B., and Haushild, W. L., 1962, Boundary form and resistance to flow in alluvial channels: Belgium, Internat. Assoc. Sci. Hydrology Bull., 5 p.

Simons, D. B., and Richardson, E. V., 1960, Resistance to flow in alluvial channels: Am. Soc. Civil Engineers Proc., v. 86, no. HY5, 27 p. Also published with closure in ASCE Trans., v. 127, pt. 1, no. 3360, 1962, p. 927–1006.

Simons, D. B., and Richardson, E. V., 1961, Forms of bed roughness in alluvial channels: Am. Soc. Civil Engineers Proc., v. 87, no. HY3, 19 p. Also published with closure in ASCE Trans., v. 128, pt. 1, no. 3414, 1963, p. 284–323.

——— 1963, A study of variables affecting flow characteristics in alluvial channels: Federal Inter-Agency Sed. Conf., 2d, Proc., ARS, Misc. Pub. 970, p. 193–207.

——— 1966, Resistance to flow in alluvial channels: U.S. Geol. Survey Prof. Paper 422–J (in press).

Simons, D. B., Richardson, E. V., and Haushild, W. L., 1961, Variable depth-discharge relations in alluvial channels: U.S. Geol. Survey Prof. Paper 424–C, p. C45–C47.

——— 1962, Depth-discharge relations in alluvial channels: Am. Soc. Civil Engineers Proc., v. 88, no. HY5, 16 p.

Simons, D. B., Richardson, E. V., and Nordin, C. F., Jr., 1965, Sedimentary structures generated by flow in alluvial channels—a symposium: Soc. Econ. Paleontologists and Mineralogists Spec. Pub. 12, p. 34–52.

——— 1965, Bed load equation for ripples and dunes: U.S. Geol. Survey Prof. Paper 462–H, 9 p.

EQUIPMENT AND SANDS

The flumes and related equipment used are in the hydraulic laboratory adjacent to the Engineering building on the main campus at Colorado State University. The bed materials were selected from natural river sands found within a few hundred miles of Fort Collins.

EQUIPMENT

Most of the data were collected in a recirculating flume 8 feet wide, 2 feet deep, and 150 feet long. The flow could be varied from 0 to 22 cfs (cubic feet per second) by use of two pumps and a valve control on the discharge lines. The slope of the plywood channel could be adjusted from 0 to 1.5 percent by screw jacks. A schematic diagram of this flume is shown in figure 1.

Many data relative to the effect of temperature and fine sediment on resistance to flow and sediment transport were collected in a recirculating flume 2 feet wide, 2½ feet deep, and 60 feet long that has ½-inch clear-plastic sidewalls and a ¼-inch stainless-steel plate floor. The flow could be adjusted from 0 to 8 cfs, and the slope, from horizontal to 10 percent. A schematic diagram of this flume is shown in figure 2.

Each flume has specific entrance conditions, wall roughness, and flow characteristics which may affect the flow and transport variables. A given run, therefore, cannot be reproduced exactly in another flume. These recirculating flumes with constant-head tailboxes most nearly duplicate flow conditions in alluvial channels, except for highly variable flow of sediment from tributaries.

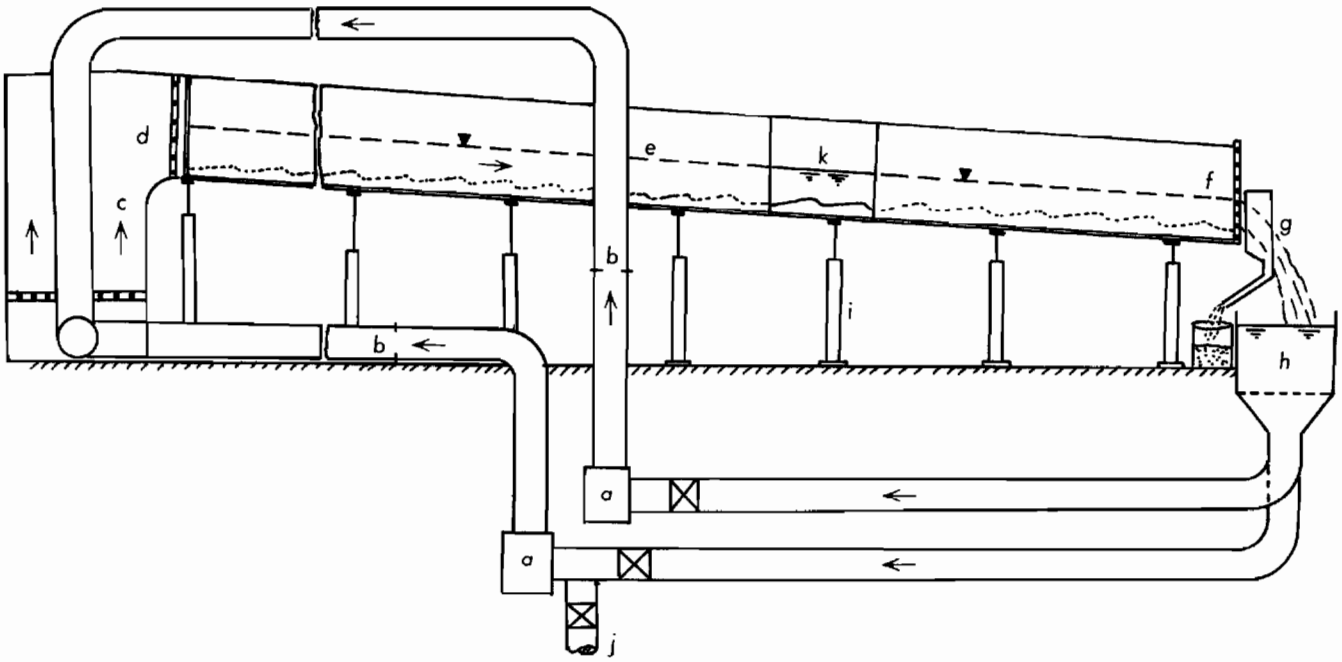

FIGURE 1.—The 8-foot-wide flume. After Simons, Richardson, and Albertson (1961, p. 21). *a*, pumping units; *b*, orifices; *c*, headbox and diffuser; *d*, baffles and screens *e*, flume (8×2×150 ft); *f*, tailgate; *g*, total-load sampler; *h*, tailbox; *i*, jacks supporting flume; *j*, connection to storage sump; *k*, transparent viewing window.

SANDS

The sands used for the 10 sets of experiments were obtained from 5 sources: a deposit of decomposed sandstone near Denver, Colo.; the Elkhorn River near Waterloo, Nebr.; the Cache la Poudre River at Fort Collins, Colo.; the North Platte River near Scottsbluff, Nebr.; and the Black Hills Silica Sand Corp., Hill City, S. Dak. These national sands were modified by sieving or washing away components of different sizes for some of the experimental sets.

The sands used as bed material in the experiments are identified by their median fall diameter. Table 1 lists each sand, where it was obtained, the kind of processing used, and the general character of the experiments. A particle-size distribution curve (size in millimeter versus percent finer than indicated size) is given in figures 3 and 4 for each sand. Figure 5 is a composite of photographs of each sand to show roundness, gradation, and relative size.

OPERATION PROCEDURE

The general operation procedure was the same for both flumes and for the various sand sizes. In a natural stream, depth is dependent on discharge, slope, bed roughness, and shape of channel. In a flume, only discharge and shape of channel can be controlled precisely, and slope only approximately. Slope and

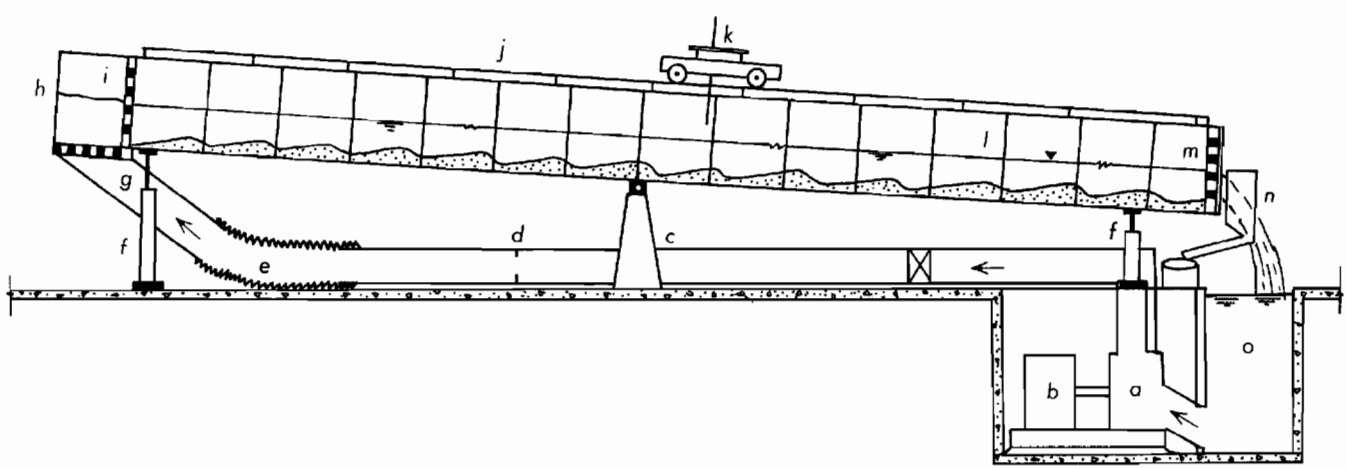

FIGURE 2.—The 2-foot-wide flume. After Simons, Richardson, and Haushild (1963, p. 3). *a*. pumping unit; *b*, motor; *c*, center support; *d*, orifice; *e*, flexible connection *f*, jacks; *g*, manifold diffuser; *h*, headbox; *i*, baffles and screens; *j*, rails; *k*, instrument carriage; *l*, flume (2×2.5×60 ft); *m*, tailgate; *n*, total-load sampler; *o*, tailbox.

TABLE 1.—*General information about the sands used in the experiments*

Median size (mm)	Gradation σ	Source of sample	Method of obtaining and processing sand	Type of study	Width of flume used (ft)
0.19	1.30	Decomposed sandstone near Denver, Colo.	The sandstone was run through a hammermill to break up the large chunks and then washed to remove the clay binder.	General	8
.27	1.56	Elkhorn River near Waterlou, Nebr.	0.28-mm sand wet screened to remove material coarser than 2.0-mm	do	8
.28	1.67	do	Sand scooped from middle of flowing river by dragline. No processing.	do	8
.45	1.60	Cache la Poudre River at Fort Collins, Colo.	Washed, passed a No. 8 sieve and retained on a No. 200 sieve	do	8
.93	1.54	North Platte River near Scottsbluff, Nebr.	Washed, passed a No. 4 sieve and retained on a No. 16 sieve	do	8
.32	1.57	Elkhorn River near Waterloo, Nebr.	From 0.27-mm sand. Coarser sand retained as fines were washed away in overflow.	Effect of viscosity by varying temp.	2
.33U	1.25	Black Hills Silica Sand Corporation, S. Dak.	Passed a No. 40 sieve and retained on a No. 60 sieve	Effect of gradation	2
.33G	2.07	do	6 sand sizes mixed to obtain a wide size-gradation range	do	2
.47	1.54	Cache la Poudre River at Fort Collins, Colo.	From 0.45-mm sand. Coarser sand retained as fines were washed away in overflow.	Effect of viscosity by varying concentration of fine sediment.	8
.54	1.52	do	From 0.45-mm sand. Coarser retained as fines were washed away in overflow.	do	2

depth reach equilibrium in accordance with the bed roughness for specific flow conditions.

The procedure followed for some runs involved recirculating a given discharge of water-sediment mixture in the flume at a preselected slope until equilibrium conditions were established. Equilibrium here should be defined as a condition of statistically uniform velocity, concentration, and slope with respect to both time and space in the flume where the variables are observed. Even though discharge can be held relatively constant, depth, slope, and sediment discharge in the final equilibrium condition (several hours or days after the start of the run) could be consider-

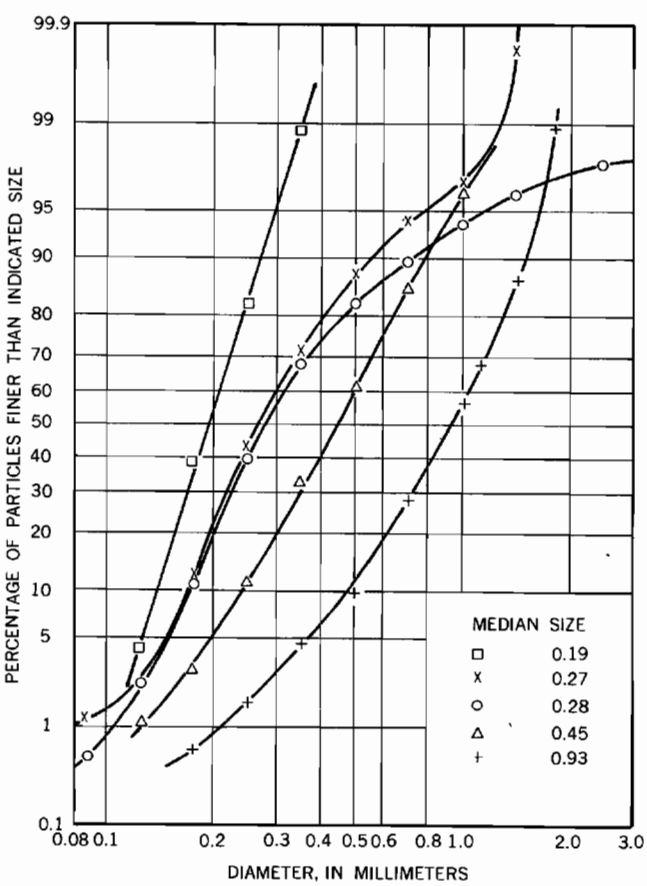

FIGURE 3.—Particle-size distribution curves for bed materials having median sizes of 0.19, 0.27, 0.28, 0.45, and 0.93 mm.

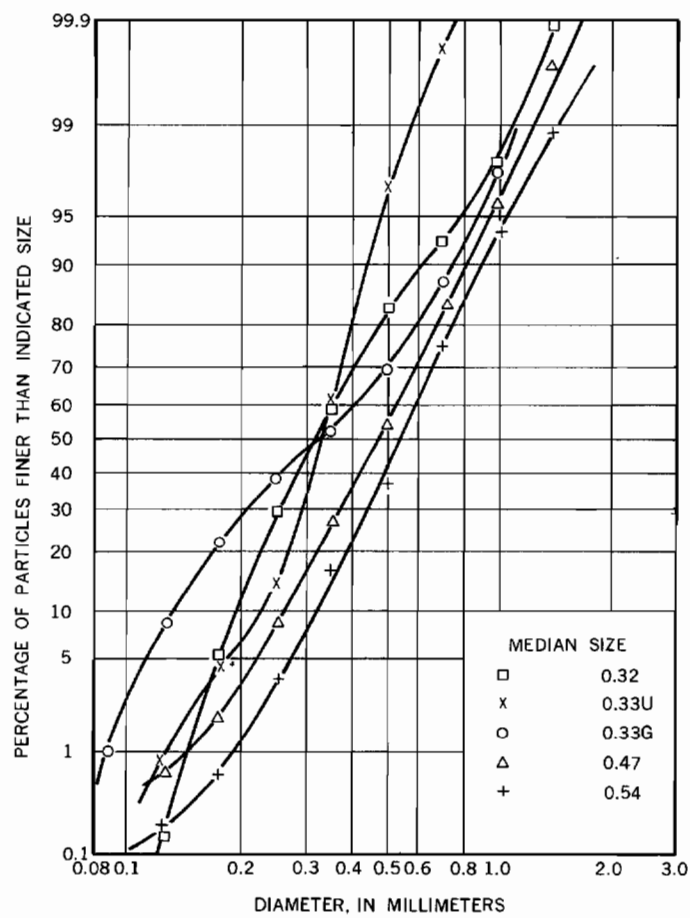

FIGURE 4.—Particle-size distribution curves for bed materials having median sizes of 0.32, 0.33U, 0.33G, 0.47 and 0.54 mm.

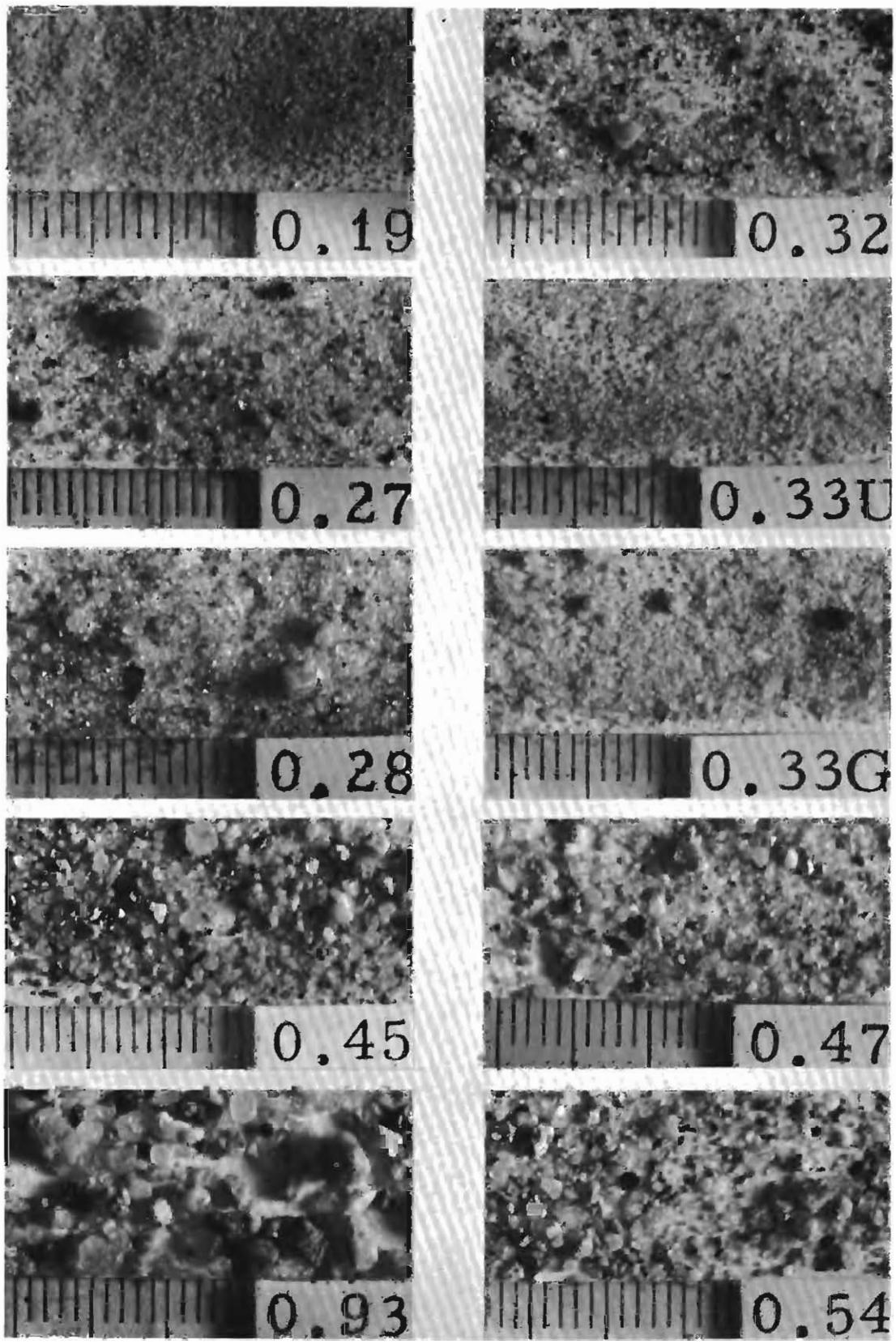

FIGURE 5.—Representative sand particles of bed materials used for the 10 sets of experiments. The number in the lower right corner of each photograph is the median diameter of the sand, in millimeters. The scale also is in millimeters. See table 1 for further description of each sand.

ably different from those in the initial condition. For some runs depth was kept constant either by adjusting the tailgate slope or discharge. For some other runs slope was kept constant either by adjusting the tailgate or the discharge, or both.

For runs having a relatively high rate of sediment discharge and requiring a short time to reach equilibrium (slopes greater than 0.006 ft per ft), the slope was preset by adjusting the tailgate and allowing the bed to adjust itself by scour and fill. For runs with Froude numbers greater than 1, the tailgate was often completely removed. For runs having a low rate of transport (slopes less than 0.006 foot per foot), the desired preset slope was established by planing or screeding the bed and then adjusting the tailgate to make the slope of the water surface parallel to the bed.

The nonequilibrium flow caused by change of bed roughness was eliminated by continuing the run until the average bed slope and the average slope of the water surface became parallel by natural adjustment of the sand bed. Equilibrium flow was considered as established, and collection of the data started, when (1) the bed configuration was consistent in the full length of the flume, excluding the sections influenced by entrance or exit conditions, and (2) the average water- and bed-surface slopes remained constant and parallel with respect to time. The time required to establish equilibrium conditions varied with the slope and the discharge. Some runs on flat slopes required 3 or 4 days to achieve equilibrium, whereas runs on steeper slopes established equilibrium within 2 or 3 hours. In each run, the flume was operated continuously until equilibrium had been reached and the necessary data collected. To insure the achievement of equilibrium conditions, most runs were continued longer than the required time as indicated by observations of variables likely to change prior to equilibrium.

The general procedure was different for the 0.47-, 0.54- and 0.32-mm sands. After equilibrium had been established and the data collected for a given run, the run was continued and, for the 0.47- and 0.54-mm sands, bentonite was either added or extracted from the flow, or, for the 0.32-mm sand, the temperature was changed. The new run was then continued until equilibrium was again established, and the necessary data collected. This procedure of adding or extracting bentonite or changing the temperature without stopping the flow was continued for a series of runs.

DESCRIPTION OF EXPERIMENTAL VARIABLES AND PARAMETERS

Following the operating procedure discussed led to the establishment of equilibrium conditions for a given run. Two or more measurements of slope made some time apart were required prior to the data-collection phase to insure that equilibrium had been established. In this investigation, slope observations were not started until visual inspection showed that a relatively systematic bed configuration and, consequently, a uniform resistance to flow had been established the full length of the test section.

When the rough movable boundary occurred in the flume, flow and transport values varied considerably during a given run. As a result, representative average values for all the basic variables had to be obtained by making successive observations during a relatively long period of time. The frequency and the time period over which the observations were made depended mainly on the bed form. For example, a few slope observations over a short time were sufficient to give a reliable average for the rippled condition; but many observations over a long time were required for the dune condition.

The following kinds of data were collected and are reported in tables 2–11 ("Basic Data" section):

1. Water surface slope.
2. Depth of flow.
3. Water discharge.
4. Water temperature.
5. Suspended-sediment concentration.
6. Concentration of total bed-material discharge.
7. Size graduation of sediment.
8. Bed configuration.

Several of these measured variables can be used to compute other variables and parameters useful for evaluating flow and transport characteristics in the flume channel. These variables include:

1. Mean velocity.
2. Velocity profile.
3. Shear velocity.
4. Sediment discharge.
5. Kinematic viscosity.
6. Shear at bed.
7. Reynolds number.
8. Froude number.
9. Resistance factors.

The inherent errors of each computation are proportional to the errors in the observation data. More specifically, the composite error (ΔX) of the computed variable or parameter will be

$$\Delta X = \frac{m_1 X_1 \pm m_2 X_2 \pm \ldots + m_n X_n}{\sqrt{n}},$$

where X_1 to X_n is the error of specific observation data, m_1 to m_n is the exponent of the respective X's, and n is the number of X's.

WATER-SURFACE SLOPE

The water-surface slope (col. 2, tables 2–11) was determined by observing the water-surface elevation with a level and a mechanical point gage, and also with a differential bubbler gage (Barron, 1963). The slopes computed using data from both methods were in close agreement.

The mechanical point-gage method consisted of reading the level of the water surface every 5 feet along the centerline of the flume. The point gage was mounted on a four-wheeled carriage that traveled on rails mounted on the walls of the flume. Levels were run on the gage at all locations for which water-surface readings were required. Three to eight sets of water-surface readings were made for each run after equilibrium was reached and during the period of data collection. The elevations for each point along the centerline may be plotted separately or averaged to obtain a mean slope. The average for each of the points was used to compute a least-squares regression for the runs with the 0.45-mm sand. The slope was determined graphically for the runs using the other sands. A study of the two methods indicated that both were sufficiently precise to yield slope values with no more error than is inherent in other variables.

Slope measurements taken after attainment of equilibrium conditions were used to determine the average slope. Also, water-surface elevations reflecting nonuniform flow at the entrance and exit of the flume were discarded.

The bubbler gage continuously recorded the difference in elevation of the water surface to within 0.001 foot between two points, and from this difference the water-surface slope was computed. The bubbler-gage connections to the 8-foot-wide flume were 100 feet apart. The continuous record of slope, as computed from the bubbler-gage headings, was used to determine when equilibrium conditions were established. The bubbler gage was not used in the 2-foot-wide flume or in the 8-foot-wide flume for the 0.45-mm sand.

Any error in the mean-slope value reported for each run can be attributed to two major sources: (1) the plus or minus 0.001 foot accuracy for the bubbler gage or the individual point-gage readings, and (2) the variation about the mean for a series of readings for the bubbler gage or the point gage. If the error for the bubbler gage is 0.001 foot in 100 feet, the absolute error for the gage is $\frac{10^{-5}}{S}$. For the finer sands, this alone would be 5–10 percent for slopes where sediment particles move occasionally. A 0.001-foot error in the point-gage reading is much less significant when plotted with several other readings. The variation about the mean for bubbler-gage readings is caused mostly by the effect of the bed forms moving near the orifices to the bubbler gage in the flume. Variation in the point-gage readings at a specific location is also due to the movement or shape of bed forms near the point-gage readings. This variation may cause errors of as much as 15–20 percent, depending on the size of the bed forms, the relative slope, and the number of observations.

DEPTH OF FLOW

The average depth of flow (col. 3, tables 2–11) was determined by observing the difference in elevation between the water surface and the sand bed with a point gage. Observations were made at preselected intervals down the length of the flumes. The selection of the interval depended upon the bed configuration that existed for the run, the intervals being closer spaced for a dune-bed configuration than for an antidune or a ripple-bed configuration. Only those depths observed in the part of the flume having uniform slope were used to establish the average depth. Because of the rapid changes in water-surface elevation at a point and the softness of the bed, especially for runs in the lower flow regime, many depth observations were required to obtain a reasonably accurate average value.

This method of observing depth was used for all the sands except the 0.45-mm size. Observations of depth for the 0.45-mm sand were made by determining the elevation of a screeded 30-to-40-foot central section of the sand bed and determining the average elevation of the water surface at times when the surface was relatively smooth. The two methods of observing depths yielded virtually the same results. The observations of average depth are considered accurate to plus or minus 0.03 foot. At a depth of 0.60 foot, the observation is therefore accurate to plus or minus 5 percent.

WATER DISCHARGE

Water discharge (col. 4, tables 2–11) was determined in the return-flow lines with calibrated orifice meters connected to water-air manometers. The orifice meters were located in the lines to avoid the possible effect of sand deposits on the calibration. They were checked periodically to determine if any change had occurred in the calibration from abrasion by the sand. The individual observations are considered accurate to plus or minus 2 percent. The mean discharge for each run is determined from the average of 5–15 readings made during the period of data collection.

"Water discharge" actually means the discharge of the water-sediment mixture. For example, a concen-

tration of 50,000 ppm (parts per million) of sediment means that 5 percent of the water-sediment mixture is sediment by weight, or nearly 2 percent of the mixture is sediment by volume. The orifice meters were calibrated in clear water. However, a study by Nobuhiro Yotsukura (written commun., 1961) proved that the use of clear water to calibrate the meters would not produce any appreciable error in the sediment concentrations used in the course of this study.

WATER TEMPERATURE

The water temperature (col. 5, tables 2–11) was measured to the nearest half of a degree centigrade with a mercury thermometer. The temperature reported for each run was based on an average of 5–10 readings obtained during the data-collection phase of each run. The average temperature recorded for each run should be correct to plus or minus 3 percent.

SUSPENDED-SEDIMENT CONCENTRATION

Suspended-sediment concentration is defined as the ratio of the weight of solids to the weight of the water-sediment mixture. Suspended sediment (Col. 6, tables 2–9, and col. 7, tables 10, 11) was sampled 95–100 feet downstream from the headbox of the 8-foot-wide flume and 35 feet downstream from the headbox of the 2-foot-wide flume with a specially designed depth-integrating sampler. The sampler consisted of a brass nozzle 3 inches long and ¼ inch in diameter attached to a "wading rod." The nozzle was connected to a flexible tube. A water-sediment sample was drawn through the tube to a container by means of a vacuum pump which was adjusted to draw in the fluid at a velocity approximately equal to the velocity of the flow. With this equipment, 5- to 8-pound samples of water-sediment mixture were collected from two to four times during each run by a mechanical integration of the flow in the cross section. The integration was attained by traversing the sampler through equally spaced verticals at an equal transit rate for each vertical.

Some suspended-sediment concentrations were found to be larger than corresponding concentrations of bed-material discharge. This difference was due, in part, to the inadequate number of suspended-sediment samples, and to the possibility that samples were taken in a region of flow where local shear stress and turbulence were much greater than average. The standard deviation given in column 7, tables 2–9, is based on the variation among the individual samples and has considerable range depending on the number of samples, the flow, and the bed conditions.

CONCENTRATION OF TOTAL-SEDIMENT DISCHARGE

The concentration of total sediment discharge (col. 9, tables 2–11) was obtained with a width-depth integrating sampler located at the nappe where the flow dropped from the flume into the tailbox. For all sands except the 0.45-mm size, on a dune-bed configuration, eight or more samples were collected during a 2-hour period. For the 0.45-mm sand size, on a dune-bed configuration, and for all sands at all other bed configurations, four to six samples were taken in a 1-hour period. Each sample consisted of 70–110 pounds of the water-sediment mixture. For all sets of data except those for the 0.45-mm sand, the mean concentration obtained for each run is considered accurate to plus or minus 5–10 percent for concentrations in excess of 100 ppm, and to plus or minus 10–50 percent for concentrations between 1 and 100 ppm. The standard deviation given in column 10 of tables 2–11 is based on the variation among the individual samples.

For the experiments using the 0.47- and 0.54-mm sand where fine sediment was added to the flow, the concentration of fine sediment was determined from a sample (about one liter) taken from the large 70- to 110-pound sample of the water-sediment mixture after the large sample settled for 1 minute. The bed-material fraction (col. 9, tables 2–11) of the total-sediment discharge was that material retained after washing on a No. 200 sieve. To obtain the total-sediment discharge, the fine-sediment concentration (col. 6, tables 2–11) must be added to the bed-material discharge (col. 9, tables 2–11). Of course, for those experiments where fine sediment was not added to the flow, the bed-material discharge was the total-sediment discharge.

SIZE GRADATION OF SEDIMENT

The median particle size and (or) the gradation distribution in terms of fall diameter of each suspended- and bed-material-discharge sample and each bed-material sample (cols. 8, 11, 12, and 13, tables 2–11) was determined by drying the total sample, splitting it into a workable size, and then analyzing it in the visual-accumulation tube (Inter-Agency Report No. 11, 1957). Each bed-material sample consisted of several 0.1-foot-diameter cores, about 0.6 foot in length, taken at random from the bed of the flume. In the sets of runs where fine sediment was added to the flow, the fine sediment was washed out of the sample before the sample was dried, split, and analyzed.

The particle-size distribution curves given in figures 3 and 4, the average median diameter of the sand, and the gradation coefficient of the bed material were determined by averaging the results of the size analysis of

the bed material for all runs of a given set and sand. The gradation (σ) is determined by the equation

$$\sigma=\frac{1}{2}\left(\frac{d_{50}}{d_{16}}+\frac{d_{84}}{d_{50}}\right),$$

in which d_{50} is the median size and d_{16} and d_{84} are the respective sizes for which 16 and 84 percent of the sample is finer than the indicated size.

BED CONFIGURATION

The general bed configuration (col. 30, tables 2–11) was noted visually and recorded photographically through the observation window in the side of the flume, at the water surface through the central measuring section of the flume, and at the bed surface in the flume. The bed-surface observations were made either through the water, if the water was sufficiently clear, or from the flume at the end of the run after the water had been carefully drained out.

A sonic depth sounder was being developed during the collection of most of these data (Richardson and others, 1961). After development of the sounder, sonic data were obtained over ripple-and-dune runs by (1) setting the sounder at a stationary point and allowing the sand wave to move past the sounder, and (2) traversing the sounder over the length of the flume at a predetermined uniform velocity.

The length, height, and velocity of the sand waves (cols. 14–16, tables 2–11) were evaluated by:

1. Observations through the wall of the flumes marked by a grid.
2. Observations in the center of the flume by point gage and foot attachment.
3. Observations by a sonic sounder.

The sonic-sounder method was only applicable when the bed configuration was ripples, dunes, or transition-dunes. The number of observations made for each run was generally considered adequate to define within plus or minus 10 percent, the mean values reported.

MEAN VELOCITY OF FLOW

The velocity of flow of a stream is usually determined from a series of velocity readings in the stream section. In the flume, however, the mean velocity (col. 17, tables 2–11) was determined from the observed values of discharge (Q), depth (D), and width (W) by use of the continuity equation,

$$V=\frac{Q}{A}=\frac{Q}{D\times W}.$$

The expected error of V from the above equation would be about 6 percent if, for example, Q and D had errors of 3–5 percent, respectively. A small error in W would be constant for all runs and thereby be canceled with respect to evaluation of other variables.

VELOCITY PROFILE

Velocity-profile data, obtained from the horizontal movements of flow at specific verticals in the flow, are reported in tables 12–21. The observations were made with a standard Prandtl pitot tube which had been calibrated in a towing tank. Tables 12–21 show the velocity at various distances above the sand bed for most runs.

The magnitude and shape of the velocity profile in open-channel flow depend on the bed roughness and on the sediment-transport characteristics. The bed roughness and transport, in turn, depend on several waves. Figure 28 shows a breaking wave. The bed material, and viscosity of the water-sediment mixture.

Except for the plane-bed run, the velocity profiles were not constant with either time or space. As the bed configuration changed with time, so did the velocity profiles. In consideration of the time required to obtain a single velocity profile (5–15 min.), there was some change in the profile during the measurement. Also, the velocity profiles did not plot as a straight line on semilogarithmic paper (V_y = B log y + C) except for those for the plane-bed runs and some made on the back of the ripples or dunes near their crest.

The profile data were plotted on semilogarithmic paper with depth (log) as the ordinate and velocity as the abscissa. A "best fit" straight line was then used to define the relation between V_y and log y (that is, $V_y=B$ log $y+C$), where B defines the slope of the line in terms of velocity per log unit, and C defines the intercept of the line at a depth of 1.0 foot above the bed in terms of velocity. The values of B and C, although of limited utility for the dune runs, are listed in columns 18 and 19 in tables 2–11.

SHEAR VELOCITY, V_*

Shear velocity (col. 20, tables 2–11) is defined as $\sqrt{gDS}$, or $\sqrt{\tau/\rho}$. The error in V_* would be about 7 percent if D and S both have errors of 10 percent, or about 5 percent if D and S have errors of 10 and 4 percent, respectively.

BED-MATERIAL DISCHARGE, q_s AND q_t

Bed-material discharge (cols. 21–22, tables 2–11) was computed from Q, C_s or C_t, and a constant. Since q_s and q_t are expressed in pounds per second per foot of width, $q_s=\frac{Q}{W}\times C_s\times 0.0000624$, and $q_t=\frac{Q}{W}\times C_t\times 0.0000624$. If Q, W, and C_s or C_t have average errors of 5, 2, and 10 percent, respectively, then the mean error for q_s or q_t is about 10 percent.

791–597 O—66——2

KINEMATIC VISCOSITY, ν

The kinematic viscosity (ν) of the water-sediment mixture (col. 23, tables 2–11) was determined from the temperature of the water and appropriate standard tables. For runs in which fine material (bentonite) was added to the flow, the "apparent" kinematic viscosity was determined from figure 6. Dynamic viscosity values were determined by testing water-bentonite mixtures in a Stormer Viscometer (Simons and others, 1963, p. 17) for 0.5-, 1-, 2-, 3-, 5-, and 10-percent concentrations and for a temperature range from 5° to 45° C. The "apparent" kinematic viscosities plotted in figure 6 were computed from the dynamic viscosity values (μ) and the density of the water-bentonite mixture (ρ); $\nu=\frac{\mu}{\rho}$.

SHEAR STRESS AT BED, τ

The shear stress (τ) or tractive force at the bed (col. 24, tables 2–11) is a parameter commonly used as a measure of the intensity of forces related to resistance to flow and transport of sediment particles. It is computed by the formula

$$\tau=\gamma DS,$$

where D and S are from columns 3 and 2, tables 2–11, respectively, and γ is the specific weight of water (62.42 lbs per cu ft at 0° C).

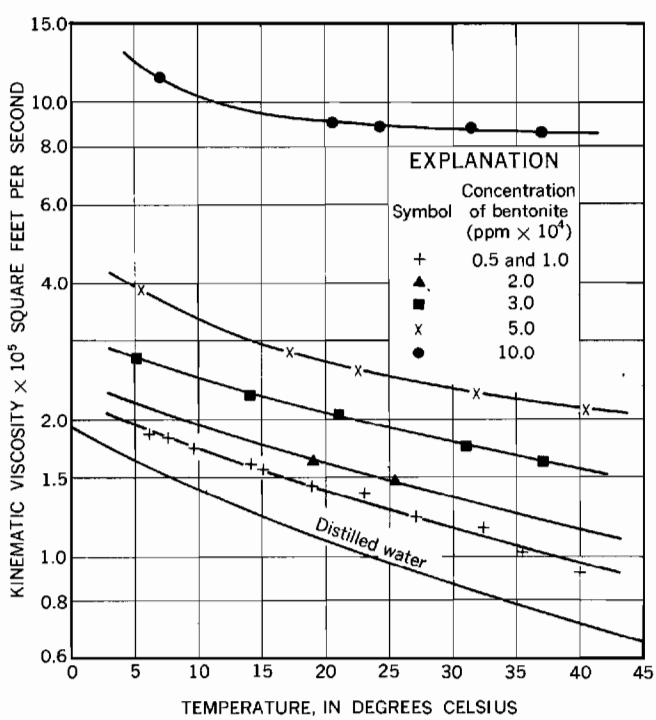

FIGURE 6.—Relationship of "apparent" kinematic viscosity of aqueous dispersions of bentonite to temperature.

REYNOLDS NUMBER, R

The Reynolds number, R (col. 25, tables 2–11) is a ratio of the viscous force to the total inertial force in the channel:

$$R=\frac{VD\rho}{\mu} \text{ or } \frac{VD}{\nu}.$$

It is commonly used as a measure of the effect of viscosity on the flow pattern.

The Reynolds number is also often used with respect to a sediment particle:

$$R=\frac{\omega d\rho}{\mu}, \text{ or } \frac{\omega d}{\nu},$$

where ω is fall velocity of the particle and d is fall diameter of the particle.

FROUDE NUMBER, F

The effect of gravity on the flow pattern is commonly related to the Froude number, F (col. 26, tables 2–11), which is the ratio of the gravity force to the total inertial force. As commonly used and reported herein,

$$F=\frac{V}{\sqrt{gD}}.$$

RESISTANCE FACTORS, f, $C/\sqrt{g}$, n

Parameters related to average resistance to flow in channels are based on the variables S, D, and V. They are:

1. Darcy-Weisbach resistance coefficient, $f=\frac{8gDS}{V^2}$.
2. The dimensionless Chezy discharge coefficient, $C/\sqrt{g}=\frac{V}{V_*}$ or $\frac{V}{\sqrt{gDS}}$. Note that the discharge coefficient is the inverse of resistance.
3. The Manning n, $n=\frac{1.49D^{2/3}S^{1/2}}{V}$, where D is nearly equal to R the hydraulic radius. These resistance factors are listed in columns 27–29, tables 2–11.

DESCRIPTION OF INDIVIDUAL RUNS

This section of the report documents pertinent laboratory notes from general and unusual observations of the flow and transport phenomena during the period in which the run was approaching equilibrium and during the collection of the routine basic data. Most notes refer to methods used to set up the runs, the bed forms, the flow characteristics, and to unusual conditions relative to data collection. Many photographs were taken to show the flow and roughness characteristics. The photographs were generally taken either through the glass wall at the side of the flume, from above the water surface, or from above the bed

surface after careful draining of the flume at the end of the run.

Notes and corresponding photographs, if any, for each run are headed by the respective run number. These make up the set of runs for a specific sand and flume size. The run numbers and the order of presentation (usually by increasing slope) correspond to the run numbers and order given in tables 2–11.

RUNS USING 0.19-MM SAND IN 8-FOOT-WIDE FLUME

The sand used in this set of runs was the finest used during the investigation. The runs were made between November 3, 1959, and January 21, 1960. The experimental variables and parameters are given in table 2, and the velocity-profile data in table 12.

Run 24.—The data are an average from two runs during which slope, discharge, depth, and temperature remained nearly the same. Beginning of motion or transport occurred at a low slope ($S = 0.00006$) because of the fine sand and the 0.94-foot depth of flow. The error in the mean slope measurement was in the order of 10–20 percent. The problem of determining when beginning of motion occurred (Rubey, 1937) was further complicated by the effect of small local irregularities on the bed. Particle movement on the bed nearly ceased as very small ripples became established. The ripples, in turn, increased roughness and depth, and decreased velocity. Equilibrium was thus established.

Run 22A.—The bed material was carefully screened to a plane, and then flow was established to a depth of 0.6 foot. Slope was increased and depth decreased by opening the tailgate in small increments until beginning of sand particle motion was observed. With $Q = 2.99$, $T = 17.5$, $S = 0.00010$, and $D = 0.48$, there was some movement of lightweight particles. The coarse light-weight particles (0.5–1 mm) which moved on the bed surface were sand grains cemented with a clay material. This coarser material collected along with the fine material into isolated ridges about 0.005 foot high.

Run 2.—The conditions for this ripple run were similar to those for run 1 (page I 12) except that depth and discharge were doubled and slope was reduced. Movement of the bed material in the form of very slowly moving ripples occurred throughout the flume. No armor plating developed, as it did in runs using coarser sands. The ripple waves seemed very fluid and soft in comparison to the troughs. Depth measurements may have been too great, owing to the ease with which the probe penetrated the surface of the sand waves. The average concentration from eight samples was used to determine bed-material discharge. Longitudinal and transverse views of the ripples are shown in figures 7 and 8. The photographs were taken after the water was slowly drained from the flume, without disturbing the ripples. The troughs between many ripples appeared flat owing to water standing in the depressions.

Run 22B.—This run was established from 22A by increasing the slope to 0.00016 and, thereby, decreasing the depth to 0.43 foot. All the particles moved occasionally, and then, very slowly as the slope was increased. Careful observation was required to detect such small amounts of movement. Slight indentations,

FIGURE 7.—Longitudinal upstream view of the flume bed, showing ripple formation at end of run 2 after slowly draining the water from the flume.

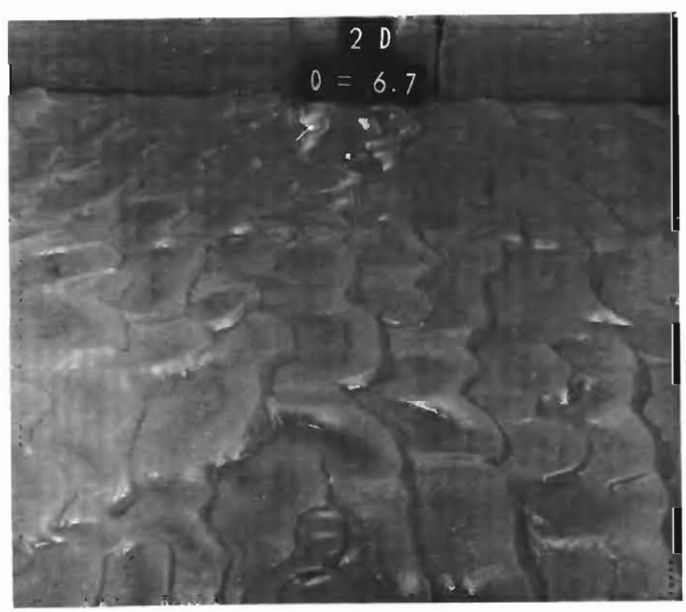

FIGURE 8.—Transverse view of ripple formation at end of run 2. The direction of flow was from left to right.

similar to those described by Bagnold (1956), formed on the bed as primary features (the beginning of ripple forms). Ripples that formed upstream from station 15 were caused by entrance effects and should not affect data relative to beginning of particle motion.

Run 26.—Some particle movement occurred over the entire flume bed. Large particles moved farther than smaller particles. These larger particles (0.2–0.3 mm) collected together and formed very small ridges spaced about the same as those ordinarily formed by ripples. It may be concluded that this segregation was responsible for the formation of ripples, except that other investigators (Brooks, 1958; Liu, 1957) reported such ridges and ripples when using a more uniform sand.

Run 25.—The conditions for this run were the same as for run 24 except that the slope was steeper. The bed was completely covered with very small ripples while the water surface was very tranquil. Ripples began to form wherever there was a slight bed irregularity, such as a large particle, and, motion having begun, continued to form progressively downstream and laterally from this point. A few coarse clay particles rolled freely on the sand surface until stopped by a depression or another large stationary particle. The ripple waves were fluidlike or soft to the probe. Figure 9 shows the smaller size of ripples formed in this run, in contrast with those formed in run 2. Note the absence of a plane with respect to the troughs of the ripples.

Run 22C.—This run was a continuation of runs 22A and 22B, but at a slightly increased slope and decreased depth. Movement of sediment was general over the entire bed, and thus ripples formed over most of the bed within about four hours after starting the run. Beginning of motion was best represented in run 22B. The rate of transport was very low; therefore, sediment samples were not taken.

FIGURE 9.—Upstream view of ripples formed during run 25. Ripples are smaller and more completely developed than those formed in run 2 (figs. 7, 8).

Run 30.—The bed was screeded prior to starting the run, and the slope of the bed was set parallel to an assumed water surface slope which would insure uniform flow over ripples at the desired depth of about 1 foot. The ripples formed a more irregular pattern than did those of runs with less shear. The water surface was tranquil or mirrorlike. The individual ripples changed shape with time and moved very slowly. The bed-material discharge, determined from nine samples, ranged from 3.1 to 4.3 ppm (parts per million), and the suspended-sediment concentration of four samples was composited and equals 7.0 ppm.

Run 1.—This run was started with the bed screeded level. Small ripples 0.3–0.4 foot long and 0.02 foot high covered the entire bed immediately after the run began. The ripples gradually increased in length and height to about 0.6 foot and 0.05 foot, respectively. Ripple crests were very soft and fluidlike in comparison with the intervening troughs. The transport rate was very low; so that the velocity of the ripples was extremely slow. The run had been in progress for about 40 hours before data were taken. The bed-material discharge, determined from eight samples, ranged from near 0 to 3 ppm. Suspended-sediment concentration was not measured.

Run 31.—Ripples formed under the flow conditions of this run were larger and had more irregular patterns than those formed at lower slope and depth. The velocity was such that sand was eroded at the headbox and moved downstream as a wave. This wave affected the water-surface slope downstream to station 45. The ripple waves in the test section seemed to be much softer than the underlying, nonmoving material. A transverse view through the flowing water (fig. 10) shows the more triangular shape of the ripples, in contrast with those shown in figure 8. The seven bed-material discharge samples ranged from 25.0 to 34.9 ppm, and the four suspended-sediment samples was composited and equals 42 ppm.

Run 27.—The shifting part of the bed was very fluid, but the underlying part was firm because of screeding. The seven bed-material discharge samples ranged from 3.1 to 5.1 ppm. Suspended-sediment movement was negligible; therefore, samples were not taken. The measured bed-material discharge was less than was expected for the given hydraulic conditions.

The pattern of ripple development for all runs suggested that flow conditions can easily be set up which

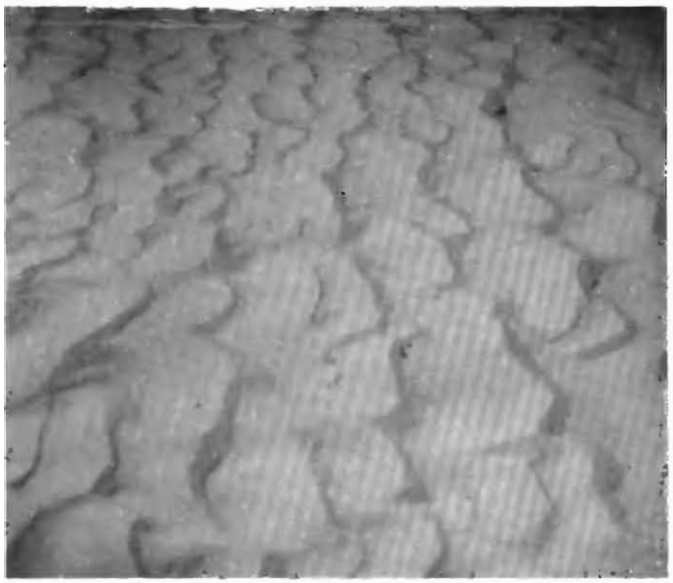

FIGURE 10.—Transverse view, through the flowing water, of ripples formed during run 31. The direction of flow is from left to right.

will form very uniform ripples of small amplitude that are nearly continuous across the flume. Then, slightly increasing shear stress by increasing depth or slope will cause larger more irregular ripples to form which are distinctly discontinuous across the flume.

Run 5.—Run 4 was not completed because of a sand wave in the flume. The bed form of run 5 was large ripples. The bed was very soft, particularly on the crest of the ripples. The large ripples and consequent transverse currents caused very small boils, which could be seen by careful observation of the water surface. Flow tended to meander through the flume and cause somewhat uneven depth of flow across the flume at a particular across section. The seven bed-material discharge samples ranged from 110 to 144 ppm, and the four suspended sediment samples ranged from 95 to 119 ppm.

Run 23.—After runs 22A–C, the bed was raked crosswise to create artificial roughness. Ripples formed overnight on the entire bed. Seemingly, the run was not in perfect equilibrium; that is, minor slope, roughness, and depth adjustments were occurring which caused nonuniform flow. The water surface was very placid, although not as smooth as before beginning of motion. The seven bed-material discharge samples ranged from 1.8 to 2.8 ppm. As indicated for run 27, the measured sediment transport rate was much less than expected when the hydraulic factors were compared with those for runs of similar hydraulic conditions. Figure 11 shows the ripple pattern which formed during run 23.

FIGURE 11.—Upstream view of ripple pattern on flume bed at end of run 23.

Run 32.—Bed roughness appeared to be small dunes with superposed ripples. The bed material to a depth of 0.1–0.2 foot was moved. Depth observations were very difficult to make because the rapidly moving material was very soft. Ripples changed shape rapidly: old ones vanished and new ones formed. Data on the length and height of ripples, from observations through the side windows, may be misleading because of the wall effect. The sonic recorder was used to determine the dimensions and velocity of the sand waves. The character of the bed configurations is indicated in figure 12.

Run 8.—Bed roughness consisted of ripples superposed on dunes. The bed was soft as with dunes,

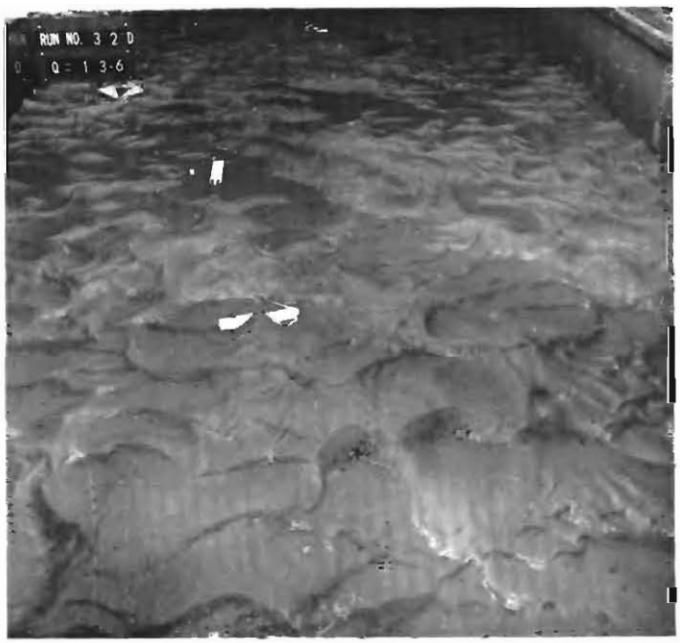

FIGURE 12.—Upstream view of bed configurations at the end of run 32. Light spots are reflection of lights on water left from incomplete drainage in ripple troughs.

particularly on the shifting parts. Boils associated with the dunes appeared on the water surface, but they were not very violent. Figure 13 is an upstream view of the bed form for this run. The upstream side of the dunes had no ripples where the depth was shallowest and the shear was greatest.

Run 28.—Conditions for this run were similar to those for run 27 except that the slope was greater. The suspended-sediment discharge was still very small. The water surface was relatively smooth, but a brickworklike pattern of ripples formed on the bed. The bed was very soft in the zone of movement. Seven samples of bed-material discharge ranged from 28.4 to 42.4 ppm.

Run 33.—The bed configuration for this run was very large widely spaced dunes. Large strong eddies carried sand from the bed to the water surface just downstream of the dune crests. These eddies resulted in boils or local crowns at the water surface, from which moved small horizontal components of flow. The backs of most dunes, according to feel with a foot plate, were covered with ripples. The velocity of flow over the crest of a few very high dunes was sufficient to plane away all roughness on the crest. Slope and depth observations were difficult to make because of the rapid change in position and shape of the dunes. Small dunes were continually forming and moving onto the crest of the large dunes, thus changing the amplitude and rate of travel of the large dunes. Bed-material discharge, determined from nine samples of flow, ranged from 606 to 1,152 ppm; four suspended-sediment concentration samples ranged from 652 to 1,460 ppm.

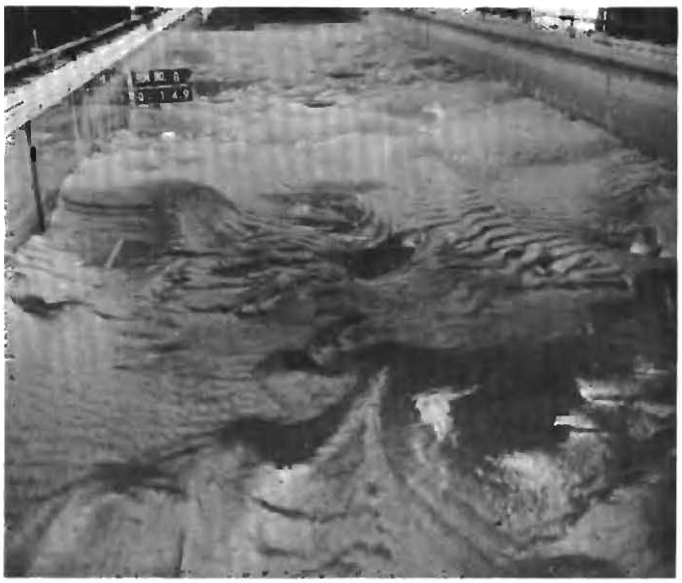

FIGURE 13.—Upstream view of ripple-dune pattern at end of run 8

Run 29.—The discharge was less than one-third, the depth was less than one-half, and the slope was nearly the same as that of run 33. The result was an increase in roughness, a decrease in velocity, and about one twenty-fourth as much sediment discharge. This effect of depth on the flow and bed-material discharge was found to be comparable to that shown by Colby (1961). The ripples moved faster and there was more sediment in suspension than in other ripple runs. The ripples, which were soft and fluid in their moving parts, formed a brickworklike pattern. The water surface was rather smooth, as in the preceding ripple runs. The eight samples of bed-material discharge ranged from 45.2 to 68.6 ppm. The four samples of suspended-sediment concentration were composited for a mean concentration of 30.6 ppm.

Run 3.—The ripples were somewhat larger in amplitude and more widely spaced than those in runs 1 and 2. The considerably increased sediment discharge caused the ripples to move faster and with greater irregularity of pattern. The irregular ripple pattern is shown in a photograph of the bed taken through the flow (fig. 14). The seven samples of bed-material discharge ranged from 61 to 120 ppm.

Run 11.—At the beginning of the run, the bed was nearly plane; during the run large regular dunes formed, which in turn caused the slope to increase. This was the first run using the fine sand for which the form, the individual element, and bed roughness as a whole, was similar to that observed in runs using coarser sands. The amplitude of the dunes was about 0.5 foot. Some ripples formed in the dune troughs

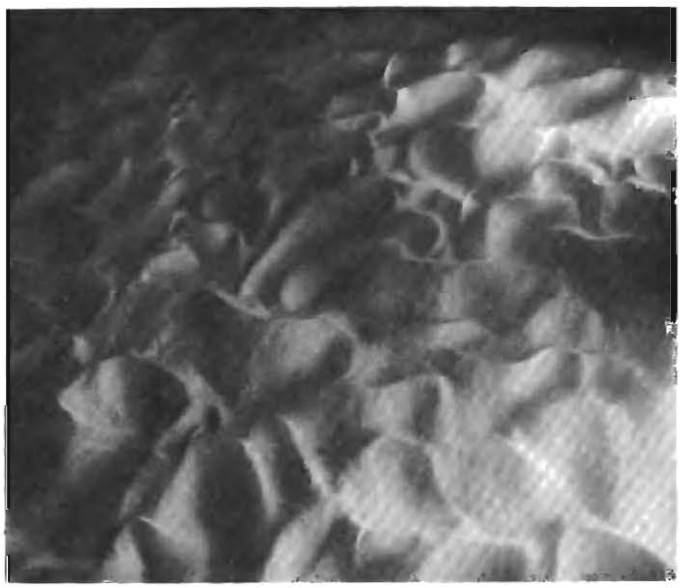

FIGURE 14.—Downstream view through flow showing rippled-bed configuration during run 3.

FIGURE 15.—Upstream view of bed configuration at end of run 11. The small surface ripples formed during shutdown of the run. Note the scour hole to the floor of the flume in the foreground.

adjacent to the walls. The bed was very firm on the back of the dunes, where the surface was planelike; and it was very soft in the trough area, where the velocity was less and the sand was being deposited. When the flow was stopped and the flume drained, more ripples were seen on the dunes than were apparent when the run was in progress. (See fig. 15). Four observations of dune velocity were made through the window to show the range of velocity of the more prominent dunes. The results were 0.085, 0.181, 0.182, and 0.480 fpm (feet per minute). The eight bed-material discharge samples ranged from 1,140 to 1,560 ppm, and the four suspended sediment samples ranged from 766 to 856 ppm.

Run 13.—Discharge was about the same as in run 12, but the tailgate was slightly opened. The resultant increased slope and decreased depth caused the downstream dunes to be partly planed out and, thus, caused decreased resistance to flow. The upstream dunes near the flume entrance were fully developed, but decreased in amplitude downstream until, at station 100, plane-bed conditions prevailed. (See fig. 16.) A few small dunes, however, remained below station 100. The water surface was very smooth over the plane-bed area. Considerable sediment was carried into suspension by eddies in the dune area. Low, more streamlined, dunes offered less resistance to flow and, hence, caused less suspension of sediment than did the regularly shaped dunes at the upper end of the flume. Eight observations of bed-material discharge ranged from 1,180 to 1,385 ppm, and four observations of suspended-sediment concentration ranged from 695 to 852 ppm.

FIGURE 16.—Typical bed conditions at end of run 13. The small surface waves were caused by slow flow at the time of shutdown.

Run 14.—The shear stress was increased from that in run 13 by increasing slope. More of the bed was plane for this run than for run 13, and the dunes at the upper end of the flume were reduced to long flat sand waves about 0.1 foot high. (See fig. 17.) The resulting decreased resistance caused a decrease in depth from that observed for run 13. When core samples of the bed were taken, a crusty surface was noted. This indicated that the sand particles were more densely packed at the surface than at the lower levels. On the whole, the bed was much firmer than that for the ripple-and-dune runs. The variation in concentration of bed-material discharge was nearly the same as for run 13. The differential-bubbler-gage record of slope showed considerable variation. However, this varying of slope was not as great as that for a dune-bed configuration because it was caused by changes in water-surface elevation as dunes moved downstream.

FIGURE 17.—Upstream view of bed conditions at the end of run 14. The small surface ripples formed during shutdown.

Run 15.—Slope was greater and depth was less than in runs 13 and 14. The bed was plane throughout the flume except for very minor long flat sand waves. The bed was very firm and had a crustlike surface. The water surface was very plane and showed neither boil activity nor standing waves. Thus, data were easy to collect for this kind of flow condition. Through the side window, small chunks of sandstone were visible only 0.1–0.2 foot below the sand surface. This was the maximum depth at which the sand moved in this bed.

Run 34.—The bed configuration for this run comprised small dunes with large ripples superposed, which caused considerable roughness of the water surface. A smoother surface would probably have resulted if depth had been greater under these conditions of roughness. Figure 18 is an upstream view of the water surface. Bed-material discharge ranged from 464 to 543 ppm for eight samples and the suspended-sediment ranged from 342 to 467 ppm for four samples.

Run 12.—The conditions for this run were very similar to those for run 11 except that both the slope and velocity were increased. Large dunes, spaced 15–30 feet apart, formed on the bed. The back of the dunes was very firm, the intervening troughs, soft. Some dunes had a rather flat avalanche face; consequently, upstream circulation over the bed in the trough was weak. This condition resulted in a lower roughness value for this run than for run 11, and a firmer bed in the trough area. Figures 19 and 20 show the water surface and the bed, respectively. Nine concentration measurements of bed-material discharge ranged from 1,180 to 1,540 ppm, and six concentration measurements of suspended sediment ranged from 887 to 1,040 ppm.

FIGURE 18.—Upstream view of water surface during run 34.

FIGURE 19.—Upstream view of water surface during run 12.

FIGURE 20.—Bed configuration at the end of run 12, viewed upstream. Note large rather streamlined dunes.

FIGURE 21.—Upstream view of ripples on low dunes characteristic of run 6. The pools of water remained after incomplete drainage at the end of the run.

Run 6.—As is shown in figure 21, the bed roughness elements for this run consisted of ripples and irregularly spaced dunes about 6 feet long. The ripples had an irregular shape which changed rapidly. Some ripples had the usual triangular shape; others were rounded and symmetrical. The water-surface slope also varied considerably between the measurement points. Several slope measurements were averaged to get a value for the representative slope of this run. An upstream view of the water surface is shown in figure 22.

Run 7.—The principal bed configuration was dunes, although ripples formed in the deeper and lower velocity parts, as is indicated in figure 23. Turbulence at the water surface seemed to be less than in run 6, although many boils were seen which carried sand to the surface. Once during the run, a dune crest was seen. Downstream from the dune crest, at the zone of separation, ripples were orientated in the upstream direction.

Run 35.—The conditions for this run were similar to those for run 34 except that slope and mean velocity were increased. The bed roughness elements were dunes with ripples superposed, but the dunes were larger than those in run 34. The water surface was not as rippled as in run 34, but much stronger eddies carried clouds of sand from the bed to the water surface. Transverse flow apparently formed long sand ridges parallel to the direction of flow. Sediment streaming off these ridges indicated greater than average sediment transport. The bed was very soft near the dune crests. A plane-bed condition with very intense sediment movement near the bed, existed on the upper part of the dunes, where the water was shallowest. Sediment transport differed widely, both from point to point on the bed and in suspension. The shapes of the dunes and ripples were very irregular and changed quickly. Thus, tracking dunes either visually through the window or with the sonic sounder was difficult. This sand was much more fluidlike and more sensitive to probing forces than were the coarser sands.

FIGURE 22.—Upstream view of water surface during run 6.

FIGURE 23.—Upstream view of bed configuration at the end of run 7.

Run 16.—The slope was steeper, the velocity greater, and the depth less than in runs 13, 14, and 15. Upstream from station 110 the bed and water surface were essentially plane; downstream from this point, standing waves were inphase with bed waves. Figure 24 shows these water-surface characteristics. The waves in the lower end of the flume had an amplitude of less than 0.1 foot and were about 3–4 feet apart.

Run 10.—This was essentially a plane-bed run. Very long and low sand waves moved down the flume. A few ripples persisted at the walls of the flume downstream from the crests of these waves. The presence

FIGURE 24.—Upstream view during run 16, taken from station 140. Standing waves can be seen in the part of the flume downstream from station 110, and plane conditions, upstream from station 110.

of the sand waves was also shown by the cycling of the bubbler gage. The bed was firm and plane except near the ends of flume.

Run 9.—The dunes formed in this run were very long and rather low but not as rounded as a sand wave. On the basis of observations though the window, some ripples apparently formed in the troughs. The back of the dunes (upstream from the crest) was very firm and plane; over which, the velocity was greater than in the deeper trough areas where the bed was irregular and very soft. Such variation in velocity caused considerable variation in elevation of the water surface at a point where the dunes passed. The water surface showed strong boils over the trough area. Nine sample measurements of bed-material discharge made in an 8-hour period ranged from 967 to 1,640 ppm. Suspended-sediment concentration in six samples ranged from 497 to 1,070 ppm—three samples taken from the back of the dune (plane area) averaged 600 ppm, and three from the trough area averaged 948 ppm.

Run 17.—The slope was increased by opening the tailgate after run 16 without stopping the flow. Velocity increased from 3.84 to 4.14 fps (feet per second), and depth decreased from 0.72 to 0.67 foot. In the first 60–70 feet the flume had a plane bed. Downstream the bed condition became one of small standing waves and then, with an increase in wave size, antidunes in the vicinity of stations 90–100. The most consistent and greatest antidune activity was downstream from station 110. The bed was very firm in the plane-bed areas and got softer with increasing wave activity in the downstream direction. See description of runs 18 and 19 for photographs showing these flow conditions.

Run 18.—Slope was increased from that for run 17 by further opening the tailgate. This resulted in a velocity increase from 4.14 to 4.33 fps and caused waves and antidunes to form from station 30 downstream to the end of the flume. Very symmetrical waves formed upstream from station 80 and extended all the way across the flume but did not break. Below station 80, waves were accented on one side of the flume or the other or extended the full width of the flume. The condition downstream from station 100 (fig. 25) was the same as that below station 80 except that interfering waves caused a choppy water surface. In the lower part of the flume, the water surface at a specific location went through the cycle of choppy, smooth, increasing wave, and breaking wave. When the waves broke, the flow in the area nearly stopped. The antidunes formed at a much lower slope than they did in runs using the coarser sands.

FIGURE 25.—Upstream view of the water surface in the area of antidune activity during run 18.

Run 19.—The slope was increased from 0.00300 (for run 18) to 0.00350, but the mean velocity remained unchanged. The antidunes traveled upstream faster than did those in runs using the 0.45-mm sand. Not more than three or four waves broke, and then, very gently. Sometimes waves built up and then subsided without breaking. Occasionally, at a section, wave interference from breaking waves upstream caused the water surface to be very choppy. As in the previous run, this choppy water surface smoothed and then waves developed again. Figure 26 shows the flow and bed characteristics during this run. View *A* shows a condition at near minimum depth (about 0.45 ft) and maximum velocity, and view *B* shows an area of deceleration where depth increases to about 0.75 foot. Both views *A* and *B* show that the stream bed remained relatively plane and uniform from scour despite the very large amount of sand being swept along near the bed. View *C* shows a breaking wave carrying a large amount of sand in suspension. The sand obscures the bed in the right part of the picture. The depth of the breaking wave is slightly less than twice the depth of the trough.

Run 39.—Conditions for this run were similar to those for run 19 except that slope and velocity were increased. Antidunes formed throughout the entire width and length of the flume. The average length of waves from crest to crest was 4.8 feet for 12 observations. The average depth was 0.50 foot in the trough (21 observations) and 0.88 foot at the crest (27 observations).

Run 20.—The intensity of turbulence due to antidune activity was nearly uniform through the flume. Most waves built up and broke, but a few waves built up and died down without breaking. Almost all waves

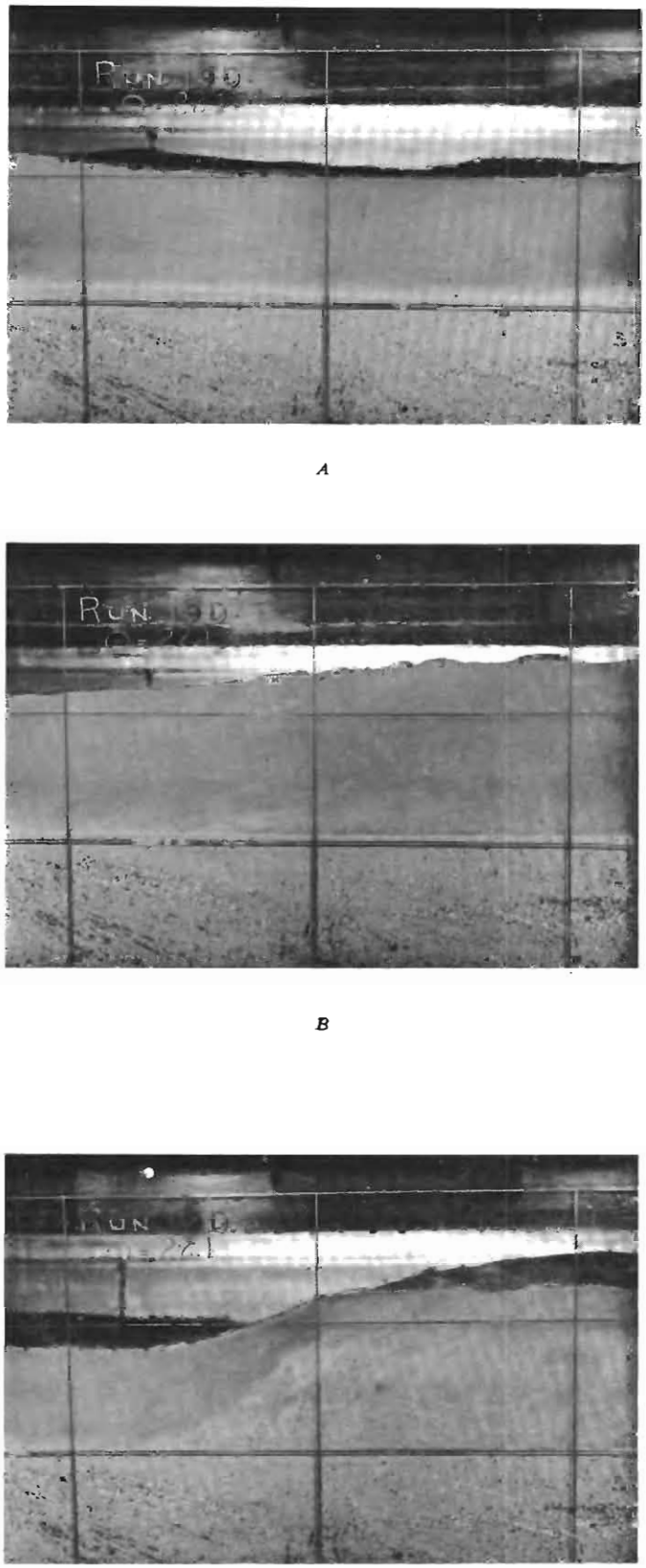

A

B

FIGURE 26.—Flow and bed characteristics of antidune conditions during run 19, photographed through window in side of the flume. *A*, The trough of a water wave. *B*, The upstream side, or deceleration area, of a wave. *C*, A breaking wave, showing heavy concentration of suspended sand.

moved gradually upstream. The amount of sediment being moved, including both that in contact with the bed and that in suspension increased considerably. The amount of sediment in suspension was sometimes so great that the position of the bed was practically impossible to distinguish through the window. In the trough the bed was firm; but where the water surface was choppy in the areas of breaking waves, the bed was soft.

Run 21.—For this run, the tailgate setting was left the same as for run 20, but the discharge was reduced from about 22 cfs to 16 cfs. Decreasing discharge caused the slope of the energy grade line and the alluvial bed to increase considerably. The antidune waves, shown in figure 27, formed both single trains occupying the full width of the flume and some double trains. A choppy water surface occasionally resulted from interference of upstream antidune waves or, when the waves were not quite at right angles to the flow and reflected off the sides of the flume, from criss-cross waves. Figure 28 shows a breaking wave. The bed surface is more irregular than it was in run 19 (fig. 26*C*). In comparison to run 19, the depth of flow in the breaking waves was more than twice the depth of flow in the trough.

Run 38.—The flow conditions for this run were nearly the same as for run 21 even though discharge, depth, velocity, and slope were increased. Antidune activity was apparent throughout the flume, and a pool and small chute formed. (See description for runs 36 and 37.) The pool, possibly the result of antidunes breaking, was only about 5 feet long, and the chute was indistinct.

Run 36.—Chute-and-pool activity was very pronounced in this run. (See fig. 29.) As many as four

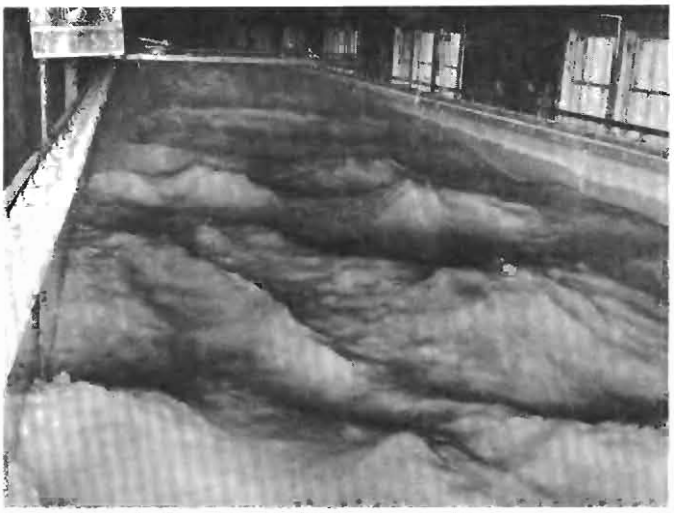

FIGURE 27.—Upstream view of antidune wave pattern during run 21

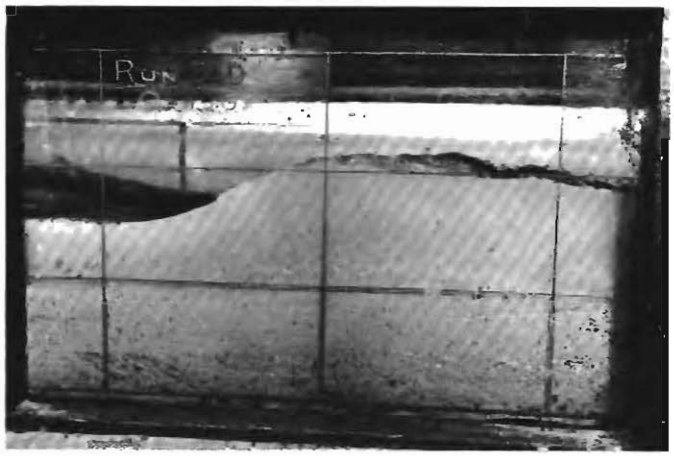

FIGURE 28.—Side view of breaking antidune during run 21.

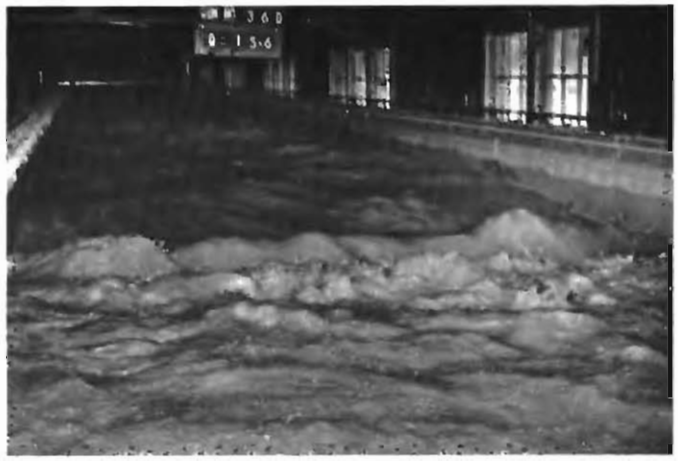

FIGURE 29.—Upstream view of chute-and-pool flow conditions during run 36. Note the air bubbles on the water surface downstream from the hydraulic jump in the foreground of the picture.

A

B

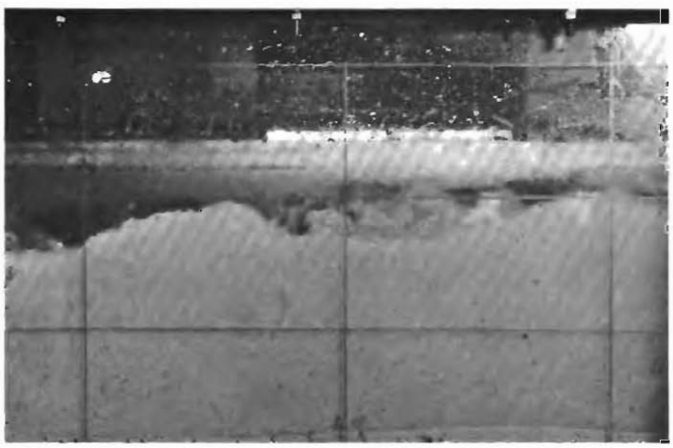

C

D

FIGURE 30.—Side views of chute-and-pool flow conditions during run 37. *A*, The chute. *B*, The hydraulic jump. *C*, The pool. *D*, The acceleration of flow toward the next chute. Photographs were taken through the window in the side of the flume.

chutes and four pools formed in the flume at one time. The gradient into the pools was very steep. The storage of water in and the release of water from the pools caused the discharge of the pump to vary. The flow in the pool sections, which were as much as 30 feet long, was 0.5–0.8 foot deep and was tranquil (Froude No. less than 1); whereas, the flow in the shorter, chute sections was 0.2–0.3 foot deep and was rapid (Froude No. more than 1). The bed elevation changed about 0.4 foot with time, but at no time was the floor of the flume exposed.

Run 37.—A chute began to form at station 50, near the lower end of the flume, and moved upstream. When it reached station 100, another chute began to form at station 50; thus, the chutes were about 50 feet apart. The chutes and pools moved upstream at a rate of about 8 feet per minute. Figure 30 shows the flow conditions during run 37. The slope of the water surface was nearly 40 percent on the steepest part of the chute.

RUNS USING 0.27-MM SAND IN 8-FOOT-WIDE FLUME

The 0.27-mm sand was obtained by wet screening the 0.28-mm sand and removing the fraction coarser than 2.0 mm (table 1). These experiments were conducted during the period March–April 1959. The experimental variables and parameters are given in table 3, and the velocity-profile data, in table 13.

Run 50A.—During this run the bed material was very close to beginning of motion. The bed was planed prior to starting flow and then once again after the water was flowing by moving the planer from upstream to downstream. Ripples formed on 3–4 percent of the bed. The formation of ripples may have been due to vibration of the flume. Vibrations of the flume caused by very small water-surface waves to form, which made precise measurement of slope difficult.

Run 50D.—The slope was increased to 0.00018, compared with 0.00007 for run 50A, and ripples formed. The mean velocity increased only a small amount (0.79 to 0.84 fps) in consideration of the large increase in slope because of the increase in bed roughness from the plane bed in run 50A to the ripples formed in this run. The rippled bed was very soft. The sand in the trough between ripples felt and looked coarser than the sand in the back and the crest of the ripples. Apparently, only the finer sand moved up the incline to form the ripple. The coarse fraction tended to armor-plate the trough and inhibit further growth of the ripples. This sorting, shown in figure 31, is opposite that indicated by Bagnold (1941) for blown sand, in which the coarsest material collects at the crest and the finest in the trough.

Run 51.—The amplitude and spacing of ripples were greater than in run 50D. The coarser particles moved, and the sand felt as if it were about the same diameter in both the trough and the crest of the ripples. Figure 32 shows that the ripples were more fully developed than those in run 50D (fig. 31) and that the coarse material was deposited at the base of the ripple face rather than being a residual in the trough of the ripple. The concentration of bed-material discharge ranged from 10 to 15 ppm for seven samples, and the suspended-sediment concentration averaged 9.0 ppm for four samples.

Run 52.—The ripples formed were slightly larger than those formed in run 51, more sand was moving, the slope was steeper, and the velocity was greater. The bed seemed very fluidlike, and all sizes of particles

FIGURE 31.—Upstream view of ripples on the bed of the flume at the end of run 50D.

FIGURE 32.—Upstream view of ripples on the bed at end of run 51. Note that the ripples are better developed than those shown in figure 31.

were in motion sometime during the run. The rate of ripple movement was difficult to determine because of the rapid change of ripple shape. Some lateral shifting occurred as the ripples moved downstream. Figure 33 shows the shape of the ripples formed under the flow conditions for run 52.

These ripples were more irregular in size and shape than those formed during run 51 (fig. 32). The sand movement over the bed was typical of ripples. It moved by sliding and bounding up the back side of the ripple and then sliding or leaping until it came to rest on the foreplane of the ripple. Some fine sand went into suspension at the ripple crest. The bed-material discharge ranged from 72 to 121 ppm for eight samples, and the suspended-sediment concentration ranged from 46 to 62 ppm for four samples.

Run 54.—The bed form was one of dunes with ripples superposed. The ripples and dunes were irregular in form and changed shape rapidly as they moved past the observation window. The bed was soft, and particles of different size were well mixed, even in the troughs. The bed was firmest on the back of the larger dunes. Bed-material discharge ranged from 163 to 287 ppm for eight samples and suspended-sediment concentrations ranged from 102 to 197 ppm for four samples.

Run 53.—The back of some of the large dunes was plane where the depth was shallow and the shear was great. Most dunes were covered with small ripples or with sand waves nearly equivalent to ripples. The flow conditions were such that a slight increase in shear would cause the bed form to change to the non-rippled dune. The bed was much softer than in runs where only ripples formed. The dunes constantly changed shape and speed as small ones caught up with the larger ones. Some lateral shifting of dunes and

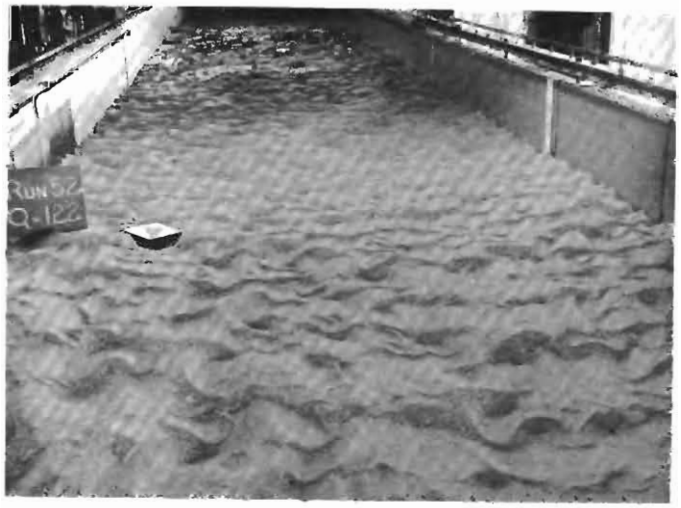

FIGURE 33.—Upstream view of ripples on the bed at the end of run 52.

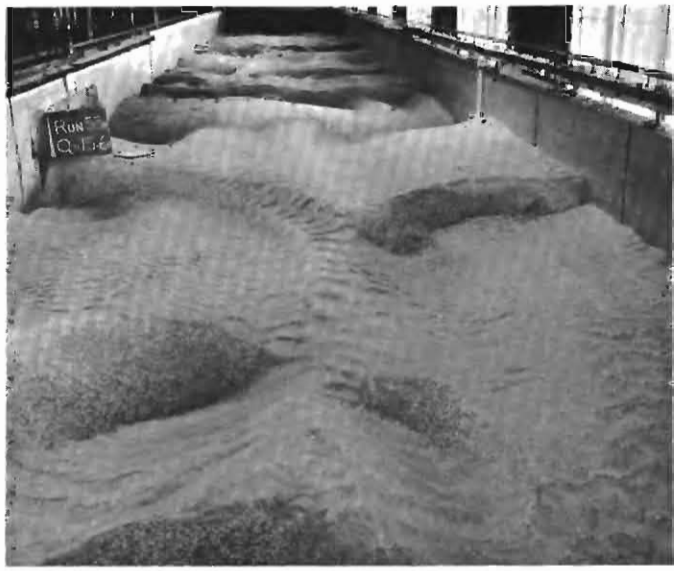

FIGURE 34.—Upstream view of the bed configuration at the end of run 53.

formation on longitudinal ridges or fins parallel to the flow also occurred. Large amounts of sediment from those fins went into suspension. The characteristic shape of the dunes, ripples, and fins is shown in figure 34.

Run 57.—The shallow depth of flow caused the bed to revert to a rippled condition even though the slope had been increased from the previous run. The ripples were fully developed and soft, particularly near the crest. The bed was firmest just downstream from the ripple troughs. The bed looked very similar to that of run 51 (fig. 32). Bed-material discharge ranged from 69 to 110 ppm for eight samples.

Run 56.—The slope was the same for this run as for run 57, but discharge, depth, and velocity were greater. The bed form changed to dunes with superposed ripples. Again, no ripples formed on the back of the larger dunes, where depth of flow was shallow, the velocity high, and the bed very firm. The "plane" flow condition on the back of the dunes caused a rather compact crust, possibly as much as one-half inch thick, to form on the dune. At places where sand was being carried into suspension, the bed was very fluidlike or soft. Figure 35 shows the irregularity of the dune and ripple pattern of run 56. The variation of concentration among sediment samples was very high. Bed-material discharge ranged from 355 to 829 ppm, and suspended-sediment discharge ranged from 252 to 852 ppm.

Run 55.—The slope of the flume for this run was not changed from that for runs 56 and 57; but as the discharge, depth, and velocity were increased, the slope increased from 0.00126 to 0.00130 as equilibrium was

FIGURE 35.—Upstream view of bed configuration at the end of run 56.

established. The dunes formed were rather large, and caused some troughs to extend to the floor of the flume. (See fig. 36.) The top layer of sand on the back of large dunes was firm, but it was very easily broken to expose the softer body of the dune. The bed was soft both at the crest and in the trough of the dunes. The condition of the water surface varied greatly with distance and time. It was very smooth and sloped downward where the velocity increased up the back side of the dune. A series of eddies and the reverse flow in the trough downstream from the dune caused a rapid increase in elevation of the water surface at the crest of the dune. Water-surface elevation varied

FIGURE 36.—Upstream view of bed configuration at the end of run 55. Note the large dual fins in the left foreground.

0.035 foot within a 5-feet distance along the flume. The reverse flow in the troughs of the dunes was further substantiated by reverse-orientated ripples in these troughs.

Run 45.—The bed was firm and felt plane except near scattered very low dunes or depressions. No eddies reached the surface from these depressions. Small symmetrical surface waves were seen near the headbox and occasionally near the tailbox.

Run 43.—The dunes formed in this run were very large. The bed was firm and very smooth on the back of dunes, and soft at the crest and through the trough of dunes. The reverse circulation in the trough of the large regularly-shaped dunes was very strong. The largest dune observed through the window, was 0.75 foot high (fig. 37). This dune probably would have been even larger if the depth of the sand bed had been greater. Some segregation of coarse and fine sand was noted, but it was not as noticeable as in runs using the 0.28-mm sand, which contained more coarse material. Again, reverse-orientated ripples frequently formed in the dune trough. Bed-material discharge ranged from 583 to 1,310 ppm for eight samples, and suspended-sediment discharge ranged from 505 to 684 ppm for three samples. Ten observations of the slope of the avalanche faces of dunes ranged from 24° to 32° and averaged 30°.

Run 44.—The dunes were longer, lower, and more irregularly shaped than those of run 43. The irregular shapes made measurement of dune velocity at the window more difficult. The back of the typical dune was firm and smooth, and the trough was soft and rather rippled. The concentration of nine bed-material discharge samples ranged from 550 to 1,060 ppm, and of four suspended-sediment samples, from 501 to 843 ppm. Concentrations of bed-material discharge were

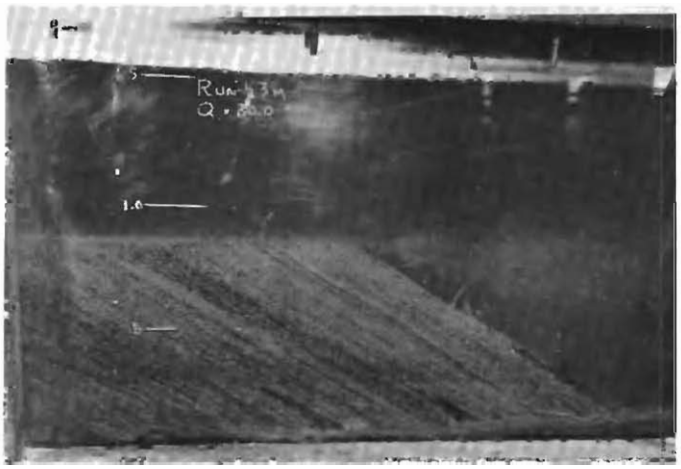

FIGURE 37.—Sliding face of the largest dune (0.75 ft) observed during run 43, viewed from window. Direction of flow is from left to right. Foreslope of the dune is 30°.

considerably lower than normal for the given flow conditions.

Run 42.—This was a dune run that was very similar to run 43. The bed-material discharge of eight samples ranged from 629 to 809 ppm, and the suspended-sediment concentration of three samples ranged from 378 to 481 ppm.

Run 46.—The slope was the same as for run 42, but a substantial increase in discharge planed the bed. Low resistance to flow resulted in a 0.2-foot reduction in depth and an increase in velocity from 2.09 to 3.68 fps. The increased tractive force caused the average bed-material discharge to increase from 704 to 1,670 ppm. The sand bed was firm and smooth, similar to the back of dunes mentioned in descriptions of previous runs. Low (about 0.05 ft) standing waves formed on the water surface throughout the flume and then dissipated. The bed level at any point varied only about 0.03 foot. The concentration of eight bed-material discharge samples ranged from 1,400 to 1,880 ppm, and the concentration of four suspended-sediment samples ranged from 771 to 1,000 ppm.

Run 58.—The depth of flow was shallow and probably inhibited dune growth. Strong vortices in the flow affected the water surface, as is shown in figure 38. The bed was firm except at the crest of the dunes. The troughs were much firmer than those in previous dune runs. The firmness in the troughs was probably caused by the shape of the trough and the height of the dune. Several minor roughness elements about the size of large ripples, but with greater length between crests were seen. After the water had been carefully drained from the flume at the end of the run, some longitudinal formations were noted. (See fig. 39.) The bed-material discharge ranged from 567 to 880 ppm for eight samples, and the suspended-sediment discharge ranged from 240 to 484 ppm for three samples.

FIGURE 38.—Upstream view of water surface during run 58.

FIGURE 39.—Upstream view of the bed configuration at the end of run 58.

Run 47.—This was an antidune run. Wave activity was slow and weak, but waves broke throughout the flume. Some waves moved upstream while others rose and fell without much migration. The concentration of seven bed-material discharge samples ranged from 4,080 to 5,900 ppm, and the concentration of four suspended-sediment samples ranged from 3,230 to 4,360 ppm.

Run 48.—Increasing the slope from 0.00280 (for run 47) to 0.00493 caused more antidune activity to occur than was noted in run 47. Considerable water was stored in the flume when waves broke, thus the level in the tailbox dropped and discharge decreased slightly. Bed level was difficult to locate in the areas where the waves were breaking, because of the large amount of suspended load. Between the breaking waves, in the rapid-flow areas, the suspended-sediment discharge was small but the bed-material discharge was very large. The surface flow conditions are shown in figure 40.

Run 39.—The antidune activity in this run was considerably more violent than that in run 48. Some chute-and-pool activity was noted. (See description of runs 36 and 37, for the 0.19-mm sand.) The discharge was nearly the same as that in run 48, but the slope was increased considerably, the depth was decreased from 0.59 to 0.55 foot, the mean velocity was increased from 4.60 to 4.93 fps, and the mean concentration of bed-material discharge was increased from 9,080 to 28,700 ppm.

Run 41.—Discharge and depth were decreased and slope was increased after run 39. The result was a typical chute-and-pool type of flow. The velocity of flow in the pools just downstream from the breaking waves was essentially zero. Suspended sediment moved in all directions in the pools, but it mainly settled to the bed. The unstable conditions caused very large variations in instantaneous values of velocity, slope, depth, suspended load, and bed load at any point in the flume. Velocity profiles could not be obtained with the available equipment. The concentration of six samples of bed-material discharge ranged from 23,200 to 46,500 ppm, and that of four samples of suspended sediment ranged from 37,400 to 51,800 ppm.

Run 40.—Increased flow and depth caused the flow conditions to be even more unstable than those of run 41. During most of the run, three pools and three chutes could be seen. The rapid flow running into a large wave or pool looked exactly like a hydraulic jump. Air was entrained in the water as the waves broke, just as air is entrained in a hydraulic jump. Many waves were nearly 1 foot high just before they broke. Sediment movement in the area of the waves was so great that the boundary between the flow and the bed could not be located—in fact, it appeared that part of the bed was moving. Figure 41 is a photograph showing a breaking wave or hydraulic jump in the foreground and a variety of flow conditions farther downstream.

FIGURE 41.—Downstream view of flow conditions (chute-and-pool flow) during run 40.

RUNS USING 0.28-MM SAND IN 8-FOOT-WIDE FLUME

These experiments were conducted during the period November 1958–February 1959. The experimental variables and parameters are given in table 4, and the velocity-profile data, in table 14.

FIGURE 40.—Downstream view of water-surface conditions during run 48. Note the breaking antidune near the center of the flume.

Run 7.—The bed was screeded in the direction of the water flow prior to the beginning of the run, so that the particles were arranged in a relatively stable pattern on the bed. A few small grains and an occasional large grain moved when the flow began. After 36 hours, a few ripples had developed near the headbox because of the irregular flow conditions, but no sediment movement was observed in the data-observation area of the flume.

Run 8.—The run was very close to beginning of motion, because small ripples formed downstream to station 40, a few formed at station 90, and a few formed near the end of the flume. In all, ripples covered about 15–20 percent of the flume bed. Ripples would probably have covered the entire bed if the run had been continued for several days.

Run 9.—The bed was raked at the end of run 8. The discharge was unchanged from run 8. Ripples soon formed over the entire bed, and these caused resistance and slope to become greater than those of run 8. The ripples generally extended transversely across the flume, but not in a perfectly straight line. (See fig. 42.) The coarse material armored the troughs and gave the sand waves a starved appearance. The armored troughs were very firm, whereas the ripple waves were soft and thus were different from dunes, which have firm backs.

Run 10.—Ripples formed which looked very much like those formed in run 9. The transverse pattern of the ripples, however, was more irregular, and the movement was more erratic. The stress on the bed seemingly was somewhat greater than that in run 9;

791-597 O—66——3

FIGURE 42.—Transverse view of rippled bed pattern at the end of run 9. Note the armor plate of coarse material in the ripple troughs and the rather regular transverse pattern of the ripples.

yet the armor of coarse material on the bed did not move. The resulting starved ripples did not yield as much sediment to transport as would normally be expected for this sediment, flow, depth, and slope. The run began about 44 hours prior to the beginning of data collection.

Run 5.—The ripples formed in this run were more fully developed than those of the previous runs, but a thick layer of coarse particles was again noted in the troughs of the ripples. The sand was scoured out around the nonmoving coarse particles, and, as a result, the particles were lowered to the zone of lowest sand movement. No suspended sediment was present, and the water surface was very smooth; consequently, the bed was clearly visible through the flow. Eight measurements of bed-material discharge ranged from 5 to 16 ppm.

Run 13.—An extensive study of the effect of time on equilibrium was done during this run. Data collected December 11, about 24 hours after the start of the run, was not significantly different from data collected on December 15. The bed roughness was made up of fully developed ripples, few of which had characteristics almost like those of dunes. These few large forms caused some disturbance of the water surface. Many ripples not only moved downstream, but also, moved laterally several tenths of a foot. The rapidly changing form of the ripples made measurement of their velocity difficult. Also, observations of the velocity of specific ripples were ruined when the observed ripple either was overtaken by a faster moving ripple from upstream, was invaded by a ripple from the side, or overtook another ripple. The ripple velocity is affected by the size of the ripple and the flow and transport conditions in the vicinity of the ripple. Bed-material discharge ranged from 58 to 88 ppm for 10 observations. The sediment from four suspended-sediment samples was composited in the laboratory, so that a range cannot be given.

Run 4.—This was a ripple run. Figure 43 is an upstream view of the ripples after the water had been carefully drained from the flume. The water surface had only a few minor surface disturbances. Little or no suspended sediment was present. Coarse particles moved slowly and intermittently, while the finer sand moved from around the larger particles.

Run 11.—The ripples were more irregular than those formed in previous runs, at flatter slopes. They were deeper and the distance was greater from crest to crest. The coarse material did not influence the shape of the ripples, and movement occurred in the same manner as in previous runs of this set. Again, the finer sand was eroded away from the coarse particles, so that the rate of transport of the coarse particles was reduced. The bed-material discharge ranged from 18 to 22 ppm for eight observations. There was no suspended sediment in the flow.

Run 33.—This run was designed to provide data to fill a gap in those for the dune range of bed roughness. Ripples formed on the dunes except on the back of the very largest dunes. The top of most dunes rose and fell as ripples caught up with the dune crest. The counter-circulation in the dune troughs was very weak. The angle of the avalanche face of the dunes ranged from 23° to 30°, depending on the form of the dune

FIGURE 43.—Upstream view of the rippled bed form at the end of run 4.

and the amount of counter-circulation in the trough. The bed was very soft at all locations. Bed-material discharge ranged from 238 to 400 ppm for nine observations, and suspended-sediment concentration ranged from 195 to 558 ppm for four observations.

Run 1.—The bed form consisted of relatively large dunes with a profuse pattern of ripples superposed. The ripple pattern was very hetrogeneous as a result of the irregular flow patterns around the dunes. Suspended-sediment concentration seemed very uniform vertically, and the eddies (boils) of the water surface downstream from the dune crests were not particularly strong. The slope for this run was poorly defined.

Run 12.—The run began about 16 hours prior to data collection. The general bed roughness was classed as ripples, but it contained a few elements which looked like poorly developed dunes. The coarse particles did not influence the roughness elements. These coarse particles either settled in the sand as the finer material was eroded away from them, rolled downstream to the next trough, or, occasionally, rolled upstream into a deeper part of the ripple trough. The upstream movement occurred only in the zone of reverse flow in the trough of a dunelike form. The bed was very soft. The water surface was rougher than that of most ripple runs, and some suspended sediment was present, indicating that the flow was approaching the dune condition. The ripples rapidly changed form, size, and shape; thus, measurement of ripple velocity was very difficult.

Run 14.—The run began December 15 and continued to December 17, when the final data were recorded. The mean slope at 0800 December 16, 1500 December 16, 0800 December 17, and 1045 December 17 was 0.00122, 0.00109, 0.00122, and 0.00118, respectively. The roughness on the bed was mainly ripples and a few larger elements resembling dunes. (See fig. 44.) Some sediment moved in suspension. The water surface was more turbulent than in the preceding ripple runs; but, despite the small quantity of suspended sediment, the streambed could still be seen through the flow. The bed was very soft. Accumulation of coarse material on the bed was not excessive. Small ripples moved over larger ones and seemed to consist of sand finer than the average in the bed.

FIGURE 44.—Upstream view of the dune-bed configuration at the end of run 14.

FIGURE 45.—Upstream view of the dune-bed configuration at the end of run 20.

Run 20.—The bed condition for this run consisted of dunes, as is shown in figure 45. The bed was very soft in the troughs but firm on the back of the dune upstream from the crest, where the depth was at a minimum and the velocity was at a maximum. The area in the trough and immediately downstream from the trough contained ripples. Some dune faces were very round, and the counter-circulation in such places was weak and intermittent. The dune face generally was of the normal type shown in figure 46. The angle of the dune face was generally between 25° and 27°, but occasionally as low as 20° or as much as 30°, depending upon the strength of the counter-circulation in the dune trough. The coarse particles rolled readily from the downstream part of the trough area up the back of the dune and then slid down the face of the dune until they came to rest. After coming to rest they were buried and were not exposed again after passage of the dune. Such large particles were never seen in suspension. Twelve measurements of bed-material discharge ranged from 365 to 754 ppm, and 3 measurements of suspended-sediment concentration ranged from 323 to 373 ppm.

Run 2.—This run was very similar to run 20 except that the dunes formed were lower and longer. The

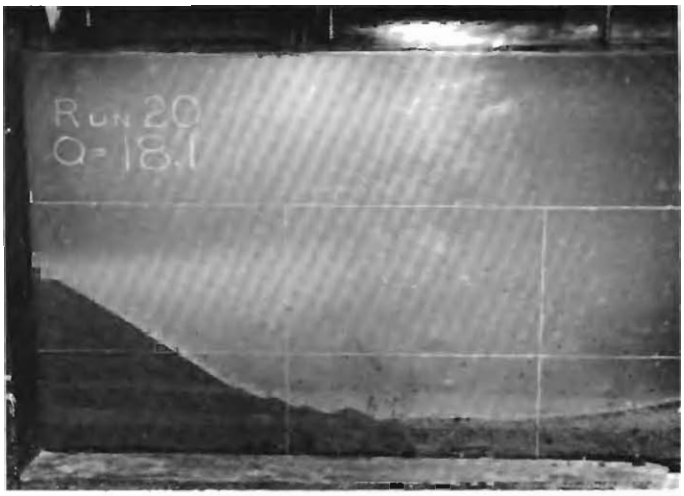

FIGURE 46.—Avalanche face of a large dune formed during run 20. Direction of flow is from left to right.

flatness of the dunes, compared with those formed in run 20, was probably due to the shallower depth and somewhat greater slope during run 20. Again, the bed was firm and crusted on the back of the dunes and soft on the dune crest and in the trough. Boils on the water surface marked the separation zone, and large-scale eddies occurred downstream from the dune crest. The slope was poorly defined.

Run 21.—Very few ripples were associated with the dune pattern for this run. As in runs 20 and 2, the distance between dunes was great, but the dune height was somewhat less than in runs 20 and 2. The water surface was relatively smooth over the back of the dunes; but it was very turbulent, because of large boils over the troughs and slightly downstream from the troughs. The water surface stood high over the trough, relative to that over the back of the dunes, because of the change of velocity head as the flow moved from one area to another.

Run 19.—Except for flow depth, which was shallower, the flow conditions and bed forms were very similar to those of runs 2 and 21. The shallower mean depth caused the eddies and turbulence to be stronger and the dunes smaller.

Run 16.—The large dunes moved faster than in preceding runs. The rate of transport of sediment by the sand waves was very high, but the limited sand depth on the bed of the flume seemingly was not adequate to allow full-scale roughness to develop—some troughs extended to the floor of the flume. The dunes traveled through the flume at all elevations. Occasionally, a dune crest formed just upstream from a short trough that extended below the average downstream bed elevation. The jet from the crest of such a low dune, in its effort to "normalize" the dune and the trough, impinged on the downstream edge of the trough and caused very rapid erosion of the trough. Rate of dune movement for a given height of dune was not constant, because the main current was sometimes directed around an area by upstream forms, and because part of the sediment in transport was sometimes captured by a dune immediately upstream from the one being observed. The slope was poorly defined.

Run 23.—This was a transitional run in which the bed forms oscillated between dunes and washed-out dunes. Dunes generally existed when resistance was relatively great and slope was steep. Then the dunes seemed to vanish, and resistance and slope decreased to the point where dunes again developed. The cycling between dunes and washed-out dunes probably resulted from the change in depth and slope that occurred when the resistance changed with a change in bed form. Some cycling may have resulted, however, from segregation of the bed material into different sizes for different dunes because it was observed that dunes of fine, coarse, and intermediate sized material passed by the observation window. Large boils resulting from eddies near the dune trough and the rapid flow over the irregular bed configuration caused the water surface to be very turbulent.

Run 17.—The slope was nearly the same as that of run 16, but the depth of flow had been reduced considerably. Dunes formed which rapidly changed shape and direction of motion. The water surface had an appearance typical to that over a dune bed. More surface turbulence, in the form of small waves, occurred than in runs with greater depth of flow.

Run 3.—With depth increased (at the same slope) over that for run 17, dune height and length increased. As in run 17, most dunes moved. Small dunes moved faster than large ones, and small dunes in shallow fast water moved faster than small dunes in deep slow water. When a small dune approached a large dune and began taking sediment from it, the large dune stopped (or nearly stopped) until the small dune caught up. The result was a new dune. The bed was firm on the back of the dunes upstream from the crest and was very soft on the crest, on the avalanche face, and in the trough. The slope for this run was poorly defined.

Run 18.—The bed condition for this run was a typical dune bed. Ripples formed in some of the deeper troughs. Large eddies formed downstream from the dune crests, or over the troughs, and carried much sand to the water surface; the suspended load was large in these areas. On the back of the dunes, upstream from the crest, particles moved mostly in contact with the bed. Suspended-sediment concentration

was small enough in this zone that both the bed and the "sheet" of moving sand could be seen.

Run 30.—The flow was tranquil, and the bed was nearly plane. An occasional dune or bar less than 0.1 foot high was seen moving through the flume. The bed was not soft, but neither was it as firm as during a plane-bed run with greater velocity. The run was classed as transitional between dunes and plane bed.

Run 34.—The depth of flow was shallow, and the bed configuration was reduced almost to ripples. Figure 47, a photograph taken after the water had been drained from the flume, shows ripples on the left and small dunes with ripples on the right. The slope was steeper than for previous runs having fully developed dunes. The suspended load was negligible, and the total load was small for this slope.

Run 22.—A plane bed and little resistance to flow were the significant characteristics of this run. The elevation of the bed varied no more than 0.01 foot about the mean. Most sediment transport was near the bed, and the coarse material rolled along at a rather uniform rate. Run 22 has nearly the same slope as run 34, but the rate of flow has been increased from 5.5 to 14.9 cfs. The increased flow caused the depth to increase from 0.44 to 0.60 foot even though the resistance decreased from 0.021 to 0.013 (Manning n). The rate of energy input, or in this case depth of flow, strongly affects other variables.

Run 15.—Reducing discharge from that of run 22 (14.92 to 12.87 cfs) caused the bed form to change to fully developed dunes. With this increased roughness, the mean depth increased from 0.60 to 0.75 foot and the mean velocity decreased from 3.11 to 2.14 fps. The dunes ranged from 0.3 to 0.5 foot in height and were as much as 30 feet apart. The wide spacing of the dunes resulted in a large variation in the amount of bed-material discharge at the tailbox. Twelve samples, collected there over a long period of time (0820–1155), had concentrations ranging from 674 to 998 ppm. Suspended sediment in four samples ranged from 358 to 419 ppm.

FIGURE 47.—Upstream view of bed configuration at the end of run 34.

Run 24.—The bed configuration was transitional between dunes and plane bed. The dunes were very irregularly spaced and had an amplitude of 0.2 to 0.4 foot. The avalanche angle of a typical dune in this run was small, and the flat trough inhibited counter-circulation. Occasionally a dune formed that had a more normal avalanche angle and a trough with some counter-circulation. The water surface was very choppy. The flow expanded, or decelerated, over the dune troughs and contracted, or accelerated, over the crests; hence, surface waves formed. Eddies in the dune troughs did not reach the water surface.

Run 25.—The bed of sand in the flume was firm and plane. It fluctuated vertically no more than 0.05 foot at the window. The water surface was smooth compared with that in the dune runs and transitional runs. A minor disturbance on the water surface was generated downstream from station 50 by a wall roughness. Figure 48 shows the flow and bed conditions of this run. Much of the material that rolled along the bed was coarser than the average bed-material size. The windrow effect, or lines of coarse particles, may have been caused by secondary circulation.

Run 28.—The flow variables and resulting plane-bed configuration were nearly the same as for run 25. Most sediment transport occurred close to the bed.

Run 29.—For this plane-bed run, slope was increased from that for run 28. As a result, velocity increased from 3.57 to 3.77 fps and sediment transport increased from 2,760 to 3,120 ppm. The bed and water surfaces, as seen through the window, slowly varied about 0.1 foot, approximating a standing-wave condition.

Run 26.—The increased slope over that of run 29 (from 0.00278 to 0.00328) resulted in a flow pattern of standing waves and an occasional breaking wave. The standing waves built up near stations 35–40 and traveled down the remainder of the flume to the tailbox. The largest waves formed near the tailbox. Waves extended the full width of the flume except when they were first forming. Some of the waves moved upstream; and, of these, some broke and some did not.

Run 32.—The flow conditions (antidunes) were similar to those described for run 31, except that wave

A

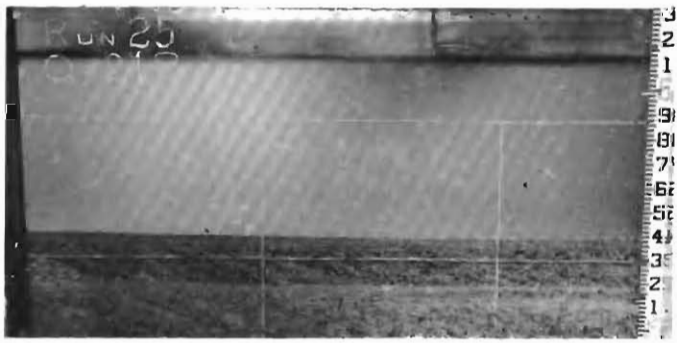

B

C

FIGURE 48.—Flow and bed conditions for run 25. *A*, Water surface during flow. *B*, View through the side window. *C*, Flume bed after draining the flume at the end of the run.

activity was not as great and the total-sediment transport was much less.

Run 27.—This was an antidune run. Much breaking-wave activity occurred, but seldom did more than three waves break at one time. Some waves moved upstream and subsided without breaking. The waves extended most of the way across the flume except when they first began to form. The coarse fraction of the bed material may be an important factor in causing the sand waves to move upstream, because much of the coarse material that eroded from the downstream part of the sand wave moved only to the upstream slope of the next sand wave.

Run 31.—Violent antidune action occurred throughout the flume. The waves were large, and as many as six or none at all may have been breaking at a given instant. Figure 49 shows the flow conditions downstream from near the middle of the flume. Near breaking waves the mean velocity of the water was reduced to nearly zero, and sediment moving into this region was lifted into suspension. As the flow accelerated and smoothed out to a plane-bed condition, the zone of maximum transport shifted toward the bed. The plane-bed condition gradually evolved into a low-standing wave, and then into a higher wave that moved upstream prior to breaking. Small rollers turned from the flow toward the bed on the upstream side of the sand waves as they broke. The bed was firm in the trough, firm on the downstream side of the waves, softer on the upstream side of the sand wave, and much softer on the crest or peak of the sand wave.

Run 35.—Conditions for this run were similar to those for run 31 except that slope was increased from

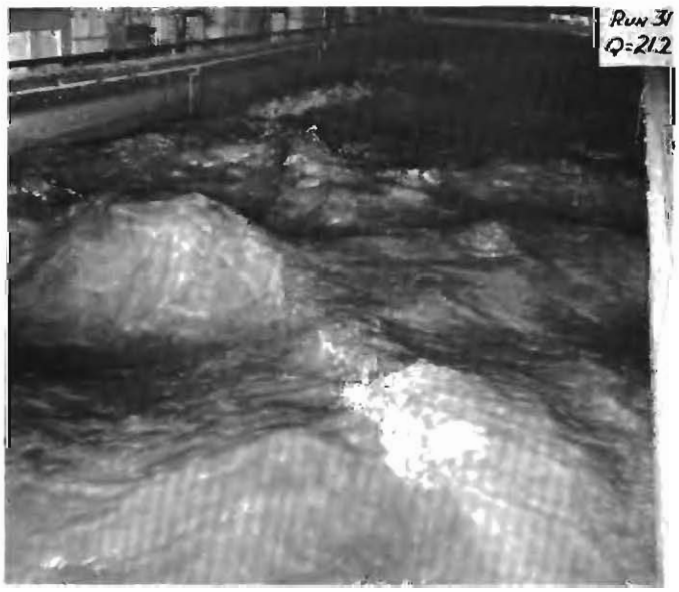

FIGURE 49.—Downstream view of antidune flow conditions during run 31.

0.00593 to 0.00815. This caused a greater number of violent antidune waves of larger amplitude to form and caused the transport rate to be more than double that in run 31. The mean velocity and depth did not change appreciably from run 31, but resistance to flow increased.

Run 37.—Discharge and depth were much less than in runs 35 and 31, and the size of the waves formed and the violence of the antidune activity were accordingly less. Breaking waves were farther apart. Many waves built up to near the breaking elevation, and then the sand appeared to be pushed out from under the water wave and the wave subsided without breaking.

Run 38.—The discharge for this chute-and-pool run was intermediate between that of runs 37 and 36. Although the slope and the tailgate setting were not changed for the three runs, the slope and the flow conditions changed considerably as a result of the change of shear stress on the bed with the change in rate of discharge. The flow conditions were very violent. A series of three or four chutes and pools formed in the length of the flume, each with rapids, large standing waves, breaking waves, and a pool, in downstream order. Figure 50 is a sketch of this phenomenon as seen through the window. The pool was like a small hydraulic jump or stilling basin, where sediment was brought into full suspension and then settled onto the bed at the lower end of the pool, at the head of the next sand wave and chute. The sediment-transport rate was higher for specific slope, depth, and bed material than was expected for the antidune roughness.

Run 36.—This run was similar to run 38 except that the discharge was increased and the chute-and-pool activity was, therefore, more intense.

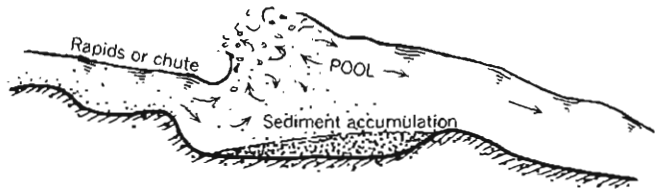

FIGURE 50.—Sketch of chute-and-pool phenomenon as viewed through the window in the wall of the flume. The vertical scale is exaggerated 3–5 times. Each chute-and-pool series is 20–30 feet long.

RUNS USING 0.45-MM SAND IN 8-FOOT-WIDE FLUME

This was the first set of runs completed for the project. The notes were not as complete as for other sets, and the data-collection system lacked some refinements which were developed later. The significant differences in data-collection methods between this set and other sets are:

1. For runs having antidune flow, depth was measured only in areas where the water surface was relatively smooth; thus, the measured depth is too shallow.
2. Fewer bed-material discharge samples were taken over a shorter period of time, causing a greater error in the mean.
3. Slope was determined by averaging the several readings taken at different times every 5 feet along the flume and then computing a least-squares regression from these averages. The slope for other sets of runs was determined by plotting each and (or) the average of several slope measurements on graph paper and then visually drawing the mean slope line through these points. The water-surface elevation from which the slope was computed for antidune runs was only obtained when the water surface was relatively smooth. The water-surface elevation and depth for the other sets of runs were taken at random times at a given flume station. A system for taking good pictures was lacking for several runs in this set.

These experiments were conducted during the period January–July 1957. The experimental variables and parameters are given in table 5, and the velocity-profile data, in table 15.

Run 14.—The flow for this run was increased from 1.84 cfs (run 13) to 3.94 cfs. The velocity increased from 0.65 to 0.81 fps, and the shear stress was below beginning of motion.

Run 13.—The bed was planed to a slope of 0.00010 prior to the beginnning of the run. The bed material did not move under the given flow conditions.

Run 17.—The flow for this run had sufficient shear stress to move particles into a configuration of ripples, which averaged 0.77 foot long and 0.04 foot high. All transport was on or very close to the bed. No sediment was in suspension.

Run 16.—The transport rate of 1.2 ppm for this run was in equilibrium with the low-ripple bed configuration. The ripple waves transported sand much finer than the sand remaining in the troughs. This made the ripples appear "starved," as in ripple runs with the 0.27- and 0.28-sands.

Run 15.—The run began March 4, 1957. Several adjustments of the tailgate were made prior to 1700 March 6, by which time ripples had formed over the full length of the flume. At 0800 March 7 the slope, transport, and bed configuration were stabilized throughout the flume. The bed slope was 0.00021, and the water-surface slope was 0.00023; thus, flow conditions were nearly uniform. The concentration of

five bed-material-discharge samples taken March 8 ranged from 0.26 to 1.38 ppm. This large range reflected the uneven transport at the end of the flume caused by the transverse pattern of waves moving in the flume.

Run 18.—The bed was not planed after run 17. The discharge was reduced from 6.22 to 3.62 cfs, and the slope was increased from 0.00020 to 0.00031. These changes did not alter the ripple-bed configuration appreciably from that of run 17. (See fig. 51.) The mean bed-material discharge was reduced from 0.7 to 0.4 ppm.

Run 2.—The bed was screeded to a slope of 0.00050 before the run began. The mean bed-material discharge was 9.4 ppm, about 10 times greater than that for the previous runs. Ripples on the flume bed had greater spacing and amplitude than those for the runs already described. The ripples were more random with respect to size, shape, and location on the bed. They no longer had a well-arranged transverse pattern, and sorting of the sand was no longer noticeable.

Run 3.—The flow conditions and ripples of this run were similar to those in run 2. The slope was increased and the velocity decreased because of increased resistance. The bed-material discharge was increased by less than 10 percent.

Run 9.—The discharge of this run was reduced from 7.90 cfs (run 3) to 3.84 cfs. The result was a ripple run with little bed-material discharge. The concentration of five bed-material discharge samples ranged from 0.8 to 1.8 ppm.

FIGURE 51.—Transverse view of the ripples formed during run 18. The flow was from right to left, and the scale is 1.3 feet long. The crests of the ripples contain finer sand than is found in the troughs.

Run 1.—This run was nearly the same as runs 2 and 3, except that the slope was increased, and this caused a reduction in the resistance to flow. The reduced resistance to flow may have been the result of the longer, relatively lower and more rounded ripples. Either the measured bed-material discharge was too high or the slope was too low compared with other runs of similar bed-material characteristics and energy of flow.

Run 5.—The bed was screeded to a slope of 0.00050 before the run began. The mean slope of the water surface was 0.00047 at the time of data collection. The flow and bed-material-discharge conditions were nearly the same as those of run 1, but the ripples were smaller.

Run 11.—The slope was set at 0.00070 until ripples formed, and then it was reduced to 0.00050. The final slope was 0.00049. Discharge was reduced from 7.93 cfs (run 5) to 1.95 cfs. The shear stress was sufficiently low that the bed-material discharge was less than 20 percent of that of run 5. The ripple pattern was very uniform, and the pattern of ripple waves was mostly perpendicular to the direction of flow.

Run 4.—The bed configuration was low dunes and ripples. The resistance to flow was less than for regular ripple conditions and resulted in greater velocity and shallower depth than in previous runs of this set. Seventeen observations of bed-material discharge ranged from 67 to 140 ppm and had an 18-ppm standard deviation from the 92-ppm mean. Either the sediment concentration was too high, or the slope measurement was too flat in comparison with "normal" conditions found from similar runs.

Run 8.—Reducing the rate of flow from that of run 4 resulted in reduced velocity, depth, and bed-material discharge. The bed configuration was ripples.

Run 7.—Bed features formed were dunes 4–8 feet long. Many of the dune troughs were 0.4 foot deep. Small ripples were seen on the crest of the dunes. Ripple waves were spaced about 0.3 foot from crest to crest and ranged from 0.02 to 0.06 foot in height. The reported concentration of bed-material discharge was about double the normal value for these flow conditions.

Run 10.—The shallow depth and low rate of flow reduced the shear stress on the bed so that apparently, only ripples formed on the flume bed. The configuration was nearly that of a staggered pattern of individual ripples.

Run 6.—The bed configuration was a transverse pattern of ripples across the flume. A diagonal pattern (about 45°) of slightly larger forms was also evident. The transverse bed waves were about 0.08 foot high and 0.7 foot apart. The diagonal waves were about

0.15 foot high and 2.5 foot from crest to crest. No sediment was in suspension.

Run 12.—The shallow depth of this run caused a low bed-material discharge and a rippled bed configuration. The shallow depth also accentuated the effect of a backwater curve from the tailgate. This backwater curve reduced the bed-material discharge near the tailgate compared with the discharge near the central part of the flume. The total measured transport may be too low by a factor of 10–20. The other measurements of basic data probably were satisfactory.

Run 19.—Dunes formed which were 3–8 feet long and almost completely covered with ripples. The dunes had a maximum height about equal to the mean flow depth. Many dune crests moving down the flume were normal to the flume walls, but some were 20–30° from the normal. The resistance to flow seemed to be less than in runs in which fully developed dunes formed.

Run 21.—Flow was increased from 4.24 cfs (run 19) to 12.12 cfs. This increase in flow caused the depth of flow to more than double and caused the velocity to increase from 1.30 to 1.58 fps. The bed-material discharge also was nearly doubled. Figure 52 is a view of the dune-bed configuration in the flume after carefully draining the flume at the end of the run. The fin or longitudinal dune in the foreground is evidence of transverse-flow components resulting from either secondary circulation or flow diversion around the upstream dunes, or both. The spacing of the ripples on the dunes varied from close in the deep troughs to wide, and even obliteration, on the crest.

Run 22.—The bed configuration and resistance to flow were nearly the same as for run 21. A small increase in flow rate caused the bed-material discharge to increase.

FIGURE 52.—Upstream view of the dune-bed configuration at the end of run 21.

FIGURE 53.—Upstream view of the dune-bed configuration at the end of run 25.

Run 25.—Low discharge and shallow depth caused the dune height to be less than in runs 21 and 22. Figure 53 shows that the dune pattern was more regular than in the previous runs. The avalanche faces were normal to the flow and averaged about 6 feet in width. The orientation of the ripples, although not continuous on the dunes, indicated the direction of flow over the dunes.

Run 20.—The flow and transport conditions resulted in a dune-bed configuration and an overall resistance to flow transitional between those of runs 25 and 21. The bed-material discharge was nearly the same as that of run 21, which had the deeper flow, because of the much higher slope.

Run 23.—The flow rate for this run was about the same as that for runs 21 and 22, but the slope was about double. The dunes had a more natural appearance than those of run 25. Compare figures 53 and 54. The dunes appeared to consist of slightly coarser material than that seen on the surface of the trough. The finer material in the trough settled out of suspension as a result of the lower velocity of flow over the trough area.

Run 24.—The dunes that formed on the bed were similar to those formed in run 23, but somewhat smaller. The resistance to flow and the bed-material discharge were greater than for the previous run.

Run 40.—The water surface was extremely turbulent, and the waves were neither symmetrical nor smooth-surfaced. Some disturbances on the surface could be correlated with points of maximum roughness on the bed. Slope measurement was difficult because of the rough water surface. The water surface in the area

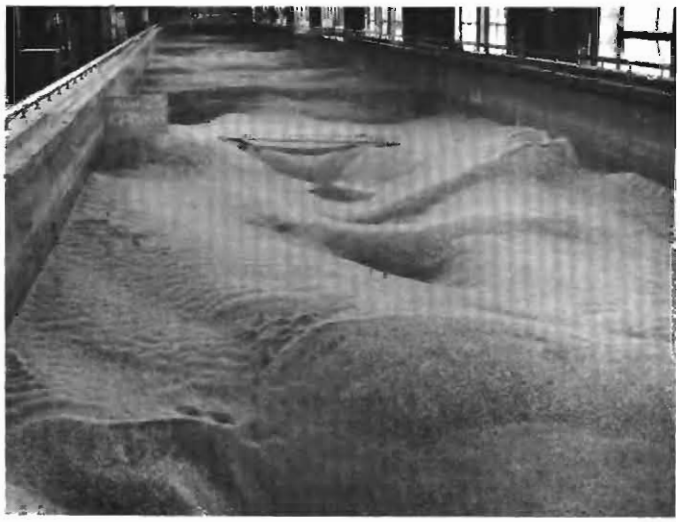

FIGURE 54.—Upstream view of the dune-bed configuration formed during run 23. Note that the dune wave and avalanche face consist of coarser material than is in the trough.

of a boil stood several hundredths of a foot higher than in the surrounding area. Both horizontal and inclined bedding planes were observed through the window as the dunes moved by at different levels. The inclined bedding planes were on the avalanche face of the dunes and appeared to be formed of material somewhat coarser than the median diameter of the bed material. The horizontal layers were composed of suspended sediment deposited in the trough of some dunes and appeared to be somewhat finer than the median diameter of the bed material.

Run 39.—Slope was 0.00364 and discharge was 2.58 cfs per foot of width. All dune roughness was planed out. A train of well-rounded standing waves traveled from near the entrance of the flume to the exit. The water surface was much smoother and the bed was firmer than in the dune runs. A train of inphase sand waves formed under the water waves, the reverse of the phenomenon observed for the dune forms. The relative variation of bed-material-discharge concentration was much less than for the dune runs.

Run 26.—This was a plane-bed run. The flow was essentially the same as described for run 39 except that no standing waves or undulations in the bed elevation occurred.

Run 28.—The flow of this run was in a transition phase. One side of the flume had low washed-out dunes, where the water surface was out of phase with the sand waves; and the other side had low standing waves, where the surface was inphase with the bed waves. The amplitude of both kinds of sand waves was much smaller than that of the water waves. The proportion of the two kinds of flow changed considerably with time.

Run 29.—Long flat dunes formed during this run, each with an avalanche face as much as 0.15 foot high. A typical observation showed smooth flow 0.25 foot deep on the back of the dune and, after the flow passed a 0.10 foot high avalanche face, turbulent flow 0.42 foot deep in the trough area. The water surface was actually 0.07 foot higher over the dune trough than over the smooth back of the adjacent dune.

Run 31.—The flow lines were relatively straight, and the water surface was relatively smooth, except for rounded standing waves which generally developed slowly into trains. Small ripples formed near the wall of the flume. They were probably due to the wall effect and did not extend into the flow more than 1 foot. Some water waves near the tailbox became steep and broke.

Run 27.—The moving bed forms were low alternate bars, which caused the flow to meander. Some standing waves formed in the flume, and occasionally a wave would break gently. The standing-wave condition seemed to alternate with the plane-bed condition. (See fig. 55.)

Run 36.—The low discharge (3.15 cfs) and shallow depth (0.19 ft) for this run accentuated formation of the alternate-bar type of flow mentioned for run 27. The bars were 0.1–0.2 foot high and generally occupied about half the flume width. Shallow flow over the bars moved sediment and deposited it at the downstream edge of the bar; thus, the bars slowly migrated downstream. In the deeper flow, which moved from side to side in the flume, around the bars, antidunes formed. Generally the antidunes were standing waves, but occasionally a wave broke. Figure 56 shows the water surface during this run and the bed condition at the end of the run, after the flume was drained.

Run 41.—A train of standing waves formed in the middle half of the flume. The standing waves were a train of sand waves under inphase water waves. The waves generally increased somewhat in height as they traveled along the flume. The waves occasionally migrated slowly upstream or downstream, but they generally were nearly stationary. The height of the water waves varied 0.20–0.25 foot from trough to crest, whereas the height of the sand waves varied 0.12–0.16 foot from trough to crest. The bed was very firm where the water surface was smooth, but it was either soft or firm under waves.

Run 30.—The flow in this run was similar to that described for run 36. The thalweg wandered from side to side along the flume and contained an occasional small antidune. The water surface was more wavy over the entire flume than it was for run 36. These waves averaged about 0.2 foot high and 1.2 feet from

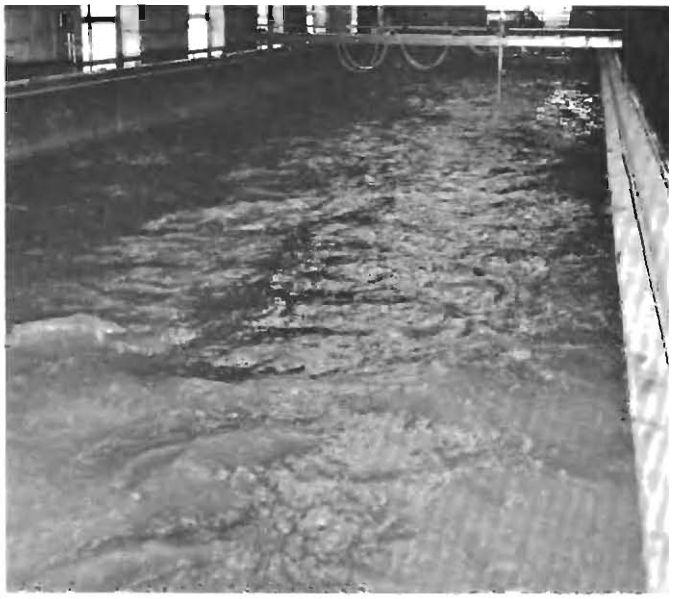

A

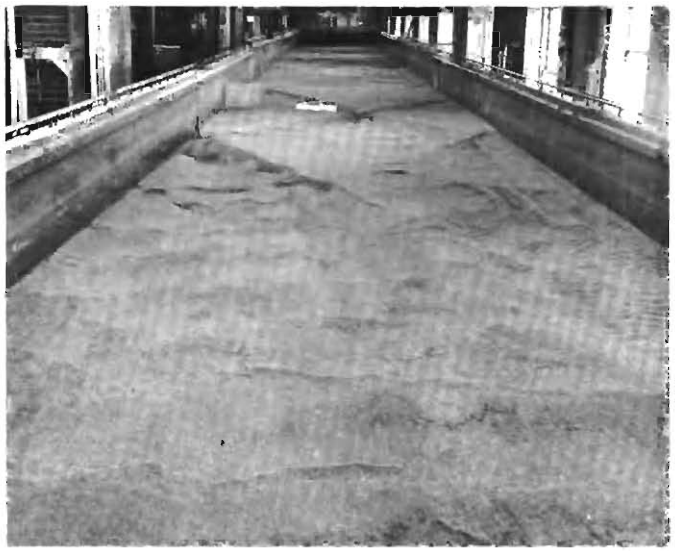

B

FIGURE 55.—Flume conditions for run 27. *A*, Water surface downstream from station 100. *B*, Diagonal bars formed by flow upstream from station 100.

A

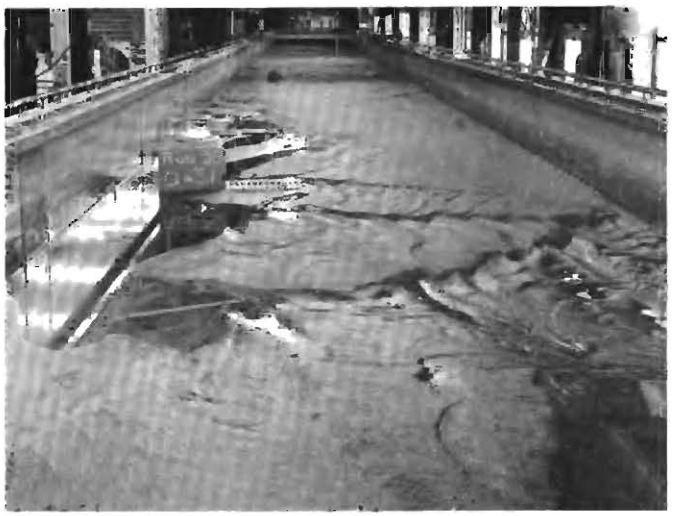

B

FIGURE 56.—Upstream views during and after run 36. *A*, The water surface. *B*, The bed after the flume was drained. Note that the main thread of streamflow is on the left side of the flume in the area of the sign and then moves downstream toward the right side of the flume toward the lower right corner of the photographs.

crest to crest. The alternate bars were 0.2–0.3 foot high on the downstream or avalanche edge. Waves on the bed under water-surface waves had a pattern similar to that of the surface waves, but they were less than half as high.

Run 35.—This run was similar to run 30 except that the alternate bars which formed were not as prominent and the standing waves were more evenly spaced in the flume. Some standing waves occasionally moved upstream, but they generally remained in one position, growing in amplitude and then gently receding.

Run 34.—The slope, depth, and velocity were greater than those of run 35. A series of standing waves formed.

Run 33.—The mean velocity was 4.60 fps compared with 2.80 fps for run 35. The standing-wave flow pattern occurred at varying rates of mean velocity for several runs. Occasionally a train of small antidunes formed and moved upstream without breaking (standing waves). These waves grew in amplitude and then gently receded to a plane bed. The resistance to flow was very low.

Run 38.—The flow was deeper than for run 33, and standing waves formed from wall to wall across the flume at approximately right angles to the flow. More waves moved upstream than moved downstream. No waves broke.

Run 37.—The flow conditions were very similar to those of run 38. The train of standing waves extended from wall to wall in the flume. The waves varied greatly in size, but never disappeared nor broke. The channel bed was very firm and, as seen through the window, appeared to be horizontally bedded. Clouds of suspended sediment extended up through about two-thirds of the flow depth.

Run 32.—The size of the water-surface waves increased with distance downstream in the flume. During most of the run, a train of antidunes existed between stations 40 and 95. These dunes continuously built up, broke, and then reformed. (See fig. 57*A*.) From station 105 to the end of the flume, the dunes and resulting water waves extended the full width of the flume (See fig. 57*B*.) The antidunes did not move upstream very much during their buildup. The waves on the bed surface under the main train of water waves were inphase with the water waves and had an amplitude about one-fourth that of the water waves. Most sediment moved near the bed, but some suspended sand was seen in the top part of the larger waves. Wave activity at the side window was mild compared with that in midstream; small inphase waves migrated downstream, and the amplitude of the bed undulations under them was about one-fourth that of the water waves. The bed undulations were still apparent after the flume had been drained at the end of the run. They extended all the way across the flume, were generally less than 0.1 foot high, and appeared to be parallel to each other and perpendicular to the flow direction.

Run 45.—The water-surface condition varied widely, from plane, to antidune waves (either breaking or standing), to trains of waves extending nearly the full length of the flume. The sand bed was firm except where the antidunes broke (see fig. 58). Very heavy concentrations of sediment moved, mostly near the bed. Analysis of data showed that the concentration was about double that ordinarily expected for the imposed hydraulic conditions.

Run 44.—Antidune waves formed just to the left of the center line of the flume, generally in a single train, but occasionally in a double train. The waves moved slowly upstream until they broke. New waves that formed downstream from the breaking position continued the process, so that net upstream movement was minor. The bed was firm except under the crest of a breaking wave. Mean flow depth for this run was shallow (0.28 ft), so a given antidune sand wave was generally higher than the adjacent trough of the water wave.

Run 42.—The flow condition and the bed configuration for this run are similar to run 44 even though the slope was steeper, the discharge, depth, and velocity were greater, and the bed-material discharge was less.

Run 43.—Wave activity was very diverse. The waves generally occupied the full width of the flume and formed and broke rather quickly compared with those formed in runs described previously. When several of these large waves broke at once, the flow velocity was greatly reduced and considerable water was stored in the flume. The result was a lowering of the water level in the tailbox and, consequently, a reduction of the discharge of the pumps. Thus, the rate and magnitude of discharge variation depended on the antidune activity.

RUNS USING 0.93-MM SAND IN 8-FOOT-WIDE FLUME

Data for these runs were collected during the period March–July 1960. The experimental variables and parameters are given in table 6, and the velocity-profile data, in table 16.

Run 19.—The bed was screeded to a plane prior to this run. Then flow was carefully increased until several particles close to incipient motion had settled into a more stable position. No sediment was moving when the hydraulic data were collected. Resistance to flow due to the stationary sand grains was computed (table 6).

Run 25.—The flow depth was the same as for run 19, but the slope was greater and, consequently, the velocity was 1.22 instead of 1.00. No sediment movement occurred.

Run 26.—Discharge was increased about 10 percent over that for run 25, and the resulting shear stress and a mean velocity of 1.32 fps were sufficient to cause some movement of particles finer than 1 mm. The movement of the grains was very random and infrequent. The rate of bed-material discharge was too low for reliable measurement.

Run 27.—Further increase in the shear stress over that in run 26 caused general movement of all particles except those larger than about 2.0 mm. The bed-material discharge, determined from a composite of six samples, was 2.8 ppm.

Run 20.—The slope for this run was the same as for run 27, but the discharge and velocity were less. The measured bed-material discharge was about 0.4 ppm, but data from other runs indicated that it should have been about 2 ppm. The slope was more than double that for run 19, and the velocity was about one-third greater. The bed seemed denser than that in run 19 because of the fact that particles fell to a lower elevation on the bed as they moved in run 20.

A

B

FIGURE 57.—Flow conditions during run 32. *A*, View downstream showing train of antidunes near station 80. *B*, View upstream from station 125 showing large antidunes occupying full width of flume, and narrower antidunes from station 95 to the head of the flume.

Run 21.—The slope and discharge were increased for this run over those for run 20. Some particles moved constantly, but the largest ones moved only occasionally. The bed was very plane, and the largest grains were gradually buried. The water surface was smooth but not as glassy as in runs 19 and 20. The measured bed-material discharge (0.4 ppm) was about one-sixth that normally expected for the given flow conditions.

Run 18.—A series of very low dunes or sand waves formed along the left wall of the flume. They tapered down to the plane bed along the right side of the flume. Some armoring occurred in the areas of greater boundary shear stress as a result of sorting of the fine material from the coarse. At least 99 percent of the bed-material discharge (21 ppm) moved in contact with the bed, so the water remained very clear.

Run 28.—The discharge was about 10 percent greater than that in run 18, but the slope remained the same. Low dunes formed in a pattern similar to that in run 18. The dunes in this run, however, extended farther across the flume than did those in run 18.

Run 29.—The slope was increased over that of run 28, but no sediment moved because of the low shear stress. The low shear stress resulted from a reduction in velocity (from 1.75 to 1.16 fps) and in depth (from 1.04 to 0.50 ft).

Run 22.—This run was nearly identical with run 29.

Run 30.—The velocity was increased to 1.25 fps by increasing both slope and discharge. Only particles less than about 1.0 mm in diameter moved.

Run 31. This was the first of the shallow-depth (about 0.5 ft) runs with the 0.93-mm sand during which there was general transport of the sand on the bed. No sand waves or dunes were seen, but some sorting of the fine and coarse material was noted. Movement of fine material occurred about 0.5 foot from the walls of the flume and was parallel to the direction of the flow. A few small depressions or pockets were eroded in the bed. No sand waves were seen downstream from such erosion pockets.

Run 15.—Very small regular dunes about 0.10 foot high formed and moved slowly downstream. These dunes were typical of those obtained with finer sands, except that they were perhaps more regular and more closely spaced. They looked like those of run 14 shown in figure 59. The water surface was calm except downstream from dune crests, where small boils were generated by eddies. The bed was easily seen through the flow, because the amount of sand in suspension was very small.

Run 23.—Conditions were similar to those in run 30 except that the velocity was 1.30 instead of 1.25 fps. No particles larger than about 1.5 mm moved. The bed-material discharge was greater over patches of finer material. Even large particles rolled across these areas and then stopped when they reached the zone of normal gradation and other large particles.

Run 32.—The bed was essentially a plane, and the bed-material discharge was 26 ppm. The bed-material discharge was nearly the same as for runs 18 and 28, but the hydraulic conditions were much different. Eight or nine bands of relatively fine material moved at equally spaced increments across the flume. Figure 60 shows the bed after the flume had been drained at the end of the run.

Run 24.—The discharge was about 10 percent less than that of run 32. The bed was plane, the depth was 0.49 foot instead of 0.52 foot, and the velocity was 1.46 fps instead of 1.50 fps. As in run 32, segregated move-

A

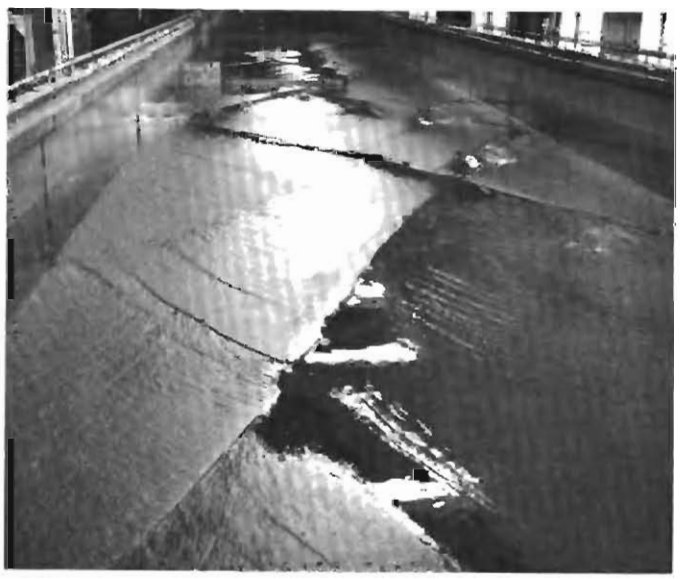

B

FIGURE 58.—Upstream views of flow conditions for run 45. *A*, Train of antidune waves (sometimes called rooster tails). *B*, Bed configuration caused by the antidune flow.

ment occurred: the bed-material discharge was mostly composed of fine particles. Some small depressions or pockets were noted.

Run 14.—The bed roughness for this run consisted of small dunes having an amplitude of less than 0.05 foot and spaced 2.5–3.0 feet apart. This state of equilibrium was reached by washing out the large dunes formed in run 13, in which discharge and slope were much larger. The sand bed was very soft, particularly on the crest of the dunes. There was little or no suspended load, and the bed roughness did not affect the water surface. The bed was plane adjacent to the flume walls. Figure 59 shows the bed after the flume had been drained at the end of the run. Evidence of differential transport can be seen in view *B*, which shows that the finer material is concentrated where the dunes are highest. Differential bed-material discharge was also indicated by the fact that the median diameter of the bed-material discharge was 0.00272 foot, whereas the median diameter of the bed material on or near the surface was 0.00325 foot;

Run 34.—The flow conditions were similar to those described for run 14 (fig. 59) but the dunes that formed were slightly more irregular in shape. The increased shear stress caused the dune velocity and bed-material discharge to increase. The average particle size in the dunes or sand waves was smaller than that in the bed as a whole.

Run 16.—The shear stress was sufficient to cause dunes to form that were more typical of natural dunes that those formed in runs 18, 28, 15, 14, and 34. The pattern of the dune faces was generally perpendicular to the direction of flow, but some advancement of the faces sometimes occurred near the centerline of the flume. Figure 61 shows the degree of dune development at the end of the run. Some sediment was carried in suspension, but not so much that the bed could not be seen through the water surface. Although the bed was very soft during flow, especially near the dune crests, the depth was much easier to measure than in runs using finer sands. As the size of the bed material increased, the avalanche face of the dunes grew steeper, recirculation downstream from the dune crest grew stronger, and the dunes moved in a more definite plane, were closer together, and had a more uniform shape.

Run 35.—The depth of flow was shallow (0.53 foot) and slope, fairly steep (0.00130). Dunes formed that appeared to have characteristics between those of dunes formed in runs 16 and 34. (See fig. 60, 61 and 62.) The steeper slope caused an increase in the bed-material discharge and the dune velocity. The resistance to flow was about midway between those in runs 16 and 34; yet, the water surface was more turbulent than in runs 16 and 34. Small boils were seen on the water surface downstream from the crest of the low dunes. Small fins of sediment that were parallel to the flow formed downstream from some avalanche faces. Many fins consisted of material finer than the average in transport.

Run 17.—This run was similar to run 16 except that the slope and, consequently, the shear stress were increased by opening the tailgate. The dunes were well formed and moved faster because the shear stress was increased. The suspended bed-material discharge con-

A

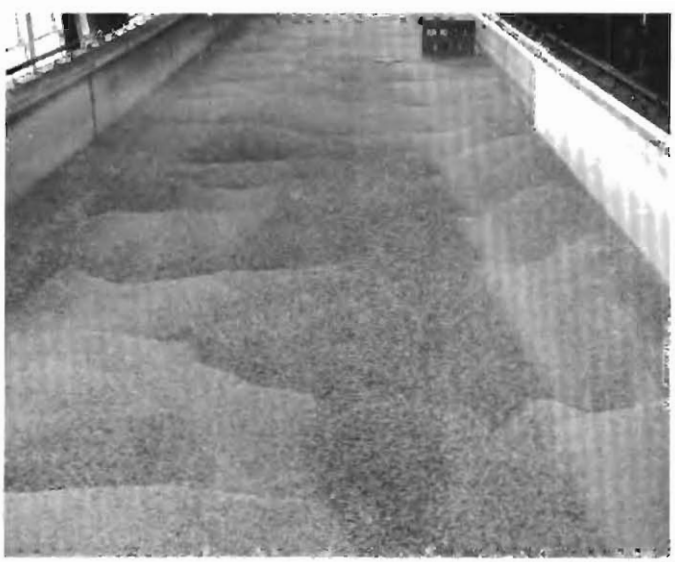

B

FIGURE 59.—Flume bed at end of run 14. *A*, View upstream. *B*, View downstream. Note in view *B* that the finer material is in the areas of maximum dune height.

sisted mainly of the finer particles, and the water was sufficiently clear that the bed could be seen through the flow. A few ripples moved on the backs of the largest dunes.

Run 33.—The bed was raked and rough-screeded prior to the beginning of this run. Because of the shallower depth of flow, the dunes that formed were not as high as those formed in run 17. The water surface was rough and choppy, and a few boils were seen downstream from the dune crests. The dune height and the resistance to flow were greater than in runs 35 and

FIGURE 60.—Upstream view of the plane bed at the end of run 32.

34. Figure 63 shows the bed at the end of run 33 and may be contrasted with figure 62, which shows the bed at the end of run 35.

Run 5.—The dunes formed were larger and more irregularly shaped than those formed at nearly the same discharge but at lesser slope in runs 16 and 17. The rate of dune movement was nearly equal to that in run 17 (table 6), but the bed-material discharge was greater because the dunes were larger. The water surface was depressed in depth over the dune crests and was expanded over the troughs. Boils due to the strong counterflow in the troughs, could be seen on the water surface downstream from the dune crests. The bed

FIGURE 61.—Upstream view of dunes formed during run 16.

FIGURE 62.—Upstream view of the dune-bed condition at the end of run 35.

with these larger dunes was softer and more fluid than in the previous runs. The suspended-sediment concentration was very small so the bed could be seen through the flow. Small fast-moving dunes moved on top of the large dunes, possibly causing the change in level of the major dune movement.

Run 10.—The slope was steeper, the depth shallower, and the bed-material discharge greater than in run 33. The result was a low dune pattern. The relatively large amount of bed-material discharge near the bed and possibly also the increased strength of secondary circulations accentuated the "fins" downstream from the dune crest. (See fig. 64.) The irregularly shaped dunes and "fins" seemed to indicate that at such shallow depths, meandering might develop if slope and transport rate were increased.

FIGURE 63.—Upstream view of low dunes on the flume bed at the end of run 33.

FIGURE 64.—Upstream view of the dune configuration at the end of run 10.

Run 37.—The flow conditions in this run were similar to those in run 6, which will be described later.

Run 36.—This was another shallow-depth run and was similar to run 10. The water surface was so turbulent that eddies, generated by the dunes, were indistinct. Waves generated in the flow by the dunes were reflected from the side walls, giving the appearance of additional roughness. The dunes were larger than those in other shallow-depth runs. The large dunes at this shallow depth caused much resistance to flow.

Run 6.—This run was similar to run 37. As can be seen in figure 65, the bed consisted of large dunes. The

FIGURE 65.—Upstream view of the dune-bed configuration formed during run 6.

A

B

FIGURE 66.—Upstream views of the flow conditions for run 11. *A*, The water surface. *B*, The bed configuration at the end of the run.

dunes were very regular in form and had small dunes or ripples on their back. The bed was soft on the crest and firmer on the back, but in general it was softer and more porous than in runs having smaller dunes. The high velocity of flow over these large dunes resulted in a very rough water surface. If the depth had been greater, the surface waves would probably have been dampened and eddies and boils would have been more conspicuous. The turbulence was sufficient to cause some larger particles to be carried in suspension, and some of these were seen "jumping" from dune crest to dune crest. Most of the moving sediment was, however, in nearly continuous contact with the bed. The dunes advanced by the processes of (1) sediment avalanching and deposition on the front of the dune crest and (2) erosion of the dune back and at the front of the trough. The amount of bed-material discharge varied greatly, depending on the position of the dune or dunes in relation to the flume exit.

Run 7.—The slope was about the same as that for run 6, but the discharge was reduced to about 10 cfs. Compared with run 6, the velocity and depth were less, the dunes were smaller, and the water surface was smoother. Boils were conspicuous on the water surface downstream from the dune crests. As in other sets of runs, the large dunes moved much slower than the small dunes. The speed was directly proportional to the size or amplitude of the avalanche face, which varied with the volume of sediment in transport. The speed was also proportional to the shear stress, to the bed-material discharge over the back of the dune, which, in turn, was affected by the position of upstream dunes, and to the exposure or elevation at which the dune moved through the flume.

Run 38.—The dunes formed in this run were similar to those formed in runs 6 and 37. Increasing the slope for this run caused the velocity of flow and the bed-material discharge to increase; consequently, the mean dune velocity was considerably greater. Many short dune troughs formed, in which the impinging flow from the crest of the dune at the upstream edge of the trough caused very rapid scour on the downstream part of the trough. The components of flow from this impingement, both forward and reverse, caused considerable suspension of sediment.

Run 11.—The bed configuration consisted of large fast-moving dunes. The water surface was turbulent, and a few random surface waves were generated. Figure 66 shows the water-surface and bed conditions of this run. As can be seen in figure 66*B*, ripples or small dunelike sand waves formed on the back of the dunes. The distance between the major dunes seemed to increase as they moved downstream. When the distance between dunes had increased to about 10 feet, either a new dune formed or the distance gradually decreased, depending on the position and shape of the dune pattern upstream.

Run 8.—This run was similar to run 7 except that the slope was steeper and the velocity was higher. The discharge was increased over that of run 7 to maintain nearly the same depth. The dunes that formed were longer, lower, and traveled faster. The characteristics of the flow on the dunes seemed to represent the beginning stages of the transition between dunes and plane bed, although the energy of the flow was much

791–597 O—66——4

less than the rapid-flow condition in which $F > 1$. The wavy water surface effectively masked the typical dune-type boils on the water surface.

Run 12.—The dunes were medium sized but moved rapidly and caused many surface waves. Some surface waves had white caps, but did not exhibit antidune characteristics. The bed increased in firmness as the velocity increased, especially on the back of the dunes. The dune shapes were sometimes observed to be very regular and consistent or, at other times and locations, change rapidly. Occasionally, a jet of flow moved over a dune that had a steep avalanche face, inpinged on the steep upstream face of the trough, or on the back of the next dune downstream, and caused very rapid erosion and the suspension of large quantities of sediment. Where such flow conditions occurred, very strong reversed flow originating from the eroding area and moving across the bottom of the trough was evident. Figure 67 shows these flow conditions.

Run 13.—The slope for this run was steeper than that for run 12. Faster flow and more bed-material discharge resulted. The water surface was very rough, and short trains of irregularly shaped waves with white caps formed. The dunes were elongated and irregular in shape. Figure 68 shows the flow conditions of the run. The suspended-sediment concentration was greater than that in run 12. The dunes moved fast and changed shape rapidly; thus, useful data on dune velocity and amplitude were difficult to obtain through observation windows.

Run 9.—The water surface was very rough, and the dunes were low and moving downstream very rapidly. This was a true transitional run. Standing waves inphase with the underlying bed configuration were common, but, more typically, the water waves were out of phase with the bed configuration. Some trains of standing waves built up and then broke.

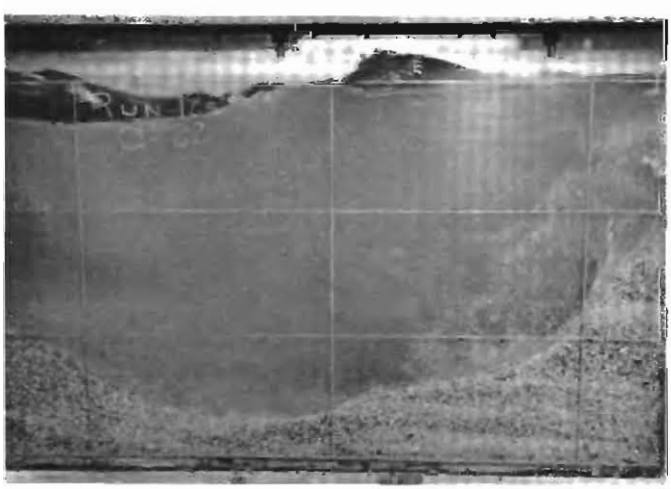

FIGURE 67.—Rapid flow from the dune crest on the left impinging on the downstream wall of the trough and causing rapid erosion and suspension of sediment during run 12.

A

B

FIGURE 68.—Upstream views of flow and bed conditions for run 13. *A*, Water-surface condition. *B*, Bed configuration at end of run.

Run 3.—The flow and roughness conditions of this run were similar to those described for run 9. Greater depth and velocity, however, caused much more suspension of sediment.

Run 1.—The water surface was very rough, and some standing waves broke. The waves were less symmetrical and wider spaced than those in runs using smaller diameter sands. The water surface indicated

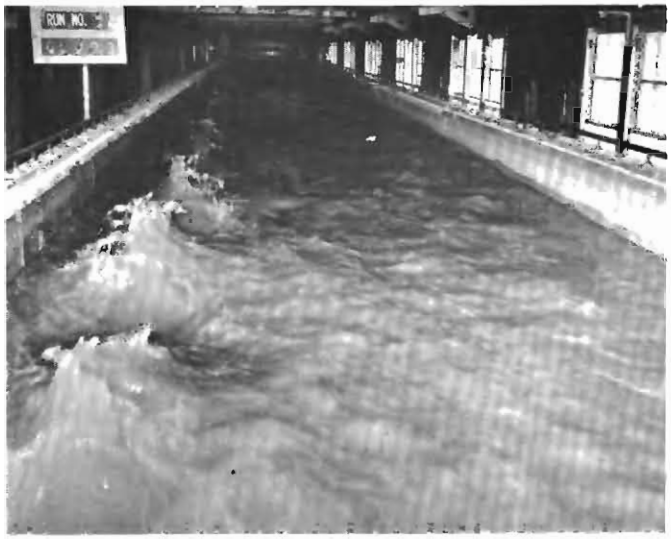

A

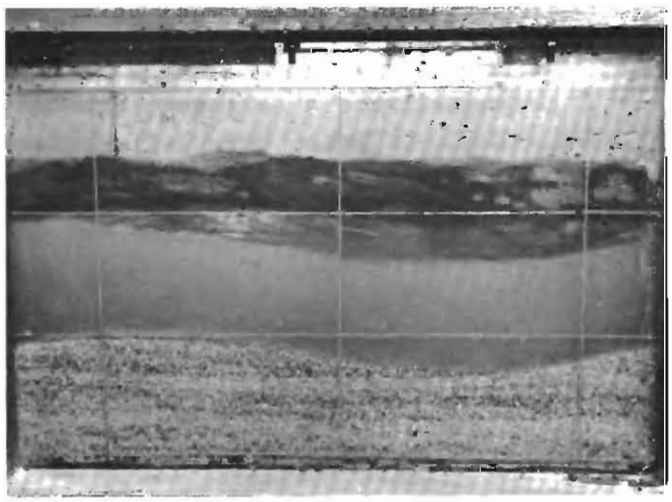

B

FIGURE 69.—Flow conditions during run 2. *A*, An upstream view of a train of rough standing waves, and the water surface. *B*, A side view of inphase water and bed surfaces typical of standing waves.

A

B

FIGURE 70.—Upstream views of flow conditions for run 4. *A*, The rough water surface. *B*, The bed configuration at end of run.

a condition of an upper regime flow, but the bed consisted of low rapidly moving dunes. Very streamlined dunes indicated a transitional condition.

Run 2.—In this run, the slope was steeper, the resistance was less, the velocity was higher, and the depth was less than in run 1. Trains of standing waves (fig. 69*A*) formed, but the waves generally disintegrated or washed out without breaking. The sand and water waves were inphase (fig. 69*B*) and generally were nearly stationary. Under these flow conditions, most sediment transport was close to the bed. As the sharpest and largest waves broke, "rooster's tails" formed on the water surface.

Run 4.—The conditions at the start of this run were the same as in run 2, except that the discharge was less. The reduced discharge caused the depth and the bed-material discharge to decrease, and the resistance to increase. The water surface was extremely rough, as is shown in figure 70. A variety of conditions, such as small elongated dunes rapidly advancing across a flat area and a few symmetrical or inphase waves, was visible from the side window. The symmetrical sand waves were very unstable and rapidly changed to dunes or planed out.

Run 41.—This was another transitional run. Sometimes the bed and water surfaces were plane, sometimes they were undulating inphase, and sometimes they

A

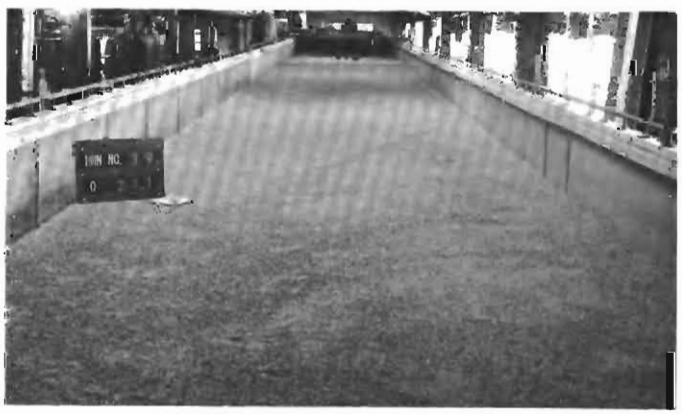

B

FIGURE 71.—Upstream views of flow conditions for runs 43 and 39. *A*, The water surface. *B*, The sand bed.

were out of phase. The out-of-phase condition was caused by small and rounded dunes having weak zones of flow separation. The resistance to flow was less than that in run 4; therefore, the water surface was smoother, and both the velocity and the bed-material discharge were greater.

Run 42.—The flow conditions over the bed were more plane than those of run 41. Small trains of large amplitude standing waves occasionally formed and then died out; but did not break. The bed was very firm except on the crest of dunes in a wave train.

Run 40.—This run differed from run 42 by having more standing waves, greater resistance to flow, and more bed-material discharge. The wave trains sometimes built up nearly to the breaking point and then moved slightly upstream without breaking.

Runs 43 and 39.—Input variables, resistance to flow, and bed-material discharge for these two runs were nearly identical. The water and bed surfaces are shown in figure 71. Small-amplitude standing waves occasionally formed on the water surface, and these affected the bed. The bed was at least as firm as that in any other run or set of runs. The firmness of the bed may have been a major factor causing the low bed-material discharge noted for these two runs. Turbulence was reduced by the pavementlike bed.

RUNS USING 0.32-MM SAND IN 2-FOOT-WIDE FLUME

The purpose of this set was to determine the effect of viscosity on resistance to flow and bed-material discharge. The viscosity of the flow was varied for each run by changing the temperature of the flow. The temperature of the flow for a given run was maintained at a specific level by immersing a steam hose into the tailbox, thus warming the water before it was pumped back to the head of the flume. The sand used was the 0.27-mm sand used in the 8-foot-wide flume, but made coarser by washing away some of the fine particles. This set of experiments was conducted during the period November 1959–April 1960. The experimental variables and parameters are given in table 7, and the velocity profiles in table 17.

The order of presenting the runs in the following discussion and in table 7 is different from that used for the preceding sets because increasing slope cannot be used if the low- and high-temperature runs for a given discharge are to be compared. The low- and high-temperature paired runs are presented in the order of increasing discharge, the low-temperature run preceding the high-temperature run. For a specific temperature, the order approximated that of increasing slope, velocity, and bed-material discharge. Only water temperature and, hence, fluid viscosity were changed for any pair of runs. Changes in slope, depth, roughness, and bed-material discharge were the direct response to the change in fluid viscosity. In some sets the first run was made with cold water, and the second with heated water; in others the procedure was reversed.

Run 1.—The run was started with the bed planed to a slope of about 0.00015. At a mean velocity of 0.90 fps, small particles moved more steadily than large ones. When large particles moved, they generally became stabilized at a lower elevation, a very short distance, from where they started. The very small ripples formed from this kind of selective movement were most evident at the lower end of the flume, mainly because the depth of the flow there was less and the velocity was higher, but also because most of the fine sediment had been moved, by selective movement, from the upper to the lower end of the flume.

Run 2.—The conditions for this run were similar to those for run 1 except that the temperature of the flow was 23.4°C in contrast to 10.0°C in run 1. The sediment transport rate was slightly greater than in run 1. Small particles moved constantly, medium particles moved intermittently, and large particles moved occasionally. The final bed form, very low ripples, caused somewhat greater resistance to flow and, in turn, lower velocity, than in run 1.

Run 3.—Fully developed ripples as much as 0.2 foot high formed on the bed. Although these ripples moved downstream very rapidly, the water surface remained generally smooth. Clouds of sand occasionally swirled off the crests of the ripples, but no true suspended sediment extended from the bed to the water surface.

Run 4.—The bed configuration of this run was ripples averaging 0.07 foot high and 0.66 foot long. The water surface was relatively smooth. Most sediment rolled or slid over the crest of each ripple. Small clouds of the finer particles were occasionally carried up into the flow. Few if any particles reached the surface, however, and the suspended concentration, for all practical purposes, was zero.

Run 30.—Large and fairly uniform ripples formed throughout the length of the flume. Suspended sediment (24 ppm) was especially noticeable downstream from the ripple crests.

Run 29.—The higher water temperature for this run caused a higher flow velocity and a higher bed-material discharge than run 30 at nearly the same slope. The dunes formed on the bed were smooth and flat and were partly covered with small ripples. Some dunes were almost indistinguishable. Ripples were the dominant bed form. Suspension of sediment was especially noticeable downstream from the ripple or dune crests. Suspended transport was only a small portion of the total transport as was attested by the smooth water surface.

Run 5.—Both dunes and ripples formed on the bed of the flume. The water surface was undulating and was much rougher than in any other run previously described in this set. The bed sloped transversely near the larger dunes. Some bed-material discharge moved as suspended sediment, but most rolled and slid rapidly over the crest of the dunes.

Run 6.—Rate of discharge was the same as in run 5, but the water temperature was 17°C higher than in run 5. Depth of flow was greater than in run 5, but slope, velocity, and bed-material discharge are all significantly less. Again the bed features comprised low dunes with small ripples superposed. (See fig. 72.) Occasionally small vortices were seen carrying sand to the surface of the flow.

Runs 27 and 28.—Fully developed dunes (and a few ripples) formed throughout the flume. In run 27 (cold water) the dunes were longer and more rounded and the water surface was smoother than in run 28 (warm water). The effect on depth, velocity, slope, and bed-material transport caused by changing water temperature seemed to be the inverse of that in the previous three pairs of runs, in which ripples were the dominant forms.

Runs 26 and 25.—The dunes formed on the flume bed in runs 26 and 25 were generally of typical shape and were out of phase with water-surface undulations—that is, the depression in the water surface was over the crest of a sand wave. Occasionally, some irregular dune troughs formed, such as an erosion pocket with both steep upstream and downstream slopes. Ripples formed in some dune troughs where the velocity was lowest. In run 25 the dunes increased in size downstream. As in runs 27 and 28, velocity and slope were higher in runs using warm water, whereas bed-material discharge was less.

Run 21.—The run was typical of the transitional regime. The bed alternately was nearly a plane or comprised long low dunes. During the near-plane condition, the water surface conformed closely to any bed irregularities. Small irregularities slowly developed into low dunes, most of which did not extend uniformly across the flume. Dunes were 0.2–0.3 foot high on the left side of the flume but only 0.1 foot high on the right side. The bed was firm though easily scoured

FIGURE 72.—Downstream view of dune-bed configuration formed during run 6.

under the plane conditions, and very soft in the vicinity of the dune crests.

Run 22.—The higher water temperature in this run resulted in a bed condition closer to that of dunes, although it was actually transitional. Long low very irregular dunes occupied about two-thirds of the flume. Most dunes were about 0.15 foot high, but at least one in each train of dunes that moved through the flume was about 0.3 foot high. The water surface was rough, and the depth of flow varied greatly. The more dune-like configuration caused the velocity and the slope to be lower and the bed-material discharge to be larger, especially the suspended part, than in run 21.

Runs 24 and 23.—These runs were similar to runs 21 and 22 except that the increased discharge resulted in a greater depth and somewhat lower velocity. The dunes formed in the warmer water (run 23) were more fully developed than those in run 22.

Run 7.—The flow conditions for this run resulted in a smooth bed form of very long waves. The water surface was rough and followed the same pattern as the bed. Much of the bed-material discharge was rapidly rolled or slid along the bed, but some went into suspension very easily like dust swept by a broom. The bed-material discharge varied rapidly. Undulation of the bed surface caused stratification in the form of thin alternate layers of fine and coarse sediment in the bed, at least in the areas near the walls of the flume.

Run 8.—The warm water caused the bed configuration to revert back to dunes from the nearly plane condition of run 7. About two-thirds of the length of the flume was covered with dunes, which started at the upper end of the flume and became progressively smaller as they moved downstream. In a few places the bed was intermittently scoured to the floor of the flume. The water surface was very rough, and the crest-to-crest distance between water waves was much less than the distance between dune crests. The downstream face of the dunes was not steep, so that any eddies downstream from the dunes were small. Figure 73 is a side view of the dune configuration and flow of run 8. Sediment streaming from the crest of the dune can be seen in the photograph.

Run 20.—Downstream from station 35, very small antidunes formed. These moved upstream very slowly but did not break. The water and sand waves were inphase because the flow was in the upper regime.

Run 19.—The higher temperature in comparison with run 20 caused the bed form and flow to change from one of mild antidunes to a plane bed. The downstream one-third of the flow surface had a slightly

FIGURE 73.—Side view of dunes and flow conditions during run 8.

wavy appearance, but the rest was very smooth. The bed was very firm except in a few upstream areas of the flume. Even though the downstream water surface became increasingly wavy, it was very smooth compared with the surface in runs having greater slope.

Runs 10 and 9.—The flow velocity and the amount of bed-material discharge were similar in these runs. The bed configuration was one of standing waves. Slope and resistance to flow were greater in run 10, seemingly because the viscosity of the water was greater (1.55 as opposed to 1.00). The standing waves were more persistent in runs 9 and 10 than in runs 19 and 20. They generally formed and remained for about 15 seconds and then gradually diminished. Figure 74 shows the long low amplitude of the inphase sand and water waves. The amplitude of the water waves was greater than that of the sand waves.

Runs 12 and 11.—The depth of flow was increased from that in runs 10 and 9, and for a given temperature a decrease in bed-material discharge and slope resulted. The bed was nearly plane in both runs, although standing waves formed in run 11. The water surface undulated gently in run 11. The magnitude of the undulations was about 0.1 foot at the downstream end of the flume. The bed-surface undulations were not as large as those of the water surface.

Runs 14 and 13.—Antidunes formed in both runs. Those formed in run 14 (cold water) were better de-

FIGURE 74.—Side view of bed and flow during run 9.

A

B

FIGURE 75.—Side views of antidune flow conditions during run 15. *A*, Dune crest (left) and zone of flow acceleration (center and right). *B*, Trough of sand and water waves (left) and breaking wave and very heavy concentration of sediment near the bed (center and right).

veloped than those formed in run 13 (warm water), and they moved upstream at about 0.2 fps compared with 0.1 fps for those in run 13. The magnitude of the antidunes and their rate of movement decreased upstream in the flume. The bed-material discharge was greater in run 14 than in run 13 because the cold water resulted in greater antidune activity and, thus, more suspension of sediment.

Runs 15 and 16.—The antidunes formed in these two runs were similar to those formed in runs 14 and 13. Bed-material discharge was greater in runs 15 and 16 than in 14 and 13 because mean velocity and depth were greater and possibly because the water temperatures were lower. The suspension of bed material developed upward from a densely transported layer at the bed and was significantly greater than in runs 14 and 13. Figure 75 shows two views of the flow conditions.

Run 17.—A chute-and-pool condition formed during this run that was nearly like that formed during runs using finer sands in the 8-foot-wide flume. Occasionally, an 8- to 10-foot-long chute formed in which flow accelerated downstream to a hydraulic jump or a strong downstream standing wave. Breaking antidunes were seen all along the flume, and often the lower 20 feet of the flume had a continuous series of breaking antidunes. The antidunes seemed to break when the crest of the sand wave was level with the water surface in the upstream trough.

Run 18.—Flow in this run appeared similar to that in run 17 except that it was not as violent and no chutes and pools formed. The water surface was very rough; so reliable measurements of depth and slope were difficult to make. Eight measurements of the velocity of the upstream movement of the antidunes ranged from 0.020 to 0.082 fps and averaged 0.052 fps.

Run 31.—This was a chute-and-pool run. The length of the chutes was possibly limited by the amount of sediment on the flume bed; that is, the lower part of the chute at the hydraulic jump may have been scoured to the floor of the flume. Nonuniform suspended-sediment concentration was indicated by analyses of four samples in which the mean concentration was 41,600 ppm and the standard deviation was 27,800 ppm. Four measurements of bed-material discharge averaged 49,300 ppm and had a standard deviation of 7,700 ppm. A comparable high-temperature run was not made.

RUNS USING 0.33-MM (UNIFORM) SAND IN 2-FOOT-WIDE FLUME

The sand used in this set of runs had a median diameter of 0.33 mm and as little size gradation as was practical to obtain. Table 1 and figures 4 and 5 have more detailed information on the character of the sand. The runs were all made with temperature of the water close to 20°C and the depth of flow close to 0.50 foot. This set of experiments was conducted during the period January–April 1961. The experimental variables and parameters are given in table 8. Velocity-profile data are given in table 18. The runs are discussed on the following pages and are listed in table 8 in chronological order by increasing slope.

Run 7.—The bed was planed smooth under quiet water and set at a slope of 0.00025 immediately prior to this run. When flow had been established, the resulting mean flow velocity was 1.14 fps. The shear stress was great enough to cause movement of sediment throughout the length of the flume but was not great enough to cause ripples to form anywhere but near the headbox.

Run 8.—The slope was increased to 0.00087, and this increase caused much sediment movement; consequently, resistance to flow increased and ripples formed. The increase in resistance made it necessary to decrease the discharge and the velocity so that a depth of 0.50 foot could be maintained. As is shown in figure 76 and

in columns 14 and 15 of table 8, the ripples had small amplitude and length. Ripples appeared to be slightly larger near the flume walls than at midstream. The bed-material discharge was only 6.6 ppm, and nearly all of it moved very close to the bed. The bed was very firm except on ripple crests, which were very soft and fluidlike.

Run 5.—A continuous flow for 3 days was required to establish equilibrium in this run. Little or no change in flow conditions occurred during the last 24 hours. The ripples were about twice as high as those formed in run 8, and their size and shape varied more widely. The bed-material discharge was 47 ppm, of which about 15 ppm was carried in suspension.

Run 11.—The bed form consisted of dunelike highs and lows almost completely covered with ripples. The high areas did not have discernible crests, as one would expect for dunes. The entire bed was soft.

Run 10.—The slope was 0.00213, more than double that for run 11. The consequent flow and transport variables achieved equilibrium with a bed form consisting of ripples superposed on dunes. Some shorter dunes, 1.5–2.0 feet long, did not have ripples on their surface. The sand bed felt soft and fluidlike.

Run 6.—The flow characteristics were similar to those expected over a dune-bed configuration. The dunes varied greatly in size and shape, and some had ripples on their surface; some even had a very round crest. Figure 77 illustrates the bed and flow conditions in run 6. The rounded shape of some of the dunes apparently resulted from the specific dune being subjected to a jet of flow from over the next upstream dune.

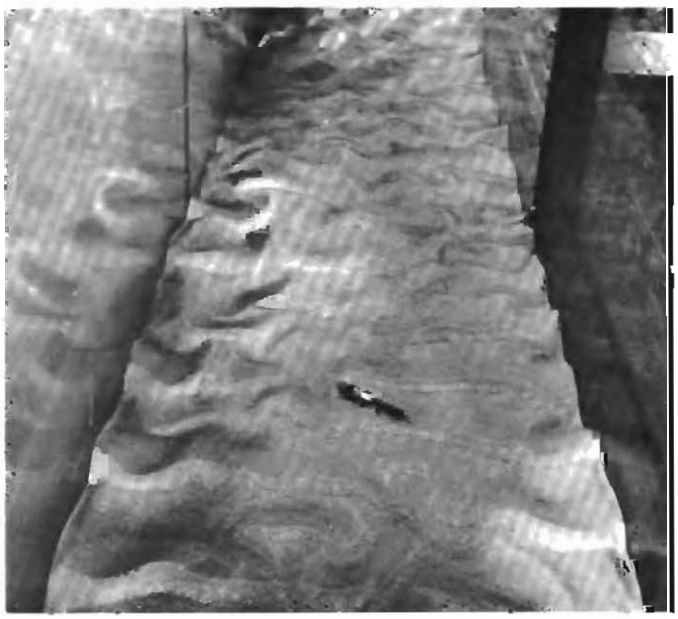

FIGURE 76.—Upstream view of rippled flume bed at the end of run 8.

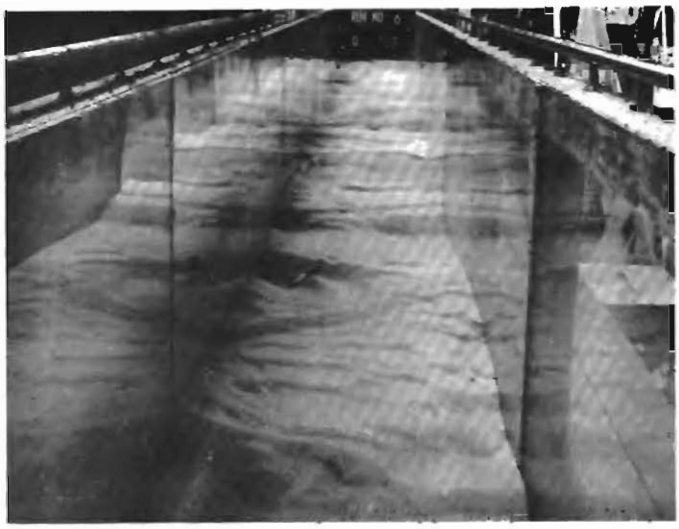

A

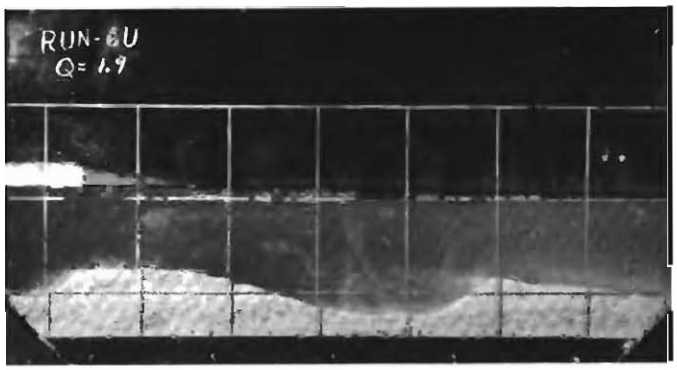

B

FIGURE 77.—Bed and flow conditions for run 6. *A*, Upstream view of the flume after the water had been drained from it at the end of the run. *B*, Side view of two dunes. The flow is from right to left.

Run 4.—The slope and depth seemed to fluctuate considerably, and, with them, the bed condition—from nearly plane to transitional dunes. The bed-material discharge remained relatively constant. The transitional dunes gradually built up from the plane-bed condition. At first they were long but had small amplitude; then they changed to short but with large amplitude. As the dunes built up, the resistance to flow increased and caused the depth and slope to increase also. The bed was softer than under normal plane-bed conditions.

Run 1.—Plane-bed conditions of flow and transport existed during this run. The resistance to flow was low, and the water surface was relatively smooth. Most sediment transport occurred in close contact with the sand bed. The average bed-material discharge was 3,090 ppm, of which only 12.7 percent was in suspension, in contrast to over 30 percent ordinarily in

suspension when dunes and ripples are present. The sand bed was very firm.

Run 9.—The flow condition varied with the size and shape of the dunes formed. At times the dunes were as much as 8–12 feet long, and at other times they averaged 3–4 feet long. The height of the long dunes was about one-half that of the short dunes. The alternating from one kind of dune to another affected slope, depth, and concentration of bed-material discharge. The mean slope for this run was greater than that for run 1, but the velocity and bed-material discharge were much less.

Run 12.—A plane-bed condition very similar to that in run 1 existed as long as the water was kept heated. When the water temperature was allowed to drop to 15°C, the bed condition converted to the one of antidunes.

Run 13.—The increase in slope and shear stress for this run caused the flow velocity and bed-material discharge to be greater than in run 12. The result was a series of standing waves which built up slowly and then gently receded or broke. The sand and water waves were inphase, and the vertical distance between the crest and trough of the water waves was about twice that of the sand waves. None of the dunes upstream from station 40 broke, and only some of those downstream from station 40 broke.

Run 2.—This was a typical antidune run of relatively mild activity. Antidunes formed and broke regularly in the downstream end of the flume, less frequently in the middle of the flume, and only occasionally in the upper end of the flume. The mild activity as the dunes broke did not cause much suspension of sand. After a series of waves broke, the bed usually planed out considerably and low-standing waves developed. The standing waves, in turn, moved upstream as they grew in size and developed into antidunes. Figure 78 illustrates the nature of the standing-waves formed in run 2.

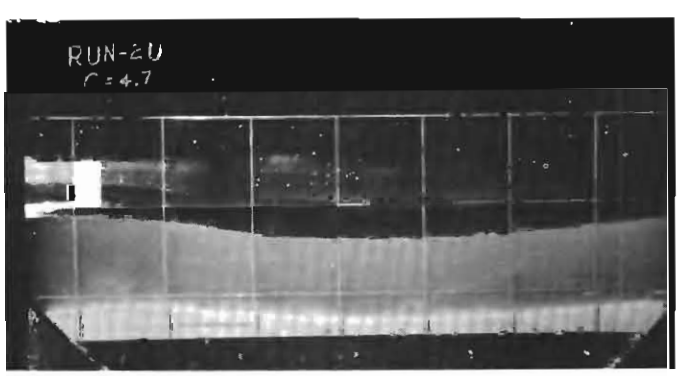

FIGURE 78.—Side view of the standing waves most typical of flow conditions during run 2. Flow is from right to left.

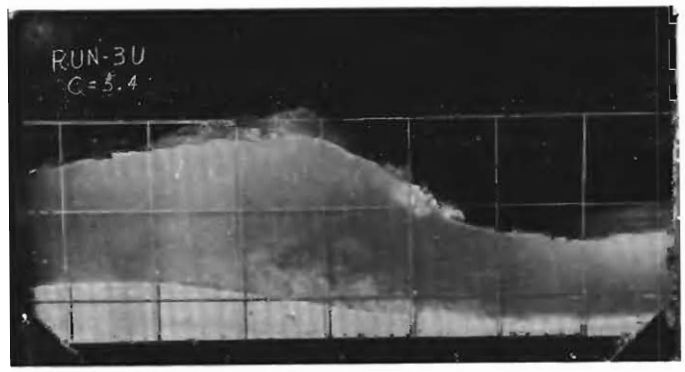

FIGURE 79. Side view of an antidune beginning to break during run 3. Flow is from right to left.

Run 3.—Antidunes were breaking somewhere in the flume at all times during this run, but they generally took longer to break than did those in run 2. The longer breaking time, plus the greatly increased frequency of breaking resulted in a large increase of suspended bed-material discharge over that in run 2. Sediment was deposited on and filled in the upstream slope of the sand waves. During and after breaking of an antidune, such deposition and filling occurred very rapidly. Figure 79 shows an antidune early in the breaking stage. The 0.1-foot-thick highly concentrated layer of sediment became a cloud of sand in the low velocity flow under the breaking crest of the water wave.

Run 14.—Increase in slope over that in run 3 caused greater velocity and more violent activity in the form of breaking antidunes. The bed-material discharge was nearly the same as that of run 3, but the part held in suspension was greater.

RUNS USING 0.33-MM (GRADED) SAND IN 2-FOOT-WIDE FLUME

The 0.33-mm graded sand as described previously, was manufactured or assembled from several size fractions to obtain a nonuniform sand having a median diameter of 0.33 mm. Flow characteristics and bed-material discharge in runs using this sand were recorded for comparison with data for runs using the uniform 0.33-mm sand. The runs in this set are likewise presented in order of increasing slope. The following data were collected during the period July–September 1961. The experimental variables and parameters are given in table 9, and the velocity-profile data, in table 19.

Run 11A.—The bed was planed smooth under several inches of quiet water prior to the beginning of the run. Flow was established at a slope of 0.00022 and a mean velocity of 1.08 fps. Some fine grains moved, mostly to positions at lower levels among coarser grains.

Particles which protruded into the flow were affected by the greatest shear stress and usually were the first to move.

Run 11B.—General movement of all particles was obtained by increasing the slope to 0.00027 and increasing the mean velocity to 1.28 fps. Ripples formed from stations 0 to 20, and some fine-grained particles moved as far as station 24. The remainder of the flume downstream from station 24 remained plane despite considerable particle movement.

Run 16.—Data collection began 36 hours after the run was begun. A uniform pattern of ripples that resembled sand waves formed. It appeared that material finer than the median size was traveling over a bed of material coarser than the median size. Figure 80 shows the bed configuration after the water had been drained from the flume at the end of the run. (Compare the ripples shown in fig. 80 (graded sand) with those shown in fig. 76 (uniform sand of same median diameter). Several samples were taken from the sand waves and from the troughs. Analysis of the composited wave samples gave a median diameter of 0.20 mm and a standard deviation of 1.96, whereas the composited trough samples gave a median diameter of 0.38 mm and a standard deviation of 2.23. This analysis confirmed the visual observation that sorted bed-material discharge existed under this kind of ripple formation.

Run 6.—The ripples formed in run 6 were more fully developed and in a more irregular pattern than those formed in run 16. (See fig. 81.) They caused greater resistance to flow and somewhat lower mean velocity than those in run 16, even though the slope had been increased from 0.00029 to 0.00047. The water surface was calm. The bed-material discharge (12 ppm) moved in almost continuous contact with the bed.

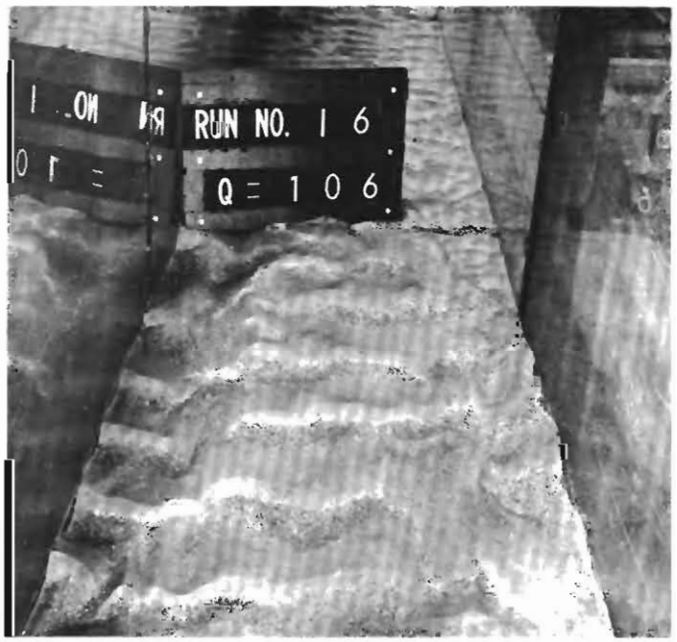

FIGURE 80.—Upstream view of ripples at the end of run 16. Note that the sand in the ripple crests is finer than that in the troughs.

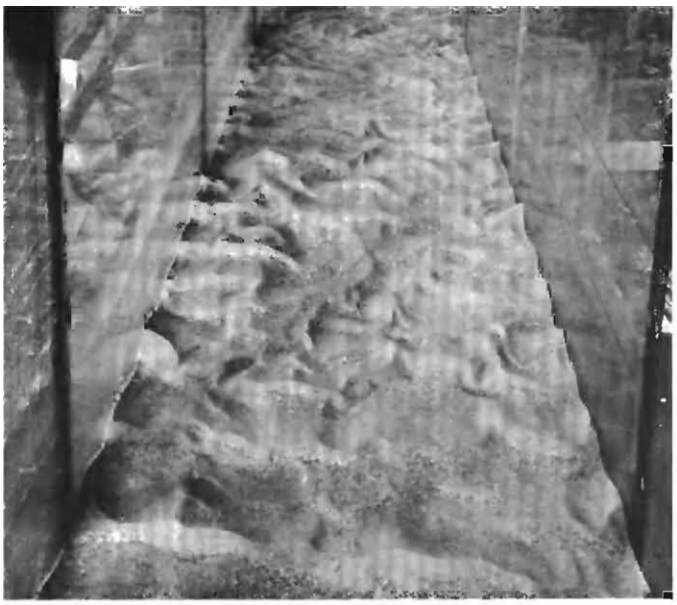

FIGURE 81.—Upstream view of ripples formed during run 6.

Run 5.—Slope and discharge were increased over those in run 6. As a result, flow velocity in this run was much greater than that in run 6, and bed-material discharge was somewhat greater. The ripples seemed very small; their growth may have been restricted by the coarse bed material. (See fig. 82.) Sediment moved by sliding or by short hops. A mixture of coarse and fine particles moved near the center of the flume, whereas only fine particles moved closer to the flume walls. The coarser material formed an armor plate, and the fine material moved as ripples. Many coarser particles moved across several ripples without stopping, whereas the fine particles moved from ripple to ripple but had a long rest period between moves.

Run 1.—Long low dunes and a few low ripples formed. (See fig. 83.) Generally, relatively low resistance to flow indicates a low percentage of suspended sediment, but this was not true for this run. The low resistance to flow in run 1 may be explained by the fact that the bed was very soft throughout the depth disturbed by the dune movement.

Run 10.—The bed form in this run was mostly one of ripples superposed on dunes. Long low dunes occasionally formed, moved slowly downstream, and then died away. The bed-material discharge was some-

FIGURE 82.—Upstream view of ripples formed during run 5.

what less than in run 1, and the suspended part was much less.

Run 8.—Small rather rounded dunes formed. Ripples on these dunes were less prominent than on those formed under similar hydraulic conditions in runs using the uniform sand.

Runs 9 and 7.—Low dunes of various sizes formed in both runs. (See fig. 84.) Some dunes had a few superposed ripples during the runs.

FIGURE 83.—Upstream view of the dune-bed configuration at the end of run 1.

FIGURE 84.—Upstream view of the dune-bed configuration formed during run 9. Most of the ripples were caused by flow disturbance during draining of the flume at the end of the run.

Run 2.—Dunes formed that were similar to those of runs 9 and 7 but were somewhat rounded because of the increased slope and velocity in run 2. (See fig. 85.) The dunes moved through the flume very rapidly, so that there was much bed-material discharge.

Run 3.—The flow pattern and bed-material discharge were characteristically those of a run in which the bed condition was transitional between dunes and plane

FIGURE 85.—Upstream view of the dune-bed configuration at the end of run 2.

bed. The bed form varied from almost plane to fast-moving low dunes which rapidly changed form. Some segregation of particles occurred, but generally the sediment was well graded throughout most of the flume.

Run 4.—The mean velocity of flow was 4.00 fps. The transitional dunes of run 3 were washed away, and a plane firm sand bed resulted. Most of the bed-material discharge was in a thin layer close to the bed.

Run 12.—The bed for this run was essentially plane, but some very small standing waves formed. These small waves can be seen in figure 86. Very heavy sediment transport took place near the bed.

Run 13.—The flow conditions for this run resulted in formation of standing waves and slow-moving antidunes, some of which broke.

Run 15.—Violent antidunes broke in series and caused considerable suspension of sediment. The water surface was too rough to allow reliable depth and slope measurements.

Run 14.—This was another antidune run, but the slope was steeper and the velocity lower than in run 15. The antidunes alternately had small and large amplitude. The small antidunes broke gently, and the large ones, vigorously.

RUNS USING 0.47-MM SAND IN 8-FOOT-WIDE FLUME

The 0.47-mm sand used in this set of runs was derived from the 0.45-mm sand by washing away of some of the fine fractions. The main purpose of the set was to determine the effect of fine sediment, C_f, on the mean-flow and bed-material-discharge parameters for a range of equilibrium-flow conditions similar to those in the set of runs using the 0.45-mm sand.

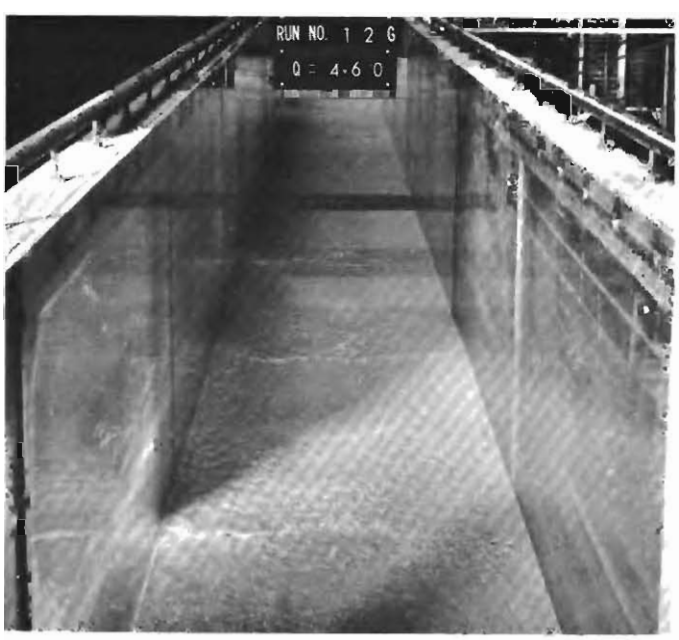

FIGURE 86.—Upstream view of bed conditions at the end of run 12.

After equilibrium was established and the data collected for a given run, bentonite was either added to or extracted from the flow to establish a new concentration of fine sediment without stopping the flow. The change in the fine-sediment concentration generally caused a change in the flow and transport conditions, and these changes, in turn, caused a change in bed roughness, depth, slope, and bed-material discharge.

Bentonite was used as the fine sediment because it is commercially available in large quantities. The particle-size distribution of the bentonite down to 2 microns is shown in figure 87. Bentonite is composed of several different clay minerals, as is shown in figure 88. The mean specific gravity of the particles is about 2.8.

As Simons, Richardson, and Haushild (1963) pointed out, aqueous dispersions of bentonite are non-Newtonian; that is, the shearing stress is not directly proportional to the rate of shear. Therefore, the term "apparent" viscosity relates the shearing stress to the rate of shear. Figure 6 shows the relations of apparent kinematic viscosity (ν) and temperature for dispersions of 0, 0.5, 1, 2, 3, 5, and 10 percent bentonite in distilled water as determined using a Stormer viscometer. One part sodium hexametaphosphate to 99 parts bentonite, the ratio used in the flume experiments, prevented flocculation of the clay particles in the dispersions. The apparent kinematic viscosity is given in column 23 of tables 10 and 11 for each run.

After equilibrium had been established in each run, samples for determination of total sediment discharge (bed material plus fine material) were collected into a tank at the end of the flume with a width-depth integrating sampler. Eight samples were taken in the lower flow regime (ripples and dunes) during a 12-hour pe-

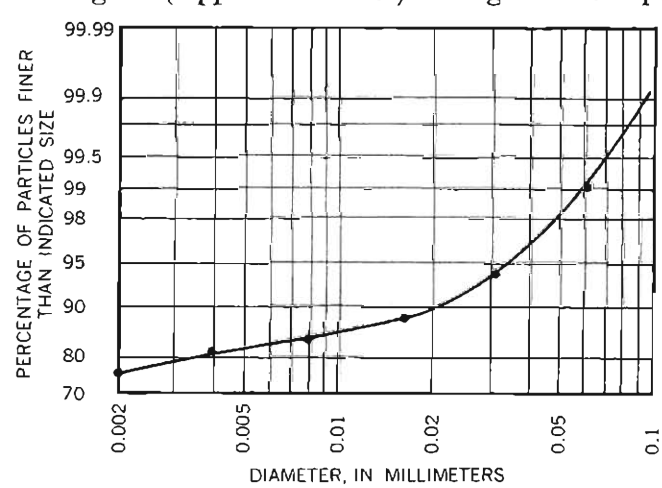

FIGURE 87.—Particle-size distribution of bentonite used in flume studies with the 0.47-mm and 0.54-mm sands. The sample was chemically and mechanically dispersed in water and analyzed by the sieve-pipette method.

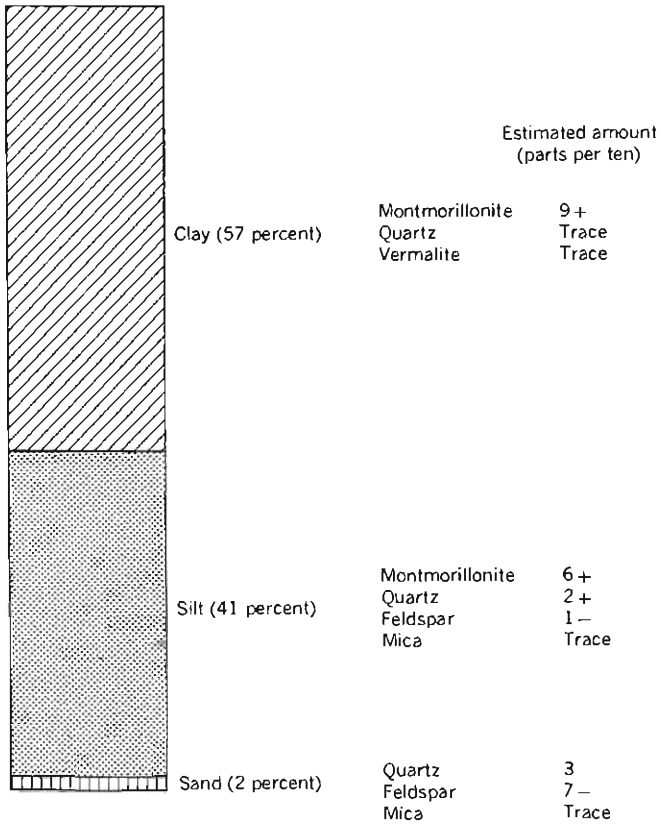

FIGURE 88.—Mineralogy of bentonite for different size classifications as analyzed with an X-ray diffractometer by Paul D. Blackman, U.S. Geological Survey, Denver. The size distribution differs from that shown in figure 87 because no chemical dispersant was used to prevent flocculation after the sample had been mechanically dispersed.

riod, and four samples were taken in the upper flow regime (plane bed, standing waves, and antidunes) during a 1-hour period. Each sample consisted of 70–110 pounds of the water-sediment mixture.

To separate the fine material, or "wash load," from the bed material, the sample was allowed to stand a few minutes so that the sand could settle. After the sand settled, the water-bentonite mixture was drained off, leaving the sand. The remaining fine material in the sand was removed by washing the sand over a No. 230 sieve. The concentration of the fines thus removed was added to the concentration of the fines removed from a pint sample of the water-bentonite mixture drained from the tank containing the flume sample. Then, all material coarser than 0.062 mm was considered bed material, and all finer material was considered fine material. The concentration of fine-material transport is listed in table 10, column 6, and bed-material transport, in column 9. The sum of these is the total concentration of sediment discharge.

Samples of concentration of suspended-sediment (col. 7, table 10) were obtained with the specially designed depth-integrating sampler in the flume section 95–100 feet downstream from the flume entrance. Generally, only one 5- to 8-pound sample was collected by the equal-transit-rate method for each run. Some concentrations were not recorded because the samples contained an excessive amount of bed material from contact of the sampler nozzle with the bed, particularly for the dune runs. Because only a single sample was collected during each run, the standard deviation could not be computed.

This set of experiments was conducted during the period January–May 1958. The experimental variables and parameters are given in table 10, and the velocity-profile data, in table 20.

The order of presenting the runs in table 10 and in the descriptions to follow is based on (a) increasing fine-sediment concentration within a series of runs, (b) increasing slope, and (c) the following order of bed form: ripples, dunes, transitional, plane, and antidunes. The run numbers were continued from the 0.45-mm set because of the close similarity of the bed material.

Runs 46, 47, 48, and 49.—These runs were made using the 0.47-mm sand and clear water. Data collected were meant to fill gaps in the data for the runs using the 0.45-mm sand. Dunes with superposed ripples were formed in all four runs. As was expected, the mean velocity increased as depth increased and as the dunes became lower and longer. Runs 47 and 48 had low shear stress and a low rate of bed-material discharge; thus, there was no suspended-sediment movement, and the sand dunes moved very slowly.

Runs 85, 86, 87, and 88.—The slope for this series of runs ranged from 0.00046 to 0.00049, and the concentration of fine-material discharge was 0, 4,800, 8,400, and 11,400 ppm, respectively. Under these conditions, ripples formed on the bed and flow velocity ranged from 1.13 to 1.20 fps. Fine material near the bottom (about 0.1 foot of flow) blocked visibility of the bed. Through the side window of the flume, however, it could be seen that the fine material was being deposited in the trough of the ripples and that the next ripple from upstream would ride over the lens of fine material; subsequent ripple troughs passed above, through or below the lens deposit. Figure 89, photographed through the window, shows ripples and lenses formed during run 88. The lenses, as well as the shape and velocity of the ripples, seemed to offer some resistance to normal sand transport. When ripples became stationary or nearly so, they became rounded and had about the same slope on the upstream and downstream faces. The stationary ripples resulted from the space between the sand grains at the surface being filled with fine sediment. The fine material definitely caused the

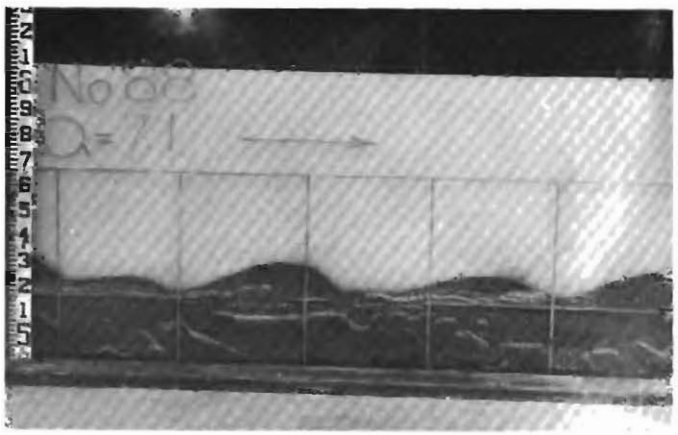

FIGURE 89.—Ripples and lenses of fine material (light colored) in the bed during run 88. The relatively round shape of the ripples can be contrasted with the normal-shaped ripples shown in figure 33.

ripple shapes and patterns to be more irregular than those formed in clear water. In collecting bed-material samples, it was noted that the layer of sand below the normal depth of movement of the ripple waves was much firmer for the fine-material runs than for the clear-water runs.

Runs 90 and 89.—The slope was greater for these runs than for runs 85–88. Both the flow and the ripples were noticeably affected by the stabilization of the bed by the bentonite. In run 89 a crusty layer underlay the ripples throughout most the flume, and the ripples were the same height as those in the previous four runs but were longer and had a higher velocity. The bed was raked smooth to a depth of about 0.15 foot prior to run 90, but it was covered with loose sand ripples riding on a layer of clay-impregnated sand during the run. The sand moved more freely, at least near the windows in run 90, than in run 89.

Runs 93, 92, and 91.—The slope was again increased for these runs and was sufficient to cause dunes and

FIGURE 90.—Upstream view of the bed configuration typical of that formed during runs 93, 92 and 91.

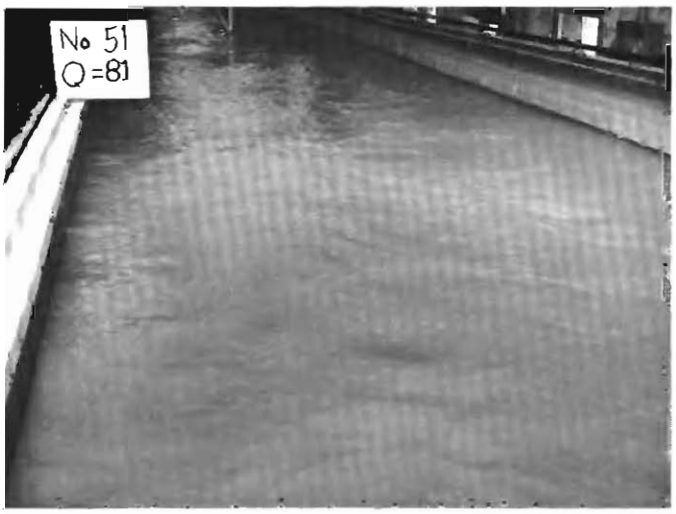

A

B

FIGURE 91.—Upstream views of the water surface during runs 51 (*A*) and 96 (*B*) contrasting the increase in turbulence with increased flow stress and resistance.

overriding ripples to form on the bed. The bed form shown in figure 90 at the end of run 92 was typical for all three runs. The water surface was turbulent, and boils formed downstream from the major dunes. Resistance to the establishment of flow equilibrium due to the fine material in the bed seemed to increase as slope increased. In each run the slope was gradually increased over a period of several hours and then slightly reduced before the final equilibrium was obtained to insure that the more compact sand-clay layer would be below the zone of dune movement.

Runs 82, 51, 52, 73, 74, 76, 75, 53, 77, and 96.—In this series of 10 runs, the slope ranged from 0.00199 to 0.00248, the water discharge ranged from 8.01 to 8.76 cfs, and the bed-material discharge ranged from 429 to 761 ppm. The bed form in all the runs was one of

dunes with varying amounts of superposed ripples. The water surface in each run showed evidence of turbulence depending on the amounts of shear stress and resistance to flow. Figure 91 shows the water surface during runs 51 and 96. The dune shape ranged from rough in a relatively regular cross pattern (run 51) to washed out in an irregular pattern (runs 82 and 96). This range in dune shape is shown in figure 92. The resistance to flow in these runs as measured by Manning n ranged from n=0.034 (run 82) to n=0.023 (run 96).

Many sizes of dunes and ripples were in motion at any given time. The small dunes often moved faster and, hence, caught up with the large dunes and drastically modified their shape, amplitude, and velocity. When a small dune caught up with a larger one, the new dune approximated the sum of the two amplitudes in height. The small dune moved faster than the large one only if it was behind the large dune. The fine sediment seemed to cause the dune form in these runs to be more irregular for a given slope and velocity of flow than that in the clear-water runs, possibly because of the cohesiveness of the mixture.

Run 94.—This was a dune run with almost no fine sediment in the flow. The shape of the dunes was normal; however, the amplitude and the spacing varied considerably. The material on the bed appeared to move more freely than in runs with a large fine-sediment concentration.

Runs 83, 54, 56, 55, 57, 58, and 95.—These runs had slopes ranging from 0.00180 to 0.00259, depths between 0.80 and 0.94 foot, bed-material discharge ranging from 588 to 1,600 ppm, and a bed form of dunes. The discharge of the water-sediment mixture ranged from 15.28 to 15.58 cfs, a variation of only 2.0 percent. Fine-material concentration increased from 0 (run 83) to 28,300 ppm (run 95). Depth, slope, and roughness decreased as concentration of fine sediment increased. The water surface was turbulent and contained many boils caused by eddies downstream from the dune crests. The most turbulent surface flow occurred in run 95. (See fig. 93.) The bed roughness in run 95 became stabilized for brief periods of time (several minutes) and, when this happened, caused choppy waves on the water surface. However, the bed was soft (no lenses of clay), and the turbulence was great enough to cause the clay to act as a wash load, even at this concentration of 28,300 ppm. In run 83 (clear-water condition), dunes had a mean height of 0.43 foot, and some dune troughs exposed the floor of the flume. Water-surface waves and the sand waves were out of phase in all runs in this series; that is, a high (or crown) on the water surface was over a low area (or trough) of the dune, and the low area on the water surface was over a dune crest.

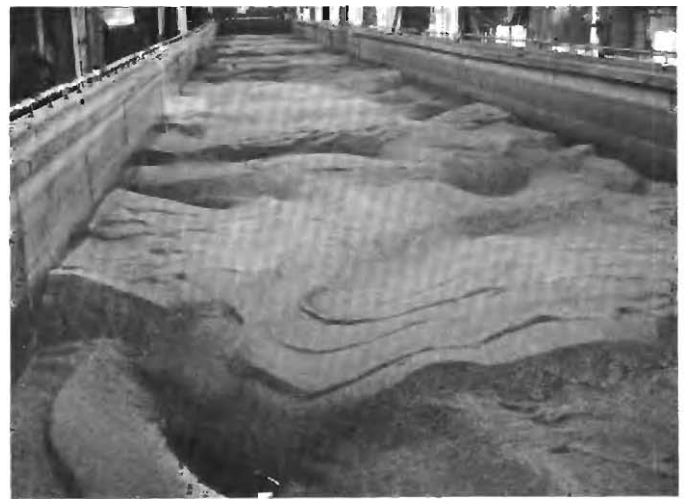

A

B

FIGURE 92.—Upstream views contrasting dune shapes resulting from the flow during runs 82 (*A*) and 96 (*B*).

Run 78.—The flow for this run was in equilibrium with large dunes moving at a rapid rate. Strong eddies from the dune crests caused the water surface to be very turbulent. (See fig. 94.) The water stood high over the trough and low over the crest of dunes, as in the preceding runs, but to an even greater extent. The flow must have been nearly transitional, as indicated by the fact that often no major dunes could be seen near the flume windows.

Run 59.—The flow stress in this run caused the dunes to be washed out; so this run, too, was transitional. The water surface was very irregular, as is shown in figure 95. The washed-out dunes formed a diagonallike crisscross pattern, which was also re-

FIGURE 93.—Upstream view of water surface during run 95. The flow, at a velocity of 2.39 fps, is over a dune-bed form.

FIGURE 94.—Upstream view of water surface during run 78.

FIGURE 95.—Upstream view of water surface during run 59.

peated for the surface waves. The bed was very soft and fluid, particularly near the dunes.

Runs 60 and 61.—These runs had plane-bed conditions. Occasionally a small dunelike form was seen, but these features were generally less than 0.01 foot in amplitude. These minor dunes seemed to extend diagonally across the flume, similar to those observed during run 59. The bed was firm except on the crest of the minor dunes. The character of the flow at the surface is shown in figure 96.

Runs 71, 72, and 70.—The flow was typically that of plane-bed runs. Some small dunes, similar to those formed in runs 60 and 61, formed during run 71; the bed was very plane in run 72; and a few small standing waves formed at the lower end of the flume during run 70. The sand bed was firm, but not as firm as in runs in which higher velocities caused standing waves to form.

Runs 63, 64, 65, 66, and 80.—The flow stress caused formation of bed features ranging from predominately standing waves during run 63 to double-train antidunes during runs 65, 66, and 80. Figure 97 shows a typical water-surface condition for this series of runs. The wave pattern in run 63 developed less vigorously and less frequently than that in run 80, in which the wave trains formed nearly continuously. The sand waves were symmetrical and inphase with the surface waves. The sand bed was firm and smooth except in the area of the breaking antidunes. For a given slope, antidune activity seemed to increase with fine-sediment concentration.

Runs 81, 62, 67, and 79.—The slope ranged from 0.00622 to 0.00651, the depth ranged from 0.53 to 0.55 foot, the mean velocity was about 4.9 fps. Standing waves formed in each run. Figure 98 shows a typical view of the flow for these runs: at times the water

FIGURE 96.—Upstream view of water surface during run 60.

FIGURE 97.—Upstream view of water surface typical of runs 64, 65, and 66.

surface was nearly plane in short reaches, and at other times low- to medium-height standing waves were evident. The bed was plane under the plane-flow areas and wavy under the standing waves with an amplitude of about one-half the amplitude of the water waves. The bed was firm at all locations. Most bed-material discharge occurred within 0.05 foot of the bed. Fine material was in the bed below the zone of sand movement.

Runs 84, 69, and 98.—Varying amounts of antidune activity occurred during this group of runs. Figure 99 illustrates the range of flow condition during run 84—from standing waves to breaking antidunes. The highest concentration of the fine material (42,000 ppm) for this set occurred in run 98. Run 98 also had the largest, most frequent, and most violent antidunes. Figure 100 illustrates the antidune activity during run 98.

Run 68.—A single train of standing waves formed during this run. The standing waves were similar but slightly larger than those of run 67. The water waves had an amplitude of about 0.05 foot and the sand waves had an amplitude of about 0.04 foot. The in-phase water and sand waves were spaced about 4 feet apart. The bed surface was firm.

Runs 100 and 99.—These two runs were nearly identical with respect to slope, depth, and velocity. Run 100 was a continuation of run 99 except that the fine-sediment concentration had been decreased by adding clear water to the flow and wasting the excess of the mixture. Run 100 had 106 ppm of fine sediment and a temperature of 13.3°C, whereas run 99 had 26,900 ppm of fine sediment and a temperature of 19.6°C. Run 100 had a plane bed and a mean bed-material discharge of 8,440 ppm; run 99 had violent antidunes and a mean bed-material discharge of 16,100 ppm. The decrease in antidune activity with the decrease in fine-sediment concentration was very striking.

Run 97.—The slope for this run was much steeper than that for runs 100 and 99, but the mean velocity was much less because of the shallower flow. The antidunes formed in run 97 were not as violent as those in run 99; and, consequently, the bed-material discharge was little more than half that of run 99.

RUNS USING 0.54-MM SAND IN 2-FOOT-WIDE FLUME

This set of runs complemented the previous set (0.47 mm sand in 8-ft-wide flume) in determining the effect of fine sediment on resistance to flow and on sediment transport. The smaller, 2-foot-wide flume, made it practical to use much higher concentrations of bentonite in the flow. The characteristics of the bentonite are described on page I 52.

As in the previous set, equilibrium was established and data were collected for a given run, then without stopping the flow, bentonite was added to or extracted from the flow to establish a new concentration of fine sediment. The change of fine-sediment concentration generally affected the fluidity, which in turn caused a change in bed roughness, velocity, depth, slope, and bed-material discharge.

Samples for determination of total-sediment-transport concentration (bed material plus fine sediment) were collected with a width-depth integrating sampler at the end of the flume. From 8 to 12 samples were taken for the ripple and dune runs, and from 6 to 8 samples were taken for the upper-regime flows. The method of analysis for separation of the fine material and bed material was described on page I 53. Depth-integrated suspended-sediment samples were not obtained for these runs.

FIGURE 98.—View of water surface typical of runs 81, 62, 67, and 79.

A

B

FIGURE 99.—Upstream views of standing waves (*A*) and breaking antidunes (*B*) during run 84.

This set of experiments was conducted during the period April–July 1959. Experimental variables and parameters are given in table 11, and velocity-profile data, in table 21.

The order for presenting this set of runs is identical with that used for presenting runs using the 0.47-mm sand.

Runs 1 and 2.—Particles of sand moved under flow conditions during these runs, but the degree of movement was not sufficient to cause ripples to form. In run 1, particles moved only occasionally; but in run 2, many particles were in motion at any given time. Before run 2 was started, the material on the bed was thoroughly raked and ripples were introduced, but the flow and the characteristics of the sediment particle

FIGURE 100.—Downstream view of the antidunes during run 98.

movement during the run caused the ripples to erode down to a plane bed after about 4 hours.

Run 3.—The flow during this run caused considerably more sediment movement than occurred during run 2. Irregular sand waves formed that were very different from ripples.

Run 4.—In spite of the low bed-material discharge of 17 ppm, a rippled bed did not develop. The bed pattern, in general, comprised sand waves; but occasionally it included a very small avalanche face, such as normally would be associated with a dune.

Runs 6 and 5.—The flow conditions in these runs caused normal steep-fronted dunes to form throughout the length of the flume. The dune fronts were continuous across the full width of the flume but were not always normal to the flume wall. If the dunes were diagonal to the flow, however, they were all in the same direction; and if they were normal to the flow, they all were normal. The continuous dune fronts caused increased resistance to flow, but not increased bed-material discharge, in contrast with the data for the 0.47-mm sand in the 8-foot-wide flume.

Run 20.—This run should be classed as transitional, although it could be called a dune run. The dunes were irregular in shape and movement; sometimes there was a long flat area with no dunes. The water surface was generally rough, with choppy waves superposed on longer waves owing to the dunelike bed configuration.

Runs 8, 8A, 8E, 8B, 8C, and 8D.—The discharge for this series of runs ranged from 3.69 to 3.84 cfs, and the fine-material concentration ranged from 0 to 63,700 ppm. Runs 8, 8A, and 8E had bed forms of typical sharp-crested dunes. However, beginning with run 8B the fine-sediment concentration was increased to 20,600

ppm, and the dunes became irregular in shape. The irregularities ranged from long stretches of very low sharp-crested dunes to large round-crested dunes. Also beginning with 8B, some bentonite was layered in the bed by the dune action. The highest concentration of fine material was during run 8D, and the dunes formed during this run were very long and low and had small rounded ripplelike waves superposed. The bed in run 8D was much firmer than that in the dune runs, but not as firm as is expected for the plane-bed condition.

Run 7.—This clear-water run had a slope nearly double that for 8D; yet the bed had a rough dune configuration in contrast to the low smooth configuration of run 8D. The average bed-material discharge was 1,250 ppm for run 7 and 521 ppm for run 8D. The relatively high bed-material discharge for run 7 was caused by the rapid movement of the dunes and by the suspension of sediment through the action of large eddies that originate from the dune crests. The water surface over the dunes was very turbulent. Small waves and boils formed over the dune trough and eddy areas and dissipated over the upstream slope of the next dune downstream.

Runs 14, 14A, 14C, and 14B.—The discharge for each of these runs was about 4.8 cfs, and the fine-sediment concentration ranged from 0 to 44,100 ppm. The bed condition varied from one of nearly normal dunes, for clear water (run 14), to plane bed, for the highest concentration of fine material (run 14B). The equilibrium slope decreased as the fine-sediment concentration increased, as in runs 8–8E.

Run 19.—This run was set up to produce dunes at a discharge rate higher than that in run 7. The depth was first set at 0.6 foot but was increased as equilibrium became established. The dunes resulting from this flow had an unusual shape, especially the short ones, in that they were high and well-rounded toward the upper end but drawn down at the lower end, where the crest is ordinarily located. The avalanche face, where present, was less than half as high as the dune. The water surface was extremely rough, because of the turbulence caused by the dunes. A short dune trapped between two relatively long dunes was severely scoured by a jet of flow from the upper dune and, therefore, rapidly changed size and shape. This run was classed as transitional between dunes and plane bed.

Run 9.—This run was transitional between dunes and plane bed. Generally one or more irregularly shaped dunes could be seen in the flume, but the conditions changed constantly. Dunes formed and then were erased by the flow. The roughness of the water surface varied with the roughness of the bed.

Run 10.—The bed in this run was plane more than 90 percent of the time. Sometimes smooth undulations developed throughout the length of flume and lasted 2–3 minutes. Occasionally a very low dune with a small avalanche face formed and moved rapidly through the flume. This kind of flow caused most of the bed-material discharge to slide and to roll along the bed.

Runs 15, 15A, 15B, and 15C.—The discharge for each of these runs was nearly 7.0 cfs, and the concentration of fine material ranged from 0 to 58,600 ppm. The flow in all the runs was considered to have standing wave form, although the waves for run 15 were often poorly defined. Unlike in dune runs 8–8D and 14–14B, an increase in fine-material concentration caused an increase in the equilibrium slope. Most bed-material discharge moved in relatively close contact with the sand bed.

Runs 13 and 11.—These were clear-water runs which had standing-wave patterns of flow. Suspended sediment moving in the cross section of flow was much less a part of the bed-material discharge than that moving close to the bed. With the recirculating system and under these flow conditions, only the top few hundredths of a foot of the bed was disturbed. Specific sand particles from the bed moved downstream, but they were immediately replaced by other particles from the moving layer. The step length and rest period differed greatly for any group of particles or between specific particles.

Runs 18, 18A, 18B, and 18C.—The discharge in this series of runs was about 7.6 cfs, and the fine-sediment concentration ranged from 0 to 58,700 ppm. The flow conditions ranged from standing waves when there was no fine sediment (run 18) to mildly breaking antidunes when the concentration of fine sediment was highest (run 18C). Equilibrium slope increased noticeably, and suspended-sediment concentration considerably, as fine-sediment concentration increased, especially when the flow shifted to the breaking antidunes of run 18C.

Runs 16A, 16B, and 16C.—The discharge in each of these three runs was about 7.8 cfs, and fine-material concentrations ranged from 11,200 to 44,500 ppm. Slopes were considerably steeper than in runs 18–18C. The flow condition was one of antidunes in all three runs. The degree of antidune activity and resistance to flow in the runs increased with increasing fine-material concentration.

Runs 17, 17A, and 17B.—The discharge in this series was nearly the same as in the 16A–C series, but the slope was greater and antidunes formed in all runs. As bentonite was being added between periods of data collection ("runs"), it was noted that antidune activity

increased with increasing concentration of the fine material. A similar condition was noted by Langbein (1942) for natural streams. This increased antidune activity caused increased resistance to flow and greater slope to maintain the depth of flow. In run 17B, three or four waves occasionally broke simultaneously, scouring out a 16- to 20-foot-long pool and creating a steep section draining the pool. Run 17B must have been transitional between antidunes and chute-and-pool flow. The increasing antidune activity caused the suspension and total transport of sand to increase rapidly.

Run 12.—This clear-water antidune run was made at high slope to allow comparison with runs having high concentrations of fine sediment.

BASIC DATA

TABLE 2.—*Experimental variables and parameters*

Run	Slope $\times 10^3$ S	Depth D (ft)	Water discharge Q (cu ft per sec)	Temperature T (° C)	Suspended concentration: Sampled C_s (ppm)	Suspended concentration: Standard deviation C_s (ppm)	Suspended concentration: Particle size d_{50} (ft$\times 10^3$)	Total bed-material discharge: Concentration C_t (ppm)	Total bed-material discharge: Standard deviation C_t (ppm)	Total bed-material discharge: Particle size d_{50} (ft$\times 10^3$)	Total bed-material discharge: Gradation σ	Bed material particle size d_{50} (ft$\times 10^3$)	Sand waves: Length L (ft)	Sand waves: Height H_s (ft)	Sand waves: Velocity V_s (ft per min)
(1)	(2)	(3)	(4)	(5)	(6)	(7)	(8)	(9)	(10)	(11)	(12)	(13)	(14)	(15)	(16)
24	0.0055	0.94	6.52	18.6	0	0	----------	0	0	----------	----------	----------	----------	----------	----------
22A	.010	.48	2.99	17.5	0	0	----------	0	0	----------	----------	----------	----------	----------	----------
2	.015	1.06	6.68	12.3	0	0	----------	0.2	----------	----------	----------	0.656	0.6	0.03	0.00098
22B	.016	.43	2.99	17.8	0	0	----------	0	0	----------	----------	----------	----------	----------	----------
26	.017	.30	2.00	19.2	0	0	----------	0	0	----------	----------	.626	----------	----------	----------
25	.018	.93	6.45	19.2	0	0	----------	.3	.2	----------	----------	.613	.4	.03	----------
22C	.018	.42	2.99	18.0	0	0	----------	0	0	----------	----------	----------	----------	----------	----------
30	.028	1.00	8.91	17.0	7	----------	----------	3.7	.5	0.321	1.80	.626	.6	.03	.024
1	.034	.58	3.42	13.6	0	0	----------	1.2	1.0	.712	1.40	.643	.5	.02	.00085
31	.043	1.02	10.62	18.1	42	----------	0.423	29	3.3	.433	1.59	.623	.6	.04	----------
27	.057	.55	4.08	18.1	----------	----------	----------	4.0	.7	.334	1.61	.623	.5	.03	----------
5	.058	1.03	12.67	16.4	105	11	.462	120	13	.499	1.62	.640	.9	.04	.080
23	.062	.44	2.99	18.1	0	0	----------	2.0	.4	.499	1.38	.597	.4	.03	.0029
32	.066	.95	13.64	18.2	----------	----------	.456	281	17	.456	1.53	.649	4.0	.10	.23
8	.070	.93	14.81	18.3	506	28	.511	519	40	.427	1.67	.630	5.4	.18	.17
28	.079	.54	4.49	18.0	----------	----------	----------	34	4.9	.518	1.32	.623	.6	.04	----------
33	.083	1.06	16.66	17.4	748	86	.482	836	174	.482	1.46	.656	8.0	.65	.13
29	.084	.56	5.08	19.1	31	----------	----------	58	7.2	.558	1.45	.643	.6	.04	----------
3	.092	.55	5.20	12.3	----------	----------	----------	84	18	.528	1.36	.659	.7	.04	.032
11	.099	1.09	20.47	18.9	795	42	.351	1,300	181	.446	1.55	.583	11.6	.39	.21
13	.100	.89	21.98	19.3	772	67	.371	1,240	68	.453	1.54	.590	13.4	.13	.20
14	.106	.86	22.12	19.4	950	56	.413	1,490	168	.522	1.43	.564	18.8	.17	----------
15	.112	.79	21.84	19.3	1,120	84	.482	2,000	71	.561	1.38	.584	20.5	.04	----------
34	.127	.52	7.00	16.6	393	58	----------	503	26	.518	1.36	.653	1.7	.04	.26
12	.130	1.02	21.96	19.7	929	58	.423	1,270	110	.436	1.54	.593	17.7	.32	.20
6	.130	.61	8.14	15.3	550	88	.429	861	157	.489	1.42	.620	5.1	.18	.10
7	.140	.68	9.66	18.0	567	140	.452	1,240	192	.499	1.56	.614	7.4	.31	.24
35	.147	.52	7.52	18.5	729	154	.462	999	131	.531	1.40	.656	4.5	.13	.24
16	.156	.72	22.14	18.8	1,350	116	.528	2,750	296	.620	1.34	.597	----------	----------	----------
10	.170	.51	11.68	19.1	861	157	.433	2,480	316	.548	1.40	.587	24.0	.10	.78
9	.194	.49	8.22	18.6	697	260	.397	1,210	230	.495	1.46	.623	5.2	.20	.15
17	.196	.67	22.19	19.1	4,030	373	.472	4,650	1,770	.544	1.30	.561	4.4	.10	----------
18	.300	.64	22.16	18.9	7,270	473	.478	9,240	820	.522	1.29	.597	4.9	.10	----------
19	.350	.64	22.19	18.7	13,400	562	.495	12,900	3,060	.522	1.33	.564	----------	----------	----------
39	.390	.61	22.33	18.8	20,100	2,080	.521	16,200	3,590	.495	1.30	----------	----------	----------	----------
20	.460	.60	22.17	18.5	23,300	4,620	.485	23,900	3,610	.512	1.33	.590	----------	----------	----------
21	.542	.50	16.13	18.7	21,900	3,690	.469	25,200	4,720	.502	1.26	----------	----------	----------	----------
38	.582	.58	22.00	17.9	31,600	10,000	.508	26,600	7,510	.522	1.33	----------	----------	----------	----------
36	.845	.51	15.54	16.8	38,800	13,900	.518	35,500	4,120	.541	1.31	.676	----------	----------	----------
37	.950	.65	21.84	17.3	57,300	14,600	.561	47,300	10,500	.512	1.31	.689	----------	----------	----------

for 0.19-mm sand in 8-foot-wide flume

Run	Mean velocity V (ft per sec)	Velocity profile: Slope B	Velocity profile: Intercept C	Shear velocity V_* (ft per sec)	Bed-material discharge: Sampled suspended g_s (lb per sec per ft)	Bed-material discharge: Total g_t (lb per sec per ft)	Kinematic viscosity $\times 10^5$ ν (sq ft per sec)	Shear stress at bed τ (lb per sq ft)	Reynolds number $\times 10^{-2}$ R	Froude number F	Resistance factor: Darcy-Weisbach f	Resistance factor: Chezy $C/\sqrt{g}$	Resistance factor: Manning n (ft$^{1/6}$)	Bed configuration
(1)	(17)	(18)	(19)	(20)	(21)	(22)	(23)	(24)	(25)	(26)	(27)	(28)	(29)	(30)
24	0.87	0.27	1.19	0.041	0	0	1.12	0.0032	730	0.16	0.174	21.4	0.012	Plane.
22A	.78	----------	----------	.039	0	0	1.16	.0030	320	.20	.0203	19.8	.012	Do.
2	.79	.38	1.16	.072	0	0	1.33	.0099	625	.14	.0656	11.0	.024	Ripple.
22B	.87	----------	----------	.047	0	0.000010	1.15	.0043	323	.23	.0234	18.5	.012	Plane.
26	.83	.24	1.18	.041	0	0	1.10	.0032	----------	----------	----------	----------	----------	Do.
25	.87	.53	1.24	.073	0	.000015	1.10	.010	725	.16	.0570	11.8	.022	Ripple.
22C	.89	.36	1.18	.049	0	0	1.14	.0047	325	.24	.0246	18.0	.013	Plane.
30	1.11	.51	1.52	.095	0.00049	.00026	1.17	.017	949	.20	.0585	11.7	.022	Ripple.
1	.74	.47	1.15	.080	0	.000032	1.28	.012	328	.17	.0928	9.3	.026	Do.
31	1.30	.76	1.86	.119	----------	.0024	1.14	.027	1,161	.23	.0669	10.9	.024	Do
27	.93	.53	1.51	.100	----------	.00013	1.14	.020	449	.22	.0934	9.3	.026	Do.
5	1.54	1.01	2.15	.139	.0104	.0119	1.19	.037	1,330	.27	.0649	11.1	.024	Do.
23	.85	.34	1.40	.093	0	.000047	1.14	.017	325	.23	.0957	9.1	.025	Do.
32	1.79	.72	2.43	.142	----------	.030	1.13	.039	1,499	.32	.0504	12.6	.021	Dune.
8	1.99	.83	2.66	.145	.058	.060	1.13	.041	1,636	.36	.0423	13.7	.019	Do.
28	1.04	.63	1.72	.117	----------	.0012	1.14	.027	491	.25	.1016	8.9	.027	Ripple.
33	1.96	.49	2.63	.168	.097	.109	1.16	.055	1,788	.34	.0590	11.6	.023	Dune.
29	1.13	.64	1.77	.123	.00123	.0022	1.11	.029	569	.27	.0949	9.2	.026	Ripple.
3	1.18	.67	1.85	.128	----------	.0034	1.33	.032	482	.28	.0936	9.2	.026	Do.
11	2.35	.45	3.13	.186	.127	.21	1.11	.067	2,300	.40	.0503	12.6	.021	Dune.
13	3.09	----------	3.85	.169	.132	.21	1.10	.056	1,498	.58	.0240	18.2	.014	Transition.
14	3.22	1.29	4.13	.171	.164	.26	1.10	.057	2,514	.61	.0226	18.8	.014	Do.
15	3.46	1.37	4.50	.169	.191	.34	1.10	.055	2,480	.69	.0190	20.5	.012	Plane.
34	1.68	.77	2.47	.146	.021	.027	1.18	.041	736	.41	.0603	11.5	.020	Dune.
12	2.69	1.33	3.84	.207	.159	.22	1.09	.083	2,514	.47	.0472	13.0	.020	Do.
6	1.67	.80	2.30	.160	.035	.055	1.22	.049	827	.38	.0732	10.4	.023	Do.
7	1.78	.83	2.51	.175	.043	.093	1.14	.059	1,061	.38	.0774	10.2	.024	Do.
35	1.81	.63	2.71	.157	.043	.059	1.12	.048	836	.44	.0601	11.5	.020	Do.
16	3.84	1.40	4.92	.190	.233	.47	1.12	.070	2,473	.80	.0196	20.2	.012	Transition.
10	2.89	1.29	4.22	.167	.078	.23	1.11	.054	1,328	.71	.0267	17.3	.014	Plane.
9	2.10	1.18	3.68	.175	.045	.078	1.12	.059	909	.53	.0555	12.0	.019	Dune.
17	4.14	----------	----------	.206	.70	.80	1.11	.082	2,502	.89	.0197	20.1	.012	Antidune.
18	4.33	----------	----------	.249	1.26	1.60	1.11	.120	2,489	.95	.0264	17.4	.014	Do.
19	4.33	----------	----------	.269	2.32	2.23	1.12	.140	2,475	.95	.0308	16.1	.015	Do.
39	4.58	----------	----------	.277	3.50	2.82	1.12	.148	2,500	1.03	.0292	16.6	.015	Do.
20	4.62	----------	----------	.298	4.03	4.13	1.12	.172	2,462	1.05	.0333	15.5	.016	Do.
21	4.03	----------	----------	.295	2.76	3.17	1.12	.169	1,796	1.00	.0430	13.6	.017	Do.
38	4.74	----------	----------	.330	5.43	4.57	1.14	.211	2,397	1.10	.0387	14.4	.017	Do.
36	3.81	----------	----------	.373	4.71	4.30	1.18	.269	1,650	.94	.0765	10.2	.023	Chute-pool.
37	4.20	----------	----------	.446	9.77	8.06	1.16	.385	2,351	.92	.0902	9.2	.026	Do.

TABLE 3.—*Experimental variables and parameters*

Run	Slope $\times 10^2$ S	Depth D (ft)	Water discharge Q (ft³ per sec)	Temperature T (° C)	Suspended concentration: Sampled C_s (ppm)	Suspended concentration: Standard deviation C_s (ppm)	Suspended concentration: Particle size d_{50} (ft×10³)	Total bed-material discharge: Concentration C_t (ppm)	Total bed-material discharge: Standard deviation C_t (ppm)	Total bed-material discharge: Particle size d_{50} (ft×10³)	Total bed-material discharge: Gradation σ	Bed material particle size d_{50} (ft×10³)	Sand waves: Length L (ft)	Sand waves: Height H_s (ft)	Sand waves: Velocity V_s (ft per min)
(1)	(2)	(3)	(4)	(5)	(6)	(7)	(8)	(9)	(10)	(11)	(12)	(13)	(14)	(15)	(16)
50A	0.007	0.96	6.09	14.5	0	0	----------	----------	----------	----------	----------	----------	----------	----------	----------
50D	.018	.91	6.09	15.8	0	0	----------	0.5	0.2	----------	----------	0.856	0.4	0.04	0.0002
51	.046	.99	9.86	16.0	9	----------	----------	12	1.7	0.705	1.71	.889	1.2	.03	.053
52	.065	.94	12.25	16.0	57	8	----------	98	16	.696	1.61	.820	1.7	.06	.096
54	.084	.93	13.62	18.3	157	40	----------	200	44	.607	1.56	.935	5.1	.17	.055
53	.108	1.02	15.58	16.9	396	100	0.584	358	67	.584	1.49	.902	6.0	.28	.29
57	.126	.48	5.11	13.9	0	0	----------	93	16	.771	1.56	.951	.7	.05	.080
56	.126	.75	11.09	15.3	407	297	.591	550	147	.623	1.58	.823	4.9	.20	.16
55	.130	1.08	17.80	18.1	534	203	.689	639	173	.646	1.48	.886	9.2	.36	.13
45	.138	.84	21.84	17.8	679	136	.541	1,270	675	.755	1.76	.951	----------	----------	----------
43	.140	1.13	19.23	17.4	556	112	.640	931	248	.686	1.60	.912	9.7	.44	.13
44	.163	1.03	21.55	16.8	623	151	.820	833	157	.630	1.56	.856	11.1	.41	.18
42	.167	.94	15.68	14.8	416	57	.902	704	70	.656	1.60	.837	8.5	.40	.086
46	.167	.74	21.76	18.5	857	98	.554	1,670	172	.853	1.64	.827	----------	----------	----------
58	.185	.46	6.75	14.2	331	129	.689	753	104	.702	1.53	.902	9.0	.15	.26
47	.280	.63	21.79	13.6	3,770	461	.600	4,760	673	.758	1.73	.863	3.4	.05	----------
48	.493	.59	21.69	15.9	10,800	1,150	.662	9,080	1,020	.646	1.53	.856	4.7	.15	----------
39	.813	.55	21.71	10.2	34,000	1,710	.627	28,700	9,460	.656	1.46	.787	5.0	.18	----------
41	.952	.45	15.41	11.0	43,300	2,020	.715	35,600	7,920	.636	1.42	.955	4.4	.12	----------
40	1.022	.60	21.35	10.8	41,400	9,470	.623	35,800	6,150	.656	1.45	1.033	----------	.12	----------

TABLE 4.—*Experimental variables and parameters*

Run	Slope $\times 10^2$ S	Depth D (ft)	Water discharge Q (cu ft per sec)	Temperature T (° C)	Suspended concentration: Sampled C_s (ppm)	Suspended concentration: Standard deviation C_s (ppm)	Suspended concentration: Particle size d_{50} (ft×10³)	Total bed-material discharge: Concentration C_t (ppm)	Total bed-material discharge: Standard deviation C_t (ppm)	Total bed-material discharge: Particle size d_{50} (ft×10³)	Total bed-material discharge: Gradation σ	Bed material particle size d_{50} (ft×10³)	Sand waves: Length L (ft)	Sand waves: Height H_s (ft)	Sand waves: Velocity V_s (ft per min)
(1)	(2)	(3)	(4)	(5)	(6)	(7)	(8)	(9)	(10)	(11)	(12)	(13)	(14)	(15)	(16)
7	0.007	1.01	6.61	13.9	0	0	----------	0	0	----------	----------	----------	----------	----------	----------
8	.011	1.00	7.76	11.9	0	0	----------	0	0	----------	----------	0.985	----------	----------	----------
9	.023	1.01	7.76	10.9	0	0	----------	2.7	1.8	----------	----------	.985	0.6	0.02	0.029
10	.041	.59	4.16	15.1	0	0	----------	1.0	.2	0.902	1.58	.866	.5	.03	.055
5	.045	1.00	10.73	16.5	0	0	----------	12	3.5	.850	2.08	.985	.7	.04	.040
13	.063	1.00	13.46	16.4	99	----------	----------	75	11	.663	1.82	.949	1.2	.06	.31
4	.069	.86	10.73	14.6	0	0	0.649	51	16	.650	2.00	.902	.8	.06	.077
11	.073	.59	4.92	14.9	0	0	----------	20	1.8	.906	1.60	.951	.6	.03	.027
33	.090	1.06	15.74	17.6	377	203	.672	330	54	.630	1.60	.853	6.2	.27	.10
[a] 1	.100	.88	12.70	16.7	403	----------	.570	405	65	.423	2.13	1.064	7.1	.29	----------
12	.108	.57	7.19	16.0	74	7	----------	150	14	.751	1.92	.886	.9	.04	.22
14	.116	.62	8.61	15.6	134	----------	----------	298	55	.725	1.71	.853	1.5	.07	.080
20	.120	1.05	18.14	15.6	347	25	.672	506	105	.607	1.62	.928	9.6	.46	.17
[a] 2	.131	.92	15.19	15.8	583	62	.354	664	158	.554	1.96	.918	11.2	.35	----------
21	.131	1.07	20.39	16.5	528	126	.518	732	101	.591	1.64	.866	9.8	.31	.16
19	.134	.65	9.90	14.9	423	82	.655	563	104	.627	1.69	.870	5.8	.20	.123
[a] 16	.134	1.02	17.23	15.8	436	89	.449	549	144	.574	1.74	.820	7.8	.34	.12
23	.134	.91	22.02	15.6	608	81	.492	1,230	248	.656	1.64	.997	11.8	.26	.38
17	.136	.65	10.01	14.7	262	44	.600	505	79	.630	1.72	.892	6.2	.25	.11
[a] 3	.136	.88	15.28	15.2	445	73	.383	733	168	.640	1.91	.843	7.6	.27	.13
18	.141	.61	11.96	14.7	439	189	.485	1,040	200	.699	1.68	.814	11.7	.24	.20
30	.142	.64	15.68	14.5	548	63	.462	1,370	102	.627	1.47	.975	----------	.04	----------
34	.150	.44	5.50	14.1	----------	----------	----------	480	127	.788	1.69	.951	1.8	.06	.095
22	.153	.60	14.92	12.7	442	53	.511	1,540	59	.755	1.62	.951	----------	----------	----------
[a] 15	.158	.75	12.87	13.0	389	34	.446	789	123	.620	1.68	.837	8.2	.35	.098
24	.172	.82	21.98	15.7	763	375	.475	2,350	351	.689	1.77	.899	16.2	.23	.36
25	.199	.72	21.85	14.7	972	328	.561	2,710	363	.804	1.64	1.031	----------	----------	----------
28	.229	.55	15.72	15.1	750	121	.586	2,760	372	.833	1.51	.873	----------	----------	----------
29	.278	.52	15.70	15.4	1,240	118	.587	3,120	135	.886	1.72	.929	----------	----------	----------
26	.328	.50	15.51	15.0	1,740	133	.573	5,060	1,160	.820	1.62	.886	2.5	.06	----------
32	.470	.58	21.76	10.8	9,490	1,360	.590	10,500	1,590	.676	1.71	.846	3.4	.07	----------
27	.533	.43	15.47	15.1	8,240	251	.557	11,500	866	.682	1.71	.916	3.1	.14	----------
31	.593	.56	21.34	10.2	16,400	634	.613	13,000	2,630	.591	1.34	.906	3.8	.22	----------
35	.815	.54	21.33	10.9	31,800	5,080	.619	27,600	3,810	.650	1.46	.903	6.0	.25	----------
37	.820	.30	8.34	11.6	7,820	941	.639	19,900	1,690	.885	1.91	.935	3.0	.13	----------
38	.930	.40	15.26	11.1	33,800	4,220	.698	36,100	6,650	.656	1.48	.912	4.5	.14	----------
36	1.007	.57	21.38	11.5	47,400	8,660	.648	42,400	11,400	.669	1.43	.984	5.7	.12	----------

[a] Slope poorly defined.

for 0.27-mm sand in 8-foot-wide flume

Run	Mean velocity V (ft per sec)	Velocity profile: Slope B	Velocity profile: Intercept C	Shear velocity V_* (ft per sec)	Bed-material discharge: Sampled suspended q_s (lb per sec per ft)	Bed-material discharge: Total q_t (lb per sec per ft)	Kinematic viscosity $\times 10^5$ ν (ft per sec)	Shear stress at bed τ (lb per ft)	Reynolds number $\times 10^{-2}$ R	Froude number F	Resistance factor: Darcy-Weisbach f	Resistance factor: Chezy $C/\sqrt{g}$	Resistance factor: Manning n (ft$^{1/6}$)	Bed configuration
(1)	(17)	(18)	(19)	(20)	(21)	(22)	(23)	(24)	(25)	(26)	(27)	(28)	(29)	(30)
50A	0.79	0.18	1.23	0.047	0	0	1.25	0.0042	607	0.14	0.0277	17.0	0.015	Plane.
50D	.84	.20	1.27	.073	0	.000024	1.21	.010	631	.16	.0598	11.6	.022	Ripple.
51	1.24	.52	1.70	.121	.0007	.00092	1.20	.028	1,023	.22	.0763	10.2	.026	Do.
52	1.63	.58	2.03	.140	.0055	.0094	1.20	.038	1,277	.30	.0592	11.6	.022	Do.
54	1.83	.66	2.22	.159	.017	.021	1.13	.049	1,506	.33	.0600	11.5	.023	Dune.
53	1.91	.45	2.18	.188	.048	.044	1.17	.069	1,665	.33	.0778	10.1	.026	Do.
57	1.33	.84	1.67	.140	0	.0037	1.27	.038	503	.34	.0881	9.5	.024	Ripple.
56	1.85	.93	2.70	.174	.035	.048	1.22	.059	1,137	.38	.0711	10.6	.024	Dune.
55	2.06	.68	2.63	.213	.074	.09	1.14	.088	1,952	.35	.0852	9.7	.027	Do.
45	3.25	1.24	4.07	.193	.116	.22	1.15	.072	2,374	.62	.0283	16.8	.015	Transition.
43	2.13	.37	2.15	.226	.084	.14	1.16	.099	2,075	.35	.0898	9.4	.029	Dune.
44	2.62	.68	3.24	.233	.105	.14	1.18	.105	2,287	.45	.0630	11.3	.023	Do.
42	2.09	.50	2.26	.225	.051	.086	1.24	.098	1,584	.38	.0926	9.3	.028	Do.
46	3.68	1.40	4.74	.199	.15	.28	1.12	.077	2,431	.75	.0235	18.4	.014	Plane.
58	1.83	.30	2.07	.166	.017	.040	1.26	.053	668	.48	.0655	11.0	.021	Dune.
47	4.32	----------	----------	.238	.64	.81	1.28	.110	2,126	.96	.0243	18.1	.014	Antidune.
48	4.60	----------	----------	.306	1.83	1.54	1.20	.182	2,262	1.06	.0354	15.0	.016	Do.
39	4.93	----------	----------	.379	5.76	4.86	1.40	.279	1,937	1.17	.0474	13.0	.018	Do.
41	4.28	----------	----------	.371	5.21	4.28	1.38	.267	1,396	1.12	.0602	11.5	.020	Chute-pool.
40	4.45	----------	----------	.444	6.91	5.98	1.38	.383	1,935	1.01	.0798	10.0	.024	Do.

for 0.28-mm sand in 8-foot-wide flume

Run	Mean velocity V (ft per sec)	Velocity profile: Slope B	Velocity profile: Intercept C	Shear velocity V_* (ft per sec)	Bed-material discharge: Sampled suspended q_s (lb per sec per ft)	Bed-material discharge: Total q_t (lb per sec per ft)	Kinematic viscosity $\times 10^5$ ν (sq ft^2 per sec)	Shear stress at bed τ (lb per sq ft)	Reynolds number $\times 10^{-2}$ R	Froude number F	Resistance factor: Darcy-Weisbach f	Resistance factor: Chezy $C/\sqrt{g}$	Resistance factor: Manning n (ft$^{1/6}$)	Bed configuration
(1)	(17)	(18)	(19)	(20)	(21)	(22)	(23)	(24)	(25)	(26)	(27)	(28)	(29)	(30)
7	0.82	0.17	0.81	0.048	0	0	1.27	0.0044	652	0.14	0.0271	17.2	0.015	Plane.
8	.97	----------	----------	.060	0	0	1.34	.0069	724	.17	.0301	16.3	.016	Do.
9	.96	.45	.84	.086	0	.00016	1.38	.014	703	.17	.0649	11.1	.024	Ripple.
10	.88	.59	.85	.088	0	.000032	1.23	.015	422	.20	.0804	10.0	.024	Do.
5	1.34	.69	1.41	.120	0	.0010	1.19	.028	1,126	.24	.0646	11.1	.024	Do.
13	1.68	1.01	1.97	.142	.0104	.0079	1.19	.039	1,412	.30	.0566	11.9	.022	Do.
4	1.56	.76	1.80	.138	0	.0043	1.25	.037	1,073	.30	.0628	11.3	.023	Do.
11	1.04	.47	1.04	.118	0	.00077	1.23	.027	499	.24	.1025	8.8	.027	Do.
33	1.86	.36	2.22	.175	.046	.041	1.15	.060	1,714	.32	.0710	10.6	.025	Dune.
1	1.80	.32	2.06	.168	.040	.040	1.18	.055	1,342	.34	.0700	10.7	.024	Do.
12	1.58	.71	1.79	.141	.0042	.0084	1.20	.038	750	.37	.0635	11.2	.021	Ripple.
14	1.74	.71	2.15	.152	.0090	.020	1.21	.045	892	.39	.0612	11.4	.021	Dune.
20	2.16	.55	2.55	.201	.049	.072	1.21	.079	1,874	.37	.0696	10.7	.025	Do.
2	2.06	----------	----------	.197	.069	.079	1.21	.075	1,566	.38	.0732	10.5	.025	Do.
21	2.38	.33	2.41	.212	.084	.116	1.19	.087	2,140	.41	.0637	11.2	.024	Do.
19	1.90	.39	2.19	.167	.033	.043	1.23	.054	1,004	.42	.0622	11.4	.022	Do.
16	2.11	.31	2.28	.210	.059	.074	1.21	.085	1,779	.37	.0791	10.1	.026	Do.
23	3.02	1.07	3.15	.198	.105	.21	1.21	.076	2,271	.56	.0344	15.2	.017	Transition.
17	1.92	.46	1.67	.169	.020	.039	1.24	.055	1,006	.42	.0618	11.4	.021	Dune.
3	2.17	.91	2.53	.196	.053	.087	1.22	.075	1,565	.41	.0655	11.0	.023	Do.
18	2.45	.56	2.51	.166	.041	.097	1.24	.054	1,205	.55	.0369	14.7	.016	Do.
30	3.06	1.06	3.95	.171	.067	.168	1.25	.057	1,567	.67	.0250	17.9	.014	Transition.
34	1.56	.34	2.01	.146	----------	.021	1.26	.041	545	.41	.0699	10.7	.021	Dune.
22	3.11	1.26	3.91	.172	.051	.179	1.31	.057	1,424	.71	.0244	18.1	.013	Plane.
15	2.14	.25	2.57	.195	.039	.079	1.30	.074	1,235	.44	.0667	11.0	.023	Dune.
24	3.35	.82	3.82	.213	.131	.40	1.21	.088	2,270	.65	.0324	15.7	.016	Transition.
25	3.79	1.29	4.89	.215	.166	.46	1.24	.089	2,200	.79	.0257	17.6	.014	Plane.
28	3.57	1.22	4.60	.201	.092	.34	1.23	.079	1,596	.85	.0255	17.7	.014	Do.
29	3.77	1.36	4.97	.216	.152	.38	1.22	.090	1,607	.92	.0262	17.5	.014	Do.
26	3.88	1.87	5.48	.230	.211	.61	1.23	.102	1,577	.97	.0281	16.9	.014	Antidune.
32	4.69	----------	----------	.296	1.61	1.78	1.38	.170	1,971	1.09	.0319	15.8	.015	Do.
27	4.50	----------	----------	.272	.99	1.39	1.23	.143	1,573	1.21	.0292	16.6	.014	Do.
31	4.76	----------	----------	.327	2.73	2.16	1.40	.207	1,904	1.12	.0378	14.6	.016	Do.
35	4.93	----------	----------	.376	5.29	4.60	1.38	.275	1,929	1.18	.0466	13.1	.018	Do.
37	3.48	----------	----------	.281	.51	1.30	1.35	.154	773	1.12	.0523	12.4	.017	Do.
38	4.77	----------	----------	.346	4.03	4.27	1.37	.232	1,393	1.33	.0421	13.8	.016	Chute-pool.
36	4.69	----------	----------	.430	7.91	7.08	1.36	.358	1,966	1.09	.0672	10.9	.022	Do.

TABLE 5.—*Experimental variables and parameters*

Run	Slope $\times 10^2$ S	Depth D (ft)	Water discharge Q (cu ft per sec)	Temperature T (° C)	Suspended concentration: Sampled C_s (ppm)	Suspended concentration: Standard deviation C_s (ppm)	Suspended concentration: Particle size d_{50} (ft$\times 10^3$)	Total bed-material discharge: Concentration C_t (ppm)	Total bed-material discharge: Standard deviation C_t (ppm)	Total bed-material discharge: Particle size d_{50} (ft$\times 10^3$)	Total bed-material discharge: Gradation σ	Bed material particle size d_{50} (ft$\times 10^3$)	Sand waves: Length L (ft)	Sand waves: Height H (ft)	Sand waves: Velocity V_s (ft per min)
(1)	(2)	(3)	(4)	(5)	(6)	(7)	(8)	(9)	(10)	(11)	(12)	(13)	(14)	(15)	(16)
14	0.015	0.61	3.94	10.2	----	----	----	0	0	----	----	----	----	----	----
13	.019	.35	1.84	9.0	----	----	----	0	0	----	----	----	----	----	----
17	.020	.98	6.22	12.0	----	----	----	.7	.2	----	----	----	0.8	0.04	----
16	.021	.81	5.11	12.0	----	----	----	1.2	.6	0.728	2.70	----	.7	.06	----
15	.023	.80	5.07	11.0	----	----	----	.7	.5	.837	2.68	1.44	----	----	----
18	.031	.58	3.62	11.3	----	----	----	.4	.1	----	----	----	.7	.04	----
2	.036	.82	7.90	11.0	----	----	----	9.4	.3	.968	2.47	1.35	1.2	.07	----
3	.039	.85	7.90	11.5	----	----	----	10	5.6	.935	2.79	1.48	1.4	.09	----
9	.040	.55	3.84	12.0	----	----	----	1.4	.8	.361	3.80	1.54	.7	.06	----
1	.042	.80	7.85	9.0	----	----	----	23	7	1.160	3.95	1.44	2.0	.10	----
5	.047	.75	7.93	11.0	----	----	----	27	10	.863	2.77	1.52	1.0	.07	----
11	.049	.35	1.95	11.5	----	----	----	4.7	3.9	----	----	1.46	.8	.06	----
4	.057	.69	7.94	10.0	----	----	----	92	18	1.030	2.29	1.51	4.2	.15	----
8	.060	.51	3.83	12.0	----	----	----	7.6	2.5	.846	2.78	1.39	.7	.06	----
7	.078	.70	7.98	11.5	----	----	----	268	20	.637	3.36	1.46	4.4	.20	----
10	.088	.33	1.95	10.5	----	----	----	16	4.1	1.400	1.64	1.54	.8	.08	----
6	.088	.46	3.90	9.5	----	----	----	42	16	1.440	1.86	1.64	1.6	.10	----
12	.106	.29	1.95	11.7	----	----	----	1.0	.8	.771	3.70	1.54	.9	.06	----
19	.112	.41	4.24	18.0	----	----	----	208	52	.951	3.28	1.57	6.4	.26	----
21	.114	.96	12.12	16.0	189	----	0.31	380	34	.820	2.81	1.36	4.8	.31	----
22	.124	1.00	13.54	15.7	----	----	1.33	554	102	.791	2.58	1.25	7.5	.52	----
25	.189	.42	4.91	17.0	----	----	----	378	77	1.100	2.03	1.50	6.3	.26	----
20	.193	.61	8.14	16.4	388	----	.43	508	61	.663	2.84	1.61	5.4	.36	----
23	.247	.65	13.34	16.0	558	----	.46	856	206	.755	2.43	1.40	6.6	.41	----
24	.289	.62	8.73	17.0	----	----	1.11	917	711	.820	2.29	1.23	5.5	.31	----
40	.301	.81	21.41	19.0	917	----	.44	2,460	657	.810	1.97	1.41	7.4	.31	----
39	.364	.55	20.64	19.0	747	----	.49	3,960	338	1.010	1.92	1.51	3.7	.10	----
26	.366	.34	14.45	17.0	----	----	.44	4,580	275	1.140	1.87	1.54	----	----	----
28	.366	.40	11.19	16.0	3,970	----	1.08	4,230	594	1.110	1.84	1.65	2.6	.05	----
29	.369	.30	4.54	17.4	----	----	1.31	1,850	241	1.190	2.08	1.48	6.4	.23	----
31	.432	.44	14.85	17.5	----	----	1.51	4,750	409	1.250	1.80	1.58	3.2	.06	----
27	.436	.33	7.91	18.0	----	----	1.12	4,100	291	1.210	1.98	1.66	10.2	.19	----
36	.446	.19	3.15	19.0	323	----	.65	1,370	795	1.350	2.10	1.50	.9	.03	----
41	.466	.54	21.62	18.7	907	----	.65	4,340	785	1.380	1.76	1.14	3.9	.14	----
30	.492	.27	5.33	17.2	----	----	1.38	3,550	457	1.350	1.85	1.57	6.0	.12	----
35	.494	.25	5.58	17.0	2,680	----	1.02	4,610	330	1.330	1.71	1.48	2.2	.07	----
34	.546	.28	8.44	17.5	682	----	.59	5,690	1,050	1.450	1.77	1.31	2.5	.08	----
33	.607	.27	10.02	16.0	----	----	1.71	6,810	442	1.360	1.85	1.26	2.8	.10	----
38	.619	.50	21.38	19.0	732	----	.68	6,230	844	1.590	1.83	1.36	3.8	.09	----
37	.620	.43	18.87	18.5	752	----	.66	5,570	688	1.740	1.83	1.65	3.8	.08	----
32	.656	.37	14.96	18.0	----	----	1.56	6,180	764	1.670	1.84	1.35	3.7	.29	----
45	.862	.28	5.58	18.9	250	----	.66	9,630	1,440	1.590	1.61	1.33	1.6	.11	----
44	.898	.28	10.83	19.4	3,020	----	.98	15,100	4,160	1.570	1.60	1.74	3.0	.21	----
42	.986	.31	13.43	20.0	4,520	----	1.21	11,400	1,890	1.720	1.65	1.30	3.6	.25	----
43	1.01	.43	21.42	18.5	----	----	----	11,500	232	1.280	1.80	1.57	5.8	.27	----

for 0.45-mm sand in 8-foot-wide flume

Run	Mean velocity V (ft per sec)	Velocity profile: Slope B	Velocity profile: Intercept C	Shear velocity V_* (ft per sec)	Bed-material discharge: Sampled suspended q_s (lb per sec per ft)	Bed-material discharge: Total q_t (lb per sec per ft)	Kinematic viscosity $\times 10^5$ ν (sq ft per sec)	Shear stress at bed τ (lb per sq ft)	Reynolds number $\times 10^{-2}$ R	Froude number F	Resistance factor: Darcy-Weisbach f	Resistance factor: Chezy $C/\sqrt{g}$	Resistance factor: Manning n (ft$^{1/6}$)	Bed configuration
(1)	(17)	(18)	(19)	(20)	(21)	(22)	(23)	(24)	(25)	(26)	(27)	(28)	(29)	(30)
14	0.81	0.221	0.90	0.054	----------	0	1.40	0.0057	353	0.18	0.0359	14.9	0.016	Plane.
13	.65	.108	.67	.046	----------	0	1.46	.0041	156	.19	.0405	14.0	.016	Do.
17	.80	.161	.92	.071	----------	.000034	1.34	.012	585	.14	.0788	10.1	.026	Ripples.
16	.79	.261	.98	.067	----------	.000048	1.34	.0086	478	.15	.0568	11.9	.021	Do.
15	.79	.32	.98	.077	----------	.000028	1.38	.011	458	.16	.0759	10.3	.025	Do.
18	.78	.22	.86	.076	----------	.000011	1.36	.011	333	.18	.0761	10.2	.023	Do.
2	1.20	----------	----------	.097	----------	.00058	1.38	.018	713	.23	.0528	12.3	.021	Do.
3	1.16	.36	1.49	.103	----------	.00062	1.36	.021	725	.22	.0635	11.2	.023	Do.
9	.88	.30	1.33	.084	----------	.000042	1.34	.014	361	.21	.0732	10.5	.023	Do.
1	1.23	.35	1.68	.104	----------	.00141	1.46	.021	674	.24	.0572	11.8	.021	Do.
5	1.32	.41	1.79	.107	----------	.00167	1.38	.022	717	.27	.0521	12.4	.020	Do.
11	.70	.30	1.21	.074	----------	.000071	1.36	.011	180	.21	.0902	9.4	.024	Do.
4	1.44	.36	1.86	.113	----------	.0057	1.41	.025	705	.31	.0489	12.8	.019	Dune.
8	.93	.36	1.40	.099	----------	.00023	1.34	.019	354	.23	.0911	9.4	.025	Ripple.
7	1.43	.22	1.80	.133	----------	.0167	1.36	.034	736	.30	.0688	10.8	.023	Dune.
10	.75	.38	1.32	.097	----------	.00024	1.39	.018	178	.23	.1330	7.8	.028	Ripple.
6	1.07	.64	1.65	.114	----------	.00128	1.43	.025	344	.28	.0911	9.4	.025	Do.
12	.85	.41	1.45	.099	----------	.000015	1.35	.019	183	.28	.1096	8.5	.025	Do.
19	1.30	.56	1.87	.122	----------	.0069	1.14	.029	468	.36	.0700	10.7	.021	Dune.
21	1.58	1.05	1.75	.188	0.0179	.036	1.20	.068	1,264	.28	.1129	8.4	.031	Do.
22	1.70	.61	1.91	.200	----------	.058	1.21	.077	1,405	.30	.1105	8.5	.031	Do.
25	1.47	.32	2.25	.160	----------	.0145	1.17	.050	528	.40	.0946	9.2	.025	Do.
20	1.68	.61	2.06	.195	.025	.032	1.19	.073	861	.38	.1075	8.6	.028	Do.
23	2.57	.32	2.75	.227	.058	.089	1.20	.100	1,392	.56	.0626	11.3	.022	Do.
24	1.76	.85	2.57	.240	----------	.062	1.17	.112	933	.39	.1490	7.3	.033	Do.
40	3.32	.49	3.83	.280	.153	.41	1.11	.152	2,423	.65	.0570	11.8	.022	Do.
39	4.71	1.80	5.90	.254	.120	.64	1.11	.125	2,334	1.12	.0232	18.6	.013	Standing wave.
26	5.38	1.61	5.03	.200	----------	.52	1.17	.078	1,563	1.63	.0111	26.9	.008	Plane.
28	3.52	1.60	5.60	.217	.35	.37	1.20	.091	1,173	.98	.0304	16.2	.014	Transition.
29	1.89	1.15	3.35	.189	----------	.066	1.16	.069	489	.61	.0798	10.0	.022	Dune.
31	4.24	1.60	5.32	.247	----------	.55	1.16	.119	1,608	1.13	.0272	17.1	.013	Standing wave.
27	2.99	1.17	4.32	.215	----------	.25	1.14	.090	866	.92	.0415	13.9	.016	Transition.
36	2.04	.73	----------	.165	.0079	.034	1.11	.053	349	.82	.0525	12.4	.016	Do.
41	5.05	1.60	6.40	.285	.153	.73	1.12	.157	2,435	1.21	.0254	17.7	.013	Standing wave.
30	2.47	1.70	4.34	.207	----------	.148	1.16	.083	575	.84	.0561	11.9	.018	Transition.
35	2.80	2.07	4.93	.199	.117	.201	1.17	.077	598	.99	.0406	14.0	.015	Do.
34	3.73	1.99	5.73	.222	.045	.37	1.16	.095	900	1.24	.0283	16.8	.013	Standing wave.
33	4.60	1.62	5.48	.230	----------	.53	1.20	.102	1,035	1.56	.0200	20.0	.011	Do.
38	5.38	1.78	6.70	.316	.122	1.04	1.11	.193	2,423	1.34	.0275	17.0	.014	Do.
37	5.54	1.99	6.15	.293	.111	.82	1.12	.166	2,127	1.49	.0224	18.9	.012	Transition.
32	5.03	1.29	5.95	.280	----------	.72	1.14	.151	1,633	1.46	.0247	18.0	.012	Antidune.
45	2.50	1.51	4.75	.279	.0109	.42	1.11	.151	631	.83	.0995	9.0	.024	Do.
44	4.78	1.79	6.80	.285	.255	1.28	1.10	.157	1,217	1.59	.0283	16.8	.013	Do.
42	5.36	2.20	7.20	.314	.47	1.19	1.08	.191	1,539	1.70	.0274	17.1	.013	Do.
43	6.18	----------	----------	.374	----------	1.92	1.12	.271	2,373	1.66	.0292	16.6	.014	Do.

TABLE 6.—*Experimental variables and parameters*

Run	Slope $\times 10^2$ S	Depth D (ft)	Water discharge Q (cu ft per sec)	Temperature T (°C)	Suspended concentration: Sampled C_s (ppm)	Suspended concentration: Standard deviation C_s (ppm)	Suspended concentration: Particle size d_{50} (ft$\times 10^3$)	Total bed-material discharge: Concentration C_t (ppm)	Total bed-material discharge: Standard deviation C_t (ppm)	Total bed-material discharge: Particle size d_{50} (ft$\times 10^3$)	Total bed-material discharge: Gradation σ	Bed material particle size d_{50} (ft$\times 10^3$)	Sand waves: Length L (ft)	Sand waves: Height H_s (ft)	Sand waves: Velocity V_s (ft per min)
(1)	(2)	(3)	(4)	(5)	(6)	(7)	(8)	(9)	(10)	(11)	(12)	(13)	(14)	(15)	(16)
19	0.013	1.01	8.06	19.8	0	0	----	0	0	----	----	----	----	----	----
25	.022	1.01	9.88	19.3	0	0	----	0	0	----	----	----	----	----	----
26	.022	1.02	10.80	19.0	0	0	----	0	0	----	----	----	----	----	----
27	.028	1.01	11.86	22.7	0	0	----	2.8	----	----	----	2.79	----	----	----
20	.028	1.03	10.91	19.6	0	0	----	.4	.2	----	----	----	----	----	----
21	.030	1.01	12.06	20.5	0	0	----	.4	----	----	----	----	----	----	----
18	.037	1.01	13.42	18.0	0	0	----	21	3.6	2.64	1.43	3.15	2.1	0.04	0.06
28	.037	1.04	14.53	20.7	0	0	----	28	8.7	2.95	1.37	3.02	3.7	.05	.07
29	.043	.50	4.62	18.9	0	0	----	0	0	----	----	----	----	----	----
22	.043	.49	4.49	19.0	0	0	----	0	0	----	----	----	----	----	----
30	.050	.51	5.06	18.9	0	0	----	----	----	----	----	----	----	----	----
31	.054	.50	5.42	16.8	0	0	----	4.2	.2	----	----	3.22	----	----	----
15	.059	1.05	16.25	19.7	4.1	----	----	65	30	2.58	1.45	3.28	2.6	.09	.14
23	.062	.49	5.10	19.2	0	0	----	----	----	----	----	----	----	----	----
32	.064	.52	6.25	16.7	0	0	----	26	9.8	2.79	1.38	2.98	----	----	----
24	.068	.49	5.71	19.3	0	0	----	15	3.7	----	----	----	----	----	----
14	.071	.58	7.41	17.4	----	----	----	63	17	2.72	1.38	3.25	2.8	.03	.07
34	.080	.54	7.08	19.5	----	----	----	73	20	2.56	1.40	2.82	2.9	.02	.12
16	.112	1.04	16.85	19.4	12	----	----	140	50	2.69	1.44	3.18	3.6	.16	.13
35	.130	.53	7.64	17.1	----	----	----	201	52	2.82	1.48	3.02	2.9	.06	.20
17	.136	1.00	16.83	19.2	30	----	----	211	58	2.89	1.50	3.08	3.5	.18	.18
33	.145	.56	8.18	19.0	14	----	----	253	84	2.53	1.54	2.99	3.3	.08	.18
5	.183	.93	16.41	17.5	80	37	2.62	308	65	2.62	2.42	2.98	5.2	.28	.17
10	.192	.46	6.90	19.0	12	----	----	450	126	2.76	1.53	3.22	3.9	.12	.24
37	.275	1.11	22.58	18.0	260	117	1.38	601	259	2.35	2.40	2.43	6.6	.34	.27
36	.304	.55	8.96	17.3	56	----	----	519	70	2.69	1.62	3.07	3.5	.13	.32
6	.313	1.04	22.30	19.1	281	135	2.23	537	227	2.16	2.81	2.92	5.8	.31	.45
7	.339	.59	10.10	18.3	357	124	1.54	822	199	3.12	1.84	3.38	4.5	.19	.44
38	.356	1.02	22.69	18.9	422	220	.94	1,080	274	2.41	2.14	2.48	6.3	.30	.58
11	.393	.92	22.22	18.3	614	----	----	1,180	630	2.39	2.74	3.15	7.4	.32	.60
8	.430	.57	11.20	17.4	313	121	1.30	1,490	646	2.80	1.53	2.89	5.9	.17	.59
12	.437	.89	22.19	18.5	656	116	2.34	1,900	737	2.49	2.33	3.02	4.8	.23	1.16
13	.587	.82	22.09	18.4	1,190	572	2.79	2,750	840	2.63	1.84	3.02	6.2	.25	2.30
9	.600	.49	11.32	18.5	498	214	2.65	2,620	724	3.05	1.64	3.17	2.7	.12	1.37
3	.65	.60	16.46	17.3	2,820	1,360	2.87	3,110	723	2.85	2.02	3.08	3.2	.19	----
1	.71	.68	22.33	19.3	3,770	529	1.87	4,020	724	2.21	2.28	3.28	----	----	----
2	.92	.53	22.07	18.2	2,320	563	1.79	6,140	2,420	2.82	1.75	3.02	4.9	.31	----
4	.94	.51	15.64	18.0	2,340	875	2.82	5,090	1,600	2.76	2.11	3.08	4.5	.11	----
41	1.12	.44	15.67	21.7	2,230	170	1.48	9,480	785	2.68	1.96	3.41	----	----	----
42	1.16	.44	20.44	20.4	1,610	741	2.16	7,320	1,280	2.95	1.51	2.66	----	----	----
40	1.23	.38	15.53	19.6	1,470	498	1.51	10,200	1,740	3.47	1.34	2.72	----	----	----
43	1.26	.44	20.63	21.0	2,500	488	2.30	7,000	1,060	3.45	1.42	2.49	----	----	----
39	1.28	.43	20.88	20.5	2,300	520	2.10	7,010	460	3.35	1.50	3.35	----	----	----

for 0.93-mm sand in 8-foot-wide flume

Run	Mean velocity V (ft per sec)	Velocity profile: Slope B	Velocity profile: Intercept C	Shear velocity V_* (ft per sec)	Bed-material discharge: Sampled suspended q_s (lb per sec per ft)	Bed-material discharge: Total q_t (lb per sec per ft)	Kinematic viscosity $\times 10^5$ ν (sq ft per sec)	Shear stress at bed τ (lb per sq ft)	Reynolds number $\times 10^{-2}$ R	Froude number F	Resistance factor: Darcy-Weisbach f	Resistance factor: Chezy $C/\sqrt{g}$	Resistance factor: Manning n (ft$^{1/6}$)	Bed configuration
(1)	(17)	(18)	(19)	(20)	(21)	(22)	(23)	(24)	(25)	(26)	(27)	(28)	(29)	(30)
19	1.00	0.41	1.52	0.065	0	0	1.09	0.008	927	0.18	0.0335	15.4	0.017	Plane.
25	1.22	.48	1.78	.085	0	0	1.10	.014	1,120	.21	.0384	14.4	.018	Do.
26	1.32	.54	2.00	.085	0	0	1.11	.014	1,212	23	.0330	15.6	.017	Do.
27	1.47	.60	2.02	.095	0	.00026	1.02	.018	1,456	.26	.0337	15.4	.017	Do.
20	1.32	.61	2.07	.097	0	.000034	1.09	.018	1,247	.23	.0432	13.6	.019	Do.
21	1.49	.67	2.22	.098	0	.000038	1.07	.019	1,406	.26	.0345	15.2	.017	Do.
18	1.66	.62	2.26	.110	0	.0022	1.14	.023	1,471	.29	.0349	15.1	.017	Dune.
28	1.75	.58	2.25	.111	0	.0032	1.06	.024	1,717	.30	.0326	15.7	.017	Do.
29	1.16	.40	1.80	.082	0	0	1.11	.013	523	.29	.0400	14.2	.017	Plane.
22	1.15	.42	1.77	.082	0	0	1.11	.013	508	.29	.0410	14.0	.017	Do.
30	1.25	.50	1.93	.090	0	----------	1.11	.016	574	.31	.0418	13.8	.017	Do.
31	1.36	.54	1.99	.093	0	.000177	1.18	.017	576	.34	.0374	14.6	.016	Do.
15	1.93	.58	2.40	.141	.00052	.0082	1.09	.039	1,859	.33	.0428	13.7	.019	Dune.
23	1.30	.57	2.07	.098	0	----------	1.10	.019	579	.33	.0459	13.2	.018	Plane.
32	1.50	.56	2.30	.103	0	.00127	1.18	.021	661	.37	.0381	14.5	.016	Do.
24	1.46	.60	2.30	.104	0	.00067	1.10	.021	650	.37	.0403	14.1	.017	Do.
14	1.60	.68	2.51	.115	----------	.0036	1.16	.026	800	.37	.0414	13.9	.017	Dune.
34	1.64	.73	2.47	.118	----------	.0040	1.10	.027	805	.39	.0413	13.9	.017	Do.
16	2.03	.97	2.59	.194	.00158	.0184	1.10	.073	1,919	.35	.0727	10.5	.025	Do.
35	1.80	.63	2.50	.149	----------	.0120	1.17	.043	815	.44	.0547	12.1	.020	Do.
17	2.10	.82	2.77	.209	.0039	.028	1.10	.085	1,909	.37	.0794	10.0	.026	Do.
33	1.83	.64	2.64	.162	.00089	.0162	1.11	.051	923	.43	.0627	11.3	.021	Do.
5	2.21	.67	2.33	.234	.0102	.039	1.16	.106	1,772	.40	.0898	9.4	.028	Do.
10	1.88	.37	2.79	.169	.00083	.024	1.11	.055	779	.49	.0643	11.2	.021	Do.
37	2.54	1.28	3.34	.313	.046	.106	1.14	.191	2,473	.43	.122	8.1	.033	Do.
36	2.04	.40	2.75	.232	.0039	.036	1.16	.104	967	.48	.103	8.8	.027	Do.
6	2.68	----------	----------	.324	.049	.093	1.11	.203	2,511	.46	.117	8.3	.032	Do.
7	2.14	.27	2.83	.254	.028	.065	1.13	.125	1,117	.49	.112	8.4	.029	Do.
38	2.78	1.58	4.15	.342	.075	.191	1.11	.227	2,555	.49	.121	8.1	.032	Do.
11	3.02	1.10	4.28	.341	.106	.204	1.13	.226	2,459	.56	.102	8.9	.029	Do.
8	2.46	1.26	3.78	.281	.027	.130	1.16	.153	1,209	.57	.104	8.8	.027	Do.
12	3.12	----------	----------	.354	.114	.33	1.12	.243	2,479	.58	.103	8.8	.029	Do.
13	3.37	2.03	5.40	.394	.205	.47	1.13	.300	2,445	.65	.109	8.6	.030	Transition.
9	2.89	1.30	4.38	.308	.044	.23	1.12	.183	1,264	.72	.0941	9.2	.025	Do.
3	3.43	----------	----------	.354	.36	.40	1.16	.243	1,774	.78	.0853	9.7	.025	Do.
1	4.10	----------	----------	.394	.66	.70	1.10	.301	2,535	.88	.0739	10.4	.024	Do.
2	5.20	----------	----------	.396	.40	1.06	1.13	.304	2,439	1.26	.0464	13.1	.018	Do.
4	3.83	----------	----------	.392	.29	.62	1.14	.299	1,713	95	.0841	9.8	.024	Do.
41	4.45	3.97	7.35	.398	.27	1.16	1.04	.308	1,883	1.18	.0640	11.2	.021	Do.
42	5.81	2.96	8.20	.405	.26	1.17	1.07	.319	2,389	1.54	.0389	14.3	.016	Standing wave.
40	5.11	2.49	7.42	.388	.178	1.24	1.09	.292	1,781	1.46	.0461	13.2	.017	Do.
43	5.86	2.64	8.68	.423	.40	1.13	1.05	.346	2,456	1.56	.0415	13.9	.017	Do.
39	6.07	3.34	8.46	.420	.38	1.14	1.07	.344	2,439	1.63	.0474	13.0	.018	Do.

TABLE 7.—*Experimental variables and parameters*

Run	Slope $\times 10^2$ S	Depth D (ft)	Water discharge Q (cu ft per sec)	Temperature T (° C)	Suspended concentration			Total bed-material discharge				Bed material particle size d_{50} (ft$\times 10^3$)	Sand waves		
					Sampled C_s (ppm)	Standard deviation C_s (ppm)	Particle size d_{50} (ft$\times 10^3$)	Concentration C_t (ppm)	Standard deviation C_t (ppm)	Particle size d_{50} (ft$\times 10^3$)	Gradation σ		Length L (ft)	Height H_s (ft)	Velocity V_s (ft per min)
(1)	(2)	(3)	(4)	(5)	(6)	(7)	(8)	(9)	(10)	(11)	(12)	(13)	(14)	(15)	(16)
1	0.014	0.51	0.91	10.0	0	0	----------	0	0	----------	----------	----------	----------	----------	----------
2	.017	.52	.88	23.4	0	0	----------	0	0	----------	----------	----------	----------	----------	----------
3	.112	.54	1.31	10.5	0	0	----------	55	11	0.886	1.63	----------	----------	0.20	----------
4	.086	.54	1.31	27.8	0	0	----------	61	16	.998	1.60	0.854	0.7	.07	----------
30	.110	.57	1.56	14.7	24	8.4	----------	91	22	.886	1.47	1.021	.6	.07	0.060
29	.103	.56	1.57	33.8	9.1	1.3	----------	117	43	1.248	1.43	1.019	3.3	.11	.050
5	.139	.56	1.88	10.2	56	14	0.616	226	62	.782	1.57	.837	1.0	.10	.0050
6	.118	.59	1.88	27.2	33	----------	----------	168	40	.788	1.48	.854	1.6	.10	.0083
27	.147	.58	2.28	14.3	168	----------	.626	455	238	.854	1.36	1.038	4.1	.21	.20
28	.214	.63	2.29	34.3	251	----------	.715	787	310	.913	1.48	1.035	4.5	.13	.19
26	.201	.71	2.67	13.1	80	3.1	.649	854	295	.933	1.46	1.071	4.6	.18	.14
25	.210	.66	2.64	33.1	274	101	.655	719	180	.867	1.56	1.019	4.2	.23	.28
21	.184	.58	3.13	12.4	196	49	.538	907	199	.847	1.58	1.035	----------	----------	----------
22	.166	.64	3.13	33.9	498	218	.649	1,150	286	.886	1.63	1.051	6.4	.18	.37
24	.172	.74	3.48	12.1	307	63	.695	706	206	.847	1.52	.969	6.8	.13	.26
23	.261	.73	3.48	32.8	227	72	.646	1,150	359	.894	1.52	.916	6.3	.20	.32
7	.189	.60	3.48	11.9	196	38	.613	1,410	194	.925	1.58	.950	----------	----------	----------
8	.194	.72	3.50	26.9	248	29	.567	1,820	405	.926	1.57	1.003	5.5	.24	.48
20	.566	.55	4.55	12.7	1,520	139	.708	5,600	527	1.012	1.49	1.001	----------	----------	----------
19	.417	.56	4.55	28.4	735	159	.767	4,340	383	.831	1.48	.979	----------	----------	----------
10	.710	.59	4.78	7.0	2,020	602	.636	5,180	1,040	1.015	1.54	1.001	----------	----------	----------
9	.493	.56	4.78	23.5	1,480	86	.688	5,530	870	1.184	1.63	.935	----------	----------	----------
12	.456	.67	5.32	7.9	1,480	384	.652	3,960	288	.923	1.46	1.051	----------	----------	----------
11	.408	.60	5.30	23.8	1,810	310	.672	5,250	812	1.035	1.69	1.051	----------	----------	----------
14	.865	.60	5.70	12.5	5,340	711	.767	12,300	3,500	.906	1.51	1.215	----------	----------	----------
13	.730	.60	5.70	31.7	2,100	111	.737	8,780	1,770	.991	1.43	1.049	----------	----------	----------
15	.835	.63	6.63	11.4	19,000	3,140	.793	26,100	5,810	.801	1.39	1.160	----------	----------	----------
16	.635	.62	6.64	26.7	14,700	4,820	.737	21,000	2,480	.864	1.44	1.527	----------	----------	----------
17	.970	.62	6.79	12.9	29,900	6,060	.816	29,600	5,120	.871	1.42	1.103	----------	----------	----------
18	.656	.61	6.82	27.9	17,400	2,860	.777	20,800	6,620	.886	1.62	1.231	----------	----------	----------
31	1.62	.65	6.71	14.5	41,600	27,800	.836	49,300	7,720	.833	1.47	----------	----------	----------	----------

for 0.32-mm sand in 2-foot-wide flume

Run	Mean velocity V (ft per sec)	Velocity profile		Shear velocity V_* (ft per sec)	Bed-material discharge		Kinematic viscosity $\times 10^5$ ν (sq ft per sec)	Shear stress at bed τ (lb per sq ft)	Reynolds number $\times 10^{-2}$ R	Froude number F	Resistance factor			Bed configuration
		Slope B	Intercept C		Sampled suspended q_s (lb per sec per ft)	Total q_t (lb per sec per ft)					Darcy-Weisbach f	Chezy $C/\sqrt{g}$	Manning n (ft $^{1/6}$)	
(1)	(17)	(18)	(19)	(20)	(21)	(22)	(23)	(24)	(25)	(26)	(27)	(28)	(29)	(30)
1	0.90	----------	----------	0.048	0	0	1.41	0.045	325	0.22	0.0227	18.7	0.012	Plane.
2	.86	----------	----------	.053	0	0	1.00	.0055	447	.21	.0305	16.2	.015	Do.
3	1.24	0.49	2.00	.139	0	.0023	1.39	.038	482	.30	.101	8.9	.027	Ripples.
4	1.24	.70	1.88	.122	0	.0025	.91	.029	736	.30	.0777	10.1	.023	Do.
30	1.39	----------	----------	.142	.0012	.0045	1.24	.039	639	.32	.0835	9.8	.024	Do.
29	1.43	----------	----------	.136	.00045	.0058	.80	.036	1,001	.34	.0724	10.5	.023	Dune.
5	1.72	2.14	7.18	.158	.0034	.0136	1.40	.049	688	.41	.0677	10.9	.022	Do.
6	1.62	2.10	6.91	.150	.0020	.0101	.92	.043	1,039	.37	.0683	10.8	.022	Do.
27	2.01	----------	----------	.166	.0122	.033	1.26	.053	925	.47	.0518	12.1	.019	Do.
28	1.85	----------	----------	.208	.0183	.057	.79	.084	1,475	.41	.101	8.9	.027	Do.
26	1.93	----------	----------	.214	.0069	.073	1.30	.089	1,054	.40	.0986	9.0	.028	Do.
25	2.05	----------	----------	.211	.0231	.061	.81	.087	1,670	.44	.0849	9.7	.025	Do.
21	2.74	.88	4.05	.185	.0195	.090	1.32	.067	1,204	.63	.0366	14.8	.016	Transition.
22	2.48	----------	----------	.185	.049	.114	.80	.066	1,984	.55	.0445	13.4	.018	Do.
24	2.39	----------	----------	.202	.034	.078	1.34	.079	1,320	.49	.0573	11.8	.021	Do.
23	2.43	----------	----------	.248	.025	.126	.81	.119	2,190	.50	.0830	9.8	.025	Do.
7	2.95	1.87	4.82	.191	.021	.156	1.34	.071	1,321	.67	.0335	15.4	.016	Do.
8	2.48	.84	4.11	.212	.028	.20	.92	.087	1,941	.52	.0585	11.7	.021	Do.
20	4.23	2.00	6.76	.313	.22	.81	1.31	.194	1,776	1.00	.0448	13.4	.018	Antidune.
19	4.18	3.75	7.50	.273	.107	.63	.90	.146	2,601	.98	.0425	15.3	.016	Plane.
10	4.12	1.70	6.22	.367	.31	.79	1.55	.261	1,568	.95	.0635	11.2	.021	Antidune.
9	4.35	2.91	7.26	.298	.22	.84	1.00	.172	2,436	1.02	.0375	14.6	.016	Do.
12	4.03	1.51	5.80	.314	.25	.67	1.51	.191	1,788	.87	.0484	12.8	.019	Plane.
11	4.51	2.13	6.78	.281	.31	.89	.98	.153	2,761	1.03	.0310	16.1	.015	Antidune.
14	4.86	----------	----------	.408	.97	2.24	1.32	.324	2,209	1.11	.0567	11.9	.020	Do.
13	4.84	----------	----------	.376	.38	1.59	.84	.273	3,457	1.10	.0510	12.9	.013	Do.
15	5.36	----------	----------	.412	4.00	5.49	1.36	.328	2,483	1.19	.0475	13.0	.019	Do.
16	5.42	----------	----------	.357	3.08	4.40	.93	.246	3,613	1.21	.0348	15.2	.016	Do.
17	5.58	----------	----------	.440	6.45	6.38	1.30	.375	2,661	1.25	.0497	12.7	.019	Do.
18	5.73	----------	----------	.359	3.79	4.53	.90	.250	3,884	1.29	.0314	16.0	.015	Do.
31	5.27	----------	----------	.580	8.89	10.54	1.25	.660	2,740	1.15	.0980	9.1	.027	Chute-pool.

TABLE 8.—*Experimental variables and parameters*

Run	Slope $\times 10^2$ S	Depth D (ft)	Water discharge Q (cu ft per sec)	Temperature T (° C)	Suspended concentration: Sampled C_s (ppm)	Suspended concentration: Standard deviation C_s (ppm)	Suspended concentration: Particle size d_{50} (ft$\times 10^3$)	Total bed-material discharge: Concentration C_t (ppm)	Total bed-material discharge: Standard deviation C_t (ppm)	Total bed-material discharge: Particle size d_{50} (ft$\times 10^3$)	Total bed-material discharge: Gradation σ	Bed material particle size d_{50} (ft$\times 10^3$)	Sand waves: Length L (ft)	Sand waves: Height H_s (ft)	Sand waves: Velocity V_s (ft per min)
(1)	(2)	(3)	(4)	(5)	(6)	(7)	(8)	(9)	(10)	(11)	(12)	(13)	(14)	(15)	(16)
7	0.025	0.50	1.12	20.2	0	0	----------	0	0	----------	----------	----------	----------	----------	----------
8	.087	.50	1.00	20.0	0	0	----------	6.6	2.3	1.000	1.52	1.049	0.8	0.02	0.01
5	.088	.40	1.12	20.0	15	3.5	0.610	47	17	.912	1.68	1.075	.9	.04	.05
11	.102	.52	1.41	20.1	54	5.6	.475	142	8.9	1.009	1.73	1.163	2.3	.05	.10
10	.213	.49	1.69	20.0	568	258	1.016	460	129	1.033	1.50	1.163	2.8	.06	.19
6	.240	.52	1.96	20.0	323	50	.617	732	160	.951	1.53	1.016	3.8	.13	.27
4	.270	.49	3.29	20.0	648	70	----------	2,210	426	.969	1.57	1.020	----------	----------	----------
1	.290	.51	4.01	20.0	393	8.5	----------	3,090	397	1.085	1.18	1.115	----------	----------	----------
9	.320	.52	2.62	19.8	2,070	306	.934	1,960	368	.918	1.50	1.082	4.4	.14	.43
12	.350	.51	4.24	20.0	625	80	.844	3,280	240	1.113	1.25	1.180	----------	----------	----------
13	.620	.50	4.42	20.3	761	171	1.050	4,990	386	1.180	1.25	1.120	----------	----------	----------
2	.800	.50	4.66	20.0	5,140	978	.945	7,110	1,100	1.115	1.26	1.016	5.5	.14	----------
3	.910	.52	5.40	20.3	11,000	1,780	.928	18,400	2,530	.990	1.36	1.049	6.1	.23	----------
14	1.14	.52	6.04	19.9	15,300	2,760	.885	18,400	1,070	1.015	1.46	1.082	----------	----------	----------

TABLE 9.—*Experimental variables and parameters*

Run	Slope $\times 10^2$ S	Depth D (ft)	Water discharge Q (cu ft per sec)	Temperature T (° C)	Suspended concentration: Sampled C_s (ppm)	Suspended concentration: Standard deviation C_s (ppm)	Suspended concentration: Particle size d_{50} (ft$\times 10^3$)	Total bed-material discharge: Concentration C_t (ppm)	Total bed-material discharge: Standard deviation C_t (ppm)	Total bed-material discharge: Particle size d_{50} (ft$\times 10^3$)	Total bed-material discharge: Gradation σ	Bed material particle size d_{50} (ft$\times 10^3$)	Sand waves: Length L (ft)	Sand waves: Height H_s (ft)	Sand waves: Velocity V_s (ft per min)
(1)	(2)	(3)	(4)	(5)	(6)	(7)	(8)	(9)	(10)	(11)	(12)	(13)	(14)	(15)	(16)
11A	0.022	0.50	1.06	18.3	0	0	----------	0	0	----------	----------	----------	----------	----------	----------
11B	.027	.50	1.25	18.5	0	0	----------	0	0	----------	----------	----------	----------	----------	----------
16	.029	.50	1.05	20.5	0	0	----------	3.5	1.5	0.449	1.90	1.015	0.41	0.02	0.004
6	.047	.51	1.06	22.5	0	0	----------	12	1.7	.443	2.96	.950	.50	.03	.004
5	.063	.52	1.46	22.6	8.1	3.8	----------	85	11	.985	2.14	1.100	.29	.005	.017
1	.097	.50	1.95	22.1	217	----------	0.282	507	137	.575	2.25	1.050	----------	----------	----------
10	.117	.48	1.69	23.4	56	9.9	.335	452	100	.463	2.03	1.170	----------	----------	----------
8	.120	.51	2.11	24.1	372	178	.373	1,030	345	.482	2.31	1.445	4.0	.15	.21
9	.143	.52	2.46	23.0	888	298	.429	1,520	534	.459	2.20	1.335	4.6	.15	.35
7	.163	.53	2.32	23.2	370	19	.370	1,220	391	.540	2.49	1.408	3.4	.12	.21
2	.188	.52	2.62	22.1	1,240	75	.354	2,790	542	.423	2.12	1.110	5.8	.08	.54
3	.343	.52	3.34	21.9	3,370	1,550	.459	4,320	504	.443	1.99	1.016	3.6	.03	.89
4	.433	.51	4.00	21.8	2,560	270	.420	5,100	824	.738	2.12	.950	----------	----------	----------
12	.447	.49	4.60	21.6	3,610	410	.478	7,900	603	.689	2.38	.985	----------	----------	----------
13	.695	.49	5.38	19.6	6,130	64	.443	15,100	1,100	.502	2.68	.919	4.4	.12	----------
15	.910	.52	6.46	19.6	8,820	80	.459	22,500	7,000	.557	2.20	1.082	8.3	.18	----------
14	.980	.51	6.04	19.6	3,770	73	.452	14,600	2,280	.715	2.50	1.147	4.2	.05	----------

for 0.33-mm (uniform) sand in 2-foot-wide flume

Run	Mean velocity V (ft per sec)	Velocity profile		Shear velocity V_* (ft per sec)	Bed-material discharge		Kinematic viscosity $\times 10^5$ ν (sq ft per sec)	Shear stress at bed τ (lb per sq ft)	Reynolds number $\times 10^{-3}$ R	Froude number F	Resistance factor			Bed configuration
		Slope B	Intercept C		Sampled suspended q_s (lb per sec per ft)	Total q_t (lb per sec per ft)					Darcy-Weisbach f	Chezy $C/\sqrt{g}$	Manning n (ft$^{1/6}$)	
(1)	(17)	(18)	(19)	(20)	(21)	(22)	(23)	(24)	(25)	(26)	(27)	(28)	(29)	(30)
7	1.14	----------	----------	0.063	0	0	1.08	0.0078	528	0.28	0.0248	18.0	0.013	Plane.
8	1.02	0.45	1.40	.118	0	.00021	1.08	.027	472	.25	.1076	8.6	.027	Ripple.
5	1.17	.70	1.90	.118	.00052	.0017	1.08	.027	531	.29	.0811	9.9	.023	Do.
11	1.38	----------	----------	.129	.0024	.0064	1.08	.032	664	.34	.0703	10.7	.022	Dune.
10	1.76	----------	----------	.182	.0300	.025	1.08	.064	799	.44	.0855	9.7	.024	Do.
6	1.92	----------	----------	.200	.0198	.046	1.08	.078	924	.47	.0871	9.6	.025	Do.
4	3.43	----------	----------	.206	.066	.23	1.08	.083	1,556	.86	.0289	16.6	.014	Transition.
1	4.02	1.10	5.00	.218	.049	.39	1.08	.092	1,898	.99	.0236	18.4	.013	Plane.
9	2.57	----------	----------	.231	.169	.16	1.09	.104	1,226	.63	.0648	11.1	.021	Dune.
12	4.24	----------	----------	.240	.083	.44	1.08	.111	2,002	1.05	.0256	17.7	.013	Plane.
13	4.52	----------	----------	.316	.105	.70	1.07	.193	2,112	1.13	.0391	14.3	.016	Antidune.
2	4.76	----------	----------	.359	.75	1.06	1.08	.250	2,204	1.19	.0454	13.3	.018	Do.
3	5.30	----------	----------	.390	1.86	3.16	1.07	.295	2,576	1.30	.0434	13.6	.017	Do.
14	5.93	----------	----------	.437	2.88	3.54	1.08	.370	2,855	1.45	.0434	13.6	.017	Do.

for 0.33-mm (graded) sand in 2-foot-wide flume

Run	Mean velocity V (ft per sec)	Velocity profile		Shear velocity V_* (ft per sec)	Bed-material discharge		Kinematic viscosity $\times 10^5$ ν (sq ft per sec)	Shear stress at bed τ (lb per sq ft)	Reynolds number $\times 10^{-3}$ R	Froude number F	Resistance factor			Bed configuration
		Slope B	Intercept C		Sampled suspended q_s (lb per sec per ft)	Total q_t (lb per sec per ft)					Darcy-Weisbach f	Chezy $C/\sqrt{g}$	Manning n (ft $^{1/6}$)	
(1)	(17)	(18)	(19)	(20)	(21)	(22)	(23)	(24)	(25)	(26)	(27)	(28)	(29)	(30)
11A	1.08	----------	----------	0.059	0	0	1.13	0.0069	477	0.27	0.0243	18.16	0.013	Plane.
11B	1.28	----------	----------	.066	0	0	1.12	.0084	569	.32	.0212	19.42	.012	Do.
16	1.07	0.093	1.24	.068	0	.00012	1.07	.0090	501	.27	.0326	15.67	.015	Ripples.
6	1.06	.088	.65	.088	0	.00041	1.02	.015	531	.26	.0549	12.07	.019	Do.
5	1.43	.52	1.60	.103	.00036	.0040	1.02	.020	731	.35	.0412	13.93	.017	Do.
1	1.99	.91	.97	.125	.013	.031	1.03	.030	968	.50	.0315	15.93	.015	Dune.
10	1.80	.68	2.80	.134	.0029	.024	1.00	.035	865	.46	.0446	13.39	.017	Do.
8	2.11	.52	2.40	.140	.024	.069	.98	.038	1,094	.52	.0354	15.04	.016	Do.
9	2.42	.74	2.58	.155	.068	.12	1.01	.046	1,248	.59	.0327	15.65	.015	Do.
7	2.23	.41	2.00	.167	.027	.090	1.00	.054	1,177	.54	.0447	13.38	.018	Do.
2	2.57	.86	3.60	.177	.101	.23	1.03	.061	1,300	.63	.0381	14.49	.016	Transition.
3	3.27	1.17	4.15	.240	.35	.46	1.03	.111	1,648	.80	.0430	13.65	.017	Do.
4	4.00	.95	5.00	.267	.32	.65	1.04	.138	1,971	.99	.0355	15.01	.016	Plane.
12	4.79	2.08	6.70	.265	.52	1.16	1.04	.137	2,259	1.21	.0246	18.05	.013	Standing waves.
13	5.61	----------	----------	.331	1.03	2.59	1.09	.212	2,515	1.41	.0278	16.95	.014	Antidunes.
15	6.34	----------	----------	.390	1.78	4.63	1.09	.295	3,019	1.55	.0303	16.25	.014	Do.
14	6.05	----------	----------	.401	.71	2.81	1.09	.312	2,823	1.49	.0351	15.08	.016	Do.

791-597 O—66——6

TABLE 10.—*Experimental variables and parameters*

Run	Slope $\times 10^2$ S	Depth D (ft)	Water discharge Q (cu ft per sec)	Temperature T (° C)	Suspended concentration: Fine Material C_f (ppm)	Suspended concentration: Sampled C_s (ppm)	Suspended concentration: Particle size d_{50} (ft$\times 10^3$)	Total bed-material discharge: Concentration C_t (ppm)	Total bed-material discharge: Standard deviation C_t (ppm)	Total bed-material discharge: Particle size d_{50} (ft$\times 10^3$)	Total bed-material discharge: Gradation σ	Bed material particle size d_{50} (ft$\times 10^3$)	Sand waves: Length L (ft)	Sand waves: Height H_s (ft)	Sand waves: Velocity V_s (ft per min)
(1)	(2)	(3)	(4)	(5)	(6)	(7)	(8)	(9)	(10)	(11)	(12)	(13)	(14)	(15)	(16)
[a] 46	0.084	1.11	14.54	13.1	----------	----------	----------	181	28	----------	----------	----------	6.0	0.41	----------
[a] 47	.042	.75	9.59	11.5	----------	0	----------	23	15	1.141	1.85	----------	8.2	.22	0.035
[a] 48	.052	1.23	15.26	11.5	----------	0	----------	59	11	1.148	1.85	----------	6.2	.32	.030
[a] 49	.173	1.33	21.32	11.0	----------	----------	----------	585	169	.823	1.96	----------	7.3	.35	.080
85	.047	.78	7.11	12.7	0	0	----------	6.0	4.9	1.364	1.66	1.502	1.2	.07	.0074
86	.046	.76	6.92	17.0	4,800	4,070	----------	1.6	.3	.249	3.19	1.437	1.0	.06	.0033
87	.046	.75	6.96	19.1	8,400	7,100	----------	2.3	1.4	.210	4.37	1.521	.9	.06	.0055
88	.049	.74	7.10	18.3	11,400	10,000	----------	2.5	1.2	.417	3.04	1.640	1.0	.07	.0015
[b] 90	.053	.60	6.97	17.1	6,950	6,690	----------	37	6.2	1.345	1.70	1.355	1.6	.06	.027
[b] 89	.065	.60	7.08	18.5	9,000	7,490	----------	31	8	1.361	2.50	1.509	1.6	.06	.030
93	.072	.62	7.20	14.7	1	53	----------	99	21	1.482	1.55	1.742	6.0	.17	.039
92	.090	.63	7.14	18.5	6,070	5,350	----------	106	52	1.509	1.93	1.619	4.6	.25	.050
91	.117	.58	7.12	18.0	8,400	8,050	----------	195	44	1.443	1.90	1.610	4.3	.25	.084
82	.248	.64	8.16	23.2	133	235	----------	429	98	1.463	1.64	1.679	4.1	.28	.17
51	.236	.62	8.11	13.1	584	553	----------	545	145	1.351	1.66	----------	5.6	.20	.19
52	.222	.55	8.01	16.0	1,620	1,830	----------	578	137	1.456	1.63	1.417	5.3	.26	.18
73	.222	.61	8.20	20.7	5,670	8,670	----------	662	138	1.509	1.83	1.565	5.4	.29	.26
74	.215	.65	8.18	21.0	7,970	23,800	----------	534	151	1.420	2.08	1.627	5.5	.34	.17
76	.203	.63	8.49	20.0	9,330	9,520	----------	463	122	1.387	2.00	1.456	5.7	.30	.16
75	.204	.64	8.24	21.2	9,460	22,900	----------	625	184	1.574	1.84	1.443	4.4	.28	1.5
53	.235	.57	8.01	17.2	10,700	2,750	----------	571	191	1.361	1.65	1.564	5.8	.34	.11
77	.199	.65	8.76	19.1	12,500	22,900	----------	639	154	1.246	2.91	1.581	5.1	.29	.091
96	.201	.53	8.31	18.6	25,000	28,600	----------	761	135	1.066	2.66	1.588	4.3	.24	.20
94	.237	.81	11.30	13.5	7	56	----------	480	146	1.404	1.77	1.624	5.2	.32	.28
83	.200	.91	15.58	16.2	0	503	----------	588	170	1.151	1.74	1.633	5.8	.43	.16
54	.240	.92	15.36	16.6	1,940	2,590	----------	657	271	1.253	1.74	1.469	6.5	.41	.33
56	.242	.90	15.36	22.1	2,860	----------	----------	1,100	466	1.148	1.70	----------	5.3	.29	.20
55	.237	.94	15.36	18.5	4,060	3,140	----------	765	202	1.164	1.88	1.692	5.9	.27	.23
57	.259	.87	15.39	21.3	4,320	5,010	----------	761	204	1.325	1.91	1.518	5.1	29	.29
58	.233	.90	15.28	20.1	5,270	4,220	----------	807	204	1.210	1.94	1.535	5.4	.26	.21
95	.180	.80	15.38	18.7	28,300	43,400	----------	1,640	239	1.099	2.42	1.771	8.6	.33	.31
78	.320	.72	11.52	20.3	12,000	13,300	----------	1,510	310	1.089	2.88	1.453	7.4	.39	.34
59	.326	.65	15.36	21.7	4,570	5,820	----------	2,920	820	1.312	1.73	1.535	7.50	.07	.72
60	.342	.62	21.35	21.1	3,600	4,390	----------	3,290	457	1.427	1.64	1.699	----------	----------	----------
61	.355	.61	21.32	23.2	6,170	7,910	----------	3,390	564	1.440	1.68	1.722	----------	----------	----------
71	.531	.32	8.22	21.4	3,600	3,040	----------	5,250	1,178	1.525	1.68	1.673	----------	----------	----------
72	.550	.32	8.26	20.2	7,100	7,490	----------	5,680	261	1.505	1.55	1.588	----------	----------	----------
70	.640	.30	8.14	20.2	3,910	3,840	----------	6,310	156	1.476	1.60	1.515	----------	----------	----------
63	.570	.43	15.50	21.2	3,020	4,540	----------	5,360	358	1.633	1.60	1.535	3.4	.23	----------
64	.578	.41	15.61	21.2	6,440	8,400	----------	5,480	302	1.630	1.60	1.601	3.4	.20	----------
65	.571	.42	15.60	21.6	9,090	11,600	----------	5,160	445	1.584	1.64	1.506	3.4	.20	----------
66	.575	.45	15.52	23.0	12,300	16,600	----------	5,130	836	1.647	1.76	1.526	3.3	.20	----------
80	.643	.39	15.27	21.8	12,100	14,000	----------	7,140	37	1.624	1.76	1.594	3.4	.26	----------
81	.634	.55	21.35	10.7	7	3,380	----------	4,480	672	2.076	1.61	1.584	4.4	.04	----------
62	.622	.54	21.23	24.5	4,790	7,320	----------	4,490	428	2.030	1.54	1.647	----------	----------	----------
67	.646	.53	20.87	22.7	11,200	11,400	----------	4,390	202	1.994	1.57	1.620	4.0	.10	----------
79	.651	.55	21.31	21.0	12,400	15,200	----------	5,760	1,038	2.204	1.82	1.355	3.9	.08	----------
84	.740	.41	15.36	15.0	7	3,700	----------	7,100	135	1.410	1.39	1.640	3.6	.21	----------
69	.734	.43	15.54	22.4	7,020	9,890	----------	8,280	782	1.601	1.71	1.430	3.7	.26	----------
98	.821	.44	15.80	19.0	42,000	57,700	----------	17,700	2,620	1.237	1.90	1.440	3.1	.24	----------
68	.740	.53	20.94	23.5	7,620	12,400	----------	6,760	461	2.181	1.55	1.738	4.0	.05	----------
100	.790	.51	21.42	13.3	106	4,240	----------	8,440	681	2.322	1.40	1.561	----------	----------	----------
99	.806	.50	21.27	19.6	26,900	42,300	----------	16,100	2,000	1.361	1.93	1.492	4.0	.31	----------
97	.960	.37	12.01	19.5	5,800	6,300	----------	8,960	2,310	2.165	1.50	1.597	3.4	.16	----------

[a] Run made to supply missing slope and depth data in the 0.45-mm set.
[b] Bed stabilized by bentonite.
[c] Computed on the basis of kinematic viscosity for distilled water.

for 0.47-mm sand in 8-foot-wide flume

Run	Mean velocity V (ft per sec)	Velocity profile: Slope B	Velocity profile: Intercept C	Shear velocity V_* (ft per sec)	Bed-material discharge: Sampled suspended q_s (lb per sec per ft)	Bed-material discharge: Total q_t (lb per sec per ft)	Kinematic viscosity $\times 10^5$ ν (sq ft per sec)	Shear stress at bed τ (lb per sq ft)	Reynolds number $\times 10^{-2}$ R [a]	Froude number F	Resistance factor: Darcy-Weisbach f	Resistance factor: Chezy $C/\sqrt{g}$	Resistance factor: Manning n ($ft^{1/6}$)	Bed configuration
(1)	(17)	(18)	(19)	(20)	(21)	(22)	(23)	(24)	(25)	(26)	(27)	(28)	(29)	(30)
[a] 46	1.64	0.50	1.97	0.173	----------	0.021	1.30	0.058	1,400	0.27	0.0893	9.5	0.028	Dunes.
[a] 47	1.60	.43	1.94	.101	0	.0017	1.36	.020	882	.33	.0317	15.9	.016	Do.
[a] 48	1.55	.30	1.91	.144	0	.0070	1.36	.040	1,402	.25	.0686	10.8	.025	Do.
[a] 49	2.00	----------	----------	.272	----------	.098	1.38	.144	1,928	.31	.1482	7.4	.038	Do.
85	1.13	.52	1.51	.109	0	.00033	1.31	.023	673	.23	.0740	10.4	.024	Ripple.
86	1.14	.56	1.50	.107	.22	.0000087	1.32	.022	741	.23	.0693	10.7	.024	Do.
87	1.16	.53	1.46	.105	.38	.000:2	1.37	.022	784	.24	.0660	11.0	.023	Do.
88	1.20	.64	1.52	.108	.56	.00014	1.50	.023	786	.25	.0649	11.1	.023	Do.
[b] 90	1.45	.59	1.97	.101	.36	.0020	1.39	.020	744	.33	.0390	14.3	.017	Do.
[b] 89	1.47	.62	1.81	.113	.41	.0017	1.42	.024	788	.33	.0465	13.1	.018	Do.
93	1.45	.46	2.05	.120	.0030	.0056	1.24	.028	725	.32	.0547	12.1	.020	Dunes.
92	1.43	.82	1.94	.135	.30	.0059	1.33	.035	804	.32	.0714	10.6	.023	Do
91	1.53	.71	1.96	.148	.45	.0108	1.42	.042	778	.35	.0747	10.4	.023	Do.
82	1.60	.56	2.20	.226	.015	.027	1.00	.099	1,024	.35	.1597	7.1	.034	Do.
51	1.62	.53	2.40	.217	.035	.034	1.28	.091	785	.36	.1436	7.5	.032	Do.
52	1.81	.42	2.30	.198	.114	.036	1.26	.076	833	.43	.0960	9.1	.026	Do.
73	1.67	----------	----------	.209	.55	.042	1.24	.085	961	.38	.1251	8.0	.030	Do.
74	1.58	.38	2.33	.212	1.52	.034	1.31	.087	978	.35	.1442	7.4	.033	Do.
76	1.69	.37	2.50	.203	.63	.031	1.38	.080	986	.38	.1153	8.3	.029	Do.
75	1.60	----------	----------	.205	1.47	.040	1.36	.081	975	.35	.1314	7.8	.031	Do.
53	1.77	.71	2.42	.208	.172	.036	1.52	.084	870	.41	.1101	8.5	.028	Do.
77	1.68	----------	----------	.204	1.57	.044	1.52	.081	984	.37	.1181	8.2	.030	Do.
96	1.94	.68	2.84	.185	1.85	.049	1.93	.066	918	.47	.0729	10.5	.023	Do.
94	1.74	----------	----------	.249	.0049	.042	1.28	.120	1,101	.34	.1633	7.0	.036	Do.
83	2.14	.65	2.50	.242	.072	.071	1.19	.114	1,636	.40	.1024	8.8	.029	Do.
54	2.08	----------	----------	.267	.31	.079	1.25	.138	1,622	.38	.1315	7.8	.033	Do.
56	2.14	1.36	3.03	.265	----------	.132	1.11	.136	1,870	.40	.1225	8.1	.032	Do.
55	2.04	----------	----------	.268	.38	.092	1.26	.139	1,348	.37	.1378	7.6	.034	Do.
57	2.20	1.55	2.94	.269	.60	.092	1.19	.141	1,823	.42	.1199	8.2	.031	Do.
58	2.11	.47	2.83	.260	.50	.096	1.25	.131	1,758	.39	.1213	8.1	.032	Do.
95	2.39	1.30	2.89	.215	5.21	.197	2.03	.090	1,707	.47	.0649	11.1	.023	Do.
78	2.00	.76	3.18	.272	1.19	.136	1.41	.144	1,346	.42	.1484	7.3	.034	Do.
59	2.96	1.51	4.75	.261	.70	.35	1.20	.132	1,850	.65	.0623	11.3	.022	Transition.
60	4.28	2.52	6.05	.261	.73	.55	1.18	.132	2,503	.96	.0298	16.4	.015	Plane.
61	4.36	1.80	5.90	.264	1.32	.56	1.20	.135	2,660	.98	.0293	16.5	.015	Do.
71	3.21	1.90	5.43	.234	.195	.34	1.18	.106	988	1.00	.0425	13.7	.016	Do.
72	3.26	1.87	5.20	.238	.48	.37	1.31	.110	966	1.02	.0427	13.1	.016	Do.
70	3.41	1.35	5.21	.249	.24	.40	1.20	.120	947	1.10	.0425	13.7	.016	Do.
63	4.48	2.77	6.53	.281	.55	.65	1.16	.153	1,835	1.20	.0315	16.0	.014	Antidune.
64	4.76	1.95	6.26	.276	1.02	.67	1.26	.148	1,859	1.31	.0269	17.2	.013	Do.
65	4.63	3.20	6.83	.278	1.41	.63	1.34	.150	1,870	1.26	.0288	16.7	.014	Do.
66	4.34	3.02	6.53	.289	2.00	.62	1.38	.161	1,934	1.14	.0354	15.0	.015	Do.
80	4.91	1.20	5.45	.284	1.67	.85	1.43	.156	1,841	1.39	.0268	17.3	.013	Do.
81	4.85	2.27	7.17	.335	.56	.75	1.38	.218	1,933	1.15	.0382	14.5	.016	Standing wave.
62	4.89	2.35	7.13	.329	1.21	.74	1.12	.210	2,694	1.17	.0362	14.9	.016	Do.
67	4.91	2.20	6.67	.332	1.85	.71	1.36	.214	2,551	1.19	.0366	14.8	.016	Do.
79	4.82	2.60	7.30	.340	2.53	.96	1.46	.223	2,525	1.15	.0397	14.2	.017	Do.
84	4.67	2.40	7.10	.313	.44	.85	1.23	.189	1,557	1.29	.0358	14.9	.015	Antidune.
69	4.48	----------	----------	.319	1.20	1.00	1.24	.197	1,889	1.20	.0405	14.0	.016	Do.
98	4.51	----------	----------	.341	7.11	2.18	2.46	.225	1,788	1.20	.0457	13.2	.017	Do.
68	4.95	2.20	7.43	.355	2.02	1.10	1.23	.245	2,624	1.20	.0412	13.9	.017	Standing wave.
100	5.28	2.69	7.94	.360	.71	1.41	1.29	.251	2,087	1.30	.0372	14.7	.016	Plane.
99	5.32	4.46	9.41	.360	7.02	2.67	1.96	.251	2,440	1.33	.0367	14.8	.016	Antidune.
97	4.07	3.21	7.69	.338	.59	.84	1.29	.221	1,369	1.18	.0552	12.0	.019	Do.

TABLE 11.—*Experimental variables and parameters*

Run	Slope $\times 10^3$ S	Depth D (ft)	Water discharge Q (cu ft per sec)	Temperature T (° C)	Suspended concentration: Fine material C_f (ppm)	Suspended concentration: Sampled C_s (ppm)	Suspended concentration: Particle size d_{50} (ft$\times 10^3$)	Total bed-material discharge: Concentration C_t (ppm)	Total bed-material discharge: Standard deviation C_t (ppm)	Total bed-material discharge: Particle size d_{50} (ft$\times 10^3$)	Total bed-material discharge: Gradation σ	Bed material particle size d_{50} (ft$\times 10^3$)	Sand waves: Length L (ft)	Sand waves: Height H_s (ft)	Sand waves: Velocity V_s (ft per min)
(1)	(2)	(3)	(4)	(5)	(6)	(7)	(8)	(9)	(10)	(11)	(12)	(13)	(14)	(15)	(16)
1	0.016	0.61	1.06	15.9	0	----	----	0	0	----	----	----	----	----	----
2	.019	.60	1.12	17.4	0	----	----	0	0	----	----	----	----	----	----
3	.026	.62	1.21	16.9	0	----	----	.6	.2	----	----	1.585	0.5	0.03	0.0001
4	.038	.59	1.59	18.0	0	----	----	17	5.8	1.647	1.34	1.526	----	.10	.0004
6	.170	.72	2.45	18.6	0	----	----	387	124	1.539	1.66	1.640	4.6	.35	.0047
5	.201	.81	3.12	19.2	0	----	----	408	217	1.499	1.60	1.575	5.0	.26	.0080
20	.338	.72	4.74	20.2	0	----	----	2,620	785	1.621	1.52	1.716	4.3	.17	.036
8	.351	.78	3.82	18.9	0	----	----	1,200	370	1.585	1.55	1.903	3.6	.23	.012
8A	.331	.84	3.82	18.7	5,740	----	----	1,050	----	1.417	1.58	1.699	3.8	.20	.012
8E	.248	.88	3.69	23.3	14,500	----	----	720	194	1.673	1.47	1.968	3.6	.19	.0073
8B	.293	.85	3.84	21.5	20,600	----	----	904	362	1.483	1.67	1.949	3.6	.20	.010
8C	.294	.86	3.83	22.4	24,300	----	----	1,100	349	1.594	1.75	1.772	4.4	.24	.011
8D	.198	.72	3.77	25.0	63,700	----	----	521	78	1.787	2.92	1.706	----	----	----
7	.388	.72	3.42	20.6	0	----	----	1,250	415	2.224	1.55	1.804	3.3	.17	.012
14	.399	.89	4.77	19.3	0	----	----	1,790	475	1.667	1.45	1.903	4.0	.20	.021
14A	.366	.82	4.78	24.3	9,580	----	----	1,970	697	1.532	1.64	1.837	5.8	.20	.030
14C	.377	.87	4.80	22.2	22,400	----	----	1,950	556	1.739	1.64	1.837	5.8	.19	.034
14B	.339	.70	4.84	22.3	44,100	----	----	2,960	316	1.296	2.91	1.837	----	----	----
19	.408	.76	3.82	21.5	0	----	----	1,200	323	1.463	1.56	1.788	4.2	.16	.018
9	.433	.72	4.16	17.7	0	----	----	1,520	404	1.421	----	1.549	4.2	.18	.022
10	.486	.64	5.33	20.3	0	----	----	2,690	945	1.706	----	1.824	----	----	----
15	.551	.74	6.94	21.7	0	----	----	3,330	416	1.821	1.53	1.732	----	----	----
15A	.550	.75	6.99	22.5	14,200	----	----	4,350	350	1.519	1.88	1.854	----	----	----
15B	.537	.75	6.96	23.7	40,900	----	----	4,710	449	1.476	3.17	1.837	----	----	----
15C	.628	.73	6.99	24.0	58,600	----	----	7,640	1,330	1.247	2.69	1.722	----	----	----
13	.565	.72	6.37	18.1	0	----	----	3,350	299	1.847	1.60	1.713	----	----	----
11	.768	.66	7.48	19.9	0	----	----	5,690	931	2.067	1.46	1.509	----	----	----
18	.520	.71	7.62	22.6	0	----	----	3,330	717	1.870	1.61	1.870	----	----	----
18A	.508	.76	7.57	22.5	13,200	----	----	3,400	349	1.804	1.62	1.837	----	----	----
18B	.790	.69	7.59	23.3	37,900	----	----	9,730	3,990	1.558	1.61	1.837	----	----	----
18C	.900	.70	7.59	23.7	58,700	----	----	22,300	5,420	1.421	1.40	1.919	----	----	----
16A	.980	.67	7.82	23.5	11,200	----	----	5,600	520	2.198	1.33	----	----	----	----
16B	1.075	.66	7.84	25.0	31,500	----	----	10,300	1,720	1.496	1.73	1.713	----	----	----
16C	1.305	.65	7.86	25.1	44,500	----	----	15,800	1,940	1.132	2.22	1.837	----	----	----
17	1.175	.65	7.89	22.5	0	----	----	9,180	945	1.460	1.74	1.690	----	----	----
17A	1.365	.65	7.83	22.3	39,600	----	----	21,800	2,400	1.214	1.63	1.837	----	----	----
17B	1.928	.68	7.86	24.0	51,900	----	----	50,000	1,900	1.460	1.30	2.100	----	----	----
12	1.438	.64	7.84	16.9	0	----	----	26,000	10,300	1.486	1.74	1.847	----	----	----

* Computed on the basis of kinematic viscosity for distilled water.

for 0.54-mm sand in 2-foot-wide flume

Run	Mean velocity V (ft per sec)	Velocity profile		Shear velocity V_* (ft per sec)	Bed-material discharge		Kinematic viscosity $\times 10^5$ ν (sq ft per sec)	Shear stress at bed τ (lb per sq ft)	Reynolds number $\times 10^{-3}$ R^*	Froude number F	Resistance factor			Bed configuration
		Slope B	Intercept C		Sampled suspended q_s (lb per sec per ft)	Total q_t (lb per sec per ft)					Darcy-Weisbach f	Chezy $C/\sqrt{g}$	Manning n (ft $^{1/6}$)	
(1)	(17)	(18)	(19)	(20)	(21)	(22)	(23)	(24)	(25)	(26)	(27)	(28)	(29)	(30)
1	0.89	0.295	1.25	0.056	----------	0	1.20	0.0061	449	0.20	0.0315	16.0	0.015	Plane.
2	.96	.294	1.34	.061	----------	0	1.16	.0071	495	.22	.0320	15.8	.015	Do.
3	1.00	.422	1.45	.072	----------	.000023	1.17	.010	526	.22	.0413	13.9	.018	Ripple.
4	1.37	.428	1.95	.085	----------	.000864	1.14	.014	711	.31	.0309	16.1	.015	Do.
6	1.74	.825	3.13	.198	----------	.030	1.12	.076	1,115	.37	.1040	8.8	.028	Dune.
5	1.95	.645	2.62	.230	----------	.040	1.10	.102	1,438	.38	.1108	8.5	.030	Do.
20	3.36	.329	6.00	.280	----------	.40	1.08	.152	2,245	.70	.0555	12.0	.021	Transition.
8	2.51	.238	4.40	.297	----------	.146	1.11	.170	1,755	.50	.1117	8.5	.030	Dune.
8A	2.33	1.90	4.15	.299	----------	.128	1.31	.173	1,741	.45	.1313	7.8	.033	Do.
8E	2.15	----------	----------	.265	----------	.085	1.46	.136	1,884	.40	.1213	8.1	.032	Do.
8B	2.30	.98	3.64	.283	----------	.110	1.70	.155	1,878	.44	.1213	8.1	.032	Do.
8C	2.28	1.79	4.20	.285	----------	.134	1.79	.158	1,914	.43	.1249	8.0	.032	Do.
8D	2.65	----------	----------	.215	----------	.063	3.20	.089	1,985	.55	.0524	12.4	.020	Transition.
7	2.44	.370	3.15	.299	----------	.136	1.06	.173	1,640	.51	.1200	8.2	.030	Dune.
14	2.74	----------	----------	.338	----------	.272	1.10	.221	2,207	.51	.1214	8.2	.032	Transition.
14A	2.95	----------	----------	.312	----------	.30	1.27	.188	2,480	.57	.0893	9.5	.027	Do.
14C	2.82	----------	----------	.325	----------	.298	1.74	.204	2,386	.53	.1060	8.7	.030	Do.
14B	3.51	----------	----------	.277	----------	.46	2.41	.149	2,413	.74	.0400	12.7	.020	Plane.
19	2.58	.99	4.16	.315	----------	.146	1.04	.192	1,871	.52	.1192	8.2	.031	Transition.
9	2.93	.85	3.91	.317	----------	.201	1.15	.195	1,841	.61	.0938	9.2	.027	Do.
10	4.30	2.88	6.88	.315	----------	.46	1.07	.193	2,545	.95	.0430	13.6	.018	Plane.
15	4.75	2.96	7.42	.363	----------	.74	1.04	.256	3,408	.97	.0468	13.1	.019	Standing waves.
15A	4.76	----------	----------	.365	----------	.97	1.47	.258	3,508	.97	.0470	13.0	.019	Do.
15B	4.73	2.13	6.90	.360	----------	1.04	2.27	.251	3,573	.96	.0464	13.1	.019	Do.
15C	4.85	----------	----------	.385	----------	1.70	2.98	.287	3,606	1.00	.0504	12.6	.020	Do.
13	4.52	3.34	7.51	.362	----------	.68	1.14	.254	2,862	.94	.0513	12.5	.020	Do.
11	5.80	4.38	8.40	.403	----------	1.36	1.08	.314	3,507	1.26	.0386	14.4	.017	Do.
18	5.44	1.78	6.60	.346	----------	.81	1.02	.231	3,814	1.14	.0323	15.7	.016	Do.
18A	5.11	----------	----------	.352	----------	.82	1.44	.240	3,796	1.04	.0379	14.5	.017	Do.
18B	5.62	----------	----------	.419	----------	2.35	1.70	.340	3,870	1.19	.0446	13.4	.018	Do.
18C	5.54	----------	----------	.450	----------	5.39	3.00	.392	3,894	1.17	.0527	12.3	.020	Antidune.
16A	5.92	----------	----------	.461	----------	1.39	1.35	.412	4,002	1.27	.0485	12.8	.019	Standing waves.
16B	6.03	----------	----------	.480	----------	2.57	1.93	.446	4,160	1.30	.0506	12.6	.020	Antidune.
16C	6.14	----------	----------	.524	----------	3.95	2.32	.532	4,168	1.34	.0582	11.7	.021	Do.
17	6.21	----------	----------	.495	----------	2.31	1.02	.475	3,949	1.36	.0509	12.5	.020	Do.
17A	6.17	----------	----------	.535	----------	5.43	2.27	.554	3,917	1.35	.0600	11.5	.021	Do.
17B	5.87	----------	----------	.651	----------	12.51	2.60	.820	4,060	1.25	.0983	9.0	.027	Do.
12	6.27	----------	----------	.543	----------	6.49	1.17	.571	3,400	1.39	.0599	11.6	.021	Do.

TABLE 12.—*Velocity-profile data for 0.19-mm sand in 8-foot-wide flume*

[The lateral section used for measuring was 95-115 ft. from the headbox. w.s.=water surface]

Run	2.0 ft from left wall of flume		4.0 ft from left wall of flume		6.0 ft from left wall of flume	
	Distance above sand bed (ft)	Velocity (fps)	Distance above sand bed (ft)	Velocity (fps)	Distance above sand bed (ft)	Velocity (fps)
24			0.936	w.s.		
			.910	1.24		
			.810	1.19		
			.710	1.15		
			.610	1.12		
			.510	1.10		
			.410	1.05		
			.310	1.05		
			.260	1.02		
			.210	1.02		
			.160	.97		
			.110	.94		
			.080	.91		
			.050	.86		
			.020	.76		
2	1.030	w.s.	1.025	w.s.	1.050	w.s.
	1.000	1.08	1.000	1.16	.983	1.11
	.800	1.11	.800	1.15	.783	1.10
	.600	1.08	.600	1.11	.583	1.03
	.400	.99	.400	1.03	.385	1.00
	.200	.87	.200	.96	.185	.84
	.100	.78	.100	.80	.085	.78
	.075	.78	.070	.69	.043	.75
	.050	.71	.050	.46	.023	.71
	.025	.68	.025	.35		
26			.274	w.s.		
			.250	1.05		
			.230	1.03		
			.190	1.00		
			.150	.98		
			.110	.93		
			.080	.90		
			.050	.84		
			.020	.77		
25	.909	w.s.	.890	w.s.	.912	w.s.
	.859	1.23	.864	1.26	.901	1.27
	.709	1.22	.764	1.22	.801	1.21
	.559	1.10	.614	1.13	.651	1.12
	.409	1.04	.464	1.13	.501	1.07
	.309	.98	.364	.99	.351	1.07
	.259	.94	.214	1.01	.251	.91
	.209	.88	.164	.87	.201	.92
	.159	.82	.114	.89	.151	.83
	.109	.78	.084	.81	.121	.76
	.079	.73	.054	.70	.091	.67
	.049	.69	.024	.68	.071	.62
	.019	.63			.051	.58
22C	.415	w.s.	.401	w.s.	.418	w.s.
	.390	.93	.375	1.11	.405	1.12
	.360	.84	.325	1.07	.305	1.03
	.310	.84	.275	1.01	.255	.99
	.260	.83	.225	.99	.205	.95
	.210	.83	.175	.96	.145	.92
	.160	.79	.125	.90	.105	.87
	.110	.77	.100	.88	.080	.79
	.085	.73	.075	.84	.055	.75
	.060	.70	.050	.77	.030	.69
	.035	.62	.010	.66	.010	.62
	.010	.58				
30	1.027	w.s.	.971	w.s.	.972	w.s.
	.988	1.52	.910	1.55	.940	1.48
	.818	1.53	.810	1.53	.870	1.52
	.718	1.55	.660	1.50	.720	1.39
	.618	1.49	.510	1.40	.570	1.43
	.518	1.41	.410	1.31	.420	1.30
	.418	1.32	.310	1.25	.320	1.19
	.318	1.24	.210	1.16	.220	1.06
	.218	1.16	.160	1.12	.150	.98
	.168	1.13	.110	.98	.100	.91
	.118	1.14	.070	.50	.060	.83
	.078	1.04			.030	.70
	.048	1.03				
	.018	.95				
1	.564	w.s.	.535	w.s.	.523	w.s.
	.547	.88	.506	1.15	.492	1.09
	.447	.76	.406	1.07	.392	1.09
	.347	.76	.306	.91	.292	.91
	.247	.68	.206	.91	.192	.84
	.197	.68	.156	.77	.142	.76
	.147	.58	.106	.77	.092	.80
	.097	.52	.056	.52	.042	.76
	.047	.52	.006	.38		
31	1.048	w.s.	1.028	w.s.	.976	w.s.
	1.020	1.82	.980	1.86	.910	1.85
	.950	1.82	.880	1.80	.810	1.83
	.850	1.76	.730	1.78	.710	1.77
	.750	1.74	.580	1.76	.560	1.71
31—Con.	0.650	1.64	0.480	1.60	0.410	1.61
	.550	1.61	.380	1.60	.310	1.56
	.450	1.53	.280	1.48	.210	1.41
	.350	1.34	.180	1.39	.160	1.30
	.250	1.20	.130	1.31	.110	1.23
	.200	1.14	.080	1.19	.070	1.15
	.150	1.11	.040	.97	.040	1.11
	.110	.88			.020	1.07
	.090	.64				
	.070	.40				
	.040	.31				
27	.479	w.s.	.516	w.s.	.517	w.s.
	.429	1.34	.472	1.35	.455	1.31
	.379	1.31	.422	1.31	.405	1.28
	.329	1.31	.372	1.28	.355	1.23
	.279	1.26	.322	1.23	.305	1.19
	.229	1.16	.272	1.19	.255	1.14
	.179	1.15	.222	1.15	.205	1.08
	.129	1.08	.192	1.06	.155	1.05
	.079	.93	.162	1.08	.105	.92
	.049	.84	.132	1.02	.075	.85
	.019	.80	.102	.92	.045	.85
			.072	.84	.015	.86
			.042	.66		
5	1.063	w.s.	1.028	w.s.		
	1.028	2.11	.998	2.00		
	.828	2.10	.798	2.02		
	.628	1.96	.598	1.92		
	.428	1.79	.398	1.74		
	.328	1.68	.298	1.68		
	.228	1.54	.198	1.50		
	.128	1.42	.148	1.43		
	.078	1.24	.098	1.24		
	.028	1.07	.073	1.19		
			.048	.93		
23	.372	w.s.	.371	w.s.	.365	w.s.
	.350	1.24	.344	1.32	.348	1.36
	.300	1.19	.294	1.29	.298	1.29
	.250	1.08	.244	1.25	.248	1.23
	.200	1.05	.194	1.16	.198	1.20
	.150	1.03	.144	1.12	.148	1.16
	.100	.92	.094	1.06	.098	1.12
	.075	.90	.069	1.02	.073	1.06
	.050	.82	.044	.98	.048	1.03
	.025	.79	.019	.90	.023	.98
32	.868	w.s.	.922	w.s.	.893	w.s.
	.820	2.41	.890	2.47	.860	2.43
	.720	2.39	.790	2.41	.780	2.40
	.620	2.36	.690	2.40	.680	2.36
	.520	2.29	.590	2.33	.580	2.30
	.420	2.02	.490	2.23	.480	2.15
	.320	1.96	.390	2.16	.380	2.10
	.220	1.90	.290	2.07	.280	2.00
	.170	1.86	.240	2.02	.180	1.82
	.120	1.76	.190	1.95	.130	1.72
	.080	1.70	.140	1.90	.090	1.53
	.050	1.56	.110	1.80	.050	1.35
	.020	1.46	.080	1.70	.020	1.30
			.050	1.67		
			.020	1.37		
8	.990	w.s.	.812	w.s.	.926	w.s.
	.948	2.48	.775	2.69	.900	2.61
	.898	2.48	.625	2.63	.800	2.61
	.748	2.39	.425	2.50	.700	2.59
	.548	2.33	.225	2.29	.500	2.45
	.348	2.12	.125	2.07	.300	2.32
	.248	1.95	.075	1.98	.200	2.27
	.148	1.68	.050	1.88	.100	1.91
	.098	1.44	.025	1.38	.050	1.66
	.048	1.38			.025	1.33
	.023	1.30				
28	.557	w.s.	.460	w.s.	.475	w.s.
	.455	1.49	.430	1.50	.445	1.48
	.335	1.34	.380	1.48	.395	1.44
	.255	1.28	.330	1.46	.345	1.37
	.205	1.15	.280	1.47	.295	1.33
	.155	1.08	.230	1.43	.245	1.31
	.105	.93	.180	1.31	.195	1.26
	.075	.79	.130	1.21	.145	1.18
	.045	.55	.080	1.17	.095	1.09
			.030	1.08	.065	.97
			.020	.97	.035	.93
					.010	.87
33	.980	w.s.	.870	w.s.		
	.920	2.57	.820	2.62		
	.820	2.59	.720	2.57		
	.720	2.56	.620	2.50		

TABLE 12.—*Velocity-profile data for 0.19-mm sand in 8-foot-wide flume*—Continued

Run	2.0 ft from left wall of flume		4.0 ft from left wall of flume		6.0 ft from left wall of flume	
	Distance above sand bed (ft)	Velocity (fps)	Distance above sand bed (ft)	Velocity (fps)	Distance above sand bed (ft)	Velocity (fps)
33—Con.	0.620	2.54	0.520	2.47		
	.520	2.52	.420	2.44		
	.420	2.49	.320	2.40		
	.320	2.45	.220	2.23		
	.220	2.37	.170	2.18		
	.120	2.26	.120	2.08		
	.070	2.04	.090	2.03		
	.030	1.43	.060	1.94		
			.030	1.90		
29	.513	w.s.	.480	w.s.	.528	w.s.
	.490	1.60	.445	1.58	.495	1.60
	.440	1.59	.345	1.55	.395	1.49
	.339	1.55	.245	1.42	.295	1.31
	.340	1.52	.195	1.30	.245	1.28
	.290	1.44	.145	1.26	.195	1.17
	.240	1.35	.095	1.12	.145	1.11
	.190	1.29	.065	1.09	.095	.98
	.140	1.19	.035	1.00	.065	.83
	.100	1.12	.010	.91	.035	.65
	.060	1.08			.015	.46
	.030	1.01				
	.010	.92				
3	.516	w.s.	.490	w.s.	.575	w.s.
	.475	1.58	.444	1.60	.547	1.61
	.375	1.55	.344	1.57	.447	1.59
	.275	1.47	.244	1.44	.347	1.51
	.175	1.35	.144	1.15	.247	1.47
	.125	1.25	.094	1.02	.197	1.40
	.075	1.07	.069	.97	.147	1.38
	.050	.95	.044	.97	.132	1.26
	.025	.40	.019	.97	.097	1.20
					.072	1.09
11	.793	w.s.	.948	w.s.	1.236	w.s.
	.721	3.09	.885	3.07	1.180	3.20
	.621	3.07	.785	2.98	1.080	3.18
	.421	3.05	.685	3.03	.880	3.15
	.221	3.03	.485	2.91	.680	3.03
	.121	2.88	.285	2.91	.480	2.86
	.071	2.75	.185	2.86	.280	2.75
	.046	2.60	.135	2.75	.180	2.66
	.021	2.44	.085	2.64	.130	2.60
			.050	2.45	.080	2.49
			.025	2.29	.055	2.37
					.030	2.12
13	.900	w.s.	.886	w.s.	.851	w.s.
	.800	3.69	.850	3.74	.798	3.80
	.650	3.65	.750	3.70	.698	3.77
	.450	3.60	.650	3.70	.598	3.69
	.350	3.48	.450	3.64	.398	3.64
	.250	3.27	.350	3.50	.298	3.49
	.150	3.06	.250	3.40	.198	3.24
	.100	2.88	.150	3.17	.098	2.97
	.050	2.50	.100	2.98	.048	2.41
	.025	2.20	.050	2.63	.023	2.26
			.025	2.42		
14	.856	w.s.	.872	w.s.	.890	w.s.
	.807	3.90	.810	4.11	.810	3.98
	.707	3.84	.710	4.00	.710	3.91
	.507	3.68	.510	3.86	.510	3.75
	.307	3.43	.310	3.54	.310	3.43
	.207	3.27	.210	3.30	.210	3.07
	.107	3.09	.110	2.87	.110	2.80
	.057	2.73	.060	2.13	.060	2.44
	.027	2.43	.030	.95	.030	2.20
15	.780	w.s.	.785	w.s.	.745	w.s.
	.710	4.13	.710	4.49	.710	4.33
	.610	3.97	.610	4.31	.610	4.29
	.410	3.70	.410	4.14	.510	4.20
	.310	3.54	.310	3.95	.310	3.80
	.210	3.25	.210	3.71	.210	3.54
	.110	3.05	.110	3.20	.110	3.34
	.060	2.54	.060	2.91	.060	3.00
	.030	2.23	.030	2.17	.030	2.73
34	.498	w.s.	.495	w.s.	.485	w.s.
	.450	2.24	.450	2.29	.460	2.24
	.370	2.02	.380	2.24	.360	2.12
	.300	1.88	.310	2.20	.310	2.07
	.230	1.85	.260	2.01	.260	1.98
	.180	1.80	.210	1.81	.210	1.81
	.130	1.86	.170	1.73	.160	1.75
34—Con.	0.090	1.72	0.130	1.70	0.120	1.58
	.060	1.44	.100	1.83	.080	1.51
	.030	1.38	.070	1.85	.050	1.43
			.030	1.76	.020	1.29
12	.924	w.s.	.859	w.s.	1.162	w.s.
	.875		.800		1.100	3.43
	.775		.700	3.93	1.050	3.41
	.675		.600	3.64	.850	3.31
	.575	3.60	.400	3.45	.650	3.26
	.475	3.51	.200	3.03	.450	3.16
	.375	3.37	.100	2.55	.250	2.76
	.275	3.26	.050	2.11	.150	2.55
	.175	3.02	.025	1.39	.100	2.39
	.075	2.41			.050	2.21
	.025	2.10			.025	2.16
6	.641	w.s.	.511	w.s.	.620	w.s.
	.622	2.52	.490	2.46	.600	2.33
	.522	2.42	.390	2.46	.550	2.24
	.422	2.28	.290	2.40	.450	2.30
	.322	2.21	.240	2.36	.250	2.00
	.222	2.07	.190	2.23	.050	1.84
	.122	1.78	.140	2.10		
	.072	1.38	.090	1.86		
	.047	1.15	.040	1.59		
	.022	.75	.015	.87		
7	.727	w.s.	.647	w.s.	.651	w.s.
	.697	2.27	.621	2.30	.625	2.50
	.597	2.25	.521	2.26	.525	2.47
	.397	2.00	.321	2.06	.425	2.36
	.297	1.84	.221	1.96	.325	2.23
	.197	1.79	.171	1.88	.225	2.08
	.147	1.83	.121	1.84	.125	1.64
	.097	1.60	.071	1.77	.075	1.48
	.047	1.43	.021	.91	.050	1.39
	.012	1.07			.025	.64
35	.349	w.s.	.522	w.s.	.522	w.s.
	.317	2.68	.480	2.25	.475	2.40
	.297	2.73	.410	2.16	.405	2.22
	.267	2.75	.340	2.13	.335	2.14
	.237	2.82	.280	2.13	.265	2.06
	.207	2.79	.240	2.10	.205	2.00
	.177	2.77	.200	2.15	.165	1.97
	.147	2.68	.160	2.11	.125	1.84
	.117	2.63	.120	1.93	.085	1.68
	.087	2.49	.090	1.97	.055	1.53
	.057	2.22	.060	1.98	.025	1.36
	.027	2.09	.030	1.78		
16	.700	w.s.	.705	w.s.	.695	w.s.
	.625	4.70	.650	4.75	.625	4.64
	.500	5.00	.550	4.63	.525	5.02
	.300	4.09	.400	5.01	.375	4.28
	.200	3.82	.300	4.18	.275	4.02
	.150	3.82	.200	3.95	.175	3.90
	.100	3.68	.150	3.82	.125	3.68
	.075	3.37	.100	3.52	.075	3.28
	.050	3.28	.075	3.37	.050	3.12
	.025	2.74	.050	3.20	.025	2.60
			.025	2.69		
10	.452	w.s.	.438	w.s.	.458	w.s.
	.393		.425		.395	3.66
	.323		.325	3.68	.325	3.52
	.223	3.60	.225	3.43	.225	3.42
	.173	2.39	.175	3.31	.175	3.19
	.123	3.17	.125	3.13	.125	3.06
	.073	2.96	.100	2.98	.100	2.98
	.048	2.66	.075	2.80	.075	2.85
	.023	2.12	.050	2.76	.050	2.64
			.025	2.58	.025	2.57
9	.411	w.s.	.441	w.s.	.385	w.s.
	.400	2.95	.397	3.30	.350	3.15
	.350	2.99	.347	3.25	.300	3.09
	.300	2.94	.247	3.04	.200	2.81
	.250	2.86	.197	2.87	.150	2.68
	.200	2.67	.147	2.67	.100	2.49
	.150	2.67	.122	2.54	.075	2.38
	.125	2.59	.097	2.31	.050	2.28
	.100	2.51	.072	2.15	.025	2.04
	.075	2.43	.047	1.98		
	.050	2.35	.022	1.73		
	.025	2.15				

TABLE 13.—*Velocity-profile data for 0.27-mm sand in 8-foot-wide flume*

[The lateral section used for measuring was 95–115 ft from the headbox. w.s.=water surface]

Run	2.0 ft from left wall of flume		4.0 ft from left wall of flume		6.0 ft from left wall of flume	
	Distance above sand bed (ft)	Velocity (fps)	Distance above sand bed (ft)	Velocity (fps)	Distance above sand bed (ft)	Velocity (fps)
50A	0.965	w.s.	0.960	w.s.	0.975	w.s.
	.920	1.25	.925	1.22	.920	1.24
	.600	1.21	.600	1.15	.600	1.19
	.400	1.18	.400	1.15	.400	1.15
	.300	1.14	.300	1.13	.300	1.12
	.200	1.11	.200	1.07	.200	1.10
	.150	1.05	.150	1.06	.150	1.07
	.100	1.04	.100	1.05	.100	1.06
	.075	1.03	.075	1.03	.075	1.02
	.050	.98	.050	1.02	.050	.99
	.025	.96	.025	.96	.025	.96
50D	.890	w.s.	.900	w.s.	.915	w.s.
	.835	1.28	.845	1.25	.860	1.23
	.600	1.23	.600	1.25	.600	1.23
	.400	1.21	.400	1.22	.400	1.22
	.300	1.16	.300	1.19	.300	1.19
	.200	1.13	.200	1.15	.200	1.14
	.150	1.09	.150	1.12	.150	1.10
	.100	1.07	.100	1.09	.100	1.09
	.075	1.05	.075	1.07	.075	1.06
	.050	1.03	.050	1.03	.050	.94
	.025	.99	.025	.99	.025	.92
51	.995	w.s.	.960	w.s.	----------	----------
	.950	1.69	.920	1.67	----------	----------
	.800	1.64	.800	1.66	----------	----------
	.600	1.58	.600	1.60	----------	----------
	.400	1.49	.400	1.52	----------	----------
	.300	1.36	.300	1.48	----------	----------
	.200	1.27	.200	1.41	----------	----------
	.150	1.16	.150	1.38	----------	----------
	.100	1.08	.100	1.36	----------	----------
	.075	1.05	.075	1.28	----------	----------
	.050	1.01	.050	1.24	----------	----------
	.025	.99	.025	1.24	----------	----------
52	.965	w.s.	1.100	w.s.	.940	w.s.
	.925	1.68	.970	----------	.890	2.07
	.800	1.66	.800	1.98	.600	1.98
	.600	1.60	.600	1.84	.400	1.86
	.400	1.41	.400	1.66	.300	1.80
	.300	1.36	.300	1.60	.200	1.74
	.200	1.23	.200	1.54	.150	1.67
	.150	1.19	.150	1.49	.100	1.61
	.100	1.05	.100	1.47	.075	1.31
	.075	1.05	.075	1.45	.050	1.36
	.050	1.03	.050	1.38	.025	1.17
	.025	1.00	.025	1.40	----------	----------
54	.830	w.s.	.890	w.s.	1.050	w.s.
	.800	2.26	.870	2.16	1.000	2.24
	.600	2.20	.800	2.12	.800	2.15
	.400	2.20	.600	2.10	.600	2.08
	.300	2.07	.400	2.04	.500	2.04
	.200	2.07	.300	1.99	.400	1.95
	.150	2.07	.200	1.76	.300	1.76
	.100	2.05	.150	1.76	.200	1.65
	.075	1.94	.100	1.76	.150	1.58
	.050	1.83	.050	1.70	.100	1.40
	.025	1.80	.025	1.70	.075	1.36
	----------	----------	----------	----------	.050	1.24
	----------	----------	----------	----------	.025	1.24
53	.940	w.s.	.950	w.s.	1.130	w.s.
	.700	2.14	.800	2.19	1.020	2.27
	.650	2.14	.600	2.17	1.000	2.23
	.400	2.11	.400	2.13	.800	1.99
	.300	2.04	.300	2.08	.600	1.98
	.200	1.88	.200	1.99	.400	1.82
	.150	1.82	.150	1.90	.300	1.67
	.100	1.79	.100	1.64	.200	1.64
	.075	1.75	.075	1.30	.150	1.59
	.050	1.65	.050	1.21	.100	1.57
	.025	1.41	.025	.70	.075	1.52
	----------	----------	----------	----------	.050	1.49
	----------	----------	----------	----------	.025	1.49
57	.489	w.s.	.494	w.s.	.444	w.s.
	.445	1.42	.450	1.27	.400	1.48
	.300	1.20	.300	1.12	.300	1.43
	.200	1.10	.200	.85	.200	1.35
	.150	1.01	.150	.70	.150	1.13
	.100	.74	.100	.63	.100	.88
	.075	.66	.075	.52	.075	.90
	.050	.82	.050	.37	.050	.74
	.025	.60	.025	.30	.025	.66
56	.800	w.s.	.750	w.s.	.730	w.s.
	.760	2.30	.725	2.57	.700	2.58
	.600	2.30	.600	2.57	.500	2.56
	.400	2.27	.400	2.37	.400	2.19
	.300	2.23	.300	2.26	.300	1.89
	.200	2.13	.200	2.11	.200	1.49
	.150	1.96	.150	1.71	.150	1.30
	.100	1.89	.100	.92	.100	.96
56—Con.	0.075	1.86	0.075	1.23	0.075	0.86
	.050	1.52	.050	1.96	.050	.70
	.025	1.31	.025	1.58	.025	.60
55	1.540	w.s.	.980	w.s.	.930	w.s.
	1.500	2.52	.910	2.47	.875	2.48
	1.350	2.47	.800	2.48	.675	2.46
	1.150	2.41	.600	2.56	.475	2.44
	.950	2.41	.400	2.59	.375	2.28
	.750	2.39	.300	2.60	.275	2.35
	.550	2.30	.200	2.60	.175	2.42
	.450	2.23	.150	2.59	.125	2.46
	.350	1.91	.100	2.53	.075	2.26
	.300	1.88	.075	2.40	.025	2.35
	.250	1.76	.050	2.24	----------	----------
	.200	.96	.025	1.73	----------	----------
	.150	1.00	----------	----------	----------	----------
	.100	1.03	----------	----------	----------	----------
	.075	1.00	----------	----------	----------	----------
	.050	1.00	----------	----------	----------	----------
	.025	1.00	----------	----------	----------	----------
45	.785	w.s.	.810	w.s.	.815	w.s.
	.720	4.04	.760	3.77	.765	3.86
	.550	3.95	.550	3.71	.550	3.68
	.400	3.78	.400	3.58	.400	3.53
	.300	3.56	.300	3.34	.300	3.39
	.200	3.26	.200	3.25	.200	3.26
	.150	3.17	.150	2.85	.150	3.05
	.100	3.05	.100	2.57	.100	2.81
	.075	2.84	.075	2.39	.075	2.65
	.050	2.73	.050	2.21	.050	2.56
	.025	2.32	.025	1.72	.025	2.41
43	.670	w.s.	1.470	w.s.	1.315	w.s.
	.525	2.24	1.450	2.04	1.295	2.37
	.400	1.95	1.350	2.00	1.175	2.36
	.300	1.86	1.150	1.97	.975	2.34
	.200	1.84	.950	1.94	.775	2.33
	.150	1.82	.750	1.90	.575	2.31
	.100	1.90	.550	1.53	.375	2.26
	.075	1.90	.350	1.61	.275	2.18
	.050	1.90	.250	1.55	.175	2.11
	.025	1.90	.150	1.55	.125	1.91
	----------	----------	.100	1.55	.075	1.69
	----------	----------	.075	1.56	.050	1.66
	----------	----------	.050	1.54	.025	1.65
	----------	----------	.025	1.48	----------	----------
44	.784	w.s.	.945	w.s.	.860	w.s.
	.700	2.77	.875	----------	.750	2.86
	.600	2.95	.675	3.33	.650	2.82
	.400	3.11	.475	3.14	.450	2.77
	.300	3.13	.275	3.04	.350	2.64
	.200	3.11	.175	2.89	.250	2.56
	.150	3.08	.125	2.69	.200	2.43
	.100	3.00	.100	2.68	.150	2.31
	.075	2.82	.075	2.33	.100	2.19
	.050	2.27	.050	2.23	.075	2.08
	.025	2.15	.025	2.23	.050	2.05
	----------	----------	----------	----------	.025	2.05
42	.915	w.s.	.890	w.s.	.925	w.s.
	.885	----------	.855	2.05	.890	2.33
	.700	2.20	.600	1.68	.600	2.34
	.500	2.18	.400	1.68	.400	2.33
	.400	2.18	.300	1.76	.300	2.29
	.300	2.05	.200	1.77	.200	2.18
	.200	2.09	.150	1.79	.150	2.01
	.150	2.09	.100	1.79	.100	1.82
	.100	1.98	.075	1.75	.075	1.54
	.075	1.90	.050	1.68	.050	1.16
	.050	.95	.025	1.38	.025	1.14
	.025	1.07	----------	----------	----------	----------
46	.687	w.s.	.717	w.s.	.682	w.s.
	.660	4.77	.700	4.60	.600	4.13
	.600	4.64	.600	4.50	.400	3.96
	.400	4.39	.400	4.17	.300	3.85
	.300	4.17	.300	4.09	.200	3.54
	.200	3.96	.200	3.63	.150	3.40
	.150	3.68	.150	3.40	.100	3.21
	.100	3.68	.100	3.10	.075	3.09
	.075	3.54	.075	2.94	.050	2.90
	.050	3.30	.050	2.82	.025	2.70
	.025	2.88	.025	2.23	----------	----------
58	.440	w.s.	.370	w.s.	----------	----------
	.430	1.97	.350	----------	----------	----------
	.300	2.06	.300	----------	----------	----------
	.200	2.10	.200	1.65	----------	----------
	.150	2.16	.150	1.62	----------	----------
	.100	2.07	.100	1.69	----------	----------
	.075	1.99	.075	1.58	----------	----------
	.050	1.77	.050	1.59	----------	----------
	.025	1.61	.025	1.51	----------	----------

TABLE 14.—*Velocity-profile data for 0.28-mm sand in 8-foot-wide flume*

[The lateral section used for measuring was 95–115 ft from the headbox. w.s. = water surface]

Run	2.0 ft from left wall of flume		4.0 ft from left wall of flume		6.0 ft from left wall of flume	
	Distance above sand bed (ft)	Velocity (fps)	Distance above sand bed (ft)	Velocity (fps)	Distance above sand bed (ft)	Velocity (fps)
7	0.985	w.s.	0.990	w.s.	0.985	w.s.
	.970	0.82	.890	0.86	.970	0.80
	.940	.81	.790	.76	.940	.80
	.840	.82	.690	.74	.840	.80
	.740	.76	.490	.73	.740	.78
	.540	.68	.390	.72	.540	.77
	.340	.67	.290	.70	.340	.75
	.240	.58	.240	.70	.240	.72
	.140	.51	.190	.68	.140	.71
	.090	.51	.140	.68	.090	.69
	.040	.50	.090	.66	.040	.66
	.010	.46	.065	.64	.010	.50
			.040	.58		
			.030	.54		
			.020	.52		
			.010	.49		
9	.980	w.s.	1.000	w.s.	1.015	w.s.
	.900	.84	.950	.78	.965	.85
	.700	.78	.700	.74	.775	.79
	.550	.76	.550	.68	.625	.76
	.400	.73	.400	.65	.475	.68
	.300	.71	.300	.60	.375	.59
	.200	.66	.200	.47	.275	.55
	.150	.53	.150	.37	.175	.50
	.100	.43	.100	.33	.150	.44
	.075	.35	.075	.30	.100	.37
	.050	.35	.050	.30	.075	.34
	.025	.34	.025	.30	.050	.28
					.025	.25
10	.580	w.s.	.580	w.s.	.580	w.s.
	.530	.70	.540	.74	.540	.71
	.400	.58	.450	.65	.450	.63
	.300	.49	.350	.52	.350	.61
	.250	.44	.250	.50	.250	.51
	.200	.43	.200	.42	.200	.44
	.175	.38	.150	.40	.150	.35
	.150	.25	.100	.34	.100	.30
	.125	.21	.075	.26	.075	.23
			.050	.23	.050	.19
			.025	.21	.025	
5	1.025	w.s.	.982	w.s.		
	.950	1.35	.940	1.39		
	.750	1.27	.750	1.35		
	.550	1.18	.550	1.29		
	.400	1.08	.400	1.20		
	.300	.98	.300	1.02		
	.200	.76	.200	.85		
	.150	.61	.150	.78		
	.100	.50	.100	.75		
	.075	.48	.075	.75		
	.050	.50	.050	.71		
	.025	.57	.025	.70		
13	1.020	w.s.	1.013	w.s.	.993	w.s.
	.960	1.81	.960	1.87	.930	1.88
	.750	1.77	.750	1.79	.750	1.86
	.550	1.56	.550	1.63	.550	1.77
	.400	1.53	.400	1.60	.400	1.72
	.300	1.43	.300	1.55	.300	1.49
	.200	1.08	.200	1.29	.200	1.28
	.150	.74	.150	1.18	.150	1.02
	.100	.64	.100	1.05	.100	.72
	.075	.72	.075	1.05	.075	.62
	.050	.48	.050	1.05	.050	.58
	.025	.35	.025	1.05	.025	.55
4	.820	w.s.	.895	w.s.	.885	w.s.
	.780	1.66	.850	1.75	.835	1.69
	.650	1.62	.700	1.72	.700	1.66
	.500	1.56	.550	1.64	.550	1.60
	.350	1.51	.400	1.46	.400	1.50
	.250	1.49	.300	1.27	.300	1.28
	.200	1.38	.200	1.09	.200	1.14
	.150	1.35	.150	.95	.150	1.04
	.100	1.33	.100	.59	.100	.93
	.075	1.31	.075	.57	.075	.86
	.050	1.30	.050	.46	.050	.73
	.025	1.30	.025	.43	.025	.61
11	.521	w.s.	.644	w.s.	.522	w.s.
	.480	.88	.600	.88	.480	.94
	.400	.87	.450	.86	.400	.93
	.300	.82	.350	.76	.300	.85
	.200	.70	.250	.66	.200	.76
	.150	.62	.200	.60	.150	.72
	.100	.58	.150	.52	.100	.64
	.075	.54	.100	.51	.075	.59
	.050	.50	.075	.50	.050	.55
	.025	.48	.050	.47	.025	.51
			.025	.44		

Run	2.0 ft from left wall of flume		4.0 ft from left wall of flume		6.0 ft from left wall of flume	
	Distance above sand bed (ft)	Velocity (fps)	Distance above sand bed (ft)	Velocity (fps)	Distance above sand bed (ft)	Velocity (fps)
33	1.005	w.s.	0.930	w.s.	1.035	w.s.
	.950	2.11	.875	2.12	.970	2.15
	.800	2.11	.600	1.98	.800	2.24
	.600	2.09	.400	2.00	.600	2.24
	.400	2.09	.300	1.95	.400	2.16
	.300	2.09	.200	1.94	.300	2.10
	.200	2.07	.150	1.86	.200	2.00
	.150	2.01	.100	1.86	.150	1.77
	.100	1.93	.075	1.75	.100	1.68
	.075	1.86	.050	1.70	.075	1.65
	.050	1.82	.025		.050	1.59
	.025	1.66			.025	1.51
1	.740	w.s.	1.010	w.s.	.892	w.s.
	.690	2.04	.960	1.69	.870	1.89
	.590	2.04	.860	1.74	.770	1.85
	.490	2.00	.760	1.80	.670	1.94
	.390	2.06	.660	1.85	.620	1.62
	.340	2.08	.560	1.79	.570	1.73
	.290	2.08	.460	1.72	.520	1.74
	.240	2.08	.360	1.69	.470	1.69
	.190	2.02	.260	1.48	.420	1.74
	.140	1.93	.210	.96	.370	1.74
	.090	1.84			.320	1.73
	.040	1.70			.270	1.54
					.220	1.61
					.170	1.55
					.120	1.29
					.070	1.13
					.020	1.03
12	.628	w.s.	.601	w.s.	.580	w.s.
	.580	1.58	.550	1.66	.530	1.65
	.500	1.51	.400	1.48	.450	1.57
	.400	1.43	.300	1.40	.350	1.48
	.300	1.24	.200	1.19	.250	1.39
	.200	1.18	.150	1.16	.200	1.33
	.150	1.15	.100	1.08	.150	1.27
	.100	1.09	.075	.84	.100	1.10
	.075	.99	.050	.73	.075	.99
	.050	.84	.025	.70	.050	.99
	.025	.82			.025	.99
14	.580	w.s.	.610	w.s.	.580	w.s.
	.530	1.95	.550	1.86	.530	1.94
	.450	1.86	.450	1.77	.450	1.94
	.350	1.84	.350	1.66	.350	1.91
	.250	1.82	.250	1.46	.250	1.78
	.200	1.78	.200	1.40	.200	1.65
	.150	1.72	.150	1.33	.150	1.61
	.100	1.47	.100	1.32	.100	1.56
	.075	1.44	.075	1.33	.075	1.39
	.050	1.28	.050	1.36	.050	1.30
	.025	1.15	.025	1.35	.025	1.16
20	.960	w.s.	1.030	w.s.	.960	w.s.
	.930	2.46	.990	2.51	.920	2.31
	.750	2.50	.750	2.47	.750	2.30
	.500	2.51	.550	2.41	.550	2.21
	.400	2.41	.400	2.21	.400	2.15
	.300	2.36	.300	2.08	.300	2.18
	.200	2.10	.200	2.02	.200	2.21
	.150	1.86	.150	1.91	.150	2.06
	.100	1.72	.100	1.72	.100	2.08
	.075	1.48	.075	1.60	.075	2.07
	.050	1.25	.050	1.46	.050	1.93
	.015	.57	.025	1.30	.025	1.85
21	.855	w.s.	1.025	w.s.	1.025	w.s.
	.815	2.67	.980	2.46	.960	2.33
	.575	2.67	.750	2.39	.800	2.36
	.375	2.71	.550	2.39	.600	2.33
	.275	2.67	.400	2.39	.400	2.35
	.175	2.67	.300	2.39	.300	2.32
	.125	2.67	.200	2.31	.200	2.23
	.075	2.65	.150	2.29	.150	2.10
	.050	2.48	.100	2.22	.100	1.98
	.025	2.16	.075	2.21	.075	1.97
			.050	2.09	.050	1.88
			.025	1.70	.025	1.13
19	.515	w.s.	.510	w.s.	.615	w.s.
	.490	1.98	.475	2.10	.580	2.05
	.400	1.95	.400	2.11	.400	2.04
	.300	1.97	.300	2.08	.300	2.01
	.200	1.91	.200	2.02	.200	1.93
	.150	1.91	.150	2.00	.150	1.85
	.100	1.84	.100	1.98	.100	1.81
	.075	1.77	.075	1.97	.075	1.80
	.050	1.64	.050	1.91	.050	1.73
	.025	1.47	.025	1.88	.025	1.46

TABLE 14.—*Velocity-profile data for 0.28-mm sand in 8-foot-wide flume*—Continued

Run	2.0 ft from left wall of flume		4.0 ft from left wall of flume		6.0 ft from left wall of flume	
	Distance above sand bed (ft)	Velocity (fps)	Distance above sand bed (ft)	Velocity (fps)	Distance above sand bed (ft)	Velocity (fps)
16	0.915	w.s.	0.875	w.s.	0.895	w.s.
	.850	2.21	.800	2.45	.800	2.10
	.600	2.15	.600	2.47	.600	2.02
	.450	2.18	.450	2.43	.450	1.84
	.300	2.20	.300	2.34	.300	1.81
	.200	2.15	.200	2.32	.200	1.83
	.150	2.14	.150	2.29	.150	1.74
	.100	2.10	.100	2.31	.100	1.68
	.075	2.01	.075	2.22	.075	1.54
	.050	1.51	.050	2.10	.050	1.47
	.025	1.40	.025	1.80	.025	1.42
23	.950	w.s.	.945	w.s.	1.158	w.s.
	.900	3.13	.900	3.14	1.100	3.18
	.700	3.02	.700	2.98	1.000	3.16
	.500	2.91	.550	2.85	.900	3.10
	.400	2.80	.400	2.70	.800	3.08
	.300	2.75	.300	2.64	.700	2.98
	.200	2.55	.200	2.57	.600	2.90
	.150	2.13	.150	2.51	.500	2.70
	.100	1.93	.100	2.31	.400	2.61
	.075	1.76	.075	2.23	.300	2.44
	.050	1.56	.050	2.14	.200	2.10
			.025	2.12	.100	1.34
					.050	.30
					.025	.30
17	.925	w.s.	.595	w.s.	.690	w.s.
	.870	1.84	.540	1.72	.635	1.62
	.700	1.66	.400	1.70	.550	1.50
	.500	1.58	.300	1.56	.400	1.48
	.400	1.57	.200	1.52	.300	1.14
	.300	1.54	.150	1.52	.200	1.10
	.250	1.36	.100	1.46	.150	1.08
	.200	1.29	.060	1.35	.100	1.07
	.175	1.28	.050	1.03	.075	1.04
	.150	1.27	.025	.98	.050	1.04
	.125	.54			.025	1.03
	.100	.52				
3	1.180	w.s.	.805	w.s.	.870	w.s.
	1.015	2.50	.750	2.33	.800	2.21
	.815	2.50	.600	2.33	.700	2.21
	.665	2.50	.450	2.26	.550	2.21
	.465	2.40	.300	2.21	.400	2.18
	.365	2.21	.200	2.16	.300	2.04
	.265	1.95	.150	2.12	.200	1.95
	.200	1.28	.100	1.90	.150	1.88
	.150	.63	.075	1.78	.100	1.80
	.100	.74	.050	1.74	.075	1.60
	.075	.58	.025	1.74	.050	1.55
	.050	.62			.025	1.55
	.025	.66				
18	.740	w.s.	.750	w.s.	.600	w.s.
	.700	2.16	.720	2.84	.560	2.85
	.550	2.05	.600	2.81	.450	2.84
	.400	1.60	.500	2.76	.300	2.80
	.300	1.37	.400	2.56	.200	2.73
	.200	1.59	.350	2.47	.150	2.69
	.150	1.59	.300	2.03	.100	2.57
	.100	1.23	.275	1.70	.075	2.45
	.075	1.25	.250	1.19	.050	2.33
	.050	1.26	.225	.79	.025	2.13
	.025	1.25				
30	.665	w.s.	.625	w.s.	.720	w.s.
	.620	3.76	.580	3.68	.675	3.76
	.500	3.59	.400	3.68	.500	3.76
	.400	3.40	.300	3.49	.400	3.49
	.300	3.30	.200	3.40	.300	3.40
	.200	3.10	.150	3.20	.200	3.20
	.150	2.88	.100	2.99	.150	2.64
	.100	2.70	.075	2.76	.100	2.07
	.075	2.64	.050	2.51	.075	1.70
	.050	2.51	.025	2.07	.050	1.70
	.025	2.23			.025	1.48
34	.450	w.s.	.395	w.s.	.345	w.s.
	.425	1.79	.360	1.98	.320	1.96
	.325	1.78	.300	1.96	.250	1.94
	.225	1.68	.250	1.87	.200	1.90
	.175	1.55	.200	1.87	.150	1.75
	.125	1.39	.150	1.77	.100	1.66
	.100	1.35	.100	1.72	.075	1.64
	.075	1.36	.075	1.61	.050	1.64
34—Con.	0.050	1.36	0.050	1.61	0.025	1.61
	.025	1.37	.025	1.61		
22	.630	w.s.	.610	w.s.	.595	w.s.
	.580	3.55	.560	3.59	.560	3.43
	.500	3.50	.500	3.58	.500	3.33
	.400	3.38	.400	3.50	.400	3.27
	.300	2.98	.300	3.31	.300	3.12
	.200	2.87	.200	3.07	.200	2.94
	.150	2.85	.150	2.92	.150	2.75
	.100	2.67	.100	2.73	.100	2.55
	.075	2.56	.075	2.66	.075	2.43
	.050	2.31	.050	2.40	.050	2.14
	.025	1.93	.025	2.20	.025	1.89
15	.810	w.s.	.595	w.s.	.515	w.s.
	.750	2.32	.550	2.47	.470	2.43
	.550	2.29	.400	2.44	.400	2.40
	.400	2.18	.300	2.38	.300	2.31
	.300	2.01	.200	2.31	.200	2.25
	.200	1.83	.150	2.25	.150	2.25
	.150	1.85	.100	2.14	.100	2.25
	.100	1.89	.075	2.07	.075	2.19
	.075	1.94	.050	1.88	.050	2.16
	.050	1.94	.025	1.82	.025	2.10
	.025	1.90				
24	.650	w.s.	.810	w.s.	.800	w.s.
	.610	3.68	.760	3.70	.750	3.56
	.550	3.78	.550	3.70	.550	3.42
	.400	3.82	.400	3.68	.400	3.17
	.300	3.78	.300	3.62	.300	3.09
	.200	3.68	.200	3.48	.200	3.07
	.150	3.45	.150	3.29	.150	2.97
	.100	3.23	.100	3.10	.100	2.78
	.075	2.96	.075	2.98	.075	2.74
	.050	2.64	.050	2.79	.050	2.61
	.025	2.31	.025	2.48	.025	2.43
25	.670	w.s.	.670	w.s.	.700	w.s.
	.550	4.74	.650	4.74	.650	4.46
	.400	4.46	.550	4.53	.550	4.46
	.300	4.39	.400	4.46	.400	4.24
	.200	4.17	.300	4.24	.300	4.09
	.150	4.01	.200	4.01	.200	3.93
	.100	3.85	.150	3.85	.150	3.85
	.075	3.40	.100	3.50	.100	3.59
	.050	3.20	.075	3.40	.075	3.40
	.025	2.76	.050	3.20	.050	2.88
			.025	2.88	.025	2.76
28	.550	w.s.	.550	w.s.	.550	w.s.
	.500	4.39	.500	4.32	.500	4.32
	.400	4.24	.400	4.16	.400	4.08
	.300	4.08	.300	4.08	.300	3.93
	.200	3.93	.200	4.01	.200	3.85
	.150	3.76	.150	3.68	.150	3.59
	.100	3.40	.100	3.59	.100	3.49
	.075	3.30	.075	3.30	.075	3.30
	.050	3.10	.050	3.10	.050	3.20
	.025	2.76	.025	2.64	.025	2.76
29	.540	w.s.	.490	w.s.	.490	w.s.
	.490	4.24	.440	4.67	.440	4.81
	.440	4.39	.400	4.32	.400	4.39
	.400	4.39	.300	4.32	.300	4.39
	.300	4.16	.250	4.24	.250	4.16
	.250	4.08	.200	4.08	.200	4.01
	.200	4.01	.150	3.93	.150	4.08
	.150	3.76	.100	3.59	.100	3.68
	.100	3.49	.075	3.40	.075	3.59
	.075	3.10	.050	3.20	.050	3.40
	.050	3.20	.025	2.76	.025	3.10
	.025	2.88				
26	.505	w.s.	.485	w.s.	.475	w.s.
	.470	4.81	.430	4.81	.410	4.60
	.400	4.46	.300	4.53	.300	4.46
	.300	4.46	.200	4.32	.200	4.32
	.200	3.93	.150	4.16	.150	4.08
	.150	3.76	.100	3.49	.100	3.93
	.100	3.59	.075	3.40	.075	3.76
	.075	3.10	.050	3.30	.050	3.40
	.050	2.64	.025	2.07	.025	2.88
	.025	2.37				

TABLE 15.—*Velocity-profile data for 0.45-mm sand in 8-foot-wide flume*

[The lateral section used for measuring was 95-115 ft from the headbox. w.s.=water surface]

Run	Distance above sand bed (ft)	Velocity (fps)	Distance above sand bed (ft)	Velocity (fps)	Distance above sand bed (ft)	Velocity (fps)
	2.6 ft from left wall of flume		*4.0 ft from left wall of flume*		*6.8 ft from left wall of flume*	
14	0.613	w.s.	0.613	w.s.	0.621	w.s.
	.563	0.84	.563	0.86	.571	0.83
	.463	.83	.463	.84	.471	.85
	.363	.81	.363	.80	.371	.82
	.263	.76	.263	.79	.271	.77
	.213	.75	.213	.76	.221	.75
	.163	.73	.163	.75	.171	.73
	.113	.69	.113	.70	.121	.69
	.063	.59	.063	.64	.071	.65
	.013	.46	.013	.41	.021	.47
13	.356	w.s.	.363	w.s.	.353	w.s.
	.306	.63	.313	.63	.303	.56
	.256	.62	.263	.62	.253	.56
	.206	.61	.213	.61	.203	.56
	.156	.60	.163	.59	.153	.53
	.106	.58	.113	.58	.103	.52
	.081	.57	.088	.57	.078	.49
	.056	.56	.063	.57	.053	.47
	.031	.53	.038	.54	.028	.46
	.006	.48	.013	.45	.003	.40
17	.902	w.s.	.937	w.s.	.938	w.s.
	.852	.91	.887	.92	.888	.90
	.802	.91	.837	.92	.838	.89
	.602	.90	.637	.91	.638	.89
	.402	.87	.437	.90	.438	.87
	.202	.81	.237	.83	.238	.86
	.152	.79	.187	.78	.188	.83
	.102	.75	.137	.74	.138	.80
	.077	.74	.112	.74	.113	.78
	.052	.73	.087	.73	.088	.75
	.027	.71	.062	.72	.063	.74
	.002	.70	.037	.70	.038	.74
			.012	.69	.013	.68
	1.2 ft from left wall of flume					
16	0.792	w.s.	.787	w.s.	.813	w.s.
	.742	0.97	.737	.94	.763	.98
	.692	.98	.687	.94	.713	.98
	.492	.96	.487	.92	.513	.87
	.292	.87	.287	.88	.313	.80
	.192	.82	.187	.80	.213	.74
	.142	.78	.137	.79	.113	.65
	.092	.73	.087	.77	.063	.60
	.067	.69	.062	.69	.138	.53
	.042	.67	.037	.67	.013	.45
	.017	.62	.012	.60	.413	.86
	.010	.60				
	2.6 ft from left wall of flume					
15	0.776	w.s.	.804	w.s.	.771	w.s.
	.726	0.95	.754	.97	.721	.94
	.676	.90	.704	.92	.671	.94
	.476	.87	.604	.90	.471	.92
	.276	.86	.504	.90	.271	.82
	.176	.75	.404	.86	.171	.77
	.126	.73	.304	.82	.121	.71
	.101	.69	.204	.77	.096	.63
	.076	.65	.104	.65	.071	.58
	.051	.63	.079	.52	.046	.58
	.026	.67	.054	.46	.021	.46
			.029	.43	.010	.35
			.004	.30		
					5.4 ft from left wall of flume	
18	.673	w.s.	.697	w.s.	0.656	w.s.
	.623	.74	.647	.80	.606	.82
	.573	.78	.597	.80	.556	.79
	.473	.78	.497	.79	.456	.79
	.373	.77	.397	.78	.356	.79
	.273	.72	.297	.77	.256	.76
	.173	.67	.197	.68	.156	.74
	.073	.60	.097	.58	.106	.69
	.048	.52	.072	.51	.056	.62
	.023	.49	.047	.49	.031	.57
	.010	.39	.022	.43	.010	.46
	1.8 ft from left wall of flume					
2	0.703	w.s.				
	.603	1.34				
	.503	1.32				
	.403	1.27				
	.303	1.25				
	.203	1.24				
	.103	1.22				
	4.0 ft from left wall of flume				*4.0 ft from left wall of flume*	
[a] 2	0.727	w.s.	.861	w.s.	0.758	w.s.
	.627	1.44	.761	1.44	.658	1.44
	.527	1.38	.661	1.43	.558	1.43
	.427	1.29	.561	1.39	.458	1.46
	.327	1.29	.461	1.31	.358	1.42
	.227	1.26	.411	1.27	.258	1.37

Run	Distance above sand bed (ft)	Velocity (fps)	Distance above sand bed (ft)	Velocity (fps)	Distance above sand bed (ft)	Velocity (fps)
	4.0 ft from left wall of flume		*4.0 ft from left wall of flume*		*4.0 ft from left wall of flume*	
[a] 2—Con.	0.127	1.24	0.361	1.28	0.158	1.28
			.261	1.24	.058	.87
			.161	1.09		
			.061	.95		
3	.741	w.s.				
	.641	1.42				
	.577	1.43				
	.513	1.43				
	.449	1.38				
	.385	1.29				
	.321	1.29				
	.257	1.29				
	.193	1.20				
	.161	1.16				
	.129	1.13				
	.097	1.16				
	.065	1.11				
	.033	1.02				
	1.2 ft from left wall of flume		*2.6 ft from left wall of flume*			
9	0.551	w.s.	0.587	w.s.	0.543	w.s.
	.501	1.25	.537	1.20	.493	1.20
	.401	1.23	.437	1.18	.393	1.11
	.351	1.20	.337	1.13	.343	1.08
	.301	1.18	.287	1.05	.293	1.02
	.251	1.18	.237	.99	.243	.97
	.201	1.16	.187	.97	.193	.90
	.151	1.11	.137	.94	.143	.87
	.101	.99	.087	.84	.093	.84
	.051	.87	.037	.55	.043	.84
	.026	.84	.012	.49	.018	.80
	5.4 ft from left wall of flume		*6.8 ft from left wall of flume*			
9	0.581	w.s.	0.540	w.s.		
	.531	1.22	.490	1.25		
	.431	1.11	.390	1.23		
	.381	1.08	.290	1.16		
	.331	1.05	.240	1.11		
	.281	1.02	.190	1.08		
	.231	.90	.140	1.05		
	.181	.87	.090	1.02		
	.131	.80	.040	.97		
	.081	.73	.015	.87		
	2.0 ft from left wall of flume		*4.0 ft from left wall of flume*		*6.0 ft from left wall of flume*	
1	0.650	w.s.	0.650	w.s.	0.650	w.s.
	.625	1.62	.625	1.63	.625	1.62
	.525	1.59	.525	1.60	.525	1.62
	.425	1.55	.425	1.49	.425	1.55
	.325	1.50	.325	1.45	.325	1.52
	.225	1.41	.225	1.39	.225	1.44
	.125	1.36	.125	1.35	.125	1.30
	.025	1.33	.025	1.34	.025	1.01
	2.5 ft from left wall of flume				*5.5 ft from left wall of flume*	
5	0.737	w.s.	.667	w.s.	0.743	w.s.
	.637	1.65	.567	1.70	.643	1.78
	.537	1.62	.467	1.63	.543	1.70
	.437	1.57	.367	1.62	.443	1.70
	.337	1.57	.317	1.60	.343	1.70
	.287	1.51	.267	1.60	.243	1.53
	.237	1.45	.217	1.57	.193	1.55
	.187	1.43	.167	1.49	.143	1.49
	.137	1.25	.117	1.42	.093	1.35
	.087	1.13	.067	1.33	.043	1.25
	.037	.94	.042	1.25		
	7.0 ft from left wall of flume					
5	0.757	w.s.				
	.657	1.68				
	.557	1.67				
	.457	1.65				
	.357	1.65				
	.257	1.62				
	.207	1.55				
	.157	1.35				
	.107	1.29				
	.057	1.02				
	1.2 ft from left wall of flume		*2.6 ft from left wall of flume*		*4.0 ft from left wall of flume*	
11	0.310	w.s.	0.357	w.s.	0.314	w.s.
	.260	1.00	.311	1.00	.274	1.02
	.210	.97	.261	1.02	.224	.97
	.160	.90	.211	.84	.174	.94
	.135	.90	.186	.90	.149	.90
	.110	.87	.161	.84	.124	.90
	.085	.87	.136	.80	.099	.84
	.060	.80	.111	.77	.074	.80
	.035	.77	.086	.77	.049	.80
	.010	.69	.061	.74	.024	.77
			.036	.74		
			.011	.60		

See footnote at end of table, p. I 86.

TABLE 15.—*Velocity-profile data for 0.45-mm sand in 8-foot-wide flume*—Continued

Run	Distance above sand bed (ft)	Velocity (fps)	Distance above sand bed (ft)	Velocity (fps)	Distance above sand bed (ft)	Velocity (fps)
	5.4 ft from left wall of flume		*6.8 ft from left wall of flume*		*4.0 ft from left wall of flume*	
11—Con.	0.390	w.s.	0.271	w.s.		
	.340	1.00	.221	0.99		
	.290	.90	.171	.97		
	.240	.90	.121	.90		
	.215	.90	.096	.87		
	.190	.87	.071	.84		
	.165	.87	.046	.80		
	.140	.80	.021	.80		
	.115	.84	.001	.49		
	.090	.77				
	.065	.77				
	.040	.77				
	.015	.69				
	1.2 ft from left wall of flume		*2.5 ft from left wall of flume*			
4	0.648	w.s.	0.648	w.s.	0.661	w.s.
	.548	1.87	.548	1.81	.561	1.76
	.448	1.84	.448	1.79	.461	1.76
	.348	1.79	.348	1.78	.361	1.72
	.298	1.81	.298	1.73	.261	1.55
	.248	1.76	.248	1.78	.211	1.57
	.198	1.72	.198	1.72	.161	1.53
	.148	1.65	.148	1.62	.111	1.53
	.098	1.51	.098	1.62	.061	1.49
	.048	1.47	.048	1.58	.011	1.47
	5.5 ft from left wall of flume		*7.0 ft from left wall of flume*			
4	0.665	w.s.	0.678	w.s.		
	.565	1.73	.578	1.55		
	.465	1.73	.478	1.53		
	.365	1.70	.378	1.43		
	.265	1.62	.278	1.42		
	.215	1.53	.228	1.42		
	.165	1.51	.178	1.35		
	.115	1.45	.128	1.33		
	.065	1.29	.078	1.31		
	.015	1.25	.028	1.29		
	1.2 ft from left wall of flume		*2.6 ft from left wall of flume*			
8	0.461	w.s.	0.444	w.s.	.493	w.s.
	.411	1.29	.393	1.33	.450	1.25
	.311	1.27	.293	1.31	.350	1.22
	.261	1.20	.243	1.27	.300	1.20
	.211	1.08	.193	1.25	.250	1.18
	.161	1.05	.143	1.16	.200	1.11
	.111	.99	.093	1.11	.150	1.02
	.061	.87	.043	1.02	.100	.99
	.011	.73			.050	.84
	5.4 ft from left wall of flume		*6.8 ft from left wall of flume*			
8	0.421	w.s.	0.511	w.s.		
	.419	1.25	.461	1.27		
	.319	1.22	.361	1.25		
	.219	1.18	.261	1.11		
	.169	1.08	.211	1.08		
	.119	1.02	.161	1.02		
	.069	.97	.111	.99		
	.019	.84	.061	.90		
			.011	.35		
	2.5 ft from left wall of flume		*4.0 ft from left wall of flume*		*6.1 ft from left wall of flume*	
7	0.632	w.s.	0.698	w.s.	0.606	w.s.
	.532	1.60	.598	1.88	.506	1.75
	.432	1.62	.498	1.93	.406	1.65
	.332	1.60	.398	1.79	.306	1.65
	.232	1.62	.298	1.84	.206	1.62
	.182	1.53	.198	1.82	.156	1.60
	.132	1.58	.158	1.84	.106	1.49
	.082	1.57	.098	1.79	.056	.84
	.032	1.29	.058	1.78	.006	.49
	1.2 ft from left wall of flume		*2.6 ft from left wall of flume*		*4.0 ft from left wall of flume*	
10	0.279	w.s.	0.302	w.s.	0.245	w.s.
	.229	1.08	.252	0.99	.195	1.18
	.179	1.02	.202	.94	.145	1.11
	.154	.99	.177	.90	.120	1.05
	.129	.94	.152	.90	.095	.97
	.104	.90	.127	.84	.070	.94
	.079	.87	.102	.84	.045	.90
	.054	.80	.077	.80	.020	.87
	.029	.35	.052	.80	.010	.73
	.004	.28	.027	.77		
			.002	.35		
	5.4 ft from left wall of flume		*6.8 ft from left wall of flume*			
10	0.273	w.s.	0.346	w.s.		
	.223	1.13	.296	1.08		
	.173	1.11	.246	1.08		
	.148	1.08	.196	.99		
	.123	1.02	.171	.99		
	.098	.99	.146	.97		
	.073	.97	.121	.94		
	.048	.90	.096	.87		
	.023	.80	.071	.84		
	.008	.65	.046	.69		
			.021	.42		

Run	Distance above sand bed (ft)	Velocity (fps)	Distance above sand bed (ft)	Velocity (fps)	Distance above sand bed (ft)	Velocity (fps)
	1.2 ft from left wall of flume		*2.5 ft from left wall of flume*		*4.0 ft from left wall of flume*	
6	0.445	w.s.	0.500	w.s.	0.457	w.s.
	.395	1.45	.450	1.47	.350	1.42
	.345	1.43	.400	1.45	.250	1.31
	.295	1.42	.350	1.38	.200	1.23
	.245	1.40	.300	1.33	.150	1.16
	.195	1.33	.250	1.29	.100	1.02
	.145	1.31	.200	1.23	.050	.97
	.095	1.02	.175	1.20	.025	.69
	.070	.84	.150	1.11		
	.045	.65	.125	1.05		
			.100	.90		
	5.5 ft from left wall of flume		*7.0 ft from left wall of flume*			
6	0.477	w.s.	0.486	w.s.		
	.427	1.38	.436	1.31		
	.377	1.33	.386	1.23		
	.327	1.33	.336	1.27		
	.277	1.20	.286	1.18		
	.227	1.16	.236	1.20		
	.177	1.11	.186	1.13		
	.127	.99	.136	1.05		
	.102	.94	.086	.94		
	.077	.87	.061	.84		
	.052	.69	.036	.65		
	4.0 ft from left wall of flume					
12	0.237	w.s.				
	.189	1.22				
	.139	1.16				
	.114	1.11				
	.089	1.08				
	.064	1.05				
	.039	.97				
	.014	.90				
	2.0 ft from left wall of flume		*4.0 ft from left wall of flume*		*6.0 ft from left wall of flume*	
19	0.423	w.s.	0.433	w.s.	0.285	w.s.
	.408	1.49	.418	1.42	.270	1.58
	.308	1.58	.318	1.53	.170	1.67
	.208	1.51	.268	1.55	.120	1.63
	.158	1.42	.218	1.42	.095	1.51
	.108	1.33	.193	1.55	.070	1.45
	.083	1.22	.168	1.47	.045	1.33
	.058	1.20	.143	1.42	.020	1.20
	.033	.80	.118	1.35	.010	.94
			.093	1.25		
			.068	1.16		
			.043	1.18		
			.018	1.18		
21	1.016	w.s.	.760	w.s.	1.095	w.s.
	.916	1.58	.660	1.92	.995	1.70
	.866	1.60	.560	1.86	.895	1.75
	.816	1.60	.460	1.75	.795	1.70
	.716	1.58	.360	1.58	.745	1.65
	.616	1.62	.260	1.51	.695	1.61
	.416	1.67	.160	1.51	.595	1.60
	.316	1.20	.060	1.38	.495	1.55
	.266	1.11	.010	1.27	.395	1.22
	.216	.73			.295	1.22
	.166	.55			.195	1.22
	.116	.49			.145	.99
					.095	.69
20	.555	w.s.	.740	w.s.	.655	w.s.
	.540	1.81	.720	1.70	.635	1.75
	.440	1.84	.620	1.88	.535	1.90
	.340	1.79	.520	1.85	.435	1.91
	.240	1.58	.470	1.79	.335	1.91
	.140	1.47	.420	1.72	.285	1.85
	.090	1.35	.370	1.72	.235	1.73
	.040	1.20	.320	1.68	.185	1.63
	.015	.97	.270	1.68	.160	1.65
			.220	1.57	.135	1.55
			.170	1.43	.110	1.47
			.145	1.60	.085	1.38
			.120	1.56	.060	1.29
			.095	1.38	.035	1.16
			.070	1.40	.010	1.05
			.045	1.13		
			.010	.87		
23	.660	w.s.	1.080	w.s.	.700	w.s.
	.610	2.78	1.030	2.44	.650	2.62
	.510	2.88	.930	2.44	.550	2.68
	.410	2.82	.830	2.50	.450	2.70
	.310	2.86	.730	2.48	.350	2.60
	.210	2.78	.630	2.46	.250	2.76
	.160	2.76	.580	2.40	.200	2.70
	.110	2.70	.530	2.37	.150	2.64
	.060	2.62	.480	2.40	.100	2.60
	.035	2.60	.455	2.54	.050	2.31

TABLE 15.—*Velocity-profile data for 0.45-mm sand in 8-foot-wide flume*—Continued

Run	Distance above sand bed (ft)	Velocity (fps)	Distance above sand bed (ft)	Velocity (fps)	Distance above sand bed (ft)	Velocity (fps)
	2.0 ft from left wall of flume		*4.0 ft from left wall of flume*		*6.0 ft from left wall of flume*	
23—Con.	0.010	2.37	0.430	2.40	0.025	2.16
			.405	2.37	.010	1.88
			.330	2.44		
			.230	2.29		
			.130	2.42		
22	.965	w.s.	1.088	w.s.	1.114	w.s.
	.865	1.75	.988	1.95	1.014	1.98
	.765	1.85	.888	1.92	.914	1.94
	.665	1.75	.788	1.94	.814	2.05
	.465	1.68	.588	1.79	.714	2.03
	.265	1.67	.388	1.72	.514	1.73
	.215	1.60	.288	1.65	.464	1.63
	.165	1.55	.238	1.62	.414	1.33
	.115	1.55	.188	1.35	.314	1.27
	.065	1.55	.138	1.51	.214	1.20
			.088	1.47	.114	1.13
			.038	1.22	.010	.84
25	.484	w.s.	.351	w.s.	.270	w.s.
	.409	1.78	.301	2.02	.220	2.11
	.384	1.78	.251	1.98	.170	2.09
	.334	1.76	.201	1.91	.120	2.10
	.284	1.68	.151	1.94	.070	2.09
	.234	1.73	.126	1.92	.045	1.91
	.184	1.78	.101	1.91	.020	1.73
	.159	1.76	.076	1.76	.005	1.67
	.134	1.79	.051	1.72		
	.109	1.78	.026	1.58		
	.084	1.72				
	.059	1.55				
	.034	1.45				
24	.570	w.s.	.750	w.s.	.294	w.s.
	.470	2.80	.650	1.95	.194	2.94
	.370	2.82	.600	1.82	.144	2.92
	.320	2.66	.500	1.68	.094	2.70
	.270	2.56	.400	1.67	.044	2.50
	.220	2.48	.300	1.79	.019	2.05
	.170	2.48	.250	1.76		
	.120	2.36	.200	1.68		
	.070	2.22	.150	1.20		
	.020	2.12	.100	.77		
			.050	.73		
			.023	.60		
40	1.300	w.s.	.936	w.s.	.728	w.s.
	1.280	3.96	.900	3.08	.650	3.42
	1.180	3.83	.700	3.36	.600	3.67
	.980	3.64	.500	3.30	.550	3.60
	.780	3.87	.400	3.34	.450	3.44
	.580	3.45	.300	3.08	.350	3.75
	.480	2.15	.200	3.18	.250	3.79
	.380	1.82	.100	3.05	.150	3.71
	.280	.00	.050	2.62	.100	3.32
	.180	.00	.025	2.05	.050	2.92
					.025	2.56
39	.570	w.s.	.540	w.s.	.640	w.s.
	.550	5.45	.500	5.60	.600	5.40
	.500	5.19	.400	5.34	.550	5.10
	.400	5.22	.300	5.20	.450	5.00
	.300	5.04	.200	4.59	.350	4.80
	.200	4.85	.100	4.04	.250	4.74
	.100	4.27	.050	3.63	.150	4.20
	.050	3.74	.025	2.52	.100	3.85
	.025	2.54			.050	3.41
					.025	1.18
26	.500	w.s.	.460	w.s.	.485	w.s.
	.480	4.71	.450	4.47	.465	4.53
	.410	4.26	.350	4.48	.405	4.62
	.310	3.83	.250	4.23	.305	4.27
	.210	3.73	.200	4.07	.205	4.21
	.160	3.65	.150	3.98	.155	3.78
	.110	3.50	.100	3.50	.105	3.61
	.060	2.98	.050	3.24	.055	3.19
	.040	2.46	.030	2.96	.035	2.62
	.020	1.35	.010	1.25	.015	2.68
28	.408	w.s.	.343	w.s.	.395	w.s.
	.358	5.10	.323	4.25	.345	4.35
	.308	5.10	.273	3.85	.295	4.17
	.258	4.32	.223	3.86	.245	3.89
	.208	4.55	.173	3.74	.195	3.75
	.158	3.87	.123	3.73	.145	3.58
	.108	3.98	.073	3.71	.120	3.39
	.058	3.49	.023	3.09	.095	3.35
					.070	3.21
					.045	2.78
					.020	1.35
29	.304	w.s.	.370	w.s.	.325	w.s.
	.254	2.70	.320	2.96	.275	2.44
	.204	2.60	.270	2.64	.225	2.35
	.154	2.54	.270	2.35	.175	2.42
	.129	2.31	.220	2.37	.125	2.24
	.104	2.40	.170	2.66	.100	1.98

Run	Distance above sand bed (ft)	Velocity (fps)	Distance above sand bed (ft)	Velocity (fps)	Distance above sand bed (ft)	Velocity (fps)
	2.0 ft from left wall of flume		*4.0 ft from left wall of flume*		*6.0 ft from left wall of flume*	
29—Con.	0.079	1.97	0.145	2.52	0.075	1.98
	.054	1.78	.120	2.40	.050	1.92
	.029	1.35	.095	2.38	.025	1.31
	.004	.73	.070	2.19		
			.045	1.92		
			.020	1.60		
31			.335	w.s.	.370	w.s.
			.325	4.87	.300	4.61
			.275	4.84	.250	4.38
			.225	4.61	.200	4.38
			.175	4.60	.150	3.91
			.125	4.38	.100	4.09
			.075	3.87	.050	3.64
			.050	3.33	.025	3.50
			.025	2.29		
27	.293	w.s.	.323	w.s.	.319	w.s.
	.243	3.75	.273	3.71	.269	3.83
	.193	3.55	.223	3.64	.169	3.19
	.143	3.41	.173	3.51	.119	2.78
	.093	3.24	.123	3.46	.069	2.28
	.068	3.02	.073	2.74	.044	1.79
	.043	2.82	.048	2.39	.019	1.25
	.018	2.00	.023	2.36		
36	.190	w.s.	.170	w.s.	.160	w.s.
	.130	1.97	.150	2.44	.140	2.31
	.115	2.06	.130	2.24	.115	2.44
	.090	1.87	.105	2.08	.090	2.42
	.065	1.95	.080	1.87	.065	2.42
	.040	1.53	.055	1.67	.040	2.21
	.020	1.53	.030	1.05	.020	2.31
	.010	1.47	.020	1.38	.010	1.73
			.010	1.55		
	2.5 ft from left wall of flume					
41	0.614	w.s.	.510	w.s.	.499	w.s.
	.550	5.50	.490	6.09	.479	5.74
	.500	5.50	.450	5.82	.450	5.65
	.400	5.40	.350	5.61	.350	5.30
	.300	5.19	.250	5.39	.250	5.35
	.200	4.86	.200	5.02	.200	5.03
	.150	4.80	.150	4.82	.150	4.75
	.100	4.17	.100	4.38	.100	4.43
	.050	3.74	.050	3.77	.050	3.85
	.025	1.45	.025	2.64	.025	3.35
	2.0 ft from left wall of flume					
30	0.225	w.s.	.281	w.s.	.265	w.s.
	.175	3.06	.231	3.31	.225	3.13
	.150	2.90	.181	3.27	.200	2.72
	.125	2.62	.131	2.90	.175	3.06
	.100	2.60	.081	2.54	.150	2.98
	.075	2.46	.056	2.60	.125	2.97
	.050	2.12	.031	1.87	.100	2.76
	.025	1.68	.006	2.25	.075	2.60
					.050	2.12
					.025	1.25
35	.260	w.s.	.203	w.s.	.229	w.s.
	.200	3.76	.173	3.12	.200	3.45
	.175	3.71	.173	3.57	.175	3.23
	.150	3.52	.148	3.17	.150	3.28
	.125	3.25	.123	3.16	.125	3.01
	.100	3.40	.098	3.18	.100	2.86
	.075	2.54	.073	2.82	.075	2.64
	.050	2.44	.048	2.12	.050	1.90
	.025	2.06			.025	1.72
34	.280	w.s.	.250	w.s.	.300	w.s.
	.200	4.33	.200	4.53	.250	4.23
	.150	3.97	.150	4.27	.200	4.20
	.100	3.58	.100	3.60	.150	3.90
	.050	3.44	.050	3.27	.100	3.59
	.025	3.39	.025	2.54	.050	3.16
					.025	2.52
33	.340	w.s.	.305	w.s.	.300	w.s.
	.280	4.34	.225	4.52	.250	4.40
	.230	4.45	.175	4.30	.190	4.40
	.180	4.08	.125	3.85	.150	4.33
	.130	3.97	.075	3.50	.100	3.76
	.080	3.74	.050	3.10	.050	3.50
	.055	3.52	.025	2.83	.025	3.06
	.030	3.10				
38	.510	w.s.	.500	w.s.	.490	w.s.
	.450	6.13	.450	5.57	.450	6.13
	.400	6.08	.350	5.70	.400	6.06
	.300	5.70	.250	5.50	.350	6.19
	.200	5.19	.200	5.33	.250	5.69
	.150	5.18	.150	5.02	.200	5.45
	.100	5.09	.100	4.89	.150	5.30
	.050	5.02	.050	4.73	.100	4.83
	.025	3.89	.025	3.56	.050	4.56
					.025	3.44

TABLE 15.—*Velocity-profile data for 0.45-mm sand in 8-foot-wide flume*—Continued

Run	Distance above sand bed (ft)	Velocity (fps)	Distance above sand bed (ft)	Velocity (fps)	Distance above sand bed (ft)	Velocity (fps)
	2.0 ft from left wall of flume		*4.0 ft from left wall of flume*		*6.0 ft from left wall of flume*	
37	0.500	w.s.	0.500	w.s.	0.480	w.s.
	.450	6.10	.450	5.65	.425	5.20
	.350	5.81	.425	5.71	.400	5.20
	.250	5.75	.325	5.54	.350	5.49
	.200	5.75	.225	5.15	.300	5.49
	.150	5.20	.125	4.66	.200	4.95
	.100	4.57	.075	4.38	.100	4.56
	.050	3.77	.050	3.60	.050	4.32
	.025	1.58	.025	3.15	.025	4.06
32			.345	w.s.	.380	w.s.
			.275	5.44	.340	5.03
			.225	5.24	.290	5.25
			.175	4.93	.240	5.25
			.125	4.81	.190	4.85
			.075	4.53	.140	4.62
			.050	4.29	.090	4.53
			.025	3.95	.050	4.03
					.025	2.60
45	.185	w.s.	.190	w.s.	.215	w.s.
	.160	3.94	.160	4.08	.200	3.97
	.135	3.95	.135	3.85	.175	3.87
	.110	3.79	.110	3.79	.150	3.68
	.085	3.58	.085	3.52	.125	3.50
45—Con.	0.060	3.49	0.060	3.63	0.100	3.26
	.035	3.34	.035	3.31	.075	2.98
	.010	2.94	.010	2.72	.050	2.48
					.025	1.65
44	.302	w.s.	.300	w.s.	.255	w.s.
	.200	5.70	.239	5.40	.210	5.29
	.175	5.70	.214	5.30	.185	5.11
	.125	4.81	.189	5.45	.135	4.93
	.075	5.20	.164	5.02	.085	4.66
	.050	4.45	.139	5.15	.060	4.79
	.025	4.36	.089	4.39	.035	3.97
			.064	4.25		
			.039	4.15		
			.024	3.67		
42					.295	w.s.
					.275	5.85
					.225	5.84
					.175	5.21
					.150	5.20
					.125	5.42
					.100	5.31
					.075	4.76
					.050	4.23
					.025	3.68

[a] These profiles taken 80, 100, and 124 feet from headbox.

TABLE 16.—*Velocity-profile data for 0.93-mm sand in 8-foot-wide flume*

[The lateral section used for measuring was 95–115 ft from the headbox. w.s.=water surface]

Run	2.0 ft from left wall of flume		4.0 ft from left wall of flume		6.0 ft from left wall of flume	
	Distance above sand bed (ft)	Velocity (fps)	Distance above sand bed (ft)	Velocity (fps)	Distance above sand bed (ft)	Velocity (fps)
19	0.980	w.s.	0.974	w.s.	0.972	w.s.
	.930	1.47	.894	1.58	.930	1.49
	.830	1.50	.697	1.55	.830	1.51
	.680	1.50	.547	1.52	.680	1.48
	.530	1.44	.397	1.41	.530	1.45
	.380	1.38	.297	1.35	.380	1.40
	.230	1.32	.197	1.30	.280	1.36
	.130	1.22	.147	1.25	.180	1.27
	.080	1.11	.097	1.13	.130	1.25
	.040	1.04	.057	1.00	.080	1.13
	.020	.94	.027	.93	.050	1.02
					.020	.91
25			.982	w.s.		
			.905	1.82		
			.855	1.81		
			.755	1.75		
			.655	1.74		
			.555	1.70		
			.455	1.66		
			.355	1.62		
			.255	1.51		
			.155	1.47		
			.105	1.33		
			.065	1.28		
			.030	1.10		
26			1.008	w.s.		
			.955	1.98		
			.855	1.97		
			.755	1.92		
			.655	1.91		
			.555	1.86		
			.455	1.78		
			.355	1.70		
			.255	1.67		
			.155	1.55		
			.105	1.47		
			.065	1.39		
			.030	1.15		
27			1.005	w.s.		
			.975	2.02		
			.875	1.97		
			.775	1.97		
			.625	1.93		
			.525	1.87		
			.475	1.83		
			.375	1.77		
			.275	1.71		
			.175	1.67		
			.125	1.55		
			.075	1.35		
			.035	1.09		
			.005	.69		
20			.980	w.s.		
			.950	2.00		
			.900	2.00		
			.800	2.01		
			.700	1.96		
			.600	1.92		
			.500	1.86		
			.400	1.81		
20—Con.			0.300	1.75		
			.200	1.64		
			.150	1.57		
			.100	1.44		
			.050	1.25		
			.030	1.16		
			.010	.80		
21					0.985	w.s.
					.955	2.23
					.905	2.21
					.805	2.17
					.705	2.14
					.605	2.10
					.505	2.06
					.405	1.99
					.305	1.86
					.205	1.80
					.165	1.79
					.125	1.68
					.085	1.53
					.045	1.31
					.025	1.19
					.015	1.01
18	.900	w.s.	1.060	w.s.	1.012	w.s.
	.870	2.23	1.030	2.23	.982	2.29
	.770	2.22	.900	2.22	.882	2.30
	.670	2.18	.750	2.13	.782	2.27
	.520	2.10	.650	2.13	.682	2.25
	.370	2.06	.550	2.06	.582	2.22
	.270	1.94	.450	1.97	.482	2.16
	.170	1.81	.350	1.92	.382	2.07
	.120	1.72	.250	1.88	.282	1.98
	.070	1.63	.200	1.84	.182	1.91
	.020	1.06	.150	1.74	.132	1.81
			.100	1.49	.082	1.68
			.060	1.37	.052	1.65
			.030	1.23	.022	1.41
28	1.045	w.s.	1.040	w.s.	1.025	w.s.
	.995	2.25	.950	2.33	.975	2.30
	.895	2.21	.750	2.27	.825	2.30
	.695	2.15	.550	2.19	.675	2.25
	.495	2.06	.400	2.12	.575	2.17
	.395	2.00	.300	2.02	.475	2.13
	.295	1.97	.200	1.90	.375	2.09
	.195	1.84	.150	1.83	.275	2.00
	.145	1.78	.100	1.72	.175	1.85
	.095	1.72	.060	1.60	.125	1.75
	.055	1.56	.030	1.40	.075	1.64
	.025	1.44			.035	1.46
29			.480	w.s.		
			.450	1.65		
			.400	1.64		
			.350	1.63		
			.300	1.60		
			.250	1.53		
			.200	1.49		
			.150	1.45		
			.100	1.40		
			.070	1.34		
			.040	1.21		

TABLE 16.—*Velocity-profile data for 0.9-3mm sand in 8-foot-wide flume*—Continued

Run	2.0 ft from left wall of flume		4.0 ft from left wall of flume		6.0 ft from left wall of flume	
	Distance above sand bed (ft)	Velocity (fps)	Distance above sand bed (ft)	Velocity (fps)	Distance above sand bed (ft)	Velocity (fps)
29—Con.			0.020	1.10		
			.010	1.01		
22			.459	w.s.		
			.429	1.65		
			.379	1.62		
			.329	1.61		
			.279	1.59		
			.229	1.54		
			.179	1.52		
			.129	1.41		
			.079	1.32		
			.044	1.25		
			.024	1.16		
30			.496	w.s.		
			.466	1.78		
			.416	1.75		
			.366	1.74		
			.316	1.68		
			.266	1.66		
			.216	1.61		
			.166	1.56		
			.116	1.49		
			.076	1.38		
			.046	1.28		
			.026	1.13		
			.008	.99		
31	0.485	w.s.	.505	w.s.	0.500	w.s.
	.450	1.80	.470	1.80	.470	1.80
	.420	1.78	.400	1.76	.420	1.78
	.370	1.76	.340	1.74	.370	1.77
	.320	1.74	.290	1.68	.320	1.77
	.270	1.72	.240	1.63	.270	1.68
	.220	1.64	.190	1.60	.220	1.68
	.170	1.62	.140	1.48	.170	1.62
	.120	1.49	.090	1.43	.130	1.55
	.080	1.45	.050	1.23	.090	1.45
	.050	1.29	.020	1.08	.060	1.37
	.020	.96			.040	1.24
					.020	1.12
15	.935	w.s.	1.013	w.s.	1.077	w.s.
	.900	2.48	.950	2.50	1.050	2.60
	.750	2.51	.750	2.41	.950	2.52
	.550	2.51	.550	2.26	.750	2.39
	.400	2.40	.400	2.26	.550	2.30
	.300	2.24	.300	2.01	.400	2.14
	.200	2.18	.200	1.91	.300	2.08
	.150	2.13	.150	1.91	.200	1.98
	.100	2.09	.100	.88	.150	1.93
	.060	1.87	.060	1.85	.100	1.80
	.030	1.82	.030	1.83	.060	1.73
					.030	1.75
23					.480	w.s.
					.450	1.87
					.400	1.83
					.350	1.82
					.300	1.76
					.250	1.70
					.200	1.64
					.150	1.62
					.120	1.55
					.090	1.48
					.060	1.40
					.030	1.20
					.010	.95
32	.510	w.s.	.490	w.s.	.500	w.s.
	.490	2.03	.470	2.08	.470	2.01
	.440	2.03	.430	2.06	.420	2.02
	.390	2.05	.380	2.00	.370	2.00
	.340	2.01	.330	1.97	.320	1.98
	.290	1.99	.280	1.95	.270	1.95
	.240	1.97	.230	1.90	.220	1.92
	.190	1.91	.180	1.84	.170	1.85
	.140	1.86	.130	1.75	.130	1.80
	.100	1.76	.090	1.67	.100	1.71
	.070	1.65	.060	1.55	.070	1.63
	.040	1.51	.030	1.29	.040	1.47
	.030	1.39	.010	1.22	.010	1.21
	.010	1.23				
24					.490	w.s.
					.460	1.98
					.410	2.01
					.360	1.92
					.310	1.91
					.260	1.88
					.210	1.78
					.160	1.73
					.110	1.60
					.070	1.49
					.040	1.37
					.020	1.21
14	0.562	w.s.	0.548	w.s.	0.577	w.s.
	.540	2.16	.530	2.17	.560	2.13
	.480	2.13	.480	2.18	.520	2.14
	.430	2.10	.430	2.16	.470	2.14
	.380	2.06	.380	2.13	.420	2.09
	.330	2.03	.330	2.08	.370	2.08
	.280	1.94	.290	1.99	.320	1.99
	.240	1.92	.250	1.98	.280	1.98
	.200	1.85	.210	1.97	.240	1.92
	.160	1.80	.180	1.89	.200	1.86
	.130	1.72	.150	1.84	.160	1.79
	.100	1.66	.120	1.77	.130	1.70
	.070	1.56	.090	1.68	.100	1.62
	.040	1.35	.060	1.62	.070	1.54
	.020	1.26	.030	1.49	.040	1.41
					.020	1.37
34	.540	w.s.	.530	w.s.	.510	w.s.
	.510	2.21	.500	2.28	.480	2.30
	.460	2.20	.450	2.24	.430	2.27
	.410	2.18	.400	2.18	.380	2.24
	.360	2.15	.350	2.13	.330	2.12
	.310	2.10	.300	2.11	.280	2.04
	.260	2.02	.250	1.99	.230	2.04
	.210	1.98	.200	1.90	.180	1.92
	.160	1.88	.150	1.86	.130	1.82
	.110	1.78	.110	1.79	.080	1.71
	.060	1.66	.070	1.58	.050	1.60
	.030	1.47	.040	1.38	.030	1.45
	.010	1.31	.020	.96	.010	1.22
16	1.006	w.s.	.993	w.s.	.995	w.s.
	.950	2.55	.966	2.71	.900	2.74
	.800	2.46	.866	2.66	.700	2.66
	.700	2.44	.666	2.60	.500	2.50
	.600	2.39	.466	2.36	.400	2.40
	.500	2.26	.316	2.13	.300	2.23
	.400	2.15	.216	1.94	.250	2.30
	.300	2.00	.166	1.88	.200	2.07
	.200	1.90	.116	1.83	.150	2.02
	.150	1.76	.066	1.75	.100	1.95
	.100	1.57	.016	1.43	.060	1.94
	.060	1.37			.030	1.79
	.030	1.30				
35	.580	w.s.	.560	w.s.	.550	w.s.
	.540	2.20	.510	2.43	.520	2.42
	.490	2.21	.460	2.42	.470	2.44
	.440	2.28	.410	2.34	.420	2.36
	.390	2.24	.360	2.32	.370	2.32
	.340	2.25	.310	2.36	.320	2.29
	.290	2.16	.260	2.26	.270	2.14
	.240	2.16	.210	2.20	.220	2.06
	.190	2.12	.160	1.98	.170	1.97
	.140	2.00	.110	1.47	.120	1.78
	.110	1.86	.070	1.12	.070	1.58
	.080	1.81	.040	.98	.040	1.48
	.050	1.56	.010	.93	.010	1.33
	.010	.74				
17	1.196	w.s.	.948	w.s.	.890	w.s.
	1.160	2.67	.900	2.66	.860	2.99
	1.060	2.62	.800	2.65	.790	2.96
	.960	2.55	.700	2.57	.690	2.91
	.860	2.51	.600	2.55	.590	2.90
	.760	2.47	.500	2.55	.490	2.87
	.660	2.44	.400	2.47	.390	2.84
	.560	2.34	.300	2.33	.290	2.71
	.460	2.21	.200	2.12	.240	2.60
	.360	2.11	.150	2.00	.190	2.37
	.310	2.11	.100	2.02	.140	2.32
	.260	2.08	.060	1.99	.090	2.18
	.210	1.88	.030	1.84	.060	2.11
	.160	.84			.030	1.85
	.160	.64				
	.060	.58				
33	.500	w.s.	.460	w.s.	.510	w.s.
	.470	2.34	.420	2.63	.450	2.56
	.440	2.30	.370	2.67	.400	2.52
	.390	2.31	.320	2.65	.350	2.48
	.340	2.26	.270	2.61	.300	2.30
	.290	2.23	.220	2.53	.250	2.31
	.240	2.18	.170	2.42	.200	2.18
	.190	2.15	.120	2.36	.150	2.16
	.140	2.15	.080	2.20	.100	2.01
	.090	2.05	.050	2.08	.060	2.00
	.050	1.88	.020	1.79	.030	1.80
	.020	1.62				
5	1.105	w.s.	1.025	w.s.	.955	w.s.
	1.050	2.85	1.000	2.74	.875	2.71
	.950	2.75	.845	2.65	.675	2.76
	.750	2.52	.695	2.61	.525	2.64
	.600	2.52	.545	2.40	.375	2.47
	.500	2.48	.395	2.26	.275	2.51

TABLE 16.—*Velocity-profile data for 0.93-mm sand in 8-foot-wide flume*—Continued

Run	2.0 ft from left wall of flume		4.0 ft from left wall of flume		6.0 ft from left wall of flume	
	Distance above sand bed (ft)	Velocity (fps)	Distance above sand bed (ft)	Velocity (fps)	Distance above sand bed (ft)	Velocity (fps)
5—Con.	0.400	2.44	0.295	2.13	0.175	2.36
	.300	.71	.195	1.95	.125	2.23
	.200	.52	.145	1.58	.075	2.01
	.150	.51	.095	.58	.050	1.98
	.100	.41	.055	.58	.025	2.14
	.060	.45	.025	.73		
	.030	.49				
10	.380	w.s.	.452	w.s.		
	.350	2.63	.390	2.72		
	.300	2.63	.340	2.70		
	.250	2.60	.300	2.67		
	.210	2.59	.260	2.70		
	.170	2.56	.220	2.47		
	.140	2.53	.180	2.47		
	.110	2.49	.140	2.49		
	.080	2.37	.100	2.49		
	.050	2.32	.070	2.47		
	.020	2.25	.030	2.52		
37			.950	w.s.		
			.860	3.26		
			.760	3.10		
			.610	3.03		
			.460	2.99		
			.310	2.69		
			.210	2.50		
			.110	2.07		
			.060	1.29		
			.030	1.09		
36	.425	w.s.	.450	w.s.	0.425	w.s.
	.380	2.67	.420	2.24	.370	1.66
	.330	2.69	.390	2.66	.320	2.70
	.280	2.76	.340	2.52	.270	2.61
	.230	2.49	.290	2.35	.220	2.27
	.180	2.58	.240	2.36	.170	2.43
	.130	2.51	.190	2.36	.120	2.61
	.080	2.47	.140	2.26	.080	2.55
	.050	2.43	.090	2.43	.050	2.51
	.020	2.15	.050	2.12	.020	2.80
			.020	2.05		
6	1.010	w.s.	.965	w.s.		
	.950	3.53	.900	3.20		
	.800	3.53	.700	3.11		
	.650	3.37	.550	3.20		
	.500	3.11	.400	2.94		
	.460	2.64	.300	3.11		
	.300	1.74	.200	2.64		
	.200	2.42	.150	2.85		
	.150	2.08	.180	2.42		
	.100	2.16	.050	1.70		
	.060	2.04				
	.030	2.23				
7	.411	w.s.	.505	w.s.	.555	w.s.
	.350	3.19	.470	3.23	.520	2.81
	.300	3.18	.420	3.19	.420	2.75
	.250	3.13	.370	2.98	.320	2.76
	.200	3.06	.320	2.82	.220	2.70
	.150	3.03	.270	2.54	.170	2.57
	.100	2.57	.220	2.44	.120	2.66
	.060	2.30	.170	1.97	.080	2.60
	.030	2.40	.120	1.53	.050	2.55
			.100	1.82	.020	2.48
			.060	1.84		
			.030	1.76		
38			1.010	w.s.		
			.880	3.64		
			.800	4.02		
			.650	3.68		
			.500	3.52		
			.350	3.39		
			.200	2.60		
			.100	2.41		
			.060	.51		
11	.870	w.s.	.900	w.s.	.830	w.s.
	.750	4.09	.850	3.90	.750	3.34
	.700	4.09	.700	4.09	.650	3.98
	.550	3.75	.550	4.02	.450	4.16
	.400	3.98	.400	3.90	.300	3.59
	.300	3.82	.300	3.75	.200	2.70
	.200	3.59	.200	3.53	.150	2.55
	.150	3.53	.150	3.57	.100	1.34
	.100	3.06	.100	3.18	.060	1.80
	.060	2.60	.060	3.34	.030	1.75
	.030	0.80	.030	2.88		
8	0.550	w.s.	0.422	w.s.	0.372	w.s.
	.500	3.20	.390	3.52	.350	3.20
	.450	3.24	.340	3.52	.300	3.20
	.410	3.31	.300	3.52	.250	3.52
	.370	3.23	.260	3.20	.210	3.12
	.330	3.07	.220	3.08	.170	3.12
	.290	3.00	.180	2.77	.130	2.94
	.250	2.91	.140	2.60	.090	3.20
	.210	2.94	.100	2.41	.060	3.28
	.170	2.71	.060	2.37	.030	.76
	.130	2.61	.030	2.41		
	.090	2.35				
	.060	2.07				
	.030	.88				
13	.410	w.s.	.750	w.s.	.540	w.s.
	.350	5.92	.550	4.85	.450	4.96
	.250	5.42	.450	4.85	.350	4.63
	.150	4.52	.350	4.09	.250	3.95
	.100	4.29	.250	4.22	.150	3.54
	.050	4.22	.150	3.52	.100	3.52
			.100	3.37	.050	3.12
			.050	2.64		
9					.500	w.s.
					.450	3.75
					.400	3.52
					.350	3.83
					.300	3.45
					.250	3.52
					.200	2.42
					.150	2.65
					.100	2.93
					.060	3.03
					.030	2.75
41	.440	w.s.	.400	w.s.	.420	w.s.
	.410	6.72	.360	5.64	.350	5.96
	.360	6.24	.310	5.78	.300	5.17
	.310	5.21	.260	5.56	.250	4.85
	.260	3.95	.210	4.85	.200	5.12
	.210	3.60	.160	4.58	.150	4.70
	.160	3.25	.110	3.94	.100	4.46
	.120	2.52	.060	2.94	.060	3.82
	.090	2.05	.030	2.18	.030	3.20
	.060	1.14				
	.030	2.17				
42	.430	w.s.	.430	w.s.	.470	w.s.
	.390	6.88	.380	7.20	.430	7.35
	.340	6.80	.330	6.88	.380	7.13
	.290	6.61	.280	6.68	.330	6.95
	.240	6.38	.230	6.49	.280	6.74
	.190	6.12	.180	6.21	.230	6.46
	.140	5.82	.130	5.74	.180	6.25
	.100	5.42	.090	5.17	.130	5.63
	.060	4.96	.060	3.95	.090	4.02
	.030	3.52	.030	1.36	.060	1.12
					.030	0.38
40	.360	w.s.	.340	w.s.	.300	w.s.
	.310	6.17	.300	6.61	.280	6.53
	.260	5.92	.260	6.25	.260	5.79
	.210	5.60	.210	6.08	.210	5.37
	.160	5.01	.160	5.74	.160	5.17
	.110	3.95	.110	5.32	.110	4.70
	.060	2.66	.060	4.75	.060	4.19
	.030	1.36	.030	2.18	.030	1.36
43	.410	w.s.	.420	w.s.	.400	w.s.
	.380	7.02	.380	7.23	.360	7.61
	.330	6.91	.330	7.23	.310	7.44
	.280	6.76	.280	7.02	.260	7.30
	.230	6.53	.230	6.65	.210	7.02
	.180	6.37	.180	6.27	.160	6.63
	.130	5.87	.130	5.92	.110	6.04
	.080	5.27	.090	5.52	.060	5.01
	.030	3.12	.060	4.40	.030	3.45
			.030	5.13		
39	.470	w.s.	.410	w.s.	.450	w.s.
	.430	7.09	.390	7.35	.420	7.41
	.390	6.84	.340	7.16	.400	7.37
	.340	6.63	.290	6.99	.350	7.23
	.290	6.76	.240	6.68	.300	7.06
	.240	6.41	.190	6.30	.250	6.64
	.190	6.16	.140	5.87	.200	6.37
	.140	5.64	.100	5.46	.150	5.78
	.100	5.32	.060	4.22	.100	4.64
	.060	2.64	.030	2.18	.060	3.89
	.030	1.36			.030	.58

TABLE 17.—*Velocity-profile data for 0.32-mm sand in 2-foot-wide flume*

[w.s.=water surface]

Run	0.5 ft from left wall of flume		1.0 ft from left wall of flume		1.5 ft from left wall of flume	
	Distance above sand bed (ft)	Velocity (fps)	Distance above sand bed (ft)	Velocity (fps)	Distance above sand bed (ft)	Velocity (fps)
3	0.522	w.s.			0.500	w.s.
	.480	2.04			.450	1.76
	.410	2.04			.350	1.66
	.310	2.04			.250	1.54
	.210	2.04			.150	1.30
	.110	2.04			.100	1.22
	.060	2.04			.050	1.10
	.035	2.04			.025	.91
	.023	1.95				
	.010	1.94				
4	.600	w.s.	0.610	w.s.	.550	w.s.
	.550	1.49	.510	1.73	.500	1.59
	.450	1.56	.410	1.72	.400	1.61
	.350	1.45	.310	1.58	.300	1.57
	.250	1.40	.210	1.52	.200	1.31
	.150	1.28	.180	1.54		
	.125	1.24	.135	1.24		
	.100	1.17	.110	1.13		
	.075	1.05	.080	.97		
	.040	1.09	.060	.90		
	.025	.85	.019	.74		
5	.570	w.s.	.575	w.s.	.660	w.s.
	.520	6.57	.525	6.63	.610	5.90
	.420	6.68	.425	6.69	.510	6.20
	.320	6.28	.325	6.41	.410	5.98
	.220	6.02	.225	6.21	.310	5.69
	.120	5.29	.125	5.12	.210	5.20
	.095	4.85	.075	4.12	.160	5.16
	.070	4.70	.050	4.28	.110	4.07
	.045	4.60	.025	4.60	.085	3.80
	.024	4.64			.060	3.64
					.025	2.81
6	.595	w.s.	.675	w.s.	.650	w.s.
	.545	5.88	.625	6.56	.600	5.75
	.445	5.96	.525	6.60	.500	5.97
	.345	5.86	.425	6.68	.400	5.91
	.245	5.72	.325	6.42	.300	5.86
	.145	5.30	.225	6.07	.200	5.56
	.095	5.18	.175	5.60	.150	5.24
	.045	2.76	.150	5.25	.125	4.35
	.020	1.42	.125	4.78	.100	4.15
			.100	4.45	.075	3.96
			.075	3.64	.050	3.72
			.050	2.88	.021	2.76
			.026	2.29		
21			.545	w.s.		
			.495	3.80		
			.445	3.69		
			.345	3.64		
			.245	3.44		
			.195	3.28		
			.145	3.29		
			.120	3.01		
			.095	3.28		
			.070	3.07		
			.045	2.75		
			.020	1.75		
7	.615	w.s.	.600	w.s.	.610	w.s.
	.565	3.96	.550	3.96	.565	3.67
	.465	4.05	.450	4.14	.465	3.99
	.365	3.70	.350	4.06	.365	3.98
	.265	3.68	.250	3.99	.265	3.63
	.165	3.36	.150	3.47	.165	3.21
	.115	3.37	.100	3.28	.115	2.86
	.090	3.00	.075	2.96	.090	2.63
	.065	2.86	.050	2.94	.065	2.75
	.040	2.60	.022	2.13	.040	2.27
	.019	.87			.019	1.05
8	.562	w.s.	.620	w.s.	.675	w.s.
	.512	3.65	.570	3.60	.625	2.88
	.412	3.97	.520	3.69	.525	3.14
	.312	3.98	.470	4.41	.425	3.57
	.212	3.51	.420	4.35	.325	3.84
	.112	3.61	.320	4.01	.225	3.32
8—Con.	0.062	3.26	0.220	3.88	0.175	3.35
	.037	3.15	.120	3.70	.125	3.33
	.019	2.27	.070	3.69	.075	3.21
			.045	3.00	.050	2.62
			.020	2.62	.025	2.20
20	.511	w.s.	.506	w.s.	.592	w.s.
	.500	5.63	.450	6.03	.440	5.93
	.400	5.76	.400	5.98	.400	5.79
	.300	5.66	.300	6.08	.300	5.68
	.200	5.27	.200	5.80	.200	5.11
	.150	5.27	.150	5.36	.150	5.01
	.100	4.74	.100	4.91	.100	4.64
	.075	4.53	.075	4.77	.075	4.50
	.050	4.06	.050	4.31	.050	3.92
	.025	3.39	.025	3.31	.025	3.64
	.010	2.50	.012	2.60	.009	2.85
19			.585	w.s.		
			.535	5.93		
			.435	5.86		
			.335	5.63		
			.235	5.36		
			.185	5.13		
			.135	4.55		
			.085	4.09		
			.060	2.48		
			.035	1.56		
			.010	1.98		
10	.531	w.s.	.540	w.s.	.529	w.s.
	.450	5.81	.475	5.21	.475	5.80
	.350	5.70	.375	5.15	.375	5.61
	.250	5.24	.275	4.83	.275	5.29
	.150	4.91	.175	4.80	.175	4.96
	.100	4.85	.125	4.58	.125	4.66
	.050	4.18	.075	4.48	.075	4.48
	.025	3.66	.050	3.96	.050	4.08
	.012	2.17	.025	3.05	.025	3.38
			.009	2.16	.008	2.36
9	.585	w.s.	.544	w.s.	.544	w.s.
	.535	5.77	.486	6.14	.444	5.81
	.435	5.85	.436	6.00	.344	5.61
	.335	5.83	.386	6.09	.294	5.48
	.285	5.76	.336	6.07	.244	5.47
	.235	5.63	.286	5.82	.194	5.30
	.210	5.38	.236	5.91	.144	5.08
	.185	5.28	.186	5.68	.219	4.65
	.160	5.26	.136	5.31	.094	4.36
	.135	4.93	.111	5.18	.074	3.96
	.110	4.62	.086	4.82	.050	3.04
	.085	4.42	.061	4.20	.025	2.11
	.060	3.78	.036	3.16	.011	1.85
	.035	1.92	.011	1.75		
	.008	1.15				
12	.643	w.s.	.632	w.s.	.642	w.s.
	.575	5.20	.575	5.25	.575	5.22
	.475	5.27	.475	5.26	.475	5.28
	.375	5.16	.375	5.24	.375	5.21
	.275	4.96	.275	5.18	.275	5.02
	.175	4.80	.175	4.98	.175	4.74
	.125	4.56	.125	4.60	.125	4.46
	.075	4.04	.075	4.26	.075	4.12
	.050	3.70	.050	3.84	.050	3.81
	.025	3.20	.025	3.41	.025	3.13
	.010	2.30	.011	2.27	.009	2.40
11	.546	w.s.	.562	w.s.	.540	w.s.
	.525	5.98	.525	6.03	.525	6.01
	.475	6.07	.475	5.86	.475	6.14
	.375	6.09	.375	5.61	.375	6.03
	.275	5.86	.275	5.45	.275	5.88
	.175	5.37	.175	5.08	.175	5.48
	.125	5.24	.125	4.80	.125	5.61
	.075	4.59	.075	4.40	.075	4.97
	.050	4.05	.050	3.90	.050	4.58
	.025	2.89	.025	3.15	.025	3.61
	.010	1.88	.012	2.60	.009	1.68

791-597 O—66——7

TABLE 18.—*Velocity-profile data for 0.33-mm (uniform) sand in 2-foot-wide flume*

[w.s.=water surface]

Run	0.5 ft from left wall of flume		1.0 ft from left wall of flume		1.5 ft from left wall of flume	
	Distance above sand bed (ft)	Velocity (fps)	Distance above sand bed (ft)	Velocity (fps)	Distance above sand bed (ft)	Velocity (fps)
8			0.435	w.s.		
			.390	1.29		
			.340	1.24		
			.290	1.26		
			.240	1.17		
			.190	1.17		
			.140	.95		
			.090	.90		
			.065	.80		
			.040	.71		
			.015	.72		
5			.456	w.s.		
			.420	1.66		
			.400	1.62		
			.350	1.58		
			.250	1.44		
			.200	1.35		
5 Con.			0.150	1.31		
			.100	1.25		
			.060	1.13		
			.030	.83		
1			.520	w.s.		
			.495	4.60		
			.445	4.70		
			.395	4.60		
			.345	4.55		
			.295	4.49		
			.245	4.40		
			.195	4.19		
			.145	4.06		
			.095	3.83		
			.045	3.42		
			.020	3.11		

TABLE 19.—*Velocity-profile data for 0.33-mm (graded) sand in 2-foot-wide flume*

[w.s.=water surface]

Run	Distance above sand bed (ft)	Velocity (fps)	Distance above sand bed (ft)	Velocity (fps)	Distance above sand bed (ft)	Velocity (fps)
	0.5 ft from left wall of flume		*1.0 ft from left wall of flume*		*1.5 ft from left wall of flume*	
16			0.510	w.s.		
			.490	1.25		
			.450	1.25		
			.400	1.19		
			.350	1.16		
			.300	1.13		
			.250	1.13		
			.200	1.10		
			.150	1.10		
			.100	1.10		
			.060	1.10		
			.040	1.19		
			.020	1.22		
6			.548	w.s.		
			.528	0.62		
			.493	.63		
			.480	.60		
			.430	.60		
			.380	.61		
			.330	.59		
			.280	.58		
			.230	.58		
			.180	.56		
			.130	.53		
			.090	.52		
			.060	.52		
			.040	.51		
			.020	.50		
	1.0 ft from left wall of flume					
5	0.493	w.s.	.533	w.s.		
	.490	1.40	.510	1.39		
	.460	1.36	.460	1.37		
	.410	1.42	.410	1.44		
	.360	1.39	.360	1.38		
	.310	1.34	.310	1.33		
	.260	1.30	.260	1.28		
	.210	1.26	.210	1.25		
	.160	1.14	.160	1.20		
	.110	1.07	.110	1.11		
	.070	.93	.070	1.05		
	.040	.79	.040	.90		
	.020	.68	.020	.77		
	0.5 ft from left wall of flume					
1	0.480	w.s.	.498	w.s.	0.530	w.s.
	.430	2.62	.460	2.63	.490	2.51
	.380	2.62	.410	2.66	.440	2.64
	.330	2.59	.360	2.66	.390	2.67
	.280	2.51	.310	2.56	.340	2.64
	.230	2.43	.260	2.56	.290	2.61
	.180	2.33	.210	2.50	.240	2.49
	.130	2.23	.160	2.38	.190	2.36
	.080	1.98	.110	2.25	.140	2.15
	.050	1.83	.060	2.07	.090	2.02
	.030	1.56	.020	1.89	.050	1.77
	.020	1.38	.010	1.64	.030	1.36
					.020	1.15

Run	Distance above sand bed (ft)	Velocity (fps)	Distance above sand bed (ft)	Velocity (fps)	Distance above sand bed (ft)	Velocity (fps)
	1.0 ft from left wall of flume		*1.0 ft from left wall of flume*		*1.0 ft from left wall of flume*	
10	0.444	w.s.				
	.425	2.51				
	.375	2.51				
	.325	2.43				
	.275	2.47				
	.225	2.37				
	.175	2.30				
	.125	2.31				
	.075	1.95				
	.060	1.99				
	.040	1.90				
	.020	1.62				
8	.515	w.s.	0.640	w.s.		
	.495	2.59	.620	1.94		
	.440	2.69	.550	1.85		
	.390	2.66	.500	1.78		
	.340	2.59	.450	1.74		
	.290	2.51	.400	1.68		
	.240	2.44	.350	1.67		
	.190	2.37	.300	1.63		
	.140	2.36	.250	1.54		
	.090	2.15	.200	1.49		
	.050	1.90	.150	1.44		
	.030	1.78	.100	1.43		
	.020	1.62	.060	1.43		
			.040	1.43		
			.020	1.43		
9	.534	w.s.	.560	w.s.	0.621	w.s.
	.514	1.98	.540	2.66	.601	2.06
	.490	2.09	.490	2.81	.540	2.08
	.440	2.11	.440	3.00	.490	2.08
	.390	2.11	.390	2.88	.440	2.04
	.340	2.11	.340	2.97	.390	2.04
	.290	2.15	.290	2.98	.340	1.98
	.240	2.13	.240	3.02	.290	1.96
	.190	2.00	.190	2.97	.240	1.92
	.140	1.91	.140	2.75	.190	1.61
	.090	1.78	.100	2.39	.140	1.60
	.060	1.65	.060	2.14	.090	1.39
	.040	.99	.040	1.97	.060	1.36
	.020	1.14	.020	1.80	.040	1.31
					.020	1.33
7	.630	w.s.				
	.600	1.93				
	.540	1.92				
	.490	1.85				
	.440	1.81				
	.390	1.77				
	.340	1.75				
	.290	1.72				
	.240	1.72				
	.190	1.64				
	.140	1.60				
	.090	1.58				
	.060	1.58				
	.040	1.41				
	.020	1.31				

TABLE 19.—*Velocity-profile data for 0.33-mm (graded) sand in 2-foot-wide flume*—Continued

Run	Distance above sand bed (ft)	Velocity (fps)	Distance above sand bed (ft)	Velocity (fps)	Distance above sand bed (ft)	Velocity (fps)
	1.0 ft from left wall of flume		*1.0 ft from left wall of flume*		*1.5 ft from left wall of flume*	
2			0.528	w.s.		
			.485	3.40		
			.450	3.36		
			.400	3.23		
			.350	3.12		
			.300	3.09		
			.250	2.96		
			.200	2.94		
			.150	2.97		
			.100	2.85		
			.060	2.73		
			.040	2.61		
			.020	2.08		

Run	Distance above sand bed (ft)	Velocity (fps)	Distance above sand bed (ft)	Velocity (fps)	Distance above sand bed (ft)	Velocity (fps)
	1.0 ft from left wall of flume		*1.0 ft from left wall of flume*		*1.5 ft from left wall of flume*	
3			0.540	w.s.		
			.490	3.88		
			.440	3.75		
			.390	3.82		
			.340	3.45		
			.290	3.52		
			.240	3.52		
			.190	3.45		
			.140	3.12		
			.090	2.84		
			.040	2.64		
			.020	2.18		

TABLE 20.—*Velocity-profile data for 0.47-mm sand in 8-foot-wide flume*

[The lateral section used for measuring was 95-115 ft from the headbox. w.s.=water surface; r.f., reversed flow as indicated by negative pressure on manometer]

Run	2.0 ft from left wall of flume		4.0 ft from left wall of flume		6.0 ft from left wall of flume	
	Distance above sand bed (ft)	Velocity (fps)	Distance above sand bed (ft)	Velocity (fps)	Distance above sand bed (ft)	Velocity (fps)
46	0.938	w.s.	1.489	w.s.	1.576	w.s.
	.843	1.94	1.400	2.24	1.481	2.05
	.743	1.95	1.200	2.27	1.381	2.05
	.643	1.92	1.000	2.26	1.181	1.86
	.543	1.86	.800	2.10	.981	1.68
	.443	1.74	.600	r.f.	.781	1.62
	.343	1.23	.225	r.f.	.581	1.62
	.293	0.96	.050	r.f.	.481	1.31
	.243	1.00	.025	.35	.381	.25
	.193	0.94			.281	r.f.
	.143	1.56			.081	r.f.
	.093	1.49			.006	r.f.
	.068	1.22				
	.043	1.31				
	.018	1.30				
47	.710	w.s.	.659	w.s.	.803	w.s.
	.673	1.78	.618	1.98	.753	1.92
	.573	1.74	.518	1.95	.653	1.88
	.473	1.70	.418	1.94	.553	1.87
	.373	1.65	.318	1.92	.453	1.78
	.273	1.63	.268	1.89	.353	1.72
	.223	1.62	.218	1.82	.303	1.74
	.173	1.55	.168	1.81	.253	1.70
	.148	1.46	.118	1.80	.228	1.65
	.123	1.44	.093	1.80	.203	1.63
	.098	1.44	.068	1.77	.178	1.62
	.073	1.56	.043	1.69	.153	1.58
	.048	1.56	.018	1.62	.128	1.56
	.023	1.48			.103	1.53
					.078	1.38
					.053	1.18
					.028	1.15
48	1.232	w.s.	1.247	w.s.	1.011	w.s.
	1.147	1.91	1.157	1.81	.918	1.84
	1.047	1.88	.957	1.81	.718	1.86
	.847	1.85	.757	1.79	.518	1.84
	.647	1.81	.557	1.75	.318	1.89
	.447	1.79	.357	1.75	.218	1.77
	.347	1.78	.257	1.49	.168	1.75
	.247	1.70	.207	1.30	.118	1.74
	.197	1.71	.157	1.08	.093	1.69
	.147	1.69	.132	.90	.068	1.66
	.122	1.66	.107	.77	.043	1.56
	.097	1.58	.082	.79	.018	1.28
	.072	1.51	.057	.92		
	.047	1.43	.032	1.05		
	.022	1.28				
49	1.240	w.s.	1.220	w.s.	1.710	w.s.
	1.180	3.02	1.160	2.93	1.675	3.21
	1.130	3.07	1.100	2.93	1.475	3.21
	.930	2.99	.900	2.97	1.075	3.12
	.730	2.89	.700	2.97	.875	2.86
	.530	2.81	.500	2.87	.675	
	.430	2.51	.300	2.58	.575	
	.330	1.84	.200	2.34	.475	
	.286	1.10	.150	2.16	.425	
	.255	.96	.100	2.20	.375	
	.230	.63	.075	2.41	.350	
	.205	.63	.050	1.86	.325	
	.180	.42			.275	
	.130	r.f.			.075	
	.030	r.f.			.035	
85	.795	w.s.	.770	w.s.	.775	w.s.
	.750	1.47	.700	1.43	.700	1.43
	.600	1.36	.550	1.36	.550	1.36

Run	2.0 ft from left wall of flume		4.0 ft from left wall of flume		6.0 ft from uleft wall of fl me	
	Distance above sand bed (ft)	Velocity (fps)	Distance above sand bed (ft)	Velocity (fps)	Distance above sand bed (ft)	Velocity (fps)
85 Con.	0.450	1.28	0.400	1.31	0.400	1.30
	.350	1.22	.300	1.23	.300	1.28
	.250	1.15	.200	1.16	.200	1.13
	.200	1.03	.150	1.08	.150	1.12
	.150	.93	.100	.99	.100	1.05
	.100	.86	.080	.97	.080	1.01
	.080	.93	.060	.86	.060	.99
	.060	.93	.040	.78	.040	.90
	.040	.89	.020	.72	.020	.82
	.020	.93				
86	.800	w.s.	.810	w.s.	.800	w.s.
	.750	1.40	.750	1.43	.750	1.41
	.550	1.40	.550	1.32	.550	1.31
	.400	1.24	.400	1.24	.400	1.22
	.300	1.21	.300	1.21	.300	1.16
	.200	1.13	.200	1.07	.200	1.02
	.150	1.02	.150	1.02	.150	.98
	.100	.91	.100	.99	.100	.87
	.080	.77	.080	.96	.080	.85
	.060	.65	.060	.92	.060	.84
	.040	.51	.040	.34	.040	.71
	.020	.57	.020	.34	.020	.30
87	.785	w.s.	.775	w.s.	.770	w.s.
	.750	1.45	.750	1.41	.740	1.59
	.550	1.34	.550	1.26	.550	1.45
	.400	1.25	.400	1.15	.400	1.36
	.300	1.13	.300	1.16	.300	1.28
	.200	1.03	.200	1.05	.200	1.14
	.150	.98	.150	1.05	.150	1.07
	.100	.90	.100	.88	.100	1.03
	.080	.92	.080	.86	.080	.99
	.060	.74	.060	.83	.060	r.f.
	.040	.45	.040	.80	.040	r.f.
	.020	.00	.020	.74	.020	r.f.
88	.780	w.s.	.775	w.s.	.740	w.s.
	.730	1.49	.725	1.48	.710	1.49
	.550	1.43	.550	1.39	.550	1.44
	.400	1.29	.400	1.33	.400	1.28
	.300	1.24	.300	1.20	.300	1.14
	.200	1.09	.200	1.06	.200	1.09
	.150	1.01	.150	.91	.150	.97
	.100	.93	.100	.78	.100	.82
	.075	.88	.075	.73	.075	.74
	.050	.72	.050	.56	.050	.61
	.025	.50	.025	.61	.025	.51
90	.600	w.s.	.595	w.s.	.570	w.s.
	.550	1.65	.550	1.84	.530	1.95
	.400	1.59	.400	1.76	.400	1.91
	.300	1.55	.300	1.62	.300	1.83
	.200	1.49	.200	1.63	.200	1.79
	.150	1.45	.150	1.52	.150	1.74
	.100	1.38	.100	1.45	.100	1.56
	.075	1.35	.075	1.37	.075	1.47
	.050	1.12	.050	1.24	.050	1.26
	.025	.90	.025	1.57	.025	.63
89	.625	w.s.	.630	w.s.	.620	w.s.
	.600	1.58	.600	1.69	.590	1.79
	.500	1.53	.500	1.65	.500	1.76
	.400	1.41	.400	1.63	.400	1.72
	.300	1.36	.300	1.59	.300	1.69
	.200	1.23	.200	1.47	.200	1.57
	.150	1.12	.150	1.36	.150	1.52
	.100	1.08	.100	1.25	.100	1.46
	.075	.97	.075	1.19	.075	1.34

TABLE 20.—*Velocity-profile data for 0.47-mm sand in 8-foot-wide flume*—Continued

Run	2.0 ft from left wall of flume		4.0 ft from left wall of flume		6.0 ft from left wall of flume	
	Distance above sand bed (ft)	Velocity (fps)	Distance above sand bed (ft)	Velocity (fps)	Distance above sand bed (ft)	Velocity (fps)
89—Con.	0.050	0.51	0.050	1.08	0.050	1.22
	.025	.42	.025	.50	.025	1.03
93	.640	w.s.	.540	w.s.	.530	w.s.
	.600	1.80	.500	1.95	.500	2.07
	.500	1.81	.400	1.93	.350	2.00
	.400	1.79	.300	1.86	.250	1.86
	.300	1.74	.200	1.82	.150	1.78
	.200	1.67	.150	1.76	.100	1.67
	.150	1.62	.100	1.72	.075	1.43
	.100	1.64	.075	1.68	.050	.99
	.075	1.57	.050	1.60	.025	.88
	.050	1.48	.025	1.46		
	.025	1.40				
92	.755	w.s.	.740	w.s.	.515	w.s.
	.700	1.84	.700	1.79	.470	1.80
	.550	1.81	.500	1.74	.400	1.78
	.450	1.68	.400	1.63	.300	1.74
	.350	1.31	.300	1.46	.200	1.58
	.250	1.08	.200	1.32	.150	1.22
	.200	1.06	.150	1.27	.100	.73
	.150	1.06	.100	1.23	.075	.76
	.100	1.10	.075	1.12	.050	.82
	.075	.96	.050	.97	.025	.86
	.050	.90	.025	.88		
	.025	.95				
91	.605	w.s.	.530	w.s.	.660	w.s.
	.550	1.84	.490	1.50	.620	1.93
	.450	1.78	.350	1.53	.500	1.90
	.350	1.64	.250	1.51	.400	1.82
	.250	1.28	.200	1.43	.300	1.76
	.200	1.28	.150	1.35	.200	1.66
	.150	.97	.100	1.19	.150	1.62
	.100	.71	.075	1.05	.100	1.55
	.075	1.03	.050	.98	.075	1.45
	.050	.82	.025	.74	.050	1.38
	.025	.92			.025	1.19
82	.765	w.s.	.795	w.s.	.620	w.s.
	.740	2.03	.750	2.12	.560	2.37
	.600	1.84	.550	2.13	.450	2.44
	.500	1.72	.400	2.13	.350	2.44
	.400	1.64	.300	1.91	.250	2.36
	.350	1.68	.200	1.80	.200	2.41
	.300	1.53	.150	1.74	.150	2.16
	.250	.81	.100	1.82	.100	.99
	.200	.00	.075	1.78	.075	.33
	.150	.00	.050	1.46	.050	.48
	.100	.00	.025	.59	.025	.30
	.075	.39				
	.050	.61				
	.025	.63				
51	.364	w.s.	.417	w.s.	.550	w.s.
	.304	2.62	.357	2.12	.520	2.11
	.254	2.63	.307	2.05	.470	2.13
	.204	2.53	.257	1.97	.420	2.10
	.154	2.61	.207	2.22	.370	2.23
	.104	2.39	.157	2.22	.320	2.08
	.079	2.23	.107	2.25	.270	2.10
	.054	.88	.082	1.97	.220	2.13
	.029	.69	.057	1.54	.170	2.10
			.042	.76	.120	2.23
			.027	.69	.095	2.08
					.070	1.81
					.045	1.65
					.020	1.51
52	.897	w.s.	.560	w.s.	.507	w.s.
	.847	2.09	.500	2.08	.490	2.17
	.697	1.77	.350	2.09	.460	2.13
	.597	1.64	.250	2.13	.410	2.23
	.497	1.19	.200	2.02	.360	2.12
	.397	.59	.150	1.98	.310	2.12
	.347	.86	.100	1.85	.260	2.11
	.297	.84	.075	1.61	.210	2.07
	.272	.72	.050	1.30	.160	2.04
	.247	.79	.025	.80	.110	1.97
	.222	.90			.060	1.95
	.197	1.14			.035	1.96
	.147	.00			.015	1.93
	.097	r.f.				
	.047	r.f.				
	.022	r.f.				
73	.802	w.s.	.482	w.s.	.402	w.s.
	.750	2.23	.430	2.23	.350	2.48
	.650	2.26	.400	2.57	.300	2.50
	.550	2.16	.300	2.41	.250	2.47
	.450	2.08	.200	2.33	.200	2.59
	.350	1.93	.150	2.29	.150	2.56
	.300	1.51	.100	2.20	.125	2.51
	.250	.37	.080	1.90	.100	2.50
73—Con.	0.200	0.37	0.060	1.59	0.075	2.27
	.150	.35	.040	.58	.050	2.27
	.125	.38	.020	.50	.025	1.48
	.100	.44				
	.075	.41				
	.050	.41				
	.025	.41				
74	.695	w.s.	.635	w.s.	.570	w.s.
	.640	2.40	.600	1.98	.520	2.23
	.570	2.55	.450	1.97	.400	2.20
	.470	2.57	.350	1.74	.300	2.15
	.370	2.55	.250	1.68	.250	2.08
	.320	2.50	.200	1.66	.200	1.97
	.270	2.29	.150	1.58	.150	1.93
	.220	.37	.100	1.39	.100	1.97
	.170	.35	.080	.66	.080	2.00
	.130	.35	.060	.57	.060	1.93
	.100	.35	.040	.57	.040	1.80
	.080	.33	.020	.62	.020	1.66
	.060	.31				
	.040	.30				
	.020	.28				
76	.625	w.s.	.625	w.s.	.690	w.s.
	.580	2.29	.580	2.33	.650	2.44
	.460	2.43	.460	2.36	.530	2.39
	.360	2.46	.360	2.33	.430	2.29
	.260	2.53	.260	2.30	.330	2.30
	.210	2.34	.160	2.26	.280	2.27
	.160	2.10	.110	2.13	.230	.61
	.135	1.93	.085	2.13	.180	.74
	.110	1.62	.060	2.05	.130	.66
	.085	.53	.040	1.94	.100	.55
	.060	.44	.020	1.90	.075	.55
	.040	.43			.050	.67
	.020	.53			.025	.73
75	.655	w.s.	.640	w.s.	.630	w.s.
	.590	2.16	.590	1.84	.600	2.26
	.500	2.24	.550	1.76	.500	2.23
	.400	2.23	.450	1.70	.400	2.20
	.300	2.31	.350	1.66	.300	1.91
	.250	2.30	.250	1.86	.250	1.62
	.225	2.21	.200	2.02	.200	.84
	.200	1.66	.150	1.98	.150	.74
	.175	.43	.100	1.76	.125	1.07
	.150	.43	.075	.69	.100	.51
	.125	.43	.050	.47	.075	.52
	.100	.41	.025	.61	.050	.58
	.080	.41			.025	.63
	.060	.39				
	.040	.44				
	.020	.50				
53	.600	w.s.	.464	w.s.	.472	w.s.
	.570	2.33	.434	2.31	.437	2.24
	.490	2.39	.364	1.95	.367	2.24
	.390	2.35	.314	1.75	.317	2.19
	.290	1.97	.264	1.63	.267	2.06
	.240	1.71	.214	1.67	.217	1.94
	.190	1.78	.164	1.64	.167	2.09
	.140	1.71	.114	1.76	.117	2.08
	.100	1.64	.089	1.71	.092	1.96
	.075	.83	.064	1.63	.067	1.89
	.050	.35	.039	1.53	.042	1.67
	.025	0	.014	1.21	.017	.54
77	.690	w.s.	.895	w.s.	.510	w.s.
	.620	2.36	.855	2.13	.470	2.48
	.450	2.36	.825	2.10	.400	2.48
	.350	2.27	.725	2.07	.300	2.46
	.250	2.21	.625	1.97	.250	2.43
	.200	2.07	.525	1.97	.200	.51
	.150	1.90	.425	1.78	.150	.50
	.125	1.64	.325	1.64	.125	.50
	.100	1.51	.275	1.57	.100	.75
	.080	.52	.225	1.25	.080	.67
	.060	.43	.175	.54	.060	.67
	.040	.42	.135	.54	.040	.66
	.020	.43	.100	.50	.020	.57
			.075	.50		
			.050	.51		
			.025	.54		
96	.350	w.s.	.525	w.s.	.545	w.s.
	.315	2.39	.495	2.56	.500	2.44
	.250	2.38	.400	2.55	.400	2.34
	.200	2.37	.300	2.40	.300	2.37
	.150	2.36	.200	1.55	.200	2.44
	.100	2.33	.150	.96	.150	2.36
	.075	2.27	.100	.50	.100	2.24
	.050	2.00	.075	.57	.075	2.15
	.025	1.28	.050	.79	.050	1.78
			.025	.84	.025	1.16

TABLE 20.—*Velocity-profile data for 0.47-mm sand in 8-foot-wide flume*—Continued

Run	2.0 ft from left wall of flume		4.0 ft from left wall of flume		6.0 ft from left wall of flume	
	Distance above sand bed (ft)	Velocity (fps)	Distance above sand bed (ft)	Velocity (fps)	Distance above sand bed (ft)	Velocity (fps)
94	0.745	w.s.	0.755	w.s.	0.840	w.s.
	.680	2.59	.700	2.13	.800	2.02
	.550	2.57	.550	2.21	.700	1.98
	.400	2.56	.400	2.15	.550	2.02
	.300	2.52	.300	2.04	.400	2.13
	.200	2.37	.200	2.04	.300	2.20
	.150	2.07	.150	1.90	.200	2.04
	.100	.87	.100	1.68	.150	2.11
	.075	.80	.075	.81	.100	1.98
	.050	.80	.050	.63	.075	1.86
	.025	.99	.025	.69	.050	1.78
					.025	.79
83	1.095	w.s.	.845	w.s.	.965	w.s.
	1.015	1.00	.800	2.43	.900	2.81
	.845	.99	.650	2.43	.800	2.80
	.645	.92	.500	2.45	.650	2.77
	.545	.90	.400	2.45	.500	2.65
	.445	2.53	.300	2.48	.400	2.46
	.395	2.02	.200	2.48	.300	2.27
	.345	.49	.150	2.33	.250	1.25
	.295	.43	.100	2.23	.200	.92
	.270	.45	.075	2.26	.150	.72
	.245	.50	.050	2.04	.100	.46
	.220	.66	.025	.96	.075	.41
	.170	.29			.050	.79
	.130	.39			.025	.66
	.100	.54				
	.075	.74				
	.050	.58				
	.025	.58				
54	.873	w.s.	.815	w.s.	.888	w.s.
	.833	3.01	.755	2.53	.825	2.88
	.783	3.01	.655	2.42	.775	2.80
	.533	2.93	.555	2.47	.725	2.87
	.433	2.61	.455	2.59	.675	2.78
	.333	2.51	.355	2.43	.575	2.86
	.283	1.37	.255	2.07	.475	2.76
	.233	1.00	.205	1.60	.375	2.71
	.183	1.71	.155	1.46	.275	2.57
	.133	1.23	.105	.65	.225	2.27
	.083	1.56	.080	.65	.175	1.90
	.058	.61	.055	.80	.125	1.23
	.033	.68	.030	1.08	.075	1.23
	.018	.96			.050	.96
					.025	.69
56	.830	w.s.	.690	w.s.	1.015	w.s.
	.800	2.61	.650	2.56	.975	2.62
	.750	2.46	.600	2.76	.900	2.71
	.600	2.46	.550	2.94	.800	2.71
	.500	2.22	.500	3.02	.700	2.76
	.400	2.00	.400	3.02	.500	2.71
	.300	1.44	.300	2.94	.400	2.78
	.250	1.48	.200	2.82	.300	2.85
	.200	1.48	.150	2.60	.200	2.64
	.150	1.44	.100	2.41	.150	2.01
	.125	1.25	.050	2.02	.100	.50
	.100	.92	.025	1.84	.075	.41
	.075	.41			.050	.30
	.050	.57			.025	.41
	.025	.79				
55	1.054	w.s.	.585	w.s.	1.060	w.s.
	1.024	2.64	.535	2.50	1.030	3.28
	.874	2.52	.485	2.67	.830	3.25
	.724	2.41	.385	2.66	.630	3.20
	.574	2.46	.285	2.50	.530	3.13
	.474	2.13	.235	2.42	.430	2.75
	.374	1.91	.185	2.32	.380	2.50
	.324	1.66	.135	2.32	.330	1.23
	.274	1.48	.100	2.30	.280	1.28
	.224	1.62	.075	2.37	.230	1.28
	.174	1.46	.050	1.51	.180	1.36
	.124	1.72	.025	1.38	.130	1.07
	.099	1.91			.105	1.07
	.074	2.02			.080	1.42
	.049	2.08			.055	1.42
	.024	1.84			.030	1.50
57	.885	w.s.	.970	w.s.	1.250	w.s.
	.825	2.66	.880	2.60	1.160	2.89
	.625	2.57	.680	2.34	.960	2.50
	.425	2.46	.480	2.37	.760	2.29
	.325	2.34	.380	2.30	.560	2.15
	.225	1.90	.330	2.36	.460	1.88
	.175	1.62	.280	2.33	.360	2.00
	.125	1.91	.230	1.93	.310	.69
	.100	2.61	.180	.50	.260	.45
	.075	.84	.130	.50	.210	.45
	.050	.88	.105	.63	.160	.41
	.025	.84	.080	.63	.120	.41
			.055	.72	.090	.41
			.030	.96	.060	.45
57—Con.					0.025	0.30
58	0.720	w.s.	0.960	w.s.	.900	w.s.
	.680	2.74	.920	2.87	.860	2.76
	.550	2.82	.700	2.63	.730	2.67
	.450	2.78	.500	2.51	.630	2.67
	.350	2.89	.400	2.33	.430	2.60
	.250	2.65	.300	2.48	.330	2.29
	.200	2.73	.250	2.37	.230	2.26
	.150	2.73	.200	2.07	.180	2.21
	.100	2.65	.150	2.10	.155	1.93
	.075	2.57	.125	1.98	.130	.88
	.050	2.24	.100	1.91	.105	.45
	.025	2.20	.075	2.04	.080	.50
			.050	2.04	.055	.41
			.025	1.84	.030	.57
95	.680	w.s.	.630	w.s.	1.130	w.s.
	.630	2.96	.580	2.66	1.080	2.97
	.550	2.98	.400	2.65	.900	2.87
	.400	2.89	.300	2.59	.700	2.64
	.300	2.92	.200	2.19	.550	2.34
	.200	2.87	.150	1.90	.400	2.13
	.150	2.80	.100	1.86	.300	2.02
	.100	2.80	.075	1.72	.200	1.78
	.075	2.54	.050	1.74	.150	1.44
	.050	2.11	.025	1.46	.100	1.16
	.025	1.90			.075	1.10
					.050	.99
					.025	.96
78	.870	w.s.	.625	w.s.	.610	w.s.
	.800	2.61	.530	2.99	.560	2.29
	.650	2.61	.500	2.92	.400	2.33
	.500	2.65	.400	2.84	.300	2.26
	.400	2.65	.300	2.75	.200	2.20
	.300	2.56	.200	2.81	.150	2.60
	.250	2.30	.150	2.78	.100	2.67
	.200	1.51	.100	2.59	.075	2.67
	.175	1.19	.075	2.20	.050	2.60
	.150	1.19	.050	.92	.025	1.22
	.125	1.25	.025	.92		
	.100	1.07				
	.075	1.04				
	.050	1.19				
	.025	1.19				
59	.510	w.s.	.535	w.s.	.640	w.s.
	.490	4.13	.495	4.17	.610	3.50
	.440	4.01	.415	4.05	.550	2.99
	.340	3.93	.315	3.85	.450	2.99
	.290	3.81	.265	4.01	.350	3.20
	.240	3.68	.215	3.77	.300	3.30
	.190	3.85	.165	3.68	.250	3.63
	.150	3.77	.115	3.20	.200	3.50
	.125	3.50	.090	2.07	.150	2.88
	.100	3.35	.065	2.64	.125	2.99
	.075	3.10	.040	2.64	.100	2.94
	.050	2.51	.015	1.22	.075	2.88
	.025	0.00			.050	.74
					.025	.88
60	.635	w.s.	.605	w.s.	.590	w.s.
	.605	5.69	.565	5.42	.560	5.42
	.505	5.69	.465	5.24	.460	5.24
	.405	5.47	.365	5.24	.360	4.93
	.305	4.99	.265	4.87	.260	4.74
	.255	4.60	.215	4.67	.210	4.32
	.205	4.53	.165	4.53	.160	4.31
	.155	4.01	.135	4.31	.110	3.93
	.105	3.50	.105	4.17	.085	3.59
	.080	2.99	.080	3.77	.060	3.10
	.060	2.37	.055	1.90	.040	2.76
	.040	.88	.035	.88	.020	1.48
	.020	.88	.015	.88		
61	.590	w.s.	.550	w.s.	.600	w.s.
	.560	5.58	.540	5.42	.560	5.24
	.460	5.51	.460	5.33	.460	5.21
	.360	5.30	.360	5.12	.360	4.93
	.260	4.99	.260	4.93	.260	4.60
	.210	4.90	.210	4.67	.210	4.43
	.160	4.60	.160	4.46	.160	4.28
	.110	4.31	.110	4.39	.110	4.17
	.085	4.09	.085	4.39	.085	3.85
	.060	3.64	.060	4.24	.060	3.50
	.040	3.50	.040	3.89	.040	2.99
	.020	3.20	.020	3.40	.020	1.90
71	.340	w.s.	.286	w.s.	.345	w.s.
	.310	4.46	.230	4.31	.310	4.31
	.280	4.31	.190	4.31	.280	4.21
	.230	4.31	.160	4.17	.230	4.17
	.180	4.09	.130	4.01	.180	3.89
	.140	3.93	.100	4.17	.140	3.68
	100	3.50	.080	3.77	.100	3.20
	.080	3.10	.060	3.63	.080	2.88

TABLE 20.—*Velocity-profile data for 0.47-mm sand in 8-foot-wide flume*—Continued

Run	2.0 ft from left wall of flume		4.0 ft from left wall of flume		6.0 ft from left wall of flume	
	Distance above sand bed (ft)	Velocity (fps)	Distance above sand bed (ft)	Velocity (fps)	Distance above sand bed (ft)	Velocity (fps)
71—Con.	0.060	1.90	0.040	3.50	0.060	2.64
	.040	.63	.020	3.20	.040	1.90
	.020	.63	.020	2.99	.020	.00
72	.310	w.s.	.320	w.s.	.360	w.s.
	.270	4.39	.275	4.31	.330	4.17
	.220	4.24	.225	4.17	.300	4.17
	.170	4.17	.175	4.01	.250	3.93
	.130	3.96	.125	3.85	.200	3.81
	.100	3.93	.100	3.85	.160	3.68
	.080	3.63	.080	3.68	.130	3.50
	.060	3.30	.060	3.50	.100	3.20
	.040	2.23	.040	3.20	.080	2.99
	.020	1.48	.020	1.70	.060	2.64
					.040	.00
					.020	.00
70	.305	w.s.	.260	w.s.	.275	w.s.
	.290	4.46	.240	4.53	.240	4.39
	.240	4.39	.200	4.46	.200	4.31
	.200	4.39	.160	4.31	.160	4.09
	.160	4.39	.130	4.09	.130	4.01
	.130	4.17	.100	4.01	.100	3.93
	.100	4.09	.080	3.77	.080	3.77
	.080	3.77	.060	3.68	.060	3.68
	.060	3.68	.040	3.20	.040	3.50
	.040	3.40	.020	2.51	.020	3.30
	.020	2.76				
63	.400	w.s.	.450	w.s.	.405	w.s.
	.350	4.80	.400	4.93	.355	5.12
	.300	4.53	.350	4.31	.255	5.64
	.250	4.31	.300	4.93	.205	5.06
	.200	4.67	.250	3.77	.155	4.74
	.150	4.53	.210	5.24	.105	5.06
	.100	3.68	.180	4.24	.085	4.67
	.080	3.85	.150	3.68	.065	4.81
	.060	2.64	.120	3.59	.045	4.09
	.040	.00	.100	1.90	.025	1.90
	.020	1.48	.080	2.23		
			.060	0		
			.040	0		
			.020	0		
64	.320	w.s.	.255	w.s.	.250	w.s.
	.270	4.87	.205	5.36	.200	5.96
	.220	4.31	.155	6.01	.150	4.60
	.170	4.60	.105	5.24	.100	4.60
	.120	3.68	.095	4.93	.080	4.74
	.090	4.01	.075	4.39	.060	4.60
	.060	3.20	.055	4.46	.040	4.39
	.040	4.60	.035	4.93	.020	4.09
	.020	.88	.015	3.40		
65	.325	w.s.	.355	w.s.	.425	w.s.
	.305	5.12	.305	4.74	.355	5.42
	.255	4.67	.255	4.81	.305	5.06
	.205	5.30	.205	4.31	.255	4.87
	.155	3.68	.155	4.09	.205	4.67
	.105	3.93	.105	3.85	.155	4.24
	.075	3.40	.075	4.60	.105	3.59
	.055	3.10	.055	3.30	.075	4.46
	.035	2.76	.035	.88	.055	1.22
	.015	0	.015	.63	.035	.63
					.015	.63
66	.330	w.s.	.345	w.s.	.405	w.s.
	.300	4.81	.295	4.93	.350	5.47
	.270	5.06	.245	4.74	.300	4.46
	.240	4.57	.195	4.39	.250	4.99
	.200	4.24	.145	3.40	.200	5.64
	.160	4.60	.120	4.17	.150	4.09
	.130	4.24	.095	4.24	.125	4.24
	.100	4.81	.070	3.68	.100	3.68
	.080	4.24	.045	1.90	.075	1.70
	.060	3.93	.020	2.07	.050	0.00
	.040	2.07			.025	0.00
	.020	2.07				
80	.295	w.s.	.430	w.s.	.395	w.s.
	.250	5.18	.400	6.20	.375	5.65
	.200	4.40	.350	5.10	.275	5.50
	.150	4.50	.300	4.90	.225	5.10
	.125	4.50	.250	4.50	.175	5.80
	.100	3.70	.200	5.38	.125	5.20
	.075	4.30	.150	4.70	.100	3.85
	.050	4.00	.100	4.25	.075	3.00
	.025	3.82	.075	.85	.050	.64
			.050	.85		
			.025	3.65		
81	.500	w.s.	.505	w.s.	.545	w.s.
	.485	6.45	.420	6.38	.515	6.36
	.385	6.31	.360	6.31	.435	6.16
	.285	6.21	.260	6.01	.335	5.91
	.185	5.42	.210	5.96	.235	5.53
	.135	5.06	.160	5.64	.185	5.47
	.085	4.53	.110	5.47	.135	4.93
	.060	4.09	.085	5.18	.085	4.39
81—Con.	0.035	3.77	0.060	4.60	0.060	4.31
	.015	0	.035	4.67	.035	3.10
			.015	3.77	.015	.63
62	.535	w.s.	.540	w.s.	.530	w.s.
	.505	6.45	.500	6.01	.490	6.11
	.435	6.26	.440	6.31	.430	6.01
	.335	6.06	.340	6.01	.330	5.75
	.235	5.80	.240	5.53	.230	5.64
	.185	5.58	.190	5.36	.180	5.36
	.150	5.91	.140	4.87	.130	5.12
	.125	5.53	.105	4.67	.105	4.87
	.100	4.99	.080	4.09	.080	4.87
	.075	4.67	.060	3.77	.060	4.31
	.055	4.39	.040	1.70	.040	3.93
	.035	4.17	.020	1.22	.020	1.36
	.015	3.93				
67	.465	w.s.	.485	w.s.	.515	w.s.
	.430	6.41	.445	6.21	.480	6.16
	.380	6.11	.345	6.11	.430	6.01
	.330	6.06	.295	5.91	.330	5.59
	.280	5.85	.245	5.80	.280	5.47
	.230	5.53	.195	5.59	.230	5.36
	.180	5.42	.145	5.47	.180	5.12
	.130	4.87	.095	4.99	.130	4.81
	.105	4.60	.070	4.09	.100	4.67
	.080	3.77	.045	4.24	.075	4.09
	.060	3.59	.025	.63	.050	3.30
	.040	1.90			.025	.87
	.020	.87				
79	.520	w.s.	.565	w.s.	.550	w.s.
	.480	6.50	.475	6.31	.480	6.31
	.400	6.36	.400	6.01	.430	6.41
	.300	6.21	.300	5.96	.330	6.01
	.250	6.06	.250	6.01	.280	5.85
	.200	5.53	.200	5.58	.230	5.53
	.150	5.06	.150	5.58	.180	5.58
	.100	4.24	.100	4.99	.130	5.30
	.075	4.24	.075	4.74	.080	4.53
	.050	.88	.050	4.53	.060	4.46
	.025	1.07	.025	.63	.040	3.77
					.020	3.10
84	.340	w.s.	.385	w.s.	.285	w.s.
	.300	6.15	.350	5.90	.250	5.15
	.250	6.50	.300	5.85	.200	4.50
	.200	6.05	.250	5.65	.150	5.25
	.150	5.50	.200	5.65	.100	4.10
	.100	5.40	.150	4.91	.080	4.10
	.080	5.30	.100	4.50	.060	3.60
	.060	4.90	.080	4.40	.040	3.10
	.040	4.25	.060	3.30	.020	.65
	.020	1.38	.040	1.45		
			.020	.65		
68	.404	w.s.	.458	w.s.	.500	w.s.
	.380	6.69	.430	6.64	.480	6.31
	.330	6.69	.380	6.36	.430	6.31
	.280	6.69	.330	6.26	.380	6.16
	.230	6.26	.280	6.31	.330	6.06
	.180	6.21	.230	6.11	.280	6.01
	.130	5.75	.180	5.85	.230	5.80
	.100	6.06	.130	5.53	.180	5.53
	.080	5.69	.100	5.12	.130	5.06
	.060	5.36	.080	5.06	.100	4.74
	.040	5.24	.060	4.99	.080	4.39
	.020	4.31	.040	4.09	.060	3.59
			.020	.69	.040	3.77
					.020	1.48
100	.470	w.s.	.515	w.s.	.515	w.s.
	.430	7.38	.450	7.05	.450	6.69
	.300	6.61	.300	6.65	.300	6.46
	.200	6.31	.200	6.26	.200	6.01
	.150	6.06	.150	6.06	.150	5.47
	.100	5.69	.100	5.36	.100	5.24
	.075	5.18	.075	4.74	.075	4.60
	.050	4.31	.050	3.77	.050	3.85
	.025	2.76	.025	1.49	.025	3.77
99	.400	w.s.	.520	w.s.	.480	w.s.
	.300	7.43	.500	7.05	.350	7.00
	.200	7.05	.400	7.17	.250	5.91
	.150	7.35	.300	6.65	.150	5.85
	.100	5.53	.200	4.60	.100	5.85
	.050	4.24	.150	5.18	.050	1.23
			.100	4.17		
			.050	r.f.		
97	.302	w.s.	.250	w.s.	.311	w.s.
	.287	5.18	.232	5.58	.251	5.36
	.237	5.06	.182	5.30	.201	5.24
	.187	4.67	.132	5.12	.151	5.06
	.137	5.47	.082	4.60	.101	4.74
	.087	5.91	.052	2.99	.076	4.01
	.057	4.74	.022	2.07	.051	3.93
	.017	3.30			.020	2.37

TABLE 21.—*Velocity-profile data for 0.54-mm sand in 2-foot-wide flume*

[w.s.=water surface. Measurement taken 1.0 ft from left wall of flume]

Run	Distance above sand bed (ft)	Velocity (fps)
1	0.605	w.s.
	.565	1.22
	.500	1.16
	.400	1.14
	.300	1.06
	.200	1.02
	.150	.96
	.100	.94
	.075	.90
	.050	.81
	.025	.74
	.010	.63
2	.600	w.s.
	.565	1.26
	.500	1.22
	.400	1.22
	.300	1.18
	.200	1.13
	.150	1.11
	.100	1.07
	.075	1.01
	.050	.99
	.025	.88
	.010	.75
3	.610	w.s.
	.581	1.46
	.575	1.50
	.500	1.31
	.400	1.26
	.300	1.25
	.200	1.13
	.150	1.07
	.100	1.02
	.075	.99
	.050	.90
	.025	.77
	.010	.60
4	.548	w.s.
	.530	1.85
	.520	1.78
	.500	1.78
	.400	1.77
	.300	1.73
	.200	1.65
	.150	1.57
	.100	1.47
	.075	1.46
	.050	1.41
	.025	1.29
	.010	1.16
6	.622	w.s.
	.600	2.07
	.569	2.16
	.500	2.28
	.400	2.30
	.300	2.69
	.200	2.61
	.150	2.99
	.100	3.20
	.075	2.77
	.050	2.04
	.025	1.56
6 Con.	0.010	1.36
5	.774	w.s.
	.745	2.36
	.500	2.42
	.400	2.40
	.300	2.38
	.200	2.24
	.150	2.12
	.100	2.13
	.075	2.11
	.050	1.82
	.025	1.28
	.010	1.19
20	.700	w.s.
	.682	4.67
	.600	5.36
	.500	5.30
	.400	5.12
	.300	4.60
	.200	3.85
	.150	3.30
	.100	2.88
	.075	1.48
	.050	1.22
	.025	1.22
8	.808	w.s.
	.770	2.99
	.700	3.40
	.600	3.59
	.500	3.77
	.400	3.68
	.300	3.40
	.200	3.10
	.150	2.64
	.100	.88
	.075	.88
	.050	1.48
	.025	2.64
8A	.796	w.s.
	.760	3.40
	.700	3.10
	.600	3.30
	.500	3.50
	.400	3.68
	.300	3.10
	.200	2.99
	.150	2.76
	.100	2.07
	.075	2.37
	.050	2.23
	.025	.88
8B	.833	w.s.
	.785	2.51
	.700	2.76
	.600	2.76
	.500	3.10
	.400	3.20
	.300	3.10
	.200	2.76
	.150	2.76
	.100	3.20
8B Con.	0.075	3.20
	.050	2.99
	.025	.88
8C	.832	w.s.
	.780	3.20
	.700	3.20
	.600	3.50
	.500	3.50
	.400	3.40
	.300	3.20
	.200	3.30
	.150	3.20
	.100	3.20
	.075	2.51
	.050	1.22
	.025	.88
7	.558	w.s.
	.510	3.05
	.400	3.04
	.300	2.96
	.200	2.81
	.150	2.76
	.100	2.75
	.075	2.76
	.050	2.75
	.025	2.56
	.010	2.02
19	.643	w.s.
	.605	3.59
	.570	3.97
	.500	4.00
	.400	4.05
	.300	4.41
	.200	3.47
	.150	3.40
	.100	3.23
	.075	2.99
	.050	2.82
	.025	2.64
	.010	2.12
9	.630	w.s.
	.610	3.30
	.500	3.40
	.400	3.30
	.300	3.30
	.200	3.54
	.150	3.40
	.100	3.25
	.075	3.10
	.050	2.82
	.025	2.37
10	.638	w.s.
	.600	5.80
	.500	5.96
	.400	5.91
	.300	5.75
	.200	5.36
	.150	5.18
	.100	4.53
	.025	3.96
	.050	2.15
10 Con.	0.025	1.36
15	.748	w.s.
	.680	6.41
	.600	6.50
	.500	6.46
	.400	6.41
	.300	6.21
	.200	5.91
	.150	5.42
	.100	4.93
	.075	4.09
	.050	3.30
	.025	2.07
15B	.754	w.s.
	.670	6.06
	.600	6.06
	.500	6.11
	.400	6.11
	.300	6.06
	.200	5.75
	.150	5.58
	.100	4.99
	.075	4.46
	.050	4.01
	.025	3.20
13	.707	w.s.
	.672	6.26
	.600	6.31
	.500	6.36
	.400	6.36
	.300	6.21
	.200	5.30
	.150	5.47
	.100	4.74
	.075	3.85
	.050	2.07
	.025	1.22
11	.664	w.s.
	.636	7.67
	.600	7.63
	.500	7.50
	.400	7.20
	.300	7.01
	.200	6.16
	.150	5.52
	.100	3.48
	.075	2.60
	.050	1.51
	.025	1.53
18	.752	w.s.
	.670	6.16
	.600	6.16
	.500	6.16
	.400	6.11
	.300	5.85
	.200	5.36
	.150	5.12
	.100	4.39
	.075	3.59
	.050	4.66
	.025	4.60

REFERENCES

Bagnold, R. A., 1941, The physics of blown sand and desert dunes: London, Methuen and Co., 145 p.

——— 1956, The flow of cohesionless grains in fluids: Royal Soc. [London] Philos. Trans., v. 249, no. 964, p. 256–260.

Barron, E. G., 1963, New instruments for surface-water investigations: U.S. Geol. Survey Water-Supply Paper 1669–Z, p. Z4–Z8.

Brooks, N. H., 1958, Mechanics of streams with movable beds of fine sand: Am. Soc. Civil Engineers Trans., v. 123, p. 526–549.

Colby, B. R., 1961, Effect of depth of flow on discharge of bed material: U.S. Geol. Survey Water-Supply Paper 1498–D, 12 p.

Gilbert, G. K., 1914, Transportation of debris by running water: U.S. Geol. Survey Prof. Paper 86, 263 p.

Langbein, W. B., 1942, Hydraulic criteria for sand-waves: Am. Geophys. Union Trans., p. 615–618.

Liu, H. K., 1957, Mechanics of sediment-ripple formation: Am. Soc. Civil Engineers Jour., v. 83, paper 1197, 23 p.

Richardson, E. V., Simons, D. B., and Posakony, G. J., 1961, Sonic depth sounder for laboratory and field use: U.S. Geol. Survey Circ. 450, 7 p.

Rubey, W. W., 1938, The force required to move particles on a stream bed: U.S. Geol. Survey Prof. Paper 189–E, 21 p.

Simons, D. B., Richardson, E. V., and Albertson, M. L., 1961, Flume studies using medium sand (0.45 mm): U.S. Geol. Survey Water-Supply Paper 1498–A, 76 p.

Simons, D. B., Richardson, E. V., and Haushild, W. L., 1963, Some effects of fine sediment on flow phenomena: U.S. Geol. Survey Water-Supply Paper 1498–G, 45 p.

U.S. Inter-Agency Report No. 11, 1957, The development and calibration of the visual-accumulation tube: Minneapolis, Minn., St. Anthony Falls Hydraulic Laboratory.

○